Geochemical and mineralogical evaluation of toxic contaminants mobility in weathered coal fly ash: as a case study, Tutuka dump site, South Africa

By

Segun Ajayi **Akinyemi**

B. Sc (Hons.) M.Sc (UWC)

A Thesis Submitted in fulfilment of the requirement for the Degree of

Doctor of Philosophy in Applied Geology

of

The University of the Western Cape

Supervisors: Prof. L. F. Petrik, Dr A. Akinlua and Dr M. W. Gitari.

May 2011.

DECLARATION

I declare that **Geochemical and mineralogical evaluation of toxic contaminants mobility in weathered coal fly ash: as a case study, Tutuka dump site, South Africa** is my own work, that it has not been submitted before for any degree or examination in any other university, and that all the sources I have used or quoted have been indicated and acknowledged as complete references.

Segun Ajayi Akinyemi **May 2011**

Signed: ……..

ACKNOWLEDGEMENTS

Every worthwhile goal requires a journey. In the same way every journey must have a destination. My arrival at this destination has been made possible only through the assistance, guidance and prayers of so many people who are hereby gratefully acknowledged. Firstly, I will like to give the Almighty God all the glory, honour and adoration for seeing me through this great journey.

To my supervisors, Professor Leslie F. Petrik, Dr Akin Akinlua and Dr Wilson M. Gitari, I say a big thank you for your untiring efforts and interest in this work. You introduced me to the world of Environmental Geochemistry and ensured that I receive water, care and nourishment from time to time. Your self-belief in me was indeed a great motivation. From time to time, you are ever willing to attend to my "don't knows". The fruit of your support is evident, and I am indeed very grateful.

To the Department of Earth Sciences, University of the Western Cape, Bellville, South Africa, the Head of the department, Prof. Charles Okujeni and all the members of staff, I say a big thank you for the good and cordial working relationship I enjoyed during my studies.

To the Environmental and Nano Science Research Group, Department of Chemistry, University of the Western Cape, Bellville, South Africa South Africa, thank you for awarding me a PhD bursary. To the SASOL/ESKOM thank you for providing me with postgraduate grant and making your facilities available for this research study.

This study would not have been completely satisfying without the cordial and good working relationship I had with my colleagues in the Environmental and Nanoscience Laboratory, including Ojo Olanrewaju Fatoba; Omotola Oluwafunmilayo Babajide; Ziboneni Godongwana; Qiling Ying Naidoo; Nicholas Mulei Musyoka; Godfrey Madzivire; Grace Nyambura Muriithi; Monday Alegbe; Olushola Rotimi Adeniyi; Kasongo Wa Kasongo; Alexander Ilchev; Bonelwa Mabovu; Sammy Nyale; Paul Chuks Eze; Waheed Saban; Guillaume Ndayambaje; Nomso Hintsho; Nosipho Khuse and others. Your contributions are highly appreciated. The leadership role and cooperation from our post-doctoral fellows; Richard Odunayo Akinyeye; Alexander Nechaev; Gillian Balfour; Ravi Vadapalli are gratefully acknowledged.

I wish to thank all the ministers and members of the Church of God where I derived spiritual nourishment. The Redeem Christian Church of God, Victory Center, and lately, Household of God Centre: you served as a river to keep me evergreen. Most especially, Pastor and Pastor (Mrs) Sola Oduwole; Pastor (Dr) Olanrewaju Fatoba; Pastor Rasak Olowu; Pastor Monday Alegbe; Pastor Tolu Balogun; Pastor (Mrs) Oluwatoyin Olukunle; Deaconess Abiodun Folakemi Fatoba; Deaconess Caroline Akinyeye; Deacon Oluwafemi Adewumi; Deacon Ademola Adeshina; Dr Jelili Babajide; Brother George Chigwanda. I am indeed very proud of you.

My brothers and friends both here in South Africa and in Nigeria, I say thank you for always being there for me from time to time. Mr. Kehinde Kayode Agbele; Mr. Oluwaseun Adejuwon Fadipe; Engr. Tajudeen Fatayo; Mr. Rasak Afolabi; Dr Bamikole Amigun; Dr Tunde Ojumu; Dr Niyi Isafiade; Dr Solomon Adekola; Chief (Hon.) Femi Alfred Aluko; Mr. Tajudeen Temitope Afolabi; Ayodeji Olatunde Egunlusi; Mr. Jemiseye Kayode; Busuyi Adewale Egunlusi etc. (you are too many to be all mentioned by name), your contributions are noticed. Thank you.

I also thank Ms. Riana Rossouw, ICP-MS Laboratory in the University of Stellenbosch for multi element analysis. I wish to express my heartfelt gratitude to Prof. Richard Madsen, University of Missouri, USA for his assistance on statistical evaluation of the analytical data.

I am grateful to the management of the University of Ado-Ekiti, Nigeria for granting me the permission to undertake this study.

Finally, to all my family members, I say thank you. I am particularly grateful to my parents, “Madam Julianah Eeguntola Egunlusi-Akinyemi and Chief Shittu Fatumi Akinyemi-Kojere” for my education and upbringing. It is delightful to see you alive as I progress in life. Painfully, Mummy passed away at the climax of this work, may her soul rest in peace. My beloved siblings “Dr Mathew Adelusi Egunlusi; Mr. Oluwadamilare Festus Egunlusi; Mr. Omotuyise Benjamen Egunlusi**”**, I missed you greatly during the period I was away studying for this degree. I know you missed me more. All my other family members are equally gratefully acknowledged. Thanks for the love and care.

DEDICATION

This project is dedicated to

The

Almighty God,

My beloved parent

Late Chief and Mrs. Shittu Fatumi Akinyemi-Kojere

And

My beloved family members

For your prayers, love, understanding and endurance during my absence from home during this course of study.

Geochemical and mineralogical evaluation of toxic contaminants mobility in weathered coal fly ash: as a case study, Tutuka dump site, South Africa

Segun Ajayi Akinyemi

KEYWORDS

Coal fly ash

Dry disposed fly ash

Weathering/ageing

Unsaturated weathered ash

Mineral phases

Bulk chemistry

Pore water chemistry

Insoluble mineral phase

Dissolved soluble salts

Acid susceptibility

Soluble buffering constituents

Amphoteric behaviour

Modified sequential extraction scheme

Chemical partitioning

Metals mobility

Major oxides

Major elements

Trace elements

Anion species

Geochemical and mineralogical evaluation of toxic contaminants mobility in weathered coal fly ash: as a case study, Tutuka dump site, South Africa

Segun Ajayi Akinyemi

ABBREVIATIONS

ICP-AES = Inductively coupled plasma-optical emission

ICP-MS = Inductively coupled plasma- mass spectrometry

AAS = Atomic absorption spectrometry

XRF = X-ray fluorescence

XRD = X-ray diffraction

FTIR = Fourier transform infrared rays

SEM /EDS= Scanning electron microscopy and energy dispersive spectroscopy

COD = Coefficient of divergence

Rho = Spearman's correlation coefficient

^{o}C = degree Celsius

Mt = Million tonnes

mg/kg = Milligram per kilogram

Kt = Kilo tonnes

ppm = Part per million

mol/ l = Mole/litre

mg/L = Milligram per litre

Ingress CO_2 = Ingressed carbon dioxide

NO_3 = Nitrate

Ingress O_2 = Ingressed oxygen

% = Percent

SO_4^{2-} = Sulphate

LOI = Loss on ignition

PO_4 = Phosphate

BCR = Community Bureau of Reference

Cl^- = Chloride

ABSTRACT

The management and disposal of huge volumes of coal combustion by products such as fly ash has constituted a major challenge to the environment. In most cases due to the inadequate alternative use of coal fly ash, the discarded waste is stored in holding ponds, slag heaps, or stock piled in ash dumps. This practice has raised concerns on the prospect of inorganic metals release to the surface and groundwater in the vicinity of the ash dump. Acceptable scientific studies are lacking to determine the best ash disposal practices. Moreover, knowledge about the mobility patterns of inorganic species as a function of mineralogical association or pH susceptibility of the dry disposed ash dump under natural weathering conditions are scarce in the literature. Fundamental understanding of chemical interactions of dry disposed ash with ingressed CO_2 from atmosphere, percolating rain water and brine irrigation within ash disposal sites were seen as key areas requiring investigation. The mineralogical association of inorganic species in the dry disposed ash cores can be identified and quantified. This would provide a basis for understanding of chemical weathering, mineralogical transformations or mobility patterns of these inorganic species in the dry ash disposal scenario.

The current study therefore aims to provide a comprehensive characterisation of weathered dry disposed ash cores, to reveal mobility patterns of chemical species as a function of depth and age of ash, with a view to assessing the potential environmental impacts. Fifty-nine samples were taken from 3 drilled cores obtained respectively from the 1 year, 8 year and 20-year-old sections of sequentially dumped, weathered, dry disposed ash in an ash dump site at Tutuka - a South African coal burning power station. The core samples were characterized using standard analytical procedures viz: X-ray fluorescence (XRF), X-ray diffraction (XRD), Fourier transforms infrared (FTIR) techniques, Scanning electron microscopy/energy dispersive spectroscopy (SEM/EDS) and Acid neutralisation capacity (ANC) test. A modified sequential extraction (SE) method was used in this study. The chemical partitioning, mobility and weathering patterns in 1 year, 8 year and 20-year-old sections of the ash dump were respectively investigated using this modified sequential extraction scheme. The sequence of the extractions was as follows: (1) water soluble, (2) exchangeable, (3) carbonate, (4) iron and manganese and (5) residual. The results obtained from the 5 steps sequential extraction scheme were validated with the total metal content of the original sample using mass balance method. The distribution

of major and trace elements in the different liquid fractions obtained after each step of sequential extraction of the 59 drilled core samples was determined by inductively coupled plasma mass spectrometry (ICPMS). The data generated for various ash core samples were explored for the systematic analysis of mineralogical transformation and change in ash chemistry with ageing of the ash. Furthermore, the data was analyzed to reveal the impact of ingressed CO_2 from atmosphere, infiltrating rain water and brine irrigation on the chemistry of ash core samples. Major mineral phases in original ash core samples prior to extraction are quartz (SiO_2) and mullite ($3Al_2O_3 \cdot 2SiO_2$). Other minor mineral phases identified were hematite (Fe_2O_3), calcite ($CaCO_3$), lime (CaO), anorthite ($CaAl_2Si_2O_8$), mica (Ca (Mg, Al)$_3$ (Al_3Si) O_{10} $(OH)_2$), and enstatite ($Mg_2Si_2O_6$). X-ray diffraction results show significant loss of crystallinity in the older ash cores. The presence of minor phases of calcite and mica in dry disposed ash cores are attributed to reduction in the pore water pH due to hydration, carbonation and pozzolanic reactions. The X-ray diffraction technique was unable to detect Fe-oxyhydroxide phase and more aluminosilicate phases in ash core samples due to their low abundance and amorphous character. X-ray fluorescence results of the original ash core samples showed the presence of major oxides, such as SiO_2, Al_2O_3, Fe_2O_3, while CaO, K_2O, TiO_2, Na_2O, MnO, MgO, P_2O_5, and SO_3 occur in minor concentrations. The ratio of SiO_2/Al_2O_3 classified the original core samples prior to extraction as a silico-aluminate class F fly ash. The ternary plot of major elements in 1-year-old ash core samples was both sialic and ferrocalsialic but 8 year and 20-year-old ash core samples were sialic in chemical composition. It is noteworthy that the mass % of SiO_2 varies through the depth of the core with an increase of nearly 3 %, to 58 mass % of SiO_2 at a depth of 6 m in the 1-year-old core whereas in the case of the 8-year-old core a 2 % increase of SiO_2 to a level of 57.5 mass % can be observed at levels between 4-8 m, showing dissolution of major components in the matrix of older ash cores.. The Na_2O content of the Tutuka ash cores was low and varied between 0.6-1.1 mass % for 1-year-old ash cores to around 0.6-0.8 mass % for 8-year-old ash cores. Sodium levels were higher in 1-year-old ash cores compared to 8 year and 20-year-old ash cores. Observed trends indicate that quick weathering of the ash (within a year) leached out Na^+ from the ash dump. No evidence of Na^+ encapsulation even though the ash dump was brine irrigated. Thus the dry disposal ash placement method does not result in a sustainable salt sink for Na-containing species over time. The total content of each of the elements in 1 year and 20-year-old ash cores was normalised with their total content in fresh ash from same power station

to show enrichment and depletion factor. Major elements such as K^+, Mn showed enrichment in 1-year-old ash cores whereas Al, Si, Na^+, Ti, Ca, Mg, S and Fe showed depletion due to over time erosion. Trace elements such as Cr, Sr, P, Ba, Pb, V and Zn showed enrichment but Ni, Y, Zr showed depletion attributed to over time erosion. In 20-year-old ash cores, major elements such as Al, Na^+ and Mn showed enrichment while Si, K^+, Fe, Mg and Ca showed depletion highlighting their mobility. Trends indicated intensive flushing of major soluble components such as buffering constituents (CaO) by percolating rain water. The 1-year-old and 20-year-old coal ash cores showed a lower pH and greater loss/depletion of the soluble buffering constituents than the 2-week-old placed ash, indicating significant chemical weathering within a year. Based on ANC results the leaching behaviours of Ca, Mg, Na^+, K^+, Se, Cr, and Sr were found to be controlled by the pH of the leachant indicating high mobility of major soluble species in the ash cores when in contact with slightly acid rain water. Other investigated toxic metals such as As, Mo and Pb showed amphoteric behaviour with respect to the pH of the leachant. Chemical alterations and formation of transient minor secondary mineral phases was found to have a significant effect on the acid susceptibility and depletion pattern of chemical species in the core ash samples when compared to fresh ash. These ANC results correlated well with the data generated from the sequential extraction scheme. Based on sequential extraction results elements, showed noticeable mobility in the water soluble, exchangeable and carbonate fractions due to adsorption and desorption caused by variations in the pore water pH. In contrast, slight mobility of elements in the Fe and Mn, and residual fractions of dry disposed fly ashes are attributed to the co-precipitation and dissolution of minor amount of less soluble secondary phase overtime. The 1-year-old dry disposed ash cores were the least weathered among the 3 drilled ash cores. Therefore low concentration of toxic metals in older ash cores were ascribed to extensive weathering with slower release from residual mineral phases over time. Elements were found to associate with different mineral phases depending on the age or depth of the core samples showing greater heterogeneity in dispersion. For instance the average amount of total calcium in different mineral associations of 1-year-old ash cores is as follows; water soluble (10.2 %), exchangeable (37.04 %), carbonate (37.9 %), Fe and Mn (7.1 %) and residual (2.97 %). The amount of total Na^+ in different mineral phases of 1-year-old ash cores followed this trend: water soluble (21 %), exchangeable (11.26 %), carbonate (2.6 %), Fe and Mn (4.7 %) and residual (53.9 %). The non-leachable portion of the total Na^+ content (namely that contained in

the residual fraction) in the 1-year-old ash core samples under conditions found in nature ranged between 5-91 %. This non-leachable portion of the Na^+ showed the metastability of the mineral phases with which residual Na^+ associates. Results showed older ash cores are enriched in toxic elements. Toxic elements such as As, B, Cr, Mo and Pb are enriched in the residual fraction of older ash cores. For instance As concentration in the residual fraction varied between 0.0003-0.00043 mg kg^{-1} for 1-year-old ash cores to around 0.0003-0.0015 mg kg^{-1} for 20-year-old ash cores. This suggests that the older ash is enriched in toxic elements hence dust from the ash dump would be toxic to human health. The knowledge of mobility and ecotoxicological significance of coal fly ash is needed when considering its disposal or reuse in the environment. The mobility and ecotoxicology of inorganic metals in coal fly ash are determined by (i) mineralogical associations of inorganic species (ii) in-homogeneity in the ash dumps (iii) long and short term exposure to ingress CO_2 and percolating rain water. Management issues such as inconsistent placement of ash in the dumps, poor choice of ash dump site, in-homogeneity in brine irrigation, no record of salt load put on the ash dumps and lack of proper monitoring requires improvement. The thesis provides justification for the use of the modified sequential extraction scheme as a predictive tool and could be employed in a similar research work. This thesis also proved that the dry ash disposal method was not environmental friendly in terms of overall leaching potential after significant chemical weathering. Moreover the study proved that the practice of brine co-disposal or irrigation on ash dumps is not sustainable as the ash dump did not act as a salt sink.

TABLE OF CONTENTS

DECLARATION……...II
ACKNOWLEDGEMENTS…….III-IV
DEDICATION……...V
KEYWORDS…….VI
ABBREVIATIONS……..VII
ABSTRACT …….VIII-XI
TABLE OF CONTENTS……..XII-IX
List of Figures...…….....XX-XXV
List of Tables……...…XXVI-XXVII
CHAPTER ONE……..1
INTRODUCTION……...1
1 Background information and motivation……..1
1.1 Statement of the problem……...3
1.2 Objectives……..5
1.3 Research questions…….5
1.4 Scope and delimitations of study……...6
1.5 Study area……..7
1.6 Research hypothesis……...7
1.7 Research approach…….7
1.8 Thesis layout……..9
CHAPTER TWO……...11
Literature Review of Fly ash……..11
2. Introduction to coal as a source material for fly ash..……11
2.1 Coal formation process...…….12

2.1.1 South African coal reserve and its distribution…….14
2.1.2 Coal composition and types……..15
2.1.3 Mineralogy, major and trace elements in coal……..……17
2.1.4 Coal texture and structure…….21
2.1.5 Uses of coal……...22
2.2 Coal fired power generation technologies……...23
2.2.1 Conventional coal fired power station……..23
2.2.2 Cyclone furnaces……...24
2.2.3 Environmental impacts of coal fired electrical generation……...25
2.3 Electricity generation……...26
2.4 Need for research into fly ash……..26
2.4.1 Coal fly ash……...28
2.4.2 Classification of fly ash……30
2.4.3 Physical properties of coal fly ash……31
2.4.4 Physico-chemical properties of fly ash…….33
2.4.5 Disposal of fly ash……39
2.4.6 Weathering processes of fly ash……...41
2.4.7 pH and neutralizing capacity of fly ash……44
2.4.8 Leaching of fly ash……...46
2.5 Utilization of fly ash……50
2.5.1 Construction work and industry……...51
2.5.2 Road and pavement utilization…….53
2.5.3 Construction materials utilizing light weight aggregate……...54
2.5.4 Use of fly ash to neutralize AMD…….55
2.5.5 Use of fly ash for Agricultural purposes……...57
2.5.6 Réclamation and revegetation of damaged areas……..59

2.5.7 Application of zeolite synthesis from fly ash……...60
2.5.8 Utilization of coal fly ash in geopolymeric material……61
2.5.9 The effect of fly ash disposal on a soil and ground water system……62
2.6 Selective sequential extraction techniques…….....64
2.6.1 Concept of sequential extraction scheme and its applications……64
2.6.2 Exchangeable fraction……..67
2.6.3 Carbonate (acido-soluble) fraction……...68
2.6.4 Iron and manganese hydroxide fraction……...68
2.6.5 Residual fraction…….....70
2.6.6 Harmonization of sequential extraction protocol: BCR scheme…….....71
2.6.7 Drawbacks of sequential extraction procedure……74
2.6.7.1 Lack of selectivity of reagents……...74
2.6.7.2 Readsorption and redistribution……75
2.6.7.3 Sample pre-treatment……76
2.6.7.4 Methodology……..78
2.8 Total metal digestion……79
CHAPTER THREE……...83
Geology and stratigraphy of the Tutuka Ash dump site……83
3. Introduction……...……83
3.1 Description of Tutuka Power Station……...84
3.2 Dry ash disposal system at Tutuka Power Station…….....86
3.3 Weather and climate of Tutuka ash dump site…….....87
3.4 Stratigraphy and depositional setting of Karoo Super group……...88
3.5 Local geology of Tutuka ash dump site…….....91
3.6 Geophysical survey of Tutuka ash dump site…….....91
3.7 Lithostratigraphy of the Tutuka ash dump site…….....96
3.8 Summary and conclusions……...99

CHAPTER FOUR……100
Analytical techniques and experimental protocols……..…100
4. Description of the Tutuka ash dump..……..…100
4.1 Sampling techniques…….……..…101
4.1.1 Borehole positions……..……101
4.1.2 Pre-treatment and storage of drilled core ash samples……103
4.2 Standard Experimental Methods……104
4.2.1 Moisture content determination……..104
4.2.2 Determination of loss on ignition (LOI) of drilled core samples……105
4.2.3 Sample pre-treatment for wet chemical extraction procedures……...105
4.2.4 Pore water chemistry of drilled weathered cores……...106
4.2.5 Sequential extraction procedure……..……..106
4.2.5.1 Common procedure for steps 1- 4……106
4.2.6 Total acid digestion……..……..108
4.2.7 Acid neutralization capacity experiment (ANC)……109
4.2.8. Standard analytical and instrumental techniques……..….111
CHAPTER FIVE……112
Results and Discussion 1……112
Physicochemical and mineralogical analysis of drilled cores……..112
5. Introduction……..……112
5.1 Optimum moisture content of dry disposed ash cores……..113
5.2 Mineralogy of the dry disposed ash cores……..114
5.3 Bulk chemical composition of 2 week, 1 year, 8 year and 20-year-old dry disposed ash cores.……122
5.4 Enrichment and depletion of major and trace components in dry disposed ash……132
5.5 FTIR analysis of 2 week and 20-year-old dry disposed ash cores…….....136
5.6 SEM and EDS analytical results……138

5.7 pH and EC of the extracted interstitial pore water……140

5.8 Anion and cation constituents of the extracted interstitial pore water……...145

5.9 Up flow percolation test (Column leaching test) results...…….151

5.10 Summary and conclusions……...152

CHAPTER SIX……...154

Results and Discussion 2…….154

Inorganic metal leaching and acid susceptibility of weathered dry disposed fly ashes……..154

6. Introduction…….……154

6.1 Bulk mineralogy of fresh and unsaturated weathered ash cores……....156

6.2 Bulk chemistry of fresh ash and unsaturated weathered ash cores……157

6.3 Pore water chemistry of fresh ash and unsaturated weathered fly ashes……...158

6.4 Acid neutralization capacity test results…….....160

6.5 Chemical characterization of the leachates……....163

6.6 Summary and conclusions…….173

CHAPTER SEVEN…….175

Results and Discussion 3…….175

Chemistry of the major species and its impacts on the chemistry of trace toxic species (such as As, Se, B, Cr, Mo and Pb) in weathered drilled ash cores ……..175

7. Introduction…..……175

7.1 Chemical sequential extraction scheme results……..…….176

7.1.1 Analysis of water soluble fraction……..176

7.1.1.1 Aluminium and silicon…….176

7.1.1.2 Iron and manganese…….178

7.1.1.3 Calcium and magnesium……..181

7.1.1.4 Sodium and potassium……184

7.1.2 Analysis of exchangeable and carbonate fractions……..……185

7.1.3 Fe and Mn, and residual fractions……...……195

7.2 Distribution pattern of major elements in the five geochemical phases of 1-year-old ash core samples…….207

7.2.1 Aluminium and silicon……207

7.2.2 Iron and manganese……210

7.2.3 Calcium and magnesium…….210

7.2.4 Sodium and potassium……211

7.3 Total metal concentration of major elements in weathered ash cores ..……212

7.4 Statistical assessment of data quality……215

7.4.1 Fractionation scheme and efficiency of fractionation for major elements…….216

7.5 Markers for major elements in fly ashes for environmental applications……..221

7.5.1 Major element patterns by age and depth of dry disposed ash core samples…..…...……221

7.6 Summary and conclusions…….228

CHAPTER EIGHT……..231

Results and Discussion 4…….231

Chemical partitioning and mobility of As, Se, B, Cr, Mo and Pb in weathered drilled ash cores aged 1 year, 8 year and 20 year……231

8. Introduction……..231

8.1 Total content of trace elements in weathered drilled core ash samples ……...233

8.2 Chemical sequential extraction scheme results for trace toxic elements……...235

8.2.1 Analysis of water soluble fraction..……235

8.2.1.1 Arsenic and selenium ……..235

8.2.1.2 Molybdenum and chromium ……..……..238

8.2.1.3 Lead and boron ……...……241

8.2.2 Analysis of exchangeable fraction...……...244

8.2.2.1 Arsenic and selenium ……....244

8.2.2.2 Molybdenum and chromium ……..…….....246

8.2.2.3 Lead and boron ……..……..……...248

8.2.3 Analysis of carbonate fraction……250

8.2.3.1 Arsenic and selenium ……...……...250

8.2.3.2 Molybdenum and chromium ……..……..……253

8.2.3.3 Lead and boron …….…….…….255

8.2.4 Analysis of Fe and Mn fraction……..257

8.2.4.1 Arsenic and selenium ……..……257

8.2.4.2 Molybdenum and chromium ……..……259

8.2.4.3 Lead and boron ……..…….261

8.2.5 Analysis of residual fraction……...263

8.2.5.1 Arsenic and selenium ……..…….263

8.2.5.2 Molybdenum and chromium ……...……...…….265

8.2.5.3 Lead and boron…...…….....……...267

8.3 Distribution of trace elements in the five leached fractions……..269

8.3.1 Water soluble fraction…….272

8.3.2 Exchangeable and carbonate fractions……272

8.3.3 Iron and manganese fraction…….....273

8.3.4 Residual fraction…….274

8.4 Fractionation scheme and efficiency of fractionation for trace elements……..275

8.5 Trace element patterns by age and depth of dry disposed fly ash……....279

8.6 Summary and conclusions…….....282

CHAPTER NINE……....284

Conclusion and recommendations…….....284

9. Overview……..……284

9.1 Insight from physico-chemical and mineralogical analysis of weathered drilled ash cores……...285

9.1.1 Pore water chemistry…….……..285

9.1.2 Mineralogical composition by XRD/FTIR…….286

9.1.3 Elemental composition by XRF and total digestion……...286

9.1.4 Morphology by SEM……..287

9.2 Acid susceptibility by ANC tests……..……288
9.3 Mineralogical partitioning by chemical sequential extraction…….……289
9.4 Integration of findings……...……294
9.5 Main scientific contributions of the dissertation……...295
9.6 Recommendations……295
9.7 Future work……295
9.8 Output from the dissertation…….296
9.8.1 Contribution at conferences..…….296
9.8.2 Manuscripts and publication authored from PhD study……296
REFERENCES.....297
APPENDIX……335
Appendix A. Analytical techniques…….....335
i. pH measurements.…….....335
ii. Electrical conductivity (EC) measurement……..336
iii. Total dissolved solids (TDS)…….....336
iv. Bulk chemical composition by X-ray fluorescence (XRF).……...337
v. Mineralogical analysis by qualitative and quantitative X-ray diffraction (XRD).…….....338
vi. Fourier Transform Infra-Red analysis of drilled core Samples.……...340
vii. Scanning electron microscopy-energy dispersion spectroscopy.…….....341
viii. Ion chromatography (IC)…….....342
ix. Inductively coupled plasma mass spectroscopy (ICP-MS) ….……..344
x Up flow percolation test (Column leaching test)……..……346

LIST OF FIGURES

Figure 3.1. Topographical map of the area and facilities surrounding the Tutuka power station (in relation to topography, ash dump, coal stockyard, dirty dam, sewage plant and solid waste site) ……84

Figure 3.2. Tutuka locality site map ash dump, water dam to the north and small water body to the east. Scale 1:1000 m…….85

Figure 3.3. Photograph of dry ash disposal system at Tutuka Power Station……86

Figure 3.4. Stratigraphy and inferred depositional settings of the southern Karoo Basin……..89

Figure 3.5. Geological profile of borehole at Tutuka Ash dump site……....93

Figure 3.6. Ash-1 and Ash-1B traverses used in the electrical resistivity surveys of dry disposed fly ash dump at Tutuka Power Station…….....94

Figure 3.7. Electric resistivity profile at line ASH-1 on Tutuka: Profile length: 1700 m……94

Figure 3.8. Electrical resistivity profile at Line ASH-1b on Tutuka: Profile length: 1700 m……95

Figure 3.9. Graphic log and physical sample description by depth for borehole AMB 79……96

Figure 3.10. Graphic log and physical sample description by depth for borehole AMB81……..97

Figure 3.11. Graphic log and physical sample description by depth for borehole AMB 83……98

Figure 4.1. Horizontally lay down dry disposed ash in Tutuka ash dump site……....100

Figure 4.2. Map of Tutuka ash dump showing the positions of the geophysics lines (1:50000) and drilling points (core drilled bore holes) marked as anomaly positions……....101

Figure 4.3. Estimated boreholes positions in relation to the electrical resistance profile results.....102

Figure 4.4. Air flush barrel and drilled core ash sample inside barrel……..103

Figure 4.5. Sampling of drilled core ash samples in Zip lock sample bags and storage in a lid plastic container……...103

Figure 4.6. Schematic diagram of research approach…….……104

Figure 5.1. % moisture content of dry disposed fly ash as a function of depth…….113

Figure 5.2. XRD spectra for 2-week-old (T 87) dry disposed ash cores...……..115

Figure 5.3. XRD spectra for 1-year-old (AMB 83) dry disposed ash cores ...……....115

Figure 5.4. XRD spectra for 8-year-old (AMB 81) dry disposed ash cores ..…….116

Figure 5.5. XRD spectra for 20-year-old (AMB 79) dry disposed ash cores ...……..116

Figure 5.6. Bulk XRD mineral mean peak heights in 1-year-old Tutuka ash samples.……...117

Figure 5.7. Bulk XRD mineral mean peak heights in 8-year-old Tutuka ash samples...…….118

Figure 5.8. Bulk XRD mineral mean peak heights in 20-year-old Tutuka ash samples...……...119

Figure 5.9. Ternary oxide plots for classification of the 2-week-old drilled ash cores..…….130

Figure 5.10. Ternary oxide plots for classification of the 1-year-old drilled ash cores..…….130

Figure 5.11. Ternary oxide plots for classification of the 8-year-old drilled ash cores.……..131

Figure 5.12. Ternary oxide plots for classification of the 20-year-old drilled ash cores..……...131

Figure 5.13. FT-IR Spectrum of 20-year-old dry disposed fly ash core (at 1 m depth) sample……..136

Figure 5.14. FT-IR Spectrum of 20-year-old dry disposed fly ash core (at 10 m depth) sample……..137

Figure 5.15. FT-IR Spectrum of 2-week-old dry disposed fly ash (at 1 m depth) sample…….....137

Figure 5.16. SEM photomicrograph of fly ash samples: (a) 2-week-old (1 m depth) (b) 20-year-old drilled ash core (9 m depth)……..…….139

Figure 5.17. pH and EC of pore water versus depth for 20-year-old drilled ash core (n=3)…...141

Figure 5.18. pH and EC of pore water versus depth for 8-year-old drilled ash core (n=3)..…...142

Figure 5.19. pH and EC of pore water versus depth for 1-year-old drilled ash core (n=3).……143

Figure 5.20. (a) pH of pore water versus depth and (b) EC of pore water versus depth for 2-week-old drilled ash core (n=3)…….144

Figure 5.21. Concentration of Cl^-, SO_4, NO_3 and PO_4 by depth in the pore water for 20-year-old dry disposed fly ash…….146

Figure 5.22. Concentration of Cl^-, SO_4, NO_3 and PO_4 by depth in the pore water for 1-year-old dry disposed fly ash…….147

Figure 5.23. Concentration of some chemical species (As, Mo, K and Na) by depth in the pore water for 20-year-old drilled ash core…….....149

Figure 5.24. Concentration of some chemical species (Ca, Se, Fe, B and Mg) by depth in the pore water for 20-year-old drilled ash core……..150

Figure 6.1. XRD spectra of fresh ash (FA) used for ANC test…...…….156

Figure 6.2 (a). Major elements in water soluble extract of fresh ash (FA) and unsaturated weathered ashes…..…….158

Figure 6.2 (b). Trace elements in water soluble extract of fresh ash (FA) and unsaturated dry disposed ashes……..…….159

Figure 6.3 a & b. Variations of pH as a function of acid susceptibility behaviours of fresh as(FA) unsaturated weathered ash as a function of pH……161

Figure 6.4 (a & b). EC as function of acid susceptibility of fresh ash (FA) and unsaturated weathered ash…..…….162

Figure 6.5 (a). Acid leaching behaviour of major elements (Na and K) from the unsaturated dry disposed fly ashes at different depths as determined at different pH.……164

Figure 6.5 (b). Acid leaching behaviour of major elements (Ca and Mg) from the unsaturated dry disposed fly ashes at different depths as determined at different pH.……165

Figure 6.5 (c). Acid leaching behaviour of major elements (Al and Si) from the unsaturated dry disposed fly ashes at different depths as determined at different pH.…….166

Figure 6.6 (a). Acid leaching behaviour of trace elements (Cr, Se and Sr) from the fly ashes at different depths as determined at different pH.…….169

Figure 6.6 (b). Acid leaching behaviour of trace elements (As, Mo and Pb) from the fly ashes at different depths as determined at different pH.……...170

Figure 6.7a. The extractability of major elements in de-ionized water and acid leaches……171

Figure 6.7b. The extractability of trace elements in de-ionized water and acid leaches…….172

Figure 7.1. Aluminium and silicon trend in water soluble fraction of drilled cores of different ages and depths……..……..179

Figure 7.2. Iron and manganese trend in water soluble fraction of drilled cores of different ages and depths ...……....180

Figure 7.3. Calcium and magnesium trend in water soluble fraction of drilled cores of different ages and depths…….……..182

Figure 7.4. Sodium and potassium trend in water soluble fraction of drilled cores of different ages and depths ……...183

Figure 7.5. Aluminium and silicon trend in exchangeable fraction of drilled cores of different ages and depths……..……..186

Figure 7.6. Iron and manganese trend in exchangeable fraction of drilled cores of different ages and depths……..……...187

Figure 7.7. Calcium and magnesium trend in exchangeable fraction of drilled cores of different ages and depths……..……..188

Figure 7.8. Sodium and potassium trend in exchangeable fraction of drilled cores of different ages and depths……..……..189

Figure 7.9. Aluminium and silicon trend in carbonate fraction of drilled cores of different ages and depths……190

Figure 7.10. Iron and manganese trend in carbonate fraction of drilled cores of different ages and depths……...……191

Figure 7.11. Calcium and magnesium trend in carbonate fraction of drilled cores of different ages and depths……..……...192

Figure 7.12. Sodium and potassium trend in carbonate fraction of drilled cores of different ages and depths……..……...193

Figure 7.13. Aluminium and silicon trend in Fe and Mn fraction of drilled cores of different ages and depths……..……...199

Figure 7.14. Iron and manganese trend in Fe and Mn fraction of drilled cores of different ages and depths……200

Figure 7.15. Calcium and magnesium trend in Fe and Mn fraction of drilled cores of different ages and depths……..……..201

Figure 7.16. Sodium and potassium as a function of depth in Fe and Mn fraction of drilled cores of different ages……...202

Figure 7.17. Aluminium and silicon trend in residual fraction of drilled cores of different ages and depths……203

Figure 7.18. Iron and manganese trend in residual fraction of drilled cores of different ages and depths……...……204

Figure 7.19. Calcium and magnesium trend in residual fraction of drilled cores of different ages and depths……..……...205

Figure 7.20. Sodium and potassium trend in residual fraction of drilled cores of different ages……..……206

Figure 7.21. Distribution of Al, Si, Fe and Mn in geochemical phases of 1-year-old fly as…...208

Figure 7.22. Distribution of Ca, Mg, Na and K in geochemical phases of 1-year-old fly ash…209

Figure 7.23. Relationship of K in the exchangeable, carbonate and Fe and Mn fractions with depth of dry disposed fly ash……...223

Figure 7.24. Relationship of Mn in water soluble fraction with the age of dry disposed fly ash……226

Figure 7.25. Relationship of Mn in the exchangeable, carbonate, Fe and Mn and residual fractions with the age of dry disposed fly ash……..……227

Figure 8.1. Arsenic and selenium trend in water soluble fraction of drilled cores of different ages and depths…….……...237

Figure 8.2. Molybdenum and chromium trend in water soluble fraction of drilled cores of different ages and depths...……..240

Figure 8.3. Boron and lead trend in water soluble fraction of drilled cores of different ages and depths……...……243

Figure 8.4. Arsenic and selenium trend in exchangeable fraction of drilled cores of different ages and depths…….……...245

Figure 8.5. Molybdenum and chromium trend in exchangeable fraction of drilled cores of different ages and depths...……..247

Figure 8.6. Boron and lead trend in exchangeable fraction of drilled cores of different ages and depths (Pb is not detected in the 8-year-old core).....…….……249

Figure 8.7. Arsenic and selenium trend of depth in carbonate fraction of drilled cores of different ages and depths……251

Figure 8.8. Molybdenum and chromium trend in carbonate fraction of drilled cores of different ages and depths……..……..254

Figure 8.9. Boron and lead trend in carbonate fraction of drilled cores of different ages and depths……...……256

Figure 8.10. Arsenic and selenium trend in Fe and Mn fraction of drilled cores of different ages and depths…….……...258

Figure 8.11. Molybdenum and chromium trend in Fe and Mn fraction of drilled cores of different ages and depths……...…….260

Figure 8.12. Boron and lead trend in Fe and Mn fraction of drilled cores of different ages and depths (Boron was below detection limit in the 1-year-old)……..……..263

Figure 8.13. Arsenic and selenium trend in residual fraction of drilled cores of different ages and depths (Selenium is not detected in the 1-year-old core)...……..264

Figure 8.14. Molybdenum and chromium trend in residual fraction of drilled cores of different ages and depths (Molybdenum is not detected in the 8-year-old ash cores)…….....……..266

Figure 8.15. Boron and lead trend in residual fraction of drilled cores of different ages and depths……...……268

Figure 8.16. Distribution of As, Se, Mo and Cr in five fractions of 1-year-old ash cores……...270

Figure 8.17. Pb and B distribution in five fractions of 1-year-old ash cores……..271

Figure 8.18. Relationship of As in residual fractions with the age of dry disposed fly ash……282

Figure Ai. Hanna HI 991301 pH meter with portable pH/EC/TDS/Temperature probe…….335

Figure Aii. Phillips PANalytical pw1480 X-ray spectrometry using Rhodium tube as X-ray source……...337

Figure Aiii. Phillips PANalytical XRD instrument with pw 3830 X-ray generator operated at 40 kV and 25 mA……..339

Figure Aiv. Perkin Elmer Spectrum 100 series (FT-IR spectrometer), Universal ATR accessory spectrometer…….341

Figure Av. Ion chromatography system-Dionex ICS-1600 (RFIC)……343

Figure Avi. ICP Optical Emission Spectrometer (Varian 710-ES)…….345

LIST OF TABLES

Table 2.1. Percentage distribution of Coal resources and reserves in the differential coal fields in South Africa…….....15

Table 2.2. Characteristic of the coal fed into European power station…….....19

Table 2.3. Average concentrations and range of major and minor elements in eastern US bituminous coal……..20

Table 2.4. ASTM Standards classification of fly ash……31

Table 2.5 Normal range of chemical composition for fly ash……...34

Table 2.6. Typical concentrations of trace element in fly ash……...34

Table 2.7. Thermal transformation of mineral phases……...38

Table 4.1 Drilled core of different ages and depth intervals used for the study…….102

Table 4.2. List of chemical reagents of analytical grade used in the study…….……109

Table 5.1. Summary of the statistical analysis of the peak heights of various mineral phases in Tutuka fly ashes (1 year, 8 year and 20-year-old dry disposed fly ash……..…….120

Table 5.2. Chemical composition of drilled core taken from 2-week-old section of the dry disposed fly ash dump……..125

Table 5.3. Chemical composition of drilled core taken from 1-year-old section of the dry disposed fly ash dump…….…….126

Table 5.4. Chemical composition of drilled core taken from 8-year-old section of the dry disposed fly ash dump…….127

Table 5.5. Chemical composition of drilled core taken from 20-year-old section of the dry disposed fly ash dump……..128

Table 5.6. Chemical composition of fresh and composite weathered ash core……...…132

Table 5.7. Chemical composition and calculated enrichment/depletion factors for 1 year and 20-year-old dry disposed ash cores……...135

Table 5.8. Mass balance showing the concentration (mg/kg) and percentage (%) of salts captured in the Tutuka fly ash after the percolation of 50 L brine solution……...152

Table 6.1. Concentration of trace elements (ppm) in fresh ash (FA) and unsaturated dry disposed coal fly ashes……...…….157

Table 6.2. Anion constituents (mg/L) leaching into water soluble fraction of fresh ash (FA) and unsaturated weathered ash samples in 30 minutes……..160

Table 7.1a. The concentration (mg/kg) of major elements in 1-year-old ash samples as determined by triple acid digestion…….213

Table 7.1b. The concentration (mg/kg) of major elements in 8 year and 20-year-old ash samples as determined by triple acid digestion……...……..214

Table 7.2. Recoveries obtained in analysis of the NIST SRM 2689 (Class F fly ash) subjected to triple acid digestion……..215

Table 7.3. Statistical analysis of five fractions in 25 sub samples from 1-year-old ash….……216

Table 7.4a. Major elements distribution in five step sequential scheme and total metal content in samples taken at 1 m, 3 m, 5 m and 7 m depths in Tutuka 1-year-old ash cores..…….218

Table 7.4b. Major elements distribution in five step sequential scheme and total metal content in samples taken at 9 m, 12 m, 15 m and 18 m depths in Tutuka 1-year-old ash cores...……...219

Table 7.4c. Major elements distribution in five step sequential scheme and total metal content in samples taken at 22m, 27m, 29m and 31m depths in Tutuka 1-year-old ash cores...…….220

Table 7.5. Relationship of major element in different solubility medium with depth of dry disposed fly ash……222

Table 7.6. Relationship of major element in different solubility medium with age of dry disposed ash cores……...225

Table 8.1. Trace elements distribution in a total acid digested weathered drilled ash cores.…..234

Table 8.2. Statistical analysis of five fractions in 25 sub samples from 1-year-old ash….…….275

Table 8.3. Trace metals distribution in five step sequential scheme and total metal content in samples taken at various depths in 1-year-old ash cores……...……..277

Table 8.3 contd. Trace metals distribution in five step sequential scheme and total metal content in samples taken at various depths in 1-year-old ash cores...……..278

Table 8.4. Relationship of trace elements in different solubility with depth of weathered dry disposed fly ashes……279

Table 8.5. Relationship of trace elements in different solubility medium with depth of dry disposed fly ashes……281

CHAPTER ONE

Introduction

This chapter gives a brief introduction to ash disposal and its environmental implications then brings concept of species mobility, leaching, weathering and sequential extraction scheme and its applications, background information and motivation. The statement of the problem, research objectives, methodology that was adopted and thesis layout are presented.

1. Background information and motivation

The increasing need for production of electricity to meet the nation's energy demand, abundant coal reserve, and low operational cost of the coal-fired power generating stations has made electric power generating companies in South Africa (i.e. SASOL and ESKOM) to rely solely on coal as their fuel source. Coal fly ash is a solid residue of coal combustion processes from electrical power generating stations (Burgers, 2002; Bezuidenhout, 1995; Petrik *et al*., 2003). Fly ash is a non-volatile, incombustible, thermally altered mineral matter comprising of the inorganic components that were originally contained in coal (Scheetz *et al*., 1998) and is the most abundant residue from coal combustion during power generation. Other waste residues produced during combustion include flue gas desulphurization (FGD) sludge, fluidized bed boiler (FBB) waste, and bottom ash (Andriano *et al*., 1980).

During combustion, the inorganic mineral impurities in the coal such as clay, feldspars and quartz are thermally fused and float out of the combustion chamber with exhaust gases. As the fused material rises, it cools and solidifies into spherical glassy particles called fly ash (Basham *et al*., 2007). The properties of the ash depend on the physicochemical properties of coal and the coal burning process. Other factors according to Saikia *et al*. (2006) which include the source of coal and the ash disposal method used, will impact upon the release of contaminants to the environment. Coal in South Africa can produce up to > 40 % of its weight as coal ash after combustion (Breslin and Duedall, 1983). This solid residue (coal ash) obtained from coal combustion process is composed of 70 % fly ash and the remaining portion is bottom ash (Fulekar and Dave, 1986).

Fly ash can be reused as additive to cement, concrete, ceramic products, construction fill, road base, and mineral filler in asphaltic mix (Fulekar and Dave, 1986). It is also useful as a soil stabilizer in agricultural lands (Ghodrati *et al*., 1995). Despite all these beneficial routes of fly ash reuse, huge quantities of coal fly ash are still stored in piles and ash dump sites. Thus the coal-fired power stations are faced with fly-ash disposal problem. The ESKOM Report (2009), show that ESKOM generates about 37 Mt of fly ash annually which only 5 % is currently utilized, the rest being disposed in ash dams, landfills or ponds (Petrik *et al*., 2003). The largest proportion of coal ash is stored in the form of waste-heaps, which create a serious and acute environmental problem (Kalembkiewicz *et al*., 2008). The production of ash is continuously increasing, and its disposal is expensive (Lecuyer *et al*., 1996). Previous studies have shown that sub bituminous coal contains trace elements (As, B, Ba, Be, Bi, Cd, Co, Cr, Cs, Cu, Ga, Ge, Hg, Li, Mn, Mo, Ni, Pb, Rb, Sb, Se, Sn, Sr, Ta, Th, Tl, U, V, W, Y, Zn, Zr and Rare Earth Element) and some of them (i.e. As, B, Ge, Se, Pb, Mo, Zn and Tl) are reported to be potentially toxic elements (Querol *et al*., 1995). All these elements remain in fly ash after coal combustion. Toxic constituents in fly ash include As, Be, B, Cd, Cr (III), Cr (VI), Co, Pb, Mn, Hg, Mo, Se, Sr, Tl and V along with dioxins and polycyclic aromatic hydrocarbon (PAH) compounds (Aljoe *et al*., 2007; Huffman *et al*., 1994; Davison *et al*., 1974). It has been proven that the concentrations of these inorganic toxic metals depend on the source of parent coal and combustion process (Kim *et al*., 2003; Wang *et al*., 2004a). It has been reported that soluble salt content in fly ashes is closely related to the coal properties and the age of the fly ash and also to the pH and other environmental conditions (Plank and Martens, 1973). The coal fly ash generated in power stations is alkaline as a result of the presence of soluble basic oxides, such as CaO and MgO (Kutchko *et al*., 2006; Choi *et al*., 2002; Saikia *et al*., 2006).

The quantity and nature of inorganic metals and metalloids released from fly ash at the ash dump sites are related to the composition of the parent coal burnt, the combustion conditions and ash disposal system utilised at the power station. Chemical species such as anions and cations as well as toxic elements are possibly leached in significant quantities from the stockpiles or ash heaps by the waste water derived from the ash slurry, or brines used for dust suppression, or by subsequent infiltration of rain water. The principal processes affecting the leaching process when fly ashes interact with water are dissolution of primary solids and precipitation of secondary minerals, as well as redox, sorption and hydrolysis reactions. The release of trace elements from

a typical fly ash is considered to be sometimes complex process, strongly dependent on the resulting pH due to interaction with the leaching solutions (Jankowski *et al*., 2006).

The knowledge of mobility and ecotoxicological significance of coal fly ash is needed when considering its disposal or reuse in a natural environmental setting. The mobility and ecotoxicology of inorganic metals in coal fly ash are determined by (i) the physicochemical conditions under which the fly ash is stored (ii) the total leachable metal content in fly ash (iii) the distribution and mineralogical fractionation of metals (Jegadesaan *et al*., 2008). Most often, the mineralogical distribution of metals in the fly ash appears to play a major role in metal leachability and mobility. The mobility of trace metals in coal fly ash when in contact with infiltrating rain water, ingressed O_2 and CO_2 over an extended period may cause serious environmental indication. The associated chemical interactions within ash dumps might lead to progressive chemical alteration, elevated concentration of enriched toxic elements which can contaminate both groundwater and surface water in the environment. Therefore fly ash should be disposed safely to prevent pollution to the environment (Van der Berg *et al*., 2001; Theis and Wirth, 1977).

The dissolution of toxic and non-toxic trace elements locked in different physicochemical forms in coal fly ashes is envisaged to occur when coal fly ash weathers. It has been reported that the non-toxic elements that are soluble will first leach out in when in contact with water or weak acids (Green and Manahan, 1978) but in the long-term, leaching of toxic trace elements is associated with slow mobility of elements from glass, magnetite and related minerals (Hulett *et al*., 1980). Thus the chemical interactions of coal fly ashes with infiltrating rain water, ingressed O_2 and ingressed CO_2 at the ash dumps might take a long time to mobilise or entrap trace metals from the fly ash solid phase. This might eventually lead to salt precipitation or entrapment of toxic elements by the formed secondary minerals. Previous studies have revealed the alteration of aluminosilicate phases to non-crystalline glass during weathering of coal fly ash (Zevenbergen et al., 1999).

1.1 Statement of the problem

There are a number of studies showing that the process of mineral transformation during the weathering/ageing of coal or municipal solid waste incineration (MSWI) ashes is similar to that of volcanic ashes in nature. Yet, the time frames are quite different: while volcanic ashes need

several thousands of years for clay mineral development, there is evidence that e.g. clay illite is formed from glass phases in MSWI bottom ash after only 12 years or that clay-like amorphous material can be formed in micro-scale throughout the surfaces of coal ash particles after 8 years of natural weathering (Zevenbergen *et al*., 1999; Zevenbergen *et al*., 1998; Zevenbergen *et al*., 1996). Natural weathering of MSWI for a period of about 90 days reduced the leaching of heavy metals, stabilised the bottom ash pH, minimising the solubility of metal hydroxides, and this enabled the residue to be used as secondary building material (Chimenos *et al*., 2000).

Based on these studies on volcanic material, coal or MSWI ashes it is presumed that weathered fly ashes, like those stored in Tutuka ash dump site used in this study, would have been subject to similar weathering and mineral transformation processes. The chemical interactions amongst the coal fly ash, rain water, ingressed O_2 from atmosphere for an extended period, might eventually lead to mineralogical transformations, affect the metal partitioning and mobility, and affect the acid neutralization capacity (ANC) of coal fly ash. The weathering process of coal fly ash could lead to dissolution of primary mineral phases, precipitation of secondary mineral phases and heavy metal fixation. The precipitation and dissolution of mineral phases therefore would significantly affect the mobility and release mechanism of toxic metals in coal fly ash under natural environmental settings. This highlighted that weathering process would alter the chemistry of fly ash and ultimately affect the inorganic metals present in different physicochemical forms in the coal fly ash. Many of these prior studies were done on Class C ash or other waste residues and few studies exist on South African class F ash.

Moreover, there are two ash disposal placement methods: dry or wet ash disposal methods. Acceptable scientific studies are lacking to determine the best ash disposal practices. Today, there are many ash dump sites undergoing long-term chemical interaction with the ingressed O_2, ingressed CO_2 from atmosphere and percolating rain water. The challenge is to understand the speed and the extent of the mineral transformations, chemical partitioning and mobility, acid neutralisation capacity of unsaturated zones and the potential metal release of weathered dumped ash in South Africa. This is very crucial for conducting risk assessments of the rate and extent of toxic element that may leach from coal fly ash dumps and storage piles. The application of sequential extraction scheme, mineralogical evaluation, and acid neutralisation capacity (ANC)

tests will serve as techniques to determining the mineralogical associations and mobility patterns of inorganic species in weathered dry disposed ash core.

1.2 Objectives

In general, the objective of this study is to apply five steps sequential extraction scheme modified from a previous study (Tessier *et al*., 1979), to identify and quantify the mineralogical association of inorganic metals in weathered coal fly ash of different ages. Among the trace metals of interest are As, B, Cr, Pb, Mo, and Se. These inorganic toxic in coal fly ash are known to have varying degrees of toxicity.

In specific terms, the objectives of the study are:

1. To understand the degree of chemical weathering over time by comparing the fresh ash with dry disposed fly ash in a land fill.
2. To elucidate weathering patterns along the depths and over time in dry disposed fly ash.
3. To reveal mobility patterns of inorganic elements and various mechanisms controlling their mobility in a dry disposed ash scenario.
4. To understand the impacts of chemical weathering on the acid neutralisation capacity (ANC) of dry disposed fly ash.
5. To reveal the extent of leaching of chemical species to ground water system.

1.3 Research questions

Wet and dry methods of ash handling are recognised worldwide as common practice for disposal of waste combustion by-products from coal-fired power stations. Research questions relating to the dry ash disposal method and its potential for overall leaching of chemical species during considerable chemical weathering has been identified. Fundamental understanding of chemical interactions of dry disposed ash with ingressed CO_2 from atmophere and percolating rain water within ash disposal sites was seen as a key area requiring investigation. The following considered research questions are essential to this investigative study.

This study aim to address the following research questions:

(i) does demineralization, for example due to percolating rain water, lead to release of the salts from ash dump to groundwater system in the vicinity of the ash dump?

(ii) what are the chemical processes leading to the secondary mineral formation and what factors control these processes?

(iii) can mineralogical associations of inorganic species in weathered fly ash be identify and quantify?

(iv) what are the various mechanism controlling the mobility of the chemical species?

(v) is dry ash disposal method a good practice in term of overall leaching of species?

This study is about finding the correct methodology to get the answer needed for the above stated necessary research questions.

1.4 Scope and delimitations of study

In this study, the water soluble fraction was included in the modified sequential extraction scheme originally proposed by Tessier et al. (1979). This was to account for the easily mobilised inorganic elements associated with the water soluble fraction of the dry disposed ash. Fifty nine ash core samples taken from 1 year, 8 year and 20-year-old section of Tutuka ash dump were characterised with standard analytical technique. This is to understand the effect of chemical weathering on the chemical alteration and mineralogical transformations. Comparative study was conducted on the fresh ash sample from the same power station to understand the degree of chemical weathering. Acid neutralisation was conducted on the 20-year-old unsaturated weathered ash core samples to understand the effect of weathering on the acid neutralisation capacity. A modified 5 steps sequential extraction scheme was applied on the weathered ash taken from 3 drilled cores to understand the mineralogical association of inorganic elements.

The delimitations of the present study are: (i) inorganic species associated with the sulphide fraction of the dry disposed fly ash is not considered in this study. (ii) One of the limitations of these methods is the liquid/solid ratios of the ash/water system which do not correspond with the ratios of water to ash at the ash dump and neither is contact time factored in and (iii) analysis towards understanding pollution levels of the monitoring water bore hole in the vicinity of the Tutuka ash dump. (iv) The sequential extraction scheme was not carried out on the 2-week-old ash dump because its chemistry and mineralogy is quite similar to the fresh ash from the same power station which forms other part of another study (Fatoba, 2011).

(v) A modified chemical sequential extraction scheme was not applied on multiple ash cores due to high cost of sample analysis.

1.5 Study area

Dry ash disposal method is the practice used by coal fired generation station located at Tutuka Power Station, Mpumalanga province, South Africa (see Figure 3.3). The dry disposed weathered ash core was sequentially/stacked together at different stage of weathering in the Tutuka ash dump site.

1.6 Research hypothesis

The mineralogical association of inorganic species in the dry disposed ash cores can be identified and quantified. This would provide a foundation for understanding the chemical weathering, mineralogical transformations or mobility patterns of these inorganic species in the dry ash disposal scenario.

1.7 Research Approach

The physical and chemical characterization of the fresh and weathered ash samples were performed in the laboratory. The physical and chemical characterization techniques used include:

(i) X-ray fluorescence (XRF)

(ii) X-ray diffraction (XRD)

(iii) Fourier transform infrared spectroscopy (FT-IR).

Morphological and structural characterizations were performed on both the fresh and weathered ash samples with scanning electron microscopy (SEM). The data generated for various coal fly ash samples were explored for the systematic analysis of mineralogical transformation and change in ash chemistry with ageing of the ash.

The pH, electrical conductivity (EC) and total dissolved solid (TDS) in the pore water of the ash samples were measured. The readily soluble species in the pore water was determined with ICP analysis. The anion species such as SO_4, Cl^-, PO_4 and NO_3 were analysed in interstitial water of the ash samples with Ion Chromatography technique (IC). The data generated was applied to reveal the impact of ingressed CO_2 from atmosphere and infiltrating rain water on the chemistry

of fly ash samples. It was further applied to show possible chemical reaction taking place at various sections of the drilled weathered ash dump under natural environmental settings.

The sequential extraction (SE) method used in this study was modified from the previous work done by Tessier *et al*. (1979) and Jegadesaan *et al*. (2008); the water soluble extraction step was added in this present study. The following five-fraction (steps) was adopted for the determination of the inorganic metal speciation in weathered coal fly ash: (a) Water-soluble fraction (b) Exchangeable fraction (c) Carbonate fraction (d) Amorphous Fe and Mn fraction and (e) Residual fraction. Chemical reagents that were specific towards the various physicochemical forms and arranged in order of increasing strength were prepared to extract inorganic elements from weathered coal fly ash in order to establish the mineralogical association of the elements. The results obtained from the 5 steps sequential extraction scheme were validated with the total metal content of the original sample prior to sequential extraction scheme to calculate the mass balance.

Previous studies on the determination of acid neutralisation capacity (ANC) of refuse derived fuel (Brannvall *et al*., 2009), municipal solid waste (MSW), municipal solid waste incinerator (MSWI), bottom ash and fly ash (Lo and Liao, 2007; Yeyehis *et al*., 2009) show that the formation of secondary minerals during weathering of disposed ash samples has significant effect on acid neutralisation capacity and leaching behaviour of chemical species. Acid neutralization capacity of both fresh and weathered coal fly ashes was analysed and evaluated with the aid of multivariate data analysis (principal component analysis). The acid neutralisation capacity (ANC) test was carried out in this study based on the methodology of the European standard prEN14429 (prEN14429, 2003).

The data generated from the sequential extraction scheme for drilled weathered ash core samples of different ages was used for statistical assessment of fractionation efficiency**.** Statistical analysis was done using SAS 9.2 (SAS Institute Inc. Cary, NC. USA), the variations of elements concentration per physicochemical form in the drilled weathered ash core samples were assessed by means of the coefficient of divergence (COD). The COD is self-normalizing. If two samples are similar in chemical composition the COD approaches zero, otherwise the COD approaches one (Smichowski *et al*., 2008). The Spearman's correlation coefficient was used to determine the major and trace elements pattern by age and depth.

1.8 Thesis layout

This thesis is structured into nine chapters.

- Chapter one introduces ash disposal and its environmental implications introduces concept of species mobility, leaching, weathering and the sequential extraction scheme. The statement of the problem, objectives, research questions, scope and delimitation of study, study area, research hypothesis, research approach and techniques used are briefly highlighted.
- Chapter two gives a general literature review on coal fly ash and the effect of environmental factors on its weathering process. General properties of coal fly ash are discussed alongside the factors that influence the mobility of inorganic metals in coal fly ash. A review of the characterization techniques, sequential extraction scheme applications and challenges for the future with respect to speciation of inorganic metals in coal fly ash are discussed. A review of the toxic inorganic elements in weathered coal fly ash is also covered.
- Chapter three gives an overview of the description of the Tutuka Power Station, dry ash disposal system, stratigraphy and depositional setting, local geology, geophysical survey, lithostratigraphy of ash dump, and the climate and weather conditions of the weathered coal fly ash dump located at coal-fired power stations in the Mpumalanga Province, South Africa.
- Chapter four covers the experimental protocols applied. This provides a brief synopsis on the different analytical techniques and general experimental procedure for the chemical preparation and characterization of the coal fly ash. This also provides the necessary methodology and the applied geochemical principles for the evaluation of inorganic metals in coal fly ash.
- Chapter five presents the experimental results obtained from the physicochemical and mineralogical characterization of both fresh and weathered (old) ash samples. This reveals the possible effect of chemical weathering on the chemistry and mineralogical composition of the fly ash.

- Chapter six presents the experimental results of the comparative study of acid neutralization capacity (ANC test) of both fresh and unsaturated weathered coal fly ash. The effect of chemical weathering on the acid susceptibility of the fly ash is discussed.
- Chapter seven presents the experimental results on the application of modified sequential extraction scheme originally developed by Tessier *et al*. (1979) for the determination of major metals partitioning. This chapter further discussed the chemistry of major elements impact on the chemistry of toxic elements in weathered ash core.
- Chapter eight presents the experimental results obtained from the application of the modified sequential extraction scheme originally developed by Tessier *et al*. (1979) for the determination of trace metals partitioning into mineral fractions in weathered coal fly. The chapter further evaluates the potential environmental risk of the toxic trace elements to the groundwater underneath the ash dump site.
- Chapter nine gives the summary of the main scientific contributions of the dissertation, conclusions drawn and recommendations for future research.

CHAPTER TWO

Literature Review of Fly ash

In this chapter, the origin and formation, chemical composition and mineralogy of coal were discussed. The available coal combustion technologies, physicochemical and mineralogical properties of coal fly ash, disposal system, and fly ash utilization are reviewed. This review also uses evidence from the literature to consider the usefulness and limitations of sequential extraction and total acid digestion and thereby to assess its role in determining metal partitioning in coal fly ash.

2. Introduction to coal as a source material for fly ash

Coal is derived from incompletely decomposed vegetation remnants which have been concealed under layers of sediment, squeezed by huge pressure over hundreds of million years ago (Dakyns, 2009). Coal is an extremely complex material. In addition to organic matter, coal contains water (up to 40 or more percent by weight for some lignitic coals), oils, gases (such as methane), waxes (used to make shoe polish), and maybe most importantly, inorganic matter (Hobbs *et al*., 1993). It is not only a resource of great economic significance, but a rock of strong attraction to the student of earth history. Although coal forms less than one percent of the sedimentary rock record, it is of principal importance to the Bible-believing geologist. Coal may be considered; therefore, as comprising some organically formed materials with a variety of chemical and physical properties. Besides, coal is unusual in that it has gone through several biochemical alteration processes. The original plant or animal debris has enormous morphological and chemical mixture even before being integrated into the peat. Likewise, once deposited in the peat, a range of biochemical processes take place (peatification), which again may considerably rework the morphological, physical, and chemical character of the existing organic material, as well as introducing new materials (precipitates). In the end, burial diagenesis (coalification) with increasing temperature has a considerable effect on all the individual particles, and on the coal as a whole. The accumulation of the organic matter that lithifies to coal occurs in swampy areas where organic matter deposition exceeds the rate of decomposition. The preservation of organic matter occurs under anaerobic conditions where the corrosion of organic material is inhibited because of a water table that is very close to the surface of the deposit.

During this process, many of the distinct coal fractions became increasingly alike in many (but not all) properties, which have led some to believe the existence of a 'coal molecule' (Scott, 2002). Two theories have been proposed to describe the formation of coal. The popular theory held by many uniformitarian geologists is that the plants which make up the coal were accumulated in large freshwater swamps or peat bogs at some stage in many thousands of years (http://www.icr.org/article/origin-coal/). This primary theory which supposes growth-in-place of vegetable material is called the *autochthonous theory (*Teichmuller and Teichmuller, 1975; Stach *et al*., 1982). The next theory suggests that coal strata accumulated from plants which had been quickly transported and deposited under flood conditions. This second theory which claims transportation of vegetable remains is called the *allochthonous theory.*

2.1 Coal formation process

Peat forming environments are poorly drained; they have a high water table (intermittently or permanently covered with water) and contain stagnant, anoxic (oxygen-poor) water that inhibits microscopic organisms, such as bacteria and fungi, from decomposing plant materials (see also Chapter 2 in Francis, 1961; Mukhopadhyay, 1994). Over a long period of time, the debris accumulates, partially decomposes, and becomes peat. As the peat is buried, the weight of overlying sediments exerts increasing pressure and temperature on it, driving off water and gases and changing the peat into coal (Speight, 1994). This transition from peat to anthracite is characterized by a number of chemical changes: 1. The disappearance of cellulose. 2. Decreasing proportions of hydrogen and oxygen. 3. Increasing proportion of carbon and greater proportion of carbon atoms bonded into benzene ring structure (aromatic carbon). 4. Decreasing proportion of volatile matter. (This is the material removed when the coal is heated at a temperature > 700 °C in an inert atmosphere. It includes hydrocarbons, carbon dioxide and carbon monoxide).

The past decade has witnessed great strides in the accumulation of information about the origin, chemical and physical structure, and composition of coal. These advances were made possible in part by the development of new analytical techniques, and in part by cooperative research between geologists, chemists, physicists, and biologists. Based on a review of the literature, the consensus is that coal was formed predominantly from lignin (Breger, 1958). Coalification involves the genetic and metamorphic history of coal beds. The plant materials that form coal may be, in part, simply incorporated, or they may be present in vitrinized or fusinized form. Materials contributing to coal differ in their response to diagenetic and metamorphic agencies

and the three essential processes of coalification are called incorporation, vitrinization, and fusinization (Schopf, 1948**)**. The nature of the process of metamorphosis of peat to form coal has been doubtful for many years. One theory suggests that *time* is the most important factor in coalification. The theory, nonetheless, has become not accepted because it has been recognized that there is no systematic increase in the metamorphic rank of coal with increasing age. There are some obvious contradictions: lignites representing low metamorphic rank occur in some of the oldest coal-bearing strata while anthracites representing the highest metamorphic rank occur in some of the youngest strata. A second theory supposes *pressure* to be the foremost factor in coal metamorphosis. The theory is refuted by numerous geological examples where metamorphic rank does not increase in highly deformed and folded strata. In addition, laboratory experiments exhibit that increase of pressure can essentially *impede* the chemical alteration of peat to coal.

A third theory (by far the most popular) suggests the *temperature* is the important factor in coal metamorphosis. Geological examples (an igneous intrusion into coal seams and underground mine fires) reveal that elevated temperature can cause coalification. Laboratory experiments have also been fairly successful. One experiment (Hill, 1972) produced a substance like anthracite in a few minutes by using a rapid heating process with much of the heat being generated by the cellulosic material being altered. Thus, the metamorphosis of coal does not need millions of years of applied pressure and heat, but can be formed by swift heating. It has been usually accepted that the variation in rank of South African coal is essentially due to the metamorphic effect of dolerite dykes and sills. However, no acceptable explanation could be given for the fact that true anthracite has not been formed adjacent to dykes and transgressive sills in those South African coal fields where the rank of the coal is normally low. In these areas, the coal close to the intrusives is often referred to as "burnt"(Snyman and Barclay, 1989). A detailed examination of the contact metamorphism of South African coal by dolerite intrusive shows that a dyke or sill affects the coal to variable distances, generally from 0.6 to 2 times the thickness of the intrusive, and that this distance is independent of the rank of the coal outside the contact aureole. This is explained by an initial event of contact metamorphism while the coal was still in the lignite stage of coalification, followed by burial metamorphism during which the paleogeothermal gradient increased in an easterly direction (Snyman and Barclay, 1989). This regional increase in paleogeothermal gradient is probably related to the large-scale magmatic activity that culminated in the extrusion of the Drakensberg basalts and the break-up of Gondwanaland.

2.1.1 South African coal reserve and its distribution

The Karoo Sequence of Carboniferous to Jurassic age hosts all the South African coal deposits and was formed in the great Gondwana basin. During the later part of the Paleozoic the geomagnetic pole positions suggest that the climate in South Africa changed from glacial to glacial to periglacial. South African coal, in common with other Gondwana coals, was therefore formed in a cold to cool climate, in contrast with the Carboniferous Laurasian coals that owe their origin to tropical rain forests (Stach *et al*., 1982). South Africa has more than 70 per cent of the coal resources of Africa, and coal forms the back-bone of the South African industry (Daniel, 1991; Snyman and Botha, 1993). In terms of the norms generally accepted for the Carboniferous coals of the Northern Hemisphere, South African coal has long been regarded as "abnormal". However, these apparent abnormalities can be adequately explained in terms of the petrography which in turn reflects the conditions of peat formation and the subsequent metamorphism under a steep palaeogeothermal gradient (Snyman and Botha, 1993).

The coal deposits of South Africa were formed at some stage in the Permian age immediately after retreat of glaciation. This makes it nearly certain that the climate was temperate rather than subtropical and may describe the differences involving the plant life in South Africa at that time and the flora of the North American carboniferous era. The prevalence of the inertinite maceral group in South African coals is suggestive of drier swamp conditions in which decaying processes as well as peatification played a more principal role than in the formation of the humic coals of Europe (Mackowsky, 1968). South African coals were considered to be deposited in deltaic or fluvial environments where fluctuations in water level could have caused deposition of huge quantities of mineral matter. South African coals commonly have not reached a very high rank although in Natal anthracites are established. This rank enhance seems to be due to metamorphism brought about by dolerite intrusions rather than by stratigraphic depth. The most important coal fields recline in the Highveld area of the Orange Free State, South-eastern Transvaal and Natal. Other coal fields are situated in the Northern part of the country, the Waterberg field on the Botswana border and the Limpopo and Pafuri fields on the boundaries of Rhodesia and Mozambique. At present 19 coal fields are notable in South Africa. Those numbered 1 to 9 (Table 2.1) occur in the Vryheid Formation of the main Karoo basin; those numbered 10 to 14 in tectonically controlled basins to the north and east of the main basin (Table 2.1), and number 15 is in the Molteno Formation in the south (Table 2.1).

Table 2.1. Distribution of coal resources and estimated remaining recoverable reserves as at the end of 2000 in South Africa

Coal field	Recoverable Reserves (Bredell, 1987)	Run-of Mine (ROM) production (1982-2000)	Remaining (2000)
	Reserves (Mt)		
Witbank	12460	2320.23	10139.77
Highveld	10979	972.49	10006.51
Utrecht	649	64.47	584.53
Klip River	655	85.26	569.74
Vryheid	204	81.8	122.2
South Rand	730	22.03	707.97
Vereeniging-Sasolburg	2233	334.91	1898.09
Orange free state	4919	0.22	4918.78
Ermelo	4696	101.11	4596.89
Waterberg (Ellisras)	15487	384	15103
Somkhele & Nongoma	98	15.18	82.82
Kangwane	147	0.96	146.04
Springbok flats	1700	0	1700
Southpansberg	267	6.11	260.89
Limpopo (Tuli)	107	0	107
Total	**55333**	**4388.77**	**50944.23**

Source : Bredell (1987) and South African Coal Statistics and Marketing Manual (2001).

The latter is uneconomical at present, and the relative importance of the other coal fields in terms of resources and reserves is also given in Table 2.1. It is noteworthy, the southpansberg coal field is subdivided into three viz; W. Southpansberg, C. Southpansberg and E. Southpansberg.

2.1.2 Coal composition and types

Coal is classified by rank according to their percentage of fixed carbon and heating value. Fixed carbon is the carbon residue that remains when coal is heated-without combustion- to drive off volatile matter. The volatile matter includes gases and vapours released by coal when heated. Usually, a coal's heating value and percentage of carbon (except in anthracite) have an inverse relationship with the moisture and volatile matter content. A Btu (British thermal unit) is the standard unit of measurement for heating value and is defined as the amount of heat required to raise the temperature of 1 pound of water 1 degree Fahrenheit (°F). There are basically four types of coal, each of which varies in terms of its heating value, its chemical composition, ash content, and geological origin. The four types of coal are lignite, sub bituminous, bituminous, and

anthracite is the highest rank of coal. Hendrickson (1975) provides the following description of some of these coal types: Lignite, the lowest rank of coal, was formed from peat which was compacted and altered. Its colour has become brown to black, has a fibrous, earthy texture and is commonly has a high moisture content, low heating value(less than 8,300 Btus). And it is composed of recognizable woody materials imbedded in pulverized (macerated) and partially decomposed vegetable matter. Lignite displays jointing, banding, a high compared with the higher coals. Sub bituminous coal is difficult to distinguish from bituminous and is dull, black colored, shows little woody materials, is banded, and has developed bedding planes. Sub bituminous coal has moisture content less than that of lignite, and a heating value that ranges from 8,300 to 11,500 Btus. The coal usually splits parallel to the bedding. It has lost some moisture content, but is still of relatively low heating value. Bituminous coal is dense, compacted, banded, brittle, and displays columnar cleavage and a dark black colour. It is more resistant to disintegration in air than are sub bituminous and lignite coals. It has low moisture and S content (Liu *et al*., 2005), carbon content that ranges from 69 to 86 %, volatile matter content range from 15 to 50 %, and its heating value that ranges from 10,500 to 15,500 Btus. The principal components of bituminous coal fly ash are silica, alumina, iron oxide, and calcium, with varying amounts of carbon, as measured by the loss on ignition (LOI) (Adriano *et al*., 1980). Several varieties of bituminous coal are recognizable. Anthracite is the highly metamorphosed coal, is jet black in colour, is hard and brittle, breaks with a conchoidal fracture, and displays a high lustre. It has a carbon content that ranges from 86 to 98 % and a slightly lower heating value than bituminous coal due to a low volatile matter content(less than 7 %). Neither peat nor graphite is coal, but they are the initial and end products of the progressive coalification process. Coals vary greatly in their composition. Many researches have been done on coal deposits throughout the world because of the environmental interest in the trace elements. Studies on occurrence and distribution of trace elements in coal showed that their affinities differ from one deposit to another (Querol *et al*., 1996). Of 1200 coals categorized by the Bituminous Coal Research Institute, no two had exactly the same composition (Hendrikson, 1975).

Trace elements are concentrated mainly in the heavy accessory minerals and organic matter in coal. In decreasing order of significance, the trace elements in coal may occur as: element-organic compounds; impurities in the mineral matter; major components in the mineral matter;

major and impurity components in the inorganic amorphous matter; and elements in the fluid constituent (Vassilev *et al*., 1997a). Typical compositions of dry, ash-free coal by mass include 65-95 % carbon, 2-7 % hydrogen, up to 25 % oxygen and 10 % sulphur, and 1-2 % nitrogen (Essenhigh, 1976). Inorganic mineral matters as high as 50 % has been observed, but 5-15 % is more typical. Moisture levels commonly vary from 2-20 %, but values as high as 70 % have been observed (Hobbs *et al*., 1993). Coal occurs in association with diverse types of inorganic minerals such as alumino-silicates (clay minerals), carbonates (calcite and dolomite), sulphides (pyrite), chlorides, and silica (quartz). Some elements such as sulphur occur in both the organic and inorganic coal fractions. The inorganic minerals, deposited along with the plant material, are inherent and make up 5 to 10 % of the coal. The inorganic constituents in coal are responsible for a series of technological and environmental problems related to coal mining, coal processing such as preparation, combustion, pyrolysis, gasification and liquefaction, and utilization of coal wastes (Vassilev, 1994, Querol *et al*., 1995). The sulphur and nitrogen content are important as emissions of their chemical oxides during coal burning can cause acid rain. Unrestrained emissions from coal combustion resulted in widespread damage to forests and lakes in Europe, the USA and Canada. There exist some relationship between the coal ranks and chemical and mineral composition. The low-rank coals (Cdaf <75wt %) are relatively rich in moisture, volatile matter, ash, H, N, O and S, and their ashes are abundant in MgO, CaO and SO_3. The high-rank coals demonstrate increased contents of SiO_2, $A1_2O_3$, Fe_2O_3, K_2O, Na_2O and TiO_2. (Vassilev *et al*., 1996b). The coal ash is abundant in aluminosilicates as the contents of the Fe oxides are relatively similar to the sum of the alkaline earth oxides. The minerals identified in the coal are mainly quartz, kaolinite, pyrite and calcite and, to lesser extents, dolomite, ankerite, illite, chlorite, opal, feldspars, marcasite, gypsum, melanterite and hematite (Liu *et al*., 2005; Vassilev and Vassileva, 1998).

2.1.3 Mineralogy, major and trace elements in coal

The mineralogy of the constituents of coal is dependent upon the geology of the surrounding environment of the coal deposits (Scheetz and Earle, 1998). The minerals contained in coal can be subdivided into siliceous or non-siliceous. The former consist, for the most part, of aluminium silicates (mainly mica and kaolin), whereas SiO_2 is combined with basic oxides of sodium, potassium, calcium and magnesium. In coal there is also free silica mainly as α-quartz. The ratio between combined and free silica ranges from 2:1 to 4:1 (Ferraiolo *et al*., 1990). The non-

siliceous fractions consist mainly of pyrite and other trace sulfates (copper, lead, arsenic, mercury, zinc and silver), carbonates and chlorides. Table 2.2 shows the mean proximate, elemental and mineralogical analyses of the coal sampled from European power station, which is characterized by high sulfur and mineral matter contents. The major mineral phases in coal are kaolinite ($Al_2Si_2O_5(OH)_4$), illite ($K(Al,Mg)_3SiAl_{10}(OH)$), gypsum ($CaSO_4.2H_2O$), pyrite (FeS_2), marcasite (FeS_2), quartz (SiO_2), microcline ($KAlSi_3O_8$), albite-anorthite ($(Na,Ca)(AlSi)_4O_8$) and calcite ($CaCO_3$) (Querol *et al*., 1995; Silva *et al*., 2010). The accessory minerals include a wide variety of minerals, such as: I-S (illite-smectite) interlayered clays and iron sulphates with different degrees of hydration: szomolnikite ($FeSO_4.2H_2O$), rozenite ($FeSO_4.4H_2O$), melanterite ($FeSO_4.7H_2O$) and jarosite ($(Na,K)Fe_3(SO_4)_2(OH)_6$, galena(PbS), pyrrhotite, magnetite, hematite, goethite, chromite, rutile, anatase, dolomite, corundum, gibbsite, biotite, chlorite, zircon, enstatite, garnet, alunite, barite, polyhalite, aragonite, ankerite, witherite, apatite, halite and sylvite (Vassilev, 1994). The inorganic constituents in coal include the following solid and fluid components(Vassilev and Vassileva, 1996a): (1) crystalline (mineral) matter such as crystals, grains, and aggregates of various minerals, as well as some cryptomere, metamict, and gel minerals (for example, opal, chalcedony, allophane, and some zircon, phosphates, Fe and Mn hydroxides with imperfect crystal lattices); (2) noncrystalline (amorphous) matter, namely glass, metamict, metacolloid and gel phases (for instance, volcanic and cosmic materials, and some phosphates, hydroxides, silicates); (3) fluid matter (pore and surface moisture, and inorganic gas-liquid inclusions) associated with both inorganic and organic solid constituents.

Bulgarian sub bituminous and bituminous composed mainly of quartz, kaolinite, illite, muscovite, feldspars, pyrite, and calcite as inorganic matter (Vassileva and Vassilev, 2006). Whereas the inorganic matter in lignite coal are mainly quartz, kaolinite, gypsum, calcite, and pyrite (Vassileva and Vassilev, 2005b). Coals enriched in illite, mica, chlorite, spine & dolomite, siderite and hexahydrite, and partly in quartz, kaolinite and Fe oxyhydroxides, are of higher rank, while coals with increased contents of montmorillonite, feldspars, zeolite, Al oxyhydroxides, calcite, pyrite, gypsum and Fe, Al and Ba sulfates are of low rank. Many trace elements are present within coal deposits, ranging from a few percent of the total composition of the coal to a fraction of a part per million (ppm); see Table 2.3 and references (Eble *et al*., 1997; National Academy Press, 1980; US Geological Survey; 1977).

Table 2.2. Characteristic of the coal fed into European power station

Proximate analysis (wt %)		Mineral content (wt % ad)[a]	
Moisture (ad)	9.3	Quartz	3.5
Ash (ad)	26.5	Kaolinite	18.0
Volatile matter (daf)	44.1	Illite	3.3
Calorific value (MJ Kg^{-1})	25.3	K-feldspar	0.8
		N-feldspar	<0.1
Ultimate analysis (wt %)		Calcite	0.3
C (daf)	75.5	Pyrite/marcasite	4.8
H (daf)	5.6	Gypsum	1.7
N (daf)	1.2		
S	5.0	Ash fusion temperature (^{o}C)	
Carbonate C	0.08	Deformation	960
Cl	0.02	Fusion	1320
F ppm	176	Fluidity	1340
Sulphur forms (wt %)			
Pyritic	1.6		
Organic	2.4		
Sulphate	1.0		

Source: Querol *et al*. (1995)

[a] Mean values from triplicate XRD measurements.

Table 2.3. Average concentrations and range of major and minor elements in eastern US bituminous coal.

Elements	Concentration %	Range %
Sulfur	2.00	10-7.40
Silicon	2.60	0.58-6.09
Aluminium	1.40	0.43-3.04
Calcium	0.54	0.05-2.67
Magnesium	0.12	0.10-0.25
Sodium	0.06	0.00-0.20
Potassium	0.18	0.020-0.43
Iron	1.60	0.32-4.32
Manganese	0.01	**
Titanium	0.08	0.002-0.32
Chlorine	**	0.00-0.56

** = No values provided or available. Reproduced from (Halstead, 1986).

The high-rank coals are abundant in ash-forming elements associated with probable detrital minerals, while low-rank coals show enrichment in ash-forming elements associated with probable authigenic minerals and organics (Vassilev *et al*., 1996a). The low-ash coals are enriched in ash-forming elements associated with probable authigenic minerals and organics, whereas higher-ash coals demonstrate enrichment in ash forming elements associated with probable detrital minerals (Vassilev *et al*., 1997a). Studies on mobility of coal showed that the volatility of trace elements in coal depends on the affinities and concentrations, and on the physical changes and chemical reactions of these elements with sulphur or other volatile elements.

The volatility also depends on the combustion technology (temperature, time of exposure, type of ash generation, etc). There is oxidation of elements with sulphide and organic affinities during coal combustion and consequently they may show volatile behaviour because of the temperature rise accompanying oxidation or because of reaction with Cl, F, Na or S compounds which can induce volatility in some elements such as As, Se and Cd. These trace elements if not volatilized, are present in ash as oxides and sulphates which can easily be extracted from the ash by water leaching (Querol *et al*., 1996).

2.1.4 Coal texture and structure

Investigation of the microscopic texture and structure of peat and coal contributes to the understanding of the origin of coal. Cohen (1970) initiated a relative structural study between modern autochthonous mangrove peats and a rare modern allochthonous beach peat from southern Florida. Most autochthonous peats had plant fragments viewing random orientation with a dominant matrix of finer material, while the allochthonous peat showed current orientation of elongated axes of plant fragments generally parallel to the beach surface with a characteristic lack of the finer matrix. The poorly sorted plant debris in the autochthonous peats had a massive structure due to the intertwining mass of roots, while the allochthonous pert had characteristic micro lamination due to the absence of intergrown roots. Following this study Cohen remarked: "A peculiar enigma which developed from study of the allochthonous peat was that vertical microtome sections of this material looked more like thin sections of Carboniferous coal than any of the autochthonous samples studied." Cohen noted that the characteristics of his allochthonous peat (orientation of elongated fragments, sorted granular texture with general lack of finer matrix, micro lamination with lack of matted root structure) are also general characteristics of Carboniferous coals. The structure of this material can be observed by looking at thin sections of coal under the microscope in either transmitted or reflected light. With the aid of modern spectroscopic techniques (x-ray diffraction and nuclear magnetic resonance spectroscopy) and knowledge of elemental analysis and the functional groups in coal, general structures can be proposed. Currently it is believed that all coals, except anthracite, are composed of units containing 1-3 condensed benzene rings linked by carbon chains containing various functioning groups.

2.1.5 Uses of coal

Coal is a solid hydrocarbon and can also be used in the same way the liquid hydrocarbon, oil, is used when burn. It can be used as fuel and in the chemical industries. Coal is often associated with the Industrial Revolution; coal remains an enormously important fuel and is the most common source of electricity world-wide. In the South Africa, for example, the burning of coal generates over half the electricity consumed by the nation. South Africa is the world's third largest coal exporting country, exporting 25 % of its production internationally. South Africa uses 53 % of the balance of its coal production for electricity generation, 33 % for petrochemical industries (Sasol), 12 % for metallurgical industries (Iscor) and 2 % for domestic heating and cooking. Eskom is the 11th largest electricity generator in the world, while Sasol is the largest coal-to-chemicals producer (http://www.mbendi.com/indy/ming/coal/af/sa/p0005.htm#5).

Coal at a time was mainly used to heat homes, to power railroad locomotives and factories. But recently, coal is used to generate electricity, for steel manufacturing and industrial process. When coal is burned at around 1400 ^{o}C, the water in the pipes on the surrounding wall of the boiler room gets vaporized into superheated high-pressure steam due to the intense heat. The steam drives the turbine which is connected to the generator and causes the turbine to rotate at high speeds, creating a magnetic field inside wound wire coils in the generator. This pushes an electric current through the wire coils out of the power plant through transmission lines. It is mainly these incombustible materials that form the ash that remains after combustion of the coal. It takes one pound of coal to generate about one kilowatt-hour of electricity is used to power train car, a single train car of coal (100 tons) lasts on 20 minutes in a medium sized power plant.

Coal is also used in making coke for use in steel blast furnaces. When coal is heated in the absence of air, a porous, carbon-rich material called "coke" is formed. Bituminous coal (also called metallurgical coal or coking coal) is distinguished by the peculiar characteristic that instead of forming a char, it goes "plastic" when strongly heated in the absence of air. Gases given off by the hot coal cannot easily escape and the coal expands like foam, forming coke. When cooled, this material is quite strong and is used when iron and steel are made. Coke is one of the constituents needed to properly heat the furnace (limestone and iron ore are two other constituents used). In industrial process heating, coal is used to heat boilers and ovens. The cement, glass, ceramic, and paper industries all use coal for this purpose. Coal is used in the

manufacture of synfuels (synthetic natural gas). There are several processes to convert coal into gas, which is a more convenient fuel for transport and domestic applications. Coal tar is a product of the destructive distillation of bituminous coal. Coal tar can be distilled into many fractions to yield a number of useful organic products, including benzene, toluene, xylene, naphthalene, anthracene, and phenanthrene. These substances, called the coal-tar crudes, form the starting point for the synthesis of numerous products-notably dye, drugs, explosives, flavorings, perfumes, preservatives, synthetic resins, and paints and stains. The residual pitch left from the fractional distillation is used for paving, roofing, waterproofing, and insulation.

2.2 Coal fired power generation technologies

The use of electricity has been an essential part of the South Africa economy for the last four decades. Coal power, an established electricity source that provides vast quantities of inexpensive, reliable power has become more important as supplies of oil and natural gas diminish. ESKOM, South Africa power utility company has a nominal capacity about 44, 193 MW. It generates approximately 95 % of electricity used in South Africa and almost 45 % of electricity used in Africa continent (ESKOM Abridge Report, 2009). The most economical method available is the use of abundant supplies of low-quality coal in Mpumalanga and the Northern Province; most of their power stations were sited next to the coal deposits. Coal power is a rather simple process. In most coal fired power plants, chunks of coal are crushed into fine powder and are fed into a combustion unit where it is burned. Heat from the burning coal is used to generate steam that is used to spin one or more turbines to generate electricity. ESKOM used conventional or pulverized coal fired power generation technology. Cyclone furnaces is another coal fired power generation technology available for use in electricity generation stations.

2.2.1 Conventional coal fired power station

In the 1920s, the pulverized coal firing was developed. This process brought advantages that included a higher combustion temperature, improved thermal efficiency and a lower requirement for excess air for combustion. The idea of burning coal that has been crushed into a fine powder stems from the conviction that if the coal is made fine as much as necessary, it will burn roughly as easily and efficiently as a gas. The feeding rate of coal according to the boiler demand and the amount of air available for drying and transporting the pulverized coal fuel is controlled by

computers. Pieces of coal are crushed between balls or cylindrical rollers that move between two tracks or "races." The raw coal is then fed into the pulveriser along with air heated to about 650 º F from the boiler. As the coal gets crushed by the rolling action, the hot air dries it and blows the usable fine coal powder out to be used as fuel. The crushed coal from the pulverizer is delivered to the boiler, usually by a conveyor belts. Air is blown into the boiler to burn the coal, creating heat energy.

The burning of coal heats water in the boiler to produce high pressure steam (transferring the heat energy from combustion into the steam). The combustion of coal in the boiler creates hot gases (including CO_2) and ash. The ash is disposed of and the hot gases are released into the atmosphere. The steam drives turbines that generate the electricity while the 'smoke' from the boiler is carefully filtered to remove as much of the unwanted emissions as possible. The steam passes through the blades of a turbine, causing the blades to rotate (like a fan). In the process, the steam's heat energy is converted to kinetic (movement) energy. The spinning turbine blades are attached to a shaft (axle) that also spins a generator shaft. The low-grade coal produces a large amount of ash, which is returned to the ground and isolated from the environment in long-term storage.

2.2.2 Cyclone furnaces

In the 1940s, the cyclone furnace was developed. This new technology allowed the combustion of poorer grade of coal with less ash production and greater overall efficiency. Cyclone furnaces were developed after pulverized coal systems and require less processing of the coal fuel. They can burn poorer grade coals with higher moisture contents and ash contents to 25 %. The crushed coal feed is either stored temporarily in bins or transported directly to the cyclone furnace. The furnace is basically a large cylinder jacketed with water pipes that absorb the some of the heat to make steam and protect the burner itself from melting down. A high powered fan blows the heated air and chunks of coal into one end of the cylinder. At the same time additional heated combustion air is injected along the curved surface of the cylinder causing the coal and air mixture to swirl in a centrifugal "cyclone" motion. The whirling of the air and coal enhances the burning properties producing high heat densities (about 4700 to 8300 kW/m^2) and high combustion temperatures.

The hot combustion gases leave the other end of the cylinder and enter the boiler to heat the water filled pipes and produce steam. Like in the pulverized coal burning process, all the fuel that enters the cyclone burns when injected once the furnace is at its operating temperature. Some slag remains on the walls insulating the burner and directing the heat into the boiler while the rest drains through a trench in the bottom to a collection tank where it is solidified and disposed of. This ability to collect ash is the biggest advantage of the cyclone furnace burning process. Only 40 % of the ash leaves with the exhaust gases compared with 80 % for pulverized coal burning. Cyclone furnaces are not without disadvantages. The coal used must have relatively low sulfur content in order for most of the ash to melt for collection. In addition, high power fans are required to move the larger coal pieces and air forcefully through the furnace and more nitrogen oxide pollutants are produced compared with pulverized coal combustion. Finally, the actual burner requires yearly replacement of its liners due to the erosion caused by the high velocity of the coal.

2.2.3 Environmental impacts of coal fired electrical generation

Many of the commonly held concepts about the environmental impacts of coal fired electrical generation are listed below. However, we believe that the benefits far outweigh any potential negative impacts.

1. Coal mining causes severe erosion, resulting in the leaching of toxic chemicals into nearby streams and aquifers, and destroys habitants.

2. About two-thirds of sulfur dioxide, one-third of carbon dioxide emissions and one quarter of the nitrogen oxides emissions in the U.S. are produced by coal burning.

3. Coal burning also results in the emission of fine particles matter into the atmosphere. Nitrogen oxide and fine airborne particles exacerbate asthma, reduce lung function and cause respiratory diseases and premature death for many thousands of Americans.

4. Smog formed by nitrogen oxide and reactive organic gases causes crop, forest and property damage. Sulfur dioxide and nitrogen oxides both combine with water in the atmosphere to create acid rain. Acid rain acidifies the soils and water killing off plants, fish, and the animals that depend on them.

Combustion generated pollutants, such as oxides of nitrogen (NO_x), of sulfur (SO_x), and particulates, if uncontrolled and emitted into the atmosphere represent environmental and health hazards, such as acid rain. Environmental regulations supported by intensive research and developments have reduced pollutant emissions significantly. Improvements in efficiency and emissions come by increasing steam pressure and temperature in the steam cycle, and by increased turbine inlet temperature in the gas turbine cycle (Beer, 2010). Coal gasification produces a fuel gas that is capable of being used in the gas turbine. By integrating coal gasification with gas turbine and steam cycles, advantage can be taken of high efficiency and low pollutant emission while using coal, an inexpensive, secure and indigenous fuel in many countries throughout the world. A potential supplementary advantage of the Integrated Gasification Combined Cycle (IGCC) is the capability of capturing carbon dioxide (CO_2) from the fuel gas and making it ready for high-pressure pipeline transportation to a carbon sequestration site (Beer, 2010). This will be key to the commercial and clean co-production of electricity and hydrogen from coal.

2.3 Electricity generation

Power stations work by harnessing a suitable raw energy source and turning it into electrical energy that can be sent to homes and industry. There are several steps involved in the electricity generation. The generator is made up of an electro-magnetic and wire coils, so as the generators spins it creates and electrical current, converting the kinetic energy from the shaft into electrical energy. The electrical energy is increased in voltage and fed into a high-voltage transmission network (transmission towers). Electricity is transported to substations and then into the distribution network that delivers electricity via poles and wires to your home and businesses. After passing through the turbine, the steam losses pressure and temperature. The steam is further cooled in a heat exchanger to condense it back into water. Waste heat from condensing steam is released into the atmosphere. Pure water from the condenser is pumped at high pressure back into the boiler and re-used to create steam. All processes occur simultaneously.

2.4 Need for research into fly ash

Mahlaba *et al*. (2011) conducted comprehensive characterisation of hydraulic placed fine coal ash from SASOL synfuels. The authors reported that no indication of appreciable leaching was given by X-ray Fluorescence (XRF) results except calcium and silicon. Also, evidence of

immobilised pollutants from saline brines in weathered fine coal ash was obtained. However, the study did not inform us about; how much of pollutant from saline brines was retained? And the physicochemical forms or mineral phases holding the pollutants from saline brine were not revealed.

Tiruta-Barna *et al*. (2006) reported the laboratory-scale and field pilot experimental studies conducted to assess the leaching behaviour of ash compacted layers in a use scenario. The authors conclude scenario factors like carbonation and rainfall play an important role on the leaching behaviour at field scale. This study only takes into account leachate from the water soluble fraction. Other physico-chemical forms scavenging metals in coal ash were not investigated in their study.

In 2000, the Journal of Hazardous Materials published a special edition represent eight papers on the fly ash characterization and utilization. The following remarks is made in the preface to the special issue: Of the hundreds of millions of metric tons of fly ash that are produced annually on a worldwide basis, only a small portion e.g., 20 to 40 % of the fly ash is re-used for productive purposes, such as an additive or stabilizer in cement. The remaining amount of fly ash produced annually must either be disposed in controlled landfills or waste containment facilities, or stockpiled for future use or disposal. As a result of the cost associated with disposing these vast quantities of fly ash, a significant economical incentive exists for developing new and innovative, yet environmentally safe; applications for the utilization of coal fly ash (Schakelford, 2000).

Petrik *et al*. (2003) commented on the use of fly ash in South Africa. Only 5 % of the 20 million tonnes ash produced in 2003 by coal burning power station in Mpumalanga province was used in non-landfill applications. Although, the annual coal fly ash production has increased on yearly basis. In the year 2009, the production has reached up to 36.7 million tonnes per annum (ESKOM Abridge Report, 2009); the amount utilized compare to production has remained relatively constant.

Scheetz and Earle (1998) report on the use of fly ash in America. In 1996, 43.12 million tons of fly ash went to landfills or equivalent repositories. Only 27.4 % of the fly ash was used in non-landfill applications, this assertion was corroborated by Hower *et al*. (1999). Scheetz and Earle (1998) challenge the Science community with the following remarks: Fly ash was imparted with

an excess energy, either chemical or stored surface energy, which can be utilized to participate in chemical reactions, if properly activated. The challenge for the scientific community is to exploit these resources, as low tech materials, to solve large-volume societal-environmental needs.

Kruger (1997) also made related comment in a published article discussing coal fly ash beneficiation "to a better understanding of the fundamental characteristics of ash; for example, to what degree do surface characteristics control the reactivity, and what beneficiation techniques are applicable to maximize a particular characteristic? Can fly ash be beneficiated to enrich it as a pre-concentration step for the recovery of gallium? Is a particular fraction more suited to producing slow-release fertilizers? How can beneficiation play a role in selecting a portion of fly ash more appropriate to geopolymerisation? Knowledge of the needs in the market-place and the symbiotic relation between research and product development is paramount in creating these new opportunities for fly ash (Kruger, 1997).

Malhotra *et al*. (2002) commented on the use of fly ash in the United State of America in the year 2000. The authors estimated that about 63 million tons of fly ash and about 17 million tons of bottom ash are produced every year. Only about 30 % of the fly ash produced is used. Out of which 20 % is used in the concrete industry, which has reached a maximum consumption figure. The authors challenge researchers to find a low cost but high volume application of fly ash, and to convert ashes into value added products (Malhotra *et al*., 2002).

Satapathy (2000) reported that the generation of fly ash is very high in India (80 million tons per year); however the utilization is only 6 %. Foner *et al*. (1999) highlight the role of developing new application of fly ash, by pointing out that by the year 2001 Israel will produce about 1.3 million tonnes of coal ash per annum and, of this, only about 600 000 tonnes can be utilized by the cement industry (Foner *et al*., 1999).

Nathan *et al*. (1999) estimated the figures as 1.2 million tons and 800 000 tons respectively by the year 2000. Spears and Lee (2004) estimated about 40 Mt in 2000 for Europe of which less than 50 % was utilized. The waste ends in lagoons, ash mounds, and landfill sites.

2.4.1 Coal fly ash

Coal fly ash is a complex mixture of different minerals and high amounts of toxic elements are associated with these minerals, which are leached during different environmental conditions

(Fernandez-Turiel *et al*., 1994). Fly ash is mainly a result of the mineral compounds which are contained in the coal: a certain amount of unburned residue is also usually present within this particulate matter (Ferraiolo *et al*., 1990). Coal fly ash has potential to contaminate both surface and groundwater with toxic inorganic pollutants such as arsenic, boron, selenium, heavy metals, etc. When ash is stored, particularly under moist condition, physical and chemical weathering is likely to occur which would lead to leaching of soluble constituents (Adriano *et al*., 1980). Safe disposal of fly ash depends on the chemistry of fly ash and physicochemical forms in which the inorganic contaminants. These are essential to predict the release rate and its concentration with respect to surface and groundwater protection. Fly ash is a by-product from burning pulverized coal in electric power generating plants. During combustion, mineral impurities in the coal such as clay, feldspars, quartz and shale fuse in suspension and float out of the combustion chamber with exhaust gases. As the fused material rises, it cools and solidifies into spherical glassy particles called fly ash (Basham *et al*., 2007). Fly ash is generally captured from the chimneys of coal-fired power plants by means of electrostatic precipitators, bag houses or mechanical collection devices such as cyclones.

Fly ash is one of two types of ash that jointly are known as coal ash; the other, bottom ash, is removed from the bottom of coal furnaces. Bottom ash; represent 20 % by weight of the total ash and being constituted by agglomerate granules, such as blast furnace scoriae, which precipitate on the bottom of the combustion chamber in a tank containing cooling water. The size distribution of these particles ranges from 0.03 to 30 mm with maximum frequency (about 50 %) below 2 mm (Puccio, 1983). Fly ash particles are generally spherical in shape and range in size from 0.5 µm to 100 µm. Fly ash, representing the remaining 80 % by weight and being constituted by very fine particles entering the flue gas stream. The size distribution of these particles ranges from less than 0.01 mm to 0.5 mm; about 90 % is lower than 0.3 mm, about 60 % lower than 0.04 mm and about 10 % lower than 0.01 mm (Puccio, 1983). Fly ash material solidifies while suspended in the exhaust gases and is collected by electrostatic precipitators of filter bags. Fly ash is usually removed from flue gases through several systems such as gravity chambers, cyclones, multicyclones, wet scrubbers, electro filters, and fabric bag filters (Ferraiolo, 1990). Since the particles solidify while suspended in the exhaust gases. Fly ash consist mostly of SiO_2 which is present in two forms; amorphous which is rounded and smooth, and crystalline, which is sharp, pointed and hazardous, aluminium oxide (Al_2O_3) and iron oxide

(Fe_2O_3). Fly ashes are generally heterogeneous, consisting of a mixture of glassy particles with various identifiable crystalline phases such as quartz (SiO_2), mullite ($3Al_2O_3.2SiO_3$) and various iron oxides (Fe_2O_3). Depending upon the source and make-up of the coal being burned, the components of fly ash vary considerably (Gutierrez *et al*, 1993), but all fly ash include substantial amounts of SiO_2 (both amorphous and crystalline) and calcium oxide (CaO). Toxic constituents include arsenic, beryllium, boron, cadmium, chromium, chromiumVI, cobalt, lead, manganese, mercury, molybdenum, selenium, strontium, thallium and vanadium along with dioxins and PAH compound (Aljoe *et al*., 2007).

2.4.2 Classification of fly ash

Fly ash can be classified based on the nature of constituents present. The major and minor oxides of types C and F fly ash is shown in Table 2.4. Coal fly ashes are classified by ASTM into class F or C by their aggregate alumina, silica, and ferric oxide contents. ASTM C 618-05 (2005) defines two classes: Class C comprising ash produced from lignite or sub bituminous coal combustion with at least 50 % but less than 70 % SiO_2, Al_2O_3 and Fe_2O_3. Class C fly ash is produced from the burning of younger lignite or sub bituminous coal, in addition to having pozzolanic properties, also has some self-cementing properties. In the presence of water, Class C fly ash will harden and gain strength over time. Class C fly ash generally contains more than 20 % lime (CaO). Unlike Class F, self-cementing Class C fly ash does not require an activator. Alkali and sulfate (SO_4) contents are generally higher in Class C fly ashes. Type C fly ash is produced by burning of lignite coal and contains more lime (18 %) (Iyer, 2002). It is also worthwhile to mention that the bituminous coal produces fly ash of class C (Koukouzas *et al*., 2007). Class C fly ash usually is referred to as 'high lime ash'. Many power plants in the west and mid-western states of U. S. are fuelled with low sulfur coals from Wyoming and Montana that yield high lime fly ash (Adriano *et al*., 2002).

Class F comprising ash produced from burning of anthracite or bituminous coal combustion; with at least 70 % SiO_2, Al_2O_3 and Fe_2O_3. Class F fly ash, is a representative of those produced from Mpumalanga Province, South Africa and eastern U.S. coal. The production of class F coal ashes are from higher rank coals, which have lower calcium content. Class F fly ash contains low lime content (< 7 %) and more silica, alumina, and iron oxide (Iyer, 2002). Class F fly ash is

pozzolanic (an alumino-siliceous material which in the presence of water combines with CaOH from lime or Portland cement to form cementitious compound).

Table 2.4. ASTM Standards classification of fly ash (ASTM C618, 2005)

	Class F	**Class C**
$SIO_2 + Al_2O_3 + Fe_2O_3$, Min %	70.0	50.0
SO_3, Max %	5.0	5.0
Moisture content, Max %	3.0	3.0
LOI, Max %	6.0	6.0
Available alkalis, as Na_2O, Max %	1.5	1.5

Class F fly ash, is pozzolanic in nature and contains less than 10 % lime (CaO). Possessing pozzolanic properties, the glassy silica and alumina of Class F fly ash requires a cementing agent, such as Portland cement, quicklime, or hydrated lime, with the presence of water in order to react and produce cementitious compounds. Alternatively, addition of a chemical activator such as sodium silicate (water glass) to a Class F fly ash can lead to the formation of a geopolymer. The chief difference between Class F and Class C fly ash is in the amount of calcium and the silica, alumina, and iron content in the ash. In Class F fly ash, total calcium typically ranges from 1 to 12 %, mostly in the form of calcium hydroxide, calcium sulphate, and glassy components, in combination with silica and alumina. In contrast, Class C fly ash may have reported calcium oxide contents as high as 30-40 %. Another difference between Class F and Class C is that the amount of alkalis (combined sodium and potassium), and sulphates (SO_4), are generally higher in the Class C fly ash than in the Class F fly ash (Ahmaruzzaman, 2010). The chemical properties of the fly ash are largely influenced by the chemical content of the coal burned (i.e. anthracite, bituminous and lignite) (ASTM).

2.4.3 Physical properties of coal fly ash

Fly ash consists of fine, powdery particles predominantly spherical in shape, either solid or hollow, and mostly glassy (amorphous) in nature (Ahmaruzzaman, 2010). The fine texture of fly ash results in water permeability and infiltration rates of ash deposits being characteristically low (Cope, 1962; Townsend and Hodgson, 1973; Bern, 1976). Cope (1962) noted that lateral hydraulic conductivity in fly ash deposits can be much greater than vertical conductivity. Fly ash is generally grey in colour, abrasive, mostly alkaline, and refractory in nature. The colour of fly

ash can vary from tan to gray to black, depending on the amount of unburned carbon in the ash. The lighter the colour, the lower the carbon content of coal fly ash. Lignite or sub bituminous fly ashes are usually light tan to buff in colour, indicating relatively low amounts of carbon as well as the presence of some lime or calcium. Bituminous fly ashes are usually some shade of gray, with the lighter shades of gray generally indicating a lighter quality of ash. Pozzolans, which are siliceous or siliceous and aluminous materials that together with water and calcium hydroxide form cementitious products at ambient temperatures, are also admixtures. Fly ash from pulverized coal combustion is categorized as such a pozzolan (Ahmaruzzaman, 2010). The pozzolanic properties of fly ash when mixed with water can be another problem on ash disposal sites. Pozzolanic materials react with free lime in the presence of water to form stable cement. Class C ash characteristically has pozzolanic properties while Class F ash rarely forms cement when mixed with water (Haynes, 2009).

The carbonaceous material in fly ash is composed of angular particles. Bhanarkar *et al*. (2008) recognized factors such as differences in the coal types, boiler types, combustion conditions and pollution control equipment may influence the size distribution of the particulate matter. The particle size distribution of most bituminous coal fly ash is generally similar to that of silt(less than a 0.075 mm in diameter)(Ahmaruzzaman, 2010). Although sub bituminous coal fly ashes are also silt-sized, they are generally slightly coarser than bituminous coal fly ashes (Digioia and William, 1972). Coal fly ash composed mostly of silt-sized spherical amorphous ferro-aluminosilicate minerals and is usually characterized by low permeability, low bulk density, and high specific surface area (Petrik *et al*., 2007). As noted, fly ash contains 60-95 % of particles in the silt plus fine sand fractions and there is a lack of any aggregate formation. Accordingly, dry fly ash surfaces are liable to wind erosion especially if they have been disturbed (e.g. cultivated). The fines fly ashes particles can be carried from disposal sites and contribute to visual and dust pollution experience in adjacent townships (Junor, 1978). Indeed, wind erosion is often the most obvious pollution hazard of fly ash disposal sites. This low permeability enhances surface runoff and water erosion but will tend to reduce leaching of salts and metals to groundwater (Page *et al*., 1979). The surface area is dependent on particle size. The large surface areas of fly ash are attributable to carbonaceous particles of highly porous character (Schure et al., 1985). The specific gravity of fly ash usually ranges from 2.1 to 3.0, while its specific surface area may vary from 170 to 1000 m^2/kg (Mattigod *et al*., 1990a).

2.4.4 Physico-chemical properties of fly ash

Huge amounts of solid wastes like coal fly ash (FA) are generated during the production of electrical power. The properties of coal FA depend on the physico-chemical properties of coal, coal burning process etc., and other factors (Saikia *et al*., 2006). X-ray fluorescence is mainly used to describe the bulk chemical composition of fly ash. Coal fly ash is considered to be a ferro aluminosilicate mineral with Al, Ca, Fe, K, Na, and Si as the predominant elements in higher concentrations relative to those found in the parent coal. Aluminium, calcium and iron occur in concentrations typical of soils. Sodium is present in concentrations generally exceeding those found in soil. Fossil fuel wastes are also enriched with sulphur when compared with soil (Adriano *et al*., 1980; Mattigod *et al*., 1990a). The sulphur content of the parent coal determines the pH of fly ash which could range between 4.5 and 12 (Adriano *et al*., 1980). South Africa fly ashes are classified as class F. They are originated from sub bituminous coal tends to be lower in sulfur, higher in Ca, and generally produce alkaline ash (see Tables 5.2, 5.4, 5.5, 5.6 and 5.7). Certain elements are characteristically enriched in fly ash particles, especially As, B, Mo, S, and Se (Aitken and Bell, 1985; Page *et al*., 1979). Studies have shown that As, Cd, Cu, Mo, Pb, S, Se, Tl, and Zn concentrations generally increase with decreasing particle size (Davidson *et al*., 1974; Natusch *et al*., 1975). The main mechanism suggested to be responsible for this phenomenon involves the volatilization of elements during combustion, followed by condensation on the surface of fly ash particles as temperature decreases in emission stack.

The chemical composition of ashes from anthracite, bituminous and lignite coal are likely to vary (see Table 2.5). Holcombe (1984) suggested that variability in coal source might result in time variability of ash composition. Some of the mineral elements in coal get volatilized due to the combustion temperature. There are four types of coal each of which varies in terms of its heating value, its chemical composition, ash content, and geological origin. The types of coal are anthracite, bituminous, sub bituminous, and lignite.

Table 2.5. Normal range of chemical composition for fly ash

Component %	Bituminous	Sub-bituminous	Lignite
SiO_2	20-60	40-60	15-45
Al_2O_3	5-35	20-30	10-45
Fe_2O_3	10-40	4-10	4-15
CaO	1-12	5-30	15-40
MgO	0-5	1-6	3-10
SO_3	0-4	0-2	0-10
Na_2O	0-4	0-2	0-6
K_2O	0-3	0-4	0-4
LOI	0-15	0-3	0-5

Source: Adriano *et al*. (1980)

Table 2.6. Typical concentrations of trace element in fly ash

Element	Amount (mg kg^{-1})	Element	Amount (mg kg^{-1})	Element	Amount (mg kg^{-1})
As	2 - 312	Pb	3 – 500	Ba	0.01 - 1.0
B	10 - 5000	Mo	1.0 – 250	La	17 - 100
Cd	0.1 - 100	Ni	10 – 3000	Rb	3.0 - 200
Cu	10 – 2000	Se	0.2 – 50	Hg	0.01 - 12
Cr	3.0 - 900	Zn	10 – 1000	Cs	15 - 20

Source: Page *et al*. (1979); El-Mogazi *et al*. (1988); Bilski *et al*. (1995); Asokan *et al*. (2005).

The principal components of bituminous coal fly ash are silica, iron oxide, and calcium with varying amounts of carbon, as measured by the loss on ignition (LOI). Lignite and sub-

bituminous coal fly ashes are characterized by higher concentrations of calcium and magnesium oxide and reduced percentages of silica and iron oxide as well as lower carbon content, compared with bituminous coal fly ash (Meyers *et al*., 1976). Very little anthracite coal is burned in utility boilers, so there are only small amounts of anthracite coal fly ash. The chemical composition of coal ash is typically made up of silicon, calcium, aluminium, iron, magnesium, and sulphur oxides, along with carbon and various trace elements. These elements are found in the ash because of their high melting points and the short time the ash particles actually remain in the furnace during combustion. The above table compares the normal range of the compares the normal range of the chemical constituents of bituminous coal fly ash with those of lignite coal fly ash and sub bituminous coal fly ash. From the Table 2.5, it is lucid that lignite and sub bituminous coal fly ashes have a higher calcium oxide content and lower loss on ignition (LOI) (Koukouzas *et al*., 2007) than fly ashes from bituminous coals. Lignite and sub bituminous coal fly ashes may have a higher concentration of sulphate compounds than bituminous coal fly ashes. It is partly these trace elements and minerals that are transformed during combustion and that are used as the criteria to differentiate the classes of fly ash by ASTM C 618-95 Standards. Minor or trace metals are then concentrated in fly ash as they are released in volatile form during combustion. These elements are likely formed in the surface layer of fly ash particles rather than within the glassy particles if it melts (Steenari *et al*., 1999). The presence of these metals in higher concentration makes the disposal of fly ash an acute problem which requires attention (see Table 2.6). These elements tend to leach out to the surrounding soils when in contact with water. In addition, the leaching of elements from ash disposal is supposed to be site-specific considering variability in the climatic and weather conditions. Leaching losses from ash disposal sites are likely to be site-specific but a sparse number of studies have revealed enriched concentrations of elements such as Ca, Fe, Cd, Pb, and Sb in surrounding ground water (Haynes, 2009). Hence a proper disposal or utilization is required to reduce it negative environmental effects.

The mineralogical composition of fly ash, which depends on the geological factors related to the formation and deposition of coal, its combustion conditions, can be established by X-ray diffraction (XRD) analysis (Ahmaruzzaman, 2010). The mineral compositions of FA are formed within the coal strata or integrated in the coal during the coalification process. As the coal is combusted, mineral matter transforms to fix: ash and is thermally altered into different forms,

many of which are by themselves chemically very reactive or which can be chemically activated. The term used to describe this behavior is 'pozzolanic' (Scheetz and Earle, 1998). A pozzolan is defined as a siliceous or siliceous and aluminous material that by itself exhibits little or no cementitious properties but in the presence of moisture, chemically reacts with calcium hydroxide (lime) at standard temperature and pressure to form compounds exhibiting cementitious properties. The pozzolanic reactivity of the fly ash is dependent on a number of ash properties which include the particle density and surface characteristics of the glass phase particles (Lohtia and Joshi, 1995).

A small part of the inorganic matter is present in the form of ions associated with the organic matrix. Inorganic species are librated and transformed during coal combustion process. Carbonates are calcined and sulphides are oxidized, and the clay minerals are hydrated and decomposed. Chlorides and sulphates are formed when alkali and alkaline earth metals from either organic compounds or minerals react with combustion gases (Mattigod *et al*., 1990b; Steenari *et al*., 1999). At the same time, marcasite, pyrite, and siderite which are found in coal, on combustion alter to form ferrite and hematite phases along with sulphur dioxide and carbon dioxide respectively (see Table 2.7). Gypsum dehydrates to anhydrite and the calcium sulphate remains stable. Combustion process does not affect quartz chemically but undergoes an alpha/beta phase change at 573 ^{o}C which reduces the particle size of the individual grains (Scheetz and Earle, 1998). Although fly ash is largely non-crystalline glass, the major and minor elements in fly ash (O, Si, Al, Fe, Ca, Mg and S) form several different phases that has been characterized by X-ray diffraction in many research (Warren and Dudas, 1985; White and Case, 1990; Scheetz and Earle, 1998; Zevenbergen *et al*., 1999b; Karayigit *et al*., 2001; Illic *et al*., 2003; Koukouzas *et al*., 2006; Koukouzas *et al*., 2007; Lu *et al*., 2009; Font *et al*., 2010; Silva *et al*., 2010; Akinyemi *et al*., 2011). The X-ray diffraction technique is limited in that it can only detect mineral phases that are greater the ~3 % mass, and can only detect mineral phases that are crystalline in nature (Hareepaesada *et al*., 2010). The phases of major elemental constituents that have been commonly identified in fly ash include: quartz, mullite, glass, mica, enstatite, anorthite, lime, periclase, calcite, magnetite, hematite (Mattigod *et al*., 1990; Alonso and Wesche, 1991) and anhydrite. The fly ash contains high proportion of amorphous matrix, mainly derived from reactions in the mineral matter of the coal at high temperatures during combustion (Ward and French, 2006; Matjie *et al*., 2008). Methods of quantifying these minerals and the

glass content have been developed. Previous studies of fly ashes from South African Power stations have shown mineral phases most commonly to be detected were quartz, mullite, hematite, magnetite, magnetite (Fe_2O_3), anhydrite, port-landite ($Ca(OH)_2$), lime, periclase and titanium oxides (Bosch, 1990; Bezuidenhout, 1995; Campbell, 1999; Akinyemi *et al*., 2011).

The weathered dry disposed fly ash samples analysed in this study show similar mineralogy (see Figures 5.2, 5.3, 5.4, and 5.5). The mineral quartz (SiO_2) survives the combustion process and remains as quartz in the coal ash. The crystalline quartz (α-quartz) ranges from 1 to 9 % of fly ash and constitutes particles with a size distribution ranging from 0.5 to 5 µm (Ferraiolo *et al*., 1990). Quartz is ubiquitous in all the fly ashes and occurs as a major impurity in coal (Scheetz and Earle, 1998). As suggested by other authors (e.g. Ward and French, 2006; Matjie *et al*., 2008) the occurrence of quartz in fly ash is attributed to relict quartz grains in the coal that did not melt during the combustion process. Silva *et al*. (2010) found that some quartz react during combustion and incorporated into the glassy matrix.

Other minerals decompose, depending on the temperature, and form new minerals. The mullite present in fly ash forms by the decomposition of kaolinite (White and Case, 1990; Silva *et al*., 2010) which is entrained in coal. The clay minerals lose water and may melt, forming alumino-silicate crystalline and noncrystalline (glassy) materials. Elements such as Fe, Ca, and Mg combine with oxygen in the air to form oxide minerals, such as magnetite (Fe_3O_4), hematite (Fe_2O_3), lime (CaO), and periclase (MgO) (Solem-Tishmack and McCarthy, 1995). The magnetite should be classified as ferrite, due to the different rates of substitution of Fe^{2+} and Fe^{3+} by other ions, for example vanadium, chromium, manganese, cobalt, nickel and zinc (Kukier *et al*., 2003). Coal fly ash mineralogy mostly reflects the interaction of the decomposition products of coal sulfur with the lime to form anhydrite. Also, the mineralogy of fly ash will be significantly affected by the post-combustion handling and storage conditions. Presence of sufficient amount of lime (CaO) in fly ash mostly contain the following products of the reactions of CaO: with SOX to form anhydrite ($CaSO_4$); with atmospheric moisture and carbon dioxide to form portlandite, ($Ca[OH]_2$) and calcite, ($CaCO_3$), respectively; and with anhydrite and aluminate-rich altered clays, from the mineral matter of the coal in the presence of moisture, ettringite ($Ca_6Al_2(SO_4)_3(OH)_{12}•26H_2O$) is formed (Scheetz and Earle, 1998).

Table 2.7. Thermal transformation of mineral phases

Minerals in coal	Products following combustion
Phyllosilicates	Glass, quartz (SiO_2) and mullite ($Al_6Si_2O_{13}$)
Quartz	Glass, quartz (SiO_2)
Pyrite (FeS_2), siderite ($FeCO_3$), Iron sulphates	Hematite (Fe_2O_3) and magnetite (Fe_3O_4)
Calcite ($CaCO_3$)	Lime (CaO)
Dolomite ($CaMg(CO_3)_2$)	Lime (CaO), periclase (MgO)
Gypsum ($CaSO_4.2H_2O$)	Anhydrite ($CaSO_4$)
Ankerite ($CaMg_xFe_{(1-x)}(CO_3)_2$)	Calcium ferrite ($CaFe_2O_4$), periclase (MgO)

Source: Mattigold *et al*. (1990)

The pH of fly ash varies from 4.5 to 12 depending largely on the S content of the parent coal, type of coal used for combustion and S content of the fly ash (Carlson and Adriano, 1993). Etrringite forms in coal by-products that contain high levels of calcium and sulfate react with water to give pH above ca. 12, and include aluminium that can be solubilised at high pH (Solem-Tishmack and McCarthy, 1995). The mineralogical constituent of class F ash is determined by the bulk chemical composition. Quartz, the ferrite phase, and mullite each average less than 10 wt % of the bulk and in most cases the latter two phase average less than 5 weight percent of the bulk. The most abundant phases in a class F fly ash are the glass that results from the melting of the clays and subsequent exsolution of mullite from the melt (Scheetz and Earle, 1998). Due to the higher calcium content in class C Fly Ash, the assemblage of the resulting mineralogical phase is quite different. Quartz, ferrite phase, and the mullite are present (Scheetz and Earle, 1998).

Several atomic force microscopic studies on fly ash have been done (Mollah *et al*., 1999; Mishra *et al*., 2003; Chen *et al*., 2005). The 2-weeks-old fly ash has a spherical microscopic structure (see Figure 5.16a). The chemical weathering has significant effect on the surface morphology of fly ash (Figure 5.16b). However, not all particles are spherical (Figure 5.16). The size distribution can also be assessed by investigation of the micrograph. The present micrograph are similar to those in literature (Mollah *et al*., 1999; Fang *et al*., 1999; Sokol *et al*., 2000; Mishra *et*

al., 2003; Lin and Shih, 2003; Chen *et al*., 2005). Quantitative work by energy dispersive X-ray analyses indicates the heterogeneous nature of the fly ash particles (Mollah *et al*., 1999; Kukier *et al*., 2003; Mishra *et al*., 2003). The infrared spectra of fly ash have also been reported in the literature (Mollah *et al*., 1999; van Jaarsveld *et al*., 2003). Their result is similar to infrared spectra for fly ash used in this study (Figures 5.13-5.15). Mollah *et al*. (1999) assign the bands in their spectra. The band at 1080 cm^{-1} is assigned to the antisymmetric stretching vibration of Si-O-Si and the band at 792 cm^{-1} corresponding to the symmetric vibration (Mollah *et al*., 1999). The band at 1135 cm^{-1} is tentatively assigned to the antisymmetric stretching vibration of Si-O-Al and the band at 700 cm^{-1} to the asymmetric Si-O-O bending vibration (Mollah *et al*., 1999). The shoulder at 950 cm^{-1} is assigned to a non-bridging oxygen ion band, Si-O-Na (Mollah *et al*., 1999). The bands at 800 cm^{-1} and 481 cm^{-1} are assigned to the presence of cristobalite, and the band at 700 cm^{-1} to the presence of mullite (Mollah *et al*., 1999).

2.4.5 Disposal of fly ash

The disposal of FA as a by-product of incineration of coal constitute a problem than ash produced from burning of municipal solid wastes, rice husks and tea dusts because of its volume (Iyer, 2002). Despite the different ways of utilizing fly ash and the significant quantities being used in the range of applications as a substitute for cement in concrete, as high way road basis, and other positive uses, large amounts are not used, which makes the disposal and management of fly ash produced by coal-fired power plants a major problem in many parts of the World. For example, coal-fired plants in Yugoslavia produce approximately 5000 kt of ash per year. A 20 kt is used in cement industry and for production of paving slabs, building blocks and ready mixed concrete. The remaining ash is disposed of in ash depositories (Iyer, 2002 and Ilic *et al*., 2003).

ESKOM as an electricity production company generated about 27 million tonnes annually (www.eskom.co.za/annreport09/abridged/index.htm) in which only about 5 % of the total coal fly ash produced per year is reused (Petrik *et al*., 2003). The large volume of unused fly ash is disposed in most cases to hold ponds, landfills and slag heaps (Iyer, 2002; Petrik *et al*., 2003; Jo *et al*., 2008). In many countries, coal ash has many beneficial applications such as cement and brick materials, road base, embankment construction, and structural fill (Fulekar and Dave, 1986; Fytianos *et al*., 1998). According to Foner *et al*. (1999), Israel use to dispose or utilize ash generated from power stations by adding to cement as pozzolanic admixture; dumped at sea; and

stockpiled in embankments around the power stations but this could not continue due to maximum utilization and forbidden by law, and the disposal of ash becomes an increasing acute problem.

In South Africa, power station fly ash is disposed of in one of two ways; by dry dumping or by hydraulic deposition into dams. It has sometimes been observed that a marked hardening of the hydraulically deposited fly ash occurs, producing a very erosion-resistant surface Fourie *et al*. (1997). In a dry ash handling scenario (see Figure 4.1), the ash is partially wetted at the power station by adding approximately 10-15 % water before being transported by a conveyor belt to the disposal dumpsite. This moisture prevents the ash from blowing off the conveyor belt and a watering gun is also available in the area where the ash is being tipped to prevent it from drying out and creating a dust problem. According to Hodgson (1999), this dry ash disposal system is similar to that used in all power stations in South Africa and the most common concentration of chemicals in the effluent are sodium and sulphate. Wet ash handling involves, ash being pumped from the power station to the ash dams in ash-to-water ratios of 1:10 to 1:5 by volume (Hodgson and Krantz, 1998). Excess water on top of the ash dams is decanted through a penstock arrangement, draining water into ash water return dams. From there, water is returned to the power station to pump more ash. Wet disposal of FA (fly ash) is a simple operation and has minimal effect on the local air quality. Conversely, the amount of water required forming the FA slurry is considerable and recirculation of water is a costly practice. During wet ash handling, heavy metals (which are toxic in nature) leach from the matrix leading to change in the ash chemistry and ultimately pollute the environment. A major disadvantage of wet disposal is that it demands large areas of land, which are practically irretrievable for future use Singh and Kolay (2002).

The ash handling has significant effects on the ash chemistry and mineralogical changes. For example the pozzolanic property of a wet ash system is very different from that of a dry ash system. In wet ash handling scenario, water migrates from the inside of an ash dam to the outside, where evaporation occurs. The presence of ingressed CO_2 is necessary for pozzolanic development but wet ash dams are usually saturated with water, so no carbon dioxide of any significance can permeate the dams. Although pozzolanic action is not possible within the wet ash dams, the presence of atmospheric carbon dioxide assists in the development of a skin of

pozzolanic material. This layer covers the outer few millimetres of an ash dam and can easily be broken to expose the soft unaltered ash below. At dry ash dumps, the upper layers go through alternate wetting and drying cycles, as they are exposed to rainfall and evaporation. This cyclic exposure allows sufficient water and air to exchange to establish a pozzolanic layer of up to a metre or more on the top and along the sides of these dumps (Menghistu, 2010). The controlling factor for pozzolanic action is not so much the amount of rainfall, but the irregularity of the event. Disposal of fly ash as landfill is under pressure from environmental concerns and increasingly stringent environmental regulations are progressively increasing the cost of disposal (Haynes, 2009).

Coal fly ash frequently contains trace elements such as As, Cd, Cu, Pb, Zn, and Se, which can damage the environments if released (e.g., soil and groundwater quality (Bin-Shafique *et al*., 2006; Henry *et al*., 1980; Daniels and Das, 2006). Coal ash has found limited use (e.g., concrete and brick materials) because of environmental concerns (Choi *et al*., 2002). Indiscriminate disposal of fly ash may cause long-term adverse environmental effects (Ilic *et al*., 2003). This is due to the weathering and leaching processes it undergoes leading to release of high concentration of trace elements and the increase in the mobility of these elements (Adriano *et al*., 1980). Effect of disposal of fly ash can be ameliorated by rehabilitating ash-holding ponds or dams. This can be done by covering the ash dam with vegetation to prevent wind erosion of ash sediments. For effective revegetation, the surface of the site is usually either covered with a cap of soil or organic amendments are incorporated into the surface (Haynes, 2009).

2.4.6 Weathering processes of fly ash

After disposal of fly ash into the land fill; overtime, revegetation of ash dump produce organic debris which is incorporated into the fly ash. Simultaneously, chemical interaction of fly ash with environmental factors such as; ingressed CO_2, ingressed O_2 from atmosphere and percolating rain water cause chemical alteration and mineralogical transformation in fly ash (weathering/ageing). Fly ash weathering is similar to that of volcanic ash (Warren and Dudas, 1985; Zevenbergen *et al*., 1999a). Three types of precipitation products were identified in the ash: (i) Calcite formed through the dissolution of Ca from the ash and subsequent reaction with CO_2 absorbed by the initial alkaline leaching solutions. (ii) Iron, dissolved from the ash under acidic conditions, precipitated as amorphous coatings on fly ash particles and (iii) Aluminium

and Si dissolved from the glass of the ash was translocated and precipitated within alkaline environments as an amorphous aluminosilicate material best described as proto-imogolite (Warren and Dudas, 1985). The primary stages of weathering of alkaline ashes have been established to entail transformations of Ca (Schramke, 1992; Georgakopoulos *et al*., 2002). Calcium in unweathered ash is principally present as lime (CaO) and anhydrite ($CaSO_4$) or in an amorphous glassy phase (Rai *et al*., 1987). These phases are extremely reactive when come in contact with water and as pointed out, Ca^{2+} and SO_4^{2-} are typically the major cation and anion species leached from fly ash disposal sites. Weathering of the fly ash results in substantial declines in soluble salt levels as they are progressively leached away (Adriano *et al*., 1980). Steenari and Lindqvist (1997) suggested that optimum water-to ash ratio varies between ash types and must be optimized for each ash. In addition, postulates a number of most important chemical reactions that take place when ash comes into contact with water (self hardening).

- hydroxide formation, e.g. $CaO+H_2O \rightarrow Ca(OH)_2$
- carbonatization of hydroxides e.g. $Ca(OH)_2 + CO_2 \rightarrow CaCO_3 + H_2O$
- formation of gypsum, e.g. $CaSO_4 + 2H_2O \rightarrow CaSO_4.2H2O$
- formation of etrringite, $Ca_3Al_2O_6 + CaSO_4.2H_2O + 26H_2O \rightarrow Ca_6Al_2(SO_4)_3(OH)_{12}.26H_2O$
- formation of hydrated silicate and aluminium-silicate phases.

The rivalry between Ca-rich phases, with and without SO_4^{2-}, control the chemical reactions within the system with calcite ($CaCO_3$) and gypsum ($CaSO_4.2H_2O$) being the major minerals formed. During this reaction sequence, lime (CaO) is hydrated to portlandite ($Ca(OH)_2$) (see equation 1) which reacts with water (H_2O) to form calcite ($CaCO_3$) (see equation 2). The transformation of portlandite into calcite is very important since this reaction reduces the pH of the equilibrium solution significantly (Schramke, 1992). Specifically the pH is very high when portlandite be in the majority:

$Ca(OH_2)(s) \rightarrow Ca^{2+} + 2OH^-$ ……..equation (1)

Since CO_2 (g) originating from the atmosphere and/or microbial respiration is absorbed by the highly alkaline solution, $CaCO_3$ precipitates and solution pH is reduced:

$Ca^{2+} + CO_2 + H_2O \rightarrow CaCO_3 + 2H^+$……..equation (2)

Because of its stability, it is contemplated that calcite solubility ultimately controls equilibrium pH of alkaline ash solutions and leachates (Schramke, 1992). In the longer-term, the aluminosilicate glass material that makes up the ash matrix will weather to form non-crystalline aluminosilicate clays. Certainly, Zikeli *et al*. (2005) established that soils derived from lignite ash have many soil chemical properties similar to volcanic soils although they can contain unusually large amounts of gypsum, calcium and magnesium carbonates and organic carbon depending on the composition of the parent coal. A few studies have suggested that lignite fly ash weathering is considerably more rapid than that of volcanic ash (Zevenbergen *et al*., 1999a&b; Zikeli *et al*., 2002). For example, Zevenbergen *et al*. (1999a) established that after about 10 years of weathering, the non-crystalline clay content of coal fly ash was greater than the 250-year-old volcanic ash. It has been hypothesize that rapid formation of a clay fraction is the result of the initially very high pH in the lignite ash deposits (i.e. 11–12) which promotes rapid dissolution of aluminosilicate glass compounds.

In the light of above, due to the rapid uptake of CO_2, and calcite precipitation, the pH of ash decreases and stabilizes at around 7–8 (Schramke, 1992). This pH decrease allows Si and Al to precipitate from solution yielding amorphous aluminosilicate compounds. Most probably for fly ash initially in the pH range 7–8 or lower, weathering is much slower. The pH of a suspension of 10 gram of unweathered fly ash in 100 ml of ultra pure water is 11.33±0.006 whilst 20 yrs, 8 yrs and 1-year-old dry disposed weathered fly ash range from 7.2-10.5 (Figures 5.17-5.19). A relatively lower pH value of dry disposed weathered fly ash is due to flushing of basic soluble buffering constituents (CaO and MgO). Nevertheless, no studies have yet compared weathering rates of ashes of different composition and/or pH and this aspect needs to be fully investigated (Haynes, 2009).

A limited number of literatures are available on the investigative studies on chemical and mineralogical transformations of weathered fly ash (Yeyehis *et al*., 2009; Gitari *et al*., 2009). Yeyehis *et al*. (2009) found that the formation of secondary minerals during weathering of disposed fly ash samples has significant effect on acid neutralisation capacity and leaching behaviour of their components. Gitari *et al*. (2009a) established that contact of fly ash with water is observed to be a crucial factor in the mobilization of constituents of ash or of brine used for irrigation with time. The amorphous aluminosilicates (clay) formed during weathering are able to

adsorb much larger quantities of cations and anions than crystalline glass because they have a much greater surface area and the surfaces possess much more positive and negative charges. An implication of this clay formation is that it coats the surface of ash particles and acts as an adsorbent for any heavy metal contaminants in the ash. It could also partly form a physical barrier to leaching (Haynes, 2009). This clay material could also react with organic matter produced during revegetation of the site. Thus, the developing soil would effectively sequester C and this would result in a rapid accumulation of organic matter and formation of a large soil microbial community (Zikeli *et al*., 2004; Machulla *et al*., 2004). A few literatures investigated the chemical and mineralogical transformation of horizontally lay sub-bituminous fly ash dry disposed in a land fill (Gitari *et al*., 2009a; Akinyemi *et al*., 2011). Nevertheless, no studies have yet compare the chemical alteration and mineralogical transformation dry disposed fly ash in a land fill at different stages of weathering and various depths. This aspect is fully investigated in the current study.

2.4.7 pH and neutralizing capacity of fly ash

The initial pH of fly ash is expected to exert a great influence on the chemical weathering of fly ash. The chemical interaction of fly ash with ingressed CO_2, ingressed O_2 and rain water is expected to lower the initial pH of fly ash. Theis and Wirth (1977) suggested that the relative amounts of lime and amorphous Fe oxides on the surface define the ultimate acidic or basic character of fly ash in solution. As noted above, the Class C (acidic) and Class F (alkaline) fly ashes significantly vary in the CaO content. A relatively slower chemical reaction is expected in acidic fly ash (low pH) due to low CaO content. In the case of Class F fly ash rapid dissolution of alumino silicate minerals occur due to high pH (i.e. high free CaO) (Moitsheki *et al*., 2010) when come in with water and ingressed CO_2 thereby lowering the initial pH of fly ash. Previous study had establish that rapid dissolution of aluminosilicate minerals glass material that make up the ash matrix occurred in alkaline fly ash which eventually weathers to non-crystalline aluminosilicate clays (Haynes, 2009). Apart from the CaO content, the amount of sulphur in fly ash also determines the pH of fly ash. Haynes (2009) found that the pH of ash varies from 4.5 to 12 depending on the sulphur content of the parent coal. The high CaO content in unweathered fly ash (high pH) could probably suggests availability/enrichment of trace metals.

Carlson and Adriano (1993) found that the pH of some alkaline ashes can exceed 12 and hypothesize that this may be a factor limiting plant growth, particularly on unweathered deposits. The chemical interaction of fly ash with environmental factors would invariably lead to flushing of soluble basic oxides (CaO and MgO) thus lowering the initial pH and subsequent metal release. Gitari and others (2009b) established that the flushing of basic soluble oxides (CaO and MgO) that act as a pH buffering constituents occur when fly ash comes in contact with water. Akinyemi *et al*. (2011) found that 1-year-old and 20-year-old coal fly ash cores showed a lower pH and greater leaching/flushing of the soluble buffering constituents than the 2-week-old placed ash. The effect of chemical interaction of fly ash with ingressed CO_2, ingressed O_2 and percolating rain water is thought to have significant effect on initial pH, metal mobility and neutralisation capacity of fly ash. The effect of weathering on the trace metal leaching is likely to be significant, because pH is a dominant parameter in metal mobility and complexation (Stumm and Morgan, 1981). This chemical interaction of fly ash with environmental factors may lead to formation of secondary minerals that can bind trace metals in weathered fly ash. Meima and Comans (1999) established reduction in leaching is due to the neutralisation of bottom ash pH and the formation of less soluble species of these elements as weathering continues.

The acid susceptibility of fly ash is expected to be governing by the amount of CaO and MgO in fly ash. As noted above, thus the Class F fly ash is thought to have fairly high acid neutralisation capacity than Class C fly ash. Hodgson *et al*. (1982) found that neutralization capacity of ashes was negatively correlated with their content of Si and Fe and positively correlated with Ca and Mg content. Similarly, Kukier and Sumner (1996) found large differences in fly ash neutralization capacity which were correlated with their Ca content. The liming ability or neutralizing capacity of ash (measured as titratable alkalinity) will vary greatly, from none to high, depending on the source of ash and also the extent to which it has weathered (Adriano *et al*., 1980). The liming ability of Class C ash (> 15 % CaO) is likely to be considerably greater than that of Class F (< 10 % CaO). That is, although Class F ash may have a high initial pH, its neutralizing capacity when in contact with soil will be lower due to its low CaO content (Haynes, 2009).

The role of ingressed CO_2 and percolating rain water in lowering the pH of the fly ash cannot be understated in weathering of fly ash. As noted above, the ingressed CO_2 react with highly

alkaline solution, calcite precipitate and solution pH reduce. Schramke (1992) established that in fly ash leachates under a natural systems, the rate of input of CO_2 (g) into the leachate is expected to control the overall rate of pH equilibrium. Yeyehis *et al*. (2009) investigated the effects of secondary mineral formation on the acid neutralisation capacity of fly ash. Nevertheless, no studies have investigated the effect of chemical weathering on the acid neutralisation capacity of dry disposed weathered fly ash in landfill. Acid neutralisation capacity of unweathered fly ash (fresh ash) is relatively high when compared to dry disposed weathered fly ash. As noted above, this can be explained by the formation of secondary minerals and depletion of basic soluble buffering constituents (CaO content) in weathered fly ash. Our results further show that the release of elements such as Ca, Mg, Na, K, Se, Cr, and Sr are controlled by the solution pH (Figures 6.5a&b and 6.6a&b). Whilst other trace metals like As, Mo and Pb showed amphoteric behaviour with respect to solution pH.

2.4.8 Leaching of fly ash

The environmental impact of coal ash production has at least two aspects: (a) emission and deposition of enormous amounts of coal ash, polluting air, water and soil with ash particles (including the problem of huge ash dumps); (b) leaching of microelements (including toxic heavy metals), but also major cations and anions from ash by atmospheric and surface waters (Popovic *et al*., 2001). The content of trace elements in coal fly ash is clearly relevant to any environmental aspect during beneficiation or usage and disposal. The heavy metals found in greatest concentration include antimony, cadmium, lead, nickel, thallium, and zinc; other toxic elements include arsenic and selenium (Wadge and Hutton, 1987; Querol *et al*., 2001). There is existence of either easily exchangeable or adsorbed molecules on the surface of the spheres of fly ash which become dissolved when fly ash comes in contact with water. This mechanism produces leachate (Jo *et al*., 2008) and the process is called leaching. Environmentally sensitive trace elements can be concentrated at or near the surface of fly ash particles during combustion. The presence of a non-porous continuous outer surface and a dense particle interior can restrict heavy metal leachability from residues. Leaching of trace elements from combustion residues is a very slow process and the solid and liquid phase equilibrium may not be attained even with long leaching times (Fishman *et al*. 1999; Saikia *et al*., 2006). Dudas (1981) found rapid dissolution of inorganic salts dominate compositional trends during the early stages of leaching

and the slow dissolution of glassy ash particles which becomes partially evident only in the later stages of leaching after most or all of the inorganic salts have dissolved.

As noted above, fly ash contains many potentially toxic trace elements; leaching test has shown that these are stable within aluminosilicate matrix (Hower *et al*., 1996). In view of that fly ash is not classified as a hazardous waste in America (Hower *et al*., 1996). The ministry of Environment in Israel, however considers the use of fly ash as landfill potentially harmful, and forbids its use as landfill (Foner *et al*., 1999), maybe in response to the greater leaching test results of Nathan *et al*. (1999). The only element that might pose a problem is hexavalent chromium (Foner *et al*., 1999). The major environmental concern with fly ash disposal is the possible leaching of heavy metals and toxic element to the underground water underneath the disposal site. Therefore, leaching characteristics is one of the major environmental concerns of fly ash (Yan and Neretnieks, 1995). The leaching behaviour is influenced by several factors (Yan and Neretnieks, 1995) therefore results can be expected to vary for fly ash samples from different sources. The composition of the spherical portion of fly ash is immune to dissolution due to its glassy structure. The elemental composition and leaching properties of this spherical portion is quite similar to glass, and is relatively inert. The reactivity of fly ash is determined by the particle size. The smaller particle has a larger specific surface area, making a large area susceptible to hydrolysis. According to studies, only about 1-3 % fly ash material is soluble in water with lignite fly ashes having a higher proportion of water soluble constituents (Keyser *et al*., 1978; Iyer, 2002). The particle size distribution being constant after the leaching process proves that the surface of fly ash particle, a few microns in thickness is wholly involved in leaching. Therefore the charge on the surface of fly ash particle and formation of the diffuse double layer plays a significant role in leaching (lyer, 2002).

The elements Mn, Ba, V, Co, Cr, Ni, Ln, Ga, Nd, As, Sb, Sn, Br, Zn, Se, Pb, Hg and S are usually volatile to a significant extent in combustion process. The elements Mn, Ba, V, Co, Cr, Ni, Ln, Ga, Nd, As, Sb, Sn, Br, Zn, Se, Pb, Hg and S are usually volatile to a significant extent in combustion process. The volatility for these elements is inversely proportional to particle size. Elements like Mg, Na, K, Mo, Ce, Rb, Cs and Nb possess a smaller volatilized fraction during coal combustion (Lyer, 2002). The volatility is directly proportional to particle size. The elements Si, As, Fe, Ca, Sr, La, Sm, Eu, Tb, Py, Yb, Y, Se, Zr, Ta, Na, Th, Ag and Zn are either

not volatilize or may show minor trends related to geochemistry of mineral matter. The volatility of trace elements increased from larger to smaller particle size and establishes an inverse relationship of volatility and particle size (Fischer *et al*., 1979). Saikia *et al*. (2006) recognised that the leaching behaviour of coal ash is controlled by the mineralogical composition of the combustion residues. The alkalinity and acidity controlled extractability of elements, such as, As, B, Be, Cd, Cr, Cu, F, Mo, Se, V and Zn. Eisenberg *et al*. (1986) found that aqueous extracts of an acidic fly ash contained concentrations of Cd, Co, Cu, Mn, Ni, Zn, As, B, Be, Cd, F, Mo, Se and V. The aqueous extracts of an acidic fly ash contain concentrations of most of the elements mentioned above. Depending on the reaction time and water/solid ratio in batch equilibration or with column length and flow rate in a dynamic leaching test, small sample can show marked differences in leachate water chemistry (Iyer, 2002).

Fly ash from the exhaust flow of a coal when in contact with water can pass through a range of chemical alteration pathway. The alteration pathway of fly ash and the composition of the water/fluid in contact are a function of the initial chemical and mineralogy composition of the fly ash. The main components of fly ash are anhydrous phases such as aluminosilicates and salts such as sulphates, oxides and chlorides formed at high temperatures in coal-fired power generating stations (Mattigod *et al*., 1990; Gitari *et al*., 2006). Some of these phases (alkali metal oxides, sulphates, and chlorides) are highly unstable at room temperature and pressure and in presence of water. When fly ash contacts water these phases will dissolve completely, more stable and less soluble mineral phases will thereafter precipitate. Hence, the concentration of some constituent species in the leachate will be controlled by the solubility of the precipitating secondary mineral phases and concentration of other species will be controlled by their availability to the leachate solutions and by their diffusive flux into solution from the leaching of the primary phases with time (Eary *et al*., 1990; Prasad *et al*., 1996; Spears and Lee, 2004).

Coal fly ash alteration may also depend on the mobility or retention of metals when constituents of the ash react with water. The mobility or retention of metals when constituents of fly ash react with water can be affected by high pH and adsorption or co-precipitation phenomena. The rate of alteration of ash can influence initial and long-term solution composition (Fishman *et al*., 1999). These studies showed that leachates from coal ash usually have high pH and an excess of elements such as As, Cd, Cu, Pb, Zn, and Se. The chemical interaction of coal fly ash with

ingressed CO_2, ingressed O_2 and percolating rain water would lower initial pH of fly ash and have significant impact on the leaching of soluble constituents of fly ash. In our studies, analysis of the extracted interstitial pore water showed Mg, Ca, Fe, K^+, Na^+, B, Cr, As, Mo, and Se are progressively leaching through the column of the ash. A significant decrease in the level of Se, Mo, B, and As was observed at the point of contact with the water level under the ash dump suggesting lateral diffusion of the these contaminants into the groundwater system (Akinyemi *et al.*, 2011). The authors also found that the 1-year-old and 20-year-old coal fly ash cores showed a lower pH and greater leaching/flushing of the soluble buffering constituents than the 2-week-old placed ash (Akinyemi *et al*. 2011).

Several studies showed that leachates from coal ash usually have high pH and an excess of elements such as As, Cd, Cu, Pb, Zn, and Se. The leachability of these elements is generally affected by their solubility and adsorption capacity, composition of coal ash, and the chemistry of the extracting water (e.g. pH and ionic strength) (Fytianos *et al*., 1998; Eisenberg *et al*., 1986; Gutierrez *et al*., 1993). Prasad *et al.* (1996) found that leachability of heavy metals from the coal fly ash is relatively low and leaching extent is dependent on the conditions of water system. Trace metal concentration in the leachate depends on fly ash weight/solution, pH, and concentration of elements, temperature, pressure, and time. In water, rapid leaching of most of the trace metals (except Cu), takes place from the surface of ash particles in lower pH range; all trace elements lie within acceptable limits.

The composition of ash can influence the constituent released during leaching. Wan *et al*. (2006) also reported that the leaching behavior of heavy metals such as zinc, lead, cadmium and copper in MSWI fly ash have a dependency relationship with the components of calcium, such as aphthitalite, calcite, anhydrite and calcium aluminate or calcium aluminosilicate. Steenari *et al*. (1999a) through leaching tests found that upon reaction of fly ash with moderate amount of water secondary mineral phases such as ettringite and calcite were formed. These compounds were shown to affect the leaching rate for calcium and sulphate as well as pH of leachates (Steenari *et al*. 1999a; Steenari *et al*., 199b). In the case of ash pond leachate, Theis and Ritcher (1979) showed that adsorption onto hydrous Fe and Mn oxides is the major solubility control for cadmium, nickel, and zinc while precipitation of discrete phases controls for chromium, copper, and lead. Complexing agents strongly influence the leachability of metals from fly ashes (solid

wastes, in general) and, in most cases, increase significantly the amounts of pollutants released into the environment. This holds true also for naturally occurring complexing agents such as humic substances. The presence of humic substances usually increases the mobility of metals in environment (Janos *et al*., 2002).

Ding *et al*. (1998) identify Ca^{2+}, K^{+} and Na^{+} as the soluble constituents of fly ash and find that a suspension of fly ash in water gives a pH of 12.2, in agreement with the present study as well as other work of Foner *et al*. (1999). The principal cations in water extracts are calcium and sodium, whereas anions are dominated by OH^{-}, CO_3 with aqueous extracts of ash saturated with $Ca(OH)_2$.(Elseewi *et al*., 1980; Menon *et al*., 1980). Bayat (1998) further determines, through leaching experiments that Na and K are almost entirely in their free ionic states, whereas Ca and Mg are only predominantly in their free ionic states. Hydroxides and sulphates are also common in the fly ash suspensions (Bayat, 1998). A number of elements, notably Ca, B, Sr, and, to a lesser extent, V, were preferentially leached so that their concentrations in the weathered ash residue are substantially lower than in fresh ash. This preferential removal leads to negative enrichment such that concentrations of other elements like Al, Ba, Fe, K, Na, Mn, Pb, and Zn are higher in leached ash than in fresh ash (Dudas, 1981).

2.5 Utilization of fly ash

ESKOM generate 36.7 million tonnes of coal combustion by products from coal-fired power stations in South Africa during 2009. Of this total, 1.84 million tonnes or 5 % of the ash produced was utilized in one form or another. The remaining 34.86 million tonnes of ash was disposed of by more traditional means (Petrik *et al*., 2003; Eskom Abridged Annual Report, 2009). Fly ash accumulates in large volumes and becomes a significant waste disposal problem because of the inconsistent trend of its utilization (Adriano *et al*., 1980). Utilization of fly ash can be in the form of an alternative to another industrial resource, process, or application. These processes and applications include, but are not limited to, addition to cement and concrete products, structural fill and cover material, roadway and pavement utilization, addition to construction materials as a light weight aggregate, infiltration barrier and underground void filling, and soil, water and environmental improvement (Halstead, 1986; Ahmaruzzaman, 2010).

Fly ash is used in the manufacture of lightweight aggregate, in road base construction, landfill liners, sewage sludge treatment and as filler in plastic composite materials. Fly ash is also used in

the ceramics industry and in the manufacture of bricks and tiles. The production of glass-ceramics from fly ash has been investigated. The process which involves melting fly ash mixed with other materials such as ground glass cullet and dolomite to control the composition and produce a glass. Lignite coal fly ash has been sintered to form ceramic materials using conventional powder processing based on milling, powder compacting and firing, without the addition of organic binders or other inorganic additives (Ilic *et al*., 2003). Utilization of fly ash has been investigated to facilitate its disposal and minimize negative environmental impacts and the chemical and leaching characteristics of coal residues must be known before utilization (Steenari *et al*., 1999b). The following is a short description of each of the previously mentioned alternative uses of fly ash and associated research that has been conducted and how it relates to each alternative use. In this section, the application of fly ash has been discussed.

2.5.1 Construction work and industry

Comprehensive research has been dedicated to the subject of fly ash admixture concrete and the properties that it exhibits. Due to the irresistible information that is obtainable on the topic of fly ash addition to concrete, it is outside the scope of this study to do anything more than draw attention to some of the existing research. Research has found that fly ash used as an additive to Portland cement has a number of positive effects on the resulting concrete. These positive effects are detailed below. Ahmaruzzaman (2010) in his work highlighted essentially three applications for fly ash in cement, including (1) replacement of cement in Portland cement concrete (2) pozzolanic material in the production of pozzolanic cements, and (3) set retardant ingredient with cement as a replacement of gypsum. One of the advantages of usage of fly ash in concrete is the reduction of construction cost by partial replacement of cement with fly ash. Other beneficial effects, include lower water demand for similar workability (Halstead, 1986), reduced bleeding, and lower evolution of heat. Fly ash is used particularly in mass concrete applications and large volume placement to control expansion due to heat of hydration and also helps in reducing cracking at early ages. Fly ash concrete provides much strong and stable protective cover to the steel against natural weathering (Ahmaruzzaman, 2010). The utilization of fly ash in concrete produces less permeability because of the spherical particles, and therefore improved packing, i.e. more dense paste and pozzolanic reaction.

The availability of high-lime fly ash containing compounds found in cement has led to high-strength concretes produced by the addition of fly ash and plasticizers. High-strength and high-performance concrete can also be made with Class F fly ash. The utilization of fly ash in concrete produces less permeability because of the spherical particles, and therefore improved packing, i.e. more dense paste and pozzolanic reaction. Class F fly ash produce concrete with lower heat of hydration compared to straight Portland cement concrete. Whereas Class C fly ash may not lower the heat of hydration. Abrasion resistance of concrete made with Class C fly ash was better than both concrete without fly ash and concretes containing Class F fly ash (Tikalsky *et al*., 1988). Naik *et al*. (1998) found that blending of Class C fly ash with Class F fly ash showed either comparable or better results than either the reference mixture without fly ash or the unblended Class C fly ash. Blending of fly ash, therefore, leads to comparable or better quality and reduced cost, due to the use of Class F versus Class C fly ash in concrete. Siddique (2004) found that Class F fly ash can be suitably used up to 50 % of cement replacement in concrete for use in precast elements, and reinforced cement concrete construction. The use of high volumes of Class F fly ash as a partial replacement of cement in concrete decreased its 28 days compressive, splitting tensile and flexural strengths, modulus of elasticity, and abrasion resistance of the concrete. The presence of CaO and $CaSO_4$ in some fly ash contributed to their utilization in soil stabilization and as fillers in road bases than in building materials (Steenari *et al*., 1999a). Both CaO and $CaSO_4$ form hydration products, such as portlandite ($Ca(OH)_2$) and ettringite ($Ca_6Al_3(SO_4)_3(OH)_{12}\cdot 26H_2O$), with significantly larger volumes than those of the reactants. Calcium oxide or calcium sulfate present in a concrete construction may thus create expansion cracks due to delayed reactions with water (Steenari *et al*., 1999a).

Fly ash increase resistance to corrosion, and ingress of corrosive liquids by reacting with calcium hydroxide in cement into a stable cementitious compound of calcium silicate hydrate (Scheetz and Earle, 1998; Ahmaruzzaman, 2010). Mehta (1996) also noted in his review paper that the agents responsible for concrete expansion and cracking are alumina-bearing hydrates, such as calcium monosulfo-aluminate and calcium aluminate hydrate, which are attacked by the sulphate ion to form ettringite and calcium trisulfoaluminate. Acidic-type interactions between sulphate ions and calcium hydroxide also lead to strength and mass loss. The original calcium hydroxide was soluble, whereas the calcium silicate hydrate is less soluble in fly ash concrete, thereby reducing the possibility of leaching of calcium hydroxide from the concrete. In addition to

calcium silicate hydrate being less soluble, reaction products tend to the filling of capillary voids in the concrete mixture, thereby reducing permeability of the concrete (Halstead, 1986; Ahmaruzzaman, 2010).

Gao *et al*. (2007) investigated the utilization of fly ash in the construction of concrete dams. The compressive strengths of dam concrete with 50 % of fly ash in 90 days are higher than those with 30 % of fly ash or without fly ash. Fly ash may decrease the deformation of dam concrete with 50 % of fly ash, and the shrinkage and expansive strain was reduced significantly–about 33 % and 40 % less than the specimens without fly ash, respectively (Ahmaruzzaman, 2010). The low-lime fly ash was used to develop chloride-resistant concrete by improving its physical resistance to the ingress of chlorides and binding capacity of these ions in the cover zone (Dhir and Jones, 1999).

2.5.2 Road and pavement utilization

Re-utilization of fly ash as a material in the construction of roadways and associated peripheral project has been a significant outlet for the past two decades. Fly ash has been used in embankment soil stabilization, sub grade base course material, as aggregate filler, a bituminous pavement additive and as mineral filler for bituminous concrete (Scheetz and Earle, 1998). Fly ash has been used in embankment soil stabilization, sub-grade base course material, as aggregate filler, a bituminous pavement additive and as material filler for bituminous concrete. Fly ash used as a soil stabilizer along roadway embankments has been beneficial practice foe a number of reasons. Fly ash soil stabilization is cost effective due to ease of availability combined with positive physical properties. Shear strength is an important characteristic for soil stabilization fly ash utilization and it generally equals or exceeds the strength of soils typically used for embankments (Lin, 1971). This strength is partially due to some fly ash having self-hardening or pozzolanic properties, which is a characteristic more common to class C fly ash and ash from atmospheric fluidized bed boilers. Use of fly ash in road works results in reduction in construction cost by about 10-20 %. Similarly, the use of fly ash in pavement construction results in significant savings due to savings in cost of road aggregates. The only major problem associated with soil stabilization is the frost susceptibility of the fly ash. If placed in a cold climate and exposed to frost, the fly ash will have to be stabilized with a lime mixture to chemically bind the entire mixture (Scheetz and Earle, 1998).

2.5.3 Construction materials utilizing light weight aggregate

Use of fly ash as a by-product aggregate in the manufacture of light weight construction products presents itself as a logical re-utilization process for a number of reasons. The main advantage is the economic saving to the manufacturer, associated with the reduced freight costs of shipping the finished products, as compared to the nonlight weight product when weight is a factor. The reduced cost is especially noticeable when products such as bricks are considered. Fly ash bricks weigh, on average, one-third less than conventional clay-fired bricks (Reidelbach, 1970), enabling a truck to carry more bricks per load, thus reducing shipping costs and improving profit margins. The second economic reason is an abundance of low cost fly ash available to make the bricks, yielding and excellent product. In the brick industry fly ash can be mix with clay to make clay-fly ash bricks. Depending on the type of soil, fly ash (20–50 %) is used along with clay to produce clay bricks which are more porous (40-50 %) than fly ash bricks (20 %). Nevertheless clay-fly ash bricks have high strength and absorb less water than fly ash bricks (Ahmaruzzaman, 2010). Even though fly ash is commonly used in cements, it has rarely been applied to bricks.

Lingling *et al*. (2005) shown that fly ash might improve the compressive strength of bricks and make them more resistant to frost. The porosity of the brick depends directly on the mineralogical composition of the raw material and the firing temperature, but generally, bricks fired at high temperatures are more vitreous and undergo the greatest changes in size and porosity (Cultrone *et al*., 2004). It has found that fly ash bricks are as durable as clay bricks and in fact in certain aggressive environments perform better than clay bricks. Fly ash can be used in the range of 40-70 %. The other ingredients are lime, gypsum (/cement), sand, and stone dust/chips. Minimum compressive strength (28 days) of 70 kg/cm^2 can easily be achieved and this can go up to 250 kg/cm^2 (in autoclaved type) (Ahmaruzzaman, 2010). A few numbers of studies show that fly ash brick is a far superior building material than burnt clay brick. The use of fly ash brick provides a stronger, more durable construction that is better protected from efflorescence and salinity with meaningful savings in construction costs. But the greater benefit lies in controlling two major ecological problems of fly ash disposal and the reduction of cultivable land that is needed for the production of burnt clay brick. The advantage of these bricks over burnt clay bricks are: Lower requirement of mortar in construction, Plastering over brick can be avoided, Controlled dimensions, edges, smooth and fine finish and can be in

different colours using pigments, cost effective, energy efficient and environment friendly (as avoids the use of fertile clay).

Fly ash in wet state with low quality was also used as raw material to replace clay to make fired bricks (Xu *et al*., 2005). The effect of fly ash with high replacing ratio of clay on firing parameters and properties of bricks were investigated. The results indicate that the plasticity index of mixture of fly ash and clay decreased dramatically with increased replacing ratio of fly ash. In addition to brick products, fly ash has been utilized in the manufacture of lightweight roofing products such as rigid roofing tiles. The roofing tiles have the advantage of being both lighter than clay products and providing a class A fire-rating making them an excellent replacement for cedar shake roofing in high fire danger areas. The manufacture of sintered fly ash light weight aggregates is an appropriate step to utilize a large quantity of fly ash (Ahmaruzzaman, 2010).

2.5.4 Use of fly ash to neutralize AMD

Acid mine drainage (AMD) in addition to being highly acidic (Bigham *et al*., 1990) often contains high concentrations of heavy metals such as Fe, Mn, Al and anions like SO_4^{2-} in addition to elements like Zn, Co, Pb, Cr, Cu, in trace concentrations. Acid mine drainage occurs in areas that have previously been mined for coal and contain pyritic materials in spoil piles or in mine shafts, where the pyritic material is in contact with both water and atmospheric influences. The spoil piles and mine shafts contain iron pyrite in the tailings that chemically react with oxygen, water and Thiobacillus bacteria, resulting in acid mine drainage according to the following set of reactions (Kimmel, 1983).

$FeS_2(s) + 7/2O_2 + H_2O = 2SO_4^{-2} + 2H^+ + Fe^{+2}$ (1)

$Fe^{+2} + 1/4O_2 + H + = Fe^{+3} + 1/2H_2O$ (2)

$Fe^{+3} + 3H_2O = Fe(OH)_3(s) + 3H^+$ (3)

$FeS_2(s) + 14Fe^{+3} + 8H_2O = 15Fe^{+2} + 2SO_4^{-2} + 16H^+$ (4)

Iron pyrite (FeS_2) combines with oxygen and water to produce sulphuric acid, hydrogen and Fe^{+2} in Equation 1. In Equation 2, Fe^{+2} reacts with oxygen, hydrogen and the Thiobacillus bacteria to

oxidize and produce Fe^{+3} and H_2O. In Equations 3 and 4 the resultant Fe^{+3} is then reduced by the iron pyrite and more Fe^{+2}) is released along with additional acid and AMD occurs.

In South Africa, most power stations producing fly ash are located near the coal mining sites, which make the AMD/fly ash treatment process viable. The current legislation in South Africa requires the mines to carry out neutralization and clarification of all AMDs before allowing them to rejoin natural water bodies. Underground coal mining operations conducted many years ago removed large volumes of coal, leaving only small pillars to maintain the structural stability of the surrounding land surface. Natural chemical weathering overtime caused the pillars to crumble and AMD to occur due to the exposure of the pyritic material, surrounding the coal seams, to the groundwater and atmosphere. Where groundwater was not present the risk of mine fires existed. Fly ash mine void filling has been carried out in both controlled circumstances and in actual field applications. Mine void filling is undertaken for numerous reasons, the first being for the control of Acid mine drainage, where the groundwater table intersects the mining rubble as previously described. The second reason for fly ash grout injection compliments acid mine drainage (AMD) control, by filling mine voids and providing support to areas where standing coal pillars are crumbling and causing land subsidence on the surface. The third use for fly ash injection is mine fire control.

A number of authors have investigated the capacity of fly ash to improve the quality of leachates generated by coal refuse (Stewart *et al*., 1997), by oxidation of a sulphide-rich mining waste (Pérez-López *et al*., 2007a; Pérez-López *et al*., 2007b) and in passive treatment of acid mine drainage (Gitari *et al*., 2007). These authors observed that generation of acidic leachates was prevented and inorganic contaminants significantly reduced. Erol *et al*. (2005) studied the ability of fly ash to remove Cu^{2+} and Pb^{2+} in aqueous solutions. These authors found that the contaminant removal capacity of the fly ash samples was directly proportional to the CaO content. Polat *et al*. (2007) investigated fly ash for neutralization of highly acidic heavy metal laden oily waste sludge while Potgieter-Vermaak *et al*. (2006) compared fly ash, limestone and fly ash as pre-treatment agents for acid mine drainage. The authors observed that fly ash can be used as a neutralization/fixation agent. Gitari *et al*. (2006) in their study reacted AMD with two South African fly ashes in a batch setup in an attempt to evaluate their neutralization and major, trace elements removal capacity. The authors recognized three factors that finally dictated the

nature of the final solution in the neutralization reactions were the FA: AMD ratio, the contact time of the reaction and the chemistry of the AMD. Gitari *et al*. (2008) examined the capacity of the fly ash to remove the major inorganic contaminants in Acid mine drainage. The authors observed that the relative quantities of soluble bases (CaO, MgO) in fly ash and hydrolyzable constituents in AMD dictated whether the final solution at a given contact time will have a dominant acidic or basic character. In addition found that Increase of pH in solution with contact time caused the removal of the metal ions mainly by precipitation, co-precipitation and adsorption.

2.5.5 Use of fly ash for Agricultural purposes

The potential utilization of fly ash in agriculture is now entrenched fact and more researchers and `users' are getting convinced with its usage in this field. The major attribute, which makes Fly ash suitable for agriculture, is its texture and its contain a considerable content of K, Ca, Mg, S and P except organic carbon and nitrogen (Page *et al*., 1979; Adriano *et al*., 1980; Aktar, 2007). Singh *et al*. (2010) found that the potential of FA as a resource material in agriculture is due to its specific physical properties like's texture, water holding capacity, bulk density, pH etc., and contains almost all the essential plant nutrients. Approximately on an average 95 to 99 % of Fly Ash consists of oxides of Si, Al, Fe & Ca and about 0.5 to 3.5 % consists of Na, P, K and S and the remainder of the ash is composed of trace elements (Aktar, 2007). Thus, it was found that this material could be used as an additive / amendment material in agriculture applications. The amount and method of FA application in soil would vary with the type of soil, the crop, grown, the prevailing agro climatic condition and also with the FA (Singh *et al*., 2010).

During investigations on fly ash disposal, many authors also experienced significant changes in the chemical and mineralogical properties of fly ash when it was subjected to chemical weathering under natural environments. Their main results can be summarized as follows: Fly ash is usually alkaline, so it may be utilized as an amendant for soils in order to correct pH or physical characteristics in the treated soils (Ferraiolo *et al*., 1990). Fly ash is a useful ameliorant that may improve the physical, chemical and biological properties of problem soils and is a source of readily available plant macro and micronutrients (Jalal and Goyal, 2006). Plant growth on fly ash-amended soils is most often limited by nutrient deficiencies, excess soluble salts and phototoxic B levels (Page *et al*., 1979; Adriano *et al*., 1980).

Fly ash usually contains virtually no N and has little plant-available P. However, newer power plants may be adding ammonia as a flue gas conditioner to limit NOX emissions which may lead to some plant-available N. Application of fly ash to soil may cause P deficiency, even when the ash contains adequate amounts of P, because soil P forms insoluble complexes with the Fe and Al in more acidic ashes (Adriano *et al*., 1980) and similarly insoluble Ca-P complexes with Class C ashes. Ferraiolo *et al*. (1990) suggest that P and N should be added to sustain good growths when fly ash is applied to soils. Amendment of K-deficient soil with fly ash increases plant K uptake, but the K in fly ash is apparently not as available as fertilizer K, possibly because the Ca and Mg in the fly ash inhibit K absorption by plants (Martens *et al*., 1970). Acidic-to-neutral fly ash has been found to correct soil Zn deficiencies, although alkaline fly ash amendment can induce Zn deficiency because Zn becomes less available with increasing pH (Schnappinger *et al*., 1975).

Fly ash application has also been shown to correct B deficiencies in alfalfa (Plank and Martens, 1974). In some cases, plant yields after fly ash application have been reduced because of B toxicity (Martens *et al*., 1970; Adriano *et al*., 1978). Soil modification with fly ash to improve B deficiencies should be cautiously monitored in order to avoid B toxicity. Fly ash often contains high concentrations of potentially toxic trace elements. Fly ash that has been allowed to weather and be leached by rainfall for several years generally has much lower soluble salt and soluble B concentrations and is more suitable for use as a soil amendment (Adriano *et al*., 1982). Plants growing on soils amended with fly ash have been shown to be enriched in elements such as As, Ba, B, Mo, Se, Sr, and V (Furr *et al*., 1977; Adriano *et al*., 1980). Though trace amounts of some of these elements are required for plant and animal nutrition, higher levels can be toxic. Even though, as an input material FA has many benefits for agriculture applications like, improvement of nutrient deficiency, effectively control various pests infesting etc., in contrast FA also contains number of toxic heavy metals and also have natural radioactivity materials in it (Singh *et al*., 2010). Elements such as Se and Mo, however, are not particularly toxic to plants and may be concentrated in plant tissue at levels that cause toxicities in grazing animals (Ferraiolo *et al*., 1990). Soils amended with high rates of fly ash may accumulate enough Mo to potentially cause molybdenosis in cattle (Doran and Martens, 1972; Elseewi and Page, 1984). After all, modification of soil with fresh fly ash may increase soil salinity (reported as soluble salts or electrical conductance-EC) and associated levels of soluble Ca, Mg, Na, and B. Amendment of

lagoon ash before or after sludge composting increased electrical conductivity (EC) and volatilization of NH_4-N, but lowered availability of PO_4-P (Lau *et al*., 2001). Mittra *et al*. (2005) reportedly used the alkaline fly ash as a soil ameliorant to correct low availability of P and high content of Al and Fe in acid lateritic soil.

2.5.6 Réclamation and revegetation of damaged areas

Fly ash proves also to be suitable for reclaiming wastelands due to damage incurred from coal mining. Fail and Wochok (1977) estimated that 1 million hectares of land remain virtual wastelands due to damage incurred from strip mining of coal. Even though the above quoted figures should have skyrockected now, due to increase exploration and exploitation of coal deposits in the World. When spoil areas are reclaimed, the quantities of fly ash required depend upon the following factors: (i) its pH (ii) the degree to which it has been weathered; and (iii) the pH of the soil to be reclaimed (Adriano *et al*., 1980). The feasibility of the reclamation is to be evaluated through specific studies on the soil characteristics (such as porosity, permeability and pedology), on the topography of the area, and on the geology and hydrology of the under- and up-ground (Ferraiolo *et al*., 1990). It is also neccessary to control filling phases concerning unloading methods, fly ash chemical characteristics (water content and pH), and chemical characteristics of superficial and under-waters (Puccio, 1983).

Abandoned ash-holding ponds, fly ash disposal sites, ash dumps, and stockpiles can be revegetated to provide a temporary cover until the ash can be utilized or a proper final disposal may be arranged. It is enviable to revegetate these sites for aesthetic purposes, to stabilize the surface ash against wind and water erosion and to reduce the quantity of water leaching through the deposit. Haynes (2009) in his study suggest some limitations to plant establishment and growth in fly ash which include a high pH (and consequent deficiencies of Fe, Mn, Cu, Zn and P), high soluble salts, toxic levels of elements such as B, pozzolanic properties of ash resulting in cemented/compacted layers and lack of microbial activity. Notwithstanding its potential limitations to plant growth in fly ash deposits, the material has significant agronomic potential. It has been used successfully as a soil amendment to improve plant growth on numerous occasions (Jala and Goyal, 2006). Its physical properties (high water holding capacity), presence of macro and micronutrients and liming capacity are some of the attributes that favour its use (Yunusa *et*

al., 2006). Most of the previously abandoned ash disposal sites have been revegetated in some way to give the site a cover and prevent wind erosion.

2.5.7 Application of zeolite synthesis from fly ash

Fly ash is a waste substance from thermal power plants, steel mills, etc. that is found in abundance in the world. In recent years, utilization of fly ash has gained much attention in public and industry, which will help reduce the environmental burden and enhance economic benefit (Wang and Wu, 2006). One possible way of reducing management cost of the disposal of huge quantities of coal fly ash generated from electricity production is the synthesis of zeolite product. Zeolite synthesis is one of the potential applications of fly ash production to obtain high values industrial products with environmental technology utilization (Querol *et al*., 1999). This process is similar to the formation of natural zeolites in volcanic deposits. Both volcanic ash and coal fly ash are fine-grained and contain a large amount of aluminosilicate glass. In natural conditions, this glass fraction may be converted into zeolites by the influence of percolating hot groundwater (Barrer, 1982), while the zeolites may subsequently be converted into analcime and feldspar, i.e.

glass→zeolite→analcime→feldspar

This process may take tens to thousands of years in natural conditions. In laboratory conditions, this conversion can be speeded up to merely days or even hours, both in the case of volcanic ash and that of coal fly ash (Steenbruggen and Hollman, 1998). The compositional similarity of fly ash to some volcanic material, precursor of natural zeolites, was the main reason to experiment the synthesis of zeolites from coal fly ash by Holler and Wirshing (1985). Since this initial study, many published articles have proposed different methods for the synthesis of zeolite from fly ash, and different application of zeolitic products. For example Lin and Hsi (1995) synthesize zeolites from waste fly ash under different conditions and evaluate its potential to adsorb copper and cadmium. Querol *et al*. (1995b) synthesize zeolites by alkaline activation of ferro-aluminous fly ash and achieved 75 % zeolites synthesis efficiency. Querol *et al*. (1997) synthesized zeolitic material from fly ash by conventional and microwave-assisted hydrothermal alkaline activation experiments. He showed that high NH_4^+ retention capacities are attained after a few minutes of equilibrium with NH_4^+-rich solutions. Querol *et al*. (1997) synthesized zeolitic material from fly ash by conventional and microwave-assisted hydrothermal alkaline activation experiments. He showed that high NH_4^+ retention capacities are attained after a few minutes of equilibrium with

NH_4^+-rich solutions. The zeolitic material may be also used for the uptake of ammonium from polluted waters but high concentration of other cations may considerably reduce the ammonium absorption efficiencies due to ion competition (Querol *et al*., 2002). Steenbruggen and Hollman (1998) synthesize zeolites from coal fly ash. The authors acknowledge that zeolitised fly ash has a better environmental quality than coal fly ash and suggests that it can be use as an immobilizer of pollutants. Moreno *et al*. (2001) found that application of zeolites into acid mine waters increases pH and causes metal bearing solid phases to precipitate and enhances the efficiency of the decontamination process. Murayama *et al*. (2002) synthesize zeolite from coal fly ash by alkali hydrothermal reaction and suggests that zeolite has the tendency to capture K^+ selectively in the cation exchange site. Inada *et al*. (2005) converted coal fly ashes into zeolites by hydrothermal alkaline treatment. The authors found that silica addition effectively enhances the formation of zeolite Na–P1, even at a high-NaOH concentration.

Moutsatsou *et al*. (2006) synthesize zeolites from Ca-rich and Ca-Si-rich fly ashes and test their potential of retaining heavy metals from contaminated soil. Fan *et al*. (2008) synthesize high quality zeolites from co-combustion ash and found it suitable for removal of heavy metals from waste water. Ojha *et al*. (2004) synthesize zeolite from fly ash and found out that the cost of synthesized zeolite was estimated to be almost one-fifth of that of commercial 13X zeolite available in the market. The fly ash zeolites had a high affinity for K^+, Ca^{2+}, and NH^{4+}, although attempts to use the treated ash to remove NH^{4+} and heavy metals from wastewater and electroplating wastes were only partially successful. Potential uses of the treated ash were limited due to the high pH that resulted from the dissolution of the zeolite minerals (Amrhein *et al*., 1996). The synthesis of Zeolitic material was done with the use of unweathered fly ash. The possibility of using huge quantities or abundance of disposed weathered fly ash for synthesis and application of Zeolite still require scientific investigation.

2.5.8 Utilization of coal fly ash in geopolymeric material

Geopolymers are also referred to as alkali-activated alumino-silicate binders and comprise three classes of inorganic polymers that, depending on the ratio of silica to alumina (silica/alumina), are based on the following three monomeric units:(−Si−O−Al−O−), Polysialate (PS), SiO_2/Al_2O_3 = 2; (−Si−O−Al−O−Si−O−), polysialatesiloxo (PSS) SiO_2/Al_2O_3 =4; (−Si−O−Al−O−Si−O−Si−O−), polysialatedisiloxo (PSDS), SiO_2/Al_2O_3 =6. The synthesis of

geopolymers can start from a variety of raw materials. Schmu¨cker and MacKenzie (2005) made use of metakaolinite to obtain geopolymers by reaction with alkali metal (Na or K) silicate. The utilisation of fly ash and clays as starting materials in the synthesis of geopolymeric materials has been reported by a number of authors (Swanepoel and Strydom, 2002; van Jaarsveld *et al*., 2002, 2003; Bakharev, 2005; Andini *et al*., 2008). The geopolymerisation reaction pathway can be classified as an inorganic polycondensation reaction and may be compared to the formation of zeolites. Most zeolite syntheses are performed under basic conditions using OH^- as a mineralising agent (Van Bekkum *et al*., 1991). All through the synthesis of geopolymers (geopolymerisation) there is a definite interaction between the pozzolanic material with alkaline media and specifically aqueous solutions of polysilicates (Van Jaarsveld *et al*., 1996).

Geopolymeric materials are attractive because excellent mechanical properties and durability can be achieved (Palomo *et al*., 1992). Thermal stability and resistance to acid attack are excellent (Andini *et al*., 2008). Bakharev (2005) found that geopolymer-based materials are much more resistant to acid attack than Portland cement based ones due to much lower Ca content. Schmu¨cker and MacKenzie (2005) shown that the geopolymer matrix composition is almost left unchanged upon heating to 1200 ºC. In reality, the reaction pathway necessitates either metakaolinite, obtained by calcining kaolinite at temperatures of 600-700 ºC, or raw silico-aluminates and alumino-silicates. Great interest also derives from the reduced energy requirement for the manufacture of new materials based on geopolymers. The applications of geopolymer-based materials range within the fields of new ceramics, cements, and matrices for hazardous waste stabilization, fire-resistant materials, asbestos-free materials and high-tech materials (van Jaarsveld *et al*., 1999).

2.5.9 The effect of fly ash disposal on a soil and groundwater system

A prospective chemical interaction between fly ash and soil is envisaged when ultimate dry disposal of fly is achieved through landfill. In these instances, soil contamination may occur, under particular anemological conditions, due to airborne particles fallout on unprotected ground or on soils which are not compatible with the chemical composition of fly ash (Ferraiolo *et al*., 1990). Soil contamination from fly ash may also be due to dissolution of toxic compound by percolating rain water, followed by underground transportation of the contaminants (Kaakinen *et al*., 1975). These effects are usually reduced or become negligible if fly ash has been previously

weathered (Ferraiolo *et al*., 1990). Several studies have been devoted on the effects of fly ash on soil. Page and others (1979) found that unfavourable changes in the soil's chemical equilibrium, such as increases in: pH up to 12, due to presence of CaO and MgO in alkaline ash; salinity especially in case of acidic ash; and hazardous levels of certain toxic elements. Ferraiolo and others (1990) recognized no appreciable changes in soil pH when mixed with acidic fly ash, even at high rates. Adriano *et al*. (1978) found increase available Ca^{2+}, Mg^{2+}, Na^{+}, and SO_4^{2-} concentration in the fly ash treated acidic and calcareous soils. Ferraiolo *et al*. (1990) suggests that unweathered fly ash should be used when specific changes in soil characteristics are expected, while weathered fly ash is more appropriate when no change is desired.

The effect of fly ash disposal sites on the surrounding environment should be considered. Due to the high solubility of some constituents, fly ash surface deposition can be a major source of water pollution (Rohrman, 1971), which has repercussions on aquatic biota (Gutenmann *et al*., 1976), through heavy metal contamination (Cherry and Guthrie, 1977). We visualize that unweathered fly ash will have a much greater potential for ground-water contamination than weathered material due to the presence of high levels of soluble salts. As noted in the previous section above, a rapid initial release of salts from fresh ash is expectedly followed by a decline in salt concentrations with time. In addition, the presence of secondary minerals in weathered ash which acts as binder to toxic inorganic metal in fly ash which caused decline in salt concentration in fly ash.

Expectedly, it could take a year or more for dry fresh ash to absorb enough water to yield leachate. By contrast, lagooned ash will yield leachate almost immediately since it is already saturated with water (Haynes, 2009). Fly ash deposited in landfills would eventually come in contact with water and generates a leachate which poses a contamination threat to ground-water system beneath the ash disposal site. Most visible effort on fly ash disposal site is to reduce the surface contamination problems such as blowing or burning debris or visible pollution of surface waters. The possibility of ground-water contamination by fly ash deposited in landfills is consequential because of the toxic metals composition of the waste. However, these inorganic metals in fly ash are highly variable depending on the composition of the feed stock coal.

Cherkauer (1980) established a significant modification of ground-water quality by sulphates, calcium and magnesium from disposed fly ash leachates. He further observed that toxic metals

contained in the ash have proven quite immobile in the ground water. Choi *et al*. (2002) confirms in their studies the influence of the ash leachate from the ash disposal mound on the ground water composition. Therefore a possible modification of ground-water quality underneath the fly ash disposal site should be carefully considered in the future work.

2.6 Selective sequential extraction techniques

At first, most analytical measurements dealt with the total content of a specific element in an analysed sample (such as lead, mercury, or cadmium, as examples of toxic elements, or cobalt, selenium, or magnesium, as examples of elements necessary for living organisms). Until recently, analytical methods allowed analysts to determine total contents only, but it was soon realised that this analytical information is not enough. As a result, to get adequate information on the activity of specific elements in the environment, more particularly for those in contact with living organisms, it is necessary to determine not only the total content of the element but also to gain a clue of its individual chemical and physical form. Speciation analysis is the process leading to the identification and determination of the different chemical and physical forms of an element existing in a sample (Kot and Namiesnik, 2000).

In the case of soils the speciation of heavy metals is generally related to their physico-chemical forms existed: simple and complex ions in interstitial solution; exchangeable ions; associated with soil organic fractions; occluded or co precipitated with metal oxides, carbonates or phosphates and other secondary minerals; ions in the crystal lattices of primary minerals (Zhu and Alva, 1993). Based on the thought of elements being associated with the different geochemical phases of soils there are numerous experimentally defined single and multiple sequential extraction procedures for the elemental speciation analysis (Novozamsky *et al*., 1993; Ure *et al*., 1993; Leleyter and Probst, 1999). Among them the most widely applied methods were those recommended by Tessier *et al*. (1979) and by the Community Bureau of Reference (BCR) (Ure *et al*., 1993). BCR is now called the Standard Measurement and Testing Program of the European Community (STM).

2.6.1 Concept of sequential extraction scheme and its applications

Metals in sediment may be present in several different geochemical phases that act as a reservoir or sinks of trace elements in the environment (Kramer and Allen, 1988). These phases include

the following broad categories: exchangeable forms; specifically adsorb forms; carbonate; secondary Fe and Mn oxides, organic matter, sulfides, and silicates. All these may occur in variety of structural forms (Tessier *et al*., 1979). The inorganic metals in combustion by-products of coal are locked into different physicochemical forms. It has been reported that the availability and mobility of elements present in fly ashes will depend on the physicochemical forms of the elements (Pe'rez-Bendito and Rubio, 1999). The concept of the sequential extraction (SE) procedure is the partitioning of a solid material into a specific phase or fraction in which it can selectively be extracted, i.e. liberated and released into solution (leached) along with the associated trace metals, by using the appropriate reagents arranged in increasing strength (Tessier *et al*., 1979; Horowitz, 1991, and Tessier *et al*., 1992). These methods are based on the rational use of a series of more or less selective reagents chosen to solubilise successively the different mineralogical fractions thought to be responsible for retaining the larger part of the trace elements (Gleyzes *et al*., 2002). Sequential extraction can provide a good insight into the sequence of metal leaching behaviour through determination of metal fractionation to different mineral phases in the solid matrix in coal fly ash (Fernández-Turiel *et al*., 1994; Querol *et al*., 1996; Goodarzi and Huggins, 2001; Sočo and Kalembkiewicz, 2007).

Several sequential chemical extraction schemes have been reported in the literature (Tessier *et al*., 1979; Smeda and Zyrnicki, 2002; So˘co and Kalembkiewicz, 2007). The procedures are usually based on the principle of successive extractions of conceptually distinct lithological or authigenic fractions representing a range of elemental forms, from the most mobile to those strongly bound to the support mineral (Fraser and Ken, 1983). The extractant converts the metal bound in the solid phase into a soluble form. The fraction of the individual element in each phase depends on the chemical reagents used as the extractant and the chemical and physical operating parameters involved, such as pH, reagent type, concentration, time of contact, particle size, stirring system temperature, and so on (Smichowski *et al*., 2005). The sequential chemical extraction procedure provides useful information in environmental studies. Over the last decade an increasing number of publications that have appeared on sequential extraction have some limitations and drawbacks (Kheboian and Bauer, 1987; Shan and Chen, 1993; Go´mez Ariza *et al*., 2000; Gleyzes *et al*., 2002). The selectivity of the chemical reagents toward specific physicochemical forms was not taken into consideration for most of the procedures reported (Gleyzes *et al*., 2002). The number of fractionation steps required depends on the purpose of the

study. In all of the sequential extraction procedures reported in literature, different chemical reagents are applied in order of increasing reactivity (Tessier *et al*., 1979; Smeda and Zyrnicki, 2002; Jegadeesan *et al*., 2008; Smichowski *et al*., 2008). The sequential chemical extraction procedure reported by Tessier *et al* in 1979 and the BCR procedure elaborated in 1993 by the Standards, Measurements and Testing Programme (SM&T) are the most representative schemes. The Tessier's scheme comprises four steps designed and widely applied to soil fractionation studies. This sequential extraction (SE) procedure is advantageous in that it enables us to evaluate the potential environmental availability of trace metals associated with sediment specific phases under various environmental conditions (Skvarla, 1998). The actual difficulty of the sequential extraction procedure is that the extraction from each step depends on the efficiency of previous step(s), and on factors such as leaching time; liquid-solid ratio and strength of the chemical reagent (Chang *et al*., 2009). Recent studies on the sequential extraction scheme are modifications stemming from a procedure developed by Tessier *et al*. (1979). The schemes were originally developed for the examination of aquatic sediments (Campos *et al*., 1998; Mester *et al*., 1998; Petit and Rucandio, 1999) but gained wide acceptance as tools for speciation of metals in contaminated soils (Campos *et al*., 1998; Wang *et al*., 2004). Recently the sequential extraction scheme has been applied to incinerated sludge ash (Kim *et al*., 2003; Feng et al., 2007), bottom ash and fly ash from municipal solid waste incinerators (MSWI) to determine the distribution of elements (Bruder-Hubscher *et al*., 2002; Smeda and Zyrnicki, 2002; Zielinski *et al*., 2007; Smichowski *et al*., 2008).

The actual difficulty of the sequential extraction procedure is that the extraction from each step depends on the efficiency of previous step(s), and some factors such as leaching time, liquid-solid ratio, and strength of the chemical reagent (i.e. pH of the medium) can influence the extracted amount of metals (Chang *et al*., 2009). In spite of these criticisms, the sequential extraction schemes remain widely used and are considered an essential tool in establishing element fractionation in soils and sediments (Gleyzes *et al*., 2002). The selective sequential extraction (SSE) scheme is advantageous in that it enables us to evaluate the potential environmental availability of trace metals associated with sediments in specific phases under various environmental conditions (Skvarla, 1998). Actually, sequential extraction provides more information than single extraction and has several advantages (Hirner, 1992). (i) Extractive procedures applied are analogous to those occurring in nature. In natural environments, soil and

sediments are subject to similar leaching procedures by natural and anthropogenic electrolyte solutions. (ii) the total sum of all fractions should be more-or-less 100 %, so the results are self checking. (iii) it is an vital tool in establishing element partitioning with natural samples. (iv) chemical extraction sequences can be use for the estimation of the potential remobilization of metals under changing environmental conditions. One of the most widely used procedures in the literature was proposed by Tessier *et al*. (1979). It partitions elements into five operationally-defined geochemical fractions including: exchangeable; carbonates (acido-soluble); Fe and Mn oxides (reducible); organic matter (oxidisable); and, residual. In this present study, water soluble fraction was added. The different reagents used for these purposes in the literature are described below according to this classification.

2.6.2 Exchangeable fraction

Metals extracted in this fraction would include weakly-sorbed metal species, particularly those retained on the soil surface by relatively weak electrostatic interactions. The metals in this fraction can be free easily by ion-exchange processes and leach very easily when the environmental conditions are disturbed by pH change or Eh change. Heavy metals in the exchangeable fraction play a very significant role in the evaluation of the environment and always act as a pollution indicator for its environmental mobility and bioavailability (Yuan, 2009). Reagents used for this purpose are electrolytes in aqueous solution, such as salts of weak acids and bases at pH 7 (Das *et al*., 1995). Reagents available for the chemical extraction of exchangeable fraction in soil and sediments includes; magnesium chloride, ammonium acetate, barium chloride, nitric acid, ammonium nitrate, ammonium chloride, etc. Extraction with acetate salts (particularly ammonium acetate) has also been used frequently in soil and sediment studies. Divalent cations should, in general, be more effective than monovalent cations in removing exchangeable ions, but NH^{4+} promotes replacement of ions in the interlayer exchange sites of vermiculite. Metal complexes formed with acetate ions are slightly more stable than chloro-complexes; this favours the exchange and reduces re-adsorption or precipitation of the extracted metals (Pickering, 1986). Because of the buffering capacity of the solution, variations in pH are reduced; however, the carbonate fraction can be attacked (Pickering, 1986). To avoid this problem, some authors reduce reagent concentration to 0.01 mol/l (Gleyzes *et al*., 2002).

2.6.3 Carbonate (acido-soluble) fraction

The fraction is susceptible to pH changes, and metal release can be achieved through dissolution of a fraction of the solid material at low pH close to 5. The two commonly used reagents for the extraction of carbonate fraction are ammonium acetate buffer with acetic acid and sodium acetate. Ammonium acetate buffer with glacial acetic acid is generally used for the extraction of this fraction. This reagent is well adapted to dissolve calcium carbonates (Tessier *et al*., 1979) but dissolution of dolomite is not total (Pickering, 1986). Moreover, lowering the pH from 7 (pH of the extracting solution used in the first step) to 5 would release the remaining specifically-adsorbed trace-metals ions that escaped extraction in the previous step (Tessier *et al*., 1979). The metal fraction recovered in these conditions may be thought to have been present as co-precipitated with carbonate minerals but also as specifically sorbed to some sites of the surface of clays, organic matter and Fe/Mn oxyhydroxides (Pickering, 1986). Barona and Romero (1996) reported that carbonate fraction showed greatest number of statistically significant correlation with metal contents in soil fractions. The authors considered it as a relevant parameter in the distribution of some metals such as Pb, Ni, Zn, and Cu in soils. Most often large proportion of total manganese can be extracted from the carbonate fraction during sequential extraction scheme. Tessier *et al*. (1979) concluded from a study on sediments that the Fe and the Mn found in this second fraction were in a reduced state and therefore were not derived from a partial attack of Fe/Mn oxides. As a matter of fact, the efficiency of the dissolution of carbonates depends on several parameters related to the sample: the grain size; the initial content and nature of carbonates; and, the sample weight and solid to liquid ratio. Pickering (1986) advises frequent adjustment of the pH during extraction and an increase in the attack time. Unbuffered acetic acid solution has also been used to dissolve the carbonate fraction. However, it is less specific and can attack silicates (Pickering, 1986).

2.6.4 Iron and manganese hydroxide fraction

Iron and manganese oxides does exist as nodules, concretions, cement between particles or simply as a coating on particles during the production process of fly ash in the boiler; a lot of toxic elements may be pooled into this fraction when the particles cool down in flue gas. Iron and manganese oxides are excellent scavengers of metals and are thermodynamically unstable under anoxic conditions (Chao, 1972; Yuan, 2009). By controlling the Eh and the pH of

reagents, dissolution of some or all metal-oxide phases can be achieved (Pickering, 1986). The most successful reagents for evaluating the total amount of metal ion associated with these minerals contain both a reducing reagent and a ligand able to retain released ions in a soluble form, the efficiency of the reagent being determined by its reduction potential and its ability to attack the different crystalline forms of Fe and Mn oxyhydroxides (Pickering, 1986). This dissolution can take place in one, two or three steps, separating amorphous or crystalline Mn and Fe oxides. The most commonly used reagents includes; hydroxylamine hydrochloride, oxalic acid and dithionite. Hydroxylamine hydrochloride is a reducing agent ($E^o = 1.87V$) and its ability to dissolve the different metallic oxides depends on pH, concentration, extracting time and temperature (Gleyzes *et al*., 2002).

Chao (1972) reported that (i) agitation time and concentration do not greatly influence the dissolution of Mn oxides, which is rather fast; (ii) dissolution of Fe oxides depends on these same factors, and is favoured by an increase of reagent concentration and agitation time; and, (iii) lowering the pH (with nitric acid, for example) favours the attack of iron oxides. He also reported that the use of a 0.1 mol/l hydroxylamine solution prepared in 0.01 mol/l nitric acid (pH 2) can selectively dissolve Mn oxides in 30 minutes while minimizing iron extraction (< 5 %). Sahuquillo *et al*. (1999) in their study of lake sediments proved that the pH of hydroxylamine hydrochloride is the most important factor that affects the precision of BCR three stage sequential extraction scheme. Chao and Zhou (1983) assert to have dissolved all amorphous iron oxides while minimizing the attack of the crystalline phase (< 1 %) using a 0.25 mol/l hydroxylamine solution in 0.25 mol/ l HCl. However with the same reagent, Hall *et al*. (1996), in a study of soils, tills and surficial sediments showed the extraction of the amorphous Fe oxyhydroxide phase which leads to significant dissolution of sphalerite and galena. Tessier *et al*. (1979) established on sediments that the total dissolution of the iron reducible fraction was achieved within 6 h. On the other hand, this procedure was considered inadequate for iron extraction (La force *et al*., 2000), particularly in the case of materials with a high Fe content (Gleyzes *et al*., 2001), for which the addition of a supplementary iron-specific step is advised (Gleyzes *et al*., 2001).

2.6.5 Residual fraction

Primary and secondary minerals containing metals in the crystalline lattice constitute the bulk of residual fraction. Metals in the residual fraction on the other hand are safer for the environment due to their lowest mobility and bioavailability. To remove elements in residual fraction is more difficult, because the structure of the crystalline lattice must be destroyed sufficiently by very strong acid or alkali (Yuan, 2009). Its destruction is achieved by digestion with strong acids, such as hydrofluoric acid, perchloric acid, hydrochloric acid and nitric acid. Studies on the sequential extraction scheme are modifications stemming from a procedure developed by (Tessier *et al*., 1979). The schemes were originally developed for the examination of aquatic sediments (Kheboian and Bauer, 1987; Mester *et al*., 1998; Campos *et al*., 1998; Petit and Rucandio, 1999), stream sediments (Borovec, 1996; Gismera *et al*., 2004), contaminated sediments (Carapeto and Purchase, 2000; Sahuquillo *et al*., 2003) but gained wide acceptance as tools for speciation of metals in soils (Barona and Romero, 1996; Kesley *et al*., 1997; Campos *et al*., 1998; Cabral *et al*., 1998; Ma and Uren, 1998; Barona *et al*., 1999; Stalikas *et al*., 1999; Shiowatana *et al*., 2001; Wang *et al*., 2002) and contaminated soils (Li *et al*., 1995; Maiz *et al*., 1997; Biester and Scholz, 1997; Davidson *et al*., 1998; Davidson et al., 1999b; Maiz *et al*., 2000; Barona *et al*., 2001; Sutherland, 2002; Scheckel *et al*., 2003; Wang *et al*., 2004; Brunori *et al*., 2005; Abollino, *et al*., 2006). Li *et al*. (1995) found that the multielement measurements can give useful information to assist in the interpretation of the possible geochemical forms and sources of the trace elements in soils. Sutherland (2002) established that the dilute HCl leach was slightly more aggressive than the sequential procedure as it removed significantly more Al, Cu, Fe, Mn and Ni; though no significant differences were observed between Co, Pb and Zn concentrations liberated by the two approaches

Recently the sequential extraction scheme has been applied to incinerated sludge ash (Bruder-Hubscher, 2002), bottom ash and fly ash from Sequential extraction procedures have been applied to sediments (Mester *et al*., 1998; Petit and Rucandio, 1999), contaminated soils (Campos *et al*., 1998), and incinerated sludge ash (Fraser and Lum, 1983). Recently, this step by step sequential extraction procedure was applied to bottom ash and fly ash from municipal solid waste incinerators (MSWI) to determine the distribution of various elements (Bruder-Hubscher *et al*., 2002; Smeda and Zyrnicki, 2002; Huang *et al*., 2007; Smichowski *et al*., 2008; Chou *et al*., 2009). Huang *et al*. (2007) found that the elements such as Ca, K, Na, Pb, Zn, Cd, Cu and Sr

have exhibited a remarkable mobility in fly ash. At the same time, the toxic elements such as Pb, Cd, Zn and Cu have a great potential to be released into the environment under normal conditions.

2.6.6 Harmonization of sequential extraction protocol: BCR scheme

Considering the diversity of the sequential extraction procedure and lack of uniformity in the scheme used by various authors which does not allow the results so far to be compared worldwide or the procedures to be validated (Gleyzes *et al*., 2002). Certainly, the results obtained by sequential extraction are operationally defined, i.e. the 'forms' of metals are defined by the determination of extractable elements using a known procedure. Consequently the significance of the analytical results is related to the extraction scheme used. This type of determination has frequently been referred to as 'speciation' even though this term strictly speaking cannot be applied to operationally defined procedures (the tern speciation rather covers the determination of specific forms, e.g. oxidation state or organometallic compounds (Quevauviller *et al*., 1992). One more problem which fraught a good comparability of data was the lack of appropriate reference materials which did not enable the quality of measurements to be controlled (Quevauviller *et al*., 1997). Due to the possibility of the many sources of pitfalls which may occur, it was expected that the use of extraction schemes would be progressively abandoned. As a result, the Community Bureau of Reference (BCR, now Standards, Measurements and Testing Programme) has launched a programme aimed at harmonizing single and sequential extraction schemes for the determination of extractable trace metals in soil and sediment, respectively (Quevauviller *et al*., 1994). This programme started in 1987 with the comparison of existing procedures tested in two interlaboratory exercises (Ure *et al*., 1993) to develop a three-step procedure using: acetic acid (step 1); hydroxylamine (step 2); and, hydrogen peroxide (step 3). A detailed description of the conditions of use at each step as well as the preparation of extracting solutions is given to avoid any difference that could impair the reproducibility of the procedure. This scheme was then applied to the certification of a sediment reference material (CRM 601), and that allowed it to be validated (Quevauviller *et al*., 1997).

In order to identify the main sources of uncertainties in extraction procedures, the influence of several factors, such as extraction pH, temperature, extraction time, reagent type and concentration was studied (Lopez-Sanchez *et al*., 1998; Sahuquillo *et al*., 1999). The study

focused mainly on the development of step 2 using $NH_2OH.HCl$ in nitric acid. It was demonstrated that pH adjustment could be a major source of irreproducibility, as the amount of nitric acid added fluctuated between laboratories. This fact was corroborated in the study of contaminated soil (Davidson *et al*., 1999). Consequently, it was proposed to add a fixed volume of diluted nitric acid for the pH adjustment. The improved version of three stage sequential procedures proposed by Rauret *et al*. (1999) also integrates an aqua regia digestion of both the sample and the residue after extraction according to the ISO 11466 procedure, for internal control. Taking into consideration the interest shown in the three stage procedure that was originally developed for sediment by soil scientist, a trial was organised by Rauret *et al*. (2000) to test its suitability on soil Certified Reference Materials (CRM 483). Their results showed good interlaboratory comparability and it was concluded that the new version of the BCR extraction protocol would be suitable for the analysis of contaminated soil samples. The three stage procedure was thereafter frequently used for case studies. The effectiveness of the BCR procedure has proved to be a useful tool for predicting short-and long-term mobility of trace elements, even in complex environmental scenarios (Pueyo *et al*., 2008). Usero *et al*. (1998) applied the three extraction techniques (Tessier *et al*. 1979; Kersten and Forstner 1986; and the Bureau Communautaire de Reference (BCR)) procedure elaborated in 1993 by the Standards, Measurements and Testing Programme (SM &T) on four marine sediments with different trace metal contents.

The Tessier procedure gives the lowest concentration values in the acid soluble and oxidable fractions for most of the metals studied. On the other hand, this method usually gave the highest values for the residual fraction. Finally, in the reducible fraction, the Kersten and Forstner procedure showed the highest values for Cu, Cr, and Fe, and the Tessier procedure gave the highest values for Zn, Mn, and Pb. Mester and others (1998) carried out the comparison of BCR sequential extraction procedure and Kersten and Forster procedure found no differences for Zn and Cd whereas significant differences have been found for Pb, above all, and for Cr, Ni and Cu relatively to the oxidisable fraction. Sutherland *et al*. (2000) applied it for the first time to road deposited sediments (RDS). The result were compared with the road-deposited sediments (RDS) data available in the literature and obtained with the original sequential extraction procedure by Tessier *et al*. (1979). Results were comparable for most metals, except for Cu. In the case of Cu, with the BCR scheme, equal amounts of this metal were extracted in the reducible and oxidisable

fractions, whereas, in the RDS literature, Cu was extracted in the oxidisable fraction in most cases (60 %). More investigation is necessary to clarify the discrepancy. Boonjob *et al*. (2009) investigated two dynamic fractionation systems as opposed to conventional steady-state BCR. The authors concluded that they are not operationally defined within the selected range of experimental conditions and sequential injection (SI) assemblies offer a significant saving of operational time with respect to classical BCR test.

Nevertheless, the application of the three-step BCR scheme to road-deposited sediment proved the validity of results available in the RDS literature that had been previously obtained using the Tessier scheme or similar procedures (Sutherland *et al*., 2000). Albores *et al*. (2000) compared the efficiency of two schemes (BCR and Tessier) to elucidate metal fractionation in sewage-sludge samples collected from a wastewater-treatment plant. The oxidisable step of the BCR scheme was more effective than that employed in Tessier's method. Davidson *et al*.(1999) applied the BCR scheme to industrially-polluted soils, but the quality of the results showed that improvements would be needed to achieve better interlaboratory comparison (Rauret *et al*., 2000). Sutherland and Tack (2003) applied optimized BCR procedure to two contaminated certified reference soils from Montana, US (SRM 2710 and SRM 2711). Fraction-specific concentrations, percentages and recoveries for Cu, Pb and Zn were used to explore differences between the optimized BCR procedure and three other sequential extraction schemes with published data for SRM 2710 and 2711 (i.e. Tessier scheme, Geological Survey of Canada scheme and the original BCR scheme). Differences between schemes are worrisome because trends varied between metals, between fractions and between reference soils. These data reinforce the need for increased adoption of standardized sequential extraction procedures and further examination of different solid media.

In recent, BCR sequential extraction scheme has been applied to variety of sample types. Mossop and Davidson (2003) compared the original BCR to the revised BCR sequential extraction procedure. Their work indicates that the revised BCR sequential extraction provides better attack on the iron-based components of the reducible matrix for a wide range of soils and sediments. Marqui *et al*. (2004) applied BCR sequential extraction procedure for the fractionation of Ni, Zn, Pb and Cd in mining wastes from old Pb-Zn mining areas He found that more easily mobilized forms (acid exchangeable) were predominant for Cd and Zn, and in the

contrast, the largest amount of lead was associated with the iron and manganese oxide fractions. Attempt was also made to compare the modified BCR sequential extraction procedure with other extraction/ leaching method. Fuentes *et al*. (2004) also compared the BCR sequential extraction procedure with DTPA (diethylenetriaminepentaacetic acid), and distilled water, respectively. The DTPA extraction procedure was found to be cheap and easy to perform and the obtained results are similar to those obtained with the sequential procedure. Ultimately, Kazi *et al*. (2005) compare BCR protocol with the Lixiviation test (DIN 38414-S4) and reported that the levels of leachable toxic metals were low compare to the amount extracted in the exchangeable fraction of the BCR sequential extraction procedure.

2.6.7 Drawbacks of sequential extraction procedure

Since their invention in the last three decades, the main drawback of sequential extraction scheme are; lack of selectivity of reagents, readsorption and redistribution of metals solubilised during the extraction, sample pre-treatment and general methodology (Shan and Chen, 1993; Gleyzes *et al*., 2002). Even though these disadvantages of elemental speciation analysis are recognised, the sequential extraction methods are unfortunately still used before the more effective methods available, especially in the case of study on the relationship between the elemental speciation and their bioavailability (Chlopecka and Adriano, 1996; Davidson *et al*., 1999).

2.6.7.1. Lack of selectivity of reagents

Preferably, reagents are formulated to dissolve selectively one physico-chemical form of the initial material, as a result stir up the solubilization of associated inorganic metals. Conversely, the lack of specificity of extractants has been established in many theoretical and experimental works, with both synthetic and natural solid materials. Kim and Fergusson (1991) underscore the complexity of interpreting the results properly, as the use of terms such as “bound to carbonates, to manganese oxides or organic metals led to metal speciation being wrongly evaluated. They demonstrated that, by using synthetic soils or Cd spiked phases the amounts of Cd extracted during the exchangeable and the acido-soluble steps were adsorbed, more or less strongly, on Fe/Mn oxides and organic matter. They concluded that certain confusion was likely to arise from the classification system used in sequential extraction methods.

Go´mez Ariza *et al*. (2000) criticized the modified Tessier *et al*. (1979) sequential extraction procedure proposed by the authors. They established that reagent selectivity was appropriate for the evaluation of metal-co precipitated phases (calcite, humic acid, kaolinite and illite) but not for the metal-sorbed phases (hausmannite and amorphous iron oxide). Tessier *et al*. (1982) specified that metals extracted with the NaOAc/HOAc-buffered solution would be specifically adsorbed on surfaces, more particularly on Fe oxides. Moreover, carbonated species of the various metals have different solubilities (for example, $KsPbCO_3=10^{-13.1}$; $KsMnCO3=10^{-9.3}$; and, $KsZnCO_3=10^{-10}$), so their dissolution during this step is sometimes incomplete. This continues during the next step using hydroxylamine, leading to an overestimation of the metals extracted in the iron and manganese fraction (reducing), especially lead (Kheboian and Bauer, 1987). Laban and Atkin (1999) emphasized the possible dissolution of unwanted phases which means results are subjected to misinterpretation. However careful and prudent consideration data and assessment of limitations can be useful for investigating occurrence and distribution of trace elements in coal and other materials.

2.6.7.2. Readsorption and redistribution

The incomplete dissolution of some phases and changes in pH could lead to the readsorption and the redistribution of some metals (Gleyzes *et al*., 2002). The extent of readsorption was found to be dependent on elements, properties of soil especially organic matter content, extracting flow rate and metal concentration level (Chomchoei *et al*., 2002). Kheboian and Bauer (1987) evaluated these problems by applying Tessier's procedure to mixed synthetic models, each being spiked with a specific trace element. The results showed a significant redistribution of Cu, Pb and Zn. Lead that was initially adsorbed on calcite was readsorbed at each step finally to appear in solution in the residual fraction. Earlier workers (Arunachalam *et al*., 1996; Raksasataya *et al*., 1996) reported the Pb redistribution on Fe and Mn oxides fraction of soil or humic substances (Raksasataya *et al*., 1996). In contrast, Belzile *et al*. (1989) reported that this redistribution was significant only for very elevated initial Pb contents. The lack of selectivity of the reagents can also be responsible for metal redistribution (Gleyzes *et al*., 2002). Martin *et al*. (1987) recognized that iron sulphide dissolution during the acid step led to the precipitation of dissolved metals with sulphide ions.

Tessier *et al*. (1979) procedure was found to have readsorption and redistribution problem. Tessier is quite useful and convenient for a qualitative analysis of metals in soils, but it is not accurate for a quantitative investigation because of the metals' mobility and redistribution in soils (Lo and Yang, 1998). Sahuquillo *et al*. (2003) examined the potential remobilization by application of modified BCR-sequential extraction procedure. The authors found that arsenic remained in the residues to a significant extent (30-55 %) and that 60-92 % of extractable amounts was released with a reduction mechanism. Gomez-Ariza *et al*. (1999) examined the readsorption and redistribution process when applied sequential extraction scheme on the oxic sediments. Its being concluded that both readsorption and redistribution occur and their extent depends on the characteristics of the sediment. Lucey *et al*. (2007) demonstrated the capacity of citrate to inhibit the resorption of plutonium from the various extractants, and confirm that there is no discernible increase in non-targeted phase dissolution, but indicate significant ligand competition with the carbonate phase. Similarly, Howard and Vander brink (1999) found addition of nitrilotriacetic acid (NTA) to each extracting solution in the sequence appears to be effective for counteracting resorption in feldspathic, calcareous, ferruginous and carbonaceous sediments. These authors concluded that sequential extraction scheme did not appear to be useful in evaluating the distribution of the metal between physico-chemical forms or in estimating the reactivity of a chemical reagent with respect to the different fractions able to adsorb trace metals.

2.6.7.3. Sample pre-treatment

In order to obtain accurate information on the chemical species in a sample, due consideration should be given to the sample collection, pre-treatment and storage steps (Das *et al*., 1995). The possible occurrence of chemical alterations during the drying step (air-drying or oven-drying) of sample preparation is an additional source of errors (Gleyzes *et al*., 2002). When materials are sampled and stored, redox potential, temperature, pH, and pressure will be changed and this relationship can be broken (Batley and Gardner, 1977). Possibly, the physicochemical composition of sample will be modified and material can therefore be restructured, which modified the speciation of metals greatly. Tack and Verloo (1996) studied the effect of high temperatures (120 ºC, 250 ºC and 450 ºC) on dredged sediment. The acid-extractable fraction of most metals was considerably affected by heating the sediment at 250 ºC and 450 ºC. Nevertheless, the amount of acid-extractable Ca remained unchanged, suggesting that the solubilization of carbonates was not affected. This problem was attributed to the destruction of

organic matter at high temperatures leading to a more efficient extraction of metals. Elevated temperature can also speed up the conversion of amorphous iron hydroxides to more crystalline forms, and associated metals are then determined in the residual fraction only (Gleyzes *et al*., 2002). Stephens *et al*. (2001) examined the leachability of metals from dredged canal sediments, the authors reported that most metals (except Cd and As) showed a redistribution from the residual phase into more mobile phases as the sediment dried and oxidized.

Davidson *et al*. (1999a) established that changes in speciation occurred when the sediment was air dried, oven-dried or frozen. The authors reported that cadmium speciation was particularly perturbed by freezing (oxidisable Cd), whilst lead was more affected by oven-drying. A few numbers of authors agree that the ideal is to work with fresh material, but this is not always possible (Batley and Gardner, 1977; Bordas and Bourg, 1998; Long *et al*., 2009). Davidson et al. (1999b) also established that reproducibility was higher for air-dried than for field-moist soils, but larger amount of metals were extracted, suggesting alterations in speciation occurred during drying. Pacifico *et al*. (2007) reported that sample pre-treatment can involve several different alterations on the sequential extraction procedure outputs, which are strictly related to sample 'type' and confirm that these techniques are strongly 'sample-dependent'. Furthermore, even though it is possible to apply SEP on wet samples, there are many aspects that could compromise the quality and the comparability of the information obtained (Förstner, 1993).

Preservation of samples is sometimes necessary, using either wet storage (cooling) or dry storage (air drying or oven drying). Wet storage at 4 ºC was established could preserve the integrity of materials if they are not stored for more than 2 weeks (Rapin *et al*., 1986). Air drying (at temperature below 40 ºC) and freeze-drying without mentioning the possible consequences, was recommended as French standard procedure (Bordas and Bourg, 1998). In contrast, oven drying was not recommended because their effects are marked (Rapin *et al*., 1986). Tang *et al*. (2011) demonstrated that the size of exchangeable Cd in contaminated soils is prone to change upon drying and liming, and that the potentially desorbable Cd is only slowly mobilized under ionic strength conditions prevailing in the field. Rubio and Ure (1993) recently review various approaches of sample pre-treatment for metal speciation in soils and sediments. The authors concluded that whatever the methods used for sample pre-treatment of the solid materials it can alter the results of the speciation. Farrah and Pickering (1993) reported that drying process

appears to promote metal distribution to phases having a stronger bonding power. The authors observed that metal distribution varies according to the drying method and treatment time. Similarly, Long *et al*. (2009) reported that oven drying causes numerous chemical alterations and of greater amplitude in speciation of copper and zinc in Municipal Solid Waste (MSW). These authors therefore concluded that none of the studied pre-treatments appeared to be suitable for keeping the original metal-fractionation distribution and that the extraction procedure should be applied to wet, sieved sample immediately after sampling, if environmentally relevant information was to be obtained.

2.6.7.4. Methodology

Metal partitioning, as determined by sequential extraction procedures, will be influenced by such factors as the choice of reagents used for the various extraction steps, the extraction sequence, the contact time with the particulate material, and the solid/extractant ratio (Tessier and Campbell, 1988). Reaction efficiencies are also influenced by operating conditions, mainly: the extraction time; the solid-to-liquid ratios; the type of agitation; the methods used for liquid/solid separation; the mass of the test sample; and, the rinsing method (Gleyzes *et al*., 2002).

Several authors have recognized that the dissolution of iron oxides was incomplete during the reductive step (Fe and Mn fraction) of Tessier's procedure (La force and Fendorf, 2000), leading to an overestimation of residual fraction. Vander Merwe *et al*. (1994) established that a high residual fraction in highly polluted sediment samples was found to be caused by incomplete dissolution during the previous steps. In the case of mercury contaminated soils,

Biester and Scholz (1997) demonstrated the insufficient selectivity of the used leachants, and the extraction time was not appropriate for the problem. Similarly, Coetzee *et al*. (1995) reported that selectivity of the reagents was insufficient to determine the actual mineralogical phase that host metals in sediments. Davidson *et al*. (1999a) examined changes in the reproducibility of data and extractability as a function of sample size in the case of an industrially-polluted soil. No improvement in the precision was found, except in the case of lead, for which the worst relative standard deviation were obtained for the lowest sample masses.

Van Benschoten *et al*. (1994) examined the effect of washing step on the contaminated iron oxide coated sandy soil. The authors found that the fraction associated with the slow metal

release correlated reasonably well with the residual metal fraction. Although sandy soils often are good candidate for soil washing, surface coatings may make metal extraction for even sandy soils difficult. Chomchoei *et al*. (2004) reported that variation of sample weight to column volume ratios do not affect the amounts of extractable metals, nor do extraction flow rates ranging from 50 to 100 µl s^{-1} show any effect on the extractability of the metals.

Despite the entire above highlighted drawbacks/pitfalls of chemical sequential extraction scheme. Rao *et al*. (2008) concluded that there are lot of advantages of chemical sequential extraction and still enormous scope for further research and developments in these areas because pollution sites are increasing throughout the world and there is urgent need of methods for faster, reliable and cost-effective pollution assessment so that suitable remedial measures can be taken up on priority basis at an appropriate time.

Furthermore, this present study used modified version of chemical sequential extraction scheme to determine mineralogical associations of inorganic elements in weathered fly ash under a real dry disposal conditions.

2.7 Total metal digestion

The estimation of the metal total concentration in fly ash still remains compulsory information. It is the first step in the way of the assessment of the environmental and biological risk associated to this material; on the basis of this information it can be decided to achieve or not more information on the metals availability (Mester *et al*., 1999). Total concentration of metals in fly ash, as well as in other matrices, is usually determined by spectroscopic methods following the sample dissolution. Atomic absorption spectrometry (AAS) and inductively coupled plasma-optical emission and mass spectrometry (ICP-AES and ICPMS) are among the most common spectroscopic methods used for determination of heavy metals in environmental samples (Sastre *et al*., 2002). ICPMS has emerged as a useful technique for trace analysis of fly ash due to its multi elements capability, high detection power and low sample consumption. The major setback of these techniques is that the solid sample required to be transformed into solution prior to the determination of the metal content (Sastre *et al*., 2002; Gungor and Elik, 2007). Therefore, sample preparation is an important step in the analysis of fly ash because of the solid nature of this earthy material.

Wet oxidation is normally carried out by digestion of the sample in a mixture of strong acids such as sulphuric, hydrochloric, hydrofluoric, nitric and perchloric acids (APHA, 1995). However, sulphuric acid is not recommended for simultaneous extraction of different metals, especially in sediments rich in alkaline earth metals, because of the formation of insoluble sulphate salts (Berrow and Stein, 1983). The addition of HF strongly influences the recovery of the microwave acid digestion of environmental samples. This acid breaks down silicates and minerals better than $HClO_4/HNO_3$ and HNO_3/HCl acid combinations (Melaku *et al*., 2005; Nemati *et al*., 2010). However, HF can give rise to problems in glassware and torch damage of ICP-MS. This problem can be avoided by using a small volume of HF acid and addition of saturated boric acid solution, to remove the excess of HF. Although the use of hydrofluoric acid (HF) is often necessary for the determination of a number of elements that are associated with siliceous minerals, its use can result in losses of trace elements during dissolution (Rönkkömäki *et al*., 2008).

In recent, hydrofluoric and perchloric acids are not recommended to use especially for routine metal analysis in laboratories (De Groot *et al*., 1982; Berrow and Stein 1983; Abreu *et al*., 1996). Hydrofluoric acid requires special attention to handle as it is dangerous and highly corrosive, while perchloric acid always poses a danger of explosion especially when the perchlorate vapour is trapped in the wooden or plastic ware of the fume exhausted system (Berrow and Stein, 1983; Alloway, 1995). Nitric acid was used either on its own or in combination with hydrochloric acids and proved to be effective (Berrow and Stein, 1983). For matrix digestion, many experimental protocols are proposed in the literature. They are fundamentally based on wet digestion procedures using different combinations of mineral acids, such as HNO_3-$HClO_4$ (Geladi and Adams, 1979; Mcquaker *et al*., 1979; Bingol and Ackay, 2005), HNO_3 (Sastre *et al*., 2002), HNO_3-HCl (Berrow and Stein, 1983; ISO, 1995; Tam and Yao, 1999; Sastre *et al*., 2002; Sandroni *et al*., 2003), HNO_3-H_2SO_4 (Sandroni *et al*., 2003), HNO_3-H_2O_2 (Wang *et al*., 2004b; Iwashita *et al*., 2007; Rönkkömäki *et al*., 2008), HNO_3-H_2O_2-HF-H_3BO_3 (Swami *et al*., 2001), HNO_3-$HClO_4$-HF (Wang *et al*., 1996; Melaku *et al*., 2005; Gungor and Elik, 2007), HNO_3-H_2O_2-HF (Ayrault *et al*., 2001; Iwashita *et al*., 2006), HNO_3-$HClO_4$-HF-H_2O_2 (Sastre *et al*., 2002), HNO_3-HCl-HF (Tuzen, 2003; Melaku *et al*., 2005; Marrero *et al*., 2007), HNO_3-$HClO_4$-HCl (Talmi and Andren, 1974), $HClO_4$-HF (Totland *et al*., 1992) and HNO_3-HF (Frenzel, 1995; Hatanpaa *et al*., 1997; Marrero *et al*., 2007; Nemati *et al*., 2010).

The conventional digestion procedures, such as wet digestion and dry ashing, are often the most time consuming stage of the analysis. These methods are labouring intensive and tedious, and often have a high contamination potential (Sastre *et al*., 2002; Sandroni and Smith, 2002). The speed and efficiency of instrumentation for reliable determination of trace elements in geological and environmental samples have improved dramatically over the last decades (Nemati *et al*., 2010). Nevertheless, sample preparation methods are still the major factor contributing to the uncertainty in the analytical results (Harasheh *et al*., 2009). The digestion of biological and mineralogical samples can be done in two different ways: open or closed digestion, the closed system generally being preferred. The advantages of a closed system are (1) less risk of contamination, (2) no losses of volatile elements, (3) less reagents needed, and (4) much faster digestion (Uhrberg, 1982).

Two important developments in sample preparation procedures have been (1) use of sealed high pressure bombs (vessels) to accelerate sample digestion and minimize contamination and loss of volatile elements and (2) use of microwave radiation to assist in digestion. Parr type acid digestion bombs are generally Teflon-lined, stainless-steel containers which, when sealed, are capable of digesting resistant materials with suitable solvents under elevated temperature and pressure conditions while retaining potentially volatile compounds. Unfortunately, Teflon-lined reaction bombs placed inside stainless-steel jackets are unusable because of their metallic construction; therefore, various jackets (containers) made of high-strength non-metallic microwave-transparent polymeric materials have been used (with the internal pressure not exceeding the design limits of the vessel shell) (Matuslewlcz, 1994). Fernando *et al*. (1986) reported the use of an acid digestion bomb (Parr), together with an HNO_3,-HCl-HF acid system at 180 ºC for 1 hour and found to be free of volatilization losses and adaptable for routine analyses. The one drawback is the 1 hour of heating time required. An additional limitation is the necessary delay in opening digestion bombs, which must first be cooled to room temperature and the internal pressure reduced to a safe level.

Parr type acid digestion brings a new dimension to sample preparation and may combine the qualities of the Parr-type Teflon bomb in retaining volatiles and the High Pressure Asher in completing effective decomposition within a short heating time characteristic of the microwave technique (Matuslewlcz, 1994). The development of microwaves oven has led to their usage in

analytical laboratories for sample digestion. Luque-Garcia and Castro (2003) reviewed comprehensively the theory of microwave digestion. Abu-Samra *et al*. (1975) first reported the application of microwaves for acid wet digestion of biological materials. Since that time many microwave assisted dissolution methods have been developed to include a variety of sample matrices such as rock (Totland *et al*., 1992; James and Palmer, 2000; Taylor *et al*., 2002), soil (Melaku *et al*., 2005), sediments (Lo and Sakamoto, 2005), sludge (Veschetti *et al*., 2000), biological and environmental samples (Bettinelli *et al*., 1989; Ayrault *et al*., 2001; Sastre *et al*., 2002), coal fly ash (Nadkarni, 1984; Mester *et al*., 1999; Das *et al*., 2001; Wang *et al*., 2004).

The use of closed microwave oven systems has become a quite popular method in the last few years (Frenzel, 1995). Microwave digestion in sealed containers followed by ICP-MS is, nowadays, one of the most versatile methods for the analysis of soil samples (Tuzen, 2003; Sandroni *et al*., 2003). The use of microwave radiation can, under certain conditions, greatly speed up the rate of mineralization of samples (such as digestion), the equilibrium of the distribution of analyte in two phases (such as extraction, desorption, adsorption, and clean-up), chemical reactions (such as chromogenic reactions), the heating rate of water (in the determination of moisture, and thermospray), and this technique has a promising future in sample preparation and low injection analysis (Jin *et al*., 1999). In addition to the reduction in analysis time, other advantages of microwave digestion over the conventional hot-plate digestion methods include reduced contamination, lower reagent and sample usage and enhanced operator safety. The microwave oven heats the contents to a high temperature very rapidly and the closed vessel helps in preventing losses due to volatilization of elements. Microwave digestion also tends to yield more controlled and reproducible results than conventional methods (Sastre *et al*., 2002; Sandroni *et al*., 2002). Microwave digestion protocols are classified according to their operational modes; open vessel microwave assisted digestion, which is more prone to sample contamination, and susceptible to losses of volatile metals and closed (pressurized) vessel procedures, which are rapid and efficient digestion techniques (Nemati *et al*., 2010).

CHAPTER THREE

Geology and stratigraphy of the Tutuka ash dump site

This Chapter briefly describes the Tutuka Power Station, ash handling method, weather and climatic conditions, stratigraphy and depositional settings of Karoo Supergroup and local geology of Tutuka ash dump site.

3. Introduction

Tutuka dry disposed ash dumpsites selected for this study are situated within the precincts of Eskom's Tutuka Power Station. It is situated 25 km north-east of Standerton which is located in the Mpumalanga Province of the Republic of South Africa. The scale of operations of Tutuka Power Station is large and the potential to pollute the environment is therefore real. Dry ash disposal method is used in the Tutuka power station. Dry ash handling involves any method that results in deposition/placement of a solid material that does not drain water except during rainfall and irrigation. The ash is transported by truck or conveyor belt at the site and disposed by constructing a dry embankment (dyke). Most of the ash generated at Tutuka power station is dry disposed in landfills covering several hectares of valuable land near the plant. At this power station, dry ash is dumped via conveyor belts on the ash dumpsite and irrigated with highly saline waste water from the water treatment plant to suppress excess dust (and as a co-disposal principle).

The underlying bedrock/geology of the ash dump site will definitely play a vital role in managing the impact of waste disposal on the environment of the site (Theis *et al*., 1987 and Adriano *et al*., 1983). Ojo (2009) demonstrated in her study that chemical interaction of dolerite bedrock with overlying wet disposed fly ash had a significant influence on the metal mobility or release into the subsurface beneath the ash dump. However this barrier may have a limited capacity for salt, hence the amount of salt migration should be controlled. It has therefore become imperative to acquire a good knowledge of the geology of ash dump sites before investigating the effects of waste dump on this environment. Ideally, natural soils at the base of the dump site with a high proportion of clay are associated with a low permeability barrier to prevent the salt to leach to the subsurface beneath the ash dam. The Tutuka ash dump site falls

within the main Karoo basin of South Africa. The objective of this chapter is to use evidence available in the literature on the geology and stratigraphy of the study area if required to support and explain the results of this investigation.

3.1 Description of Tutuka Power Station

The Tutuka Power Station, which started power generation more or less in 1985, is one of the recent power stations constructed by Eskom. A number of potential sources for ground water and surface water pollution are delineated in Figure 3.1 (Hodgson, 1999).

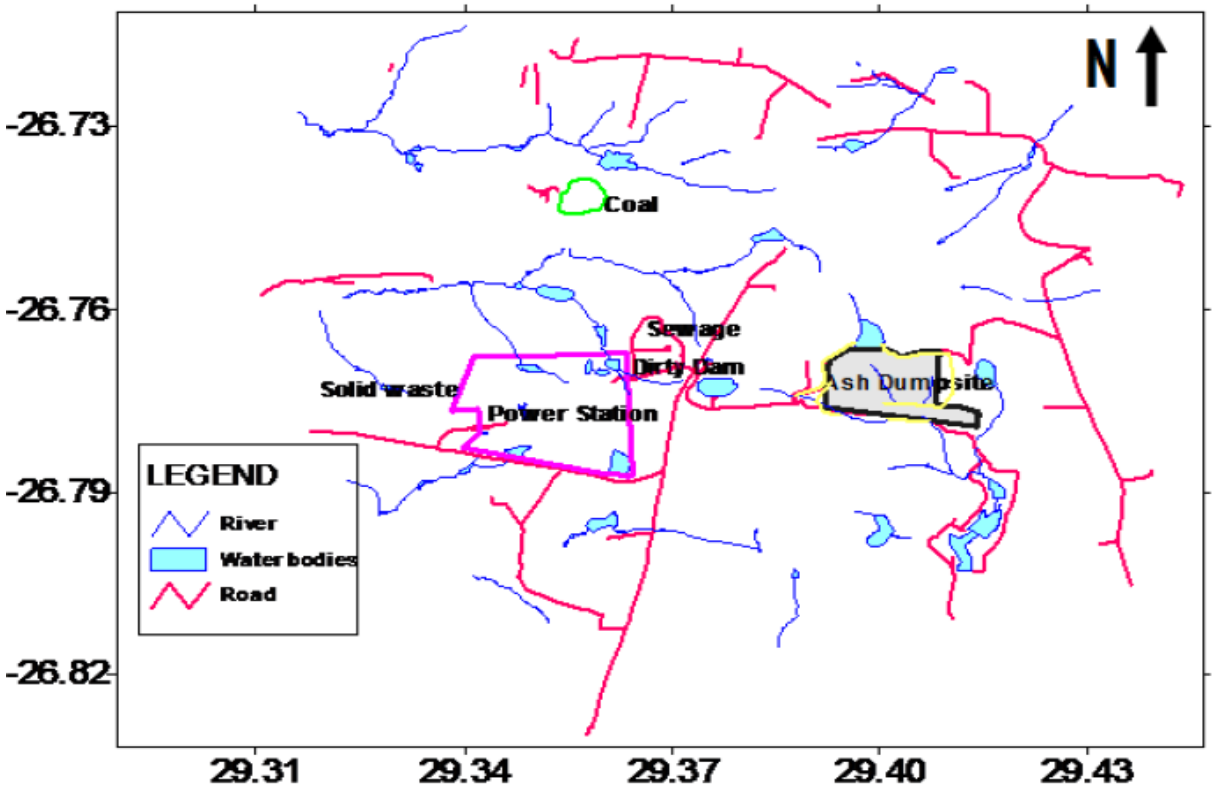

Figure 3.1. Topographical map of the area and facilities surrounding the Tutuka power station (in relation to topography, ash dump, coal stockyard, dirty dam, sewage plant and solid waste site) (After Menghistu, 2010).

Some of the more significant of these pollution sources, apart from the ash disposal site, include coal stockpiling, solid waste disposal, dirty water dams and the sewage works. The dry disposed ash dump in Figure 3.1, currently covers just about 190 ha, extending eastwards. The dry disposed ash dump is approximately 40 m above ground level on the side where dumping takes place, and slopes gently towards the west. The coal stockyard lies roughly 5 km north-west of the ash dumpsite, and covers an area of around 28 ha. Solid waste is disposed to the west of the

power station. A dirty water dam is situated in the north-eastern corner of the power station security fence, with the sewage works approximately 400 m to the north and in the same drainage system. A small water body, in the form of a wetland or pond, lies approximately 400 m to the east of the ash dump. Of concern for this study is the water dam less than 30 m north of the ash dump, more clearly delineated together with the small water body in Figure 3.2. The dam is topographically up gradient from the disposal site and groundwater flow is towards the ash dump. According to Hodgson (1999), this dam sustains a shallow groundwater table beneath the

Figure 3.2. Tutuka locality site map ash dump, water dam to the north and small water body to the east. Scale 1:1000 m (After Menghistu, 2010).

ash dump, thereby causing salt to leach excessively from the ash dump into the surrounding areas. He therefore recommended that this dam should be emptied and kept dry. Hodgson (1999) suggests that, on a regional scale, the run-off from the ash dump area is directed towards the Grootdraai Dam, which is situated approximately 9 km south of the power station. Locally, four catchments are involved. The ash disposal facility lies in its own catchment. The dirty water dam, sewage works and solid waste site are in one catchment. Run-off from the coal stockyard drains to the north, but groundwater seepage flows into the dirty water dam catchment.

3.2 Dry ash disposal system at Tutuka Power Station

Fly ash from Tutuka coal-fired power station is typically deposited by dry dumping and spread by a stacker and dozer (see Figure 4.1). The moist ash at Tutuka is transported by conveyor belt to the ash dump where it is dumped in a single or double stacking operation (Figure 3.3 b &c). No mechanical compaction of the ash is done, other than its own weight and the weight of machinery used on top of the ash dump (Figure 3.3 d, e & f). This is one of the persuasive reasons why it is assumed that ash is a porous material. In addition to the moisture added to the ash within the power station, the ash is again wetted by means of a pivot irrigation system as it is dumped off the conveyor belt to prevent the ash from drying out and creating a dust problem.

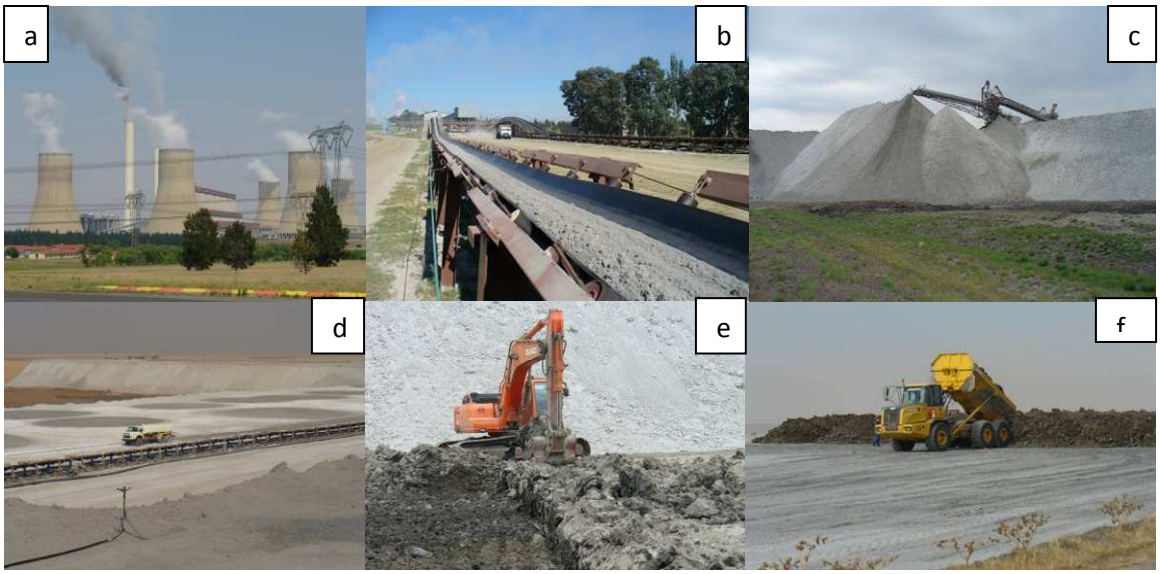

Figure 3.3. Photograph of dry ash disposal system at Tutuka Power Station (After Petrik *et al*., 2008).

Under severe windy conditions, dust does, however, still blow from the exposed ash. In addition to its less negative environmental impacts and cost effectiveness, the rehabilitation of dry ash dumps in Tutuka is viable in the early stages of the process and Eskom has achieved significant success in this respect (Burgers, 2002).

The main advantages of immediate rehabilitation are:

(i) dust and erosion are controlled/suppressed.
(ii) rain water infiltration is assumed to be minimised.
(iii) rehabilitated dumps are more aesthetically pleasing than un-rehabilitated dumps.

The ash is levelled after placement and covered with soil as soon as possible. This cover is usually in the order of 100-300 mm thick. The soil cover prevents ash from blowing off the dump and serves as a growth medium for grass. While the top surfaces of most ash dumps are slightly graded, to allow rain to run off, ponding may occur in small areas especially after heavy rainfall events. Vegetation is quickly established under these conditions when irrigated with fresh or brine/saline water, especially on the side slopes where more moisture is available from lateral seepage and run-off from the top surface of the dump.

3.3 Weather and climate of Tutuka ash dump Site

The climate and irrigation water quality plays an important role in the field soil water and salt balance. This is because the soil solution tends to get more concentrated due to higher evapo-transpirational losses, and less drainage occurs as rainfall is limited (Annandale *et al*., 2002). Similar trends are theorized in the field fly ash water and salt balance therefore understanding the climate of the Ash dump site is a requirement. The region surrounding the Tutuka ash dump site forms part of the Highveld plateau of South Africa with its characteristic flat topography and grasslands, well known for its maize and sunflower cultivation. From the monthly temperature and rainfall data recorded at the official weather station at the nearby town of Bethal 40 km north-eastern of the Tutuka ash dump site (see Menghistu, 2010), the area has a warm to cold temperate climate, characterized by two distinct seasonal weather patterns. The main wet season occurs in summer and extends from October to April, contributing to 89.9 % of the total rainfall. Most of the heavy rain in the region is associated with thunderstorms. The average annual rainfall for the area is 682 mm per annum (SA Weather Service) which is mostly concentrated in the summer months. Infrequent showers occur through the course of the winter months. Surface run-off from the area is in the order of 8 % of the annual rainfall. Groundwater recharge in undisturbed areas is in the order of 3 % of the annual rainfall (Hodgson, 1999). Temperatures in Highveld plateau of South Africa (i.e. Johannesburg) are usually fairly mild due to the city's high altitude, with the average maximum daytime temperature in January of 26° C (78.8 °F), dropping to an average maximum of around 16 °C (60.8 °F) in June. Winter is the sunniest time of the year, with cool days and cold nights. The temperature occasionally drops to below freezing at night, causing frost. The mean monthly temperature varies between 1 and 26° C (Menghistu, 2010). Summers in the Tutuka ash dump site are hot, and the winters cold. The prevailing wind

direction is north-west during the summer and east during winter. Winds are usually light to moderate. The mean annual evaporation (MAE) of the region is 1563 mm, and the mean annual run-off (MAR) 55 mm (Midgley *et al*., 1994).

3.4 Stratigraphy and depositional setting of Karoo Super group

The Karoo Super group in southern Africa occurs in the aerially extensive Main Karoo and Kalahari basins as well as in a number of subsidiary basins in South Africa, Namibia, Botswana, Zimbabwe and Mozambique. The Karoo Supergroup is subdivided into five main groups (Figure 3.4), i.e. the Dwyka, Ecca, Beaufort (comprising the Adelaide and Tarkastad subgroups), Stormberg and Drakensberg (Smith *et al*., 1993; Catuneanu *et al*., 1998). The Karoo basin evolved as a retroarc foreland basin due to accretion of the Palaeo-Pacific plate to the Gondwana plate during the late Carboniferous period (Johnson, 1991; de Wit and Ransome, 1992). The Karoo Basin is mainly underlain by a stable floor comprising the Kaapvaal Craton and the Namaqua-Natal Metamorphic Belt. It is bounded along the south by a fold-thrust belt (Cape Fold Belt) and along the east by a monoclonal downwarp. The Cape Fold Belt partly overlies less competent crust below the geophysically defined "Southern Cape Conductive Belt", interpreted by some as serpentinized basalt that was obducted against the Namaqua-Natal Belt at approximately 800 Ma (De Beer *et al*., 1982).

Following deformation and intrusion by granites (600-500 Ma) in the south, it was the site of subsidence and deposition of the Ordovician-Early Carboniferous Cape Supergroup, a precursor of Karoo Basin sedimentation. The Karoo Basin is filled with clastic and subordinate igneous rocks belonging to the Karoo Supergroup. The Karoo Basin contains an asymmetric fill of sediments and volcanics. The sediments are thickest in the south and thin northwards. The predominant sedimentary transport direction was from south to north with a minor component of fill from the north. The sediments that filled the Karoo Basin of South Africa now cover over half of the surface area of the country.

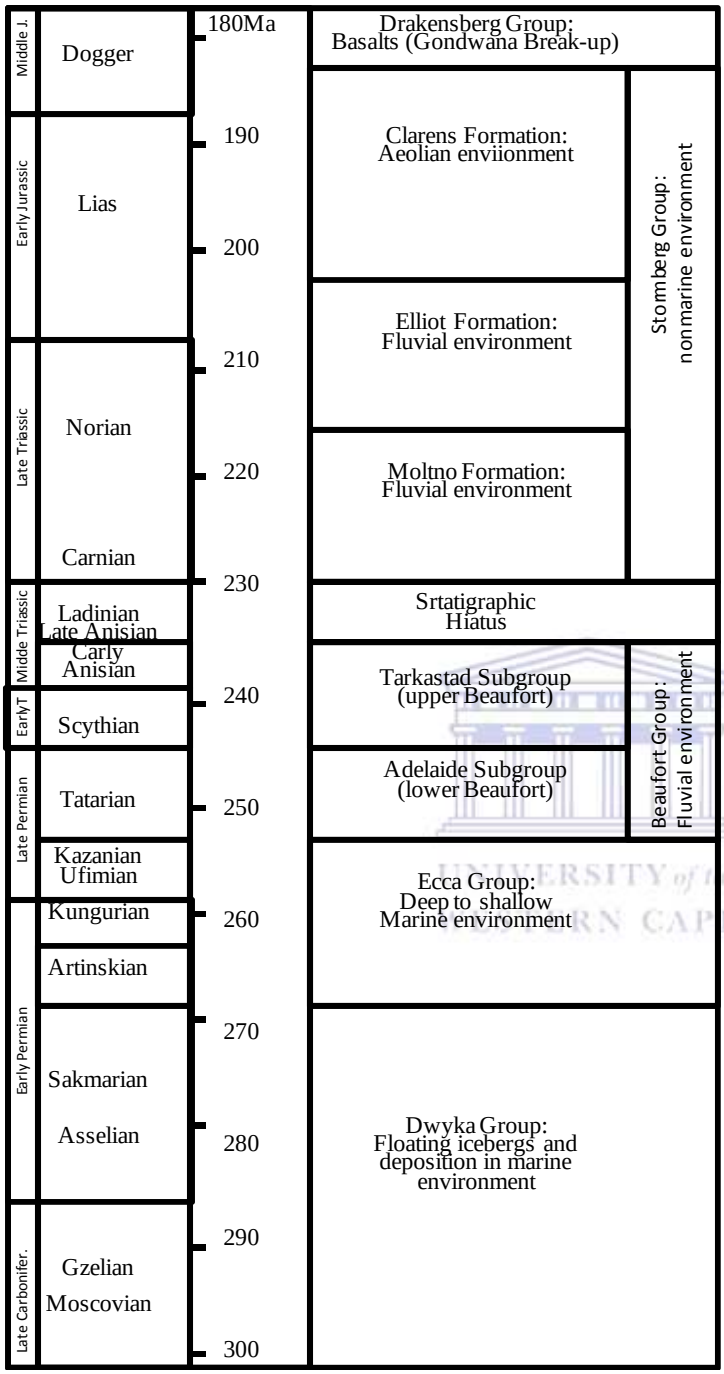

Figure 3.4. Stratigraphy and inferred depositional settings of the southern Karoo Basin (After Catuneanu *et al*. (2001) modified from Catuneanu *et al*. (1998)).

The Karoo Basin of South Africa was one of several contemporaneous intracratonic basins in south-western Gondwana that became active in the Permo-Carboniferous (280 Ma) and continued to accumulate continental sediments until the earliest Jurassic, 100 million years later. At their maximum areal extent, during the early Permian, these basins covered some 4.5 million

km^2. The present outcrop area of Karoo rocks in southern Africa is about 300 000 km^2 with a maximum thickness of some 8000 m (Smith *et al*., 1993). The strata were deposited in glacial, deep marine (including turbidite), shallow marine, deltaic, fluvial, lacustrine and aeolian environments (Johnson *et al*., 1996). The Dwyka Group (initial phase of glacigene sedimentation) forms the basal part of the succession and consists of diamictite and other glacial-related rock types deposited during the Late Carboniferous and Early Permian. The Dwyka Formation comprises a widespread fill of sub glacial till, glaciolacustrine shale, terrestrial moraine and fluvioglacial outwash (Visser, 1986; Visser and Loock, 1987). The Dwyka formations were deposited from advancing and retreating ice sheets which bordered the basin (Crowell and Frakes, 1972). The asymmetric nature of the basin as mentioned above was manifest at the adjacent of the basin southern margin; the Dwyka formation has 800 m thickness and progressively thins and pinches out northward. The deposits are overlain by the mud rock-dominated Permian Ecca Group, generally representing suspension settling. At the same time, fluvio-deltaic sand prograded into the north-eastern part of the basin while submarine fan and basin plain turbidite sand and silt as well as deltaic mud and sand were deposited in the Karoo Trough in the south. The deeper marine facies of the Dwyka and early Ecca groups including pelagic sediments, drop stones and turbidite fans, accumulated during the under filled phase of the foreland system. The shallow marine facies of the late Ecca Group corresponds to the filled phase of the basin, which was followed by an overfilled phase dominated by fluvial sedimentation (Catuneanu and Elango, 2001).

The Ecca Group is divided into three formations; the Pietermaritzburg Formation, Vryheid Formation and Volksrust Formation. The Pietermaritzburg and Volksrust Formations represent shelf shales, which merge southwards to form the Central Ecca shale facies. On the contrary, the Vryheid Formation comprises a sequence of alternating conglomerates, sandstones and shales within which the economically exploitable coal seams are present. These coarser sediments represent a regressive wedge of deltaic, fluvial and shallow marine sediments which built out into the Ecca Sea (Cadle *et al*., 1993). The coal seams accumulated in lower and upper delta plain and fluvial environments. Coal occurs in all the Karoo basins in Southern Africa, with sole exception of the Karasburg basin. However, it is at present only being economically exploited in the Vryheid formation. Sedimentation exceeded basin subsidence and the offshore muds were succeeded by prograding sandy deltas and a thick sequence (<7 km) of fluvial mud and sands

(Beaufort Group). The Beaufort and Stormberg Groups of sediments therefore reflect the change in basin evolution, depositional systems and climate during the Late Permian and Triassic Periods. Sedimentation was interrupted by a Middle Triassic lacuna before the influx of a further sequence of fluvial sands and muds (Molteno and Elliot formations). This is followed by sands and less extensive muds laid down in bajada settings (Clavens formation). Extrusion of at least 1.4 km of basaltic lavas (Drakensberg formation) during the Early Jurassic brought deposition in the Karoo basin to a close at approximately 190 Ma (Earles *et al*., 1984).

3.5 Local geology of Tutuka ash dump site

The Tutuka ash dump site is wholly underlain by sediments of the Permian Age Ecca Group of the Karoo Super group of formations, while quaternary deposits in the form of gravels containing cobbles and boulders occur along the rivers and streams in the area. The Ecca Group, which is often subdivided vertically into the Pietermaritzburg, Vryheid and Volkrust formations, overlies the Dwyka tillite conformably. By using this division, the area can be viewed as underlain by the Vryheid formation, which consists mainly of interbedded sand stones, siltstones, shales and coal. The sediments are mainly horizontally bedded, but slightly inclined in some areas, as witnessed by the gradual dip in elevation from 1650 m in the north-west to 1568 m in the south-east. The Karoo Super group has been intensely intruded by dolerite dykes and sills during the late Triassic and early Jurassic ages. As shown by the geological profile of a borehole at the Tutuka ash dump in Figure 3.5, the ash disposal site and surrounding area is largely underlain by highly-weathered and fractured dolerite at a depth of approximately 25 m. The leachate from ash dump could easily pollute water contained in the pores and fractures of the sill and hence any aquifer present in fresh siltstones, sandstones, mudstones and shales that underlie the sill. This likelihood has been previously investigated through a set of monitoring and core boreholes drilled in and around the ash dump site (see Figure 3.5).

3.6 Geophysical survey of Tutuka ash dump site

An Abem SAS 1000 terrameter and ES 464 switching unit were used for the field surveys at Tutuka ash dump site. Four multicore cables and stainless steel pegs were used with the “roll-along” surveying method. Measurement of the resistivity of the ground is carried out by transmitting a controlled current (I) between two electrodes pushed into the ground, while measuring the potential (V) between two other electrodes. Direct current (DC) or a very low

frequency alternating current is used, and the method is often called DC-resistivity. The resistance (R) is calculated using Ohm's law (After Petrik *et al*. 2008).

The RES2Dinv version 3.52-inversion program was used to invert the measured data after being manually and mathematically filtered. The 2-D model used by this program divides the subsurface into a number of rectangular blocks that will produce an apparent resistivity pseudo section that agrees with the actual measurements. A forward modelling subroutine is used to calculate the apparent resistivity values, and a non-linear least-squares optimisation technique is used for the inversion routine (After Petrik et *al*. 2008).

One profile was surveyed at Tutuka on the 21st and 22nd August 2006. The profile was surveyed using a 10 meter electrode separation with the Schlumberger-long measuring protocol. Investigation depth is approximately 80 meters. A second profile (1B) was surveyed on the 24th October 2006 with the Wenner-long measuring protocol, yielding an investigation depth of approximately 60 meters. The traverse positions are indicated in Figure 3.6. Due to steep topographical gradient at the western side of the site, topographical corrections were applied to the data on profile 1. Elevations above mean sea level were measured with a handheld GPS unit (After Petrik *et al*. 2008).

The Tutuka ash dump site is underlain by the natural bedrock consists of dolorite, shale and sandstone. A clayey topsoil of between 0.2 and 1 meter thickness is found over most of the Tutuka ash dump site. Some of this topsoil was removed for soil cover of the final ash placement elevation. The geophysics positions and resistivity traverse is shown in Figure 3.6 (After Petrik *et al*. 2008). In general it is noteworthy that the resistivity mapping shows that the dry ash system at Tutuka (Figure 3.7) is of generally high resistance (65-159 ohm.m) in ash layers, indicating a low degree of water saturation at Tutuka. This correlated with the moisture content of Tutuka ash cores (see Fig. 5.1). Profile Ash-1 (Fig. 3.7): This profile transected the ash dump from old ash placed >20 years ago on the western side of the dump with an ash depth of approximately 10 m, to fresh ash dumped within the last year (2010) on the eastern side of the dump. The shallow (near surface), approximately 18 m thick, highly resistant-layer (red-purple contours in Figure 3.7) is associated with dry disposed ashes.

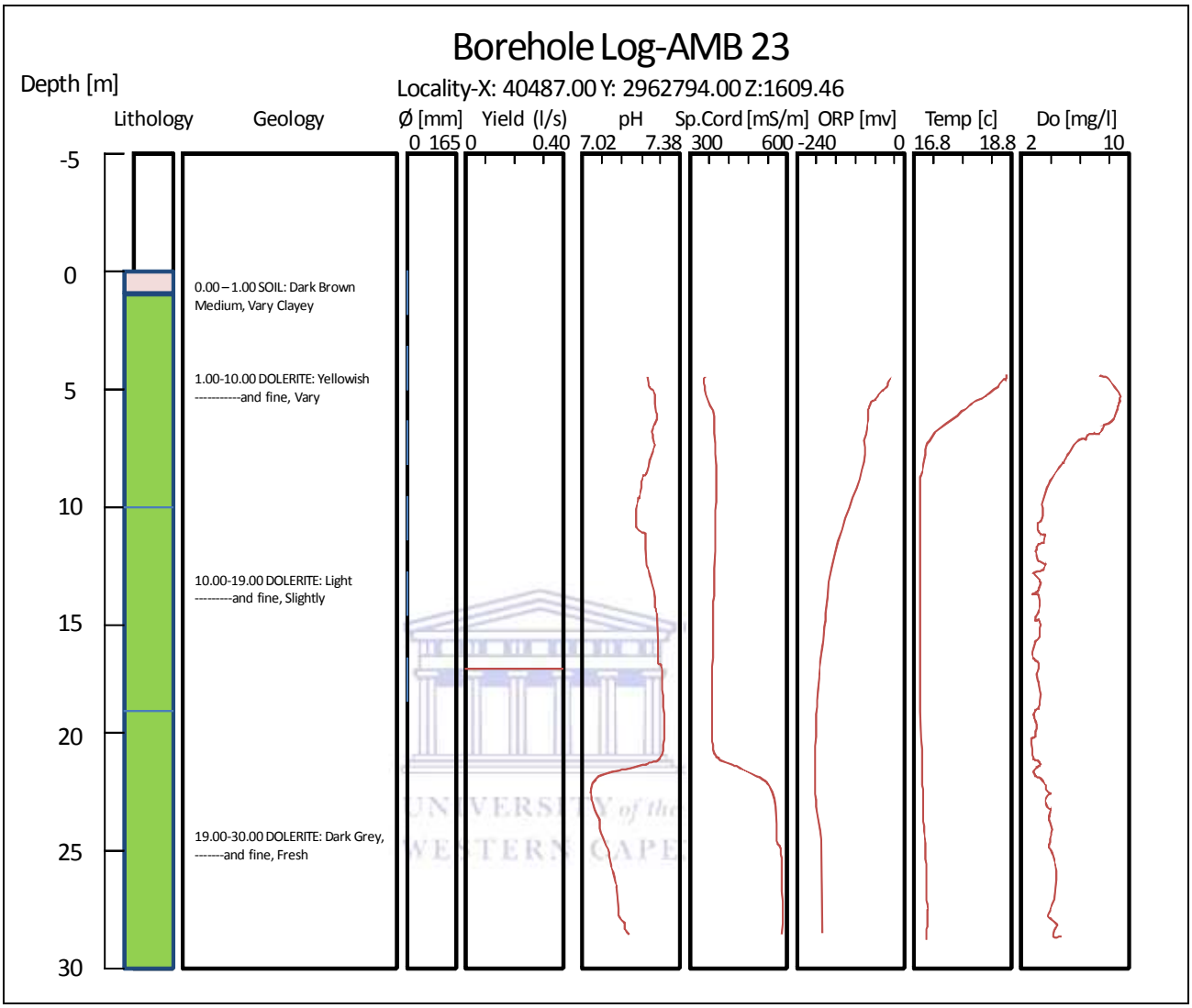

Figure 3.5. Geological profile of borehole at Tutuka Ash dump site (After Hodgson (1999)).

This highly resistant layer which disappears at a distance of 1280 m from the origin of the profile reappears at approximately 1550 m and attains its maximum thickness in the far eastern side of the resistivity section. This layer behaviour can be ascribed to the ash having different composition in that part of the profile. The more conductive nature (lower resistivity) of the ash observed in the area between 1280-1550 horizontal may result from the continuous surface irrigation with brine, causing moisture and salt saturation in this region of the dump and thus lowering the resistivity (this is possible as this is the fresh ash being deposited and conditioned with brine and has not yet reached equilibrium with the ingressed CO_2 from atmosphere for secondary mineral formation).

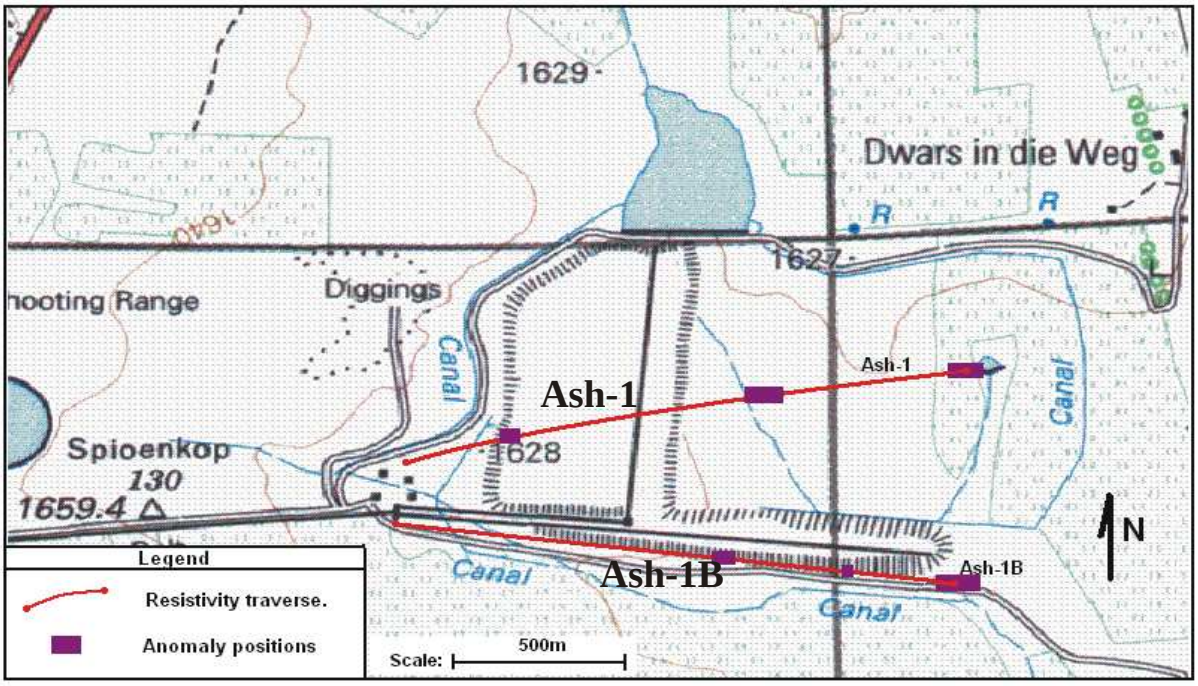

Figure 3.6. Ash-1 and Ash-1B traverses used in the electrical resistivity surveys of dry disposed fly ash dump at Tutuka Power Station (After Petrik *et al*., 2008).

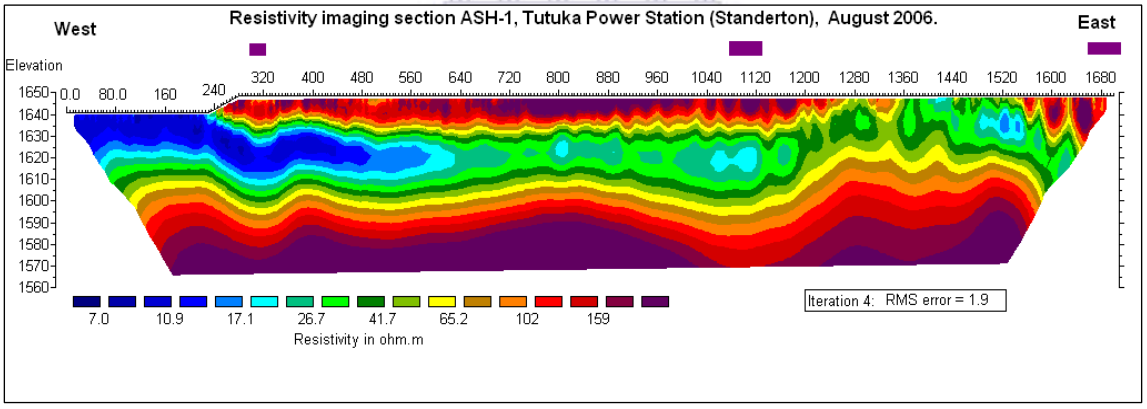

Figure 3.7. Electric resistivity profile at line ASH-1 on Tutuka: Profile length: 1700 m (After Petrik *et al*., 2008).

The resistive layer appears again at approximately 1550 meters and obtains maximum thickness in the far western side of the ash profile, which has been most recently placed (within the last year) and is the area of current dumping and had not yet been rehabilitated at the time of the survey. The more conductive (less resistive) subsurface layer (blue-yellow contours) below the ash layer is associated with a weathered dolerite sill body of approximate 30 m thickness with apparent resistivity between 7 and 60 Ohm.m. This layer reaches minimum resistivity values on

the western side of the profile where it is not covered by the ash layer and consequently exposed to a higher rate of chemical weathering. Resistivity values below 10 Ohm.m are normally associated with clayey formations.

The resistive layer below this conductor can either be fresh or less weathered dolerite or a Karoo sandstone layer. The “valley” shaped anomalies in this layer at stations 320 and 1100 metres of resistivity profile is of great interest (Figure 3.7). Positions are marked with purple squares on the model and locality map (see Figure 3.6). These anomalies are probably associated with paleo-valleys in the bedrock and are thus preferential groundwater flow paths. The valley feature at 1100 metres corresponds approximately with the old stream or drainage feature on the 1:50 000 map (Figure 3.6).

Profile Ash-1b (Figure 3.8): This model is contoured with the same resistivity contour scale as Ash-1 and the same interpretation criteria apply (see Figure 3.7). This profile (Figure 3.8) appears to be considerably less resistive indicating more brine saturated conditions at the side of the dump than the centre of the ash dump (see Figure 3.7). This low resistivity zone along the side of the dump between stations 1120 and 1600 metres correlates well with areas under constant irrigation with brine water and may also receive infiltration from the brine irrigated ash adjacent to it.

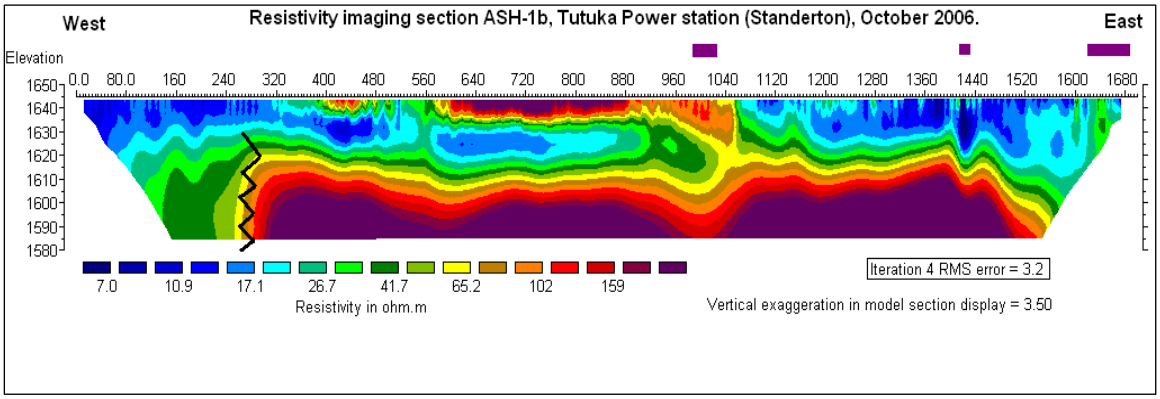

Figure 3.8. Electrical resistivity profile at Line ASH-1b on Tutuka: Profile length: 1700 m (After Petrik *et al*., 2008).

Of interest is the lateral resistivity change between stations 240 and 320 meters at a depth profile of 1630 m (Figure 3.8). This area is natural background and had no ash over layer. The lateral change visible in the substrata of this region is most probably caused by lithology of different

electrical resistivity (e.g. Dolerite sill and Karoo layer) or vertical displacement due to a geological fault. This anomaly (lateral change) might be correlated with the downward curving contours on the far eastern side of resistive profile Ash-1. The annotated section indicates the associated geology with the different modelled subsurface resistivity. It is assumed that the site is underlain by a Karoo dolerite sill and that no ash was dumped north of the existing Tutuka dump in the past. The geophysical data (Petrik *et al*. 2008) was used to optimize the site selection of the borehole positions (Figure 4.3). Sites for core drilling were selected in areas with different ash age and different salt content as interpreted from the geophysics data.

3.7 Lithostratigraphy of the Tutuka ash dump site

The complete borehole logs of AMB 79 (20-year-old), AMB 81 (8-year-old) and AMB 83 (1- yr-old) are shown in Figures 3.9-3.11. The coring procedure is reported in section 4.2.1. The coring showed that at various ages and depths differences in the ash were found varying from very hard coarse ash, to very hard fine ash, that was fractured, soft fine powdery ash and clay, mudstone or

Well ID	AMB 79	Well Log: Lithology and Construction					
		Tutuka Ash Dump					
Drilling method:		Air Flush Core		Contract No.		20 year old ash	
Coordinate		X	E29.39340	Scale	H	23	
		Y	S26.77259		V	200	
Surface Elevation (m)		0		Diameter (mm)		215	
Well depth (m)		15		Commencing date		20061130	
Casing depth (m)		11		Ending date		20061130	
Layer No.	Strata	Thick (m)	Elev. (m)	Depth (m)	Column map	Lithology	Remark
1	ASH	0.75	-0.75	0.75		Clay topsoil	
2	ASH	5.5	-6.25	6.25		solid ash	
3	ASH	0.75	-7	7		fractured porous ash	
4	ASH	1	-8	8		hard ash	
5	ASH	1	-9	9		coarse moist ash	Depth to Water level = 9.93m
6	ASH	1	-10	10		coarse ash	EC: 335 mS/m
7	ASH	1	-11	11		wet, moist ash	
8	DLRT	4	-15	15		dolorite, light brown and orange coloured clay	

Figure 3.9. Graphic log and physical sample description by depth for borehole AMB 79 (20-year-old ash dump (After Petrik *et al*., 2008).

dolerite material where the bedrock was sampled. Figure 3.9 shows AMB 79 (20-year-old) ash core was conditioned with water and depth difference in the ash were characterized with coarse ash, hard ash, fracture porous ash, coarse moist ash and wet moist ash. The depth difference of the ash was found varying in moisture content level. During coring of drilled borehole the auger came in contact with the water level at the 9.93 m depth. The ash dump was underlain by the dolerite, light brown and orange coloured clay. The AMB 81(8-year-old) ash core (Figure 3.10)

Well ID	AMB 81	Well Log: Lithology and Construction						
		Tutuka Ash Dump						
Drilling method:		Air Flush Core			Contract No.		8 Year old ash	
Coordinate		X	E29.40131		Scale	H	23	
		Y	S26.77104			V	200	
Surface Elevation (m)		0			Diameter (mm)		215	
Well depth (m)		13			Commencing date		20061130	
Casing depth (m)		0			Ending date		20061130	
Layer No.	Strata	Thick (m)	Elev. (m)	Depth (m)	Column map		Lithology	Remark
1	ASH	0.4	-0.4	0.4			top soil	
2	ASH	1.1	-1.5	1.5			hard ash	
3	FRAC	0.05	-1.55	1.55			Fracture	
4	ASH	6.95	-8.5	8.5			hard ash	
5	ASH	0.5	-9	9			brittle ash, core loss	
6	ASH	2.5	-11.5	11.5			No Core, unconsolidated ash	No water level
7	ASH	1.5	-13	13			layers to soft to drill	

Figure 3.10. Graphic log and physical sample description by depth for borehole AMB 81(8-year-old ash dump (Petrik *et al*., 2008).

was conditioned with effluent saline water and characterized by hard ash, fracture; hard ash, brittle ash and unconsolidated ash (see Figure 3.10). The drilled borehole did not come in contact with water level and underlying bedrock. Figure 3.11 shows AMB 83 (1-year-old) ash core was conditioned with effluent saline water. The drilled borehole revealed that the ash dump was characterized by soft fine ash, fracture hard ash, very coarse ash, and ash with plant debris. The drilled borehole (AMB 81) did not come in contact with water level.

Well ID	AMB 83	Well Log: Lithology and Construction						
		Tutuka Ash Dump						
Drilling method:		Air Flush Core			Contract No.		1 Year old ash	
Coordinate		X	E29.40689		Scale	H	23	
		Y	S26.77095			V	200	
Surface Elevation (m)		0			Diameter (mm)		215	
Well depth (m)		37			Commencing date		20061130	
Casing depth (m)		36			Ending date		20061130	
Layer No.	Strata	Thick (m)	Elev. (m)	Depth (m)	Column map		Lithology	Remark
1	ASH	0.5	-0.5	0.5			top soil	
2	ASH	3	-3.5	3.5			Soft ash, fine	
3	ASH	27	-30.5	30.5			Fractured hard ash: Fractures at 5.5m, 11.8m, 13m(60deg), 16m, 16.4m, 18.2m, 22m, 23m. 10cm moist ash around fractures	
4	ASH	1	-31.5	31.5			Very course very hard	
5	ASH	0.5	-32	32			ash with plant material	
6	CLAY	1	-33	33			Clay	
7	DLRT	2	-35	35			Dolorite Weathered Dry	
8	DLRT	2	-37	37			Dolorite Fresh Moist	No Water level after drilling

Figure 3.11. Graphic log and physical sample description by depth for borehole AMB 83 (1-year-old ash dump) (After Petrik *et al*., 2008).

The ash column was successively underlain by the clay, dolerite weathered dry and dolerite fresh moist. In cases where the ash dump is loose, unconsolidated and friable at deeper layers or zones though it had been irrigated continuously over time. This indicate that weak pozzolanic reactions had taken place over time and hard and soft layers were found directly adjacent to each other. Unconsolidated ash was prevalent in more recently placed areas of the dump (i.e. AMB 81). Dry

zones were found in AMB 81(i.e. 8-year-old) and AMB 83(1-year-old) where the water level was nonexistent or deeper lying. EC of core water sampled varied from 315 to 571 mS/m indicating differences in conductivity/resistance, in all likelihood due to the differences in brine irrigation regime practiced on different areas of the dump. There was not much homogeneity within each core or between different cores and many fractured zones were observed; once again highlighting the heterogeneous nature of the ash dump and the difficulty of predicting its chemical or geophysical characteristics. Thus it is not reasonable to expect predictable hydrogeological behaviour and uniform stability of ash in contact with brine flows.

3.8 Summary and conclusions

- The Tutuka ash dump site was underlain by clay, mudstone and dolerite. These bedrocks may act as barrier to migration of salt in the ash dump. However this barrier may have a limited capacity to retain salt, hence amount of salt migration should be controlled.
- The dry disposed fly ash for drilled core AMB 83 (1-year-old), AMB 81 (8-year-old) and AMB 79 (20-year-old) are characterized by ash type, texture and moisture content level. This observed inhomogeneity in the ash dump may influence the vertical distribution and mobility of metals in the ash dumps.
- The drilled cores are covered on the top section by the top soil used for rehabilitation; the leachate from these top soil cover may influence the vertical distribution of metals.
- The point of contact of ash with ground water in the drilled core AMB 79 (20-year-old) can also control the vertical distribution and mobility of metals in ash dump.
- A review of the literature draw attention to the need to apply a modified version of sequential extraction scheme drilled ash cores to elucidate the mineralogical associations of elements in the dry disposed ash dumps of different stages of weathering.

CHAPTER FOUR

Analytical techniques and experimental protocols

This chapter gives a detailed description of Tutuka ash dump, experimental approach and sampling techniques, different analytical techniques employed, research methodology, general experimental procedures for the physicochemical, mineralogical analysis of weathered drilled cores, and application of modified 5 steps sequential extraction scheme.

4. Description of the Tutuka ash dump

Figure 4.1 shows the horizontally stacked fly ash at Tutuka dump site. Tutuka ash dumps are dry disposed ash (Figure 4.1). The dry disposed fly ash shows age variation from 1-year-old to 20-year-old across the transect of the ash dump (Figure 3.6).

Figure 4.1. Horizontally stacked dry disposed ash in Tutuka ash dump site.

The dry disposed ash dumps were irrigated using waste water from the Tutuka power station and high salient effluents for dust suppression (Nyamhingura, 2009). The natural bedrock consists of dolerite, shale and sandstone. A clayey topsoil of about 1 meter thickness is found over most of

the Tutuka site. Some of this topsoil is removed for rehabilitation as soil cover of the final ash placement elevation. Most of the older sections of the surfaces of the ash dump at Tutuka is remediated and covered with a thin clayey soil (Figure 3.2) and grass. The underlying geology probably controls the flow of water leaving the ash, as well as the water level inside the ash dumps

4.1 Sampling techniques

The Tutuka ash dump sampling site is situated in the Mpumalanga Province at approximately 1.15 km in the south west of Diggings and 1.5 km west of Spioenkop (Fig. 4.2). The dry ash disposal method was used to convey the fly ash to the ash dump site conveyer. The ash dump site was delineated into two traverses based on the electrical resistivity survey (see section 3.7) and six borehole positions were established, as indicated on Figure 4.2.

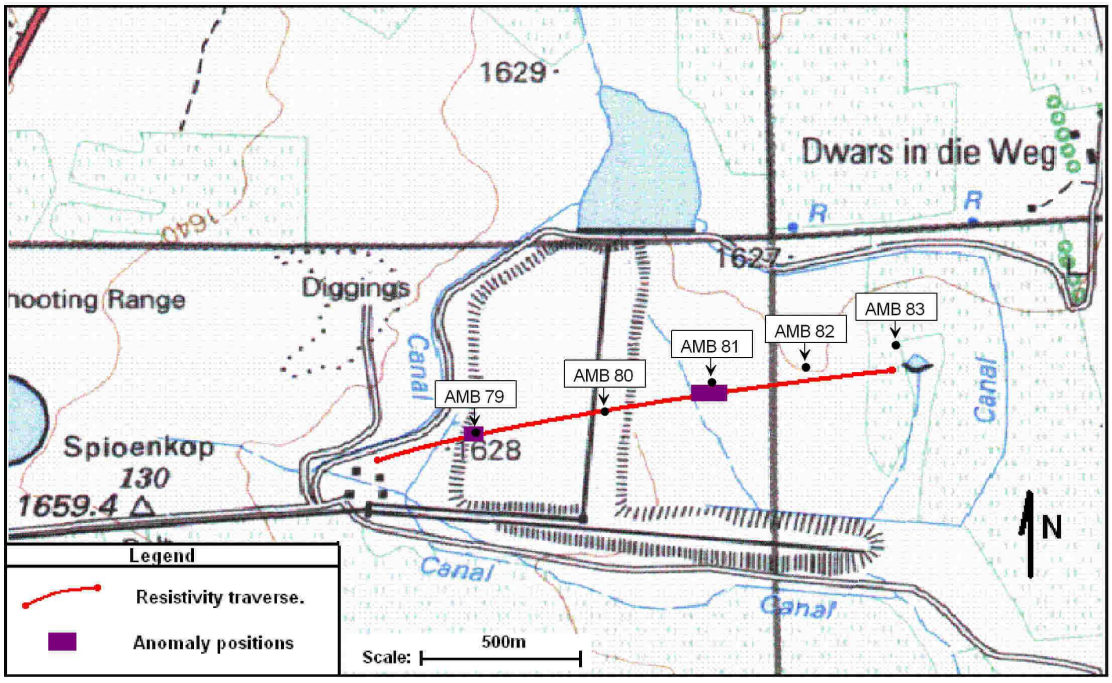

Figure 4.2. Map of Tutuka ash dump showing the positions of the geophysics lines (1:50000) and drilling points (core drilled bore holes) marked as anomaly positions (After Petrik *et al*., 2008).

4.1.1 Borehole positions

The core boreholes were drilled along the geophysics line to characterize the changes in subsurface due to difference in ash age, salt content and underlying geology (Figure 4.3).

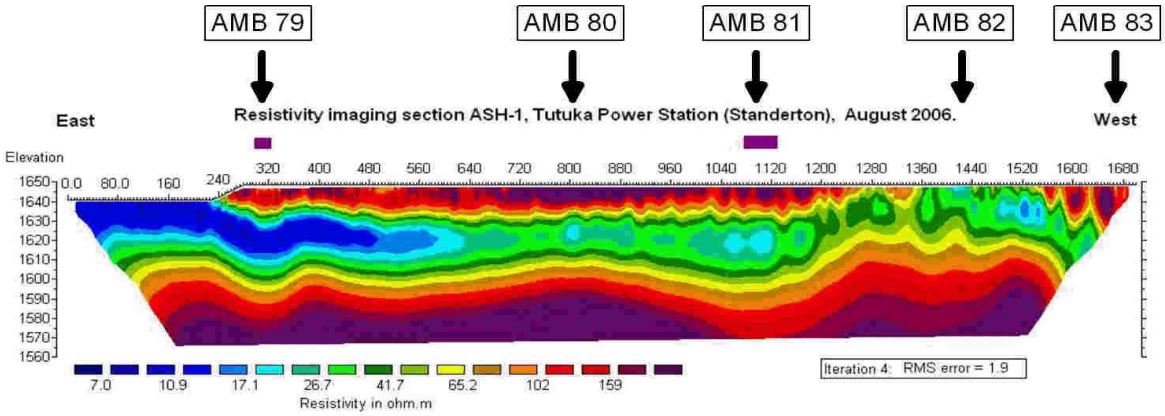

Figure 4.3. Estimated boreholes positions in relation to the electrical resistance profile results (After Petrik *et al*., 2008).

Six cores of different depth intervals were drilled in the Tutuka ash dumps of different ages: 1 year (AMB 83), 4 year (AMB 82), 8 year (AMB 81), 15 year (AMB 80) and 20 year (AMB 79) and 2-week-old (T 87) borehole was drilled in 2009. However, only results for 2-week-old (T 87), 1 year (AMB 83), 8 year (AMB 81) and 20 year (AMB 79) (see Table 4.1) are presented in this study. A combination of air flush coring and direct circulation standard air percussion drilling was used to drill the cores at the ash dump. Air flush coring uses a conventional drilling rig and compressor with a specialized drill bit that cores the ash without the need for water or lubrication for cooling of the drill bit (Fig. 4.4). The advantage of using this air drilling technique is that the coring method does not use water to cool down the drill bits as in normal rock coring therefore the ash core samples remain chemically unchanged and physically intact (Gitari *et al*., 2009a).

Table 4.1 Drilled core of different ages and depth intervals used for the study

Age of the ash core	1 year	8 year	20 year	2 week
AMB code of the ash core	AMB 83	AMB 81	AMB 79	T 87
Sampling interval (m)	1 to 29 m	1 to 13 m	1 to 15 m	1 to 25 m

An initial starter hole was drilled (215 mm diameter) using air percussion drilling through the rehabilitated cover soil to the top of the ash. The air flush coring technique was then used to drill further to the bottom of the ash dump (Fig. 4.4). Standard direct circulation air percussion of 165

mm diameter was used to drill into the underlying bedrock. Large diameter vertical boreholes were drilled in the ash dump to extract samples for evaluation. The drilling technique produced 165 mm diameter cores from which approximately 100-200 gram of fly ash sample was taken from the core inside the air flush core barrel at 1 meter sampling intervals. An intact block was extracted from the core. The borehole depths varied from 10-30 meters, depending on the depths

Figure 4.4. Air flush barrel and drilled core ash sample inside barrel.

of the ash at each drilling position. The drilled holes were completed with small concrete rings with shallow (30 cm) sanitary seals, and equipped with special tall standing lockable caps. All the completed drilled holes were clearly numbered according to the existing numbering system at the site.

4.1.2 Pre-treatment and storage of drilled core ash samples

The drilled core ash samples were stored in sealed zip lock polyethylene sample bags in the field. These sample bags were labelled accordingly and kept in plastic containers with a closed lid (Fig. 4.5). The sealed, evacuated plastic containers were kept away from any source of heat, out

Figure 4.5. Sampling of drilled core ash samples in Zip lock sample bags and storage in a lid plastic container.

of direct sunlight and away from fluctuating temperatures to avoid physico-chemical alteration of stored samples.

4.2 Standard experimental methods

The experimental approach employed in this study included the moisture content determination, pore water chemistry, total acid digestion, sequential extraction procedure, and the acid neutralisation capacity (ANC test) of all the ash core samples. The schematic diagram of the research approach is shown in Figure 4.6.

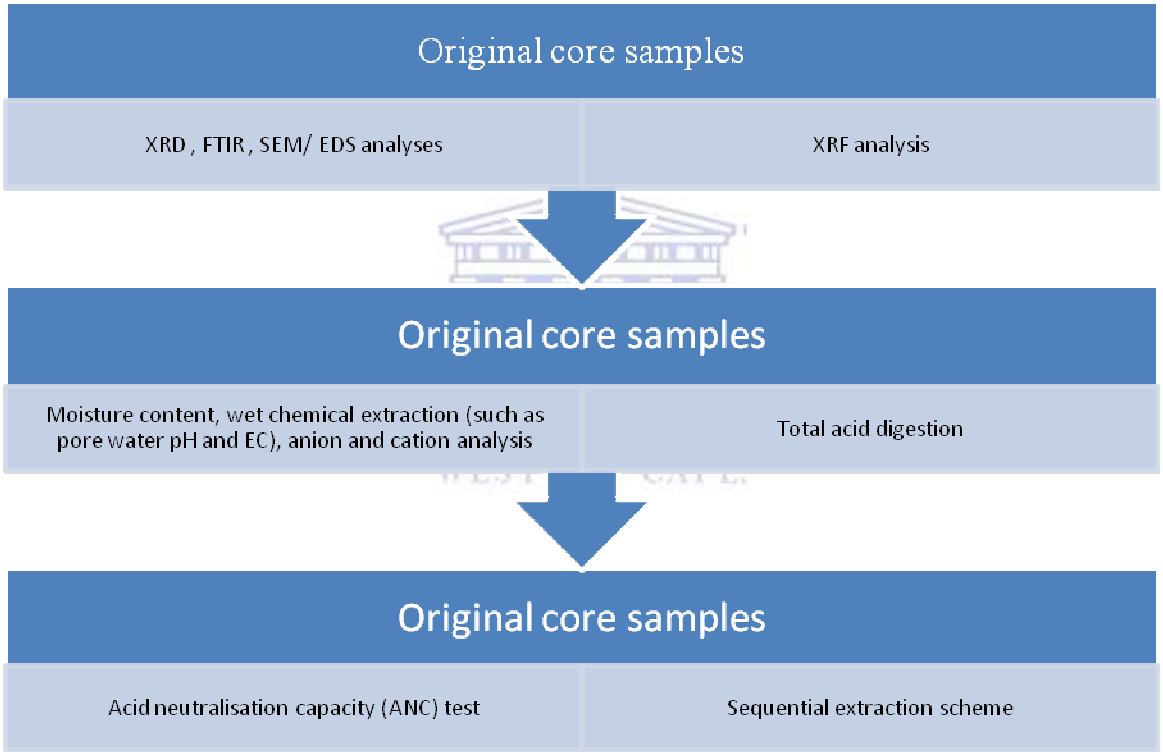

Figure 4.6. Schematic diagram of research approach.

4.2.1 Moisture content determination

Moisture content is the quantity of water contained in a material such as soils and rocks. Physical properties such as weight, density, electrical conductivity and more can be influenced easily by the moisture content. Two methods are usually employed in the determination of moisture content. These are the thermo gravimetric and the loss on drying techniques. The loss on drying technique was employed in this study according to the previous study (Ojo, 2009). The moisture content of the ash samples were determined by oven drying pre-weighed samples taken at 1 m

intervals down each of the 3 ash columns for 12 hours at 105 ^{o}C. The weight difference between the initial wet sample and the final dry sample was expressed as weight per cent of the initial wet sample and reported as moisture content per cent. The ash core samples for the rest of the determinations was air dried and therefore moisture content was not used in weight % calculations. The other data is reported on a dry mass basis.

4.2.2 Determination of loss on ignition (LOI) of drilled core samples

Loss on ignition is often taken as the measure of its organic matter, but it can only be a very rough approximation at best for most soils and rocks (Bengtsson and Enell, 1986). Heiri *et al* (2001) reported that factors such as sample size, exposure time, position of samples in the furnace and the laboratory measurements affect LOI results, with LOI at 550 °C being more susceptible to these factors than LOI at 950 °C. Loss of ignition was determined using experimental procedure reported in the study by Ojo (2009). Loss on ignition was determined by first weighing a porcelain crucible. Then 1 gram of dry mass of each sample was weighed into the crucible. The sample was then dried in an oven for 30 minutes at a temperature of 120 ºC. The crucible plus sample was then placed in a pre-heated furnace at 1000 ºC for approximately 45 minutes. The sample was allowed to cool in desiccators after being removed from the furnace and then weighed again. The procedure was repeated until a constant weight was reached.

4.2.3 Sample pre-treatment for wet chemical extraction procedures

The drilled core ash samples aged 1 year, 8 year and 20-year-old were air-dried at room temperature (25 °C) for 48 hours before used for wet chemical extraction procedure. The air dried sample treatment was considered appropriate since all analyses were not carried on ash core samples immediately after sampling. This is to minimise the modification of physicochemical form and material restructure in the ash core samples. The aliquot samples from the leachates of the ash cores after extraction were taken after the leachate was filtered through a 0.45 μm nucleopore membrane filter. The aliquot samples for cation analysis were acidified with dilute HNO_3 to pH ±2 and kept in the refrigerator at 4 °C while aliquot samples for anion analysis were kept in the refrigerator at 4 °C without adding dilute HNO_3. The samples were analysed for anions with Ion Chromatography (IC) and cations using Induced Coupled Plasma Optical Emission Spectroscopy (ICP-OES), Induced coupled plasma atomic emission

spectroscopy (ICP-AES), and Induced coupled plasma mass spectroscopy (ICP-MS). See section 4.3.4 for instrument set up and sample preparation procedure.

4.2.4 Pore water chemistry of weathered drilled ash cores

The pH of the interstitial pore water was determine to understand possible chemical reaction taking place at various sections of the drilled ash cores under natural environmental settings. The pH of interstitial/pore water was determined using 1:10 ratio of core sample: water. A sample of 10 gram respectively of each three ash cores that were taken at 1 m intervals down the profile of the ash dump were weighed and put in a beaker and suspended in 100 ml of ultra pure water. The mixture was then agitated thoroughly for 1 hour and allowed to settle for 15 minutes. The solution was filtered through a 45 µm nucleopore pore membrane filter after the pH, electrical conductivity and total dissolved solids measurement were taken with a Hanna HI 991301 pH meter with portable pH/EC/TDS/Temperature probe. The pH meter was calibrated before use with buffer solution of pH 4.0, 7.0 and 10. The pH and electrical conductivity (EC) and total dissolved solids (TDS) of the supernatant were recorded. 10 ml of the supernatant was collected and made up to 100 ml with de-ionized water in a standard volumetric flask. The solution was set aside for analysis of anions using a Dionex DX-120 ion chromatograph (IC) with an Ion Pac AS14A column and AG14-4 mm guard column. Triplicate analysis was carried out in each case.

4.2.5 Sequential extraction procedure

The five-step sequential extraction procedure applied in this study is described below. The extraction method was a modified form of the method proposed by Tessier *et al* (1979) (steps 2, 3, 4 and 5); a water soluble extraction step is added in this study. First, a water soluble fraction extraction was executed followed by exchangeable fraction extraction, carbonate fraction extraction, iron manganese fraction extraction and residual fraction was digested and analysed as set out in section 4.2.5.1. All the chemical reagents used were of analytical grade (see Table 4.2). The detailed procedures are as follows:

4.2.5.1 Common procedure for steps 1- 4

The mixtures from each step were shaken at room temperature for 1 hour with a mechanical shaker. The procedure was repeated in triplicates. The solution was allowed to settle down for 1 hour. The mixture was centrifuged at 6000 rpm for 20 minutes, and the supernatant filtered

through a 42 µm nucleopore pore membrane filter. The remaining solid portion was carefully decanted into a 100 mL plastic clear bottle without any weight loss. A 10 ml of the supernatant solution was measured into a standard volumetric flask and made up to 100 mL with ultra pure water. The solution obtained was set aside for multielement analysis with ICP-MS. The solid residue from each step was completely recovered and kept in a refrigerated condition for the next extraction method.

i. Step 1. Water soluble fractions

One gram of the fly ash samples from the ash core at various intervals in the ash horizon was weighed into 50 mL centrifuge tubes and 45 mL of ultra pure water was added. This mixture was processed as set out in section 4.2.5.1. A 42 mL of filtered supernatant was recovered. Dry weight concentration of the analytes for this sequential extraction step was calculated using the dilution factor and original weight of the sample.

ii. Step 2. Exchangeable fractions (Extraction at pH 7)

Forty-five millilitres of the 1 M ammonium acetate buffer solution at pH 7 was added to the solid residue recovered from step 1 and was processed as set out in section 4.3.5.1. A 44 mL of filtered supernatant were recovered. Dry weight concentration of the analytes for this step was calculated using the dilution factor and the weight of the residue from step 1 (i.e. difference between the mass of analytes that came out from water soluble fraction and the weight of ash sample).

iii. Step 3. Carbonate fractions (Extraction at pH 5)

Forty-five millilitres of 1 M ammonium acetate buffer solution at pH 5 was added to the 0.97 g of the solid residue recovered from step 2. This mixture was processed as set out in section 4.2.5.1. A 44 mL of filtered supernatant were recovered. Dry weight concentration of the analytes for this step was calculated using the dilution factor and the weight of the residue from step 2 (i.e. difference between the mass of analytes that came out from exchangeable fraction and the weight of solid residue from step 2).

iv. Step 4. Fe and Mn fractions

Forty-five millilitres of hydroxylamine hydrochloride (1 M) in nitric acid (0.025 M) solution was added to the 0.94 g of solid residue recovered from step 3. This mixture was processed as set out in section 4.3.5.1. A 44 mL of filtered supernatant were recovered. Dry weight concentration of

the analytes for this step was calculated using the dilution factor and the weight of the residue from step 3 (i.e. difference between the mass of analytes that came out from carbonate fraction and the weight of solid residue from step 3).

v. Step 5. Residual fractions

The solid residue recovered from step 4 was rinsed with ultra pure water and quantitatively transferred to a crucible, oven dried at 105 ºC, and weighed. 0.90 gram of dried sample was carefully transferred into the Teflon cup of a Parr bomb. A 14 mL of the combined acid ($HClO_4$: HF: HNO_3) mixed in the ratio of 3:3:1, respectively, was added and the Teflon cup placed in Parr bomb, sealed and heated to 180 °C for 3 hours in an oven. It was removed from the oven and allowed to cool down. After cooling, the solution was diluted with 40 mL of 1 % HCl and then filtered through a 42 µm nucleopore pore membrane filter. A 10 mL of the supernatant solution was measured into a standard volumetric flask and made up to 100 mL with ultra pure water. The solution obtained was set aside for multi element analysis with ICP-MS. Dry weight concentration of the analytes for this residual fraction was calculated using the dilution factor and the weight of the solid residue.

4.2.6 Total acid digestion

The total acid digestion was carried out to determine the total metal concentration in ash core samples which was used to calculate mass balance in sequential extraction scheme. The digestant selected included $HClO_4$: HF: HNO_3 mixed in the ratio of 3:3:1; the digested solutions were similar to those used in a previous study (Mester *et al*., 1999, Smeda and Zyrnicki, 2002). The respective core samples taken from 1 yr, 8 year, and 20-year-old ash dump cores were each dissolved with triple acid digestion ($HClO_4$: HF: HNO_3), and the solution thus obtained was analysed to validate the efficiency of the fractionation scheme. One-half gram samples of the drilled ash core taken at depth interval spacing of 1 m were weighed in a Teflon cup. A 7 mL mixture of combined acid ($HClO_4$: HF: HNO_3) in the ratio of 3:3:1 respectively, was added to the cup for each sample. The Teflon cup was placed in a Parr bomb, sealed, and heated to 180 °C for 3 hours in an oven. It was removed from the oven and allowed to cool. After cooling, the solution was dissolved with 40 mL of 1 % HCl and then filtered through a 42 µm pore nucleopore membrane. The solution was made up to 50 mL with same solvent (1 % HCl) in a standard volumetric flask. A 10 mL sample of the original extract was measured into a standard

volumetric flask and made up to 100 mL with ultra pure water (UP using ELGA Pure lab UHQ instrument). The procedure was repeated in triplicate. The solution obtained was set aside for multielement analysis with ICP-MS. Dry weight concentration of the analytes was calculated using the dilution factor and the weight of the original sample.

4.2.7 Acid neutralization capacity experiment (ANC)

The acid neutralisation capacity (ANC) test was carried out to determine the effect of pre-selected solution pH on the release of metals in weathered drilled ash cores. Acid neutralization capacity (ANC) test was carried out based on the methodology of the European standard prEN14429. The method is divided into two stages which are; the preliminary test to determine the acid consumption of the fly ashes; followed by the determination of acid neutralization capacity of the fly ashes. The entire chemical reagents used are of analytical grade (see Table 4.2).

Table 4.2. List of chemical reagents of analytical grade used in the study

Chemicals	Quantity	Grade	Purity %	Source
Hydrochloric acid	2.5 Litres	Analytical grade	37	Merck Chemical Pty Ltd.
Nitric acid	2.5 Litres	"	65	"
Perchloric acid	2.5 Litres	"	70	"
Hydroflouric acid	2.5 Litres	"	40	"
Ammonia acetate	500 gram	"	98	"
Hydroxylamine hydrochloride	500 gram	"	98	"
Acetic acid	2.5 Litres	"	99.5	KIMIX Chemical
Ammonia solution	2.5 Litres	"	98	KIMIX Chemical

Stage 1: Determination of acid consumption

According to the method, preliminary determination of the acid consumption has to be done to determine the volume and the concentration of acid needed to attain four different final pH values between the natural and pH 4 for each sample drawn from the three ash cores. The preliminary determination can be done by two different methods which are; (i) by titration and (ii) by arbitrary division of the maximum acid consumption for the extreme pH values. The titration procedure was considered in this research for the preliminary determination of acid consumption.

The preliminary determination of the acid consumption rates of both fresh and the weathered ashes were carried out, followed by the determination of acid neutralisation capacity of the fly ashes. The initial determination of the acid consumption was done to determine the volume of acid addition needed to attain the five required pH levels of 8, 7, 6, 5 (i.e. four different final pH values between the natural and pH 4); and 4 at which the acid neutralisation study was then done. The titration procedure was used in this study for the initial determination of acid consumption. Approximately 15 grams of the fresh ash and each of the unsaturated core samples from the 20-year-old section of the ash dump were weighed into HNO_3 acid rinsed bottles. 135 ml of de-mineralized water was added to each of the bottles, to achieve a liquid to solid ratio (L/S) of 9 (this was done in order to attain a liquid to solid ratio ranging from 10 to 11 after the addition of the acid solution). The mixtures were agitated for 1 hour. The natural pH values of the supernatant were determined after leaving the mixtures to settle down for 10 minutes. A known portion of 2 M HNO_3, analytical grade solution was added to the bottles separately and the pH values were determined after 30 minutes of agitation. This process continued for 24 hours until the specified pH intervals from a neutral pH to pH 4 were obtained. The amount of the 2 M HNO_3 required to attain each of the different pH values were recorded and used for the main acid neutralization capacity (ANC) test.

Stage 2: Main ANC experiment

The main ANC experiment was carried out using the volumes of acid determined in the initial acid consumption test. The volume and concentration of acid required to achieve each pH from natural to pH 4 was thus pre-determined. The ANC experiments were repeated, such that the volume of acid (determined in the preliminary experiments) required to achieve a certain given pH was added, so as to achieve a total volume 150 ml (plus de-mineralized water in which 15 grams of fresh fly ash had been added). The specified volume of acid was added in three portions with agitation for 30 minutes in-between additions. This procedure was repeated for each pH from natural to pH 4. The bottles were closed and the suspensions were agitated, and the pH values were measured and recorded after each timed acid addition. After the addition of the last portion of the acid, the suspensions were agitated until t = t0 + 48 hours. The pH, EC and TDS were measured before the solid residues were separated after 48 hours by filtration using a 0.45µm nucleopore pore membrane filter. The filtered supernatants were preserved with HNO_3

acid for major and trace elements analysis by Induced Coupled Plasma Optical Emission Spectroscopy (ICPOES) (see section 4.2.3).

4.2.8. Standard analytical and instrumental techniques

All the protocols for standard analytical and instrumental techniques are present in the Appendix Ai-x.

CHAPTER FIVE

Results and Discussion 1

Physicochemical and mineralogical analysis of drilled cores

This chapter presents the results obtained from the physicochemical analysis of drilled cores at Tutuka ash dump. The bulk chemical composition, mineralogy, micro-structure and pore water chemistry of waste water and high saline effluent conditioned dry disposed ash are discussed. The chemical weathering process and its consequential effect on the mobility of chemical species in a dry ash disposal scenario were elucidated.

5. Introduction

Coal fly ash is a solid residue from the combustion processes of coal for electrical power generations. The coal fly ash generated in power stations is alkaline as a result of some soluble basic oxides, such as CaO and MgO (Kutchko *et al*., 2006; Choi *et al*., 2002; Saikia *et al*., 2006). The principal processes affecting the leaching process when fly ashes interact with water are dissolution of primary solids and precipitation of secondary solids, as well as redox, sorption, and hydrolysis reactions. The release of trace elements from particular fly ashes is a slow and sometimes complex process, strongly dependent on the pH developed during interaction with the leaching solutions (Jankowski *et al*., 2006). Chemical interactions of coal fly ashes with infiltrating rain water, ingressed O_2, and ingressed CO_2 from atmosphere at ash dumps; would definitely lead to chemical alterations and mineralogical transformations. This chemical interaction would eventually mobilize species from the solid phase of fly ash. The mobilization of trace metals in coal fly ash when in contact with infiltrating rain water, ingressed O_2, and CO_2 over time poses a serious environmental concern. Therefore, fly ash should be disposed safely to prevent pollution to the environment (Van den Berg *et al*., 2001; Theis and Wirth, 1977).

This study is an attempt to understand the chemical weathering and species mobility in the dry disposed fly ash dumps irrigated with waste water and high saline effluents. A number of techniques were employed to achieve this objective. In order to have better understanding of the chemical and mineralogical changes under the real dry disposal conditions, cores were drilled from dry disposed weathered ash dumps as a function of age. Their chemical and mineralogical

analysis by depth joined to chemistry of extracted interstitial or pore water studies were applied to increase our understanding of the mobility of species under disposal conditions. A XRD mineralogical profile of a 2-week-old ash was also included for comparison. The data generated from this study was systematically explored to understand the chemical weathering and mobility of species under disposal condition.

5.1 Optimum moisture of dry disposed ash cores

The experimental protocol for this section is reported in section 4.2.1. The determined moisture content of dry disposed fly ashes is shown in Figure 5.1. There is a significant increase in % moisture content for fly samples taken at 25 m depth (2-week-old). This could be due to migration downward of moisture used for dump suppression (i.e. hydraulic). A slight variation in the moisture content in the 1-year-old ash dump indicate very little drying out during first year of dumping. For 8-year-old fly ash dump, the % moisture content shows a steady increase until 3–4 m depth intervals where there is a considerable drop in the moisture content. Noticeable uneven % moisture content is observed in 8-year-old dry disposed ash dump but a significant increase in % moisture content occur at 13 m depth.

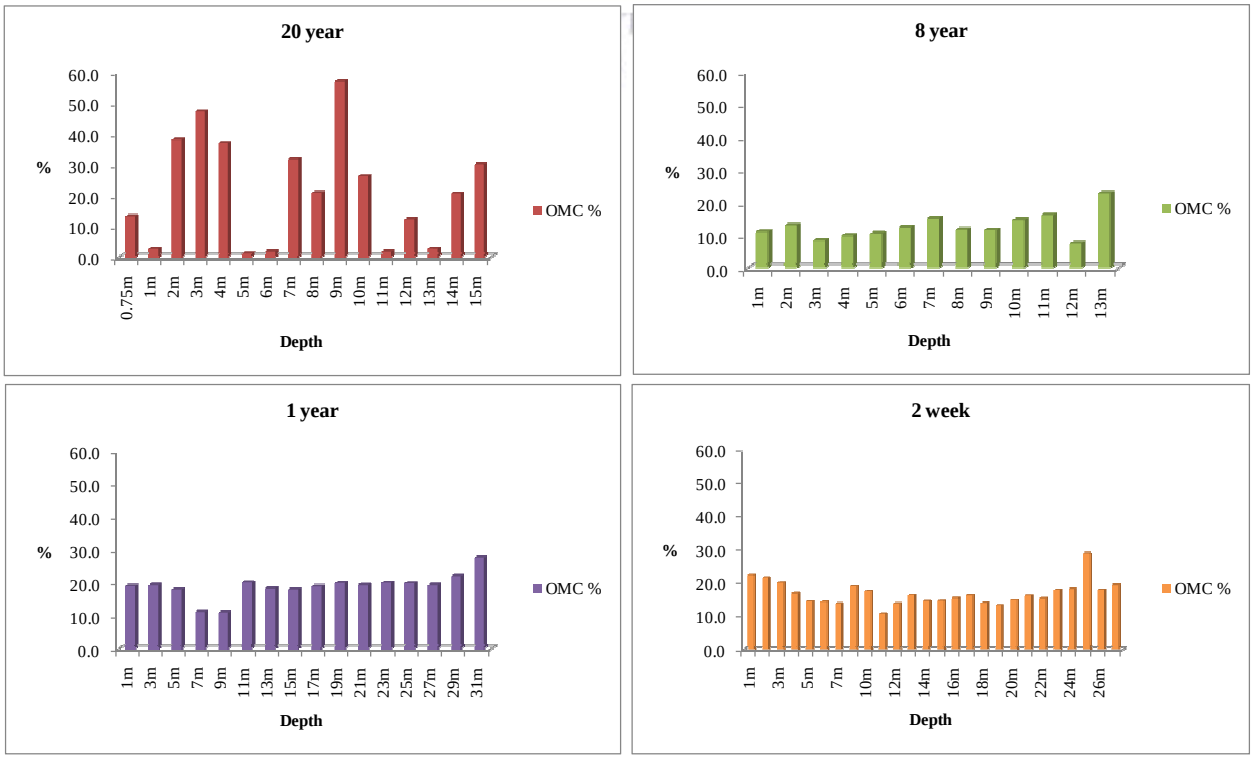

Figure 5.1. % moisture content of dry disposed fly ash as a function of depth.

This indicate that the ash dump is slowly drying out over time but still very damp at the bottom. There is a gradual increase in the % moisture content as a function of sample depth for 20-year-old ash dump which indicates continuous surface irrigation with water have caused high % moisture and salt saturation (high conductive). However, the moisture content of 20-year-old ash dump decreases between 5–6 m depths (low conductive). A significant increase in moisture content is observed for the core sample in direct contact with water level [i.e. 20 year (9 m)] (Figure 5.1). The uneven moisture content observed in 20 year, 8 year, 1 year and 2-week-old fly ash dumps could also be attributed to uneven placement conditions or varying ambient weather conditions during placement.

Generally in the weathered dry disposed ash relatively low moisture content is observed at the top sections compared to the bottom sections of the ash dumps. Noticeable uneven % moisture content is observed in 8 year and 20-year-old dry disposed ash cores compared to 2 week and 1 year ash cores. This moisture content trend essentially indicates that the older ash core samples had the highest variation in the % moisture content due to continuous surface irrigation with high saline effluents (i.e. hydration process). The % moisture content showed strong correlation with inhomogeneity in the ash dump due to textural differences (see Section 3.7) and in-homogenous brine irrigation. The high % moisture content correlate with coarse textured ash cores whilst low % moisture content correlate with fine textured ash cores. The coarse texture and high % moisture content could lead to salt saturation and thus make the ash conductive (lowering the resistivity) of the section of dump (see Section 3.6). The continuous surface brine irrigation of dry disposed ash dump would ultimately promote mobility of the chemical species.

5.2 Mineralogy of the dry disposed ash cores

The mineralogical analysis by depth of the ash dump was carried out with X- ray diffraction technique (XRD). This is to better understand the mineralogical changes (i.e. secondary phases) under the real dry disposal conditions. The experimental protocol for this section is presented in Appendix Av. The results of the XRD analysis of samples of the drilled weathered dry disposed fly ash aged 2 week, 1 year, 8 year and 20-year-old are presented in Figures 5.2 - 5.5. The main crystalline mineral phases identified are quartz (SiO_2) and mullite ($3Al_2O_3{\cdot}2SiO_2$). Other minor mineral phases identified are; hematite (Fe_2O_3), calcite ($CaCO_3$), lime (CaO), anorthite ($CaAl_2Si_2O_8$), mica ($Ca(Mg,Al)_3(Al_3Si)O_{10}(OH)_2$) and enstatite ($Mg_2Si_2O_6$).

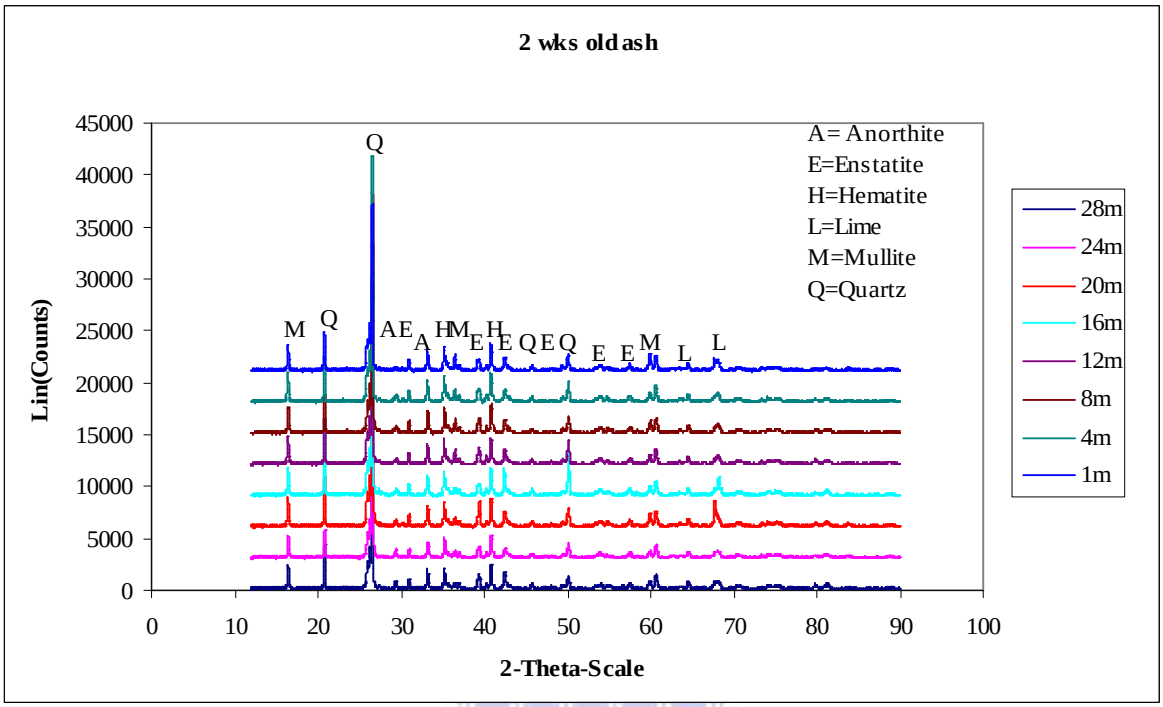

Figure 5.2. XRD spectra for 2-week-old (T 87) dry disposed ash cores.

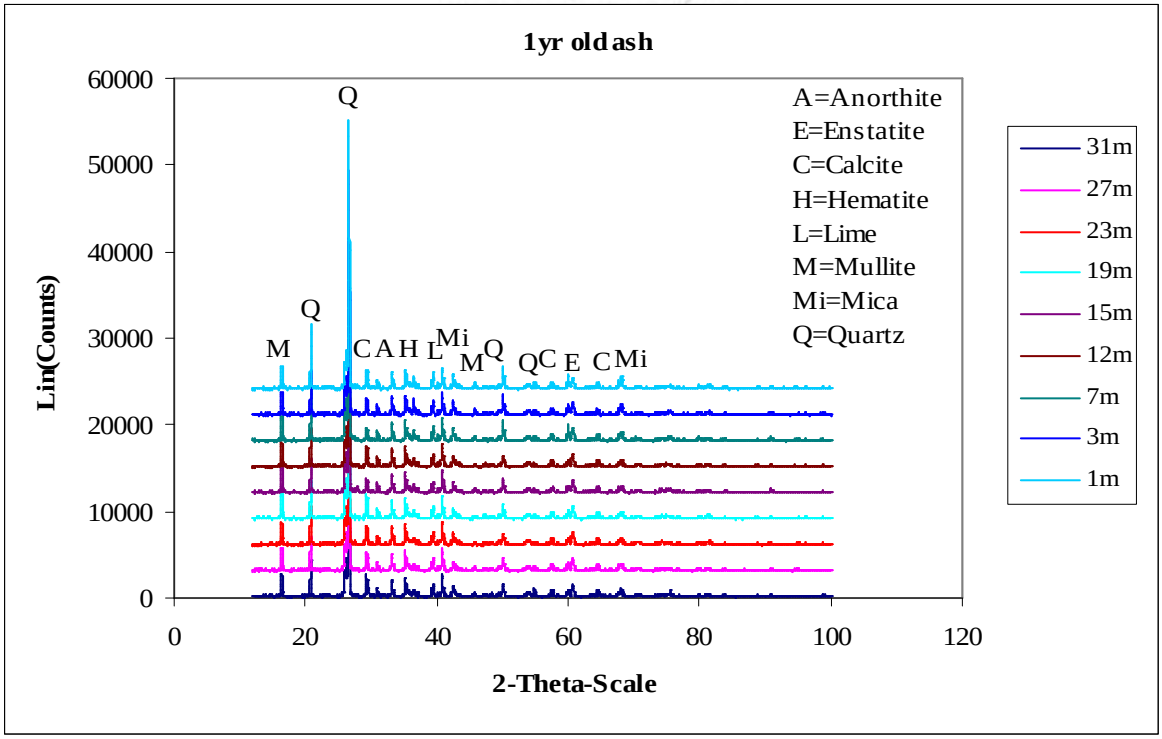

Figure 5.3. XRD spectra for 1-year-old (AMB 83) dry disposed ash cores.

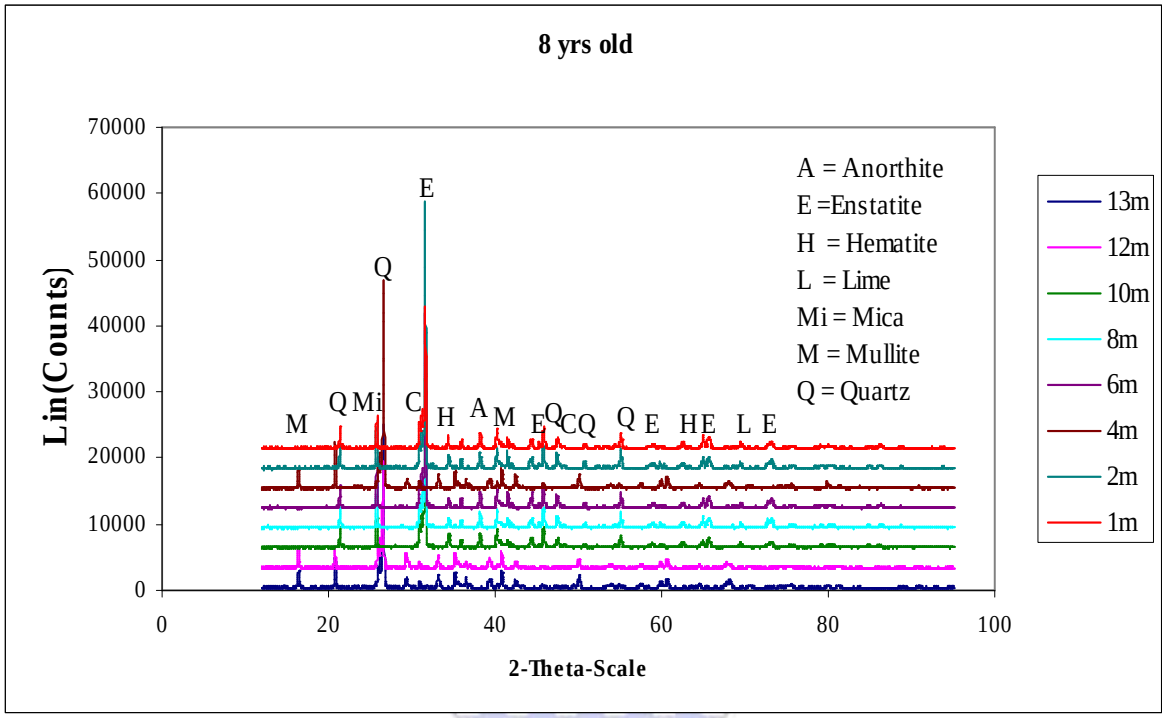

Figure 5.4. XRD spectra for 8-year-old (AMB 81) dry disposed ash cores.

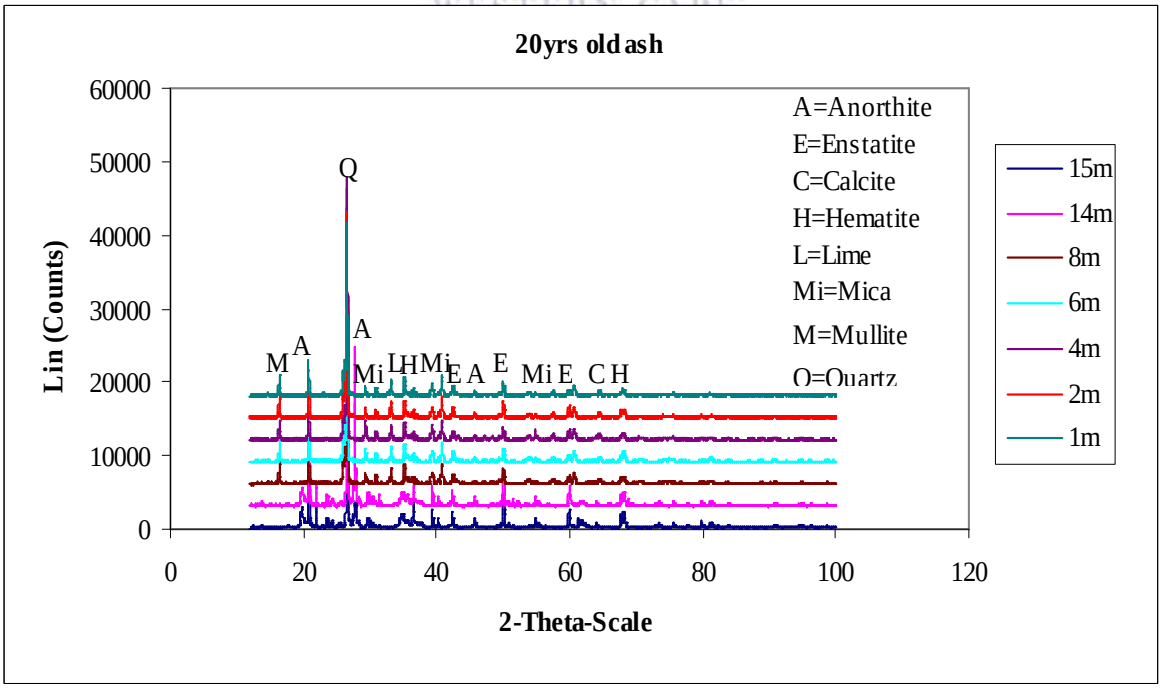

Figure 5.5. XRD spectra for 20-year-old (AMB 79) dry disposed ash cores.

This is in general agreement with mineralogy reported for other coal fly ashes (Koukouzas *et al*., 2006; Vassilev and Vassileva, 1996c; Bayat, 1998; Sakorafa *et al*., 1996; Filippidis and Georgakopoulos, 1992; McCarthy *et al*., 1984). The XRD results obtained from 2-week-old dry disposed fly ash show similar mineralogical composition to the weathered ash except for the absence of calcite and mica. Lime (CaO) presence in coal fly ash (Figures 5.2-5.5) may be due to the heat transformation of dolomite mineral or decarbonation of calcite entrained in feed stock coal (Navarro *et al*., 2009). Calcite precipitation in dry disposed fly ashes is attributed to chemical weathering due to reduction in pore water pH overtime due to CO_2 ingress. Soong *et al*. (2006) had proven that calcite precipitation in weathered fly ash is as a result of chemical interactions of calcium oxide (lime) rich fly ash with ingressed CO_2 (see Section 2.4.6). Figures 5.6-5.8 presents the summary of the mean peak heights of mineral phases determined by XRD analysis of the 1 year, 8 year and 20-year-old ash core samples drawn from different depths of the dumps respectively. The eight phases observed in every sample are considered to be characteristic phase assemblages for Class F fly ash. This assemblage presented in Figure 5.6 consisted of quartz, anorthite (residual coal minerals), mullite, calcite, hematite, mica, enstatite and lime. In the 1-year-old ash cores, the most prominent mineral phase is quartz having peak of

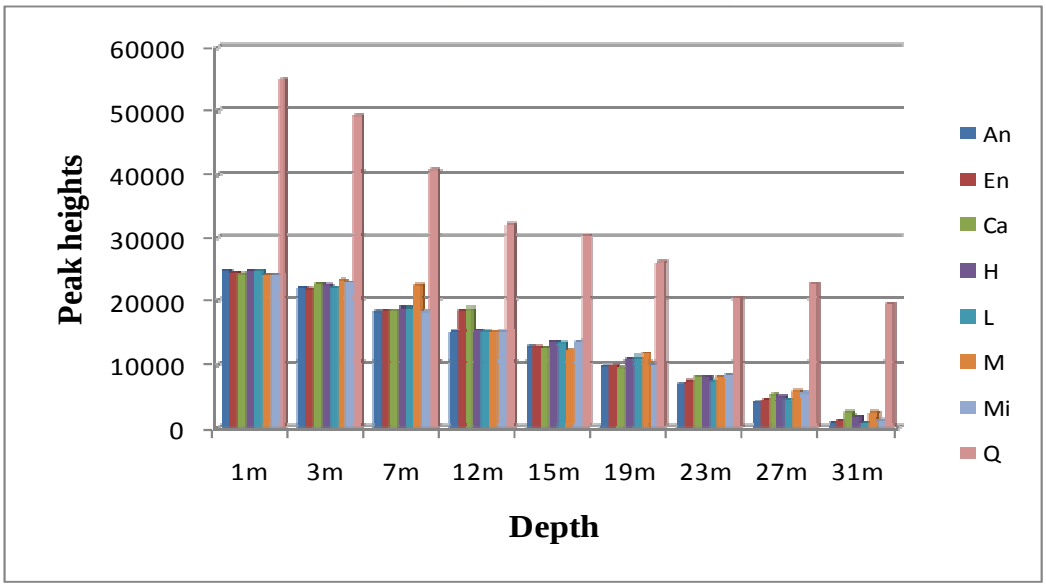

Figure 5.6. Bulk XRD mineral mean peak heights in 1-year-old (AMB 83) Tutuka ash cores (An=anorthite, En=enstatite, Ca=calcite, H=hematite, L=lime, M=mullite, Mi=mica, Q=quartz).

almost double that of the other mineral phases in all the core samples from all depths (0-31m). The peak height of quartz mineral showed a decrease trend with increasing depth of 1-year-old ash dump (Figure 5.6). This observed trend showed strong correlation with flushing/leaching of SiO_2 and Al_2O_3 in the ash dump (see Table 5.5). The Si concentration trend in the water soluble fraction of 1-year-old ash dump also confirmed this above observed trend (see Figure 7.1). Thus, the quartz mineral peak height is indicative of rapid dissolution/weathering of aluminosilicate mineral within 1 year of ash dumping. Other mineral phases such ash mullite; calcite, hematite, enstatite, lime, anorthite and mica showed similar trend in the 1 year and 20-year-old ash dumps (Figures 5.6 and 5.8). The mineral peak height in the 8-year-old section of the ash dump showed anomalous trend which may be ascribed to in-homogenous irrigation with high saline effluent (brine). This implied that 8-year-old section has received much of high saline effluents than 1 year and 20-year-old sections of the ash dump.

Stevenson and McCarthy (1985) have shown that the statistical variations in peak height on the same phase of ash samples could be used to assess the homogeneity and stability of different mineralogical phases. A statistical consideration of the variations in the ashes peak heights for the different phases was used here to appraise the mineralogical distribution and chemical heterogeneity among the coal fly ash samples.

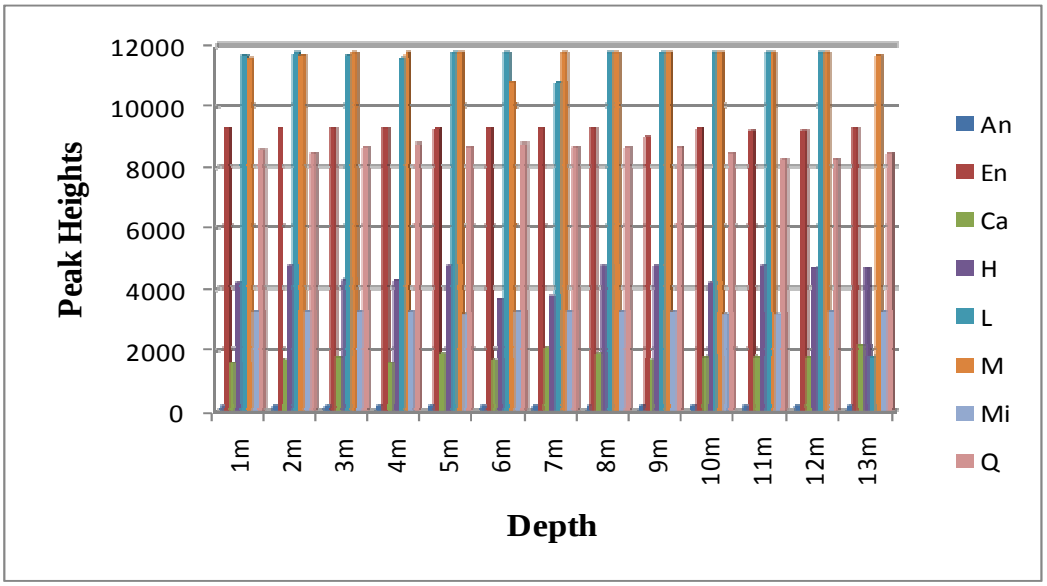

Figure 5.7. Bulk XRD mineral mean peak heights in 8-year-old (AMB 81) Tutuka ash cores (An=anorthite, En=enstatite, Ca=calcite, H=hematite, L=lime, M=mullite, Mi=mica, Q=quartz).

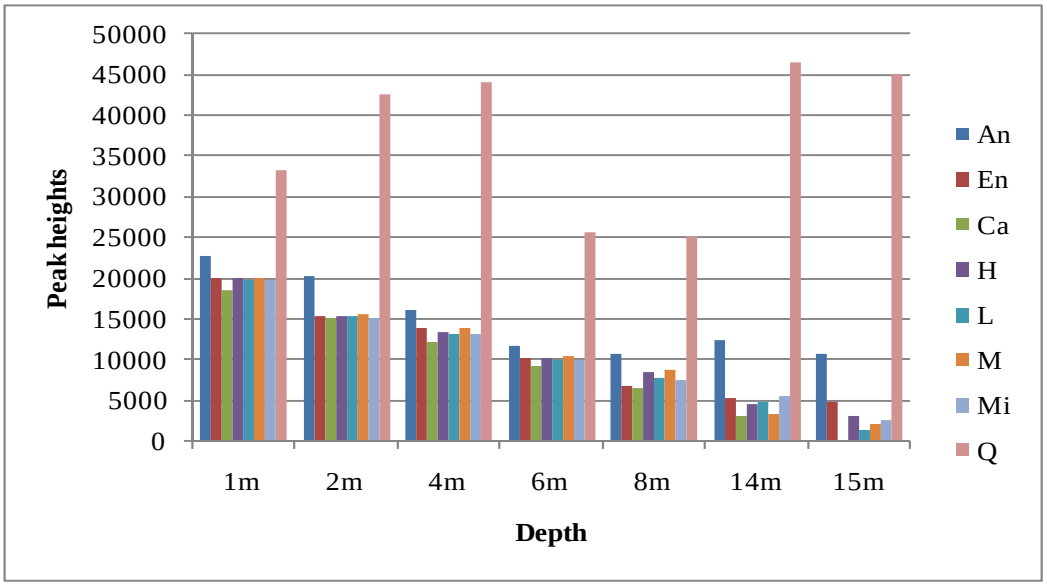

Figure 5.8. Bulk XRD mineral mean peak heights in 20-year-old (AMB 79) Tutuka ash cores (An=anorthite, En=enstatite, Ca=calcite, H=hematite, L=lime, M=mullite, Mi=mica, Q=quartz).

The statistical result is shown in the Table 5.1. The relative standard deviation (RSD) in the peak heights of 1-year-old drilled core (Figure 5.6 and Table 5.1) showed highly significant variations which could be classified into 2 groups:

< 40 % Quartz

57-65 % Anorthite, Enstatite, Mica, Mullite, Hematite, Calcite and Lime

The relative standard deviation (RSD) of quartz phase (being < 40 %) indicates less in-homogeneity among the coal fly ash mineral phases. There are however more variation (57-65 %) in the peak heights of the following mineral phases, namely anorthite, enstatite, mica, mullite, calcite and lime. The in-homogeneous distribution of the calcite mineral phase could be attributed to continuous weathering occasioned by ingress of CO_2. There is a direct relationship between the calcite mineral phase peak heights and CaO (weight %). The depletion or enrichment of CaO (weight %) in coal fly ash agreed with the peak height of calcite which is an indication of the role of lime (CaO) in the formation of calcite ($CaCO_3$). The mica mineral phase also exhibited heterogeneous distribution in the drilled weathered cores which could be attributable to continuous weathering process.

Table 5.1. Summary of the statistical analysis of the peak heights of various mineral phases in Tutuka fly ashes (1 year, 8 year and 20-year-old dry disposed cores)

1 year old core ash samples								
	An	**En**	**Ca**	**H**	**L**	**M**	**Mi**	**Q**
Mean	12776.3	13262.8	13614	13474.9	13128.2	13969	13310.4	33003.8
Stdev.	8198.9	8153.39	7813	7797.4	8057.18	7966.25	7759.5	12837.9
RSD %	64.17	61.48	57.39	57.87	61.37	57.03	58.30	38.90
8 year old ash core samples								
	An	**En**	**Ca**	**H**	**L**	**M**	**Mi**	**Q**
Mean	200.00	9261.54	1815.38	4453.85	10923.08	11692.31	3276.92	8600.00
Stdev.	0.00	83.56	170.28	381.53	2646.67	264.46	42.13	161.72
RSD %	0.00	0.90	9.38	8.57	24.23	2.26	1.29	1.88
20 year old ash core samples								
	An	**En**	**Ca**	**H**	**L**	**M**	**Mi**	**Q**
Mean	14955.4	10933.9	9302.0	10754.1	10291.0	10630.0	10513.0	37438.0
Stdev.	4862.3	5729.2	6515.9	5985.0	6284.1	6487.6	5980.7	9230.3
RSD %	32.5	52.4	70.0	55.7	61.1	61.0	56.9	24.7

[An=Anorthite, En=Enstatite, Q=Quartz, Mi=Mica, M=Mullite, Ca=Calcite, H=Hematite, L=Lime].

Mullite showed variations (57-65 %) in the peak heights which might be due to the conversion of clays that contain < 60 % of Al_2O_3. The mullite peak heights depend on the amount of SiO_2 and Al_2O_3 in the mineral phase (Figure 5.7 and Table 5.1). Anorthite is a rare compositional variety of plagioclase feldspar (calcium rich end-member of plagioclase). Anorthite has been found in other fly ashes obtained from coals in which Ca is present in inherent minerals together with other minerals with which calcium reacts.

Anorthite showed variations (57-65 %) in peak height which could be due to chemical interactions of CaO, SiO_2 and Al_2O_3 in the mineral phase of coal fly ash samples. Enstatite is a magnesium silicate mineral. Enstatite shows variations (57-65 %) in peak heights due to prevailing chemical interactions of SiO_2 and MgO in the mineral phase of coal fly ash samples. Hematite (Fe_2O_3) is a heat transformation product of pyrite in feed coal and accordingly hematite was revealed by XRD in the ash core samples. Previous studies had shown that pyrite (FeS_2) was present in the feed coal as a fine-grained mineral (Spears and Martinez-Tarazona, 1993). Hematite (Fe_2O_3) phase showed variations (≈ 57.87 %) in peak heights distribution among the

fly ash samples. This trend is an indication of the instability of the Fe containing mineral phases in the ash core samples of 1-year-old ash at the dry disposed fly ash dump site. The relative standard deviation (RSD) in the peak heights of the 8-year-old ash (Figure 5.7 and Table 5.1) showed low variations which could be classified into 3 groups:

< 3 % Anorthite, Enstatite, Quartz, Mica, Mulite,

< 10 % Calcite and Hematite

< 25 % Lime

The relative standard deviation (RSD) of anorthite, enstatite, quartz, mica and mullite (being < 3 %) indicates homogeneity among these coal fly ash mineral phases in this core. There was however more variation (< 25 %) in the mean peak heights of lime (CaO) in the 8-year-old ash samples. The in-homogeneous distribution of calcite and hematite mineral phase (< 10 %) could be attributed to continuous differential weathering occasioned by chemical interaction of fly ash with atmosphere, ingressed carbon dioxide and percolating rain water (see Section 2.4.6).

The relative standard deviation (RSD) in the peak heights of the 20-year-old ash (Figure 5.8 and Table 5.1) showed moderate variations which could be classified into 3 groups:

< 35 % Anorthite

< 60 % Enstatite, Mica and Hematite

≤ 70 % Lime, Mullite and Calcite

There is obvious similarity in the variation of mineral peak height of 20 year and 1-year-old drilled cores (Figures 5.6 & 5.8) which is attributed to in-homogeneity due to textural differences in 1 year and 20-year-old drilled ash cores (see Section 3.7). Less variation in the mineral phase peak heights is observed with the age of the ashes due to dissolution/precipitation of secondary phases (stability of mineral phases) with time. The decrease or increase in the mean peak height of some minerals in the 3 drilled ash cores suggest variation in the steady state conditions at the interface of mineral particles due to reduction in the ash pore water pH (see Section 5.8). The RSD in the mineral peak heights showed correlation with already significant change in chemistry of the 3 drilled ash core samples (see Section 5.4). This showed that significant flushing/leaching

of major components of fly ash had taken place within 1 year of ash dumping due to continuous irrigation with high saline effluents (see Table 5.3).

Bulk chemical composition as determined by XRF analysis (see Section 5.4) of all the coal fly ash samples also revealed major presence of MgO in fly ash which could result in the formation of enstatite ($Mg_2Si_2O_6$) upon concomitant depletion of quartz. Mullite and quartz were the species identified, quartz being the only original unaltered coal mineral phase present (Bandopadhyay, 2010). Mullite and hematite are products of the thermal transformation of some minerals present in the coal during combustion. Mullite ($3Al_2O_32SiO_2$) is a product of aluminosilicate transformation. It has been reported that mullite in fly ash is formed through the decomposition of kaolinite, $Al_2Si_2O_5(OH)_4$ (White and Case, 1990; Spears, 2000), which is entrapped in the parent coal.

For UK fly ashes mullite is reported to form preferentially from kaolinite, whereas illite contributes towards the glass phase (Spears, 2000). Calcite ($CaCO_3$) was found in all coal fly ash core samples. Calcite precipitation in weathered fly ash is as a result of chemical interactions of calcium oxide (lime) rich fly ash with ingressed CO_2 (Soong *et al*., 2006) during weathering. The high concentration of calcium oxide as evidenced by XRF analysis (see Section 5.3) of the core samples suggests possible secondary formation of anorthite ($CaAl_2Si_2O_8$), calcite, and lime in the fly ash dump (Bayat, 1998). Anorthite is a calcium mineral not present in coals. The formation of anorthite requires the mixing of separate calcium and aluminosilicate mineral domains. Thus, as calcium aluminosilicates are not found in fly ashes, their presence in coal-fired boiler deposits has been used to probe the mechanism of deposit formation. Studies of a range of coal fired boiler deposits, having different temperature histories, together with complementary investigations on mineral mixtures and coal ashes, have demonstrated that anorthite is formed via solid-state reactions and not by recrystallization from a homogeneous melt (Unsworth *et al*., 1988).

5.3 Bulk chemical composition of 2 week, 1 year, 8 year and 20-year-old dry disposed ash cores

The bulk chemistry by depth of the ash dump was carried out with X- ray fluorescence technique (XRF) with a view to better understand the change in ash core chemistry under the real dry disposal conditions. The experimental protocol for this section is reported in Appendix Aiv.

Tables 5.2, 5.3, 5.4 and 5.5 report the average chemical composition of 2 week, 1 year, 8 year and 20-year-old dry disposed ash cores respectively. The dry disposed ash core samples were taken from the different depth profiles from 1 m to 29 m this varied for each core (see section 4.1). The main inorganic elements in the fly ash samples as revealed by XRF are Si and Al, suggesting abundance of quartz and aluminosilicate as confirmed by XRD mean mineral peak heights (Figures 5.3 and 5.4), followed in decreasing order by Ca, Fe, Mg, Ti, Na, S, and Mg which are much less abundant. The percentage of lime (CaO) in the entire 2 week, 1 year, 8 year and 20-year-old dry disposed ash core samples range from 6.48-7.89 %, 5.24-10.02 %, 4.2-5.53 % and 2.18-6.96 % respectively. The trend showed an increase in CaO percentage at the top and middle sections of 1 year and 20-year-old, and the bottom sections of 1 year and 8-year-old ash cores.

The relative standard deviation (RSD) of the major oxide constituents in the 2 week, 1 year, 8 year and 20-year-old ash samples range from 0.93 – 10.46 %, 2.14-43.05 %, 1.46-23.40 % 3-233.27 % respectively (Tables 5.2, 5.3, 5.4 and 5.5). The chemical constituents having the least variation in the fly ash samples were SiO_2 and Al_2O_3, while the highest variation were in CaO, Na_2O, SO_3 and P_2O_5. The high variation in CaO correlates with the formation of calcite in 1 year, 8 year and 20-year- old fly ash dump. The variation in Na_2O, SO_3 and P_2O_5 is probably due to in-homogenous brine irrigation. The ratio of SiO_2/Al_2O_3 in all the drilled cores is ≥ 2 and thus can also be classified as silico-aluminate fly ash (Vassilev and Vassileva, 2007). The bulk chemical composition and classification systems of coal fly ash always include data for LOI.

The LOI value was determined at 700-1000 ºC, according to different national standards. The values are 3.98-5.38 %, 3.45-7.07 %, 3.29-7.06 % and 0.02-0.2 % in 2 week, 1 year, 8 year and 20-year-old drilled cores respectively. These are low values in general. However, the LOI contents are not equivalent concentration of organic matter in fly ash. The weathered ash is low in LOI probably due to incorporation of structural H_2O (due to hydration) and loss of CO_2 as a result of chemical and mineralogical transformations.

Vassilev and Vassileva (2007) reported that the LOI determined in fly ash poor in Ca has also overestimated OM contents due to the alteration and transformation of FAs during their storage and heating up to 1000 ºC respectively. The LOI trend dry of disposed ashes is in general agreement with previous results from the examination of flow value of mortar containing fly

ashes whose unburned carbon content was in the range of 0.4-18.0 % (Kanazu *et al*., 1998). For accurate measurements of organic matter, a conventional elemental analyzer was used to detect the concentration of carbon in the dry disposed ashes. The results are presented in Tables 5.2, 5.4 and 5.5. The average values of carbon (% C) in the 2 week, 1 year, and 20-year-old dry disposed ash cores are 1.65, 1.03 and 0.87 respectively. Whereas the relative standard deviation (RSD %) values are 19.49 %, 26.43 % and 43.34 % respectively.

The percent carbon (% C) trend showed that chemical alteration and mineral transformation caused by weathering/ageing has led to the depletion of organic matter in dry disposed fly ashes (see Tables 5.2, 5.3 and 5.5). The relative standard deviation (RSD %) also indicates significant difference in percent carbon among the dry disposed core ash of the same weathering stage (age). This could be ascribed to rapid weathering or in-homogenous irrigation of the ash dumps with high saline effluents. This suggests differential chemical weathering due to the effect of infiltrating water. Based on the ratio of detrital and authigenic minerals (DAI) some genetic information for the formation of fly ash could be deduced (Vassilev and Vassileva, 2007).

The chemical composition in this index (DAI) also symbolizes the different index mineral (IM) in coal. For example, the oxides of Si, Al, K^+, Na^+, and Ti represent minerals and phases such as quartz, feldspars, clay and mica minerals (excluding some kaolinite and illite), volcanic glass, Al oxyhydroxide, and rutile-anatase-brookite, which commonly have dominant detrital genesis in coal. On the other hand, the oxides of Fe, Ca, Mg, S, P, and Mn represent minerals such as Fe-Mn sulphides; Ca-Fe-Mg sulphates, Ca-Mg-Fe-Mn carbonates and Ca-Fe phosphates, which commonly have dominant origin in coal (Vassilev and Vassileva, 1996b).

Table 5.2. Chemical composition of drilled core taken from 2-week-old section of the dry disposed fly ash dump

Sample ID	SiO_2%	Al_2O_3%	Fe_2O_3%	MnO%	MgO%	CaO%	K_2O%	Na_2O%	TiO_2%	P_2O_5%	SO_3%	LOI%	Total	% C	SiO_2/Al_2O_3	DAI
1M	53.67	23.70	5.40	0.06	1.48	7.01	0.75	0.57	1.81	0.31	0.23	4.98	99.97	1.08	2.26	5.56
2M	53.75	23.27	5.22	0.06	1.57	7.29	0.81	0.57	1.87	0.32	0.21	5.01	99.96	1.97	2.31	5.47
3M	52.88	23.42	5.42	0.07	1.50	7.69	0.75	0.52	1.82	0.31	0.20	5.38	99.96	1.7	2.26	5.23
4M	53.24	23.60	5.50	0.06	1.48	7.48	0.77	0.51	1.83	0.32	0.20	4.98	99.97	1.23	2.26	5.31
5M	53.88	23.84	5.48	0.06	1.49	7.36	0.77	0.48	1.82	0.32	0.20	4.28	99.98	1.89	2.26	5.42
6M	53.53	23.82	5.52	0.06	1.35	7.30	0.79	0.49	1.83	0.34	0.20	4.74	99.97	1.75	2.25	5.45
7M	53.66	24.05	5.41	0.06	1.32	7.12	0.80	0.47	1.84	0.36	0.20	4.68	99.97	2.09	2.23	5.58
8M	52.86	23.93	5.37	0.06	1.38	7.37	0.81	0.47	1.88	0.37	0.20	5.26	99.97	1.37	2.21	5.42
9M	53.26	23.99	5.39	0.06	1.35	7.25	0.80	0.47	1.86	0.37	0.20	4.97	99.97	1.81	2.22	5.50
10M	52.87	24.01	5.30	0.06	1.41	7.39	0.80	0.48	1.86	0.37	0.20	5.22	99.97	1.86	2.20	5.43
11M	53.10	23.93	5.56	0.07	1.33	7.46	0.81	0.45	1.91	0.38	0.19	4.78	99.96	1.6	2.22	5.35
12M	52.52	23.74	5.38	0.07	1.62	7.54	0.81	0.45	1.88	0.38	0.18	5.38	99.96	1.96	2.21	5.23
13M	52.76	23.81	5.63	0.06	1.35	7.74	0.83	0.46	1.96	0.39	0.18	4.78	99.96	2.24	2.22	5.19
14M	53.40	24.04	5.44	0.06	1.50	7.45	0.81	0.44	1.89	0.40	0.18	4.37	99.97	1.77	2.22	5.36
15M	53.14	24.12	5.53	0.06	1.28	7.54	0.83	0.45	1.91	0.42	0.19	4.48	99.97	2.12	2.20	5.36
16M	52.54	24.08	5.41	0.07	1.37	7.70	0.83	0.45	1.90	0.42	0.20	5.00	99.97	1.27	2.18	5.26
17M	52.84	23.95	5.43	0.06	1.69	7.36	0.81	0.43	1.90	0.38	0.19	4.93	99.97	1.81	2.21	5.29
18M	52.77	24.05	5.54	0.06	1.34	7.35	0.81	0.46	1.93	0.37	0.20	5.08	99.96	1.43	2.19	5.39
19M	52.80	23.70	5.89	0.07	1.35	7.61	0.84	0.45	2.00	0.36	0.20	4.68	99.95	1.23	2.23	5.16
20M	52.59	23.77	5.77	0.07	1.35	7.74	0.80	0.46	1.97	0.36	0.20	4.87	99.95	1.33	2.21	5.14
21M	52.87	24.03	5.32	0.07	1.48	7.75	0.77	0.48	1.87	0.35	0.20	4.78	99.97	1.46	2.20	5.28
22M	54.21	24.75	5.10	0.06	1.31	6.48	0.79	0.46	1.85	0.35	0.20	4.43	99.98	1.92	2.19	6.08
23M	52.95	23.17	5.38	0.06	1.62	7.89	0.85	0.54	1.95	0.33	0.21	4.98	99.95	1.67	2.28	5.13
24M	53.65	22.96	5.36	0.06	1.60	7.51	0.86	0.61	1.93	0.31	0.23	4.88	99.95	1.3	2.34	5.30
25M	54.12	23.39	5.14	0.06	1.55	7.71	0.86	0.61	1.96	0.34	0.24	3.98	99.97	1.41	2.31	5.38
Mean	53.19	23.80	5.44	0.06	1.44	7.44	0.81	0.49	1.89	0.36	0.20	4.84	99.96	1.65	2.24	5.37
Stdv.	0.50	0.36	0.17	0.003	0.12	0.29	0.03	0.05	0.05	0.03	0.01	0.34	0.01	0.32	0.04	0.19
RSD %	0.93	1.53	3.14	4.70	8.06	3.93	3.72	10.46	2.79	8.93	7.14	7.00	0.01	19.49	1.84	3.57

RSD = Relative standard deviation; LOI = Loss On Ignition; % C = Carbon percent

Detrital/Authigenic Index (DAI) = $SiO_2+Al_2O_3+K_2O+Na_2O+TiO_2/Fe_2O_3+CaO+MgO+SO_3+P_2O_5+MnO$.

Table 5.3. Chemical composition of drilled core taken from 1-year-old section of the dry disposed fly ash dump

Sample ID	Depth Reference	Lithology	SiO_2%	Al_2O_3%	Fe_2O_3%	MnO%	MgO%	CaO%	Na_2O%	K_2O%	TiO_2%	P_2O_5%	SO_3%	LOI%	Total	% C	SiO_2/Al_2O_3	DAI
1m	Top section	Coarse ash	55.43	23.87	4.52	0.05	2.07	6.17	0.67	0.87	1.51	0.35	0.18	4.33	100.01	0.85	2.32	6.17
2m			55.03	24.65	4.42	0.05	2.11	6.21	0.71	0.87	1.59	0.39	0.21	3.76	100.00	0.96	2.23	6.18
3m			54.65	24.26	4.32	0.05	2.06	6.03	0.70	0.85	1.53	0.37	0.20	4.98	100.01	1.23	2.25	6.30
4m		Fine ash	55.14	24.69	4.18	0.04	1.80	5.80	0.72	0.87	1.54	0.35	0.21	4.65	100.01	1.17	2.23	6.70
5m			52.24	25.06	4.04	0.04	2.03	6.95	0.83	0.67	1.60	0.43	0.21	5.92	100.01	1.06	2.08	5.87
6m	Middle section		58.21	23.09	4.91	0.05	2.05	5.24	0.69	0.52	1.58	0.06	0.15	3.45	100.00	0.69	2.52	6.75
7m			55.09	24.37	4.32	0.05	1.85	5.92	0.67	0.86	1.57	0.35	0.20	4.74	100.00	1.15	2.26	6.51
8m			55.79	24.55	4.36	0.04	1.75	5.63	0.63	0.88	1.53	0.32	0.20	4.34	100.00	0.84	2.27	6.78
9m			54.85	24.20	4.92	0.05	1.65	6.03	0.62	0.95	1.72	0.33	0.20	4.46	99.98	1.05	2.27	6.25
12m		Coarse ash	47.91	23.03	5.38	0.06	1.87	10.02	1.21	0.83	2.14	0.51	0.59	6.46	100.00	0.63	2.08	4.08
13m			50.63	24.46	4.46	0.05	2.17	8.56	1.12	0.74	1.83	0.55	0.35	5.08	100.00	1.02	2.07	4.88
14m			49.03	23.92	4.64	0.05	1.80	8.91	1.11	0.82	1.99	0.55	0.61	6.57	99.99	0.55	2.05	4.64
15m			51.81	25.07	4.04	0.04	2.09	7.26	0.81	0.69	1.64	0.45	0.22	5.89	100.00	1.24	2.07	5.68
17m			51.10	24.55	4.86	0.05	1.98	8.16	0.89	0.78	1.90	0.47	0.31	4.90	99.96	1.04	2.08	5.00
18m			51.50	24.11	4.32	0.04	2.23	7.36	0.93	0.69	1.59	0.42	0.24	6.56	100.01	1.19	2.14	5.39
19m		Loose fine ash	51.03	24.27	4.19	0.05	2.22	7.67	0.90	0.71	1.71	0.49	0.28	6.45	99.99	1.34	2.10	5.27
20m			52.41	24.70	4.06	0.04	1.96	7.07	0.78	0.67	1.60	0.44	0.23	6.06	100.02	0.68	2.12	5.81
22m	Bottom section		51.41	24.71	3.80	0.04	2.17	7.06	0.71	0.69	1.62	0.51	0.23	7.07	100.02	0.67	2.08	5.73
23m			52.06	23.49	5.08	0.05	2.07	7.53	0.91	0.68	1.82	0.33	0.27	5.71	100.01	1.11	2.22	5.15
26m			50.94	24.69	3.84	0.04	2.22	7.89	0.71	0.70	1.63	0.55	0.19	6.61	100.01	1.72	2.06	5.34
27m			51.41	24.12	4.31	0.04	2.22	7.39	0.71	0.65	1.62	0.50	0.24	6.81	100.01	1.24	2.13	5.34
28m			52.40	24.33	4.59	0.04	2.05	7.45	0.67	0.67	1.65	0.48	0.23	5.45	100.00	1.12	2.15	5.37
29m			52.19	24.31	4.47	0.05	2.21	7.77	0.72	0.66	1.64	0.49	0.23	5.26	100.00	1.21	2.15	5.22
Mean			52.71	24.28	4.44	0.05	2.03	7.14	0.80	0.75	1.68	0.42	0.26	5.46	100.00	1.03	2.17	5.67
Stdev			2.37	0.52	0.39	0.00	0.17	1.13	0.16	0.10	0.16	0.11	0.11	1.01	0.01	0.27	0.11	0.70
RSD %			4.49	2.14	8.70	8.89	8.15	15.89	20.19	13.65	9.30	25.54	43.05	18.46	0.012	26.43	5.07	12.27

RSD = Relative standard deviation; LOI = Loss On Ignition; % C = Carbon percent

Detrital/Authigenic Index (DAI) = $SiO_2+Al_2O_3+K_2O+Na_2O+TiO_2/Fe_2O_3+CaO+MgO+SO_3+P_2O_5+MnO$.

Table 5.4. Chemical composition of drilled core taken from 8-year-old section of the dry disposed fly ash dump

Chemical composition of 8 years old coal fly ash																	
Sample ID	Depth Reference	Lithology	SiO_2%	Al_2O_3%	Fe_2O_3%	MnO%	MgO%	CaO%	Na_2O%	K_2O%	TiO_2%	P_2O_5%	SO_3%	LOI%	Total	SiO_2/Al_2O_3	DAI
1M	Top section	Fracture, hard ash	55.81	24.47	5.03	0.04	2.20	4.55	0.57	0.65	1.4	0.06	0.17	5.05	100.0	2.28	6.88
2M			56.76	24.7	4.98	0.04	2.08	4.73	0.60	0.69	1.41	0.06	0.14	3.81	100.0	2.28	6.88
3M			55.12	23.83	4.82	0.04	1.91	4.39	0.57	0.75	1.34	0.06	0.14	7.06	100.0	2.31	7.19
4M	Middle section		57.36	24.98	4.85	0.04	2.03	4.41	0.68	0.74	1.39	0.06	0.17	3.29	100.0	2.30	7.37
6M			57.58	25.03	4.82	0.04	1.93	4.31	0.63	0.74	1.39	0.06	0.13	3.34	100.0	2.30	7.56
7M			57.68	25.23	4.66	0.04	1.80	4.2	0.66	0.76	1.4	0.06	0.16	3.35	100.0	2.29	7.86
8M			57.37	24.25	5.08	0.04	1.89	4.34	0.64	0.77	1.34	0.06	0.12	4.13	100.0	2.37	7.33
9M	Bottom section		55.77	23.52	5.36	0.05	2.31	5.4	0.73	0.52	1.56	0.06	0.18	4.56	100.0	2.37	6.15
10M		Brittle ash	55.91	23.69	5.22	0.05	2.25	5.53	0.70	0.51	1.56	0.06	0.14	4.40	100.0	2.36	6.22
11M			56.56	23.98	5.14	0.05	2.32	5.4	0.78	0.51	1.58	0.06	0.19	3.42	100.0	2.36	6.34
12M		Unconsolidated ash	55.77	23.54	5.63	0.04	2.38	5.19	0.84	0.54	1.54	0.06	0.21	4.27	100.0	2.37	6.09
13M			56.0	23.3	5.49	0.05	2.33	5.29	0.81	0.55	1.54	0.06	0.26	4.34	100.0	2.40	6.10
Mean			56.47	24.21	5.09	0.04	2.12	4.81	0.68	0.64	1.45	0.06	0.17	4.25	100.0	2.33	6.83
Stdev			0.82	0.63	0.28	0.00	0.20	0.49	0.09	0.10	0.09	0.00	0.04	1.00	0.01	0.04	0.61
RSD %			1.46	2.62	5.52	10.88	9.23	10.12	12.68	16.29	6.12	0.00	22.49	23.64	0.01	1.75	8.89

RSD = Relative standard deviation; LOI = Loss On Ignition; % C = Carbon percent

Detrital/Authigenic Index (DAI) = $SiO_2+Al_2O_3+K_2O+Na_2O+TiO_2/Fe_2O_3+CaO+MgO+SO_3+P_2O_5+MnO$.

Table 5.5. Chemical composition of drilled core taken from 20-year-old section of the dry disposed fly ash dump

Sample ID	Depth Reference	Lithology	SiO_2%	Al_2O_3%	Fe_2O_3%	MnO%	MgO%	CaO%	Na_2O%	K_2O%	TiO_2%	P_2O_5%	SO_3%	LOI%	Total	% C	SiO_2/Al_2O_3	DAI
1m	Top section	Consolidated solid ash	57.07	23.16	4.56	0.04	2.07	5.23	0.75	0.49	1.55	0.06	0.18	4.84	100.01	0.67	2.46	6.83
2m			56.89	24.89	4.21	0.04	1.96	5.59	0.69	0.84	1.49	0.35	0.20	2.86	100.00	0.6	2.29	6.87
3m			58.82	23.91	4.66	0.04	1.99	5.05	0.68	0.51	1.56	0.06	0.16	2.56	100.00	0.67	2.46	7.15
4m	Middle section		54.02	21.01	6.52	0.06	1.86	6.96	0.82	0.60	2.03	0.07	0.48	5.49	99.91	1.13	2.57	4.92
5m			57.86	23.25	4.68	0.04	1.94	5.29	0.73	0.49	1.57	0.07	0.19	3.89	100.00	1	2.49	6.87
6m			57.32	23.07	4.53	0.04	2.10	5.27	0.74	0.48	1.53	0.06	0.17	4.71	100.01	0.84	2.48	6.83
7m			57.73	23.19	5.04	0.04	2.00	6.04	0.72	0.45	1.61	0.07	0.20	2.91	100.00	1.37	2.49	6.25
8m	Bottom section		56.76	22.75	4.96	0.04	2.16	5.87	0.71	0.45	1.57	0.06	0.19	4.49	100.01	1.6	2.50	6.20
9m		Coarse moist ash	55.13	25.38	1.57	4.38	5.91	0.48	1.75	0.56	0.04	0.07	0.63	3.90	99.80	0.87	2.17	6.35
13m		Dolerite+Clay	58.36	17.21	0.92	7.95	4.66	1.76	3.53	1.30	0.12	0.16	0.06	3.71	99.73	0.32	3.39	5.19
14m			59.97	14.82	8.49	0.08	3.02	3.24	0.77	2.41	0.96	0.14	0.03	6.02	99.96	0.29	4.05	5.26
15m			59.75	14.83	8.59	0.08	2.90	2.18	0.68	2.58	0.90	0.13	0.02	7.33	99.96	1.1	4.03	5.67
Mean			57.47	21.46	4.89	1.07	2.71	4.41	1.05	0.93	1.24	0.11	0.21	4.39	99.95	0.87	2.78	6.20
Stdev.			1.73	3.73	2.27	2.50	1.29	2.00	0.84	0.77	0.62	0.08	0.18	1.40	0.09	0.38	0.66	0.77
RSD %			3.00	17.37	46.47	233.27	47.34	45.36	79.76	82.93	49.77	76.81	86.02	31.94	0.09	43.34	23.58	12.34

RSD = Relative standard deviation; LOI = Loss On Ignition; % C = Carbon percent

Detrital/Authigenic Index (DAI) = $SiO_2+Al_2O_3+K_2O+Na_2O+TiO_2/Fe_2O_3+CaO+MgO+SO_3+P_2O_5+MnO$.

Tables 5.2 – 5.5 showed variations in the ratio of detrital and authigenic minerals (DAI) for various depth intervals of 2 week, 1 year, 8 year and 20-year-old drilled ash cores. A relatively high DAI value was recorded for the top section of 1 year and 8-year-old fly ash; both top and middle sections of 20-year-old dry disposed ash cores, middle and bottom sections of 8-year-old dry disposed ash cores. This implies that mineral with dominant detrital genesis in coal are relatively abundant in drilled ash cores from these highlighted depth intervals. A relatively low ratio of DAI values were recorded for bottom sections of 20 year and 8-year-old fly ash; middle and bottom section of 1-year-old fly ash implying that minerals with dominant origin in coal fly ash are relatively abundant at these considered depth intervals. This is as a result of chemical interaction of fly ash with the atmosphere, ingressed carbon dioxide and percolating rain water. The DAI values are 5.14 -6.08 %, 4.08-6.78 %, 6.09-7.86 % and 4.92-7.15 % in 2 week, 1 year, 8 year and 20-year-old drilled ash cores respectively. The variation in the DAI values at various depth intervals in both 1 year and 8-year-old ash cores from the Tutuka ash dump is due to differential chemical weathering. The trend shows relatively higher DAI values for 8 year and 20-year-old in comparison with 1-year-old drilled ash cores indicating minerals that have dominant detrital genesis in coal are more abundant and achieved stability with age.

Roy and Griffm (1982) classified fly ash based on the intersection of the sum of their major oxides: sialic: $SiO_2+Al_2O_3+TiO_2$; calcic: $CaO+MgO+NaO_2+K_2O$; and ferric: $Fe_2O_3+MnO+P_2O_5+SO_3$ in a ternary diagram. Based on the chemical composition of fly ash, about seven intermediate fly ash subgroups exists, such as sialic, ferrosialic, calsialic, ferrocalsialic, ferric, calcic and ferrocalcic (Vassilev and Vassileva, 2007) fly ash. Figure 5.11 shows that 1-year-old ash core samples were both sialic and ferrocalsialic in chemical composition (i.e. essentially Fe, Ca, Al and Si). Ternary diagram presented in Figures 5.9, 5.10 and 5.12 showed that 2 week, 1 year, 8 year, and 20-year-old dry disposed ash core samples were sialic in chemical composition (i.e. essentially dominated by Al and Si). These trends show that in the 1-year-old drilled cores, there is already a significant change in chemistry of ash core due to rapid weathering or due to irrigation with high saline effluents. The coal fly ash transforms into a more clay-like material due to long-term mineralogical changes occasioned by the weathering process. Recent work done by Valentim and Hower (2010) on the influence of feed and sampling systems on element partitioning in Kentucky fly ash showed that majority of coal fly ash were sialic, sialic-ferrosialic or ferrosialic depending on the coal

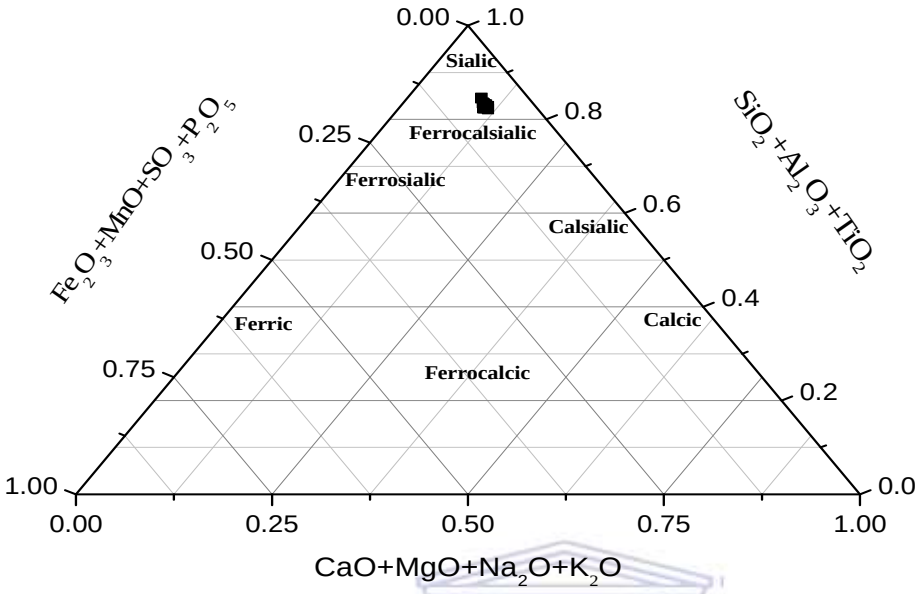

Figure 5.9. Ternary oxide plots for classification of the 2-week-old drilled ash cores.

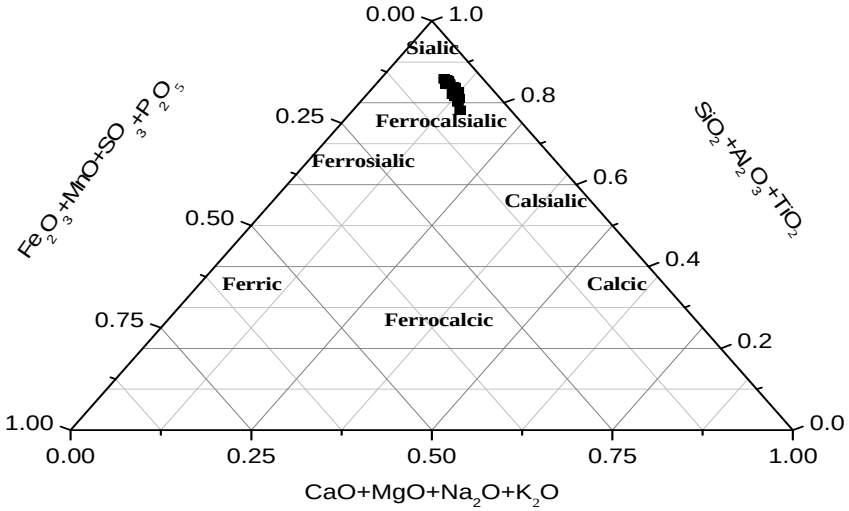

Figure 5.10. Ternary oxide plots for classification of the 1-year-old drilled ash cores.

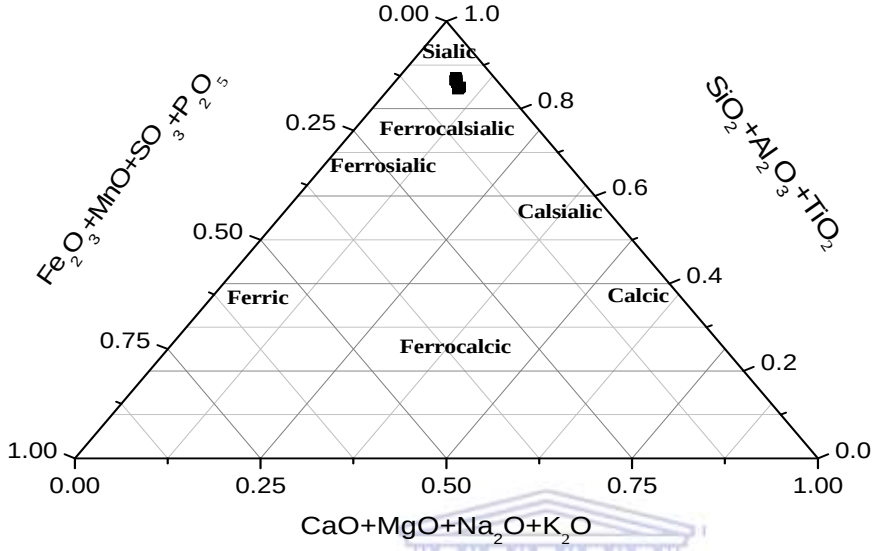

Figure 5.11. Ternary oxide plots for classification of the 8-year-old drilled ash cores.

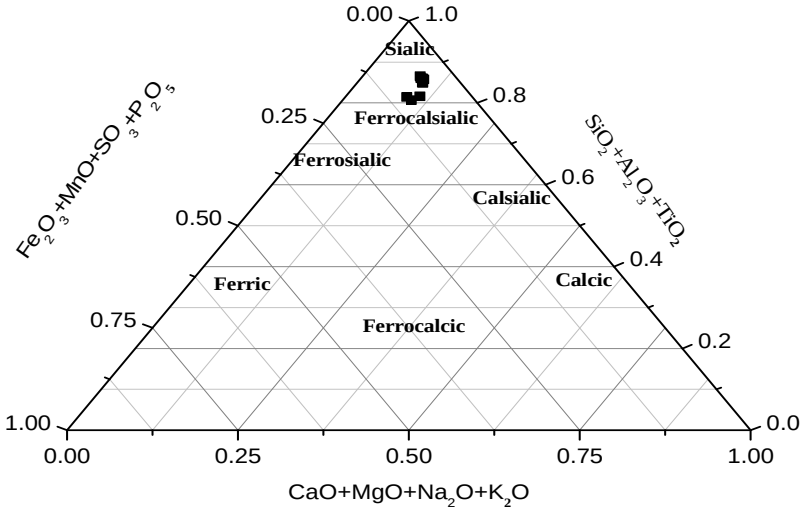

Figure 5.12. Ternary oxide plots for classification of the 20-year-old drilled ash cores.

combustion temperature, the sampling point of the ash and the ash interaction chemistry. In this study, we assumed that the first two factors were constant while the differences in classification would be mainly to the ash chemistry. The obvious disparity in the classification of the 20 year and 8 year versus the 1-year-old fly ash core samples indicates that chemical interaction of fly ash with ingressed O_2, ingressed CO_2 and percolating rain water (see Section 2.4.6) during storage have a significant impact on the overall chemistry and mineralogy.

5.4 Enrichment and depletion of major and trace components in dry disposed ash cores

The experimental protocol for results presented in this section is documented in Appendix Aiv. The XRF data for 1 year and 20-year-old drilled ash core was used to calculate enrichment and depletion of major and trace components in the fly ash under real disposal conditions. The chemical compositions of both fresh and composite weathered ash core samples (i.e. core samples taken from 9 and 10 m depths of 20-year-old section of the ash dump) from the Tutuka power station in the Mpumalanga Province, South Africa is presented in Table 5.6.

Table 5.6. Chemical composition of fresh and composite weathered ash core

Sample ID	L.O.I[a]	Al_2O_3	CaO	SiO_2	Fe_2O_3	MgO	K_2O
FA[b]	11.23	23.01	6.38	49.24	5.25	1.17	0.91
WA[c]	3.85	22.95	4.66	54.39	5.64	3.49	0.69
Sample ID	Na_2O	SO_3	CaO/SiO_2	CaO/Al_2O_3	SiO_2/Al_2O_3	SO_3/Al_2O_3	$CaO/Al_2O_3+SO_3$
FA[b]	0.32	0.29	0.12	0.28	2.13	0.01	0.27
WA[c]	0.83	0.72	0.09	0.20	2.37	0.03	0.19

L.O.I[a]. : loss on ignition, FA[b]: Tutuka fresh ash, WA[c]: weathered ash core (20-year-old).

The percentage of SiO_2 + Al_2O_3 + Fe_2O_3 in both fresh and weathered coal fly are 77.5 % and 82.98 % respectively and they contain less than 10 % lime. Thus, the ash can be classified class F according to ASTM C 618, (1993). The results of the bulk chemical composition of the ash cores revealed that the sum of the mass % composition of the major oxides (i.e. SiO_2, Al_2O_3 and Fe_2O_3) in all the ash samples was more than 70 %, $Na_2O \leq 1.5$ % (with the exception of 20-year-old drilled core samples taken at 9 m and 13 m (see Table 5.5) and loss on ignition (LOI) ≤ 8 % hence all the dry disposed fly ash dump cores can be categorized as Class F ash (ASTM C 618). The ratios of different oxides present in the fresh fly ash and weathered fly ash showed simple

relationships. The ratios of CaO/SiO_2 and CaO/Al_2O_3 and $CaO/Al_2O_3+SO_3$ are enriched in the fresh fly ash while ratios of SiO_2/Al_2O_3, SO_3/Al_2O_3 are enriched in the weathered ash core. In the longer term, the metastable amorphous aluminosilicate and amorphous Fe-oxyhydroxide (i.e. secondary phase) in fly ash (Warren and Dudas, 1985) convert to clayey material (smectite and/or halloysite) (Zevenbergen, 1999) and Fe-oxide respectively in disposal environments (Donahoe, 2004). This phenomenon might responsible for the observed enrichment and depletion of different oxides ratios in both fresh and weathered ash core. Thus, the amorphous aluminosilicate and amorphous Fe-oxyhydroxide content in weathered ash core is attributed for higher content of SiO_2 and Fe_2O_3 (see Table 5.6) and is typically formed in an alkaline environment (White, 1984). The weathered ash core is low in LOI which could be due to chemical interaction of fly ash with of ingressed CO_2 from atmosphere over time.

It is noteworthy that the mass % of the major element Si varies through the depth of the core with an increase of nearly 3 %, to 58 mass % of SiO_2 at a depth of 6 m in the 1-year-old core whereas in the case of the 8-year-old core a 2 % increase of SiO_2 to a level of 57.5 mass % can be observed at levels between 4-8 m, showing dissolution of major components in the matrix of older ash cores. This will have implications overtime for release of all the elements associated with the readily soluble glassy phase of ash. It should also be noted that there is an increase of CaO from an average of 6-7 mass % near the surface of the dump to 10 mass % CaO at 12 m depth of the 1-year-old drilled core. This also suggests dissolution of major components and its subsequent rapid transportation down the ash column with percolating rain water in the dry disposed ash. In the 20-year-old and 8-year-old drilled core, the CaO constituents have been considerably weathered. The amount of depletion in the 20-year-old drilled ash cores is generally around 4 mass % between 9-15 m, whereas in the 8-year-old drilled ash core the amount of CaO depleted throughout to levels generally < 5 mass % apart from the deeper parts of the core between 9-13 m where the mass % is approximately 5.4 mass %, showing deep and extensive chemical weathering.

The major oxides mass % in the XRF data of 1 year and 20-year-old drilled ash cores (see Tables 5.3 and 5.5) was converted to elements mass % (http://www.marscigrp.org/elconv.html). The data generated for 1 year and 20-year-old ash cores was normalized with the XRF data of the fresh ash from the same power station to give ratios which indicated the relative enrichment or

depletion of various species with respect to the fresh ash. The enrichment/depletion factors reported as ratios are presented in Table 5.7. This in turn will show the patterns of mobility or retardation of the species as a result of chemical weathering occasioned by the ingress of CO_2, O_2 and infiltration of rain water (see Section 2.4.6). In one year old ash core, elements such as K, Mn, Zn, P, Ba, Pb, V, Sr and Cr showed enrichment in the weathered ash core samples compared with fresh ash sample from the same power station. Pb showed evidence of erosion over time at the bottom of the 1-year-old ash column. Trace elements like Co showed inconsistent in the enrichment and depletion trend in the ash column. The rare earth elements such as Ce and Nd showed evidence of downward migration in the 1-year-old ash column (see Table 5.7). Major elements (such as Ti, Mg, Al, S, Na, Si, Ca) and trace elements like Ni, Y showed depletion in the 1-year-old weathered ash cores when compared with the fresh ash samples from the same power station. Chemical species such as Mg, Fe, Ca and Ti showed evidence of downward migration in the 1-year-old ash column (see Table 5.7).

In the 20-year-old ash cores, weathered ash core samples showed enrichment in major elements (such as Al, Na and Mn) and trace elements like Ni, Sr, Pb, V, Cr, and Co compared with fresh samples from the same power station. However, elements like Sr, Pb, Cr, Al and Co showed depletion at the bottom of the 20-year old ash column indicating erosion over time. Major species (such as Ti, K, Fe, Mg, Si, Al, P and Ca) and trace metals like Ba, Y, and Zr showed depletion in the 20-year-old ash cores when compared with fresh from the same power station. The Mg showed inconsistent in the enrichment and depletion trend in the 20-year-old ash column. The rare earth elements (such as Ce and Nd) showed depletion in the 20-year-old ash column. There is an obvious enrichment of Fe and K^+ at the bottom of 20-year-old ash column may be due to downward migration or contribution from the underlying dolorite/clay layers (Stucki, 2006; Mokobia *et al*., 2008).

Important feature from this section is the variation between enrichment and/or depletion factor of the elements in the 1 year and 20-year-old ash cores which is attributed to differential chemical weathering and in-homogenous continuous irrigation with high saline effluents (brine).

5.7. Chemical composition and calculated enrichment/depletion factors for 1 year and 20-year-old dry disposed ash cores

	Ba (ppm)				Pb (ppm)				V (ppm)				Zn (ppm)				Ce (ppm)				Nd (ppm)			
Depth(m)	**1 yr**	**Ratios**	**20 yr**	**Ratios**	**1 yr**	**Ratios**	**20 yr**	**Ratios**	**1 yr**	**Ratios**	**20 yr**	**Ratios**	**1 yr**	**Ratios**	**20 yr**	**Ratios**	**1 yr**	**Ratios**	**20 yr**	**Ratios**	**1 yr**	**Ratios**	**20 yr**	**Ratios**
FA	1199.9	1	1199.9	1	39.34	1	39.34	1	85.79	1	85.79	1	31.34	1	31.34	1	215.96	1	216	1	60.17	1	60.17	1
1	1496	1.25	0.61	5E-04	73	1.86	51	1.30	306	3.57	316	3.68	47	1.5	50	1.60	246	1.14	20	0.1	69	1.15	4	0.07
3	1475	1.23	3.62	0.003	85	2.16	53	1.35	298	3.47	305	3.56	40	1.3	50	1.60	52	0.21	22	0.1	25	0.36	11	0.18
5	1339	1.12	3.00	0.003	81	2.06	56	1.42	305	3.56	314	3.66	43	1.4	53	1.69	45	0.87	66	3.0	18	0.72	23	0.38
7	1414	1.18	3.19	0.003	85	2.16	62	1.58	284	3.31	240	2.80	45	1.4	53	1.69	99	0.46	61	0.9	34	0.57	9	0.39
9	1363	1.14	2.68	0.002	84	2.14	51	1.30	261	3.04	246	2.87	53	1.7	51	1.63	103	0.48	67	0.3	32	0.94	27	0.45
11	1384	1.15	3.33	0.003	75	1.91	60	1.53	320	3.73	294	3.43	49	1.6	51	1.63	69	0.67	46	0.7	22	0.69	21	0.78
13	1398.9	1.17	12.34	0.010	41.12	0.56	14	0.36	184.6	0.60	235	2.74	51.7	1.1	79	2.52	248.9	1.15	43	0.9	73	1.21	23	0.38
15	1432	1.19	14.03	0.012	45	0.53	17	0.43	216	0.72	192	2.24	49	1.2	93	2.97	260	1.20	28	0.7	83	1.14	15	0.65
	Cr (ppm)				**Y (ppm)**				**Ni (ppm)**				**Sr (ppm)**				**Zr (ppm)**				**Co (ppm)**			
Depth(m)	**1 yr**	**Ratios**	**20 yr**	**Ratios**	**1 yr**	**Ratios**	**20 yr**	**Ratios**	**1 yr**	**Ratios**	**20 yr**	**Ratios**	**1 yr**	**Ratios**	**20 yr**	**Ratios**	**1 yr**	**Ratios**	**20 yr**	**Ratios**	**1 yr**	**Ratios**	**20 yr**	**Ratios**
FA	132.14	1	132.14	1	79	1	79	1	95.79	1	95.79	1	1783	1	1783	1	404.3	1	404.3	1	24	1	24	1
1	417	3.16	116	0.88	61	0.77	69	0.87	73	0.76	115	1.20	2269	1.27	1923	1.08	164	0.41	225	0.56	14	0.58	31	1.29
3	399	3.02	215	1.63	63	0.80	45	0.57	85	0.89	109	1.14	2296	1.29	1862	1.04	195	1.19	221	0.98	24	1.00	27	1.13
5	441	3.34	247	1.87	58	0.73	48	0.61	81	0.85	110	1.15	2183	1.22	1868	1.05	185	0.95	235	0.58	24	1.00	33	1.22
7	363	2.75	300	2.27	61	0.77	53	0.67	85	0.89	112	1.17	2125	1.19	1898	1.06	209	0.52	259	0.64	26	1.08	30	1.25
9	316	2.39	260	1.97	62	0.78	67	0.85	84	0.88	113	1.18	2063	1.16	1950	1.09	223	0.55	265	0.66	21	0.81	27	1.13
11	496	3.75	285	2.16	66	0.84	51	0.65	75	0.78	107	1.12	2137	1.20	1889	1.06	190	0.85	239	0.90	25	1.19	36	1.33
13	*NA*	*NA*	138	1.04	123.9	2.03	47	0.59	73.9	0.77	90	0.94	2517	1.11	340	0.19	455.4	1.13	144	0.60	23.69	0.95	31	1.29
15	*NA*	*NA*	33	0.25	129	2.05	44	0.56	74	0.87	49	0.51	2730	1.19	197	0.11	480	1.05	161	0.40	15	0.63	20	0.65
	K (%)				**Mn (%)**				**Fe (%)**				**Mg (%)**				**S (%)**				**Na (%)**			
Depth(m)	**1 yr**	**Ratios**	**20 yr**	**Ratios**	**1 yr**	**Ratios**	**20 yr**	**Ratios**	**1 yr**	**Ratios**	**20 yr**	**Ratios**	**1 yr**	**Ratios**	**20 yr**	**Ratios**	**1 yr**	**Ratios**	**20 yr**	**Ratios**	**1 yr**	**Ratios**	**20 yr**	**Ratios**
FA	0.69	1	0.69	1	0.03	1	0.03	1	3.28	1	3.28	1	0.9	1	0.9	1	0.29	1	0.29	1	0.32	1	0.32	1
1	0.92	1.33	0.39	0.57	0.04	1.33	0.03	1	2.65	0.81	2.52	0.77	0.74	0.82	0.99	1.1	0.27	1.07	0.04	7.3	0.52	1.63	0.58	1.81
3	0.93	1.35	0.42	0.61	0.04	1.33	0.04	1.3	2.63	0.80	2.71	0.83	0.73	0.81	0.98	1.09	0.31	0.87	0.03	1.3	0.57	1.78	0.57	1.78
5	0.96	1.39	0.42	0.61	0.05	1.67	0.03	1.0	2.75	0.84	2.76	0.84	0.7	0.78	0.82	0.91	0.35	0.89	0.22	0.1	0.64	2.00	0.61	1.91
7	0.92	1.33	0.41	0.59	0.05	1.67	0.04	1.3	2.66	0.81	3.18	0.97	0.66	0.73	0.94	1.04	0.29	1.21	0.29	0.8	0.58	1.81	0.59	1.84
9	0.9	1.30	0.39	0.57	0.05	1.67	0.03	1.0	2.63	0.80	3.06	0.93	0.67	0.74	0.81	0.90	0.28	1.04	0.25	0.9	0.5	1.56	0.56	1.75
11	0.73	1.06	0.4	0.58	0.04	1.33	0.04	1.3	2.61	0.80	2.94	0.90	0.79	0.88	0.76	0.84	0.49	0.57	0.26	0.9	0.86	2.69	0.6	1.88
13	0.74	1.07	1.46	2.12	0.05	1.67	0.09	3.0	4.46	1.36	5.56	1.70	2.17	2.41	1.64	1.82	0.35	1.21	0.02	0.1	0.87	2.72	0.59	1.84
15	0.82	1.19	2.08	3.01	0.05	1.67	0.05	1.7	4.64	1.41	4.61	1.41	1.8	2.00	1.27	1.41	0.61	2.10	0.01	0.03	0.81	2.53	0.68	2.13
	P (%)				**Ti (%)**				**Ca (%**				**Al (%)**				**Si (%)**				**LOI (%)**			
Depth(m)	**1 yr**	**Ratios**	**20 yr**	**Ratios**	**1 yr**	**Ratios**	**20 yr**	**Ratios**	**1 yr**	**Ratios**	**20 yr**	**Ratios**	**1 yr**	**Ratios**	**20 yr**	**Ratios**	**1 yr**	**Ratios**	**20 yr**	**Ratios**	**1 yr**	**Ratios**	**20 yr**	**Ratios**
FA	0.13	1	0.13	1	1.55	1	1.55	1	4.56	1	4.58	1	12.76	1	12.79	1	26.37	1	26.38	1	11.3	1	11.3	1
1	0.2	1.54	0.03	0.23	1.46	0.94	1.3	0.84	4.76	0.96	3.09	0.67	14.45	0.88	19.23	1.50	24.64	0.93	26.4	0.99	3.5	0.31	4.84	0.43
3	0.21	1.62	0.03	0.23	1.5	0.97	1.48	0.95	4.42	0.97	2.84	0.92	14.68	0.98	14	1.37	24.84	0.99	26.2	0.99	2.89	0.83	2.54	0.52
5	0.19	1.46	0.03	0.23	1.48	0.95	1.43	0.92	4.67	0.95	3.66	0.80	14.23	1.03	13.81	1.01	24.29	0.92	26.3	0.99	4.09	0.36	5.49	0.49
7	0.18	1.38	0.03	0.23	1.48	0.95	1.53	0.99	4.25	0.93	4.45	0.97	14.58	0.98	13.29	1.04	25.17	0.97	25.3	0.96	2.89	0.71	4.1	0.75
9	0.17	1.31	0.03	0.23	1.45	0.94	1.51	0.97	4.05	0.89	4.22	0.95	14.59	1.00	13.43	1.05	25.21	0.96	25.8	0.98	3.4	0.30	3.9	0.95
11	0.22	1.69	0.03	0.23	1.52	0.98	1.52	0.98	5.14	0.79	4.04	0.96	14.47	1.01	13.49	1.00	23.29	0.88	25.7	0.97	4.8	0.42	4.19	0.37
13	0.55	4.23	0.07	0.54	1.83	1.18	0.88	0.57	6.11	1.34	3.33	0.82	12.94	1.01	9.11	0.71	23.63	0.90	27.3	0.94	5.08	0.45	3.71	0.89
15	0.55	4.23	0.06	0.46	1.99	1.28	0.76	0.49	6.36	1.39	1.46	0.44	12.65	0.99	9.15	0.72	22.92	0.87	28.4	0.96	5.89	0.52	7.33	0.65

5.5 FTIR analysis of 2 week and 20-year-old dry disposed ash cores

Analytical FTIR was used to characterise the absorption wavelength of the mineral component in the fly ash particles. This is used for the understanding of possible mineralogical changes in weathered ash cores. The experimental protocol for FTIR analysis is documented in Appendix Avi. The FITR analytical results are shown in Figures 5.13-5.15. The FTIR analysis at 1 m and 10 m depth for 20-year-old dry disposed ash cores was motivated by the pH profile studies which indicated three regions of suspected weathering, the shallow depths (0.75-1 m and 1-2 m) and at depths 9-10 m which are the point of contact with water (Petrik *et al*., 2008). The IR spectrum for 20-year-old fly ash (Figure. 5.13 & 5.14) show two main bands which are characteristic of the internal vibration of tetrahedral group (T=Al, Si). The first band shows absorption frequency at 2145 cm^{-1} which is associated with T-O bond asymmetric stretching vibrations while the second band at 427 cm^{-1} corresponds to T-O bond internal deformation vibrations (Criado *et al*., 2003). The presence of quartz in both the 2-week-old ash (Figure 5.15) and 20-year-old ash (Figures 5.12 & 5.13) possibly gives rise to the absorption bands at 433-427cm^{-1}, 770-764 cm^{-1}, 991-996 cm^{-1} (Criado *et al*., 2003; Fernandez-Carrasco and Vazquez, 2009; Mollah *et al*., 1999).

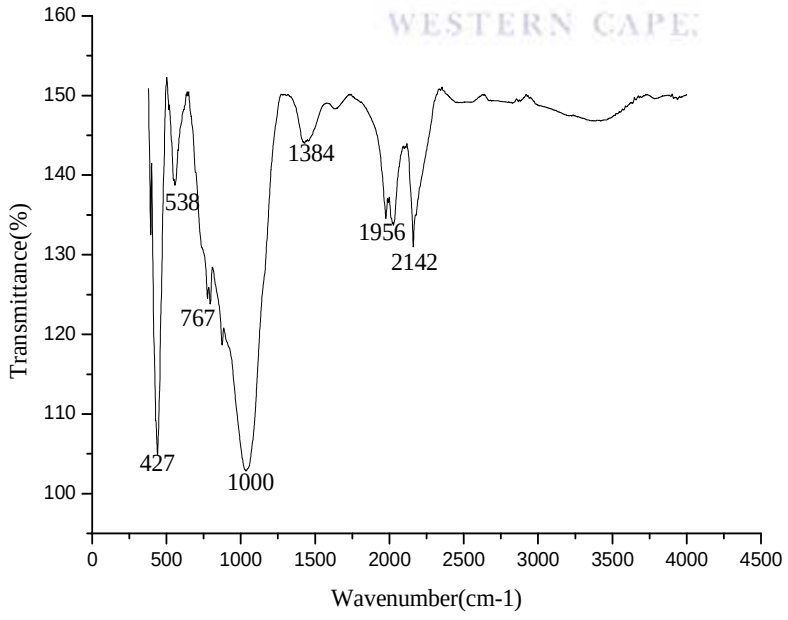

Figure 5.13. FT-IR Spectrum of 20-year-old dry disposed fly ash core (at 1 m depth) sample.

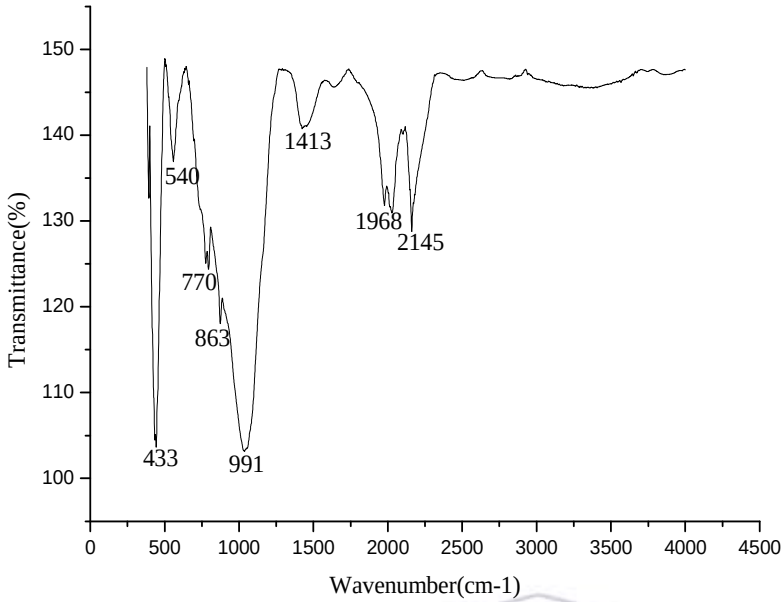

Figure 5.14. FT-IR Spectrum of 20-year-old dry disposed fly ash core (at 10 m depth) sample.

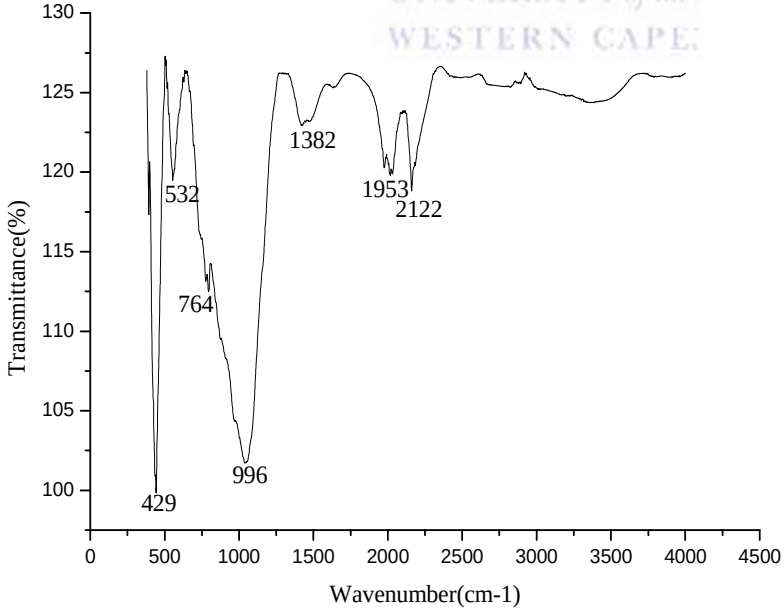

Figure 5.15. FT-IR Spectrum of 2-week-old dry disposed fly ash (at 1 m depth) sample.

The presence of mullite is possibly responsible for the series of bands at 540-532 cm^{-1} and 1413-1000 cm^{-1} (Mollah *et al*., 1999; Criado *et al*., 2003, Fernandez-Carrasco and Vazquez, 2009). No detection of calcite or mica (secondary minerals) due to their low abundances and/or amorphous character.

5.6 SEM and EDS analytical results

Analytical SEM/EDS was used to characterise morphology and chemical of individual particles of 2-week-old ash and 20-year-old weathered ash core. This is used for the understanding of formation mechanism (2-week-old ash) during combustion; and weathering mechanism (20-year-old ash) under real disposal conditions. The experimental protocol is presented in Appendix Avii. SEM photomicrograph of 2-week-old ash showed the presence of cenosphere, mineral phase and mineral aggregate such as quartz (Figure 5.16A). Agglomerated particles and irregularly shaped amorphous particles (Figure 5.16A) may have been due to inter-particle contact or rapid cooling (Kutchko and Kim, 2006). The surface of the sphere in the fresh sample exhibits a smooth appearance produced by aluminosilicate glass (Grochowiak *et al*., 2004). The size of the particles observed in this study ranged from less than 1 µm to greater than 50 µm. The majority of the particles ranged in size from approximately 1 to 10 µm and consisted of solid spheres. The cenosphere (hollow sphere) with a diameter of 20 µm tended to be at the centre of the size distribution (Figure 5.16A). The typical amorphous alumino-silicate sphere of the fly ash observed (Figure 5.16A) is attributable to the surface tension forces acting on the melt to minimize surface free energy during cooling (Mollah *et al*., 1999).

SEM photomicrograph of 20-year-old ash core sample taken at 9 m depth appears to be encrusted, etched and corroded (Figure 5.16B) due to chemical weathering (ageing). The differences in the surface morphology observed between the 2-week-old and 20-year-old ash samples are in agreement with the XRD results, which also showed the formation of secondary minerals in weathered dry disposed fly ash as a result of weathering. Figure 5.16 A&B showed elemental composition as determined by EDS; the predominant elements in the weathered and fresh fly ash samples were Si, Al, Fe, Ca, O_2, C, Ba, and K in various compounds. Aluminium was primarily associated with silicon and calcium. Lesser amounts of the C, O_2, S, Fe, Ba, and K were observed with the Al, Ca and Si.

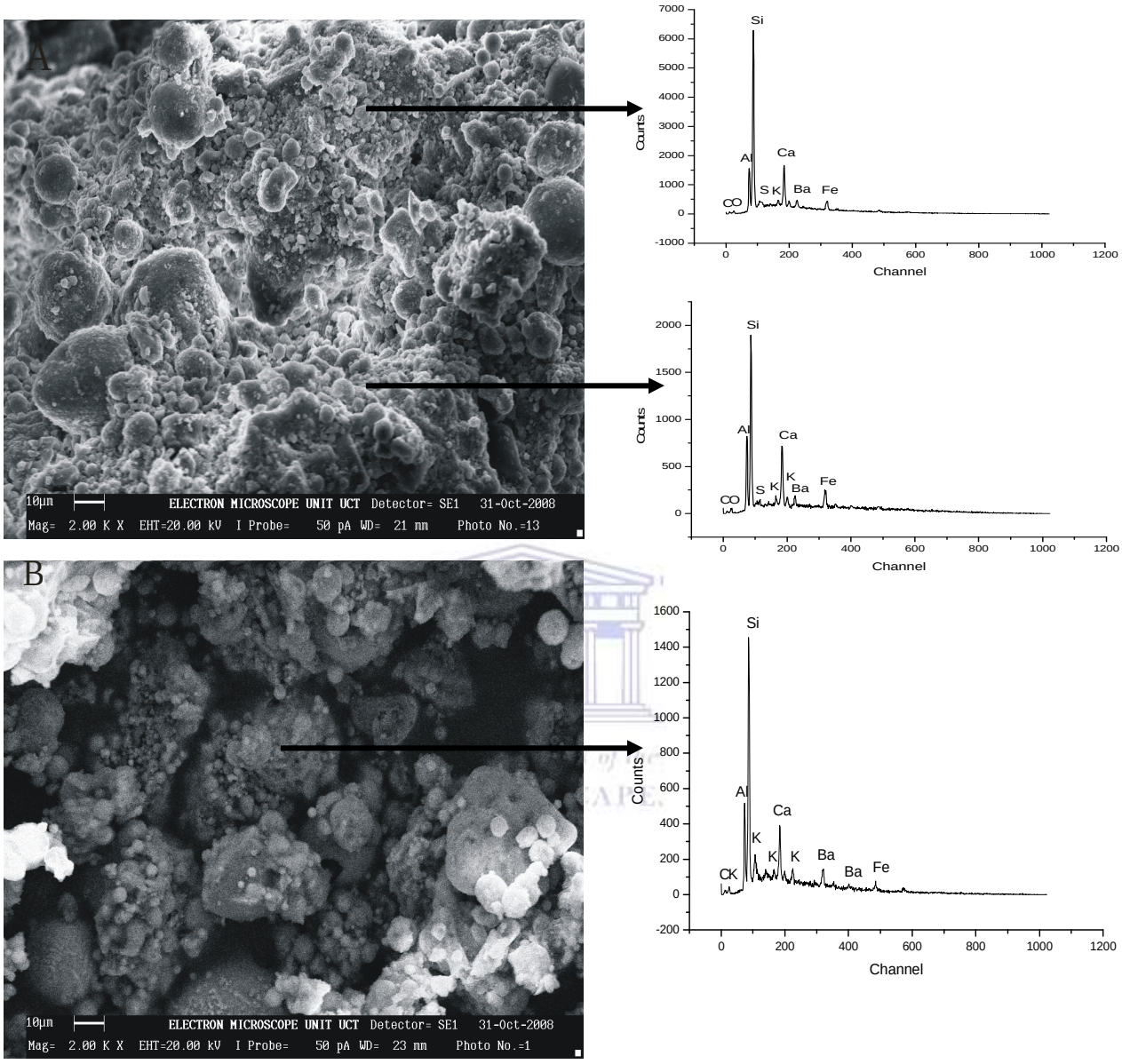

Figure 5.16. SEM photomicrograph of fly ash samples: (a) 2-week-old (1 m depth) (b) 20-year-old drilled ash core (9 m depth).

The only trace element identified was barium; it was observed only in fresh ash sample typically associated with S and O_2 (Figure 5.16A). Barium present in weathered ash sample is not associated with S and O_2 (Figure 5.16B). These trends obviously revealed the effect of long-term chemical weathering on the chemistry and quality of the weathered ash core samples from Tutuka ash dump site.

5.7 pH and EC of the extracted interstitial pore water

The experimental protocol is reported in the Appendix Ai and Aii. The results are shown in the Figures 5.17-5.20. The fresh ash sample leachates have a pH ranging between 11-12 and 0.44 $mScm^{-1}$. The pH for extracted interstitial water of 20 year, 1 year and 2-week-old dry disposed fly ashes alongside the stratigraphy by depth of each core are shown in Figures 5.16 – 5.19 respectively. The pH values of the 20-year-old ash cores is 7.2 - 9.9 whilst EC values range from 0.04 – 0.46 $mScm^{-1}$ (Figure 5.17). The pH values of the 8-year-old drilled cores is 8.95 – 10.7 while the EC values range from 0.51 – 1.03 $mScm^{-1}$. The 1-year-old ash cores has pH values of 8.7-10.6 and EC values of 0.2 – 0.7 $mScm^{-1}$ (Figure 5.18). Whereas in the case of 2-week-old ash cores, the pH values range from 9.9 – 10.9 and EC values are 0.19 – 0.25 $mScm^{-1}$ (Figure 5.18). The apparent relatively low pH values of 20 year, 8 year and 1-year-old drilled cores compared to 2-wks-old drilled cores is due to the flushing out of basic soluble constituents in fly ash caused by chemical weathering. The apparent low EC of the 2-week-old ash cores showed that it has not undergone intensive weathering process (leaching).

A review by Donahoe (2004) reports that this major drop in pH is caused by carbonation, hydrolysis and precipitation (called chemical weathering) after the depletion of portlandite ($Ca(OH)_2$). This pH range in all the ash cores is indicating the alkaline nature of a typical coal fly ash dump. A relatively low pH values are recorded at these sections i.e. [20 year (0.75-1 m, 7 m, 9-10 m and 15 m), 1 year (1-2 m, 19 m, 22 m and 28 m) and 2 week (26.5 m)]. The observed fluctuations in pH values with the depth of the ash column for 20 year, 8 year and 1-year-old ash core is probably due to the rapid dissolution and initial rapid flushing out of the soluble species in surface layers that can act as a pH buffering constituents in fly ash (Gitari *et al*., 2009a). The trend of high pH values with corresponding decrease in EC values observed in the solid ash, fractured hard ash and coarse ash is due to non-dissolution or precipitation of the soluble species in surface layers that also act as a pH buffering constituents in fly ash (Gitari *et al*., 2009a). However, there is a sharp pH increase in the region of fractured hard ash (6-7m) (Figure 5.18) and coarse ash (15-17m) (Figure 5.19). The pH of the interstitial water would have a significant effect on the mobility of trace element in fly ash (Theis and Wirth, 1977; Khanra *et al*., 1998; Jankowski *et al*., 2006). The lower pH values with corresponding increase in EC values will significantly lead to release of chemical species due to the dissolution of soluble components in

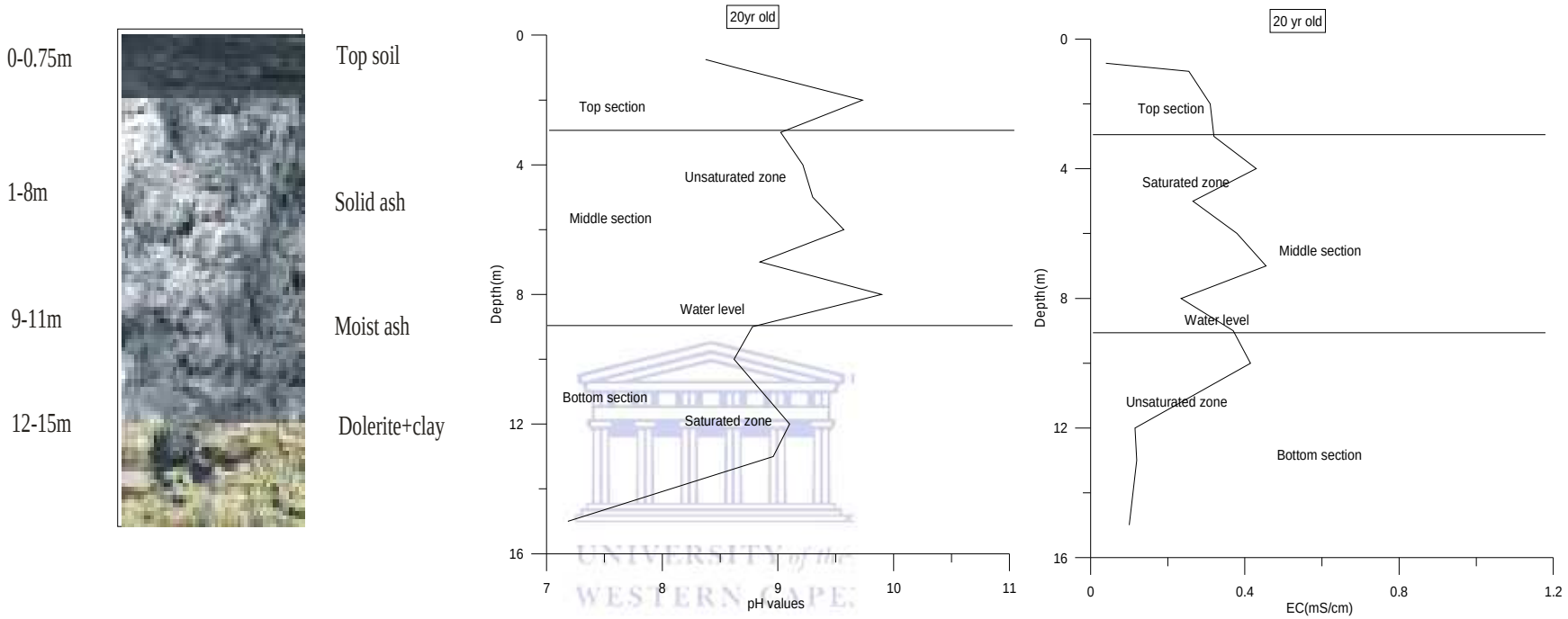

Figure 5.17. pH and EC of pore water versus depth for 20-year-old drilled ash core (n=3).

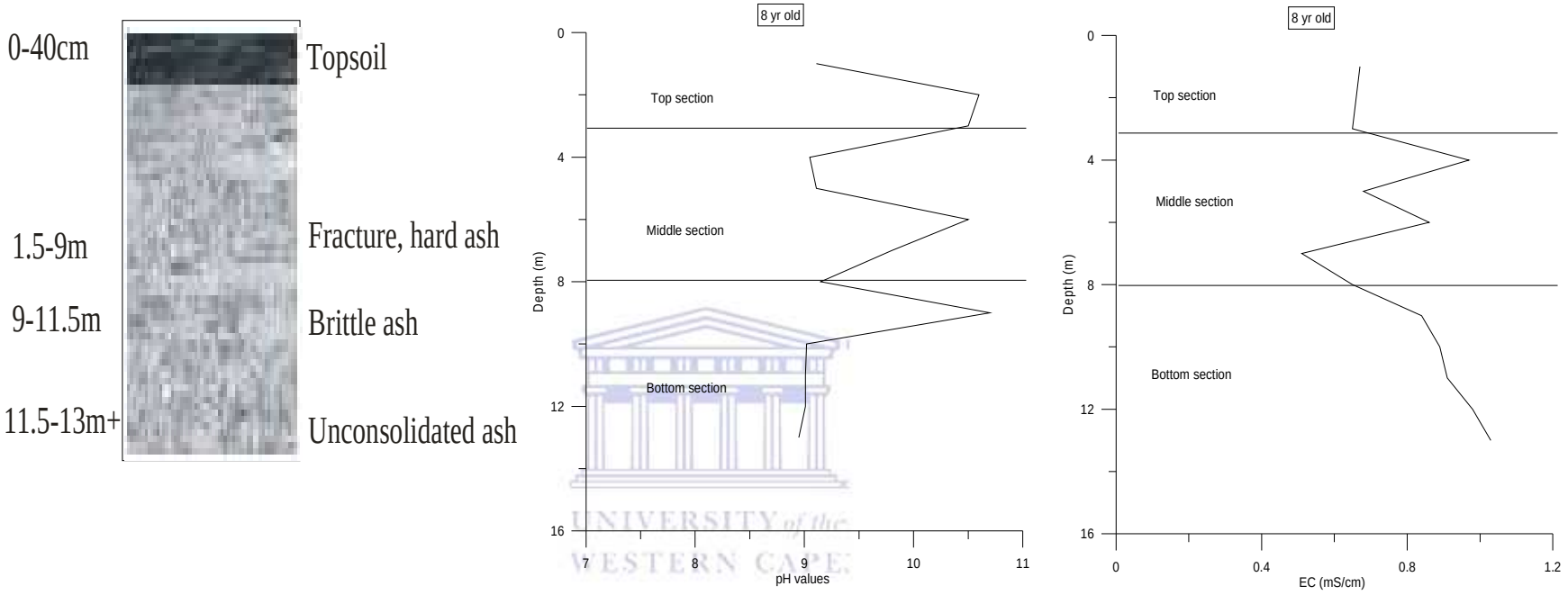

Figure 5.18. pH and EC of pore water versus depth for 8-year-old drilled ash core (n=3).

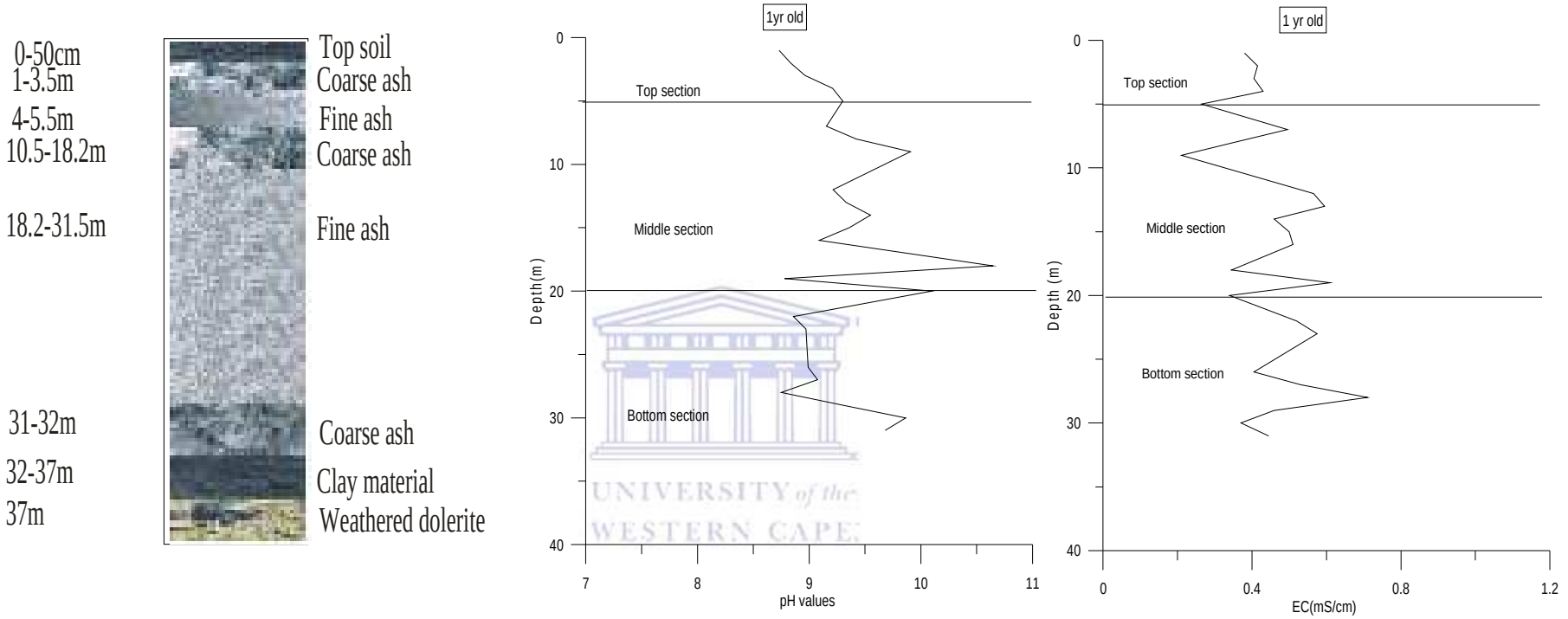

Figure 5.19. pH and EC of pore water versus depth for 1-year-old drilled ash core (n=3).

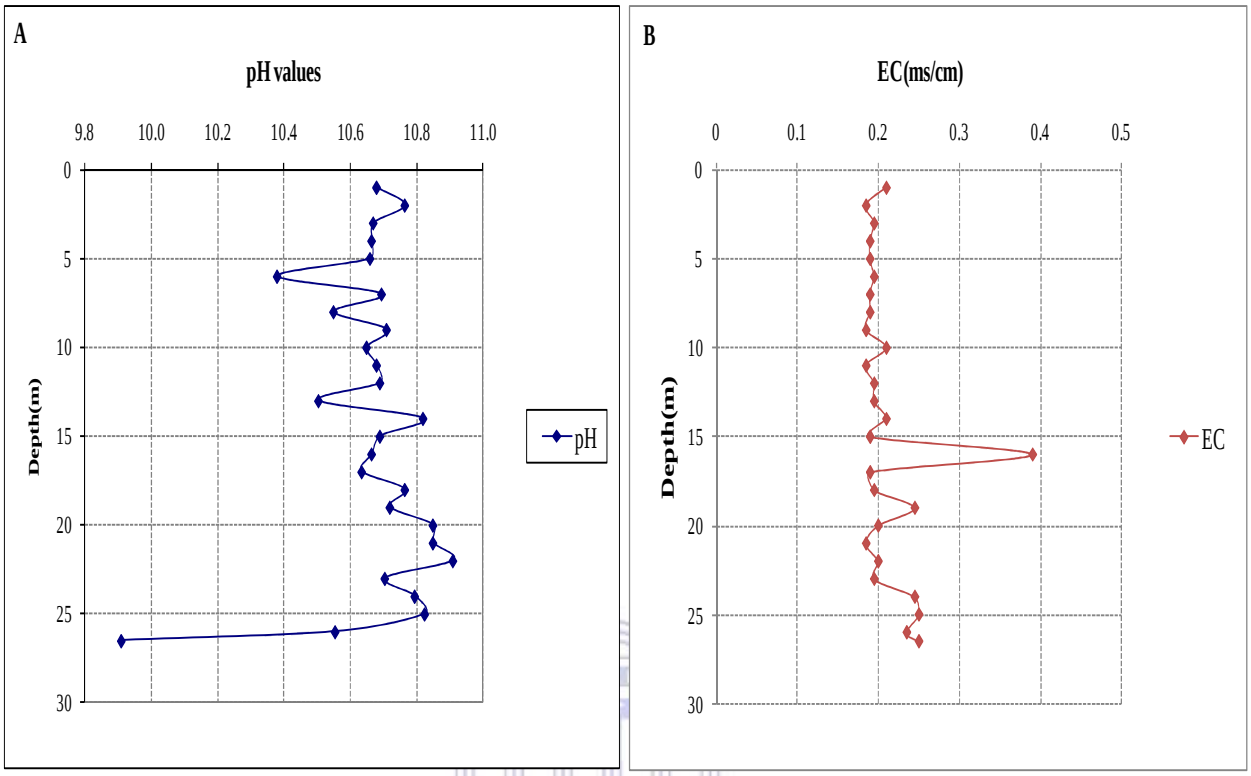

Figure 5.20. (a) pH of pore water versus depth and (b) EC of pore water versus depth for 2-week-old drilled ash core (n=3).

the ash matrix and hence leaching of the ash. The pH values within the top soil ranged from8.47-9.67, and dolerite clay (9.68) are relatively low compared to the fly ashes which ranged from 8.80-10.10 (Figures. 5.17 & 5.19). Leaching of chemical species from the surface stratum, moist ash and mixture of dolerite and clay horizons is envisaged to be intense due to the relative decrease in pH values. The high pH of the solid ash zone in the 8-year-old drilled ash core is due to non dissolution or possibly chemical precipitation of soluble components in the ash matrix and hence less leaching of chemical species (Figure 5.18). Relatively low pH trend was observed at depth sections i.e.1-13 m, 15-18 m, and 26-29 m in the 2-week-old fly ash. This slight change in pH is due to flushing of soluble buffering constituents in the 2-week-old ash cores at these depth intervals (Figure 5.20). The EC values recorded for 2-week-old ash cores shows little variation (1-15m) indicating that long term mineral transformation has not really taken place (Figure 5.20). The slight change in pH of the extracted pore water is due to chemical interaction of fly ash with ingressed CO_2, ingressed O_2 and percolating rain water (see Section 2.4.6). This observation suggests that contact with atmosphere, ingressed CO_2, microbial respiration

(Schramke, 1992) and leaching by infiltration of rain water has a profound effect on the weathering of disposed fly ash. Schramke (1992) also reported that in fly ash leachates the rate of input of CO_2 (g) into the leachate is expected to control the overall rate of pH equilibrium. The pH values have a significant effect on the release of major elements from the fly ash (Gitari *et al*., 2009b). The observed relative decrease or increase in the pH values of 1 year, 8 year and 20-year-old fly ashes could affect the release of major elements adsorbed in the mineral phases of fly ash. The relatively low pH values of the ash (7.18-10.9) could lead to dissolution or co-precipitation of the mineral phases in the ash and, hence, mobility of chemical species. In figure 5.19 the coarse ash is associated with slightly high pH values compared to fine ash which is synonymous with slightly low pH values in the column of ash. This implies that the role of texture and surface area in the weathering of fly ash, accordingly fine ash is relatively very much weathered than coarse ash from 1-year-old ash cores.

5.8 Anion and cation species in extracted pore water of drilled cores

The experimental protocol is documented in the Appendix Aviii. The results are shown in Figures 5.21-5.24. In the 20-year-old drilled core, the anion species in the extracted pore water i.e. chloride (Cl^-), sulphate (SO_4), nitrate (NO_3-N) and phosphate (PO_4) ranged from 2.64 – 19.83 mg/L, 3.89 - 228.10 mg/L, 0.39-1.24 mg/L, and 0.18-2.58 mg/L respectively (Figure 5.21). A relatively low solution concentration of anion species was observed at these sections i.e. [Cl^- (0.75-6 m, 8-13 m), SO_4 (0.75 m, 12-15 m), NO_3-N (1-10 m) and PO_4 (1-10 m)].

In contrast, a relatively high solution concentration of these anion species was observed at these sections i.e. [Cl^- (7 m, and 14 m), SO_4 (1-10 m), NO_3-N (12-15 m) and PO_4 (0.75 m, 12-15 m)]. Anion species of the extracted pore water of 1-year-old drilled core have Cl^- (13.66-66.53 mg/L), SO_4 (51.92-332.61 mg/L), NO_3-N (0.44-1.18 mg/L), and PO_4 (0.32-2.08 mg/L) respectively (Figure 5.22). A relatively low concentration of anion species were observed at these sections i.e. [Cl^- (8-9 m), SO_4 (9 m, 18 m), NO_3-N (3-9 m, 16-23 m) and PO_4 (4-12 m, 15-20 m, and 28-31 m)] which could be due to dissolution or initial leaching of soluble major components of fly ash which can acts as a scavenger.

In contrast, a relatively high solution concentration of these anion species were observed at these sections i.e. [Cl^- (1-2 m, 4-7 m, 12-31 m), SO_4 (1-8 m, 19-31 m, and 12-16 m), NO_3-N (1-2 m, 12-15 m and 26-31 m) and PO_4 (1-3 m, 13-14 m, 22 m, and 26-27 m)].

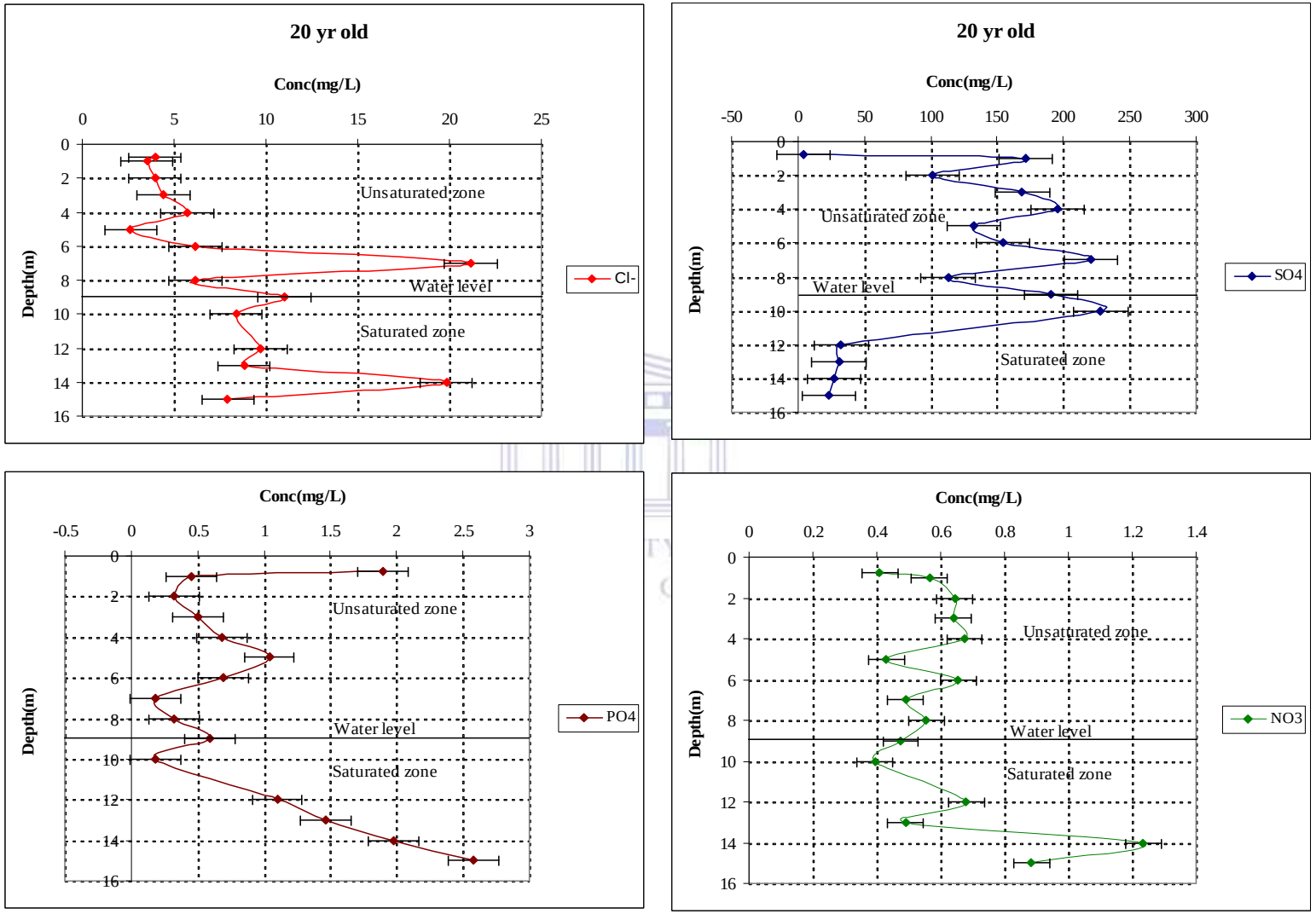

Figure 5.21. Concentration of Cl^-, SO_4, NO_3 and PO_4 by depth in the pore water for 20-year-old dry disposed fly ash.

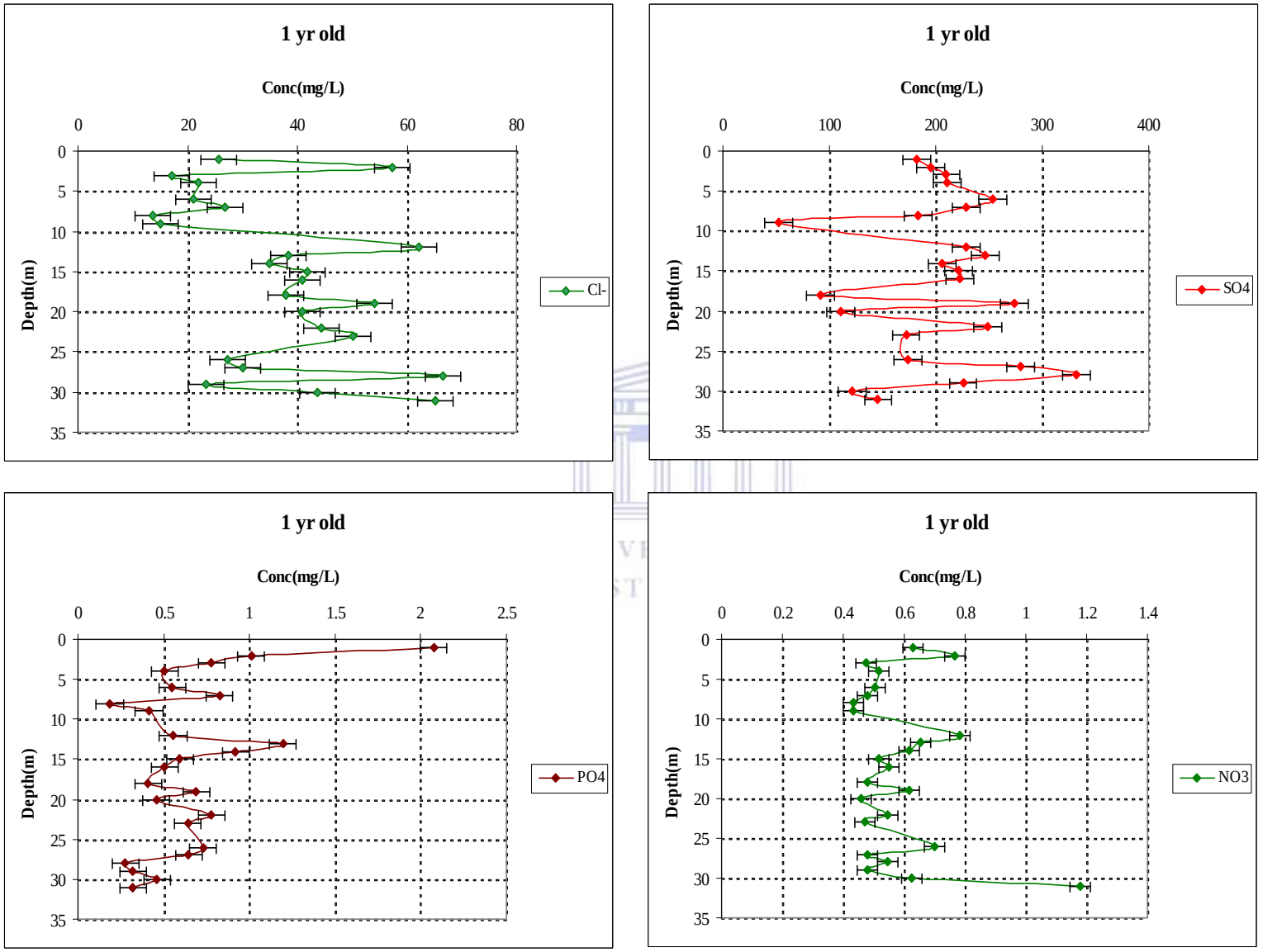

Figure 5.22. Concentration of Cl^-, SO_4, NO_3 and PO_4 by depth in the pore water for 1-year-old dry disposed fly ash.

The high solution concentration of anion species at these highlighted sections of the drilled cores could be due to dissolution of major components of fly as enhanced by the chemical interactions of fly ash with ingressed O_2, ingressed CO_2 from atmosphere and percolating rain water. Chloride and sulphate solution concentration show a progressive leaching pathway along the drilled hole and subsequent lateral diffusion at the contact with the water level (saturated zone) under the ash dump (Figure 5.21). In the pore waters, nearly all anion species show a trend of increasing concentration with depth which is interpreted as resulting from weathering reactions of the dry disposed ashes with infiltrating pore waters. The increasing concentration of anion species with increasing is due to advective transport after dissolution in the top layers.

The concentrations peak of Cl^-, PO_4 and NO_3 in the depth profiles (Figures 5.21 & 5.22), are thought to represent a time-dependent migration of these anions. This is in general agreement with the mobilization of anthropogenic input in pulverized fuel ash from decommissioned power station in the UK (Lee and Spears, 1997). Metals such as Mg, Ca, Fe, K, Na, B, Cr, As, Mo and Se were observed to be in the range of 0.00013-0.183 ppm (Figures 5.23 & 5.24). On the chemical species profile by depth, low concentrations are observed for Na, K, Mo, B, Mg, Se and Ca between 0.75-3 m (Figures. 11&12). The highest concentration was obtained at a depth of 9 m (Figs. 5.23 & 5.24). A peak in concentration was observed for Se, Mo and Mg at a depth of 9 m which represents point of maximum saturation of the ash with water and subsequent maximum dissolution of soluble salts (Gitari *et al*., 2009a). The low concentration of Se, Mo, Mg and B in the shallow depths (0.75-3 m) may be due to carbonation and conversion of the alkali and alkali earth metals into carbonates (Gitari *et al*., 2009a). Fe and As showed a somewhat high concentration at the shallow depths (0.75-3 m); both metals are typically associated with oxides and hydroxides. The progressive weathering of hematite (Fe_2O_3) in coal fly ash will definitely reduce Fe (III) to Fe (II) and probably responsible for the availability of Fe and As in the ash pore water. Decrease in pH of ash cores as weathering proceeds allow aluminium and Si to precipitate from ash pore water yielding amorphous aluminosilicate. This amorphous aluminosilicate is able to absorbed larger amount of cations and anions because they contain higher amount of negative and positive charges in neutral pH-range (Zevenbergen *et al*., 1999).

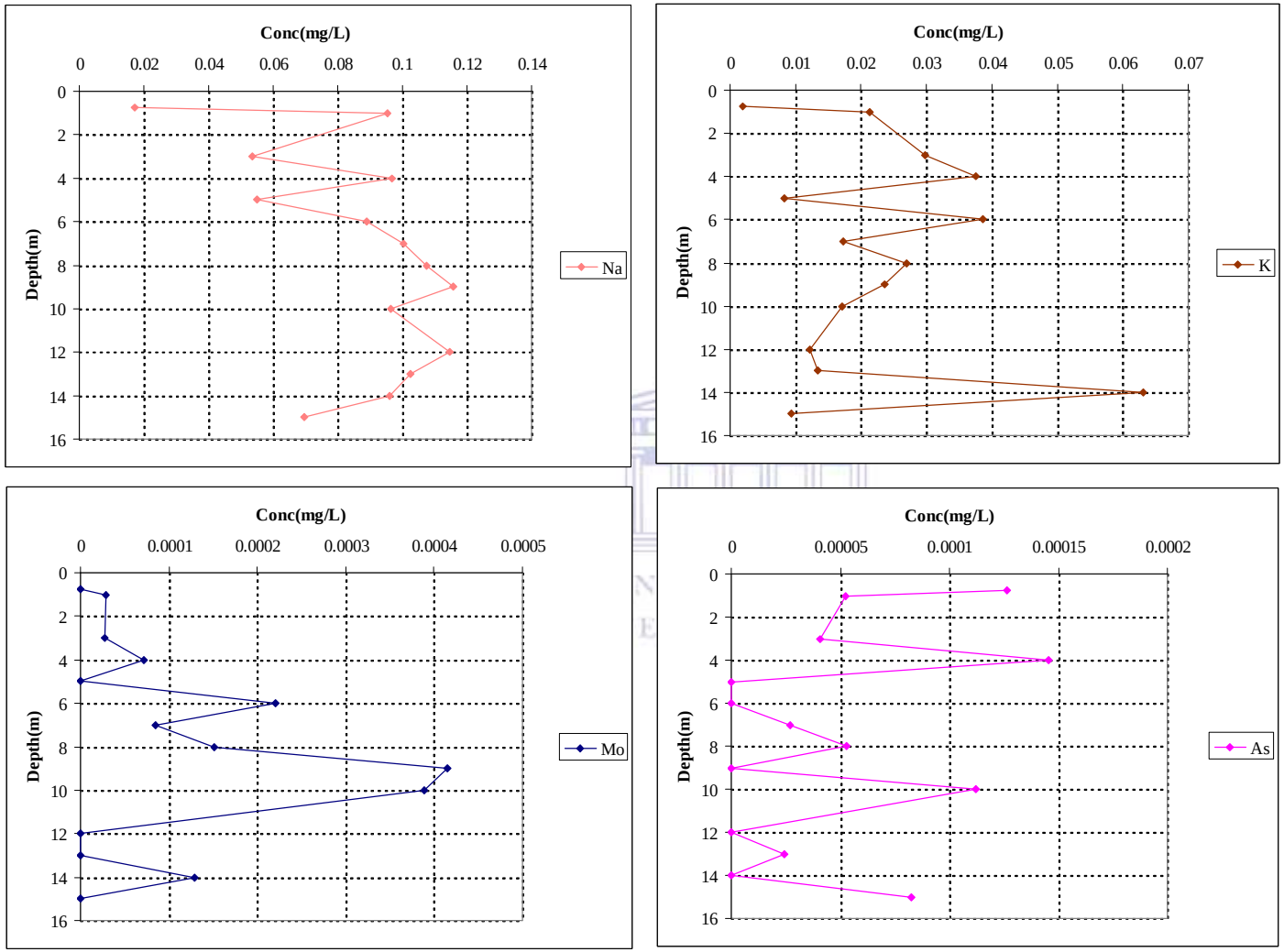

Figure 5.23. Concentration of some chemical species (As, Mo, K and Na) by depth in the pore water for 20-year-old drilled ash cores.

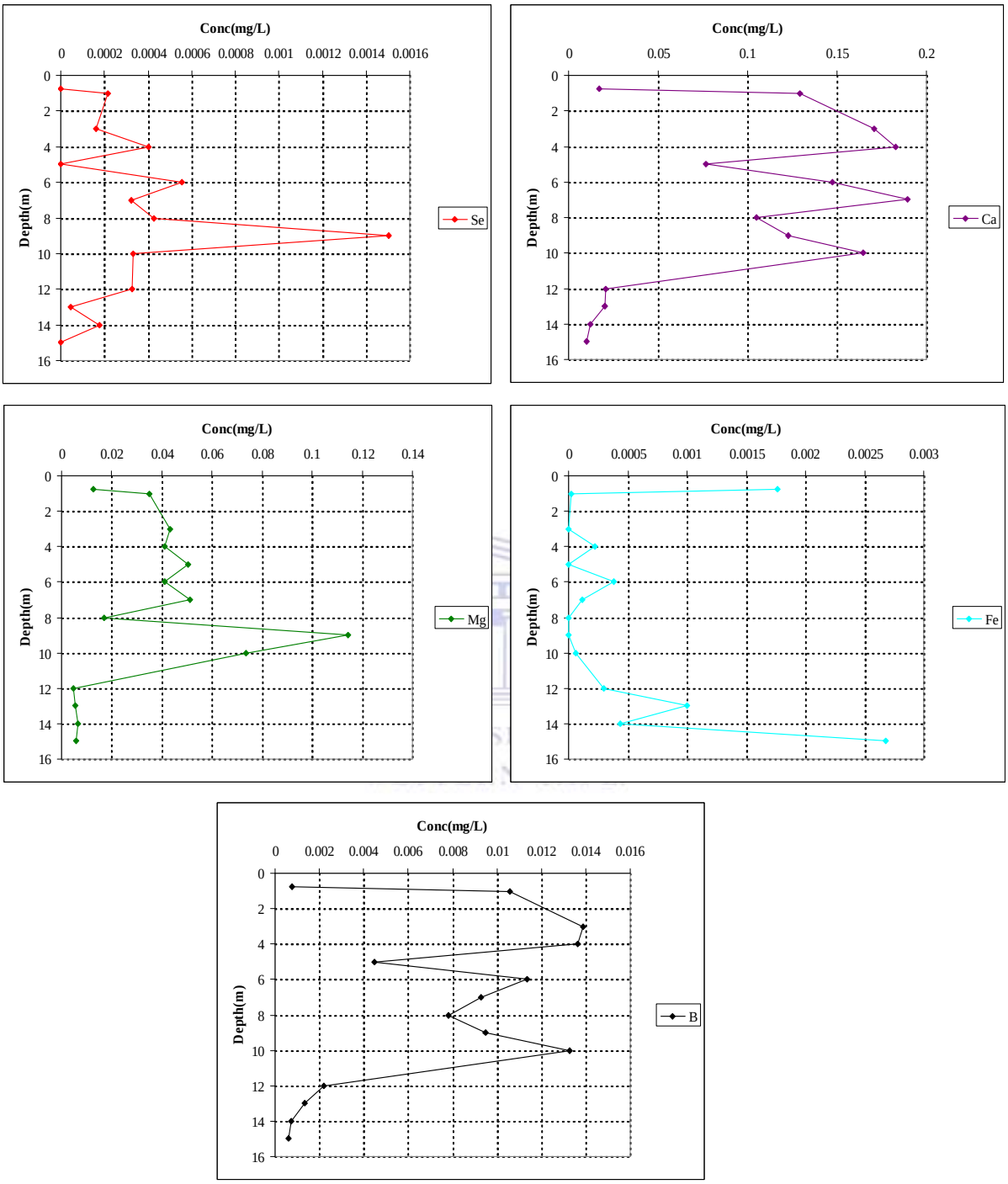

Figure 5.24. Concentration of some chemical species (Ca, Se, Fe, B and Mg) by depth in the pore water for 20-year-old drilled ash cores.

The distribution patterns of Na^+, K^+, Cl^- and SO_4^{2-} down the core show positive correlation suggesting that these chemical species are present in form of soluble sulphate or chloride salts in weathered fly ash. There is high solution concentration of anion species in the 1-year-old when compared to 20-year-old dry disposed fly ash. The lower solution concentration of anion species in 20-year-old drilled ash core is an indication of intensive leaching of major component in fly ash (soluble salts) over-time due to chemical weathering process. The mobility of chemical species in the weathered drilled ash core therefore could be controlled primarily by reduction in pore water pH. de Groot and Wijkstra (1989) in their study established the dependence of leachability of chemical species in pH of fly ash. The results further show that ash type, moisture content level of fly ash, texture of fly ash and to some extent the pH of the ash column could be factors controlling leachability of chemical species in the considered weathered drilled ash cores.

5.9 Up-flow percolation test (Column leaching test) results

This section present and discuss the results of the up-flow percolation (column) test carried out on Tutuka fresh fly ash as described in Appendix x. The up-flow percolation test was carried out to determine the leaching behaviour of species from the fly ashes under renewal of leachants. The up-flow percolation (column) test tends to simulate what happens to fly ash at the dump when water flows through the ash system from time to time. The column test has been considered as a suitable method to simulate the percolation of leaching agent through the ash dump (Ram *et al*., 2007). The choice of the up-flow mode of the leachant was to avoid channelization or preferential percolation of the leachant and to ensure complete saturation of the fly ash in the column. The dry mass of fly ash in the column, volume of leachate and the time taken for collection of leachate were used to calculate the L/S ratios used in the mass balance calculation shown in the Table 5.8.

The results show that 1.5 % and 0.2% of Na^+ and SO_4 respectively was retained in the ash after up flow percolation of the saline brines through the Tutuka fresh ash. This suggests that fresh ash from Tutuka power station is not holding salt from the saline brines and therefore is not a sustainable salt sink. This is could be explain by the leaching/flushing of major soluble components of fly ash. Percentage retained Na^+ and SO_4 in the ash increased from 1.5-1.8 % and 0.2-0.5 % respectively by the addition of antiscalant indicating that antiscalant improve salt retention capacity of the ash from Tutuka power station.

Table 5.8. Mass balance showing the concentration (mg/kg) and percentage (%) of salts captured in the Tutuka fly ash after the percolation of 50 L brine solution (Fatoba, 2011)

Species (mg/kg)	Total concentration passed through the ash (UB)	Concentration retained in the ash (TR)	% retained in the ash (TR)	Concentration retained in the ash (TRA)	% retained in the ash (TRA)
Cl	1212200	1210.3	0.9	814.6	0.7
Mg	7375	2937.5	39.8	2398.3	32.5
Na	216161	3172.8	1.5	3809.3	1.8
SO_4	442900	849	0.2	2185.6	0.5

N.B. (UB = unreacted brine; TR = Tutuka solid residue; TRA = Tutuka solid residue with antiscalant).

The XRF results of weathered ash cores showed that 1.1 % and 0.17 % of Na^+ and SO_3 respectively were retained within 8 year of dumping. Despite the obvious difficulty involve in getting the accurate % sodium and sulphate retained in the weathered drilled ash core samples. There is a close similarity between the Na^+ mass balance obtained from up flow percolation test (1.5 %) and mass % retained in the 8-year-old ash dump as determined by XRF analysis.

5.10 Summary and conclusions

The effects of chemical weathering on the dry disposed fly ash are evaluated in comparison with fresh ash from the same site. The mineralogy and micro-structural characterization results showed alteration in mineralogy and microstructure as ash ages, and revealed formation of secondary mineral phase mainly due to chemical interaction of fly ash with ingressed CO_2, ingressed O_2 from atmosphere and percolation rain water (hydration, carbonation and pozzolanic reactions) that occurred at the dump site.

1. Presence of secondary minerals (such as calcite and mica) in the weathered dry disposed ash cores is due to carbonation and hydration process occurring after disposal of fly ash. Lesser variation in the mineral phase peak heights is observed with the older ash due to long-term mineralogical transformation. Hematite (Fe_2O_3) is the major iron phase in the dry disposed fly ash from Tutuka power station

2. The pH profile of the extracted pore water as a function of age of the dump shows that the greatest weathering occurs at the shallow depth and the point of contact with water

(saturated zone). The slight change in pH of weathered drilled ash cores is probably due to rapid dissolution and initial rapid flushing out of the soluble major components that also act as a pH buffering constituents. The 1-year-old and 20-year-old coal fly ash cores showed a lower pH and greater initial leaching/flushing out of the soluble major components the 2-week-old placed ash.

3. The trends obtained from ternary plot of sum of oxides show that 20 year, 8 year and 2-week-old drilled cores are sialic while 1-year-old drilled ash cores is ferrocalsialic in composition, this significant change in chemistry of coal fly ash is probably due to chemical weathering and in-homogenous brine irrigation.

4. The Na_2O content of the Tutuka ash cores was low and varied between 0.6-1.1 mass % for 1-year-old ash cores to around 0.6 -0.8 mass % for 8-year-old ash cores. Na_2O levels were higher in 1-year-old ash compared to 8-year-old ash and observed trends indicate that weathering quickly (within a year) leaches out Na^+ from the ash dump thus the dry disposal ash placement method also does not result in a sustainable salt sink for Na-containing species over time. The non-leachable portion of the Na^+ (namely that contained in the residual fraction) ranged between 5-91 %, showing the metastability of the mineral phases with which insoluble Na associates.

5. The trend shows high detrital authigenic index (DAI) values for 8 year and 20-year-old ash cores when compared with 1-year-old ash core. This implied that minerals that have dominant detrital genesis in coal are more abundant and achieved stability (chemical unaltered) with age.

6. There is a preferential enrichment of K^+, Mn, Zn, P, Ba, Pb, V, Sr and Cr in the 1-year-old weathered ash core samples when compared to fresh ash sample from the same power station. In contrast, elements such as Ti, Mg, Al, S, Na^+, Si and Ca showed depletion in the 1-year-old ash cores.
7. A preferential enrichment of Al, Na^+, Mn, Ni, Sr, Pb, V, Cr and Co in the 20-year-old ash cores when compared with fresh ash from the same power station. However, Ti, K^+, Fe, Mg, Si, Al, P, Ca, Ba, Y and Zr in the 20-year-old ash cores. This variation in enrichment and depletion of elements in 1 year and 20-year-old ash cores is due to differential chemical weathering and in-homogenous irrigation with high saline effluents.

CHAPTER SIX

Results and Discussion 2

Inorganic metal leaching and acid susceptibility of weathered, dry disposed fly ash

This chapter presents the results of metal leaching and susceptibility of weathered ash as compared to fresh ash. The effect of weathering on buffering capacity of ash and consequently leaching of metal species were revealed and discussed.

6. Introduction

South Africa, like other developing economies, depends largely on the combustion of pulverised coal for power production. The generation of electricity by thermal conversion of low-grade (sub-bituminous) coal produces enormous quantities of fly ash. Coal fly ash is composed mostly of silt-sized spherical amorphous ferro-aluminosilicate minerals, and is usually characterised by low permeability, low bulk density and high specific surface area (Petrik *et al.*, 2007). Eskom, as the largest indigenous power production company in South Africa, generates about 37 Mt of fly ash annually (Eskom Abridged Annual Report, 2009); of which only 5 % is currently beneficially utilised, the rest being disposed in ash dams, landfills or ponds (Petrik *et al.*, 2003). Even though coal fly ash is considered a waste product, it has some valuable environmental and commercial applications due to its pozzolanic, cementitious and alkaline properties (Yeheyis *et al*., 2009). To minimise costs for the off-site dry disposal of coal fly ash, fly ash beneficiation for a variety of these environmental and commercial applications is necessary. A number of international power producers market the utilisation of coal by-products for a variety of applications, including cement/concrete, structural fill, road base, waste stabilisation, agriculture, and mine backfill (Kim, 2006). In the commercial utilisation of fly ash for such applications, fresh ash is collected from power stations. The inability of power producers to meet rising market demand for fresh ash is envisioned in the future. Thus, there is a need for adequate knowledge of the characteristics of dry, disposed ash, considering chemical and mineralogical alterations as a result of ageing or the natural weathering process, if such ash were to be utilised. Several studies have demonstrated that the process of mineral transformation during the natural weathering or municipal solid waste incineration (MSWI) of coal fly ash is comparable to that of

volcanic ash in nature (Warren & Dudas, 1985; Zevenbergen *et al*., 1994; Zevenbergen *et al*., 1999). Nevertheless, the time frames are rather different; whilst volcanic ash requires several thousands of years for clay mineral development, there is proof that clay illite is formed from glass phases in MSWI bottom ash after only 12 years, or that clay-like amorphous material can be formed in the micro scale throughout the surfaces of coal ash particles after 8 years of natural weathering (Zevenbergen *et al*., 1996; Zevenbergen *et al*., 1998; Zevenbergen *et al*., 1999).

The extent of ash utilisation has been limited because of its potential to release different metal ions, including heavy metals, during natural weathering under dry disposal conditions. The metal released could pollute the environment and contaminate groundwater in the vicinity of the ash dump. Kim (2006) reported that the potential release of heavy metals from coal utilisation by-products, when exposed to fluids such as acid rain, groundwater, or acid mine drainage, may affect their suitability for beneficial uses like bulk fill and mine remediation. Consequently, the release of heavy metals overtime due to weathering/ageing is a major concern for the utilisation/beneficiation of dry disposed fly ash. The flushing/release of soluble buffering constituents in fly ash due to natural weathering/ageing was thought to significantly affect the pH, metal mobility and mineralogical transformation of weathered fly ash (Akinyemi *et al*., 2011). Fly ash may have environmental impacts as a result of potential detrimental effects when used for landfill cover and, consequently, may pose risks to human health and the environment (Lo & Liao, 2007). The solubility of coal fly ash overtime could be affected by pH, silicate and nonsilicate distribution, magnetic and nonmagnetic fractions and humic matter (Kim *et al.*, 2002, Kukier *et al*., 2003; Kim & Kazonich, 2004).

The chemical interaction of dry disposed fly ash with ingressing CO_2 and O_2 and percolating rain water over time affects the pH and eventually leads to formation of secondary minerals (Gitari *et al*., 2009; Akinyemi *et al*., 2011). The formation of secondary minerals during weathering has significant effects on acid neutralisation capacity and leaching behaviour of fly ash components (Yeyehis *et al*., 2009). Brannvall *et al*. (2009) reported that carbon dioxide affects the pH and acid neutralisation capacity (ANC) of fly ash during ageing of refuse-derived fuel (RDF) fly ash. Several studies on the release of metals controlled by individual ion solubility have revealed that the ANC potential of ash is mostly due to the release of Ca, Mg, K, Na, Fe and Al ions (Johnson *et al*., 1995, Mizutani *et al*., 1996, Yan *et al*., 1999; Seferinoğlu, *et al*., 2003). The release of

these alkali metals might initially increase the pH of the ash leachant until they are exhausted. The release of cations, such as from Al, Be, Cd, Co, Cr, Cu, Fe, Mn, Ni, Pb and Zn but not from Ca, would be delayed until the buffering capacity of the fly ash was exhausted. As a result the neutralisation volume or buffering capacity of the fly ash affects the release of metal ions from ash when it is exposed to infiltrating rain water (Kim, 2006). The main objective of the study is to evaluate and compare the leachability of fresh and dry disposed fly ash produced from the same power station. Among the variables that may have an influence on the leaching behaviour of disposed ash, pH of the leachant solution is considered to be the most important, and was thus evaluated through acid neutralisation capacity tests. The results obtained from the acid neutralisation tests of fresh and dry disposed ash from the Tutuka power station are presented and discussed.

6.1 Bulk mineralogy of fresh and unsaturated weathered ash cores

The experimental protocol is reported in Appendix Av. The result of X-ray diffraction patterns of fresh ashes is shown in Figures 6.1 and unsaturated weathered ashes (see Figure 5.2). A detailed discussion on the mineralogical composition of unsaturated weathered ashes is presented

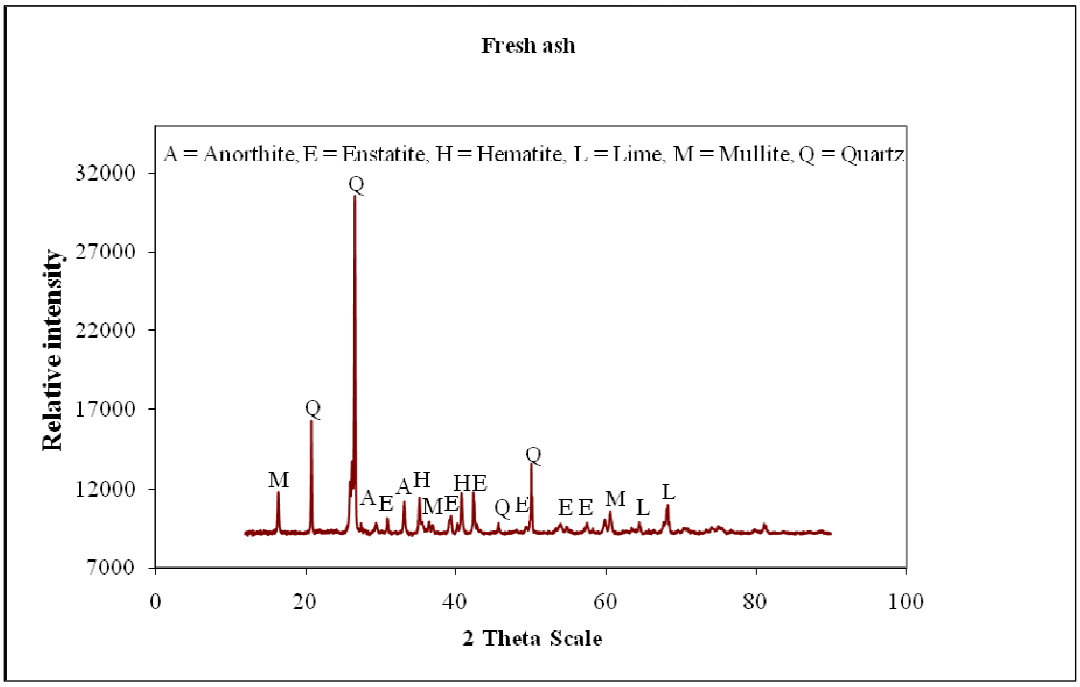

Figure 6.1. XRD spectra of fresh ash (FA) used for ANC test

in section 5.2. Calcite and mica are noticeably absent in fresh ash; however, their presence in dry disposed unsaturated ash samples (Figure 5.2) indicate a weathering/ageing process involving long-term chemical and mineralogical transformation. A few authors (Soong *et al.*, 2006; Muriithi, 2009; Muriithi *et al*., 2010) showed in their studies that the formation of calcite ($CaCO_3$) in fly ash occurred through a carbonation process which entails chemical interaction of ingressed CO_2 with the initially alkaline material present in the fly ash.

6.2 Bulk chemistry of fresh ash and unsaturated weathered ash cores

The experimental protocol is documented in Appendix Aiv. As shown in the Table 6.1, the most important trace elements of environmental concern in both fresh ash and unsaturated weathered ash include Ba, Cr, Pb, Sr, V, Ce, Zr, and Zn. Trace element concentrations of Ba, Ce, Nd, Y and Zr are relatively high in the fresh ash, indicating possible enrichment during the coal combustion process. Trace elements are associated with the surface of the ash particle due to evaporation and condensation during coal combustion.

Table 6.1. Concentration of trace elements (ppm) in fresh ash (FA) and unsaturated drilled ash core samples

Sample ID	Ba	Ce	Co	Cr	Nd	Ni	Pb	Sr	V	Y	Zn	Zr
FA	1200	216	24	132	60.2	95.8	39.3	1783	85.8	79	31.3	404
1m	1171	ND	31	116	4	115	51	1923	316	69	50	225
3m	1038	22	27	215	11	109	53	1862	305	45	50	221
5m	1064	66	33	247	23	110	56	1868	314	48	53	235
7m	1056	61	30	300	9	112	62	1898	240	53	53	259

The depletion of Ce, Ba, Nd, Zr and Y in unsaturated weathered ashes could suggest that soluble salts have already leached out of the ash dump. The precipitation of calcite and aluminosilicate minerals (e.g., mica) as revealed by XRD spectra could also have prevented or slowed the leaching rate of Ba, Ce, Nd, Y and Zr from unsaturated weathered ash through adsorption, co-precipitation, or physical encapsulation. The precipitated minerals could also serve as a barrier to the constituents of the disposed fly ash by clogging the pores of disposed fly ash and, hence, preventing their mobilisation (Yeyehis *et al*., 2009). In contrast, trace metals such as Co, Ni, Sr, V, Pb, and Zn are relatively enriched in the unsaturated weathered ash, suggesting possible weathering of other elements, leaving an enriched residue. This could be as a result of the

leaching of major soluble components, leaving non-soluble components behind. Accumulation of major oxides (i.e. Fe_2O_3, TiO_2, CaO, K_2O, Na_2O and SO_3) (see Table 5.4) and trace metals (such as Zn, Zr, Sr, Pb, Ni, Cr and Co) (see Table 6.1) in the lower layers showed progressive movement through the ash dump at a slow rate.

6.3 Pore water chemistry of fresh ash and unsaturated weathered ash cores

The experimental protocol is reported in Appendix Aix. Figures 6.2 (a) and 6.2 (b) present the elemental compositions of the water soluble extracts of fresh and dry disposed coal fly ash when in contact with de-ionised water for 30 min. The main components, such as Al, Si, Ca, Mg, Na^+, and K^+, were rapidly leached in significant amounts from both fresh ash and unsaturated weathered ash within 30 min.

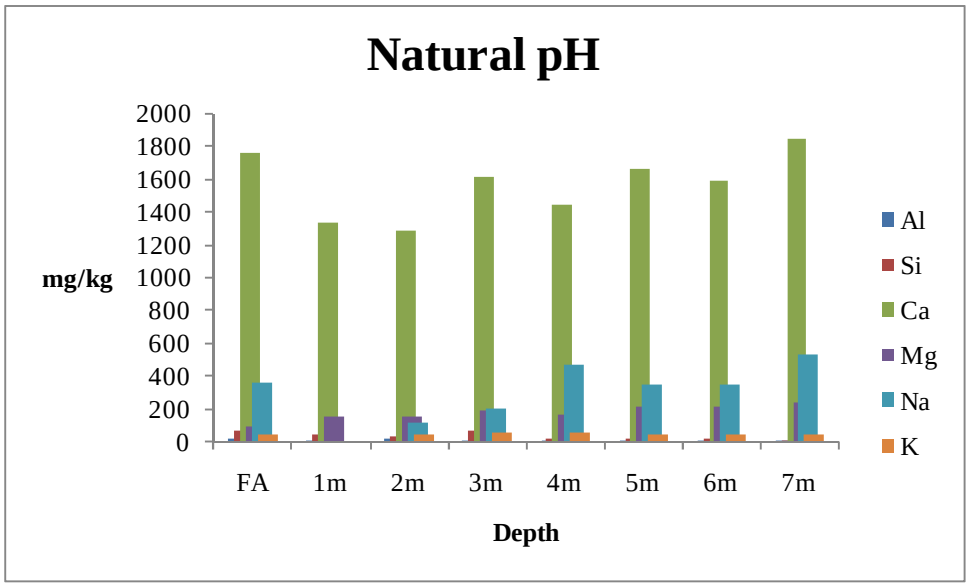

Figure 6.2 (a). Major elements in water soluble extract of fresh ash (FA) and unsaturated weathered ash.

Al and Si have concentration ranges in the aqueous extracts of fresh and dry disposed weathered ash samples of 1.83–24.69 mg kg^{-1} and 9.78–67.04 mg kg^{-1}, respectively. Ca and Mg have concentration ranges between 1290.61–1760.60 mg kg^{-1} and 150.99–241.43 mg kg^{-1}, respectively. A lower concentration of Ca in the aqueous extract of unsaturated weathered ash samples is due to lower pH and initial leaching/flushing of buffering constituents (Akinyemi *et al.*, 2011). The concentration ranges of Na^+ and K^+ are between 115.72–530.91 mg kg^{-1} and 40.63–55.24 mg kg^{-1}.

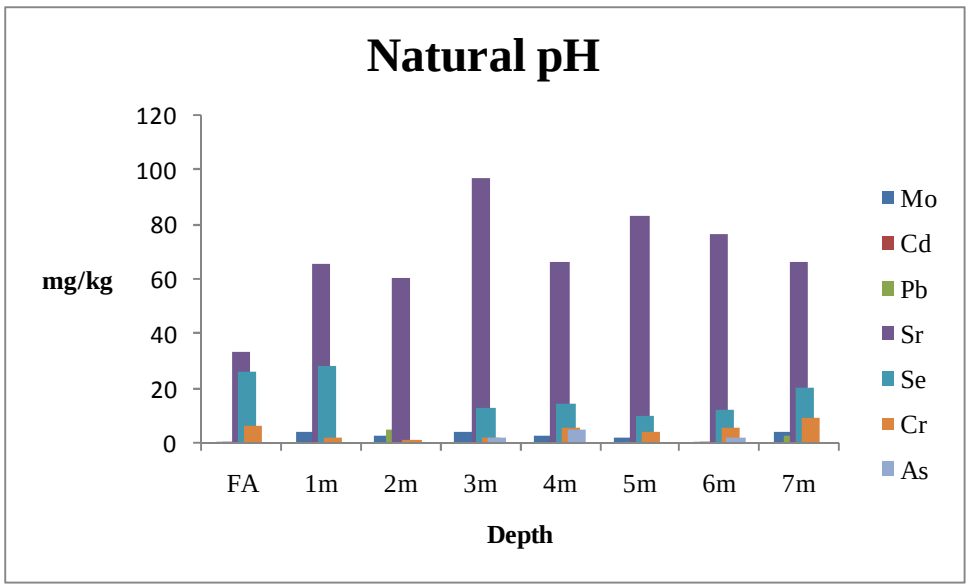

Figure 6.2 (b). Trace elements in water soluble extract of fresh ash (FA) and unsaturated dry disposed ash.

The concentration range of Sr is between 33.49–96.77 mg kg^{-1} in the aqueous extracts of the fresh and dry disposed weathered ash. Cations such as Al, Si (except at 7 m depth), and Se showed relatively lower concentrations in the aqueous extract of dry disposed weathered ash samples, which may be attributed to their slower release due to association with the less soluble mineral phase.

Figure 6.2b shows trace element concentrations in the aqueous extracts of fresh and unsaturated weathered ash. Concentration of As and Mo range between 1.67–5.12 mg kg^{-1} and 0.24–4.14 mg kg^{-1}, respectively; whereas, the concentration ranges of Se and Cr are between 9.66–28.48 mg kg^{-1} and 0.90–9.00 mg kg^{-1}, respectively. In the case of Cd and Pb, their concentrations range between 0.05–0.34 mg kg^{-1} and 0.37–4.58 mg kg^{-1}, respectively. Trace metals, such as Cd, Mo, Pb, Se and Cr, are enriched in the aqueous extract of the dry disposed weathered ash samples due to depletion of major components (i.e., CaO, Fe_2O_3, TiO_2, K_2O and P_2O_5). These trends in results show that significant concentrations of metals were released within 30 min of contact with de-ionised water. This suggests that at early stages of fly ash dry disposal, the chemical interaction of fly ash with infiltrated rain water would lead to significant leaching of elements into the surface and groundwater in the vicinity of the ash dump. Choi *et al.* (2002) have suggested that the elements in the ash particles were mainly associated with the surface and that these surface-

associated fractions might dominate leachate chemistry at the early stages of fly ash disposal when in contact with water. The water soluble anion constituents (mg/L) leaching out of fresh ash and unsaturated weathered ash samples after 30 min contact time are presented in Table 6.2. As shown in the Table 6.2, NO_3-N, Cl^- and SO_4 are the dominant water soluble anion species leaching out of fresh and dry disposed coal fly ash within 30 min.

Table 6.2. Water soluble anion constituents (mg/L) leaching out of fresh ash (FA) and unsaturated weathered ash samples in 30 min.

Sample ID	NO_3-N (mg/L)	Cl^- (mg/L)	PO_4 (mg/L)	SO_4 (mg/L)
FA	0.74±0.03	31.72±0.88	0.60±0.05	194.16±1.68
1 m	0.57±0.04	3.52±0.00	0.46±0.28	171.48±10.16
2 m	0.65±0.06	3.52±0.45	0.33±0.05	101.38±2.21
3 m	0.64±0.04	4.41±0.00	0.51±0.14	169.04±4.51
4 m	0.68±0.05	5.73±0.38	0.69±0.05	195.53±6.00
5 m	0.43±0.04	2.64±0.00	1.04±0.00	132.26±0.00
6 m	0.66±0.06	6.17±1.76	0.69±0.02	154.82±1.14
7 m	0.49±0.00	21.15±0.00	0.18±0.00	220.75±0.00

The greatest leaching was observed for sulphate, but it does not show a consistent trend in the unsaturated weathered ash samples. The concentration of sulphate is depleted from 1–3 m and 5–6 m. In contrast, it is enriched in the unsaturated weathered samples taken at 4 m and 7 m depths. Phosphate also shows a somewhat inconsistent trend in the unsaturated weathered ash samples. It is depleted between 1–3 m and at 7 m in unsaturated weathered ash samples, but an enrichment zone is observed from 4–6 m. Nitrate and chloride show lower concentrations in the unsaturated weathered ash compared with fresh ash. The observed depletion of anion species in the unsaturated weathered ash samples is possibly due to formation of less soluble salts (such as $CaSO_4$) or mineral phase thus slower the leaching rate (Figure 6.2 and Table 6.2).

6.3 Acid neutralization capacity test results

The acid consumption capacity of fresh ash (FA) and unsaturated weathered ash from Tutuka power station was evaluated to determine the volume of acid required to bring the solutions of the ash samples to pre-selected pH values. The experimental protocol for this section is reported in the section 4.3.7. This preliminary test also revealed the buffering capacity of the fly ash

samples. The equivalence volume of acid can be defined as the volume of acid added per gram of dry ash sample to bring the leachant to a predetermined pH. Acid susceptibility is a measure of the quality or state of the fly ash being affected by the acidified solution. The acid neutralisation behaviour of fresh ash and dry disposed ash is evaluated by plotting the pH and EC of each extract as a function of the equivalence volume of acid added per gram of solid ash sample (Figures 6.3 a & b and 6.4 a & b). The fresh ash (FA) showed high alkalinity (i.e., pH = 11.33) at the initial stage, when only ultra pure water had been added. The pH of dry disposed ashes with zero acid added was lower than that of the fresh ash, which is ascribed to depletion of some basic soluble oxides and hydroxides (i.e., CaO, MgO, and Na_2O) as a result of leaching and weathering over time.

Figures 6.3 a & b show that pH decreases with a corresponding increase in the volume of equivalent acid added per gram of dry fly ash. This is in general agreement with the pH behaviour described by other researchers (Paya *et al*., 1995; Glass & Buenfeld, 1999; Giampaolo *et al*., 2002; Yeyehis *et al*., 2009). This suggests that more inorganic constituents of dry disposed fly ash (with low CaO wt. %) is discharged into solution as the pH of the leachant decreases (see Figures 6.5 a & b and 6.6 a & b).

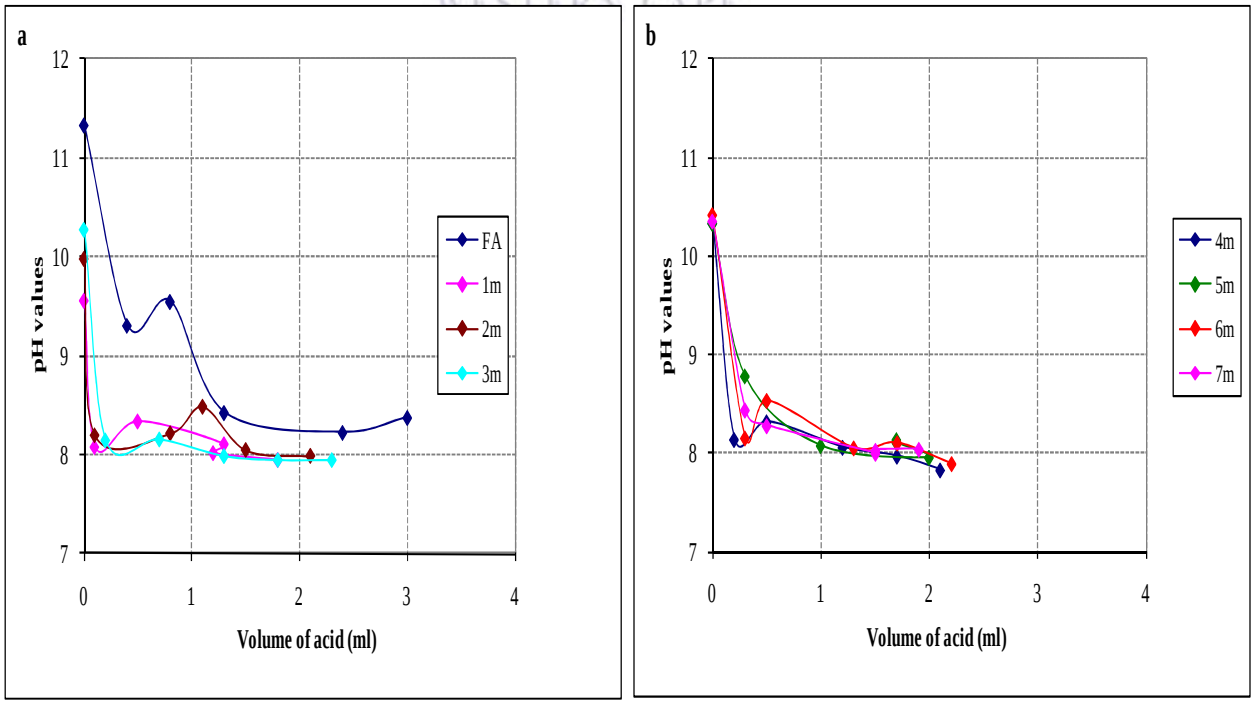

Figure 6.3 a & b. Variations of pH as a function of acid susceptibility behaviours of fresh ash (FA) unsaturated weathered ash as a function of pH

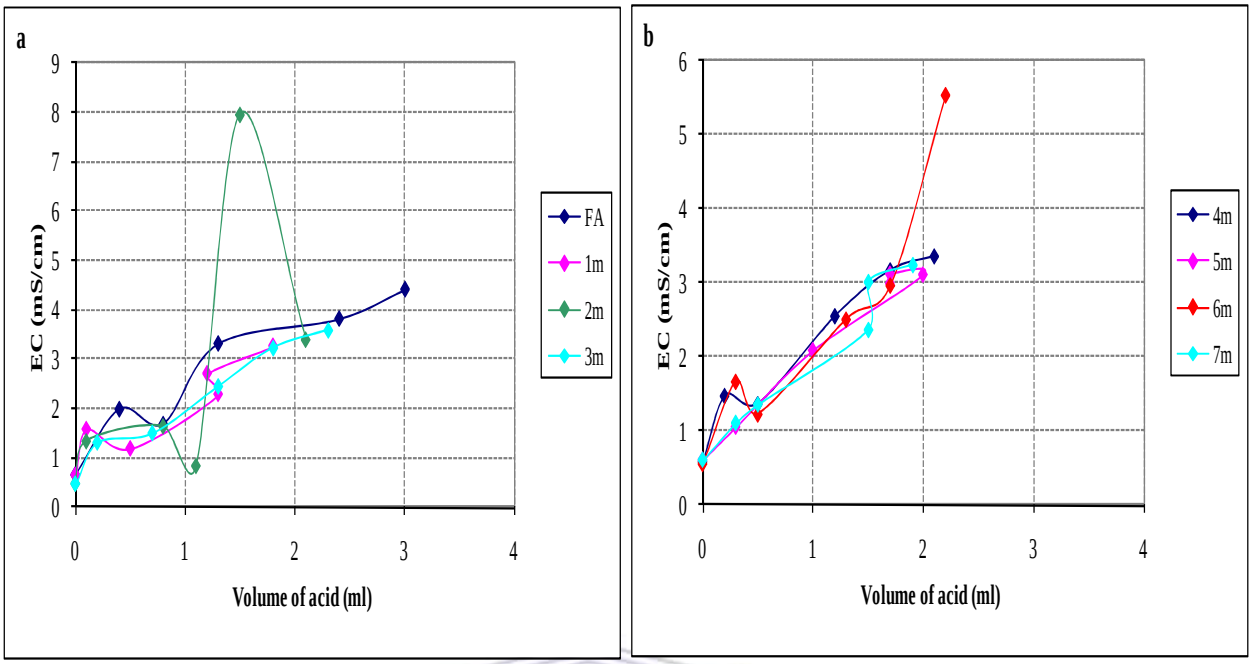

Figure 6.4 (a & b). EC as function of acid susceptibility of fresh ash (FA) and unsaturated weathered ash.

Baba *et al*. (2008) investigated leachability of metals from lignite fly ash under different acidic and temperature conditions. The authors concluded that these heavy metals concentrations increase with respect to increasing acidic conditions and temperature. The fresh bituminous fly ash sample (i.e., low CaO wt. %) used in the current study showed high alkalinity and high neutralisation capacity at the early stage as significant volumes of acid were added to achieve the pre-selected pH. The volume of equivalent acid added per gram of fly ash required to attain the specified pH therefore was higher in fresh ash than in unsaturated weathered dry disposed ashes (Figures 6.3 a & b).

It follows that unsaturated weathered ashes showed low buffering capacity at neutral pH (7.94–8), which was ascribed to the leaching away of soluble basic buffering constituents of fly ash at the disposal site. This is also due to relatively higher CaO content in fresh ash than in unsaturated weathered ashes (Table 5.4). Kukier *et al*. (2003) investigated the magnetic and non-magnetic fractions of coal fly ash. The authors concluded that calcium in the non-magnetic fraction of the alkaline fly ash led to a higher pH buffering capacity of this fraction. Although the aqueous extract of the fresh fly ash had relatively low conductivity (i.e., EC = 0.67 mS cm^{-1}) when in

contact with ultra pure water for 60 min, this value is relatively higher than that of unsaturated weathered ash.

Figures 6.4a & b show that EC increases with a corresponding increase in the equivalent volume of acid added per gram of dry fly ash. The EC increase indicates that more inorganic constituents of fly ash are released into the solution with acid addition.

The dissolution of soluble acids, such as B_2O_3, and salts containing hydrolysable constituents, such as $Fe_2 (SO_4)_3$ and $Al_2 (SO_4)_3$, can reduce the pH of the fly ash solution. The relative quantities of these soluble acids and bases in a particular fly ash will determine whether the leachate will have a dominant acidic or basic behaviour. Several studies have recognised that the pH of the aqueous extract of fly ash results from dissolution and hydrolysis of basic oxide components, such as CaO (Iwashita *et al*., 2005; Reardon *et al*., 1995). A considerably lower concentration of Si was discharged into solution at both high and low pH, indicating a slower leaching rate of silica-rich glass in fly ash particles.

The release of ions from glass can be represented by

$$SiO_2\,(glass) + 2H_2O = H_4SiO_4 \qquad (1)$$

$$M^{n+}\,(glass) + n\text{-}H_2O = M^{n+}\,(aq) + nOH^- \qquad (2)$$

where M is a metal ion in the glass matrix (Kirby & Rimstidt, 1994). Silicon clearly exhibits kinetic control, but the kinetics of silicon release to solution is slowed by the precipitation of a secondary phase (hydrous aluminosilicate) at alkaline pH (Kirby & Rimstidt, 1994; Reardon *et al*., 1995).

6.5 Chemical characterization of the leachates

The leachates from the ANC experiment were analyzed for cations with ICP-OES (see Figure Avi in the Appendix Aix). The selected major and trace elements are profiled in Figures 6.5 a-c and 6.6 a & b respectively. The concentrations of major elements from the ANC test are plotted as a function of leachant pH (Figures 6.5 a-c). In general, the release pattern of elements in fresh ash and dry disposed ash was pH dependent; with solubility of metals increasing as solution equilibrium pH decreased. Tan *et al*. (1997) reported that as the pH of the extractant decreases below neutral and into acidic ranges, the concentrations of metals rise substantially due to the

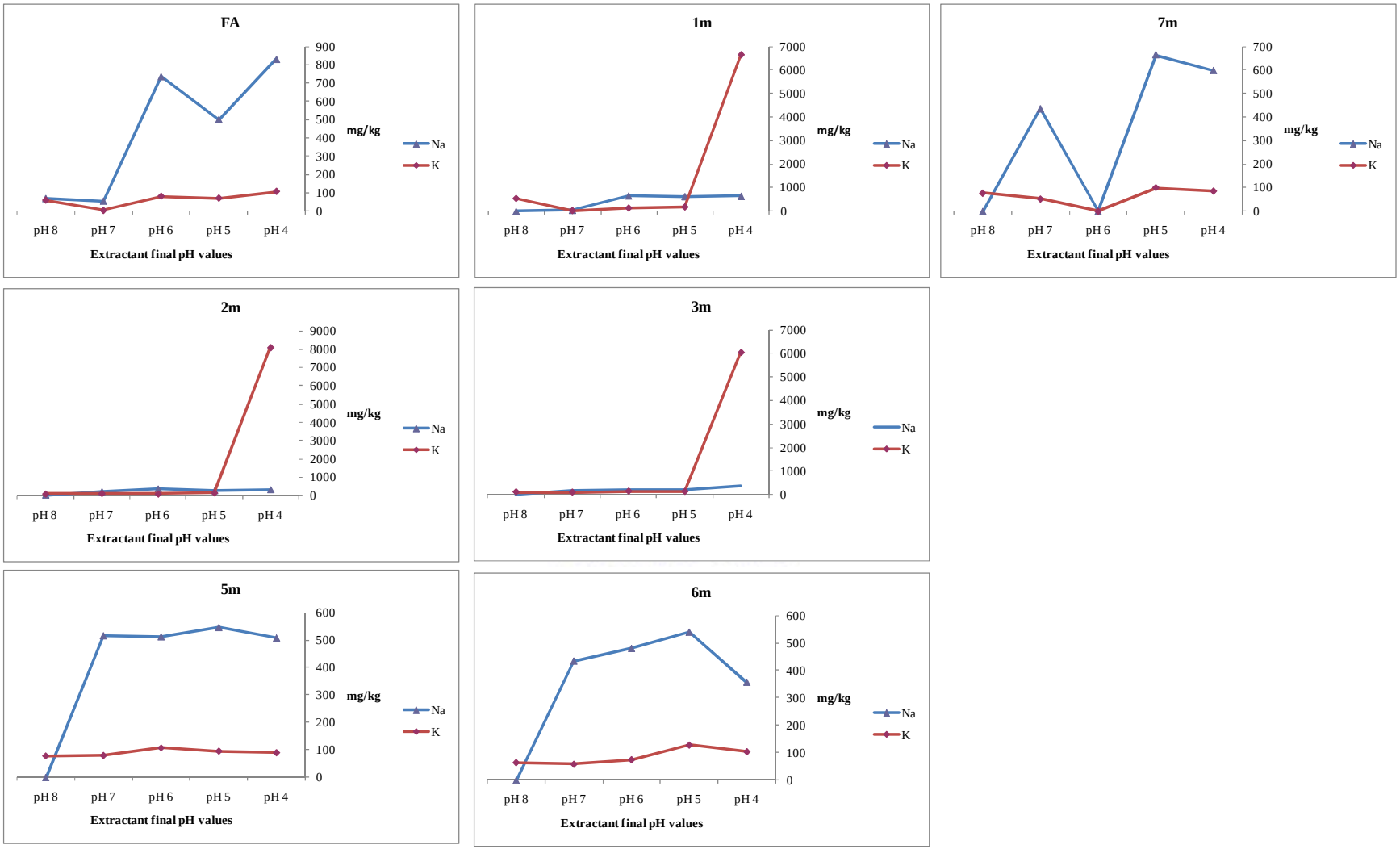

Figure 6.5 (a). Acid leaching behaviour of major elements (Na^+ and K^+) from the unsaturated dry disposed fly ash at different depths as determined at different pH

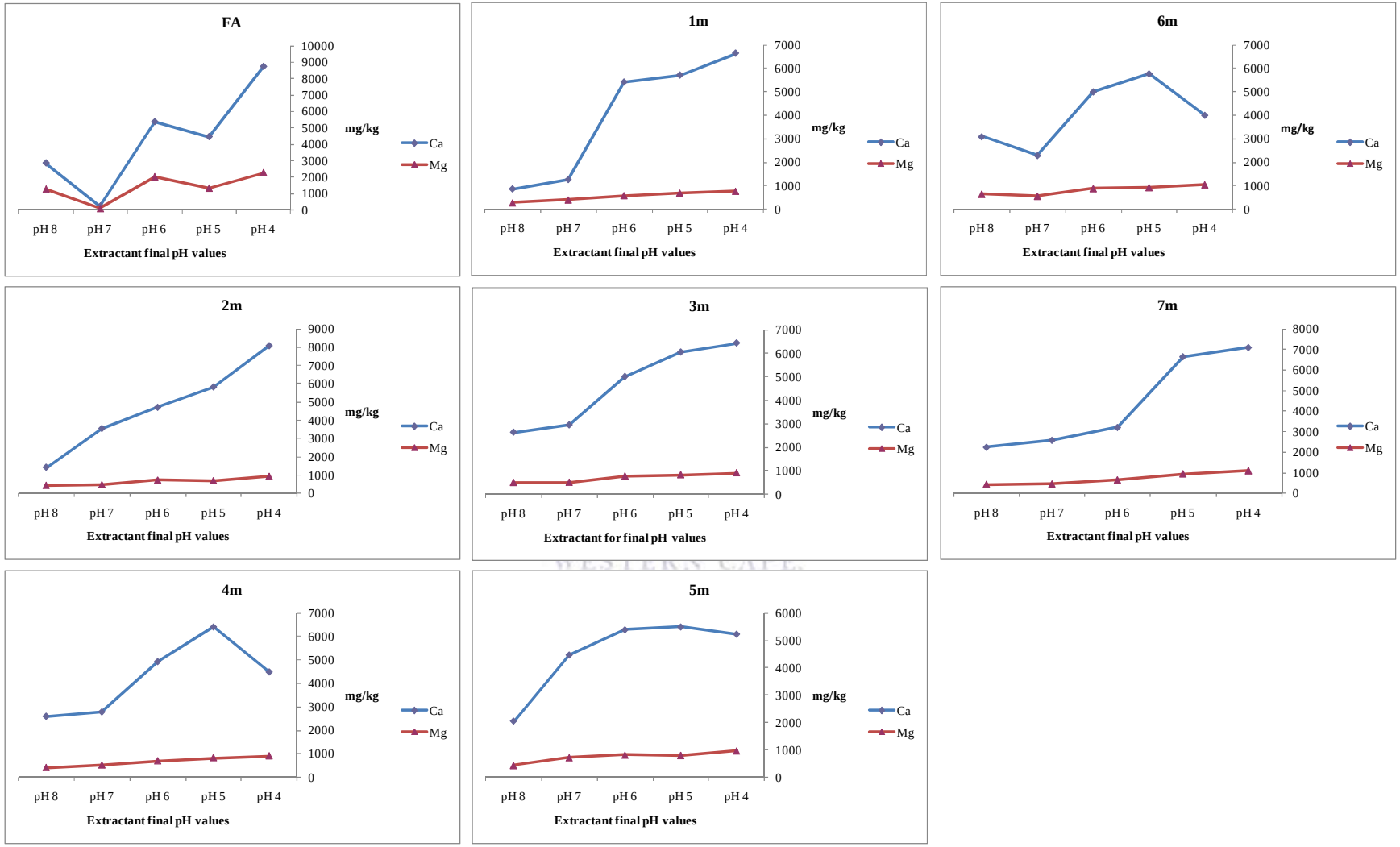

Figure 6.5 (b). Acid leaching behaviour of major elements (Ca and Mg) from the unsaturated dry disposed fly ash at different depths as determined at different pH

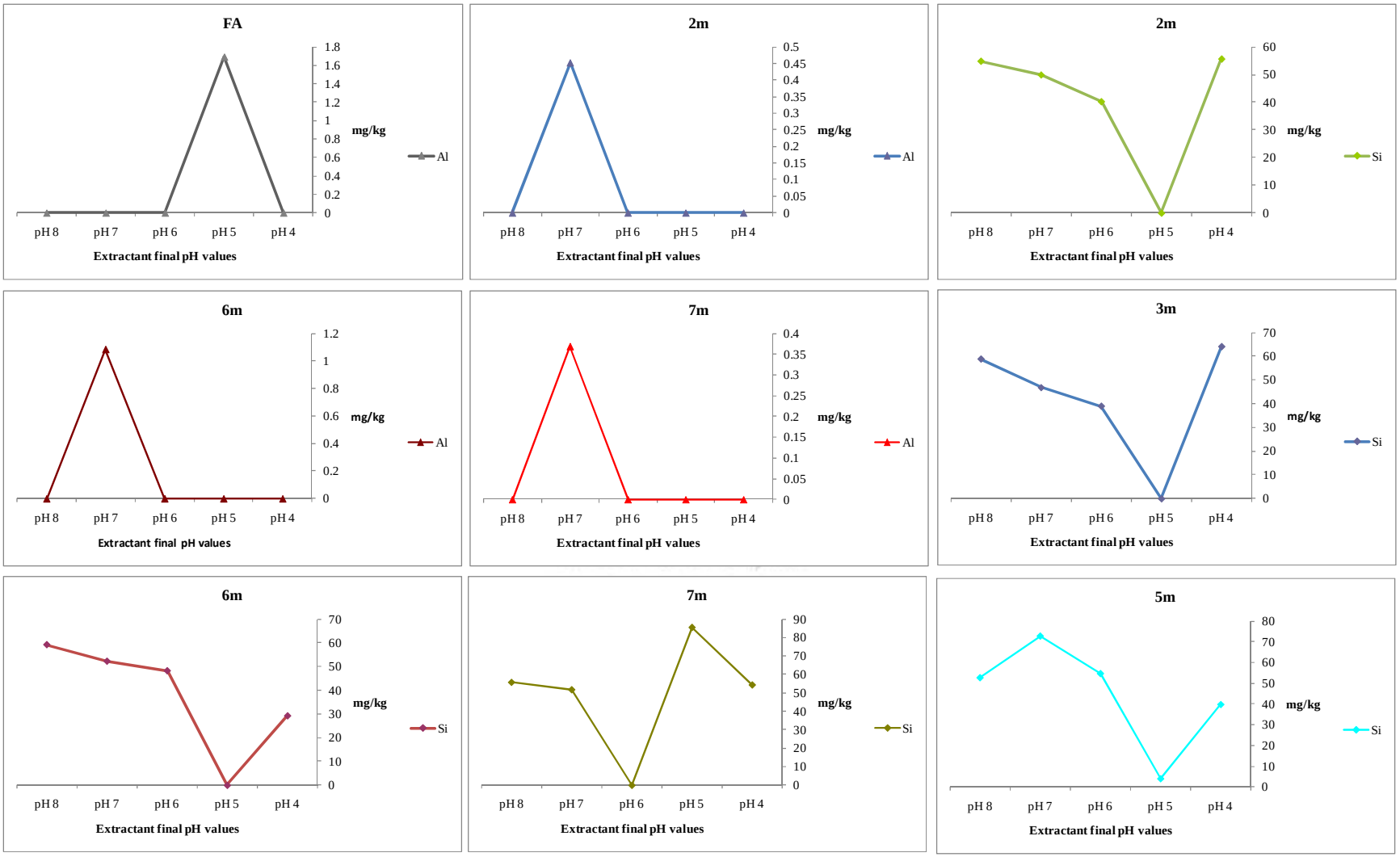

Figure 6.5 (c). Acid leaching behaviour of major elements (Al and Si) from the unsaturated dry disposed fly ash at different depths as determined at different pH

release of metals bound to carbonate fractions. The concentrations of both major and trace metals from unsaturated weathered ash are generally lower than those from fresh fly ash, which can be ascribed to loss of these elements from the dump prior to sampling as a result of leaching after rain infiltration over 20 years. Lower concentrations of elements were found in the unsaturated weathered ash than in fresh ash, even at pH 4, as well as at the inherent pH of 9.56–10.41 and 11.33, respectively. XRD analysis and water solubility experiments showed that low concentrations of metals in unsaturated weathered ash result from association of metals with less insoluble mineral phases (i.e. calcite). It could also be that all the water soluble components have leached out over 20 years of exposure to rain infiltration.

The effects of ingressing CO_2 from the atmosphere and percolating rain water (see Section 2.4.6) on the dry disposed fly ash have led to the flushing of soluble basic buffering constituents in fly ash, which could have maintained the pH of the leaching system under natural environmental conditions. The low concentration of many metals in dry disposed fly ashes could be attributed to over time leaching or slower leaching rate due to formation of secondary minerals as revealed by XRD (Figure 5.2). These secondary minerals could act as barriers to release of these species in the weathered drilled core samples. Fatoba (2008) reported that the concentration of Pb in fly ash could be attributed to adsorption processes and complex formation. Lee and Saunders (2003) in their study indicated that Pb strongly adsorbed to hydrous ferric oxide (HFO) over a wide range of pH. The authors concluded that both sorption (due to pH increase) and solid sulphide formation are important for Pb removal from solutions.

The solubility patterns of elements in fresh ash and dry disposed ash are broadly classified into four categories:

1. delayed release pattern; these metals start with a low concentration in solution but increase as pH decreases, these include Mg, K, Cr, Sr and Pb (at lower depth) (Figures 6.5a, 6.5b, 6.6a and 6.6b).
2. concentration increases linearly with decreasing pH; these include Ca, Na and Se (Figures 6.5a, 6.5b and 6.6a).
3. concentration starts at minimal values at high pH but increases to a maximum then decreases again at low pH; these include Al, Mo, As and Pb. A common feature with Mo

and As is that they can exist as oxyanions at circum-neutral and alkaline pH (6.5c and 6.6b).

4. concentration starts at maximal values at high pH but decreases to a minimum then increases again at low pH; this applies to Si (Figure 6.5c). The shape of the curve for pH-regulated silicon suggests that it is possibly released from the rapid dissolution of amorphous aluminosilicate minerals in fly ash, which occurs at alkaline (high pH) values of leachant.

The solubility pattern of Na^+ and K^+ in the leachates show a general increase in concentration with decrease in solution pH. This is a result of low CaO content and the leaching of soluble major components leaving behind non-soluble components in unsaturated weathered ash. This suggests that Na^+ and K^+ solubility in unsaturated weathered ash is controlled by pH of the solution and that their concentration in the leachant is governed mainly by their availability in the fly ash. The observed pH dependence of Na^+ and K^+ in unsaturated dry disposed fly ash generally contradicts the earlier observed non-pH-dependent behaviour of Na^+ and K^+ in solidified wastes (Tiruta-Barna *et al*., 2004; Quina *et al*., 2009).

The oxyanions of heavy metals such as Cr and Se show increased solubility with decreased solution pH. Mizutani *et al*. (1996) observed that solubility of some heavy metals in municipal solid waste (MSW) increased with corresponding decreases in leachant pH. Other heavy metals like Mo, As and Pb show somewhat different solubility behaviours with equilibrated solution pH. The solubility curve behaviours of As, Mo and Pb with respect to leachant pH are likely dependent on the oxidation states of As, Mo and Pb present in the fresh fly ash and unsaturated weathered ash. The results obtained from unsaturated dry disposed ash taken at 5 m and 6 m depths show pH-dependent behaviour of Pb, whereas incongruent behaviour is observed in the fresh and unsaturated dry disposed ash taken at 2 m and 3 m depths (Figure 6.6b). This suggests that the concentration of Pb in the leachant could also be attributed to Pb availability or concentration in the fly ash (see Table 6.1).

The solubility curves of As, Mo and Pb exhibit amphoteric behaviour, which is characterised by high solubility at low and high pH and moderate or low solubility at neutral or moderately high pH (Quina *et al*., 2009). Drever (1997) also reported in his study that the release of Cr with respect to the pH of the leachate is dependent upon the oxidation state of Cr that is present in the

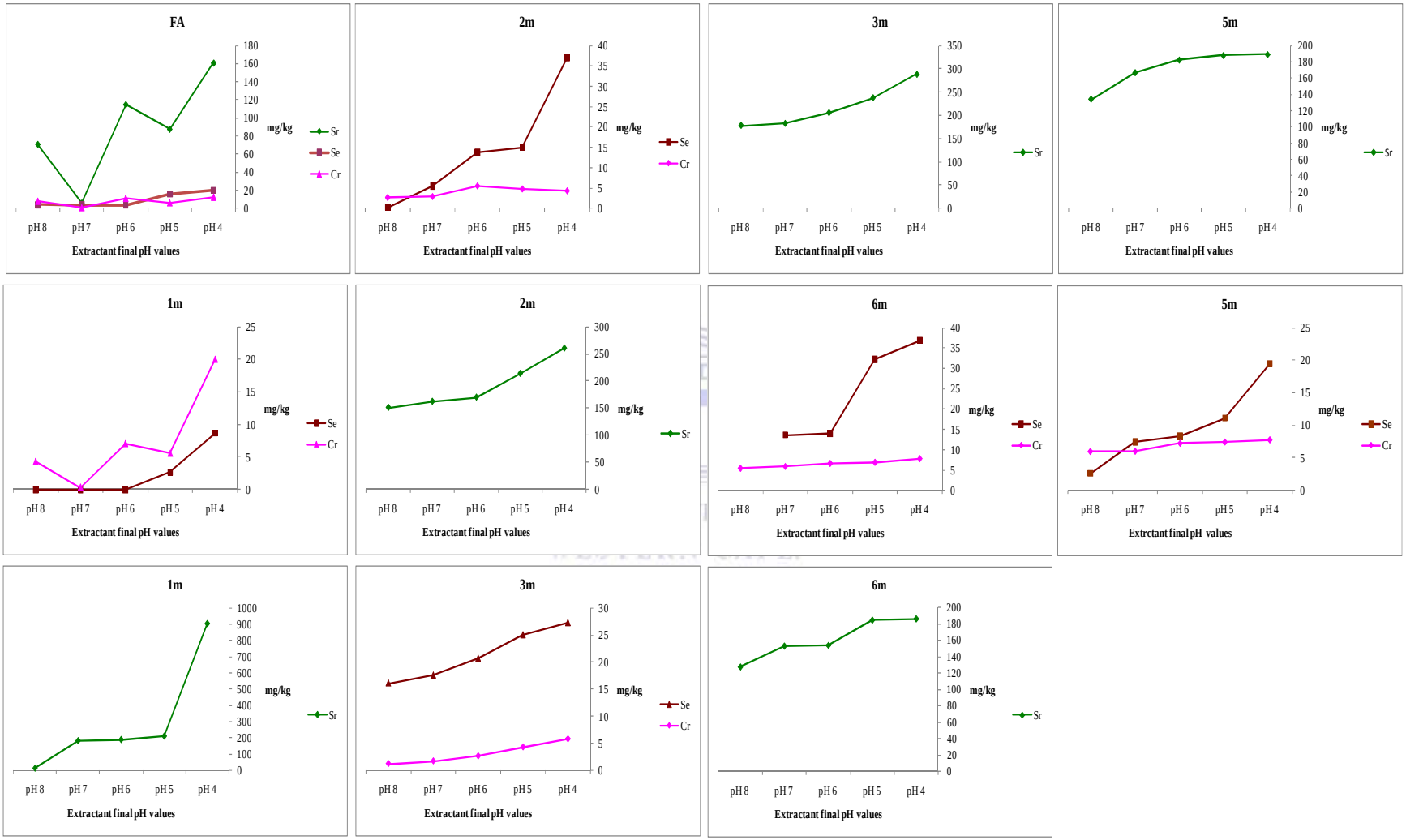

Figure 6.6 (a). Acid leaching behaviour of trace elements (Cr, Se and Sr) from the fly ashes at different depths as determined at different pH

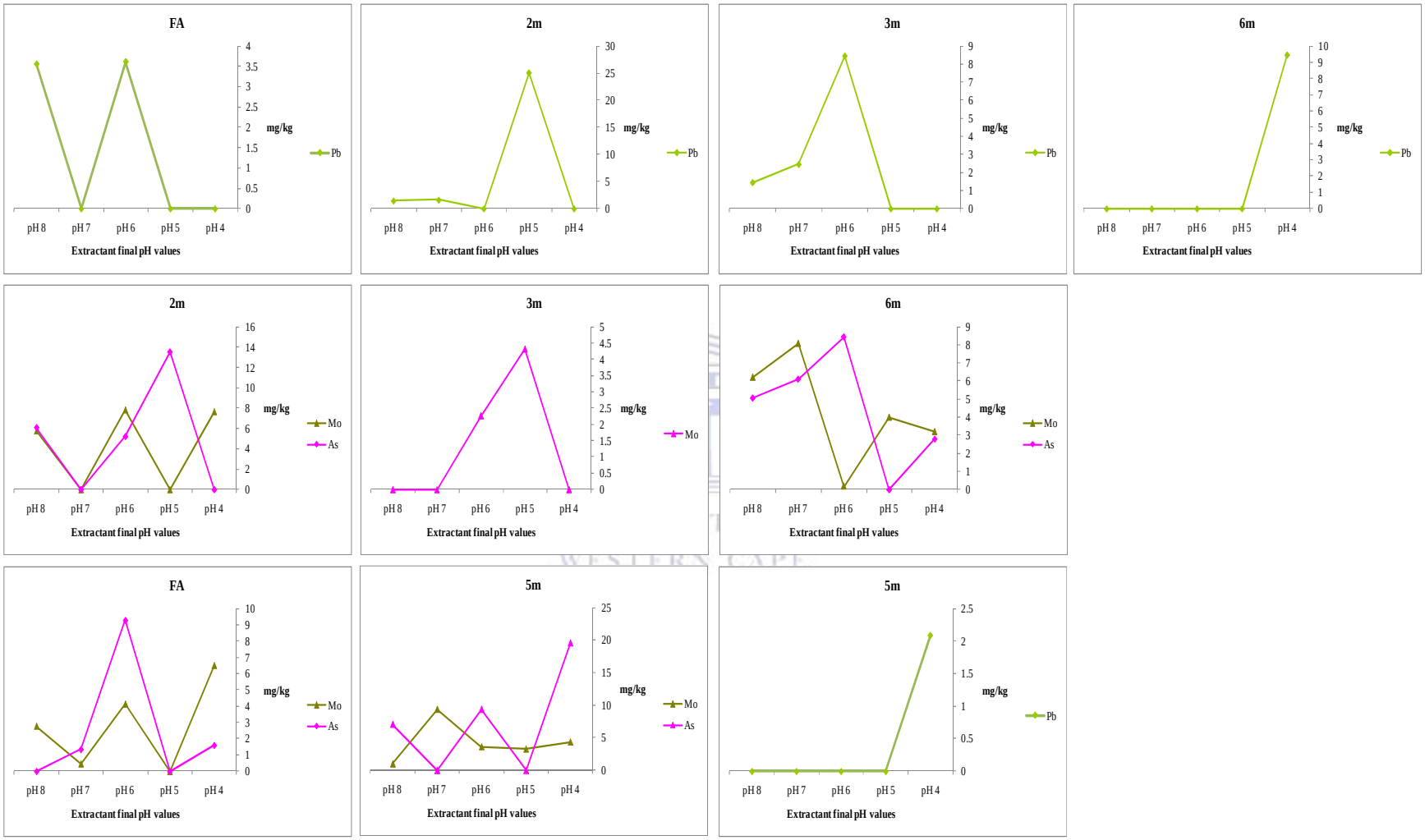

Figure 6.6 (b). Acid leaching behaviour of trace elements (As, Mo and Pb) from the fly ashes at different depths as determined at different pH

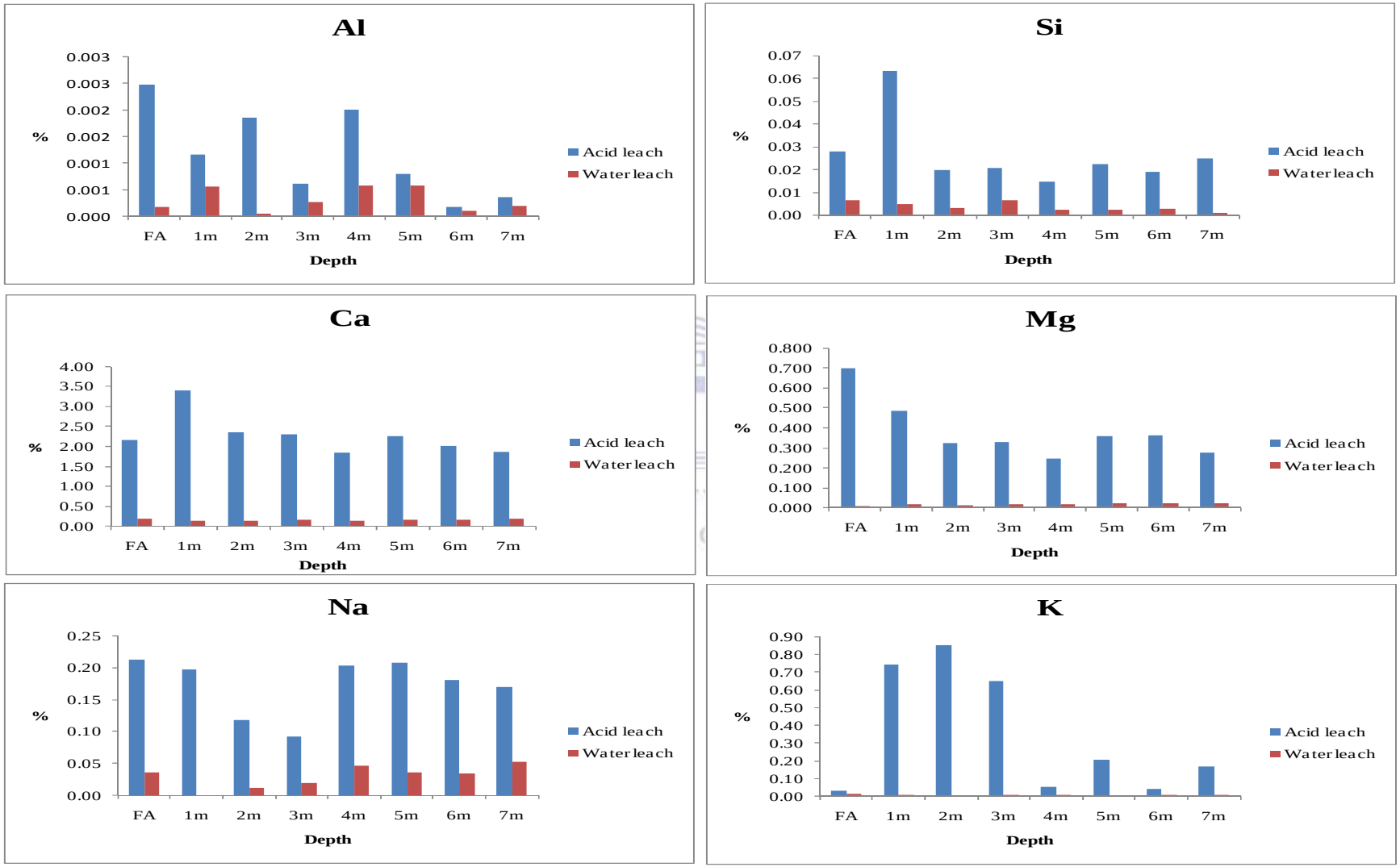

Figure 6.7a. The extractability of major elements in de-ionised water and acid leaching solutions.

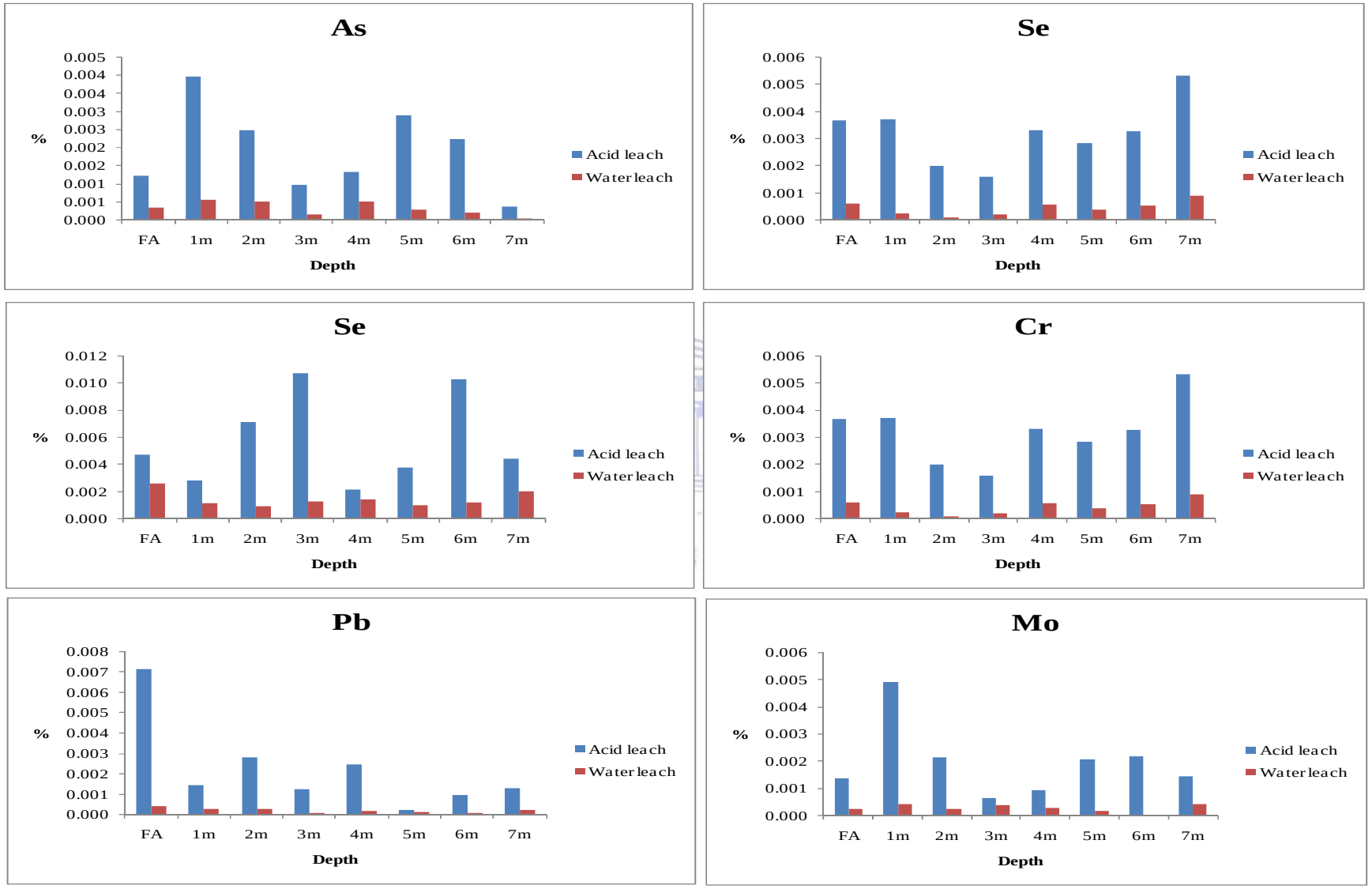

Figure 6.7b. The extractability of trace elements in de-ionised water and acid leaching solutions.

fly ash. This is in general agreement with the study on leaching of major and trace elements from MSWI bottom ash (Dijkstra *et al*., 2006). The concentration of Pb in dry disposed ashes taken at 3m, 5m and 6m depth is relatively higher than that in the fresh ash sample; this could be explained by the washing out of soluble salts, especially with slight changes in solution pH.

Vitková *et al*. (2009) in their study of smelter fly ash observed that washing out of soluble salts significantly decreased the leachability of Cd, Zn, As and Sb and increased the release of Pb, especially under acidic conditions. Figures 6.7a and 6.7b show the extractability of major and trace metals in the de-ionised water leach and acid leach tests. Both the major and trace metals show higher extractability in the acidic medium compared with de-ionised water. Metals such as Mg and Pb show less resistance to acid attack in the fresh ash, whilst Ca, K^+, Se and As show less resistance to vigorous acid attack in the unsaturated weathered ash due to initial leaching/flushing of major components in the fly ash after land filling. This suggests that contact of fresh ash and unsaturated weathered ash with a slightly acidic medium (acidified rain water) will eventually lead to higher release of metals from the fly ash to the surface and to groundwater in the vicinity of the ash dump.

6.6 Summary and conclusions

In this investigative study, a comprehensive characterisation of Tutuka fresh and unsaturated dry disposed fly ash samples was performed from the viewpoint of environmental implications of dry ash disposal system. The important features of this study are as follows:

1. Physical, chemical and mineralogical characterisation results revealed important differences between the fresh ash and dry disposed ash samples. XRD and XRF analysis results showed alteration in mineralogy and chemical composition of the fly ash after disposal.

2. XRD confirmed calcite and mica as the predominant secondary minerals formed in the unsaturated weathered dry disposed ash.

3. The unsaturated weathered dry disposed ash had lower buffering capacity at neutral pH (7.94–8.00) compared with unweathered (fresh) fly ash. This may be due to the initial leaching/flushing of soluble basic buffering constituents of fly ash at the disposal site.

4. The release of elements such as Ca, Mg, Na^p, K^+, Se, Cr and Sr is controlled by solution pH. The pH-dependent behaviour of Na and K is due to leaching and flushing of soluble major

components and is not controlled by the availability of these metals in the coal fly ash. Other trace metals, like As, Mo and Pb, showed amphoteric behaviour with respect to solution pH.

5. Chloride and sulphate anion species of water soluble extract are at equilibrium with Na and K and show significant accumulation at the bottom of unsaturated dry disposed ash. This demonstrates that the soluble salts associated with the surfaces of fly ash particles are dissolved upon chemical interaction with percolating rain water and move down through the ash just like in a chromatographic column.

6. Despite the chemical and mineralogical transformations and slight variations in the chemical composition of unsaturated weathered ashes, the overall results of the acid neutralisation capacity tests suggest that both fresh ash and unsaturated weathered ash could contaminate the surface and groundwater near the ash dump when they come in contact with slightly acidified rain.

Proper management of ash dumps is therefore very important to safeguard the environment from pollution from poisonous trace elements contained in fresh ash. Incidences of acid rain at ash dumps should be monitored regularly and control measures for pH stabilisation should be instituted.

CHAPTER SEVEN

Results and Discussion 3

Chemistry of the major species and its impacts on the chemistry of trace toxic species (such as As, Se, B, Cr, Mo and Pb) in weathered drilled ash cores

This chapter presents the results obtained from sequential extraction scheme originally developed by Tessier and others, modified and applied on dry disposed ashes at different stage of weathering/ageing. The crucial effects of chemical alteration and mineralogical transformations on the chemical partitioning, solubility and mobility of major elements in a dry disposed ash in a land fill are revealed and discussed.

7. Introduction

Major and trace species can exist in various physico-chemical forms. These forms include: exchangeable forms, carbonate, secondary Fe and Mn oxides, organic matter, sulfides, and silicates (Tessier *et al.*, 1979). The concept of the sequential extraction scheme is the partitioning of a solid material into specific phases or fractions that are selectively extracted, i.e. liberated and released into solution (leached) along with the associated trace metals. In this process, appropriate reagents are used in the order of increasing strength (Tessier *et al*., 1979; 1992; Horowitz, 1991). The sequential extraction (SE) procedure is advantageous in that it enables us to evaluate the potential environmental availability of trace metals associated with sediments in specific phases under various environmental conditions (Skvarla, 1998). The actual difficulty of the sequential extraction procedure is that the extraction from each step depends on the efficiency of previous step(s), and some factors such as leaching time, liquid-solid ratio, and strength of the chemical reagent (i.e. pH of the medium) can influence the extracted amount of metals (Chang *et al*., 2009). Sequential extraction procedures have been applied to sediments (Mester *et al*., 1998; Petit and Rucandio, 1999), contaminated soils (Campos *et al*., 1998), and incinerated sludge ash (Fraser and Lum, 1983). Recently, this step by step sequential extraction procedure was applied to bottom ash and fly ash from municipal solid waste incinerators (MSWI) to determine the distribution of various elements (Bruder-Hubscher *et al*., 2002; Smeda and Zyrnicki, 2002; and Smichowski *et al*., 2008).

This investigative study is focused on the chemical partitioning of major elements in a dry disposed fly ashes aged 20 year, 8 year and 1-year-old. The fly ash at the top of each core was laid down in the same year with ash at the bottom of each core in a land fill. The dry disposed fly ashes are markedly different in ash type, ash texture, and moisture content levels. In the present study the sequential extraction scheme was used to shed light on different solvent mediums that leach major elements in different mineral phases in coal fly ash. The five-step sequential extraction scheme adopted for the determination of the major elements partitioning in coal fly ash of different ages was based on the method of Tessier's and others (1979). The fractions are as follows: (i) water soluble fraction(deionised water) (ii) exchangeable fraction (CH_3COONH_4 at pH 7) (iii) carbonate fraction (CH_3COONH_4 at pH 5) (iv) amorphous Fe and Mn fraction ($NH_2OH{\cdot}HCl$), and (v) residual fraction (HF, $HClO_4$, HNO_3, 3:3:1). The partitioning pattern of Al, Si, Fe, Mn, Ca, Mg, Na^+ and K^+ species in the various physico-chemical forms or mineral phases as a function of depth in the ash dump investigated was used to: 1) understand the mobility patterns with depth and ages in various sections of 1 year, 8 year, and 20-year-old ash dumps; and 2) to identify and quantify the availability of the major elements in the various mineral phases.

7.1 Chemical sequential extraction scheme results

7.1.1 Analysis of water soluble fraction

A modified chemical sequential extraction scheme was applied in this study to determine major elements partitioning in the dry disposed fly ash. The experimental protocol for these results is presented in the section 4.2.5. Analysis of the water soluble fraction of the 1 year, 8 year and 20-year-old cores at different depth profile are shown in Figures 7.1-8.7. The leaching trends of the major elements (Al, Si, Ca, Mg, Fe, Mn, Na^+ and K^+) as a function of depth in the water soluble fraction of fly ash at different stage of weathering are discussed below.

7.1.1.1 Aluminium and silicon

Figure 7.1 depicts the concentration trends of Al in the water soluble fraction of 20 year, 8 year and 1-year-old fly ash. The highest concentration of Al is recorded in the 1-year-old fly ash. The concentration variation of Al in the top section, middle section and bottom section of 3 drilled ash cores evidently showed it is controlled by type, moisture content levels and textures of the coal fly ash. However, the concentration difference of Al in the top, middle and bottom sections

of the 3 drilled fly ash cores is possibly suggests Al is less mobile in dry disposed fly ash due to chemical interaction of fly ash with ingressed O_2, ingressed CO_2, and percolating rain water(weathering/ageing). A relative decrease or increase in observed in the pore water pH of the 3 drilled fly ash cores (Figures 5.17-5.19). The relatively high concentrations at the top sections of 20 year and 8-year-old ash cores which is due to dissolution of amorphous aluminium hydroxide influenced by weathering/ageing. The leaching trend of Al is controlled by the pore water pH of the ash column. The acid neutralisation capacity (ANC) results show that Al release is governed by solution pH (see Figure 6.5c). It has been reported that the leaching of Al is controlled by amorphous $Al(OH)_3$ for pH ranging between 6 and 9, and by gibbsite ($Al(OH)_3$) for pH greater than 9 (Fruchter *et al*., 1990; Roy and Griffin, 1994; Garavaglia and Caramuscio, 1994). Previous studies had shown that aluminium leaching could be influenced by the dissolution and precipitation of amorphous aluminosilicate and silicate at the slightly low pH of ash pore water (Roy and Griffin, 1984; Zevenbergen *et al*., 1994). The relatively low concentrations of Al at the bottom sections of 20 year and 8-year-old fly ash is probably influenced by Al wash off or dissolved in the saturated zone and its subsequent diffusion, transportation and possible accumulation in the extra space of the ground water, thus leaving an Al-depleted ash at these depths.

Figure 7.1 shows Si concentration trend in the water soluble fraction of fly ash of different ages. The highest concentration of Si is recorded in the 1-year-old fly ash. A slight difference in the Si concentration is recorded in the top, middle and bottom sections of 8-year-old fly ash. The difference in silicon concentration in the top, middle and bottom sections of 1 year and 20-year-old seems inconsequential suggesting that Si is less mobile is due to chemical and mineralogical transformations caused by weathering/ageing. The concentration profile of Si appears also to be influenced by the pore water pH of the ash column (see Section 5.7). It has been reported that the minerals most susceptible to weathering after the initial rapid dissolution of CaO and other soluble salts in the fly ash were amorphous aluminosilicates and silica (Seoanne and Leiros, 2001). The relatively low concentration trend of Si in spite of the relative decrease in pore water pH observed at the bottom sections of the 3 drilled fly ash cores is caused by the dissolution of quartz minerals and the subsequent diffusion of Si into the groundwater thus leaving a Si depleted fly ash. Low concentration of Si in the ash pore water might be due to dissolution of amorphous aluminosilicate minerals that do occur at slightly low pH values (7.0 - 10.0). The

release of Si in the dry disposed fly ash is governed by the solution pH (Figure 6.5c). A previous study has shown that Si concentration is governed by the solubility of quartz (SiO_2) at pH lower than 10 and by the solubility of calcium aluminosilicate at higher pH (Tiruta-Barna *et al*., 2006). It has been recognized that the higher pH of fresh ash (11.0 – 12.0) promotes rapid dissolution of aluminosilicate minerals at slightly decrease in pore water pH during weathering (Zevenbergen *et al*., 1994). It has been reported that Si concentration is consistent with SiO_2 solubility at pH lower than 10 and with wairakite ($CaAl_2Si_4O_{12}.2H_2O$) at higher pH values (Garavaglia and Caramuscio, 1994).

7.1.1.2 Iron and manganese

Figure 7.2 shows the concentrations of Fe in the extractable water soluble fraction at different stages of weathering. The highest concentration of Fe (0.01 – 0.08 ppm) was observed in the 1-year-old fly ash while the least (0.1 – 4e-5ppm) was from the 8-year-old ash cores (Fig. 7.2). The concentration difference of Fe in the top, middle and bottom sections of 20 year and 1-year-old fly ash is not significant suggesting metal immobilization. This is suggesting that the composition of the ash and whether the ash has come into contact with water do not plays a role in the trends. In contrast, a considerable difference in Fe concentration occurred in the top, middle and bottom sections of 8-year-old is influenced by the textures of coal fly ash. The relatively low concentration of Fe at the bottom section of 20-year-old ash cores (saturated zone); is possibly due to slower release due to precipitation of amorphous Fe hydroxide at a favourable pore water pH conditions or possible diffusion of Fe into the groundwater underneath ash dump. The Fe concentration in the water soluble fraction appears to be less controlled by the pore water pH of the ash column (see Section 5.7). A previous study (Garavaglia and Caramuscio, 1994) showed that Fe is in equilibrium with amorphous iron hydroxide ($Fe(OH)_3$).

Figure 7.2 shows the concentration profile of Mn in water extractable fraction of fly ash of different ages. The highest concentration of Mn is recorded in the 1-year-old fly ash. Manganese shows decreasing response with increasing depth in the water soluble fraction of 20-year-old fly ash. A slight concentration difference of manganese in the top, middle and bottom sections of 20 year and 1-year-old fly ash suggests that the composition of the ash cores and when its come into contact with the water do not plays significant role in the vertical distribution patterns.

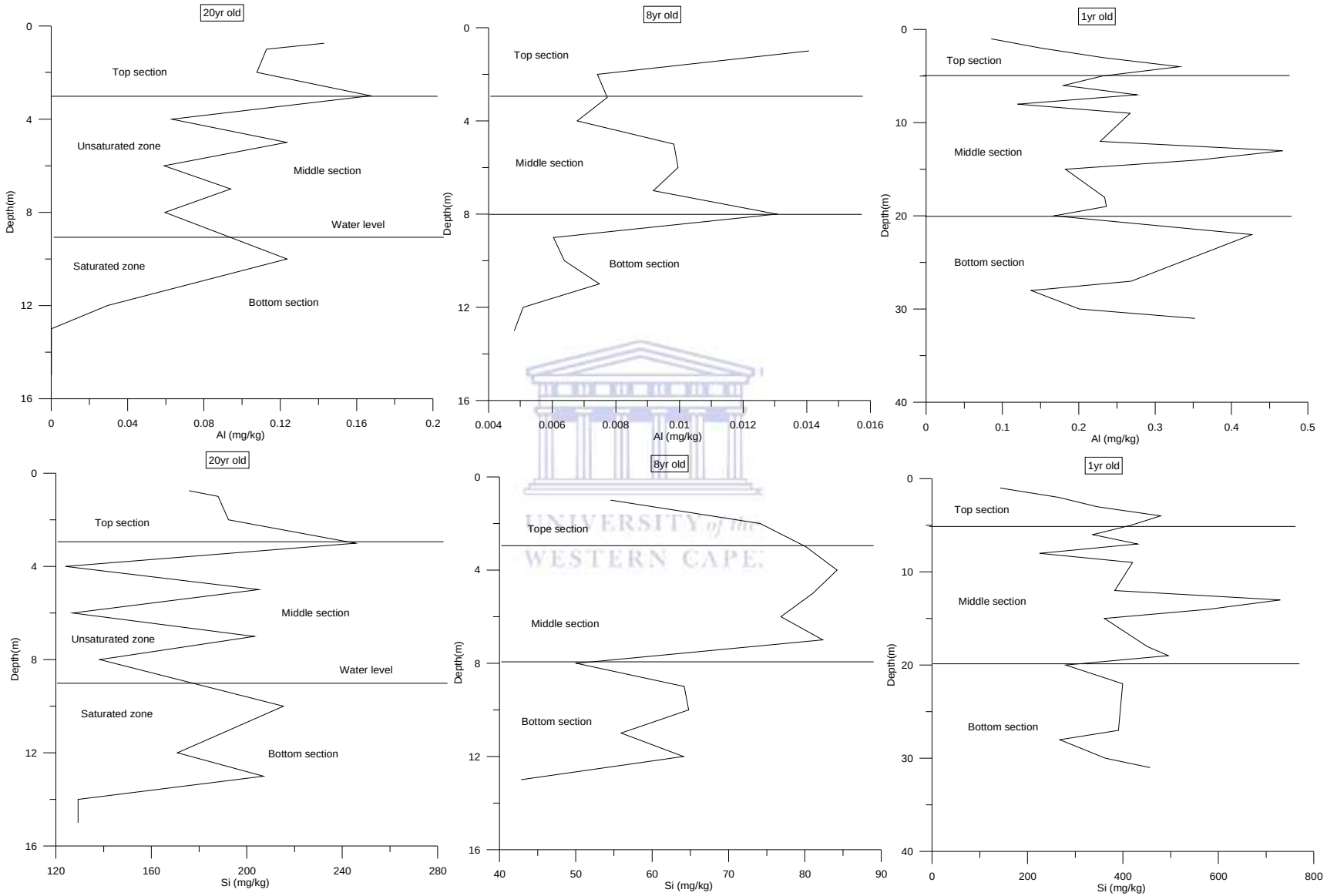

Figure 7.1. Aluminium and silicon trend in water soluble fraction of drilled cores of different ages and depths (n=3).

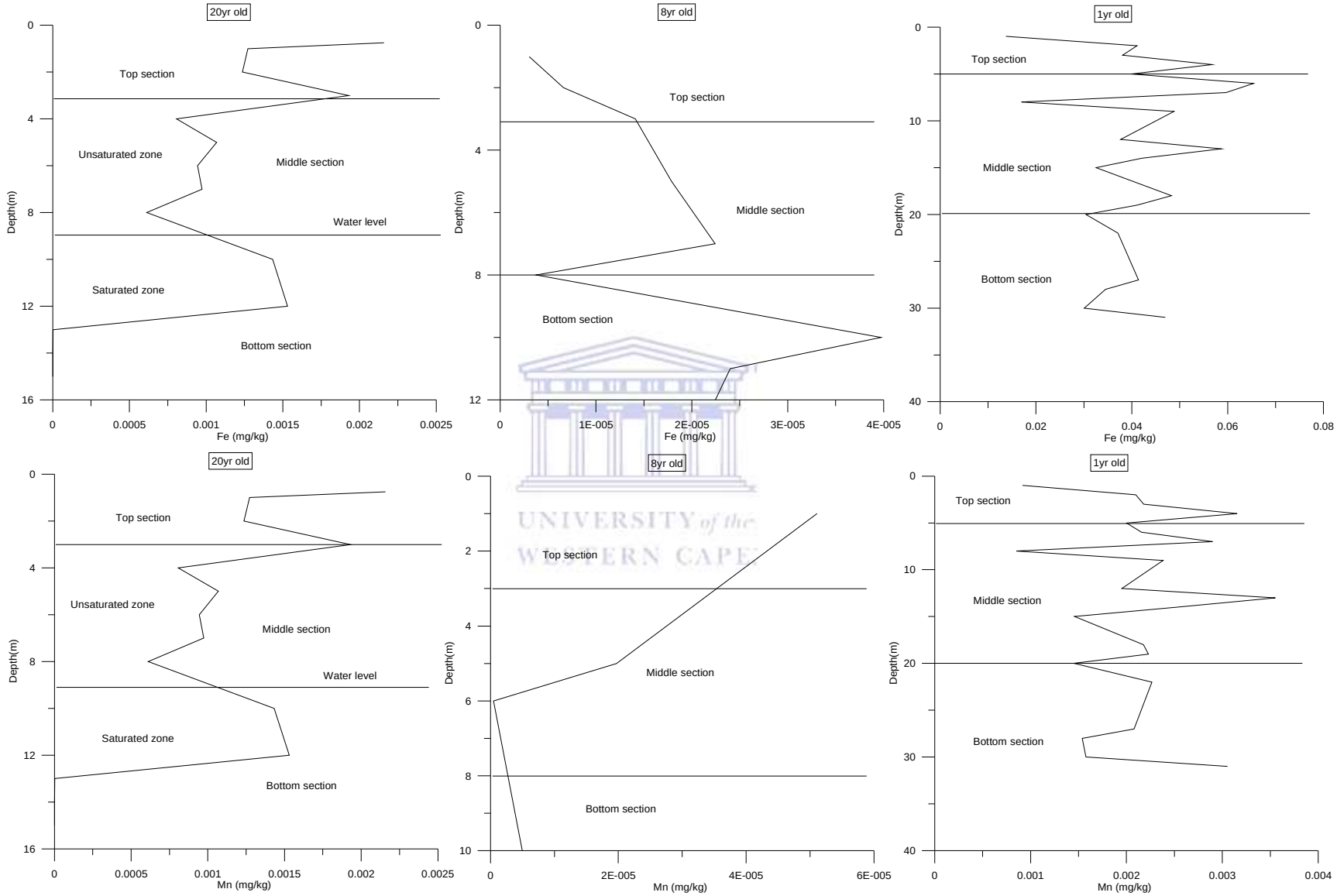

Figure 7.2. Iron and manganese trend in water soluble fraction of drilled cores of different ages and depths (n=3).

7.1.1.3 Calcium and Magnesium

Figure 7.3 shows the concentration profile of Ca in the water soluble fractions of the fly ashes at different stages of weathering. The highest concentration of Ca is recorded in the 1-year-old fly ash. Calcium concentration difference in the top, middle and bottom sections of 1 year and 20-year-old ash cores is noticeable due to leaching of major soluble components in the fly ash. A considerable high concentration observed in the bottom section of 8-year-old ash cores is influenced by pore water pH and moisture content level of the ash cores. The concentration of Ca in the water soluble fraction is controlled by the pore water pH of the ash column (see Section 5.7). The acid neutralisation capacity results of the dry disposed fly ash showed that Ca concentration is dependent on the solution pH (see Figure 6.5b). It has been reported that the dissolution of calcite ($CaCO_3$), which may have precipitated out of the solution at high pH, could lead to increase in Ca concentrations in the leachate (Johnson *et al*., 1995; Iwashita *et al*., 2005). Calcium concentration could be controlled by gypsum at pH lower than 10.5 and by wairakite at higher pH values (Garavaglia and Caramuscio, 1994).

Figure 7.3 shows Mg concentration trend in the water extractable fraction of ash cores at different stages of weathering. The highest concentration of Mg is observed in the 1-year-old ash cores. The highest concentration of Mg in the 1-year-old ash cores is due to faster release of Mg due to fly ash texture. Mg has a slight concentration difference in the top, middle and bottom sections of 1 year and 20-year-old ash cores suggesting that Mg is less mobile due to slower release. On the contrary, the concentration difference in the top, middle and bottom sections of 8-year-old ash cores is remarkable suggesting that ash moisture content level play a role in the trends. A relatively low concentration of Mg is recorded at the bottom sections of 20-year-old ash cores is most likely due to flushing of dissolved Mg into ground water. The vertical distribution of Mg in the 3 drilled cores showed that is controlled by the pore water pH. The acid neutralisation capacity results showed that Mg release in the dry disposed ash cores is influenced by solution pH.

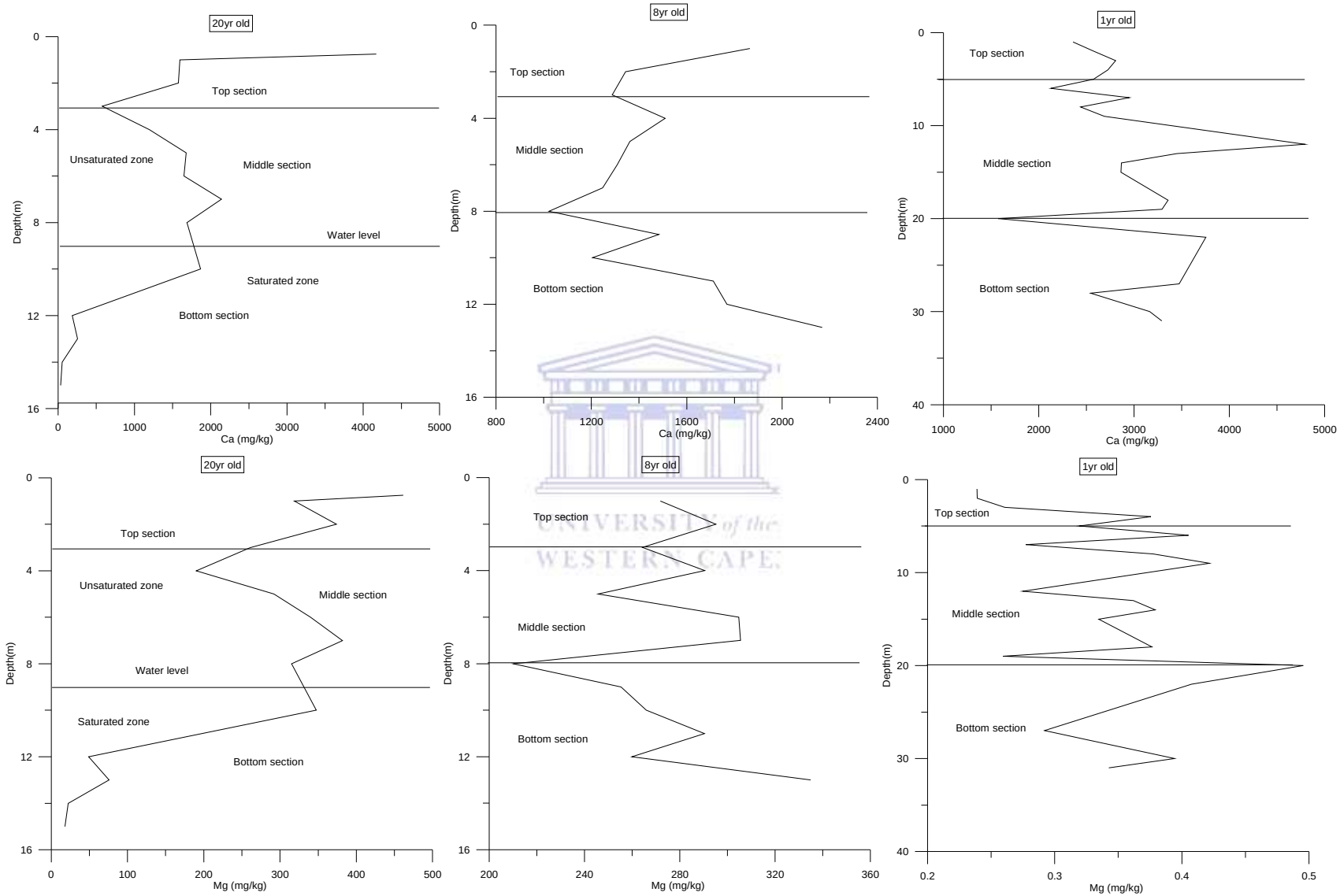

Figure 7.3. Calcium and magnesium trend in water soluble fraction of drilled cores of different ages and depths (n=3).

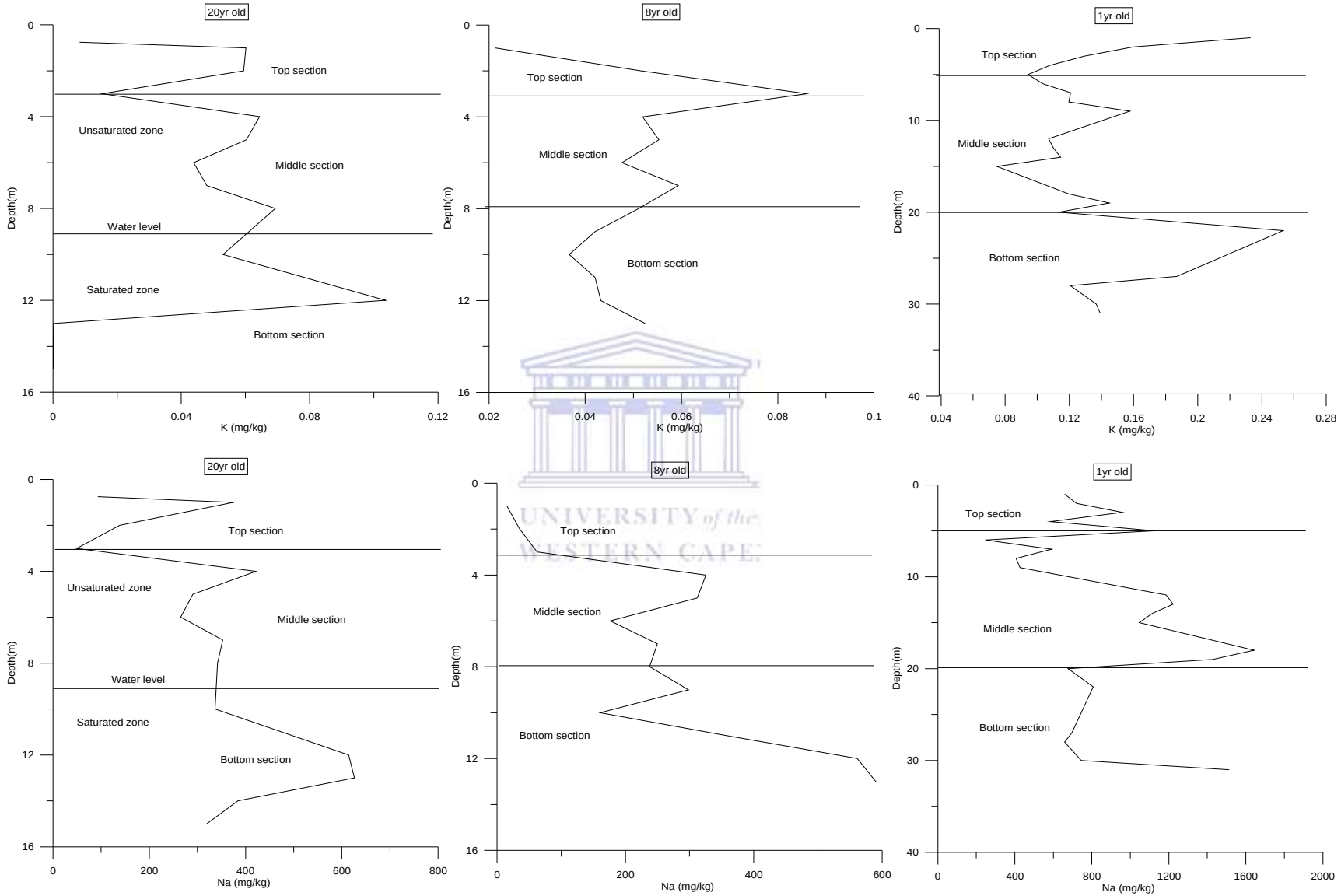

Figure 7.4. Sodium and potassium trend in water soluble fraction of drilled cores of different ages and depths (n=3).

The dissolution and precipitation of brucite and dolomite as influenced by the pH of the ash column could also control the concentration of Mg in the water soluble fraction of the fly ash. Magnesium concentration is influenced by dolomite ($CaMgCO_3$) at pH lower than 11, and then by brucite at greater pH (Garavaglia and Caramuscio, 1994). The hydrolysis of periclase (MgO) in the fly ash could lead to the formation of sparingly soluble brucite ($Mg(OH)_2$) (Tiruta-Barna *et al*., 2006).

7.1.1.4 Sodium and potassium

Figure 7.4 depicts the concentration profile of Na^+ in the water soluble fraction of fly ash at different stages of weathering. The highest concentration of Na^+ is observed in the 1-year-old ash cores. Na^+ concentration difference in the top, middle and bottom sections of 1 year, 8 year and 20-year-old ash cores is noticeable due to leaching of soluble major components in fly ash (see Tables 5.4-5.6). A relatively high concentration of Na^+ in the top section of 1-year-old ash core is influenced by weathering/ageing and leachate from top soil. The observed relatively high concentration of Na^+ at the bottom sections of 1 year and 20-year-old ash cores probably suggest the downward migration and subsequent precipitation of soluble salts. The vertical distribution patterns of Na^+ are influence by the pore water pH (see Section 5.7). It has been reported that sodium is present as soluble salts on the surface of fly ash particles but it is also present in the matrix of fly ash particles and that Na^+ is slowly released due to the dissolution of the fly ash matrix over time (Warren and Dudas, 1984).

Figure 7.4 shows the concentration trend of K^+ in the water soluble fractions of the ash cores of different ages. The highest concentration of K^+ is observed in the 1-year-old ash cores. Potassium concentration difference in the top, middle and bottom sections of 1 year, 8 year and 20-year-old ash cores is remarkable due to leaching/flushing of soluble major components in fly ash (see Tables 5.4-5.6). A relatively high concentration of K^+ in the middle and bottom sections of the 3 drilled could be the K^+ is being flushed down the core as a result of advection forces as the leachate percolates through overtime. The concentration profile of K^+ seems to be controlled by the pore water pH of the ash column (see Section 5.7). The acid neutralisation capacity results showed that Na^+ and K^+ release are controlled by the solution pH (see Figure 6.5a).

The important features of this section are Na (8-year-old ash cores) and Mn (20-year-old ash cores) which show noteworthy mobility in the water soluble fraction of fly ash. Relatively high

concentration of K and Na show that it is being flushed down the core as a result of advection forces as the leachate percolates overtime. The observed lower concentration of considered major elements in the older ashes compared with relatively young ash suggest overtime leaching of the major soluble components of fly ash due to weathering/ageing process or slower release due to association with the insoluble mineral phases.

7.1.2 Analysis of exchangeable and carbonate fractions

The inorganic metals that associate with these fractions are considered to exist as co-precipitates with carbonate minerals and strong-sorbed metal forms on the dust surface. These fractions are susceptible to pH changes, and metal release can be achieved through dissolution of a fraction of the solid material at low pH. The metals in this fraction can easily be freed by ion-exchange processes and leach very easily when the environmental conditions are disturbed by pH change or Eh change. Heavy metals in the exchangeable fraction play a very significant role in the evaluation of the environment and always act as a pollution indicator for its environmental mobility and bioavailability (Yuan, 2009).

Figures 7.5-7.8 show the trend of major elements in the exchangeable fractions at different stages of weathering of fly ash. Figure 7.5 shows concentration profile of Al and Si in the exchangeable fraction of 1 year, 8 year and 20-year-old ash cores. The highest concentration of Al and Si is recorded in the 1-year-old fly ash. Al concentration showed a remarkable difference in the middle and bottom sections of 20-year-old ash cores. But it's showed nearly constant concentration pattern in middle and bottom sections of 1-year-old ash cores.

On the contrary, Si has a slight concentration difference in the top, middle and bottom sections of 3 drilled ash cores. The obvious less mobile behaviours of Al and Si is due weathering/ageing. The marked concentration difference of Al in the top, middle, and bottom sections is due pore water pH. Acid neutralisation capacity results showed that the behaviour patterns of Si and Al are influenced by solution pH (see Figure 6.6c). The saturation point seems to have influenced the concentration of silicon at the bottom section of 20-year-old ash cores. Figure 7.6 shows concentration of Fe and Mn in the exchangeable fraction of drilled cores at different stage of

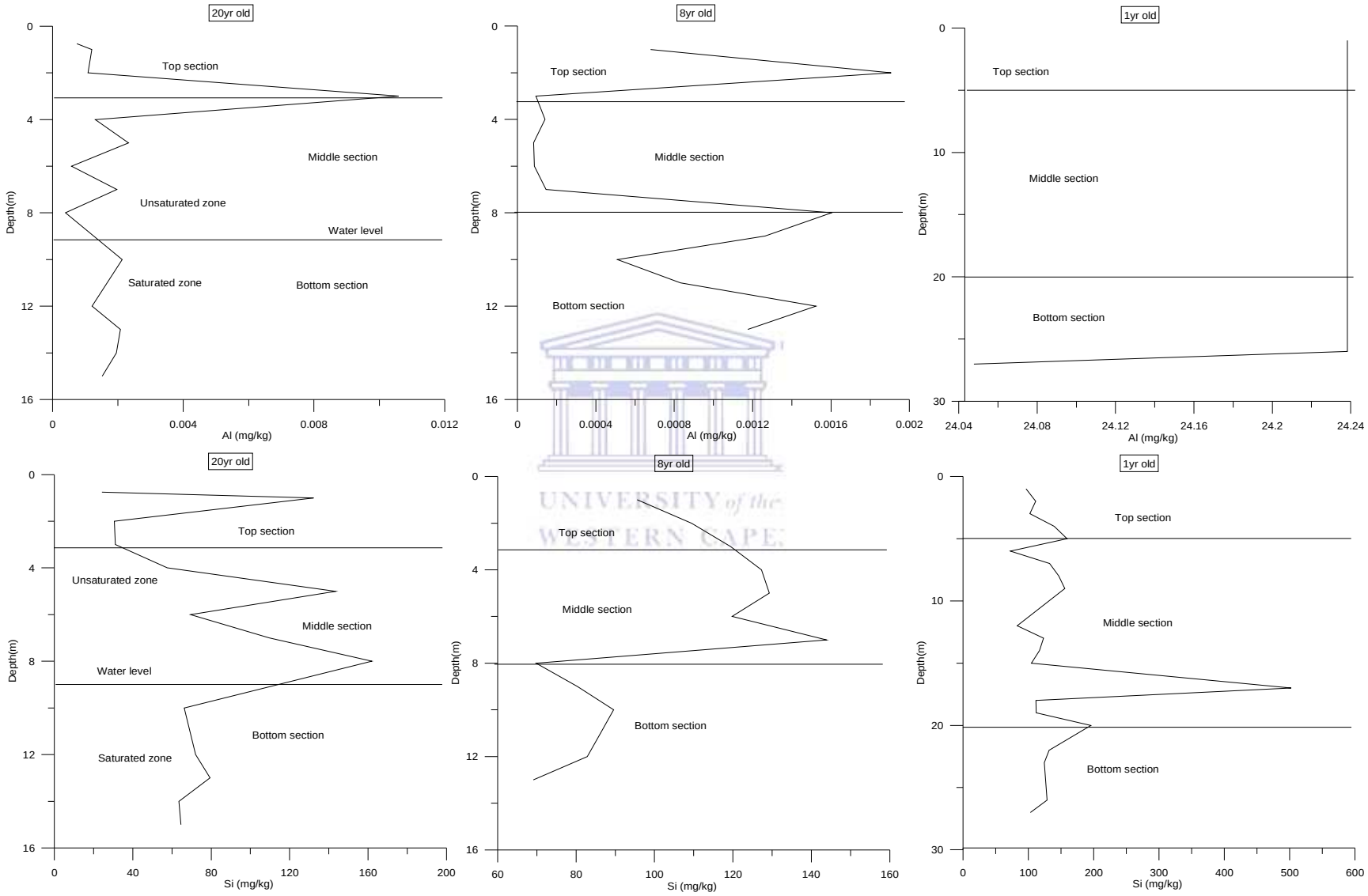

Figure 7.5. Aluminium and silicon trend in exchangeable fraction of drilled cores of different ages and depths (n=3).

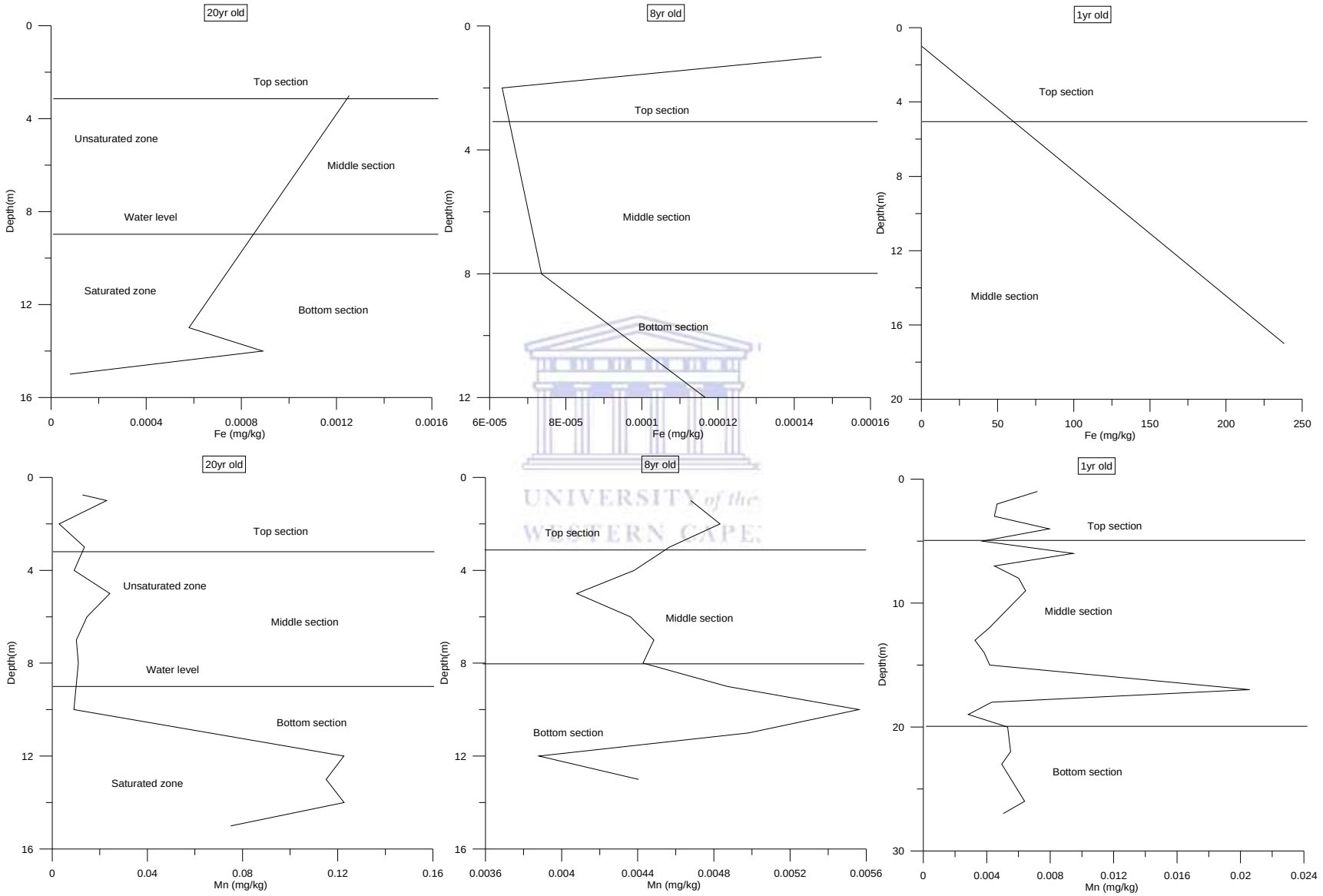

Figure 7.6. Iron and manganese trend in exchangeable fraction of drilled cores of different ages and depths (n=3).

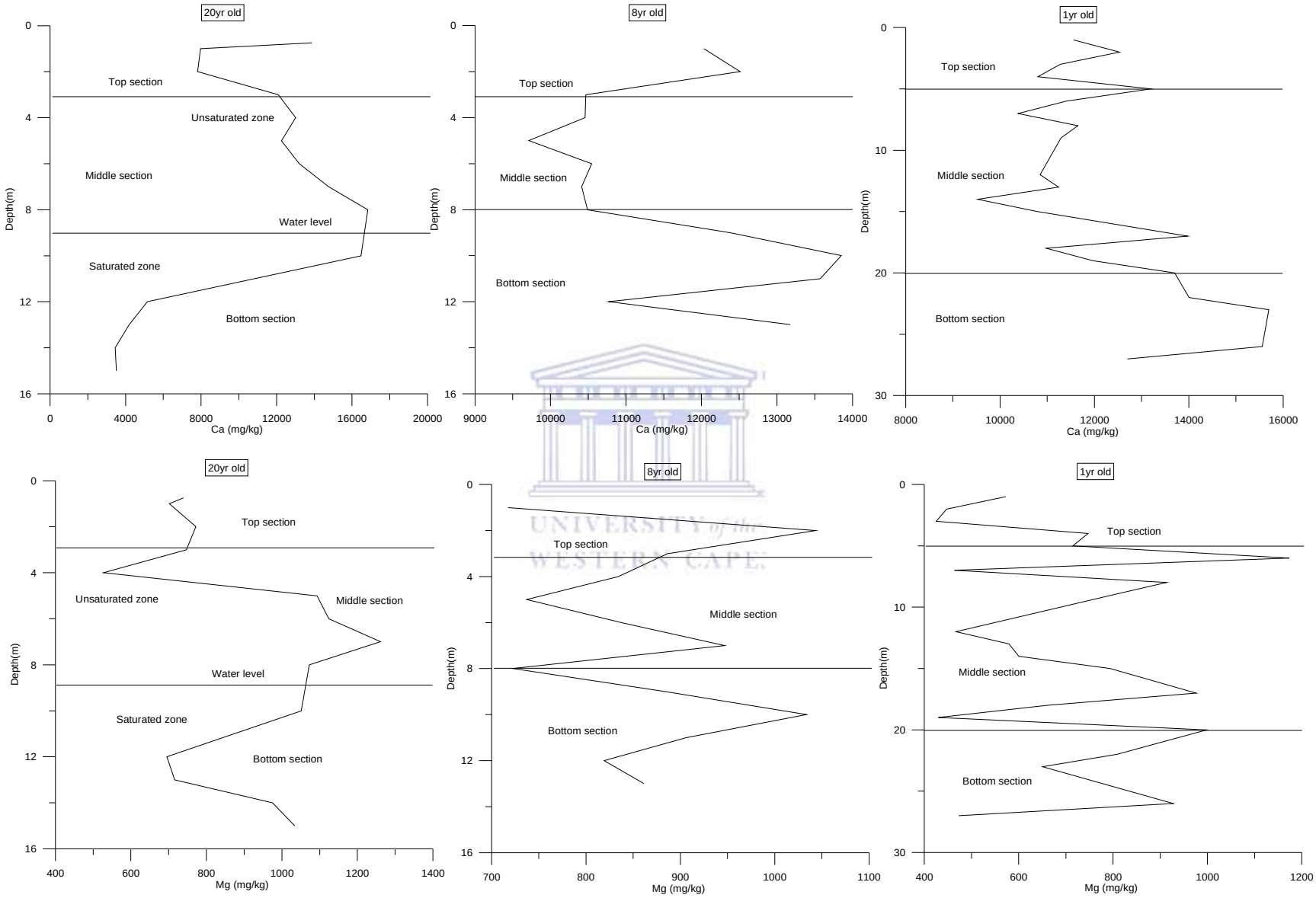

Figure 7.7. Calcium and magnesium trend in exchangeable fraction of drilled cores of different ages and depths (n=3).

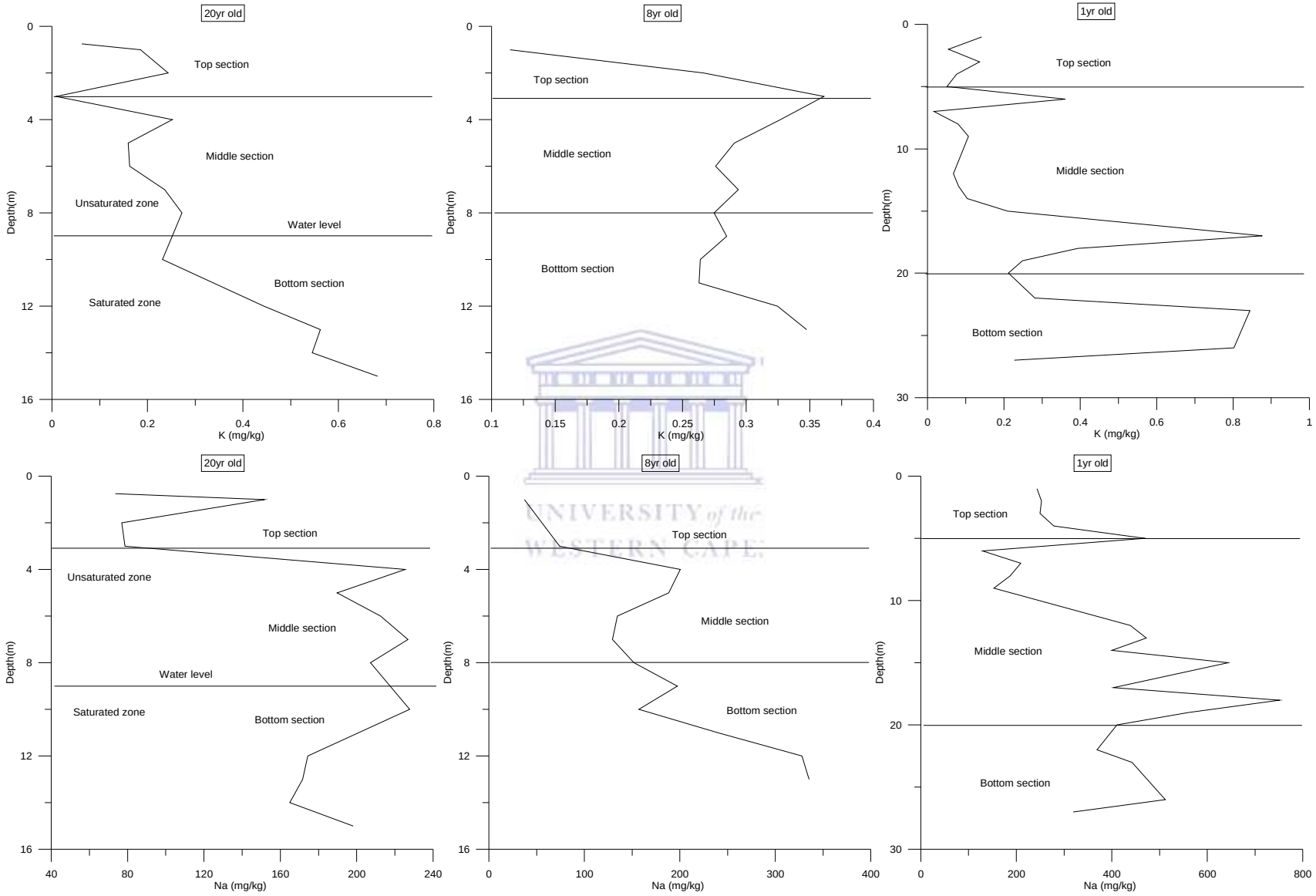

Figure 7.8. Sodium and potassium trend in exchangeable fraction of drilled cores of different ages and depths (n=3).

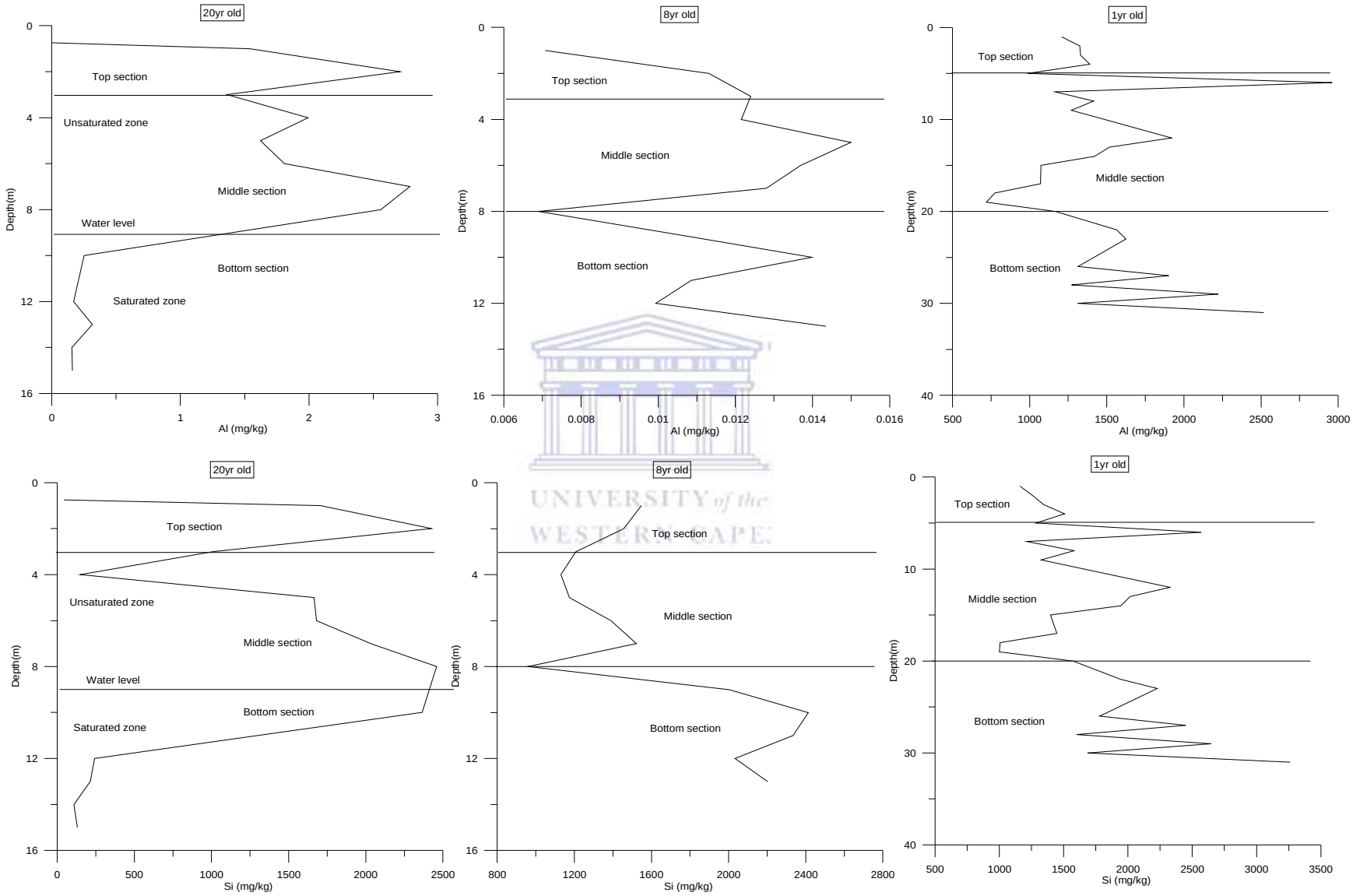

Figure 7.9. Aluminium and silicon trend in carbonate fraction of drilled cores of different ages and depths (n=3).

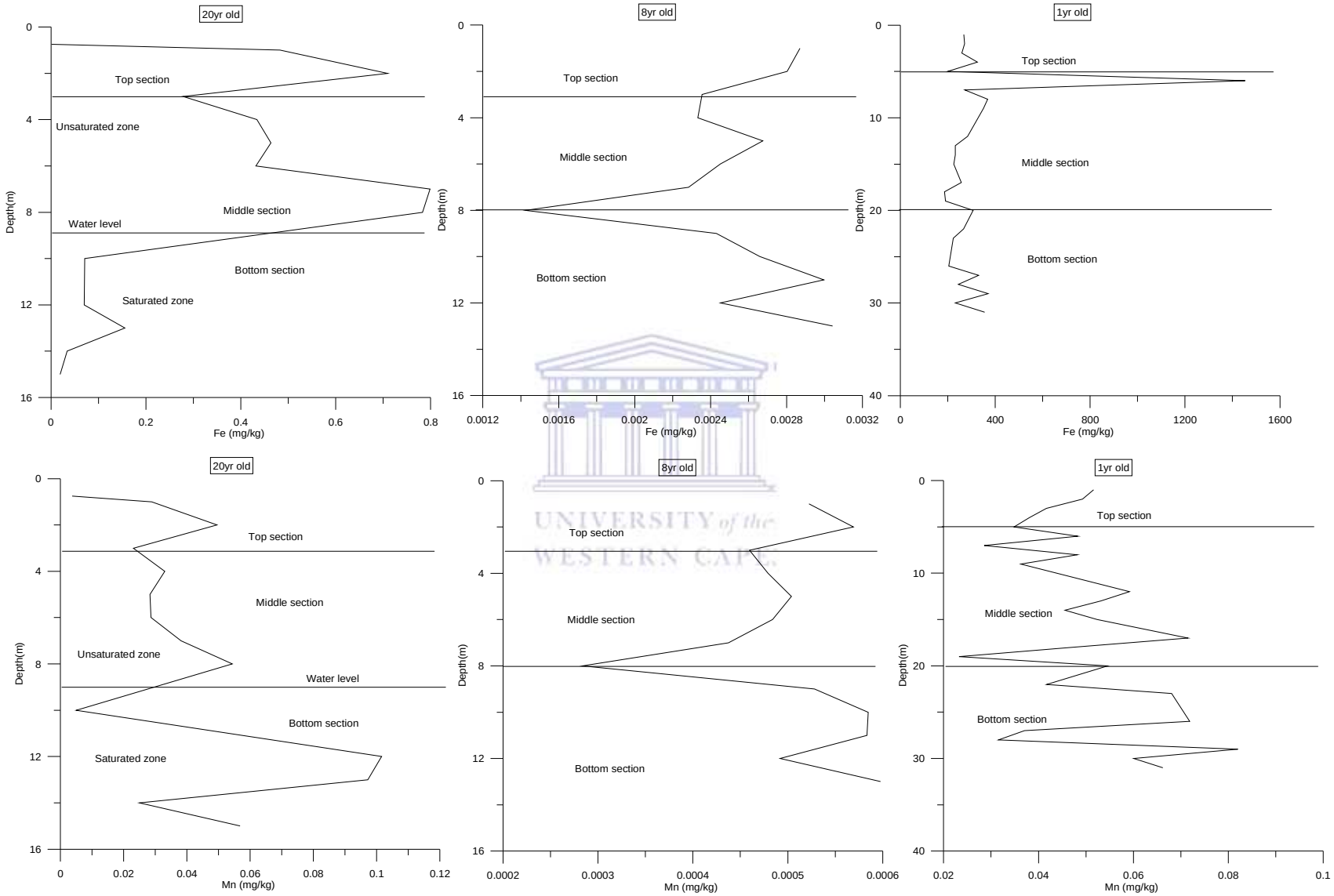

Figure 7.10. Iron and manganese trend in carbonate fraction of drilled cores of different ages and depths (n=3).

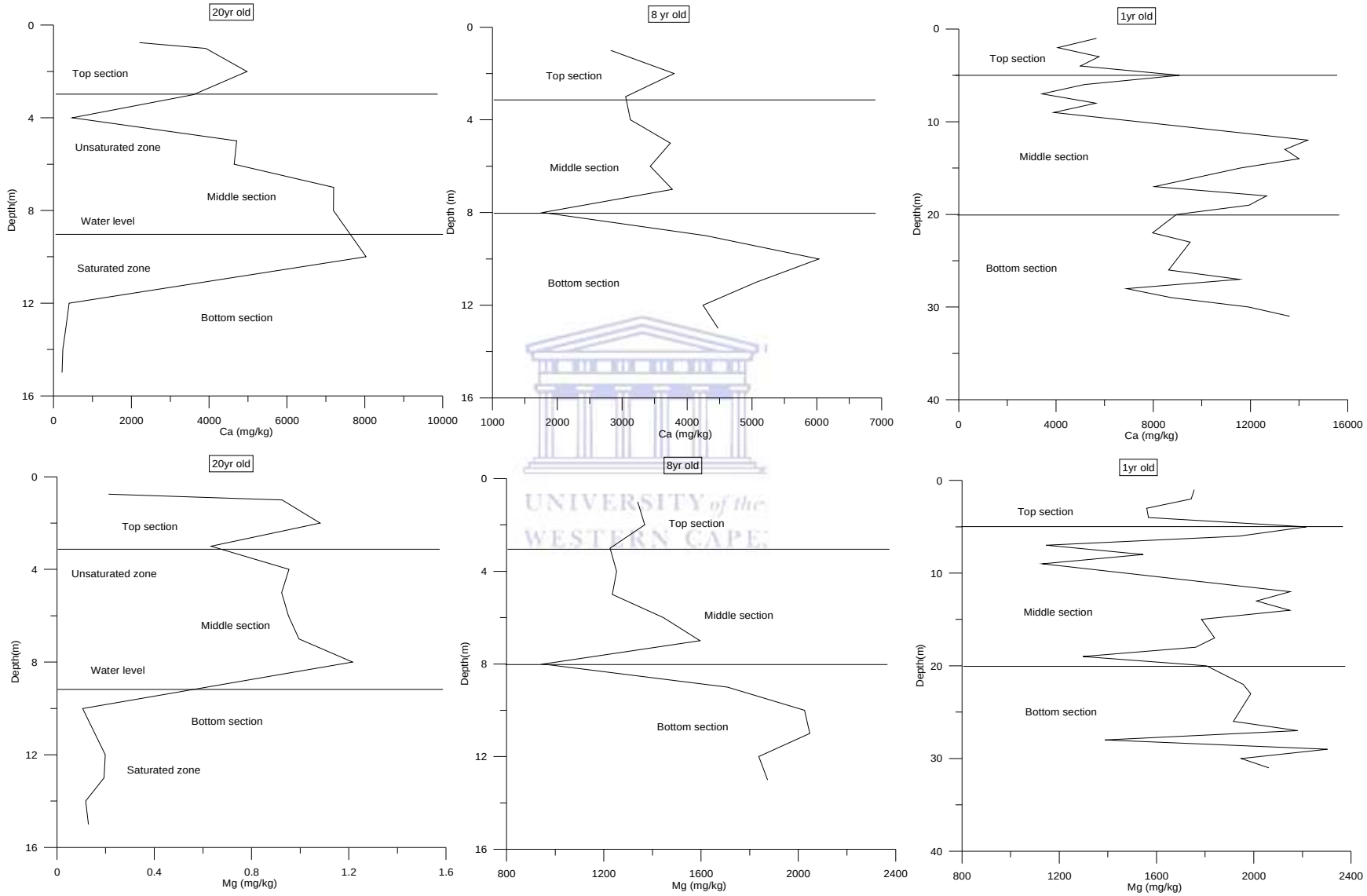

Figure 7.11. Calcium and magnesium trend in carbonate fraction of drilled cores of different ages and depths (n=3).

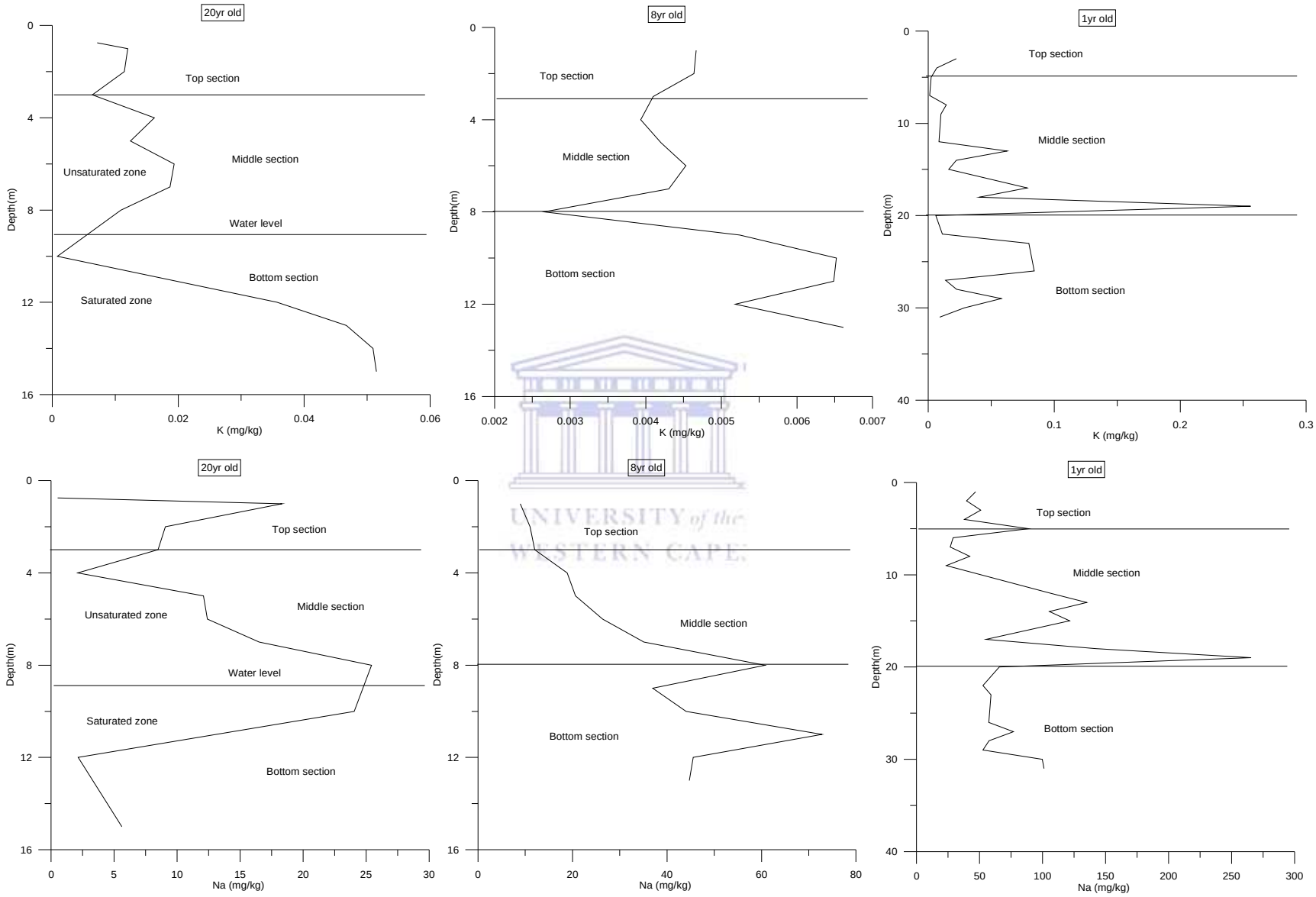

Figure 7.12. Sodium and potassium trend in carbonate fraction of drilled cores of different ages and depths (n=3).

weathering. The highest concentration of Fe and Mn is recorded in the 1-year-old ash cores. Manganese showed slight concentration difference in the top, middle and bottom sections of 3 drilled cores. At the same time, Fe show a nearly constant concentration in the top, middle and bottom sections of 3 drilled ash cores suggesting immobilization of Fe and Mn suggesting that it is not controlled by pore water pH. A relatively high concentration of Mn in the middle section (i.e. 1-year-old) and bottom sections (8 year and 20-year-old ash cores) suggest mobility/ downward migration and subsequent co-precipitation of Mn at these depths. Low concentration in the bottom sections of 1-year-old and end of bottom section of 8-year-old ash cores suggest that it has been leached out overtime at these depths. The concentration of Ca and Mg in the exchangeable fraction is shown in Figure 7.7. The highest concentration of Ca is recorded in the 1-year-old ash cores but highest concentration of Mg is recorded in 20-year-old ash cores. Relatively high concentration of Mg is recorded in the top, middle and bottom sections of 1 year, 8 year and 20-year-old fly ash. A relatively low concentration of Ca at the bottom sections of 20-year-old ash cores indicate that the concentration is influenced by point of saturation. In general trend, calcium and magnesium showed notable concentration difference in the top, middle and bottom sections of the 3 drilled ash cores is majorly suggesting that their release is influenced by pore water pH. The acid neutralisation capacity results also showed that their release is solution pH dependent (see Figure 6.5b).

The concentration of Na^+ and K^+ in the exchangeable fraction of 3 drilled ash cores is shown in Figure 7.8. The highest concentration of Na^+ and K^+ is recorded in the 1-year-old ash cores. Both Na^+ and K^+ showed increasing response with increasing depth in the 1-year-old ash cores. Potassium also showed increasing response in the exchangeable fraction of 20-year-old ash cores. In general, Na^+ and K^+ showed a marked concentration difference in the exchangeable fraction suggesting that their release is influenced by pore water pH. The concentration trend of Fe and Al (1-year-old ash) in the exchangeable fraction appears to be at variance with the other four fractions of the ash cores. Both Fe and Al showed a nearly constant high concentration at the middle section indicating no much change in redistribution that occurs in this fraction.

The trends observed in the carbonate fraction (Figures 7.9-7.12) of the 3 drilled ash cores are somewhat similar to the exchangeable fraction. The highest concentration of Al, Si, Na^+, K^+, Ca, Mg and Fe are recorded in the 1-year-old ash cores. Al and Si showed remarkable concentration

difference in the top, middle and bottom sections of 3 drilled cores. The vertical distribution patterns of both Al and Si are influenced by pore water pH. The acid neutralisation capacity results showed that their release is solution pH dependent (Figure 6.5c). Si showed increasing response with increasing depth in the carbonate fraction of 1-year-old fly ash (see Table 7.5). The concentrations of Fe and Mn in the carbonate fraction of the 8-year-old ash are different from the remaining fractions (Figure 7.10). A relatively high concentration of Mn in the top section of 8-year-old cores was influenced by leachate from top soil. Calcium and magnesium concentration trend is shown in Figure 8.11. Remarkable concentration differences of Ca and Mg were observed in the top, middle and bottom sections of 3 drilled cores due to pore water pH. The concentration of Na^+ and K^+ trend in the carbonate fraction is shown in Figure 7.12. A notable concentration difference is recorded in the top, middle and bottom sections of 3 drilled ash cores due to pore water pH (see Section 5.7). The behavioural patterns of Na^+ and K^+ in the dry disposed fly ash are governed by solution pH (see Fig 6.5a). Na^+ and Mg show increasing response with increasing depth of 8-year-old ash cores. Potassium also showed similar response pattern in the 8 year and 20-year-old ash cores respectively. The other likely factors that could influence metals concentration trend in the carbonate fraction are in-homogeneity, moisture content levels, leachate from top soil and intersection of core ash with water table.

The important features of this section are the remarkable mobility of Si (1-year-old), K (20 year and 1-year-old), Mg (8 year-old) and Na^+ (8 year and 1-year-old) in the exchangeable and carbonate fractions. This vertical distribution patterns is influenced by adsorption and desorption process due to variation in the pore water pH (see Section 5.7). Factors such as in-homogeneity in 3 drilled ash cores (see Section 3.7), moisture content levels (see Section 5.1) and point of contact with the groundwater could also promotes metal mobility. The highest concentration of the major element in the exchangeable and carbonate fractions of 1-year-old ash cores is due to overtime leaching of major soluble components in the older ashes or slower release due to association of these metals with the insoluble phases.

7.1.3 Analysis of Fe and Mn, and residual fractions

Fe and Mn oxides does exist as nodules, concretions, cement between particles or simply as a coating on particles during the production process of fly ash in the boiler, a lot of toxic elements may be pooled into this fraction when the particles cool down in flue gas. These oxides can most

likely act as excellent scavengers for trace elements and are thermodynamically unstable under anoxic conditions (Yuan, 2009). Metals in the residual fraction on the other hand are safer for the environment due to their lowest mobility and bioavailability. Primary and secondary mineral-containing metals in the crystalline lattice comprise the bulk of residual fraction. To remove elements in residual fraction is more difficult, because the structure of the crystalline lattice must be destroyed sufficiently by very strong acid or alkali (Yuan, 2009). The concentration profile of major elements in Fe and Mn fraction of dry disposed ash cores are shown in Figures 7.13-7.16. The concentration of Al and Si in the Fe and Mn fraction is shown in Figure 7.13. The highest concentration of Al and Si is recorded in the 1-year-old ash cores. The marked concentration difference of Al is recorded in the top, middle and bottom sections of 3 drilled ash cores. On the contrary, Si showed marked concentration difference in the top, middle and bottom sections of 20 year and 1-year-old ash cores. The concentration of Si in the top, middle and bottom sections of 8-year-old ash cores is nearly constant suggesting that Si is less mobile in the amorphous Fe-oxyhydroxide phase.

The concentration of Fe and Mn in the Fe and Mn fraction of dry disposed ash is shown in Figure 7.14. The highest concentration of Fe is recorded in 1-year-old ash cores but highest concentration Mn is recorded in 20-year-old ash cores. Fe showed increasing response with increasing depth in the 1-year-old ash cores. The concentration difference of Fe and Mn in the top, middle and bottom sections of 1 year and 20-year-old ash cores is noteworthy suggesting that their release could be influenced by in-homogeneity in the 3 drilled ash cores (see Section 3.8) and moisture content levels. Although a nearly constant concentration of Fe and Mn are recorded in the top, middle and bottom sections of 8-year-old ash cores indicating no much change in redistribution occurs in this fraction. The concentration trends of Ca and Mg in Fe and Mn fraction of dry disposed ash cores is shown in Figure 7.15. The highest concentration of Ca is recorded in 20-year-old ash cores.

The highest concentration of Mg is recorded in 1-year-old ash cores. The concentration of Ca and Mg difference in the top, middle and bottom sections of 1 year and 20-year-old ash cores is noticeable indicating that their release is could be due to leaching/flushing of major soluble components (see Tables 5.5 and 5.7). However, the concentration of Ca and Mg in the top section of 8-year-old fly ash is nearly constant suggesting no much change in redistribution

occurs in this fraction. The concentration profile of Na^+ in the Fe and Mn fraction of dry disposed ash is shown in Figure 8.16. The highest concentration of Na^+ and K^+ is recorded in 1-year-old ash cores. Potassium showed a decreasing response with increasing depth in the 1-year-old ash cores. On the contrary, K^+ showed increasing response with increasing depth in the 20-years-old ash cores. Na^+ and K^+ showed a marked concentration difference in the top, middle and bottom sections; suggesting that their release is influenced by ash type, ash texture, moisture content level and point of contact with groundwater. The concentrations of Al, Si, Fe, Mn, Ca, Mg, Na^+, and K^+ in the residual fractions are shown in Figures 7.17-7.20. The concentration trends of Al and Si in the residual fraction are shown in the Figure 7.20. The highest concentration of Al is recorded in 1-year-old ash cores whereas highest concentration of Si is recorded in 20-year-old ash cores. Al showed a decreasing response with increasing depth in the residual fraction of 20-year-old ash cores (see Table 7.5). A relatively high concentration of Al and Si in the top sections of 1 year and 8-year-old ash cores is influenced by the leachate from the top soil. In contrast, the relatively low concentration of Al and Si in the middle sections of 1 year, 8 year and 20-year-old ash cores due to leaching/flushing of major soluble component due to pore water pH (see Section 5.7). The acid neutralisation capacity results showed that the leaching behaviour of Al and Si is dependent on the solution pH (see Figure 6.5c). Relatively high concentration of Al and Si at the bottom sections of 8 year and 20-year-old ash cores is due to in-homogeneity in ash cores (see Section 3.7), moisture content levels (see Section 5.1) and point of contact with groundwater.

The concentration of Fe and Mn in the residual fraction of dry disposed ash is shown in figure 7.18. The highest concentration of Fe and Mn in the residual fraction is recorded in 20-year-old fly ash. A remarkable concentration difference Fe is recorded in the top, middle and bottom section of 3 drilled ash cores. This vertical distribution trend could be due to the influence of ash type, ash texture, moisture content levels and point of intersection with the ground water. Relatively high concentration of Fe and Mn in the top sections of 1 year and 8-year-old ash cores is due to influence of leachate from the top soil. The nearly constant concentration at the top section of 1-year-old ash cores suggests no much change in redistribution occur. The relatively high concentration of Fe and Mn in the bottom sections of 8 year and 20-year-old ash cores is due to lithology, moisture content levels and point of saturation. The concentration of Mn in the middle and bottom sections of 1-year-old ash cores showed that they are less mobile due to

weathering/ageing. However, the concentration difference of Ca and Mg in 20 year and Ca in 8-year-old ash cores is due to inhomogeneity in the ash dump, moisture content levels and point of saturation. These factors promote the release of Ca and Mg into the pore water system of the dry disposed ash cores. The concentration profile of Ca and Mg in the residual fraction of dry disposed ash was shown in Figure 7.19. The highest concentration of Ca and Mg is recorded in 20-year-old fly ash. A relatively high concentration of Ca and Mg in the top sections of 1-year-old ash cores is influenced by the leachate from top soil. The inconspicuous concentration difference of Ca and Mg in the 1-year-old ash cores and calcium in 8-year-old ash cores suggests that they are less mobile in the amorphous aluminosilicate phase.

The concentration of Na^+ and K^+ in the residual fraction of dry disposed ash is shown in Figure 7.20. The highest concentration of Na^+ and K^+ is recorded in 1-year-old ash cores. A relatively high concentration of Na^+ is recorded in the middle and bottom sections of 8-year-old ash cores due to down the hole leaching of major soluble component (i.e. Na_2O wt %). A fairly low concentration of Na^+ is recorded in the top section 8-year-old ash cores. Na and K show a remarkable concentration difference in the top, middle and bottom sections of 1 year, 8 year and 20-year-old ash cores is due to contact of dry disposed ash cores with the percolating rain water which caused leaching/ flushing of the major soluble components in ash cores (see Tables 5.3-5.5).

The important features of this section are major elements such as Al (20-year-old), K^+ (20 year and 1-year-old), Mn (20-year-old) and Fe (1-year-old) exhibit a remarkable mobility in the Fe and Mn, and residual fractions. These metals mobility in the Fe and Mn fraction is influenced precipitation and dissolution of Fe - hydroxide phase caused by reduction process. Other possible controlling factors are in-homogeneity in drilled ash cores, moisture content levels and point of contact with the groundwater also play out in the metal mobility. Lower concentration of Al, Si, Fe, Mg, Na^+ and K^+ in the older ashes suggests overtime leaching of major soluble components in ash cores or slower release of these metals due to association with the amorphous Fe-oxyhydroxide and amorphous aluminosilicate secondary minerals phases in dry disposed ash cores which have greatest potential to limit the mobility of metals.

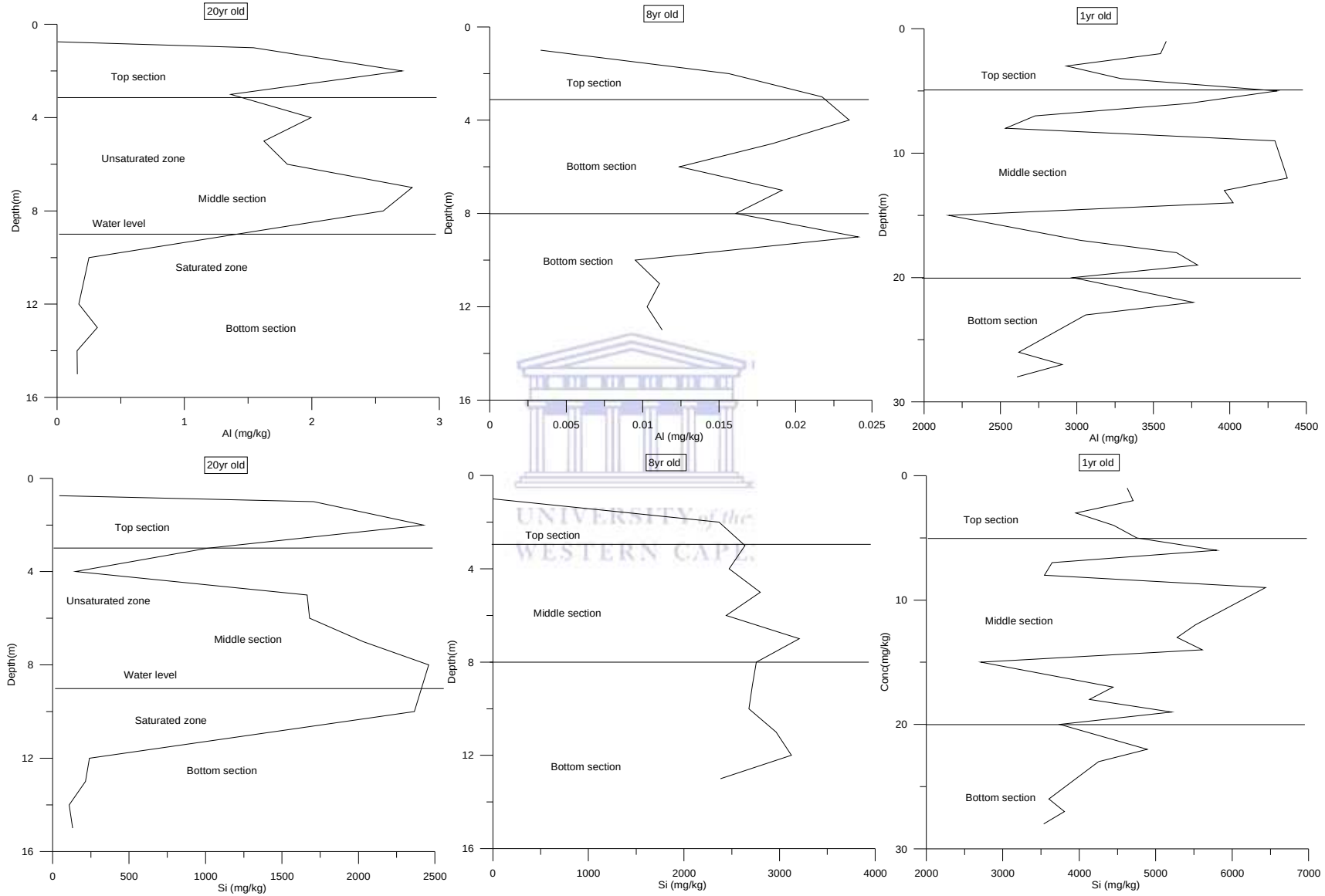

Figure 7.13. Aluminium and silicon trend in Fe and Mn fraction of drilled cores of different ages and depths (n=3).

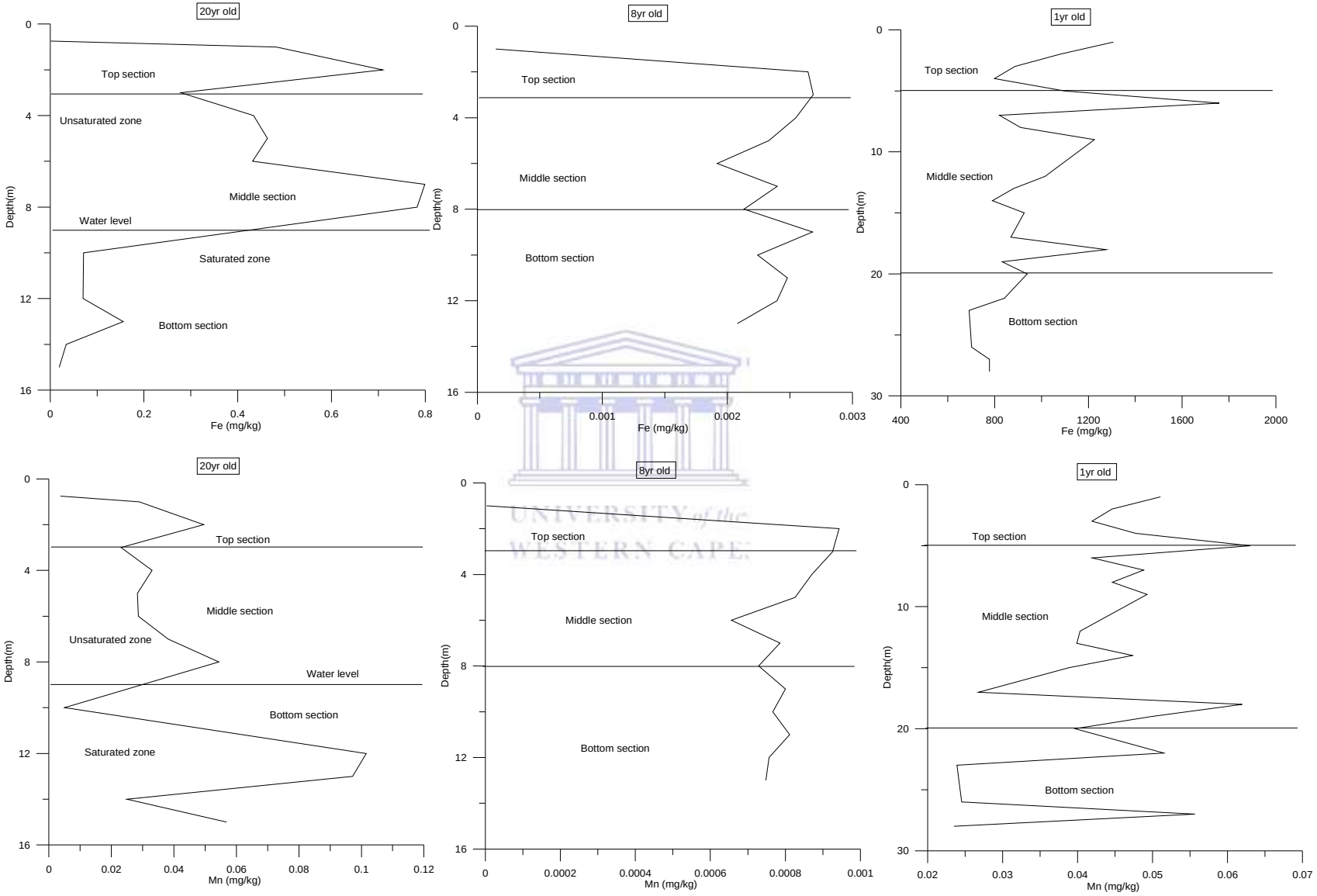

Figure 7.14. Iron and manganese trend in Fe and Mn fraction of drilled cores of different ages and depths (n=3).

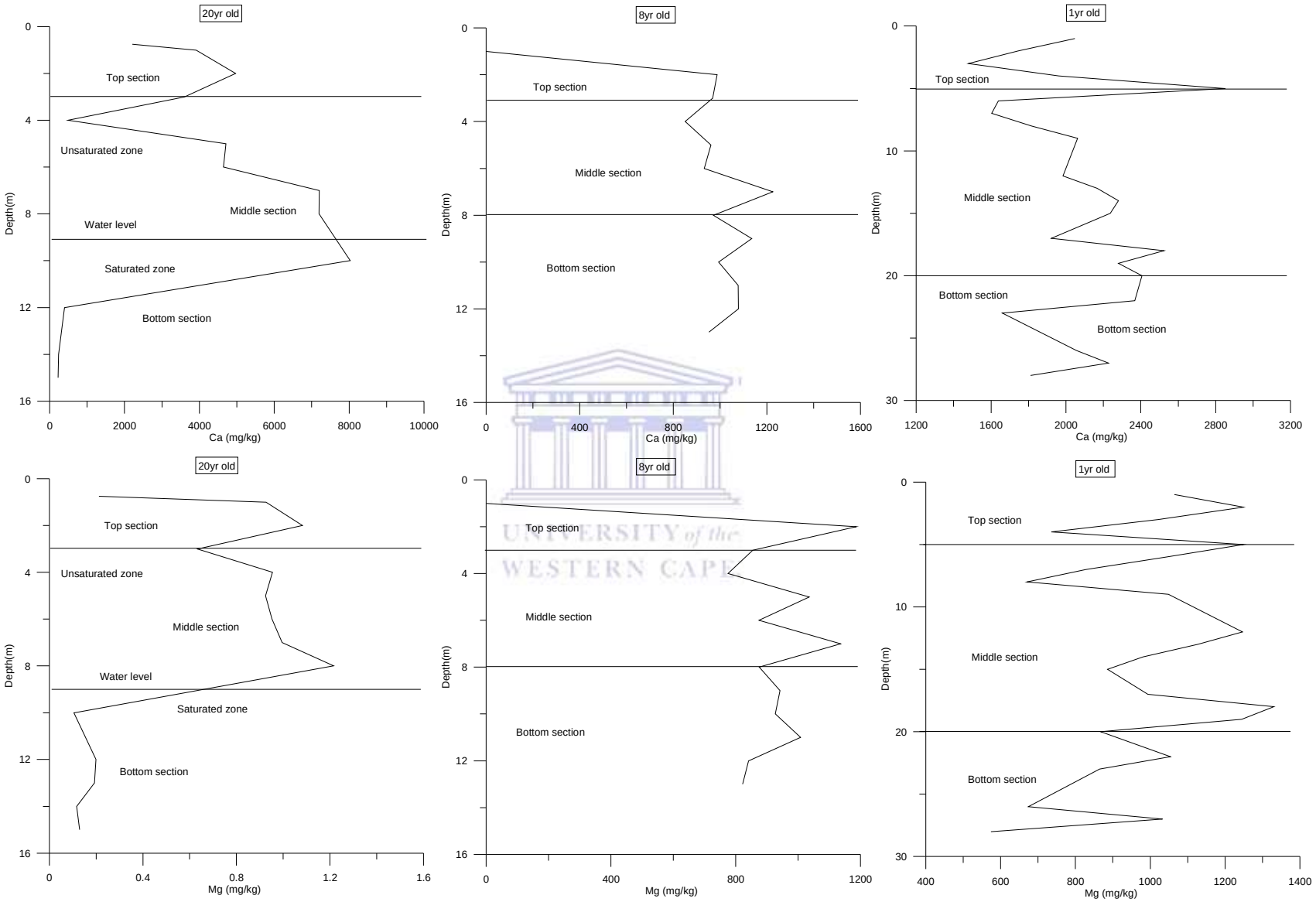

Figure 7.15. Calcium and magnesium trend in Fe and Mn fraction of drilled cores of different ages and depths (n=3).

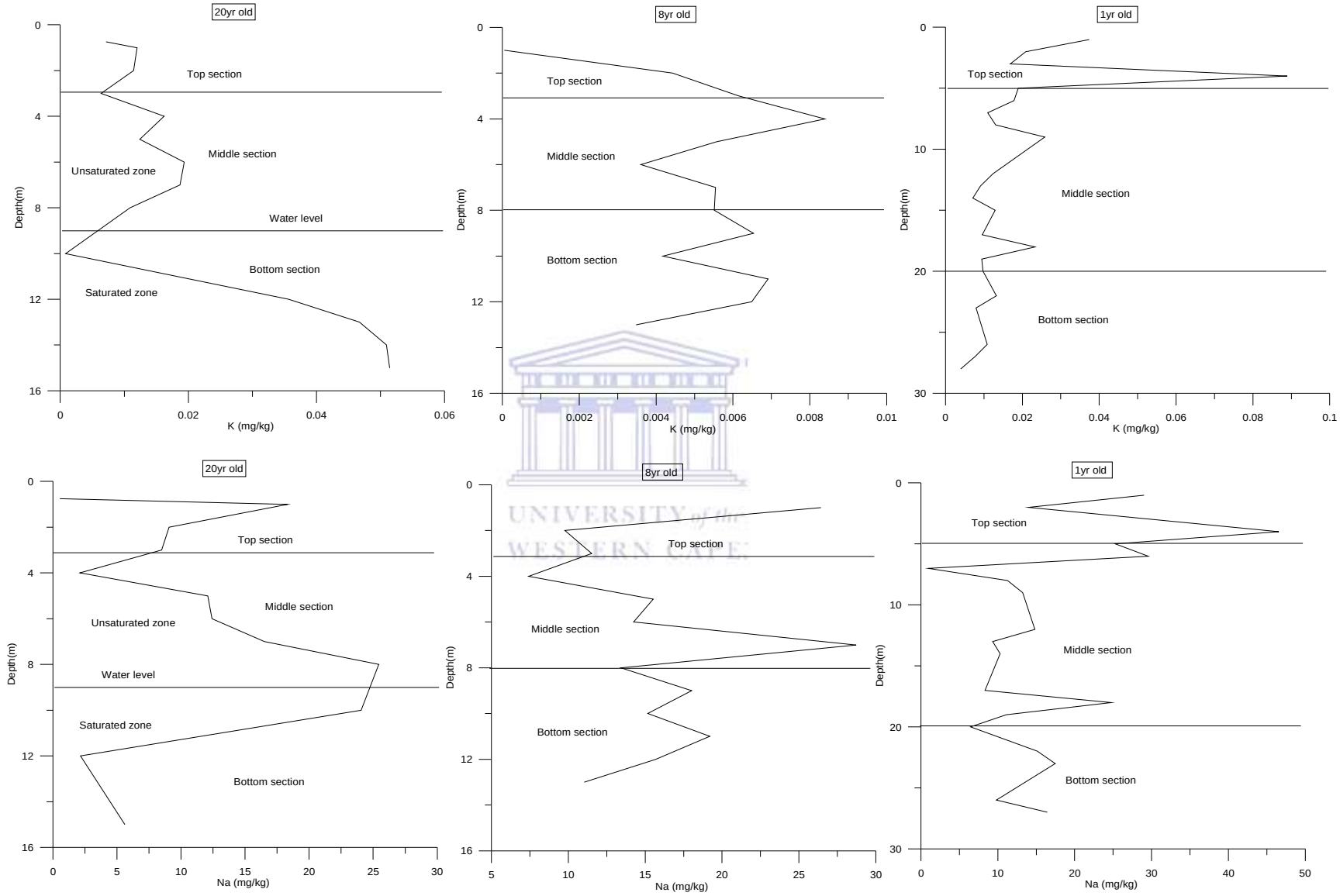

Figure 7.16. Sodium and potassium trend in Fe and Mn fraction of drilled cores of different ages and depths (n=3).

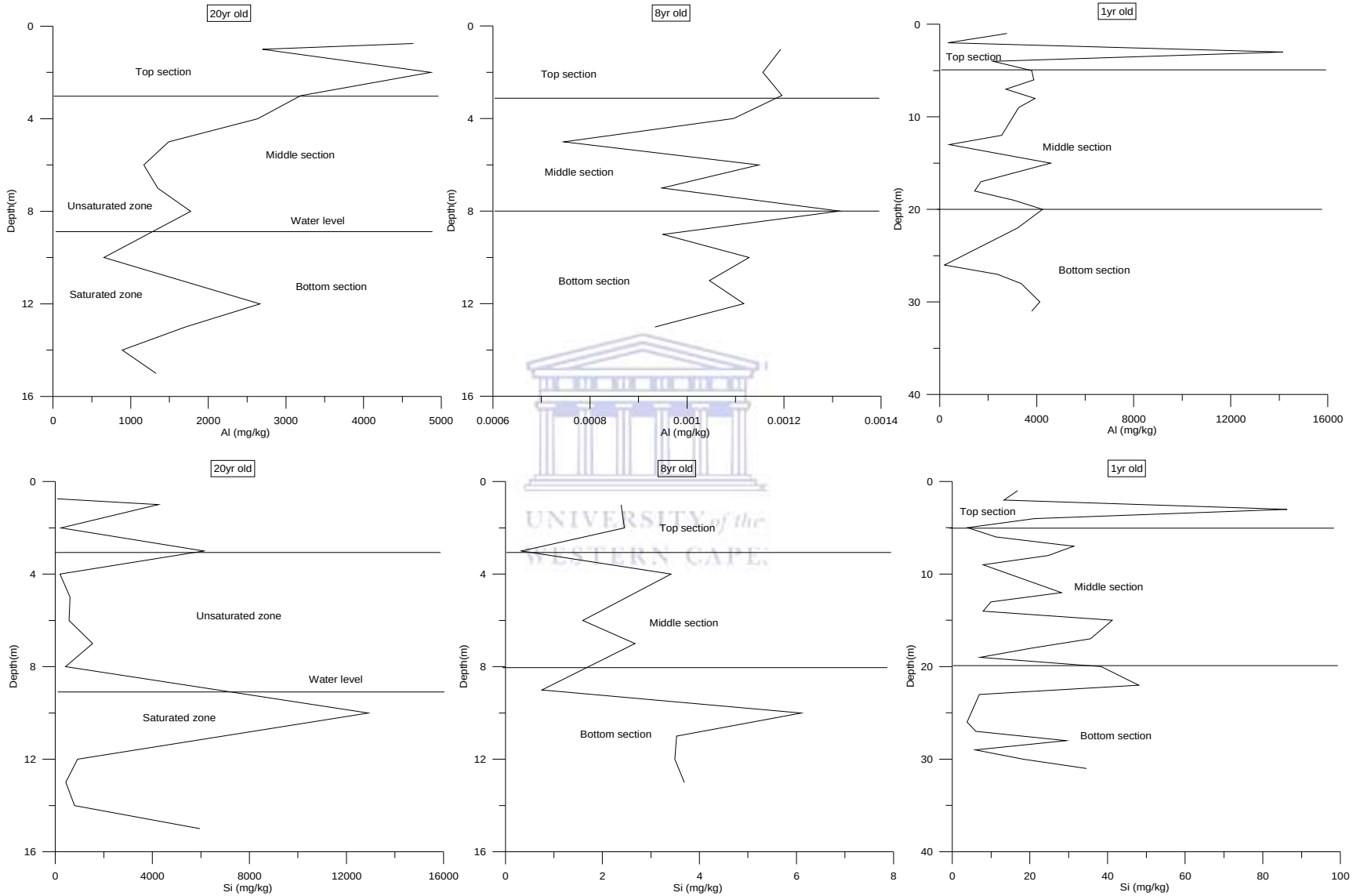

Figure 7.17. Aluminium and silicon trend in residual fraction of drilled cores of different ages and depths (n=3).

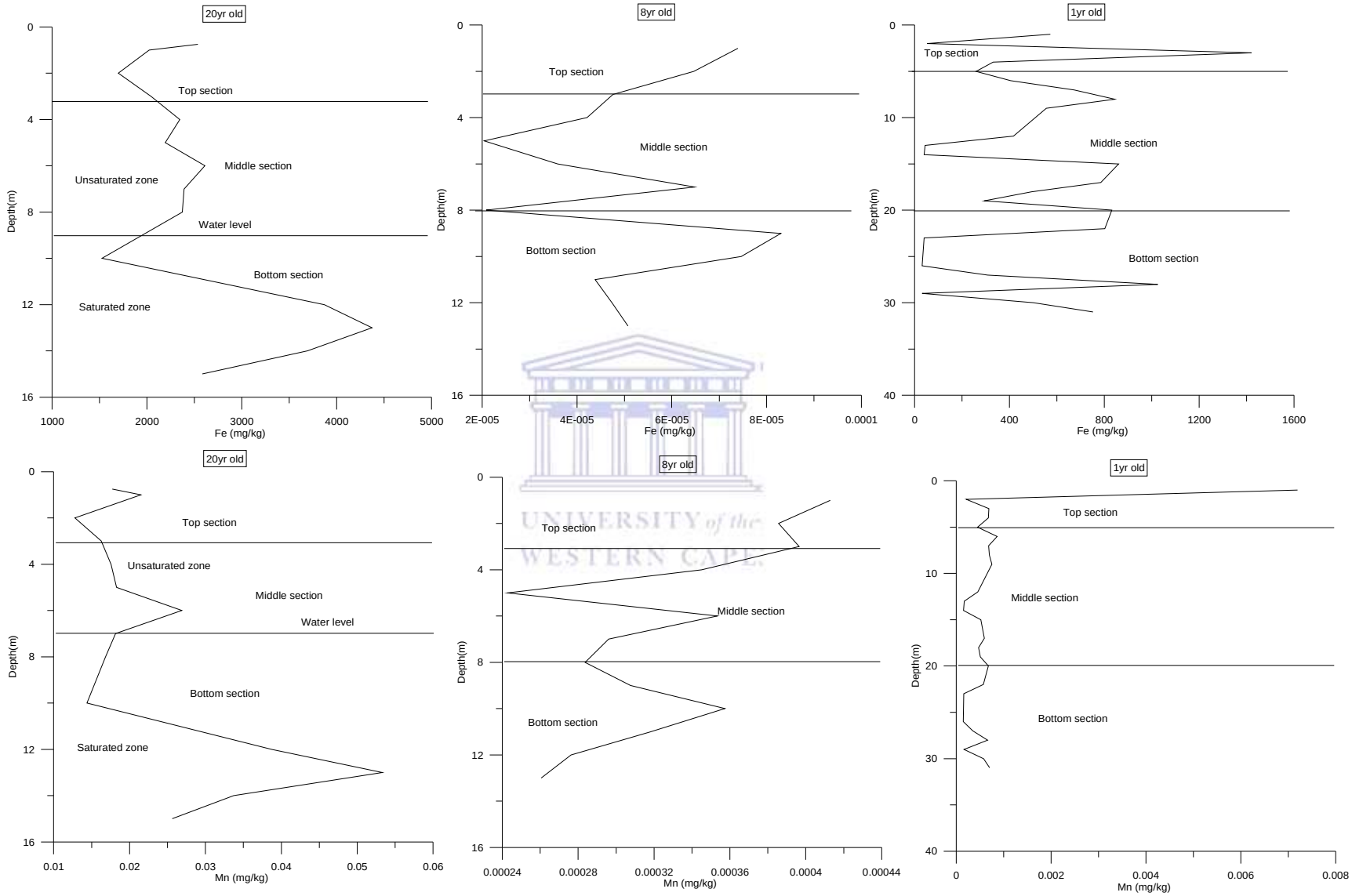

Figure 7.18. Iron and manganese trend in residual fraction of drilled cores of different ages and depths (n=3).

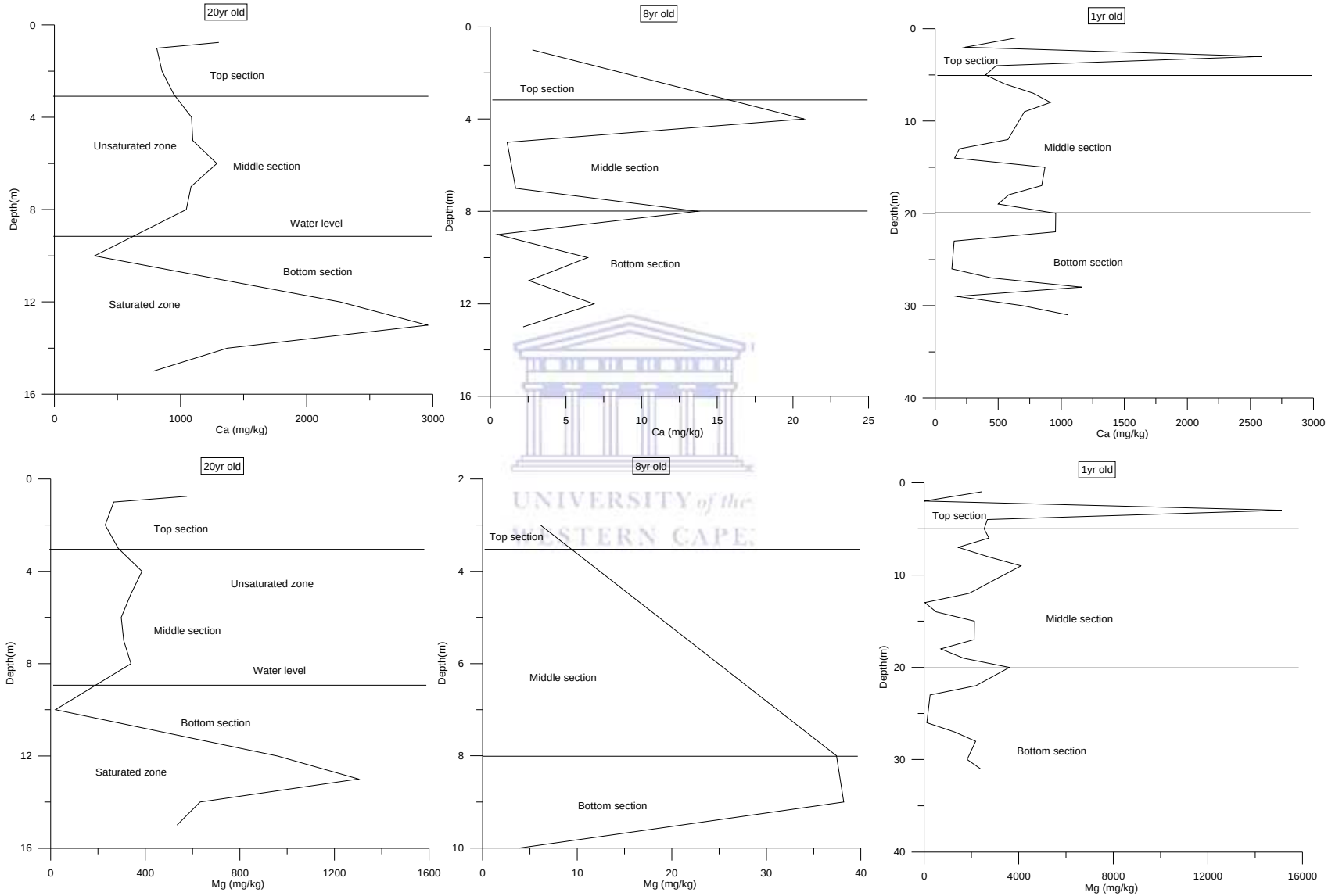

Figure 7.19. Calcium and magnesium trend in residual fraction of drilled cores of different ages and depths (n=3).

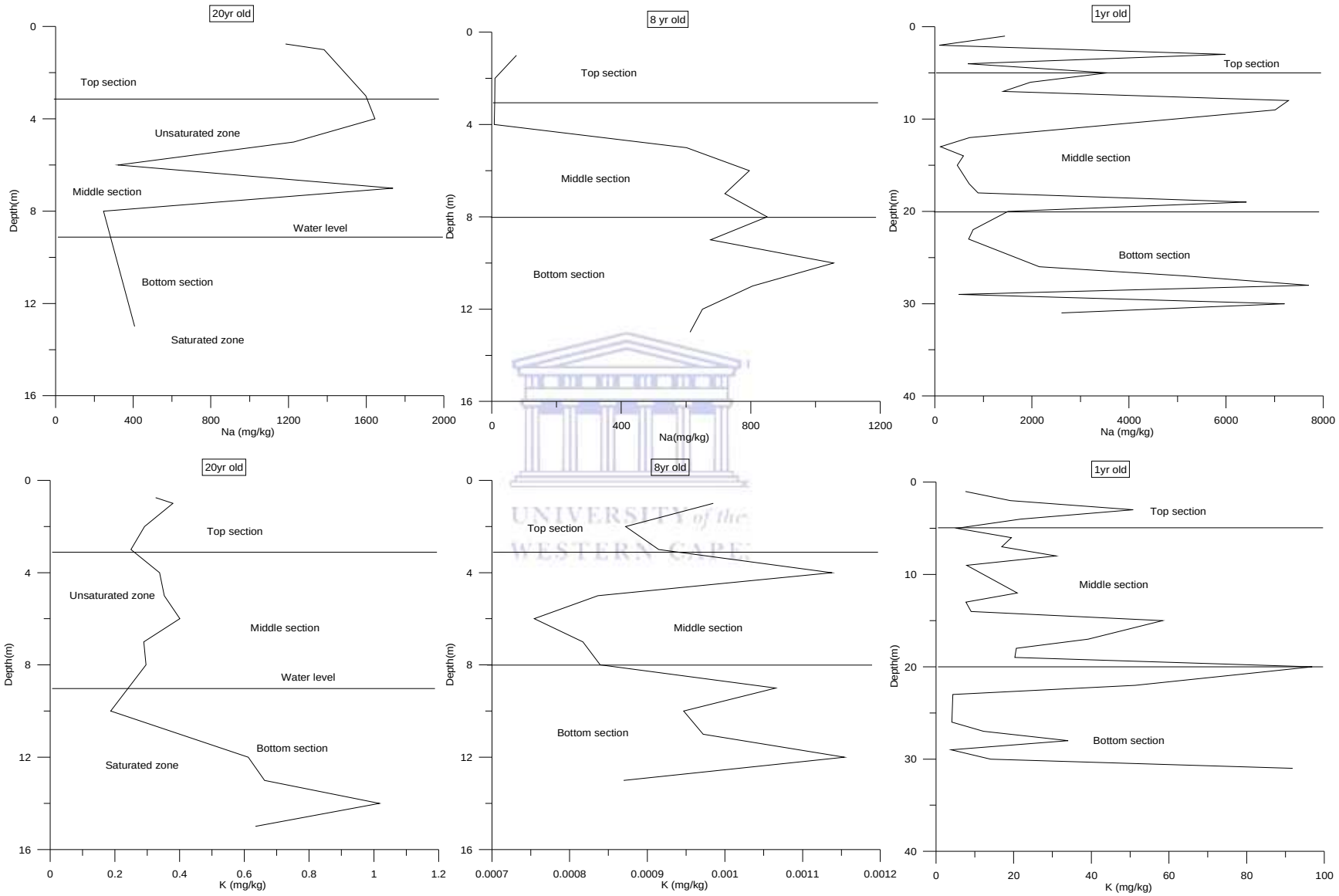

Figure 7.20. Sodium and potassium trend in residual fraction of drilled cores of different ages and depths (n=3).

7.2 Distribution pattern of major elements in the five geochemical phases of 1-year-old ash core samples

Results of the sequential extraction scheme and triple acid digestion (see Section 7.1 &7.3 respectively) for 1 year, 8 year and 20-year-old dry disposed ash cores showed that the 1-year-old ash cores has the highest concentration of considered analytes and least leached. Therefore the distribution pattern for only 1-year-old ash cores is presented in this section. The concentration of major elements in each of the five geochemical fractions of 1-year-old ash cores was calculated as a percentage of the total metal content and data obtained are presented in Figures 7.21-7.22 below to show relative values for each core with depth. The results for each element are discussed below.

7.2.1 Aluminium and silicon

Both Al and Si are major elements in the coal fly ash. The geochemical distribution pattern of Al and Si for the 1-year-old ash cores is shown in Figure 7.21. The water soluble fraction contains a negligible amount of Al which indicates it is slightly water soluble. The highest release of Al in carbonate fraction was obtained from fine ash sample (at 23 m) indicating surface area as a considerable factor in the metal release from carbonate fraction (Fig. 7.21). Al is present in all the five fractions; the range of Al in water soluble fraction and exchangeable are from 0.001-0.008 % and 0.10-0.57 % respectively. The residual fraction contains Al in the range of 0.17-1.82 % and 12.26-77-39 % in Fe and Mn fraction of coal fly ash. The leachable amount of Al in the carbonate fraction of fly ash is in the range of 9.16-39.98 %. The order of partitioning of Al in the five fractions is as follows: carbonate fraction>Fe and Mn fraction>residual fraction>exchangeable fraction>water soluble fraction. The carbonate, and Fe and Mn fractions contain notable proportion of Al in coal fly ash. The percentage leached amounts of Si were in the range of 0.74-95.83 % (carbonate fraction) and 6.40-73.33 % (Fe and Mn fraction). The sample taken at 29 m depth has highest percentage (95.83 %) of metal extracted from carbonate fraction. The leached amount of Si in the water soluble fraction is in the range of 0.16-11.58 %. The relatively high percentage leached amount of Si in the water soluble fraction could be due to rapid dissolution of amorphous aluminosilicate minerals. The major proportion of leached

Figure 7.21. Distribution of Al, Si, Fe and Mn in geochemical phases of 1-year-old ash cores.

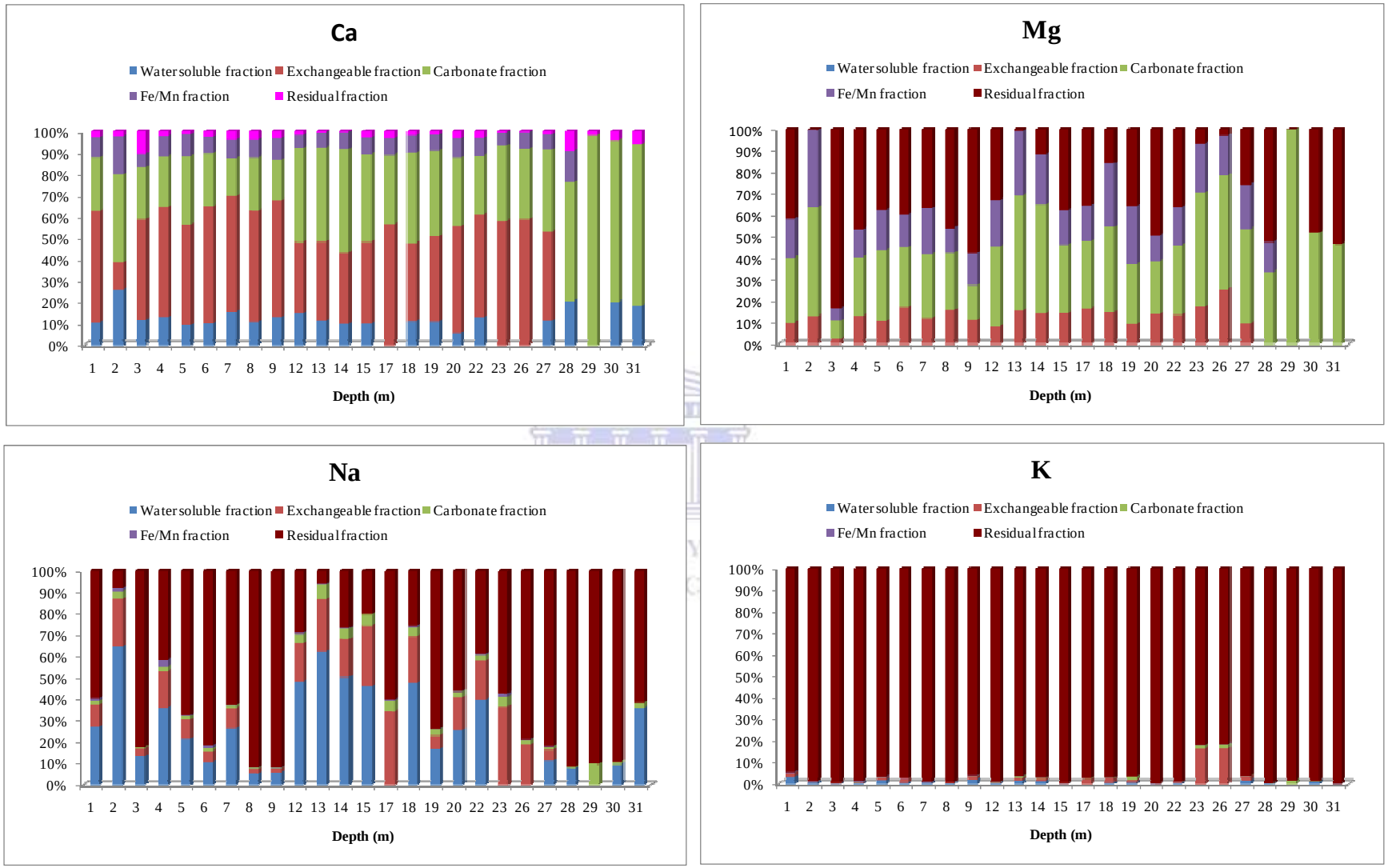

Figure 7.22. Distribution of Ca, Mg, Na and K in geochemical phases of 1-year-old ash cores.

amount of Si in the water soluble fraction is due to the relatively high pH value of coal fly ash samples which promote rapid dissolution of glass (Zevenbergen *et al*., 1994). Si ranged from 0.10-7.71 % and 0.01-0.88 % in the exchangeable and residual fractions of 1-year-old ash cores respectively. The order of partitioning of Si in the five fractions is as follows: carbonate fraction > Fe and Mn fraction > water soluble fraction > exchangeable fraction > residual fraction of 1-year-old ash cores.

7.2.2 Iron and manganese

The carbonate fraction contain notable proportion of Fe (7.22-52.76%) (Figure 7.21). It also has high leached amount in Fe and Mn fraction (27.42-65.56%) and residual fraction (1.66-51.35 %). The percentage leached amount of Fe in exchangeable fraction is in the range of 0.01-8.12 % and 0.001-0.005 % in the water soluble fraction of 1-year-old ash cores. The highest leachable amount of Fe in carbonate fraction is in sample taken at 23 m depth due to the large surface area of the ash sample (fine ash). The order of partitioning of Fe in the five fractions are as follows; carbonate fraction > Fe and Mn fraction > residual fraction > exchangeable fraction > water soluble fraction. The relatively high leached amount of Mn in the exchangeable fraction (0.02-14.80 %) showed that it is an easily mobilized fraction. It has been reported that the exchangeable fraction in the fly ash is an easily mobile fraction (Kalembkiewicz *et al*., 2008). Manganese has major proportion in the carbonate fraction (1.18-80.65 %), and in the iron and manganese fraction (0.34-57.26 %) of the 1-year-old ash cores. The leachable amount of Mn in a water soluble fraction is in the range of 0.01-3.72 %, and the remaining is locked in the residual fraction (0.02-5.63 %) of 1-year-old ash cores. The high percentage amount of Mn in the carbonate fraction suggests that its release could be influence by the pore water pH (see Section 5.8). The order of partitioning of Mn in the five fractions is as follows; carbonate fraction > Fe and Mn fraction > exchangeable fraction > residual fraction > water soluble fraction.

7.2.3 Calcium and magnesium

Calcium is present in the range of 15.64-94.47 % in the carbonate fraction. The high percentage of Ca in the carbonate fraction indicates the role of Ca in the precipitation of $CaCO_3$ in the 1-year-old ash cores. The Fe and Mn fraction contains 0.00-14.53 % leachable Ca (Figure 7.22). The leachable amount of Ca in water soluble fraction is in the range of 0.00-19.38 % and in the exchangeable fraction is 4.80-57.37 %. The remaining leachable amount (0.49-9.32 %) of Ca is

locked in the residual fraction of 1-year-old ash cores. The order of partitioning of Ca in 1-yr-old ash cores is as follows; carbonate fraction > exchangeable fraction > water soluble > Fe and Mn fraction > residual fraction. Magnesium dominates the carbonate fraction in the range of 8.6-100 % (Figure 7.22). Relatively high percentage of Mg in the carbonate fraction suggests its association with the CaMg (CO_3). However, dolomite phase was not detected by XRD spectra which could be due to its existence in the transitional phase. The significant leachable amount of Mg in the carbonate fraction suggests its association with dolomite (CaMg $(CO_3)_2$) (Garavaglia and Caramuscio, 1994). A negligible leachable amount of Mg is present in the water soluble fraction (0.001-0.009 %) of 1-year-old ash cores. Magnesium in the exchangeable fraction has a range of 1.36-20.35 % and in the Fe and Mn fraction (2.22-28.50 %). The residual fraction contains considerable proportion of Mg in the range of 0.15-75.13 %. The order of partitioning of Mg in 1-year-old ash cores is as follows: carbonate fraction > residual fraction > Fe and Mn fraction > exchangeable fraction > water soluble fraction.

7.2.4 Sodium and potassium

The leachable amount of Na^+ is primarily in the residual fraction (5.11-91.18 %). The water soluble and exchangeable fractions contain a relatively high percentage of leached Na in the range of 4.80-45.90 % and 2.21-31.29 % respectively (Figure 7.22). This relatively moderate proportion of Na^+ in water soluble fraction suggests that Na^+ is water soluble. Na accounts for 0.29-8.85 % in the carbonate fraction and 0.04-1.24 % in the Fe and Mn fraction. The order of partitioning of Na^+ in the five fractions is as follows: residual fraction > water soluble fraction > exchangeable fraction > carbonate fraction > Fe and Mn fraction. The percentage of K^+ in the residual fraction ranges from 1.54-96.66 % in the residual fraction of 1-year-old ash cores. Potassium has a range of 0.09-13.32 % in exchangeable fraction and 0.001-1.26 % in the carbonate fraction of 1-year-old ash cores. The percentage of K^+ in the water soluble fraction is in the range of 0.03-2.76 %, and in the Fe and Mn fraction (0.0 1-0.44 %). The order of partitioning of potassium in the five fractions is as follows: residual fraction > exchangeable fraction > water soluble fraction > carbonate fraction > Fe and Mn fraction.

The important feature of this section is most of the considered major elements with the exception of Na^+ and K^+ is mainly concentrated in carbonate fraction of 1-year-old ash cores. It should be noted that possible contact of the dry disposed ash cores with slightly acidic medium or slight

change in pore water pH will lead to mobility of major elements. This will ultimately have significant impact on the chemistry of the toxic metals locked in different physico-chemical forms of the dry disposed fly ash cores.

7.3 Total concentration of major elements in weathered ash core samples

The total acid digestion is used to determine the total concentration of major elements in the dry disposed fly ashes. The experimental protocol used for the results is reported in this section is presented in section 4.2.4. The results of total acid digestion of core ash samples from 1 year, 8 year and 20-year-old dry disposed ash cores are shown in Table 7.1 a & b.

The results in general show close similarities with the result of each leaching step in the sequential extraction scheme discussed in the section 8.1. Major elements trends in the total acid digestion results show a significant concentration difference in the top, middle and bottom sections of 1-year-old ash cores influence by textural differences (surface area). The concentration of Ca in the ash samples shows a consistent increase down the hole of the ash dump due to leaching of major soluble components. At the same time, Na^+ concentration increase with depth of the ash dump. Other metals (such as Al, Si, Mg, Fe, Mn and K^+) show inconsistent trend with the depth of the ash dump due to interaction with percolating rain water.

Relatively high concentrations of the major elements are recorded in the middle and bottom sections of 1-year-old ash cores characterized by fine ash (see Table 7.1a). This suggests that surface area play a noticeable role in the release of these metals from fly ash. Major elements (such as Al, Si, Mg, K, Fe and Mn) show inconsistent trend with the depth of the ash dump. On the contrary, the concentrations of Ca and Na^+ in the 8-year-old ash cores show consistent increase with depth due to leaching of major soluble components (see Table 7.1b).

The concentration seems to be controlled by pore water pH. The acid neutralisation results showed that the release of these metals is pH dependent. In addition, the ash type seemed also to contribute to the vertical distribution patterns. A relatively high concentration of Al, Si, Mg, Fe, Mn, and Na^+ is recorded in the bottom sections of 8-year-old ash cores characterized by brittle and unconsolidated fly ash. Major elements in the 20-year-old ash dump show inconsistent trend with depth. The vertical distribution patterns seem to be influenced by the ash moisture content levels and point of contact with groundwater (at 9 m for 20-year-old ash cores).

Table 7.1a. The concentration (mg/kg) of major elements in 1-year-old ash core samples as determined by total acid digestion (n=3).

Sample ID	Depth Reference	Lithology	Al (mg/kg)	Si (mg/kg)	Ca (mg/kg)	Mg (mg/kg)	Fe (mg/kg)	Mn (mg/kg)	Na (mg/kg)	K (mg/kg)
1m	Top section	Coarse ash	8254.53±57.89	6595.17±135.36	23974.17±32.40	6097.27±71.14	2258.31±56.77	0.13±0.0013	2673.82±49.85	8.44±0.02
2m			6483.14±161.80	6415.13±0.00	26090.57±302.25	4548.91±86.34	1677.29±14.56	0.14±0.00	1569.58±44.70	20.48±0.03
3m			23923.71±24.95	27847.42±186.57	25967.34±44.00	20129.30±358.72	2766.55±185.66	0.09±0.0	9313.5±469.58	55.76±6.99
4m		Fine ash	4246.43±39.16	7866.00±1.51	21163.93±16.38	6430.18±39.79	1589.17±15.29	0.09±0.002	199.99±11.41	24.39±0.039
5m			9540.70±1546.44	7110.46±3.04	28201.51±8.27	6994.61±36.04	1686.66±44.39	0.11±0.004	5656.34±42.11	6.11±1.27
6m	Middle section		10890.75±218.36	9193.36±7.36	21175.12±23.50	7557.25±23.38	3882.12±44.09	0.21±0.0002	2460.19±19.27	23.27±0.005
7m			7025.85±194.42	6394.20±6.97	19144.48±88.95	3924.36±7.70	1857.33±57.38	0.091±0.007	2463.27±0.00	19.34±0.16
8m			8055.08±7.67	6333.93±7.52	23195.65±10.29	6464.96±13.09	2155.02±32.99	0.21±0.0005	8468.28±21.37	34.47±0.005
9m			9626.44±342.21	8910.32±0.12	20743.55±49.10	7369.10±8.19	2343.55±0.29	0.11±0.002	8112.37±0.00	8.64±0.10
12m		Coarse ash	9715.89±541.35	8582.00±1.50	33005.94±170.86	6563.08±59.28	1900.94±14.98	0.11±0.0007	2699.29±11.22	22.32±0.016
13m			8097.01±141.46	82541.23±7.10	31161.04±7.13	3955.83±69.98	2861.04±35.99	0.16±0.002	2302.55±0.00	9.32±0.03
14m			5901.19±357.97	8695.56±8.81	29119.58±258.93	4407.79±54.95	2119.58±18.20	0.14±0.002	2529.875±0.00	10.29±0.04
15m			8637.08±202.99	4753.84±0.00	28998.76±98.38	6201.80±12.16	2198.76±63.74	0.1102±0.0006	2463.21±0.00	60.342±0.01
17m			6249.84±167.89	6512.54±0.20	24934.46±116.54	6182.11±54.28	2934.46±12.62	0.139±0.0004	1342.87±0.00	42.37±0.01
18m			5966.97±64.22	5893.24±0.00	31401.09±345.51	4863.54±66.46	2101.09±56.83	0.12±0.002	3791.78±49.76	22.31±0.03
19m		Fine ash	7860.42±178.00	7345.89±0.00	30639.56±33.84	5412.49±19.08	2639.56±33.84	0.08±0.0003	8932.15±0.00	23.30±0.02
20m			8849.11±98.59	5914.07±0.00	27989.78±398.59	7394.48±75.99	2189.78±34.86	0.14±0.002	2757.52±0.00	110.29±0.03
22m	Bottom section		8752.12±535.61	7845.63±0.00	30439.49±177.27	6540.14±42.89	2116.49±12.39	0.11±0.001	2403.83±0.00	57.61±0.02
23m			13339.43±24.90	6832.56±44.01	27534.78±109.48	3986.05±56.90	1054.78±51.52	0.13±0.003	1413.32±45.69	6.34±0.03
26m			4822.15±53.32	5630.99±7.54	27114.9±13.75	4557.84±21.17	1911.49±13.75	6.08±0.69	2845.89±0.00	107.02±10.17
27m			7593.74±32.90	6844.02±0.00	31239.21±63.18	5545.45±23.79	1539.21±63.18	0.11±0.0002	6468.14±50.02	14.03±0.01
28m			7323.64±104.27	5645.19±0.00	12466.90±55.28	5010.87±107.95	2466.90±38.07	0.07±0.004	8445.97±0.00	36.30±0.04
29m			2290.03±71.03	2761.59±1.43	92702.74±216.81	2556.51±56.90	430.74±20.51	0.96±0.091	595.39±0.00	4.08±0.006
30m			7321.64±33.62	227698.00±0.00	16312.26±181.15	4654.32±45.76	3127.26±19.47	0.08±0.001	8542.08±0.00	15.35±0.02
31m			6595.45±56.33	3945.90±0.72	18355.50±94.89	4738.18±23.83	1202.50±8.23	0.072±0.0003	4379.41±10.99	100.34±0.005
Mean			8294.49±109.57	19364.33±16.79	28122.89±16.67	6083.46±57.43	2120.42±38.74	0.392±0.05	4113.23±33.04	33.70±0.85

Table 7.1b. The concentration (mg/kg) of major elements in 8 year and 20-year-old ash samples as determined by total acid digestion (n=3).

8 yrs old fly ash										
Sample ID	**Depth Reference**	**Lithology**	**Al (mg/kg)**	**Si (mg/kg)**	**Ca (mg/kg)**	**Mg (mg/kg)**	**Fe (mg/kg)**	**Mn (mg/kg)**	**Na (mg/kg)**	**K (mg/kg)**
1m	Top section	Fracture, hard ash	1980.59±18.54	3979.94±8.74	18761.03±20.07	1213.83±44.58	27363.62±45.58	1485.16±49.86	181.95±24.39	2959.97±15.46
2m			2820.35±0.00	11536.92±10.11	16938.50±38.22	1372.34±185.05	25561.08±82.52	2.27±0.11	123.34±5.85	2100.52±58.04
3m			2313.18±14.24	4363.85±5.85	16188.53±51.51	1132.15±19.75	25277.65±42.24	2.18±0.07	171.56±5.98	1811.11±48.62
4m	Middle section		35556.85±0.00	4339.54±11.14	13521.33±25.59	1944.87±27.33	23664.82±283.78	2.04±0.06	560.37±0.00	2276.82±27.86
5m			45130.70±420.93	3927.12±0.00	20479.13±168.89	4080.91±92.83	29291.98±133.37	2.17±0.05	1183.95±0.00	3825.17±19.81
6m			17828.35±0.00	4794.56±3.28	13581.73±87.16	1590.48±69.47	31418.65±304.91	2.63±0.50	1169.53±7.57	2344.06±38.88
7m			17762.25±0.00	4704.36±7.51	14666.60±37.15	2067.99±59.59	25031.82±24.69	2.04±0.12	1211.73±12.96	3389.62±52.31
8m			13763.6±72.31	3994.11±11.10	18247.89±49.43	2745.44±213.94	28015.01±60.07	2.08±0.13	1338.67±19.75	3874.40±23.48
9m	Bottom section		36166.6±42.1	5502.25±15.28	30550.23±29.38	4952.35±31.91	32696.38±18.70	1.84±0.08	1234.83±13.34	2654.14±31.55
10m		Brittle ash	49605.75±0.00	5560.69±3.63	18423.71±64.45	2513.55±81.49	28860.98±25.54	3.01±0.0.17	1456.10±57.97	2403.86±16.15
11m			768.55±0.00	5439.06±10.64	11704.61±60.75	541.21±48.23	25038.58±70.63	308.68±6.19	1555.54±0.00	758.12±9.16
12m		Unconsolidated ash	33766.25±0.00	5504.39±9.96	28024.27±57.22	3020.11±545.82	36795.92±37.44	203.37±8.03	1641.43±0.00	2764.68±52.41
13m			24296.65±0.00	4897.27±7.53	27344.69±72.16	3477.84±257.13	34130.28±161.53	2.93±0.17	1607.32±55.56	2962.28±36.04
Mean			21673.82±45.86	5272.62±8.06	19110.17±58.61	2357.93±129.01	28703.59±99.23	155.42±5.04	1025.87±15.64	2624.98±33.06
20 yrs old fly ash										
Sample ID	**Depth Reference**	**Lithology**	**Al (mg/kg)**	**Si (mg/kg)**	**Ca (mg/kg)**	**Mg (mg/kg)**	**Fe (mg/kg)**	**Mn (mg/kg)**	**Na (mg/kg)**	**K (mg/kg)**
0.75m	Top section	Top soil	29295.44±385.05	4612.07±543.63	567063.85±0.00	63304.09±62.93	478164.46±57.87	0.19±0.007	393.82±7.83	2.65±0.32
1m		Solid ash	4167.24±215.43	88.98±4.57	2285.04±62.37	638.34±34.02	2013.82±38.47	0.19±0.010	773.70±0.00	2.51±0.005
2m			15003.92±0.0	37624.42±0.0	79360.32±0.20	208072.26±0.0	73163.41±59.09	093±0.00	502.7±8.44	0.0009±0.00
3m			886.59±73.02	181.65±7.80	2437.93±223.73	691.52±39.85	2260.25±192.96	18.11±3.55	232.07±16.70	12.05±0.07
4m	Middle section		1034.41±37.45	83.67±8.22	2062.32±181.36	305.39±59.25	1521.60±3.67	0.21±0.006	1634.39±49.85	80.53±0.00
5m			3584.74±56.87	51.32±8.86	2192.75±75.53	604.04±15.39	1964.27±48.20	0.19±0.006	1261.08±13.53	2.68±0.09
6m			835.25±20.36	50.01±1.29	1873.07±156.31	265.82±8.79	1360.31±44.73	0.19±0.012	1139.43±32.45	2.29±0.28
7m			360.49±14.12	1396.58±78.08	1445.96±43.02	107.61±42.52	1482.01±126.07	0.14±0.05	1391.41±0.023	1.54±0.13
8m			1781.75±0.00	8393.38±0.20	1465.91±49.85	256.91±9.00	1357.72±55.37	0.14±0.00	966.44±0.035	1.44±0.43
9m	Bottom section	Moist ash	360.92±58.42	4.99±0.00	1712.01±27.22	185.43±24.85	1210.02±147.51	6.45±0.0	866.78±0.00	61.43±0.20
10m			1111.83±37.60	316.54±49.95	1708.08±243.32	153.34±13.93	1507.37±88.65	0.17±0.017	628.33±31.83	1.99±0.31
12m		Dolerite+Clay	3568.63±50.09	47.66±0.88	2087.67±9.43	1301.49±60.18	2087.67±9.42	0.47±0.017	837.66±26.49	6.09±0.06
14m			3269.46±46.33	110.06±28.48	1421.59±38.54	976.77±32.78	1421.59±153.96	0.37±0.023	702.15±47.54	9.57±0.38
15m			2653.06±230.18	3919.38±5.98	4389.89±42.32	1865.24±58.00	4389.89±42.32	60.36±10.11	82.39±0.00	1575.59±29.63
Mean			4850.98±87.50	4062.91±52.71	47964.74±82.37	19909.16±32.96	40993.17±76.31	12.87±0.99	815.17±16.98	125.74

Whereas relatively high concentration of the investigated major elements was recorded in both top and middle sections of 20-year-old ash cores characterized by solid ash (see Table 7.1b). This suggests that moisture content levels play a major role in the metal mobility. A relatively high concentration of metals in the top section of 20-year-old ash cores is influenced by the leachate from top soil. In comparison of mean of the 1 year, 8 year and 20-year-old ash cores, there is high concentration of Al, Si, Ca, Mg, Ca and Na^+ in the 1-year-old ash cores. The Fe, Mn and K^+ showed higher concentration in the older ash cores. Their obvious low concentrations of Al, Si, Ca, Mg and Na^+ in the 8 year and 20-year-old ash cores indicate overtime leaching of major components of the ash cores or slower release due to the formed secondary mineral phase (i.e. calcite). The important features of this section are the considered major elements showed inconsistent mobility patterns by depth of the fly ashes due to in-homogeneity in 3 drilled ash cores and brine irrigation, moisture content levels and point of contact with the groundwater.

7.4 Statistical assessment of data quality

A comparison between total metal concentrations of fly ash sample with the sum of individual metal concentrations obtained from sequential extraction can be used to check for possible systematic errors arising from element losses, contamination or other undefined causes (Smichowski *et al*., 2008). In this study, a Standard Reference Material (SRM) namely NIST 2689 (Class F fly ash) was subjected to the same sequential extraction scheme presented in section 2.2. The results of the validation analysis (Table 7.2) showed recoveries as follows: Al (94.83 %); Ca (99.40 %); Fe (79.45 %); K (77.76 %); Mg (99.67 %) and Si (62.32 %).

Table 7.2. Recoveries obtained in analysis of the NIST SRM 2689 (Class F fly ash) subjected to total acid digestion.

Element	Certified (C)	Total	SD	∑Fractions	SD	Rec 1 (T/C)	Rec 2 (S/T)
Al	12.94	12.27	0.47	11.03	0.88	94.83	89.90
Ca	2.18	2.17	0.01	2.14	0.02	99.40	98.97
Fe	9.32	7.40	1.35	6.00	0.99	79.45	81.01
K	2.2	1.71	0.35	1.05	0.46	77.76	61.58
Mg	0.61	0.61	0.00	0.37	0.17	99.67	61.28
Si	24.06	15.00	6.41	8.54	4.56	62.32	56.98

**Rec1 is the recovery regarding the certified value(C). Rec2 is the recovery of the sum of fractions(S) with regard to the total metal concentration. All results are expressed in percentage.

The high reproducibility obtained for Al, Ca, and Mg indicates that the recoveries can be considered good and acceptable for this ash sample matrix. The total metal concentration of the dry disposed fly ashes aged 1 year, 8 year and 20-year-old ash cores using the certified triple acid digestion method are presented in Tables 7.1a and 7.1b.

7.4.1 Fractionation scheme and efficiency of fractionation for major elements

The 1-year-old ash cores which revealed highest concentration for the metals investigated was used for statistical assessment of fractionation efficiency. Statistical analysis was done using SAS 9.2 (SAS Institute Inc. Cary, NC. USA), the output results are indicated in Table 7.3. The variations of elements concentration per fraction between corresponding 25 ash samples were assessed by means of the coefficient of divergence (COD). The COD is self normalizing; if two samples are similar in chemical composition the COD approaches zero, otherwise the COD approaches one (Smichowski *et al*., 2008). For five fractions, we calculated 300 CODs representing all possible combinations between the twenty-five ash samples. Table 7.3 showed that major elements such as Al, Si, Mg, Fe, Mn, Na^+ and K^+ are not similar in concentrations in

Table 7.3. Statistical analysis of five fractions in 25 sub samples from 1-year-old ash cores

COD descriptive statistics for each element						
Element	N Obs	Mean	Median	Stdv.Dev.	Mininum	Maximum
Aluminium	600	0.29	0.26	0.15	0.03	0.73
Silicon	600	0.33	0.34	0.13	0.05	0.69
Calcium	600	0.29	0.28	0.12	0.03	0.61
Magnesium	600	0.28	0.25	0.12	0.05	0.66
Iron	600	0.25	0.23	0.12	0.03	0.58
Manganese	600	0.31	0.28	0.14	0.06	0.68
Sodium	600	0.48	0.47	0.22	0.06	1.00
Potassium	600	0.50	0.51	0.18	0.01	0.94
Percent recovery descriptive statistics for each element						
Element	N Obs	Mean	Median	Stdv.Dev.	Mininum	Maximum
Aluminium	25	58.30	57.68	29.22	11.60	92.01
Silicon	25	55.30	58.01	27.68	8.99	96.69
Calcium	25	70.33	68.37	20.00	41.25	98.05
Magnesium	25	43.93	38.67	31.42	4.51	98.38
Iron	25	64.90	60.95	17.01	42.83	98.04
Manganese	25	73.93	69.35	15.38	38.11	93.94
Sodium	25	71.59	77.44	24.61	17.42	99.47
Potassium	25	80.73	84.25	12.16	58.19	93.29

each of the five fractions of the twenty-five ash samples. This fact is corroborated with relatively high median value of COD for Al, Si, Ca, Mg, Fe, Mn, Na^+ and K^+. The dissimilarities in the major elements concentration in each of the five fractions are due in part to the careful adsorption of metals by different physico-chemical forms, and aqueous behaviour of metals. The second most important factor is the preferential weathering of ash core ash samples due to fluctuation in the pH of the ash column. An overview of CODs values thus indicate that the variations of Al, Si, Ca, Mg, Fe, Mn, Na^+, and K^+ are attributed to minor variations in chemical composition of fly ash influenced by the interactions of coal fly ash with ingressed CO_2, ingressed O_2, and percolated rain water. The fractionation scheme divided the total metal concentration into five partial concentrations; consequently the sum of five partial values of concentration (pseudo total) should be close to total metal concentration. The comparison between pseudo total concentration and the total metal concentration provides an indication of the performance of the extraction scheme.

The control of efficiency in the sequential extraction procedure was defined in terms of the recovery. All the recoveries were found to be good and acceptable considering the complexity of the matrix analyzed and the number of statistical manipulations performed. Table 7.3 further showed that the recoveries of the elements in 25 sub-samples from 1-year-old ash cores varied in the order Na^+ (99.47 % > Mg (98.38 %) > Ca (98.05 %) > Fe (98.04 %) > Si (96.69 %) > Mn (93.94 %) > K^+ (93.29 %) > Al (92.01 %).

Table 7.4 a-c depicted major elements in the five-step sequential fractionation scheme of the fly ash taken at 2 m depth interval in 1-year-old ash cores. The zone of greatest weathering marked the sections of relatively lowest pH values in the ash column. The sum of elements in five-step sequential fractions (pseudo-total concentration) was validated with the total metal content. There is variability (within 10 %) between sum of values obtained for different fractions (pseudo-total concentration) of Ca, Mg, Fe, Mn, and K^+ and values obtained for the same sample extracted with combined acid leach (total metal content). The higher variability (above 10 %) of Al, Si, and Na^+ in the sample taken at 3 m depth may be attributed to weight loss due to spill out of leachant at some stage in sample preparation procedure in the laboratory.

Table 7.4a. Major elements distribution in five step sequential scheme and total metal content in samples taken at 1 m, 3 m, 5 m and 7 m depths in Tutuka 1-year-old ash cores (*S1 = water soluble fraction, S2 = exchangeable fraction, S3 = carbonate fraction, S4 = Fe and Mn fraction, S5 = residual fraction)*

1m depth								
Fractions	**Al**	**Si**	**Ca**	**Mg**	**Na**	**K**	**Fe**	**Mn**
S1	0.085±14.15	142.205±8.25	2360±17.65	0.239±0.00	675.86±7.72	0.23±0.17	0.012±0.01	0.001±0.0003
S2	24.238±13.35	96.640±18.45	11535.47±162.04	572.27±31.28	243.65±10.09	0.142±0.03	0.1863±0.00	0.007±0.0003
S3	1207.78±87.21	1159.96±87.21	5668.04±147.31	1755.55±120	46.84±1.05	nd	293.96±5.03	0.0052±0.001
S4	3584.88±56.51	4625.88±333	2048.41±316.05	1064.59±89.42	29.03±33.33	0.037±0.004	9711.63±1343.15	0.0051±0.0
S5	2776.37±17.21	16.78±0.84	641.24±65.05	2429.41±0.45	29.03±0.04	7.599±54.87	1327.54±177.46	0.007±0.001
Pseudototal (mg/kg)	7593.36	6041.48	22274.06	5822.06	1446.39	8.01	11333.32	0.118
Total metal content(mg/kg)	8254.530	6595.170	23974.170	6097.270	2673.820	8.439	2258.31	0.128
Variability (%)	8.01	8.40	7.09	4.51	9.37	5.07	5.07	8.1
3m depth								
Fractions	**Al**	**Si**	**Ca**	**Mg**	**Na**	**K**	**Fe**	**Mn**
S1	207.716±0.00	346.133±11.17	2806.797±283.91	0.261±0.007	959.03±3.03	0.129±0.05	0.038±0.0001	0.002±0.0001
S2	24.238±0.00	102.243±31.89	11275.47±12.64	425.330±36.55	249.504±15.25	0.136±0.05	nd	0.004±0.0007
S3	1329±93.08	1345.084±77.48	5766.43±20.14	1559.493±7.89	50.943±11.04	0.022±0.00	259.296±25.98	0.042±0.001
S4	2932.168±243.14	3953.66±59.02	1478.786±150.02	1021.097±17.41	nd	0.017±0.004	886.954±80.32	0.042±0.007
S5	14152.461±14.29	86.260±8.99	2588.241±14.82	15122.529±0.009	5981.79±55.01	50.759±1.63	1420.549±25.25	0.001±0.0006
Pseudototal (mg/kg)	18640.99	5833.38	23915.72	18128.71	7241.28	51.06	2566.84	0.01
Total metal content(mg/kg)	23923.7090	27847.4170	25967.3370	20129.3010	9313.5000	55.7580	2766.549	0.0098
Variability (%)	22.08	79.05	7.90	9.94	22.25	8.42	7.22	7.21
5m depth								
Fractions	**Al**	**Si**	**Ca**	**Mg**	**Na**	**K**	**Fe**	**Mn**
S1	0.231±0.01	416.785±0.002	2573.604±0.001	0.3194±0.003	1125.526±0.09	0.094±0.02	0.0399±0.005	0.002±0.0003
S2	24.24±0.03	159.243±0.01	13200.15±0.006	714.47±0.005	469.004±0.002	0.05095±0.07	nd	0.0037±0.0006
S3	986.51±0.04	1283.411±12.23	9073.306±0.002	2215.659±0.001	88.89±0.001	0.0024±0.05	200.061±10.34	0.035±0.005
S4	4307.95±12.15	4753.684±0.001	2850.089±0.008	1248.736±0.001	25.279±0.001	0.0189±0.08	1098.945±0.007	0.063±0.0003
S5	3791.97±10.12	3.97±0.002	401.021±0.002	2537.403±0.001	3549.425±0.001	5.33±0.03	259.775±0.054	0.00045±0.00
Pseudototal (mg/kg)	9110.66	6617.09	28098.17	6716.59	5258.12	5.50	1558.82	0.10
Total metal content(mg/kg)	9540.70	7110.46	28201.51	6994.61	5656.34	6.11	1686.66	0.11
Variability (%)	4.51	6.94	0.37	3.97	7.04	9.99	7.58	5.39
7m depth								
Fractions	**Al**	**Si**	**Ca**	**Mg**	**Na**	**K**	**Fe**	**Mn**
S1	0.276±0.004	430.59±0.003	2948.716±10.12	0.277±0.04	590.35±0.06	0.121±0.003	0.0596±0.002	0.0029±0.0001
S2	24.238±0.002	132.639±0.004	10383.84±0.09	463.950±0.01	209.374±0.06	0.0166	nd	0.0045±0.00
S3	1166.54±0.002	1212.2108±0.002	3423.511±10..23	1147.049±0.02	26.645±1.24	0.0012±0.0001	271.63±0.001	0.029±0.0001
S4	2726.67±0.002	3644.664±0.002	1603.021±0.067	827.81±0.07	0.974±0.001	0.011±0.0002	820.545±10.23	0.049±0.0003
S5	2734.312±0.004	31.278±0.004	778.67±0.002	1432.121±0.03	1411.145±10.23	16.939±0.003	673.41±0.003	0.0007±0.00
Pseudototal (mg/kg)	6652.036	5451.377	19137.750	3871.206	2238.486	17.088	1765.647	0.085
Total metal content(mg/kg)	7025.85	6394.2	19144.48	3924.36	2463.27	19.34	1857.33	0.091
Variability (%)	5.321	14.745	0.04	1.354	9.13	11.64	4.9	6.126

Table 7.4b. Major elements distribution in five step sequential scheme and total metal content in samples taken at 9 m, 12 m, 15 m and 18 m depths in Tutuka 1-year-old ash cores (*S1 = water soluble fraction, S2 = exchangeable fraction, S3 = carbonate fraction, S4 = Fe and Mn fraction, S5 = residual fraction)*

9m depth								
Fractions	**Al**	**Si**	**Ca**	**Mg**	**Na**	**K**	**Fe**	**Mn**
S1	0.267±0.002	420.056±0.006	2688.192±0.005	0.4218±0.009	427.267±0.005	0.1577±0.003	0.049±0.0003	0.00238±0.0003
S2	24.24±0.002	155.566±0.009	11292.253±0.003	799.307±0.006	152.935±0.009	0.107±0.008	nd	0.0065±0.002
S3	1270.522±0.002	1325.008±0.007	3905.4113±0.005	1130.741±0.005	23.631±0.003	0.0102±0.002	349.768±0.05	0.0363±0.001
S4	4295.705±0.004	6437.30±0.007	2062.014±0.003	1048.442±0.002	13.253±0.002	0.0258±0.0001	1226.070±0.005	0.049±0.0001
S5	3264.94±0.001	7.959±0.003	708.703±0.008	4096.287±0.008	7009.326±0.007	7.901±0.008	555.878±0.09	0.0008±0.00
Pseudototal (mg/kg)	8855.673	8345.890	20656.574	7075.199	7626.412	8.201	2131.766	0.095
Total metal content(mg/kg)	9626.440	8910.320	20743.550	7369.100	8112.370	8.64	2343.55	0.11
Variability (%)	8.01	6.33	0.42	3.99	5.99	5.08	9.04	9.39
12m depth								
Fractions	**Al**	**Si**	**Ca**	**Mg**	**Na**	**K**	**Fe**	**Mn**
S1	0.228±0.002	382.913±0.002	4793.532±0.003	0.275±0.006	1186.041±0.002	0.107±0.004	0.0377±0.009	0.00195±0.008
S2	24.238±0.005	82.735±0.002	10845.62±0.003	467.19±0.003	438.733±0.001	0.0676±0.003	nd	0.0042±0.0001
S3	1919.549±0.002	2327.328±0.003	14360.023±0.002	2149.436±0.008	106.128±0.006	0.0087±0.0001	283.42±0.006	0.0592±0.002
S4	4376.545±0.05	5519.4244±0.003	1984.579±0.004	1246.041±0.003	14.8248±0.03	0.0124±0.006	1015.159±0.006	0.0403±0.002
S5	2558.425±0.02	28.089±0.003	576.902±0.005	1901.45±0.006	715.685±0.004	20.923±0.008	417.2009±0.002	0.00046±0.00
Pseudototal (mg/kg)	8878.98	8340.49	32560.66	5764.39	2461.41	21.12	1715.82	0.106
Total metal content(mg/kg)	9715.890	8582.000	33005.940	6163.080	2699.290	22.320	1900.940	0.111
Variability (%)	9.43	2.90	1.37	6.92	9.66	5.69	10.79	4.45
15m depth								
Fractions	**Al**	**Si**	**Ca**	**Mg**	**Na**	**K**	**Fe**	**Mn**
S1	0.183±0.001	360.891±0.003	2862.27±0.003	0.335±0.002	1046.166±0.006	0.075±0.0002	0.0325±0.002	0.00146±0.00
S2	24.238±0.004	104.7824±0.003	10788.57±0.005	793.931±0.003	643.82±0.003	0.2096±0.005	nd	0.0042±0.0001
S3	1072.342±0.001	1396.1175±0.006	11586.573±0.003	1785.24±0.0003	121.43±0.002	0.0164±0.004	225.051±0.001	0.0524±0.0003
S4	2161.893±0.005	2713.9911±0.002	2236.354±0.002	885.7972±0.001	nd	0.013±0.0002	926.264±0.005	0.0389±0.0002
S5	4575.0543±0.003	41.232±0.005	872.532±0.002	2120.471±0.003	462.534±0.003	58.325±0.0002	861.1872±0.006	0.00052±0.00
Pseudototal (mg/kg)	7833.710	4617.014	28346.301	5585.773	2273.947	58.639	2012.535	0.097
Total metal content(mg/kg)	8637.080	4753.840	28998.760	6201.800	2463.210	60.342	2198.760	0.102
Variability (%)	9.30	2.88	2.25	9.93	7.68	2.82	8.47	4.51
18m depth								
Fractions	**Al**	**Si**	**Ca**	**Mg**	**Na**	**K**	**Fe**	**Mn**
S1	0.234±0.02	451.248±0.001	3357.2024±0.002	0.2593±0.001	1642.41±0.002	0.11941±0.00	0.0412±0.002	0.0022±0.00
S2	24.238±0.001	111.662±0.003	10979.869±0.00	660.719±0.001	751.458±0.002	0.393±0.001	nd	0.0043±0.0001
S3	775.359±0.002	1005.053±0.004	12664.056±0.001	1761.1096±0.003	142.429±0.002	0.041±0.002	186.454±0.002	0.04704±0.001
S4	3651.066±0.001	4132.411±0.006	2523.868±0.005	1330.317±0.003	24.786±0.006	0.0234±0.001	1275.609±0.001	0.062±0.001
S5	1443.298±0.002	20.523±0.005	583.865±0.005	709.2466±0.002	888.245±0.001	20.702±0.001	493.615±0.002	0.00047±0.00
Pseudototal (mg/kg)	5894.19	5720.90	30108.86	4461.65	3449.32	21.28	1955.72	0.12
Total metal content(mg/kg)	5966.97	5893.24	31401.09	4863.54	3791.78	22.31	2101.09	0.123
Variability (%)	1.22	2.92	4.12	8.26	9.03	4.62	6.92	5.75

Table 7.4c. Major elements distribution in five step sequential scheme and total metal content in samples taken at 22m, 27m, 29m and 31m depths in Tutuka 1-yr-old ash cores (*S1 = water soluble fraction, S2 = exchangeable fraction, S3 = carbonate fraction, S4 = Fe and Mn fraction, S5 = residual fraction)*

22m depth								
Fractions	**Al**	**Si**	**Ca**	**Mg**	**Na**	**K**	**Fe**	**Mn**
S1	0.427±0.001	399.42±0.003	3754.66±0.001	nd	806.98±0.004	0.253±0.001	nd	0.0023±0.00
S2	24.238±0.002	131.7203±0.002	14003.703±0.006	808.427±0.003	368.928±0.003	0.281±0.002	nd	0.0055±0.0003
S3	1564.187±0.004	1941.65±0.002	7971.37±0.001	1956.466±0.002	52.643±0.003	0.011±0.002	266.102±0.003	0.0417±0.006
S4	3760.95±0.002	4889.766±0.003	2368.213±0.003	1053.97±0.002	15.158±0.006	0.0133±0.006	841.282±0.002	0.0515±0.006
S5	3215.801±0.002	48.037±0.001	954.563±0.003	2191.68±0.004	789.339±0.007	51.285±0.003	802.582±0.003	0.00057±0.00
Pseudototal (mg/kg)	8565.60	7410.59	29052.51	6010.54	2033.04	51.84	1909.97	0.10
Total metal content(mg/kg)	8752.12	7845.63	30439.49	6540.14	2203.83	57.61	2116.49	0.11
Variability (%)	2.13	5.55	4.56	8.10	7.75	10.01	9.76	7.68
27m depth								
Fractions	**Al**	**Si**	**Ca**	**Mg**	**Na**	**K**	**Fe**	**Mn**
S1	0.269±0.003	390.453±0.002	3472.779±0.003	0.292±0.002	695.178±0.002	0.187±0.002	0.0414±0.002	0.0021±0.0001
S2	24.048±0.002	103.159±0.003	12698.541±0.004	472.73±0.002	319.187±0.02	0.228±0.001	nd	0.0050±0.0002
S3	1901.387±0.002	2448.296±0.002	11546.206±0.002	2180.798±0.001	76.928±0.003	0.0139±0.001	329.982±0.003	0.037±0.0002
S4	2904.6313±0.001	3805.8711±0.002	2227.356±0.002	1032.462±0.002	16.445±0.02	0.0077±0.001	778.52±0.002	0.056±0.002
S5	2383.876±0.002	6.0480±0.004	443.989±0.002	1291.464±0.003	5136.023±0.002	12.22±0.001	308.145±0.002	0.00035±0.001
Pseudototal (mg/kg)	7214.21	6753.83	30388.87	4977.75	6243.76	12.66	1416.69	0.10
Total metal content(mg/kg)	7593.74	6844.02	31239.21	5545.45	6468.14	14.03	1539.21	0.11
Variability (%)	5.00	1.32	2.72	10.24	3.47	9.79	7.96	8.99
29m depth								
Fractions	**Al**	**Si**	**Ca**	**Mg**	**Na**	**K**	**Fe**	**Mn**
S1	nd	nd	nd	nd	nd	nd	nd	nd
S2	nd	nd	nd	nd	nd	nd	0	nd
S3	2222.79±0.002	2646.51±0.003	8757.69±0.005	2302.37±0.002	52.705±0.003	0.058±0.0002	370.797±0.001	0.0820±0.0001
S4	nd	nd	nd	nd	nd	nd	nd	nd
S5	nd	5.919±0.001	172.614±0.0005	nd	494.321±0.003	3.902±0.0005	32.186±0.005	0.000164±0.00
Pseudototal (mg/kg)	2222.79	2652.43	8930.30	2302.37	547.03	3.96	402.98	0.08
Total metal content(mg/kg)	2290.029	2761.59	9270.274	2556.51	595.39	4.08	430.74	0.09
Variability (%)	2.94	3.95	3.67	9.94	8.12	2.94	6.44	9.79
31m depth								
Fractions	**Al**	**Si**	**Ca**	**Mg**	**Na**	**K**	**Fe**	**Mn**
S1	0.352±0.001	456.794±0.003	3290.44±0.003	0.343±0.002	1513.52±0.002	0.139±0.002	0.047±0.002	0.0031±0.00
S2	nd	nd	nd	nd	nd	nd	0	nd
S3	2516.76±0.004	3261.734±0.004	13609.156±0.003	2062.20±0.003	101.236±0.001	0.009±0.00	355.813±0.0001	0.066±0.0001
S4	nd	nd	nd	nd	nd	nd	nd	nd
S5	3793.383±0.002	34.590±0.002	1054.39±0.004	2372.43±0.003	2609.66±0.002	91.83±0.002	752.514±0.002	0.0007±0.00
Pseudototal (mg/kg)	6310.50	3753.12	17953.98	4434.97	4224.42	91.98	1108.37	0.070
Total metal content(mg/kg)	6595.45	3945.9	18355.5	4738.18	4379.41	100.34	1202.5	0.072
Variability (%)	4.52	5.14	2.24	6.84	3.67	9.09	8.49	2.90

7.5 Markers for major elements in fly ashes for environmental applications

7.5.1 Major element patterns by age and depth of dry disposed ash core samples

From the statistical evaluation of the results from ICP-MS analysis on the leachates from the sequential extraction scheme on the fly ashes drawn from different ages and depths for the trace and major elements, environmental markers of the pollution trend could be identified. For each pair of variables, there is a calculated Spearman's rho and an associated p-value (denoted as rawp) for testing the null hypothesis that the correlation is zero. You can ignore the 'smallp'. The bonp is an adjusted p-value, adjusted by the Bonferroni method. The fdrp is an adjusted p-value, adjusted by the False Discovery Rate method (FDR) (Benjamini and Hochberg, 1995).

In order to evaluate for major element patterns by Age, we fix the element and the solubility at specific values. Then, stratifying by depth, we look to see if there is a relationship between age and response (i.e. concentration). Basically the statistical method showed if there is an increasing or decreasing 'trend' with age of the ash dump. The stratified test used in this study is a Cochran-Mantel-Haenszel test (CMH). Cases where the CMH test has p-values (roughly) less than 0.01 or more precisely p-values adjusted to control the false discovery rate (FDR) at a 0.05 level are shown. We looked for evidence of a correlation at each depth and then combining the evidence over the different depths. In some cases the evidence might relate to the response being consistently high (or low) in either 1 year or 20-year-old ash cores.

In the easiest-to-interpret case there will be a consistent increasing (or decreasing) pattern across ages. In order to look for patterns by depth, Spearman correlation coefficient between the recorded value and depth is the statistical method used. A significant positive correlation would correspond to increasing response with increasing depth. A negative correlation would correspond to a decreasing response with increasing depth. The correlations were calculated for each element and each age and each solubility separately. Consequently there are a large number of correlations to consider. Those strong correlations that showed significant at the 0.01 level are considered. In this case, a significant positive correlation would correspond to increasing response with increasing depth. While a negative significant correlation would correspond to a decreasing response with increasing depth.

In the previously related study, Samara (2005) calculated Pearson and Spearman correlation coefficient between elemental Total Suspended Particles (TSP) components for each sampling site. At all sites, strong correlations, significant at the 0.01 level, were observed among the crustal elements Mg, Al, Si, Ca, Ti, Mn, Fe, Sr originating mostly from soil dust and fly ash. Similarly, Pearson and Spearman correlation coefficients were calculated for trace element in atmospheric particulate matter over a coal production area; and observed strong correlation at 0.01 level (Petaloti *et al*., 2006). Spearman's rho was calculated for the major elements concentration in dry disposed fly ashes by the age and depth using SAS 9.2 (SAS Institute Inc. Cary, NC. USA). The output result is indicated in Tables 7.5 and 7.6 and graphically shown in Figures 7.23-7.25.

Table 7.5. Relationship of major element in different solubility medium with depth of dry disposed ash cores.

Spearman's correlation (Only correlations that are significantly different from 0 at the 0.01 level)											
Obs	Age	Solubility	Variable	Al	Si	K	Ca	Mg	Mn	Fe	Na
1	1	Carbonate	Depth	-	0.51846	0.57478	-	-	-	-	-
2	1	Exchangeable	Depth	-	-	0.66234	-	-	-	-	0.55195
3	1	Fe and Mn	Depth	-	-	-0.7132	-	-	-	-0.6002	-
4	8	Carbonate	Depth	-	-	-	-	0.71429	-	-	0.91209
5	8	Exchangeable	Depth	-	-	-	-	-	-	-	0.81319
6	8	Water soluble	Depth	-	-	-	-	-	-	-	0.74176
7	20	Carbonate	Depth	-	-	0.66154	-	-	-	-	-
8	20	Exchangeable	Depth	-	-	0.78462	-	-	-	-	-
9	20	Fe and Mn	Depth	-	-	0.66154	-	-	-	-	-
10	20	Residual	Depth	-0.7143	-	-	-	-	-	-	-
11	20	Water soluble	Depth	-	-	-	-	-	-0.8333	-	-
Probability (p-values)											
Obs	Age	Solubility	Variable	PAl	PSi	PK	PCa	PMg	PMn	PFe	PNa
1	1	Carbonate	Depth	-	0.0079	0.0027	-	-	-	-	-
2	1	Exchangeable	Depth	-	-	0.0011	-	-	-	-	0.0095
3	1	Fe and Mn	Depth	-	-	0.0002	-	-	-	0.0031	-
4	8	Carbonate	Depth	-	-	-	-	0.0061	-	-	<.0001
5	8	Exchangeable	Depth	-	-	-	-	-	-	-	0.0007
6	8	Water soluble	Depth	-	-	-	-	-	-	-	0.0037
7	20	Carbonate	Depth	-	-	0.01	-	-	-	-	-
8	20	Exchangeable	Depth	-	-	0.0009	-	-	-	-	-
9	20	Fe and Mn	Depth	-	-	0.01	-	-	-	-	-
10	20	Residual	Depth	0.0041	-	-	-	-	-	-	-
11	20	Water soluble	Depth	-	-	-	-	-	0.0053	-	-

**PAl= P-value associated with Spearman's rho correlation for aluminium.*

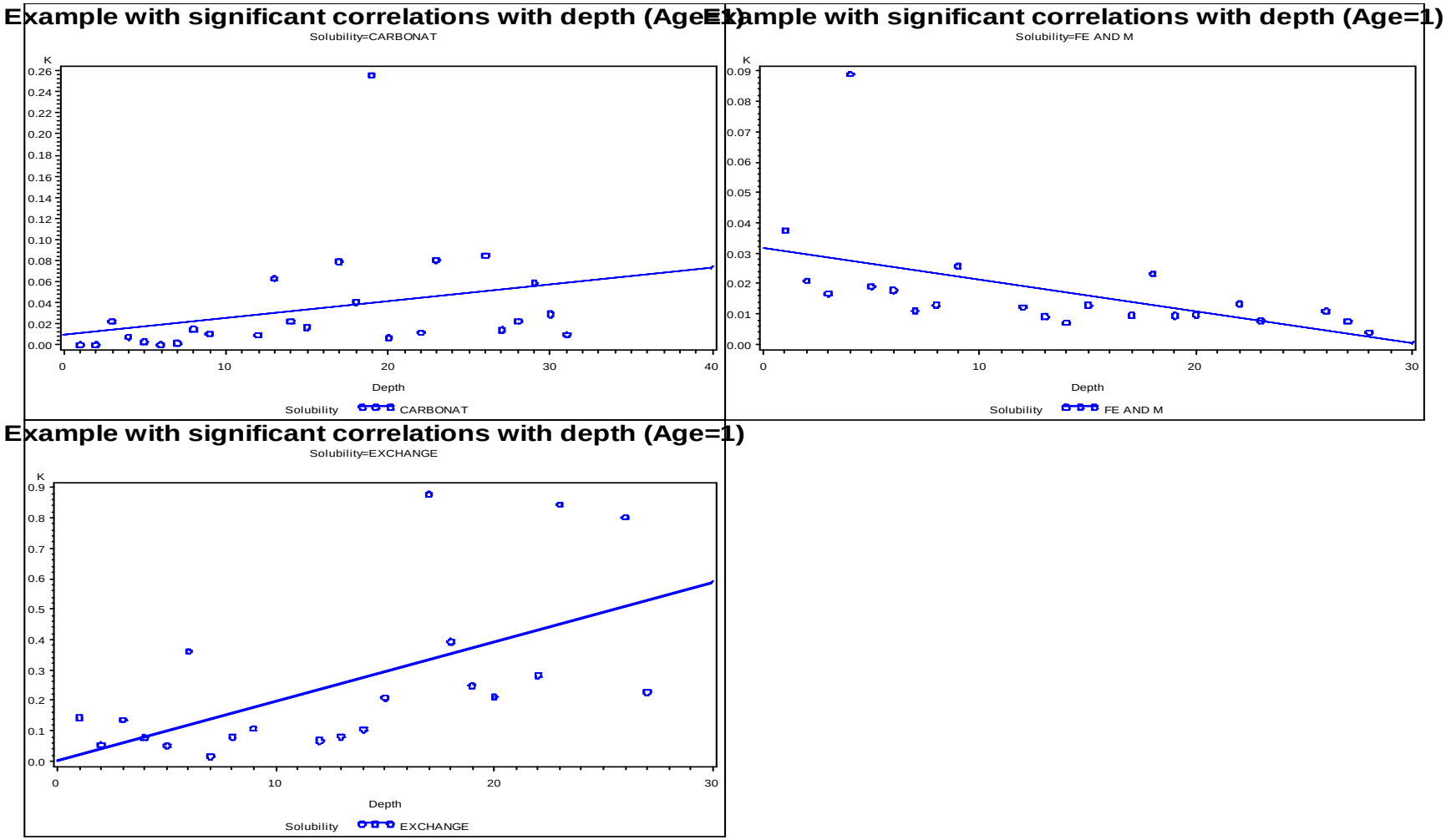

Foot note: *On the graph there is an outlier value, those values were check to determine if they were erroneous. But no acceptable explanation were found for the extreme values and consequently left them in the analysis.*

Figure 7.23. Relationship of K^+ in the exchangeable, carbonate and Fe and Mn fractions with depth of dry disposed fly ash.

Table 7.5 shows the Spearman's correlation coefficient (at 0.01 level significance) with the associated probability values of major elements such as Al, Si, K^+, Ca, Mg, Mn, Fe and Na^+ by depth of dry disposed fly ashes of different ages. Al concentration trend showed negative correlation coefficient (*rho = -0.7143 and p-value = 0.0041*) in the residual fraction of 20-year-old dry disposed fly ash. This suggests that chemical interaction of coal fly ash with ingress CO_2 at the near surface (unsaturated zone) eventually led to co-precipitation and adsorption into an insoluble mineral phase. Si concentration trend shows strong correlation coefficient (*rho = 0.51846 and p-value = 0.0079*) in the carbonate fraction of 1-year-old dry disposed ash cores. The concentration trend of Si suggests that rapid dissolution of aluminosilicate mineral occurred when fly ash chemically interacts with ingressed CO_2 and infiltrating rain water. The dissolved Si is transported into the deeper section of the ash dump by percolating rain water. The concentration trend of K^+ in the 1-year-old dry disposed fly ash, showed different correlation by depth in exchangeable, carbonate and Fe and Mn solubility (Fig. 7.23). Potassium shows strong positive correlation (*rho = 0.66234 and p-value =0.0011*) in the exchangeable fraction of 1-year-old dry disposed fly ash. Similar strong correlation pattern (*rho = 0.57478 and p-value =0.0027*) is recorded in the carbonate fraction of the 1-year-old dry disposed fly ash. An incongruent K^+ concentration trend is recorded in the Fe and Mn fraction of 1-year-old dry disposed fly ash.

Potassium shows negative correlation (*rho = -0.7132 and p-value = 0.0002*) in the Fe and Mn fraction of 1-year-old dry disposed ash cores. In the 20-year-old dry disposed ash cores, potassium show strong correlation (*rho =0.78462 and p-value = 0.0009*) in the exchangeable fraction. The concentration trend of K^+ in the carbonate fraction of 20-year-old dry disposed fly ash also shows a similar positive strong correlation (*rho = 0.66154 and p-value = 0.01*). In the Fe and Mn fraction of 20-year-old dry disposed ash cores, potassium concentration trend similarly show a positive correlation (*rho = 0.66154 and p-value = 0.01*). This suggests that chemical interaction of dry disposed fly ash with the ingress CO_2 and infiltrating rain water has led to eventual accumulation of K^+ at the deeper section of 20-year-old ash cores.

The concentration trend of Mg in the carbonate fraction of 8-year-old dry disposed ash cores showed positive strong correlation (*rho = 0.71429 and p-value = 0.0061*). This indicates leaching of dry disposed ash cores is due to weathering which has led to enrichment of Mg at the deeper section of 8-year-old ash cores. The concentration of Mn in the water soluble fraction of

20-year-old dry disposed ash cores showed negative correlation (*rho =-0.8333 and p-value = 0.0053*) with the depth of the ash dump. In the case of Fe in the Fe and Mn fraction of 1-year-old dry disposed ash cores, it's also showed a negative correlation (*rho = -0.6002 and p-value = 0.0031*) with the depth of ash dump. This may be due to overtime erosion or remobilisation of Mn in the water soluble fraction of 20-year-old ash cores and Fe in the Fe and Mn fraction of 1-year-old ash cores.

Table 7.6. Relationship of major element in different solubility medium with age of dry disposed ash cores

Cases with evidence of trend over time								
Obs	Solubility	Table	DF	Value	Prob	raw p	bon p	fdr p
1	Exchangeable	Summary for Age * Al	1	14.7425	0.0001	0.00012	0.00924	0.00103
2	Fe and Mn	Summary for Age * Al	1	5.6698	0.0173	0.01726	1.00000	0.03499
3	Water soluble	Summary for Age * Al	1	11.2845	0.0008	0.00078	0.05862	0.00451
4	Water soluble	Summary for Age * Ca	1	8.6657	0.0032	0.00324	0.24319	0.0124
5	Residual	Summary for Age * Fe	1	14.2373	0.0002	0.00016	0.01209	0.0011
6	Water soluble	Summary for Age * Fe	1	10.5891	0.0011	0.00114	0.08532	0.00533
7	Exchangeable	Summary for Age * K	1	5.7315	0.0167	0.01666	1.00000	0.03472
8	Residual	Summary for Age * K	1	8.5016	0.0035	0.00355	0.26612	0.0124
9	Water soluble	Summary for Age * K	1	8.5735	0.0034	0.00341	0.25582	0.0124
10	Carbonate	Summary for Age * Mg	1	7.0578	0.0079	0.00789	0.59192	0.02192
11	Exchangeable	Summary for Age * Mg	1	6.0905	0.0136	0.01359	1.00000	0.02998
12	Carbonate	Summary for Age * Mn	1	16.8383	<.0001	4.1E-05	0.00305	0.00073
13	Exchangeable	Summary for Age * Mn	1	6.8626	0.0088	0.0088	0.66014	0.02276
14	Fe and Mn	Summary for Age * Mn	1	15.8373	<.0001	4.1E-05	0.00305	0.00073
15	Residual	Summary for Age * Mn	1	15.334	<.0001	0.00009	0.00676	0.00088
16	Water soluble	Summary for Age * Mn	1	10.9751	0.0009	0.00092	0.06926	0.00495
17	Carbonate	Summary for Age * Na	1	10.654	0.0011	0.0011	0.08237	0.00533
18	Exchangeable	Summary for Age * Na	1	6.2114	0.0127	0.01269	0.95198	0.02888
19	Water soluble	Summary for Age * Na	1	5.7341	0.0166	0.01664	1.00000	0.03472
20	Exchangeable	Summary for Age * Si	1	6.2096	0.0127	0.01271	0.95297	0.02888
21	Fe and Mn	Summary for Age * Si	1	15.2587	<.0001	9.4E-05	0.00703	0.00088
22	Residual	Summary for Age * Si	1	6.8626	0.0088	0.0088	0.66013	0.02276
23	Carbonate	Summary for Age * Ti	1	14.3173	0.0002	0.00015	0.01158	0.0011
24	Exchangeable	Summary for Age * Ti	1	7.5741	0.0059	0.00592	0.44411	0.01776
25	Fe and Mn	Summary for Age * Ti	1	10.2762	0.0013	0.00135	0.10107	0.00595

raw p= actual probability; bon p= bonfreri probability; fdr p= false discovery rate probability.

Na^+ concentration trend in the exchangeable fraction of 1-year-old dry disposed ash cores, showed positive strong correlation (*rho =0.55195 and p-value =0.0095*) with the depth of ash dump indicating mobility. In the 8-year-old dry disposed ash cores, its showed positive correlation (*rho =0.81319 and p-value = 0.0007*) in the exchangeable fraction. Similar concentration trend of Na^+ is recorded in the carbonate fraction of 8-year-old dry disposed ash

cores. Na^+ showed positive strong correlation (*rho = 0.91209 and p-value = <.0001*) in the carbonate fraction of 8-year-old ash cores. In the water soluble fraction of 8-year-old ash cores, the concentration trend showed a positive correlation (*rho = 0.74176 and p-value = 0.0037*) with the depth of the ash dump. This is an indication of Na^+ mobility through dissolution and over time leaching of soluble salts in dry disposed fly ashes due to chemical interaction of fly ash with ingressed CO_2 and percolating rain water. Sodium was subsequently transport by the percolating rain water to the deeper section of the ash dumps. This implied that dry disposed ash cores is not holding soluble salts, these soluble salts are dissolved and leach out overtime due to weathering/ageing. Table 7.6 shows evidence of major elements (such as Al, Ca, Fe, K^+, Mg, Mn, Na^+, Si and Ti) concentration trend with time. The nicest result is for Mn (*rawp=0.00092 and fdrp =0.0045*) in the water soluble fraction of coal fly ash of different ages.

In the Figure 7.24, manganese shows increasing concentration trend with decreasing age in the water soluble of dry disposed coal fly ash. Whereas the concentration of Mn in the exchangeable, carbonate, Fe and Mn, and residual fractions show increasing concentration of Mn with increasing age of the dry disposed ash cores (Figure 7.25).

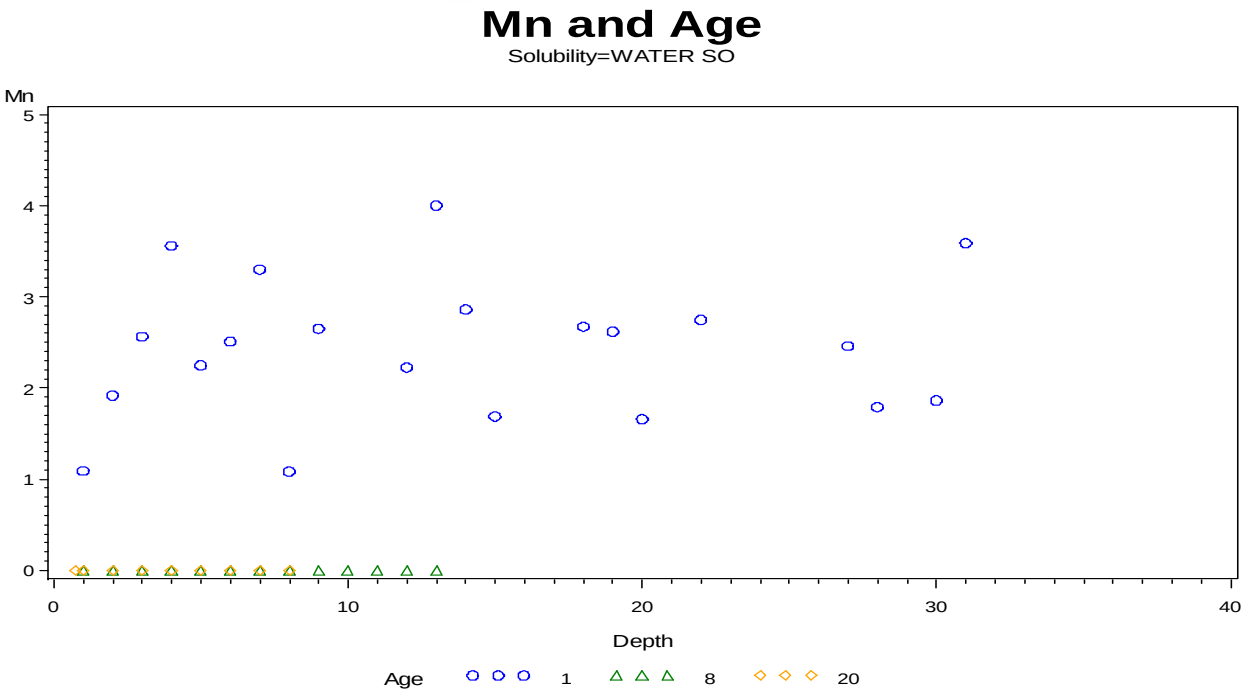

Figure 7.24. Relationship of Mn in water soluble fraction with the age of dry disposed ash cores.

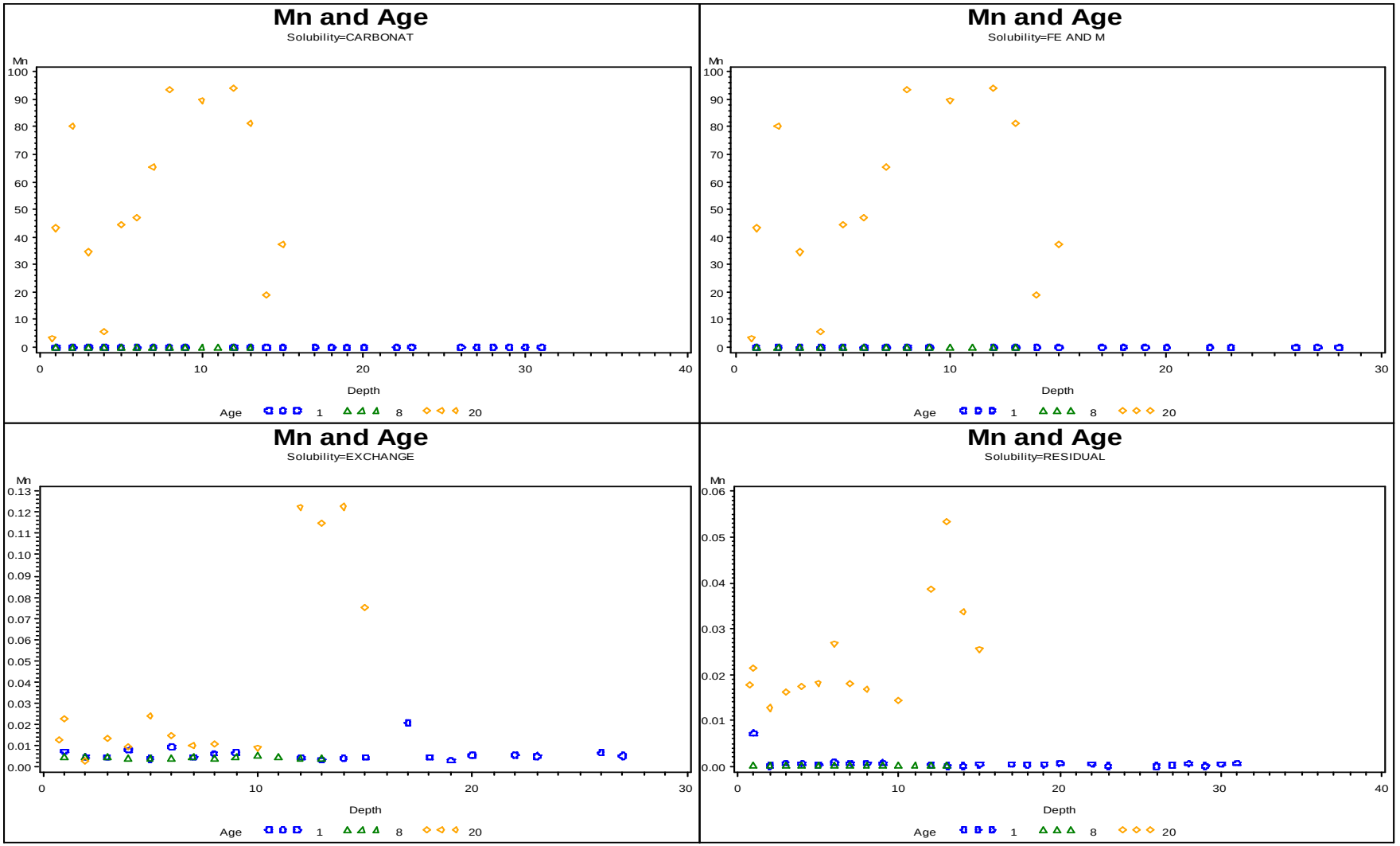

Figure 7.25. Relationship of Mn in the exchangeable, carbonate, Fe and Mn and residual fractions with the age of dry disposed ash cores.

The important features of this section are increase or decrease response of major elements by depth is an indication of the mobility of such metals in the dry disposed ash cores. The decrease response of Mn with age in the water soluble fraction indicates overtime leaching. This has led to the lower concentration of Mn in the water soluble fraction of older ash cores. The increase response of Mn with age in the other four fractions indicates dissolution of host mineral phase due to overtime weathering/ageing. The mobility of metals in the dry disposed fly ash cores is controlled by the following mechanisms; advection forces, precipitation and dissolution, and adsorption and desorption due to pore water pH variations.

7.6 Summary and conclusions

The following conclusions could be drawn from the results of the concentration profile of the investigated chemical species (Al, Si, Fe, Mn, Ca, Mg, Na^+, and K^+) using sequential extraction scheme on the ash dumps of different ages:

1. Major elements Al, Si, Fe, Mn, Ca, Mg, Na^+, and K^+ are present in Tutuka ash and partition between the water soluble, exchangeable, carbonate, iron and manganese, and residual fractions of the coal fly ash at different stages of weathering.

2. The trends of the chemical species at different stage of weathering of dry disposed ash in landfill showed high extractable percentages of Al, Si, Ca, Mg, Fe, Na^+, and K^+ in the exchangeable and carbonate fractions of the 1-year-old ash cores.

3. The average amount of the major elements in the five-fractions of 1-year-old ash core samples follows the trend: water soluble: Na^+ (21%) > Ca (10.2%) > Mn (8.4%) > Si (4.0%) > K^+ (2.58%) > Mg (0.05%) > Al (0.003%) > Fe (0.001%), exchangeable: Ca (37.04%) > Mg (12.6%) > Na^+ (11.26%) > Mn (10.3%) > K^+ (3.17%) > Si (1.6%) > Al (0.27%) > Fe (0.33%), carbonate: Mn (41.21%) > Ca (37.9%) > Mg (32.9%) > Al (29.25%) > Si (25.39%) > Fe (21.39%) > Na^+ (2.6%) > K^+ (2.23%), iron and manganese: Si (49.74%) > Al (49.61%) > Fe (44.27%) > Mn (33.76%) > Mg (17.58) > Ca (7.%) > Na^+ (4.7%) > K^+ (2.08%), and residual fraction: K^+ (81.76%) > Na^+ (53.9) > Mg (30.23%) > Fe (26.89%) > Si (19%) > Al (10.6%) > Mn (7.6%) > Ca (2.97%).

It is noteworthy that the soluble fractions (water soluble, exchangeable and carbonate) of the major elements in Tutuka ash were high and this has implications for the long-term durability of

mineral phases thus drawing into question the sustainability of the ash dump and highlighting its potential for negatively impacting the environment over time.

4. Statistical evaluation (CODs) shows that the extractability of the major elements from the five fractions of the fly ashes proved to be different, so various distribution patterns and partitioning of the major elements between different fractions over time have been observed. The recovery percentage for all the major elements in the ash samples varied between 92.01 % (Al) and 99.47 % (Na) indicating the accuracy of the sequential extraction technique.

5. The results of the sequential extractions showed (i) the chemical interaction of fly ash with ingressed CO_2 ingressed O_2, and percolating rain water at the top sections. (ii) the influence of the top soil leachate upon under laying layers of ash due to ingress of rain water (iii) the intersection of core ash with the ground water level leading to dissolution of hydrated mineral phases and ultimate diffusion of metals into the ground water system. (iii) the precipitation and dissolution of secondary hydrated mineral (compounds). (iv) in-homogeneity in the ash cores (vi) moisture content levels of ash. (v) pore water pH.

All these above highlighted factors could contribute to the extraction of the elements in the sequential fractionation of core ash samples taken from dry disposed ash in landfill at different stages of weathering. Nonetheless, relatively quick and longer term leaching as well as transformation of mineral phases and the association of specific metals with different phases at different stages of weathering were observed to occur within the depths of the Tutuka ash dump.

6. There is variability (within 10 %) between sum of values obtained for five-fractions of Al, Si, Ca, Mg, Fe, Mn, Na^+ and K^+ and total metal content in the original fly ash sample at 1 m depth of 1-year-old ash. This level of variability suggests that there is little or no sample loss, and that the mass balance calculations for the extraction scheme are good and within acceptable limits. The above 10 % variability for Al, Si, and Na^+ in the 3 m depth of 1-year-old ash cores is due to spill out of leachant at some stage in sample preparation procedure in the laboratory.

7. In this statistical evaluation study, a comprehensive Spearman's correlation coefficient was adopted for determination of environmental implications of both major and trace elements in dry ash disposal system. The important features of this section are as follows:

i. Manganese concentration in the water soluble fraction decrease with age of the dry disposed fly ash. On the other hand, its concentration in the exchangeable, carbonate, Fe and Mn and residual fractions increase with the age of dry disposed fly ash.

(ii). The increasing responses of major elements in the water soluble, exchangeable and carbonate fractions with the depth is due to leaching of major soluble components of the fly ash and suggests influence of pore water pH on the metal mobility.

(iii) The obvious decreasing responses of some major elements in the iron and manganese and residual fractions suggest immobilisation of such metals due to weathering/ ageing process. The positive correlation of Na^+ and K^+ in the easily mobilized fraction of dry disposed fly ashes suggests that the soluble salts are dissolved and subsequently transported by infiltrating rain water. This implies that the dry disposed fly ashes are not holding salt (i. e. not a salt sinks).

8. A modified chemical sequential extraction scheme was not applied on multiple ash cores due to high cost sample analysis.

CHAPTER EIGHT

Results and Discussion 4

Chemical partitioning and mobility of As, Se, B, Cr, Mo and Pb in weathered drilled ash cores aged 1 year, 8 year and 20 year

This chapter presents the results obtained from sequential extraction scheme originally developed by Tessier and others; modified and applied on dry disposed ashes at different stage of weathering/ageing. The effects of chemical alteration and mineralogical transformations on the chemical partitioning, solubility and mobility of trace elements in a dry disposed ash are revealed and discussed.

8. Introduction

The greatest quantities of industrial ashes are stored in the form of waste-heaps, which create a serious and acute environmental problem (Kalembkiewicz *et al*., 2008). The knowledge of mobility and ecotoxicological significance of coal fly ash is needed when considering its disposal or reuse in natural environmental settings. The mobility and ecotoxicology of coal fly ash are determined by (i) the physicochemical conditions under which the fly ash is stored (ii) the total leachable metal content in fly ash (iii) the distribution and mineralogical fractionation of metals (Jegadesaan *et al*., 2008). Most often, the mineralogical distribution of metals in the fly ash appears to play a major role in metal leachability and mobility. The mobilisation of trace metals in coal fly ash when in contact with infiltrating rain water, ingressed O_2 and CO_2 over time should be of environmental concerns. Chemical interactions of coal fly ash with infiltrating rain water, ingressed O_2 and CO_2 lead to chemical alteration, enrichment of toxic elements and create potential to contaminate both groundwater and surface water in the environment. Therefore fly ash should be disposed safely to prevent pollution to the environment (Van den Berg *et al*., 2001; Theis *et al*., 1977). The dissolution of nontoxic and toxic trace elements locked in different physicochemical forms in coal fly ashes is envisaged when coal fly ash is weathered. Species in soluble form will first leach out in water or weak acids (Green and Manahan, 1977) but the long term leaching of toxic trace elements is associated with slow mobility of elements from glass, magnetite and related minerals (Hulett and Weinberger, 1980). Moreover the dangers linked to the utilization of coal fly ash in the natural environmental setting with regards to the

mobility and leachability of environmentally harmful species is mainly determined by the physicochemical conditions of the fly ash dump; the sum of leachable metal content in fly ash; and the distribution or mineralogical fractionation of metals (Jegadeesan *et al*., 2008).

Sequential extraction can provide a good insight into the metal leaching behaviour through determination of metal fractionation in the solid matrix in coal fly ash. Studies on the sequential extraction scheme are modifications stemming from a procedure originally developed by Tessier *et al*. (1979). The schemes were initially developed for the examination of aquatic sediments (Tessier *et al*., 1979, Petit *et al*., 1999, Mester *et al*., 1998) but gained wide acceptance as tools for speciation of metals in contaminated soils (Campos *et al*., 1998). Recently the sequential extraction scheme has been applied to incinerated sludge ash (Wang et al., 2004), bottom ash and fly ash from municipal solid waste incinerators (MSWI) to determine the distribution of elements (Bruder-Hubscher *et al*., 2002; Smeda and Zyrnicki, 2002; Smichowski *et al*., 2008). The chemical interactions of coal fly ash with environmental factors such as ingressed O_2, ingressed CO_2 and percolating rain water can often lead to dissolution of primary mineral phases and precipitation of secondary mineral phases. These physicochemical conditions might have significant effect on the mobility and release mechanism of toxic metals in coal fly ash in natural environmental settings. They might often lead to mineralogical transformation and heavy metal fixation. The determination of As, B, Cr, Pb, Mo and Se speciation in weathered fly ash is important for conducting risk assessments of the leaching from coal fly ash dumps and storage piles.

The management of this combustion waste is of major concern because of the huge amount that is produced annually and the environmental issues arising from its disposal. Therefore, strategies to safely deal with this solid waste are necessary. In the management of this combustion by-product the focus should not only be on the prevention of environmental pollution, but also on methods that can be used to produce or manufacture value-added products from stored fly ash. The chemical composition, mineralogy and phase transformation studies are vital in predicting the environmental impact associated with fly ash disposal techniques and uses. In this study, the examination of the mineral phases present and the chemical mobility patterns in the coal fly ash irrigated with water or brine at the ash dam was conducted. The samples were collected from the dry disposed fly ash of different ages and a range of depths in order to evaluate the leaching

patterns by depth. Specifically, this study evaluated the partitioning pattern of trace elements (As, B, Cr, Pb, Mo and Se) in the various physico-chemical phases by depth in the ash dump. This information was then utilized to:

(i) elucidate the mobility patterns by depth and comparing the patterns in various sections of dry disposed fly ash of different ages.
(ii) to establish relationships between metal partitioning between the cores of different ages.
(iii) to reveal various mechanisms that control the mobility of the species by depth..

8.1 Total content of trace elements in weathered drilled core ash samples

The total acid digestion is used to determine the total metal concentration of trace metals in dry disposed fly ashes. The experimental protocol for this section is reported in section 4.2.6. The results of total acid digestion of core ash samples from 1 year, 8 year, and 20-year-old dry disposed in landfill are presented in Table 8.1.

The results in general show analogous trends with the result of each leaching step in the sequential extraction scheme discussed in the section 8.2. Trace elements like As, Se, Mo, Pb and Cr trend shows slight concentration difference in the top, middle and bottom sections of dry disposed fly ashes due to weathering/ageing. Boron revealed momentous concentration difference in the top, middle and bottom sections of dry disposed fly ashes. The concentration difference seems to be influenced by pore water pH and assisted by the ash type, ash texture, ash moisture content levels and point of contact with ground water (at 9 m for 20-year-old ash cores). A relatively high concentration of trace metals is recorded in the bottom sections of 8-year-old fly ash cores characterized by brittle and unconsolidated fly ash compared with hard fractured ash, indicating that relatively loose fly ash easily release metals. Whilst in the case of 20-year-ash cores, the relatively high concentration of the considered analytes is recorded in both top and middle section characterized by solid ash compared with moist ash, indicating that ash moisture content levels play a major role in the metal mobility in fly ash. Relatively high concentrations of the trace elements are recorded in the middle and bottom sections of 1-year-old ash cores characterized by fine ash. This suggests that surface area play a noticeable role in the release of these metals from fly ash. A relatively high concentration of metals in the top section of 20-year-old ash cores is influenced by the leachate from top soil.

Table 8.1. Trace elements distribution in a total acid digested weathered drilled ash cores (n=3)

1-year-old ash cores								
Depth	**Depth Reference**	**Lithology**	**As (mg/kg)**	**Se (mg/kg)**	**Mo (mg/kg)**	**B (mg/kg)**	**Pb (mg/kg)**	**Cr (mg/kg)**
1m	Top section	Coarse ash	0.0156±0.0001	0.0046±3.3E-05	0.0083±0.0001	0.034±0.0003	0.0158±0.0002	0.1209±0.0001
2m			0.0143±0.0001	0.0109±0.001	0.0112±0.00	0.0059±0.0002	0.006±0.0001	0.283±0.0015
3m			0.010584±0.0018	0.0045±0.0002	0.0046±0.0013	0.032±0.00034	0.00401±0.00013	0.0462±0.0031
4m		Fine ash	0.012±0.0003	0.007±0.0001	0.005±0.0001	0.03±10.005	0.0025±0.0001	0.18±0.003
5m			0.6252±0.00013	0.0058±0.0002	0.0085±0.0013	3.91±0.03	0.01423±0.0003	0.069±0.004
6m	Middle section		0.02±0.0002	0.012±0.0003	0.0038±0.004	0.31±0.03	0.097±0.0001	0.029±0.001
7m			0.0194±0.0108	0.0049±0.00	0.0130±0.0012	4.001±0.0023	0.02201±0.00015	0.1322±0.0031
8m			0.0148±0.0001	0.009±0.0001	0.0089±0.0001	1.102±0.0.2	0.01±0.0001	0.03±0.0001
9m			1.632±0.0002	0.0043±0.0001	0.5431±0.0001	3.39±0.012	0.01811±0.0061	0.10311±0.023
12m		Coarse ash	0.0146±0.0001	0.00561±0.008	0.0039±0.0013	2.65±0.0003	0.0142±0.00132	0.0904±0.0012
13m			0.011±0.0001	0.012±0.0001	0.0072±0.0001	0.21±0.0003	0.053±0.0001	0.211±0.0001
14m			0.01±0.0001	0.0089±0.00	0.0059±0.0002	0.62±0.0001	0.041±0.0002	0.06±0.0001
15m			0.0170±0.0011	0.0042±0.002	0.0081±0.008	4.74±0.001	0.0192±0.0016	0.1019±0.0091
17m			0.0142±0.0001	0.012±0.0001	0.0084±0.0003	0.56±0.003	0.063±0.00002	0.234±0.0001
18m			0.0156±0.0081	0.0045±0.0012	0.0071±0.0012	2.680.001	0.01567±0.0012	0.1034±0.0034
19m		Fine ash	0.011±0.0003	0.01±0.0001	0.0061±0.0001	0.14±0.0001	0.057±0.0002	0.175±0.00
20m			0.0089±0.0001	0.0074±0.00001	0.0044±0.0001	0.23±0.002	0.046±0.0003	0.149±0.0001
22m	Bottom section		0.01822±0.0012	0.0061±0.0013	0.0067±0.0016	2.94±0.012	0.01923±0.0023	0.0890±0.0091
23m			0.011±0.0001	0.0087±0.0001	0.01±0.0001	0.0087±0.0001	0.0599±0.0001	0.21±0.0001
27m			0.0173±0.0012	0.0045±0.0012	0.00693±0.0034	2.52±0.0023	0.0173±0.0013	0.075±0.0123
28m			0.011±0.0001	0.011±0.0001	0.0092±0.0001	0.038±0.002	0.0552±0.00	0.203±0.0001
29m			0.0363±0.0001	0.037±0.0001	0.013±0.0001	0.48±0.002	0.195±0.003	0.679±0.0001
30m			0.0104±0.0001	0.011±0.0001	0.0076±0.0001	0.41±10.23	0.054±0.0001	0.252±0.0001
31m			0.013±0.0001	0.057±0.0001	0.0045±0.0003	0.44±0.002	0.065±0.0001	0.22±0.002
Mean			0.108±0.001	0.011±0.001	0.0298±0.001	1.31±0.06	0.0402±0.001	0.160±0.001
8-year-old ash cores								
Sample ID	**Depth Reference**	**Lithology**	**As (mg/kg)**	**Se (mg/kg)**	**Mo (mg/kg)**	**B (mg/kg)**	**Pb (mg/kg)**	**Cr (mg/kg)**
1m	Top section	Fracture, hard ash	0.0039±0.0001	0.0014±0.007	0.049±0.0002	0.29±0.004	0.229±0.004	0.049±0.002
2m			0.0044±0.0003	0.0016±0.0005	0.055±0.0003	0.51±0.002	0.141±0.002	0.11±0.006
3m			0.0043±0.0003	0.036±0.0003	0.056±0.002	0.46±0.003	0.126±0.001	0.098±0.002
4m	Middle section		0.0048±0.0003	0.014±0.0001	0.058±0.0004	0.45±0.004	0.46±0.002	0.092±0.0002
5m			0.0046±0.0005	0.0015±0.0003	0.064±0.0002	0.52±0.003	0.151±0.001	0.091±0.0001
6m			0.0044±0.0001	0.0015±0.0002	0.053±0.003	0.49±0.003	0.51±0.001	0.091±0.0001
7m			0.0056±0.0006	0.0016±0.0002	0.053±0.0002	0.56±0.002	0.154±0.002	0.090±0.002
8m			0.0047±0.0002	0.0013±0.0001	0.036±0.0003	0.33±0.002	0.35±0.001	0.071±0.0003
9m	Bottom section		0.0043±0.0005	0.0063±0.002	0.069±0.0012	0.57±0.003	0.137±0.001	0.097±0.0003
10m		Brittle ash	0.0046±0.0004	0.0038±0.0002	0.081±0.003	0.76±0.005	0.82±0.004	0.11±0.002
11m			0.0047±0.0003	0.0021±0.0002	0.072±0.0003	0.67±0.004	0.151±0.004	0.12±0.0003
12m		Unconsolidated ash	0.004±0.0004	0.01±0.0004	0.07±0.001	0.58±0.002	0.12±0.002	0.096±0.0004
13m			0.0036±0.0002	0.0021±0.0002	0.089±0.0002	0.59±0.003	0.171±0.002	0.12±0.0012
Mean			0.004±0.0003	31.91±0.0009	0.062±0.0009	0.52±0.003	0.1557±0.002	0.095±0.0013
20-year-old ash cores								
Sample ID	**Depth Reference**	**Lithology**	**As (mg/kg)**	**Se (mg/kg)**	**Mo (mg/kg)**	**B (mg/kg)**	**Pb (mg/kg)**	**Cr (mg/kg)**
0.75m	Top section	Top soil	0.0089±0.0001	0.0055±0.001	0.0011±0.0003	0.025±0.001	0.068±0.003	0.11±0.003
1m		Solid ash	0.0184±0.0003	0.032±0.004	0.0027±0.0001	0.023±0.002	0.041±0.003	0.104±0.002
2m			0.0112±0.0005	0.0173±0.002	0.0018±0.001	0.059±0.002	0.033±0.002	0.079±0.0008
3m			0.011±0.0005	0.0319±0.005	0.0055±0.0007	0.097±12.34	0.05±0.003	0.117±0.005
4m	Middle section		0.017±0.0001	0.0087±0.001	0.0045±0.0004	0.029±11.23	0.06±0.001	0.105±0.0004
5m			0.019±0.0003	0.029±0.004	0.0027±0.0003	0.058±10.23	0.045±0.004	0.108±0.0003
6m			0.036±0.0004	0.0384±0.003	0.00824±0.0003	0.089±0.002	0.071±0.005	0.16±0.0001
7m			0.019±0.001	0.0046±0.0003	0.0038±0.0003	0.099±0.005	0.054±0.001	0.094±0.002
8m			0.014±0.002	0.0123±0.005	0.0046±0.0006	0.13±0.003	0.0272±0.004	0.072±0.003
9m	Bottom section	Moist ash	0.018±0.001	0.0047±0.0001	0.0043±0.0007	0.048±23.12	0.064±0.001	0.11±0.004
10m			0.015±0.0003	0.0097±0.001	0.0073±0.0003	0.025±0.0012	0.063±0.006	0.144±0.0003
12m		Dolerite+Clay	0.0046±0.001	0.0097±0.0002	0.0058±0.0002	0.025±0.005	0.01±0.002	0.17±0.0001
14m			0.0057±0.003	0.0046±0.0004	0.0061±0.0001	0.049±0.002	0.014±0.003	0.195±0.0005
15m			0.013±0.0002	0.0014±0.0001	0.0028±0.0005	0.097±0.001	0.061±0.003	0.1142±0.002
Mean			0.015±0.0008	0.015±0.0019	0.004±0.0004	0.061±0.006	0.047±0.0029	0.120±0.0016

In comparison with mean of the 1 year, 8 year and 20-year-old ash cores, there is enrichment of As, B and Cr in the 1-year-old ash cores. The Pb, Mo and Se showed enrichment in the 8-year-old ash cores suggests possible co-precipitation with secondary mineral phases. The obvious relative depletion of As, B and Cr in the older fly ashes suggests overtime leaching of major component in fly ash has impact of the trace metal levels. In contrast, the low concentration could be due to slower release ensuing from association with formed secondary mineral phase.

8.2 Chemical sequential extraction scheme results for trace toxic elements

8.2.1 Analysis of water soluble fraction

A modified sequential extraction scheme was used to determine trace toxic species partitioning in the dry disposed ashes. The experimental protocols for these results are presented in section 4.2.5. The distributions of trace elements such as As, Se, Pb, Mo, B and Cr in different leachates from the dry disposed fly ashes aged 1-year-old (0-31 meters deep), the 8-year-old (0-13 meters deep) and the 20-year-old (0.75-15 meters deep) are discussed. Figures 8.1-8.15 show each species concentration as a function of the ash core depth profile. The discussions for the variations of trace elements along the depth profile are discussed in pairs viz: As and Se, Mo and Cr, lastly B and Pb. The cumulative concentrations for each trace metal at different depths were compared with the value obtained from total acid digestion and statistically discussed.

8.2.1.1 Arsenic and selenium

Arsenic is the most poisonous trace metal that should be avoided in potable waters. Ingesting drinking water that is naturally enriched with As is the most common route of exposure to arsenic which causes skin cancer in humans. The Environmental Protection Agency specified a maximum limit of 10 ppb for As but following recent discovery of chronic effects from low exposure in Bangladesh in 2006, a new limit of 5 ppb was proposed (http://www.sos-arsenic.net/english/contamin/1.html). From Table 8.2, the total As concentration from total acid digestion showed 15.6 ppb at 1 m and 10.6 ppb at 3 m. Figure 8.1 show the concentration profile of As in the water soluble fraction of fly ash of different ages. The concentration of As in the 1-year-old ash cores ranged from 0.0002-0.0008 mg kg^{-1} (Figure 8.1). The highest concentration of As is recorded in the 1-year-old ash cores suggesting that the As has considerably leached out in the older ashes. A comparatively low concentration of As at top and bottom sections of 1-year-old ash cores suggests that it has been leached out.

Relatively high concentrations in the top sections of 8 year and 20-year-old as cores are influenced by mass transfer of leachate from top soil. A relatively high concentration of As is recorded in the middle sections of 1 year, 8 year and 20-year-old ash cores. The bottom sections of 1 year, 8 year and 20-year-old ash cores showed relatively low concentration of As in the water soluble fraction. The concentration difference of As in the 1 year, 8 year and 20-year-old ash cores is noticeable suggesting mobility this is possibly influenced by pore water pH. Acid neutralisation results showed that the release of arsenic in the dry disposed fly ash is dependent on the solution pH (see Figure 6.6a). However, As shows inconsistent patterns in the water soluble fraction by the depth of the ash dumps due to the above highlighted controlling factors.

Previous studies have shown that the concentration of As in solution can be reduced by the precipitation of calcium ortho arsenate ($Ca_3(AsO_4)_2$) at alkaline pH when considerable amounts of Ca is present in the solution (Zielinski *et al*., 2007; Wang *et al*., 2007). It has also been reported that the leaching and desorbing of As in fly ash is controlled by pH values of ash pore water (Wang *et al*., 2008). Previous studies had revealed that the formation of calcite in fly ash at high pH reduce the concentrations of As and Se by substituting the SO_4 radical with the oxyanion form of As and Se (Jankowski *et al*., 2006; Van der Hoek *et al*., 1994). It should be noted that the most abundant As containing component in the ash core was the exchangeable fraction followed by the carbonate fraction (see Figure 8.3 and 8.6). Also see the discussion for each fraction per element below.

The Se is less toxic than As. Although Se is an essential trace element needed by plants and animal, it is toxic if taken in excess and could lead to seleniosis. Water runoff from ash dumps leaches soluble Se compounds (such as selenates) into the groundwater. Figure 8.1 also shows the concentration profile of Se in the water soluble fraction of the fly ashes. The concentration of Se in the 1-year-old ash cores ranged from 0.0003-0.00075 mg kg^{-1}. The highest concentration of Se is recorded in the 1-year-old ash cores. This indicates that overtime leaching of major soluble component of fly ash has led to significant reduction in the Se concentration in the older ashes. A relatively low concentration of Se is recorded at the top and bottom sections of 1 year, 8 year and 20-year-old ash cores suggesting it have been leached out over an extended period.

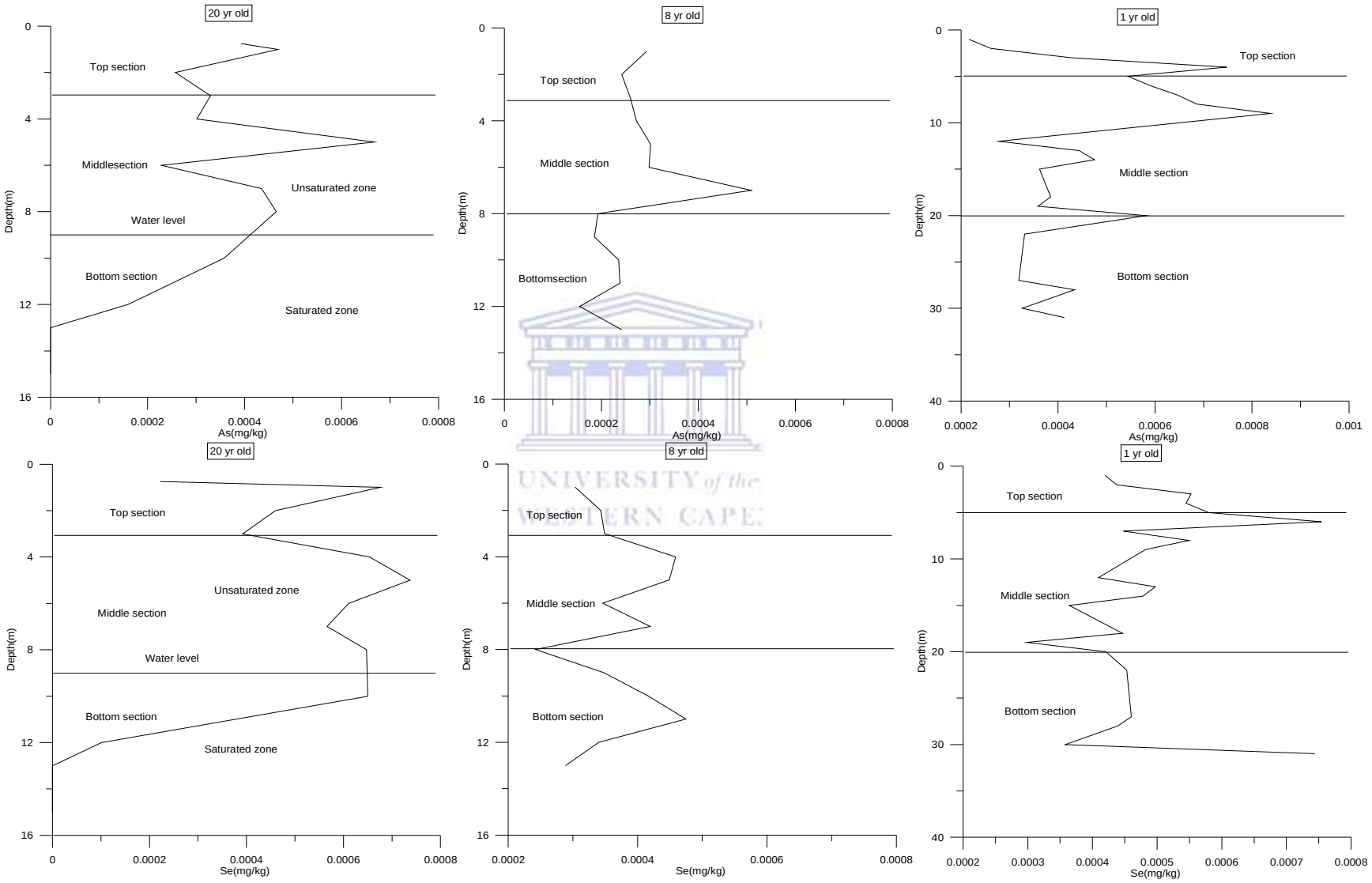

Figure 8.1. Arsenic and selenium trend in water soluble fraction of drilled cores of different ages and depths (n=3).

This obvious leaching of Se at the top sections is caused by the interaction of fly ash with ingressed O_2, ingressed CO_2 from atmosphere and percolating rain water (see Section 2.4.6). Leaching of Se is expected to decrease overtime due to the neutralisation of the ash pH, and the formation of less soluble species of these elements as weathering continues. On the contrary, the middle sections of 1 year and 20-year-old ash cores showed a comparatively high concentration. A significant concentration difference in the top, middle and bottom sections of 1 year and 20-year-old ash cores suggest that Se is mobile; is influenced by pore water pH, ash type, ash texture, ash moisture content levels and point of saturation.

It has been reported that the leaching of Se tended to increase as the pH in the aqueous phase was raised (Iwashita, 2005). Hence it is expected that Se will continuously leach until the pore water pH of the dump is neutral. It should be noted that the most abundant Se containing fraction in the ash was the exchangeable fraction, followed by the carbonate fraction (see Figures 8.3 and 8.5). Also see the discussion for each fraction per element below. Lower concentrations of As are recorded in the 1 year and 8-year-old ash cores compared with Se which is suggesting slower release of As due to its possible association with major soluble component (see Figure 8.1).

Acid neutralisation capacity results show that both As and Se release are dependent on the solution pH (see Figure 6.6a). It has been reported that As and Se showed a decline in concentrations with increasing pH (Grisafe *et al*., 1988). It had been reported that the lower concentration of As observed is due to its slower leaching rate than for Se due to the possibility of reversible sorption processes of As onto different mineral phases (Van der Hoek and Comans, 1999). Previous studies revealed that increasing pH favours As sorption whereas arsenite desorbs and becomes mobilized at very low oxidation states as it reacts with dissolved sulphide to form AsS complexes (Lee and Saunders, 2003). It had also been shown that arsenite is sorbed much less reversibly than selenites on the different mineral matrix of fly ash especially iron oxides (Van der Hoek *et al*., 1994).

8.2.1.2 Molybdenum and chromium

Figure 8.2 shows the Mo concentration in the water extractable fraction of fly ashes. The highest concentration of Mo in the water soluble fraction is recorded in 1-year-old fly ash. Relatively low concentration of Mo is observed in the top section and bottom section of 20-year-old ash cores suggesting that it have been leached out and dissolved into groundwater system

respectively. In contrast, the middle and end of bottom sections of 8 year and 1-year-old ash cores show moderately high concentration. Conversely, a comparatively low concentration of Mo is recorded in the top sections of 8-year-old ash cores. Mo concentration difference in the top and middle sections of dry disposed ash cores is not noticeable which suggest that Mo mobility is influenced by association with insoluble mineral phase caused by due to weathering/ageing. It has been reported that Mo release can be controlled by Fe and Al in solution, which reduces Mo mobility substantially at acidic condition as metal molybdates (Comans *et al*., 2000; Kukier *et al*., 2003). It should be noted that Mo is most abundant in the water soluble fraction followed by the exchangeable fraction of dry disposed ashes. It has also been reported that Mo is highly soluble and mobile under alkaline conditions and can precipitate as MoO_3 under alkaline conditions (Van der Hoek and Comans, 1999).

The concentration trend of Cr in the water soluble fraction of dry disposed fly ashes is shown in Figure 8.2. The highest concentration of Cr is recorded in the 1-year-old ash cores. A rather low concentration of Cr is recorded in the middle sections of 1 year, 8 year and 20-year-old ash cores, fairly low concentration are also recorded in the top sections. Relatively high concentration of Cr is recorded towards the end of bottom sections of 8 year and 1-year-old ash cores. The the bottom section of 20-year-old ash cores showed comparatively low concentration due to contact of ash with ground water system.

Major concentration difference of Cr in the top, middle and bottom sections of dry disposed fly ashes suggests that its release is influenced by pore water pH. Acid neutralisation capacity results showed that chromium release in unsaturated weathered ash is dependent in solution pH (see Figure 6.6b). Other likely factors controlling the vertical distribution of Cr are ash type, ash texture, moisture content levels and point of contact with groundwater system. Cr association with different fractions was highly variable (see Figures 8.2 and 8.5). Cr (VI) compounds are known to be toxic and carcinogenic (Loyaux-Lawniczak *et al*., 200), rather soluble, and produce aqueous oxyanions which can move easily through the aquifer. It has been established that both Cr (III) and Cr (VI) (Narukawa *et al*., 2007, Huggins *et al*., 1999) are present in coal combustion ash. Although Cr (III) occurs naturally in the environment, Cr (VI) in the environment is almost always related to anthropogenic activity.

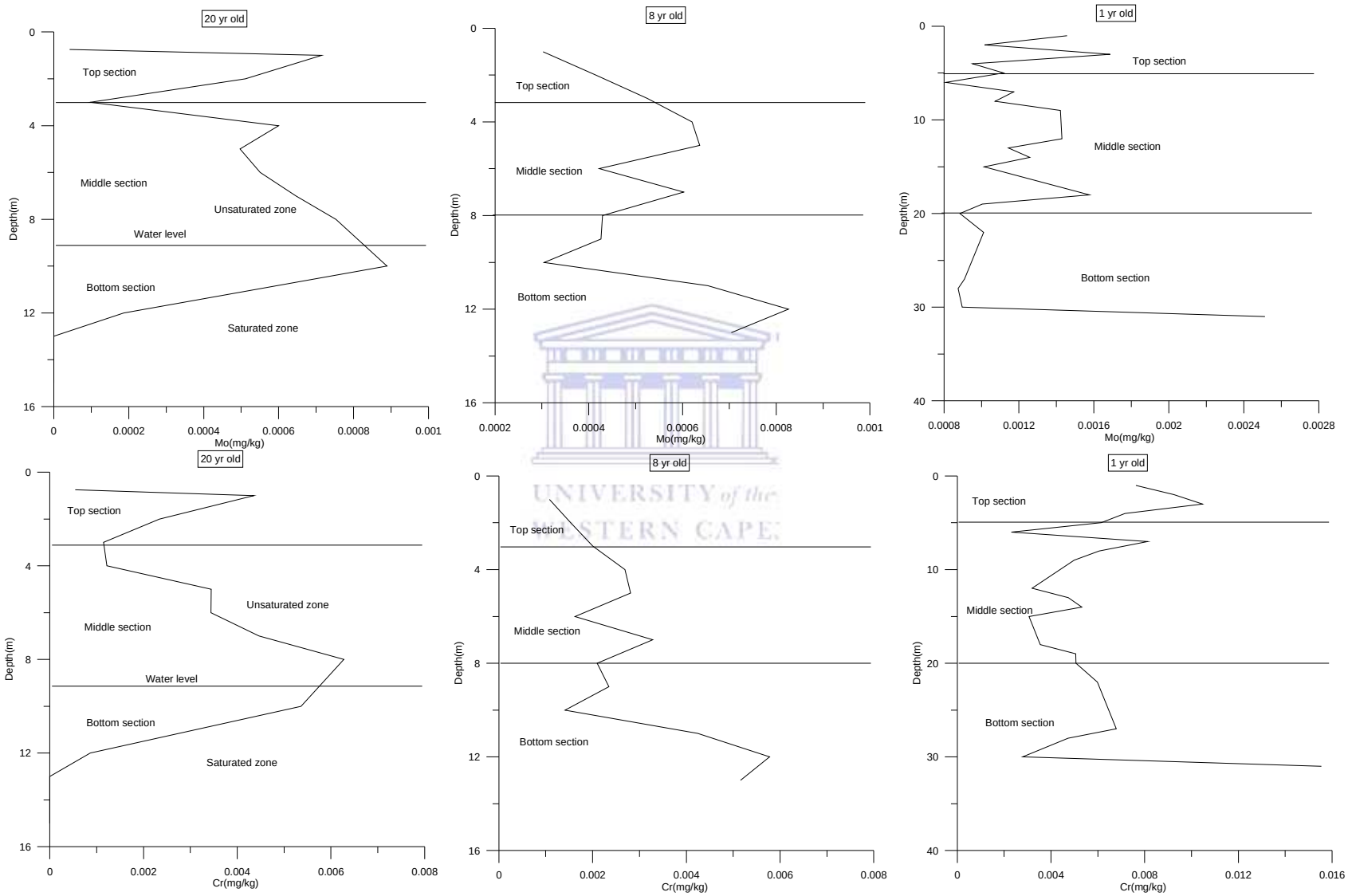

Figure 8.2. Molybdenum and chromium trend in water soluble fraction of drilled cores of different ages and depths (n=3).

Commonly occurring reductants, such as ferrous iron and organic material can transform Cr (VI) to Cr (III), but manganese oxides are the only inorganic oxidants found in the environment that cause the rapid oxidation of Cr (III) to Cr (VI) (Rai *et al*., 1989). The XRD results of 1 year and 8-year-old core ash samples indicated the presence of hematite (Fe_2O_3) which could act as reductants of Cr (VI) to Cr (III). The XRF result revealed the presence of manganese oxide (MnO) (see Tables 5.4-5.6) as the only chemical compound that can oxidise Cr (III) to most stable oxidation state (Cr (VI)) in the core samples of 1 year and 8-year-old ash dump. Shah *et al*. (2009) also documented the presence of Cr (VI) in the fly ash collected from Australian power station. The higher concentration of Cr in the 1-year-old ash cores could probably be due to the mineral stability in 8-year-old core ash samples which allowed the reduction of Cr (VI) to immobile Cr (III) in the ash. There is high potential for release of Mo and Cr in the 1-year-old ash compared to 8-year-old ash cores which is indicative of Mo and Cr fixation probably through precipitation of secondary minerals in the 8-year-old ash cores due to chemical weathering/ageing.

8.2.1.3 Lead and boron

Figure 8.3 shows the concentration profile of Pb in the water soluble fraction of fly ashes. The highest concentration of Pb is recorded in the 1-year-old ash cores. The concentration of Pb in the water soluble fraction of ash cores was lower compared with the other elements, it is generally below 0.0004 mg kg^{-1}. Low concentrations of Pb recorded at the top sections of 8 year and 1-year-old ash cores whereas the middle section shows a fairly high concentration. A rather high concentration is recorded towards the end of bottom section of 1-year-old ash cores. The concentration difference of Pb in the 20-year-old ash cores is not noticeable suggesting that it is less mobile due to weathering or ageing. Higher concentration of Pb is recorded in the water soluble fraction of the 1-year-old core compared to the 8-year-old ash cores indicates that intense long-term leaching has not yet taken place within one year of dumping the ash (Figure 8.3). Significant proportion of the Pb is associated with the carbonate and residual fraction of dry disposed fly ashes as discussed in following sections (see Figures 8.9 and 8.15). The vertical distribution of Pb is controlled by the adsorption and desorption due to variations in the pore water pH. The acid neutralisation capacity results showed that Pb release is governed by solution pH (see Figure 6.6b). Recent studies have shown that at higher pH, surfaces of the fly ash

particles are negatively charged (Lee and Saunders, 2003). This can lead to increase in the adsorption of most of Pb from the environment.

It has also been reported that Pb leaching in coal fly ash can be controlled by acidity and alkalinity of the ash pore water (Vitkova *et al*., 2009). Figure 8.3 also showed the concentration profile of B in the water extractable fraction of fly ash cores. The highest concentration of B is recorded in the 8-year-old ash cores. Although the concentrations of B were generally low; it is between 0.035-0.07 mg/kg in the water soluble fraction of dry disposed ashes. The concentration of B in the middle sections of 20 year and 1-year-old ash cores is moderately high. On the contrary, the middle section of 8-year-old ash cores showed comparatively low concentration. Relatively low concentration of B is recorded in the bottom sections of dry disposed fly ashes. A rather high concentration of B in the top section of 8-year-old ash cores is due to flushing down of leachate from top soil by advection forces. Relatively low concentration in the top section of 1-year-old and 20-year-old ash cores suggests it is has been leached out overtime due to weathering/ageing. A slight concentration difference of B in the top, middle and bottom sections of dry disposed fly ashes suggest that it is less mobile due to weathering or ageing. It has been reported that the leaching of B decreases especially under highly alkaline conditions (Iwashita *et al*., 2005). It has been reported that B is present as surface oxide precipitates or incorporated in glassy matrix of fly ash (Hullet and Weinberger, 1980; Querol *et al*., 1995a). Previous studies had shown that B exist in alkaline circum-neutral solutions in oxyanionic form and can be substituted in the ettringite structure ($Ca_6Al_2(SO_4)_3(OH)_{12}\bullet 26H_2O$) for SO_4^{2-} (Hollis *et al*., 1988; Lee and Saunders, 2003, Bruder-Hubscher *et al*., 2002). The reasonably high concentration of As, Se, Mo, Cr and Pb in the water soluble fraction of 1-year-old fly ash could be due to their presence in highly soluble form in 1-year-old ash whereas the 8-year-old ash has achieved a relative mineral stability. It has been recognized that significant increase in the extraction of As, Zn, Pb, Hg, and Se ions from the fly ash is attributed to the instability of the mineral phases (Baba *et al*., 2008).

The important features of this section are that the trace metals showed considerable mobility and downward movement primarily due to mass transfer of trace metals caused by advection forces. Factors such as inhomogeneity of ash cores, moisture content levels and point of contact with the ground water could also influenced the trace metals mobility in the water soluble fraction.

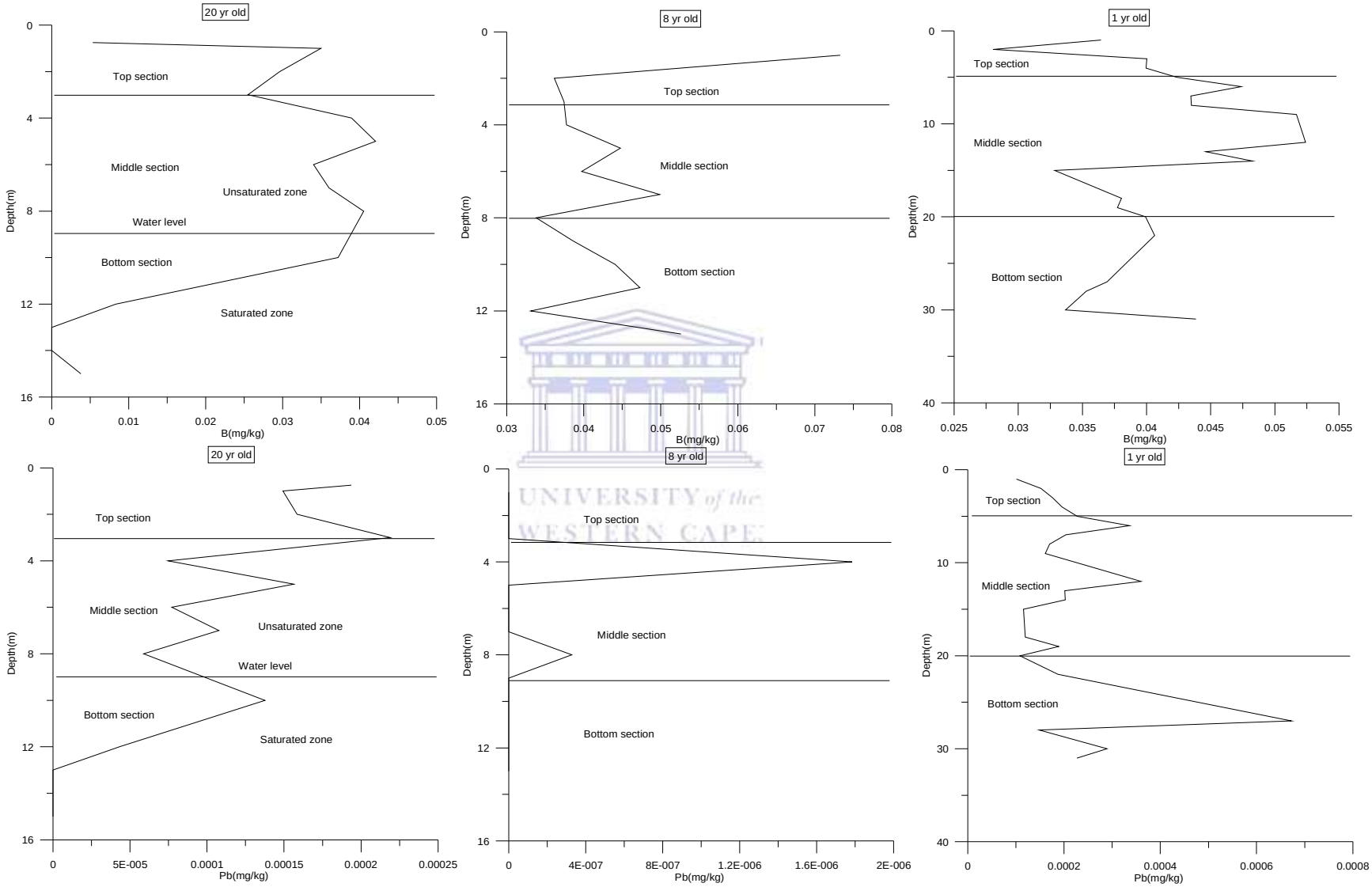

Figure 8.3. Boron and lead trend in water soluble fraction of drilled cores of different ages and depths (n=3).

8.2.2 Analysis of exchangeable fraction

8.2.2.1 Arsenic and selenium

Figure 8.4 shows concentration profile of As in the exchangeable fraction of dry disposed ash cores at different ages. The highest concentration of As is recorded in the 1-year-old ash cores. The concentration of As in the exchangeable fraction of 1-year-old ash cores ranged from 0.00019±0.00045-0.0053±0.005 mg kg^{-1}. The concentration of As in the exchangeable fraction of 8 year and 20-year-old ash cores ranged from 0.0024±0.0001-0.0038±0.0003 mg kg^{-1} and 1.24E-05±3.4E-06-0.0042±0.0005 mg kg^{-1} respectively. Relatively high concentration of As is recorded in the top sections of 20 year, 8 year and 1-year-old ash cores suggests that it is influenced by flushing down of leachates from top soil due to advection forces. The middle sections of 20 year and 8-year-old ash cores showed a rather high concentration of As in the exchangeable fraction. A relatively low concentration of As is recorded in the bottom section of 20-year-old ash cores and towards the end of bottom section of 8-year-old ash cores. Comparatively high concentration As is recorded in the middle and bottom sections of 1-year-old ash cores. The concentration difference in the top, middle and bottom sections of dry disposed fly ashes is noticeable suggesting that it is mobile. Its mobility appears to be controlled by adsorption and desorption due to variations in the pore water pH. The acid neutralisation capacity results show that As release in the dry disposed ash is governed by the solution pH. In addition the vertical distribution could also be influenced by in-homogeneity in ash cores, moisture content levels and point of saturation. The lower concentration of As in the 8-year-old ash cores is probably due to the precipitation of arsenic-bearing mineral phases which reduce its concentration in the ash pore water, hence it is not available for exchange on the adsorption sites. Previous studies have shown that the concentration of As in solution can be reduced by the precipitation of calcium ortho-arsenate ($Ca_3(AsO_4)_2$) at alkaline pH when considerable amounts of Ca is present in the solution (Zielinski *et al*., 2007; Wang *et al*., 2007).

The concentration of Se trend in the exchangeable fraction of 1 year, 8 year and 20-year-old ash cores is shown in Figure 8.3. The highest concentration of Se is recorded in the 1-year-old ash cores suggesting it have been leached out in the older ash cores. The concentration of Se in the exchangeable fraction ranges from 0.0016±0.012-0.0032±0.0003 mg kg^{-1} in the 1-year-old ash cores. The concentration of Se in the exchangeable fraction of 8 year and 20-year-old ash

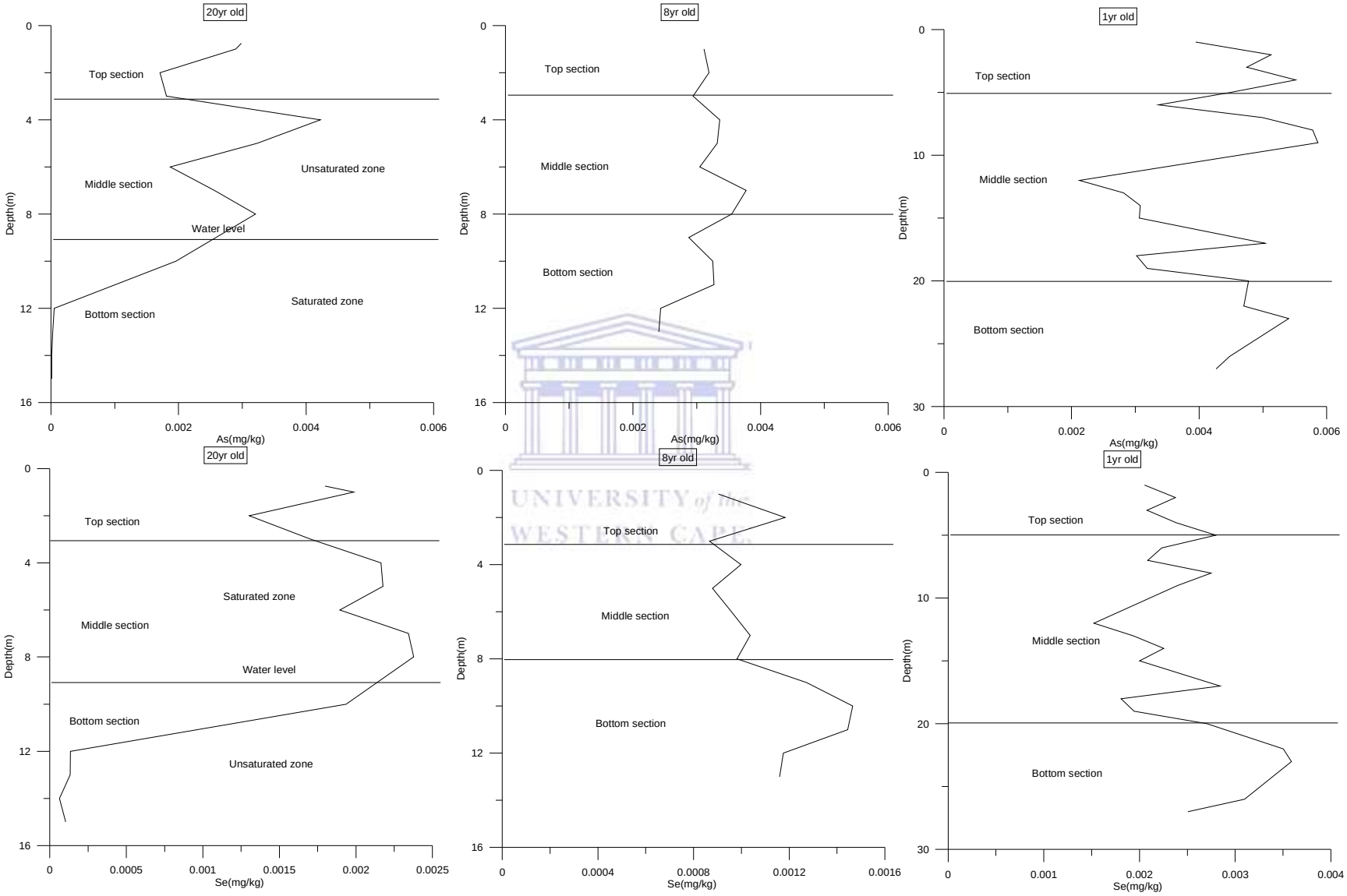

Figure 8.4. Arsenic and selenium trend in exchangeable fraction of drilled cores of different ages and depths (n=3).

ranged from 0.00087±0.00003-0.0015±0.0003 mg kg^{-1} and 6.35E-052.3E-06±-0.0024±0.0004 mg kg^{-1} respectively. The lower concentration of Se in the 8-year-old fly ash compared with 1-year-old indicates considerable leaching had occurred within 8 years of dumping of the fly ash. A reasonably low concentration of Se is recorded in the top and middle sections of 8 year and 1-year-old ash cores. In contrast, a comparatively high concentration of selenium is recorded in the bottom sections of 1 year and 8-year-old ash cores. Se showed moderately high concentration in the top and middle sections of 20-year-old ash cores; while a fairly low concentration of Se is recorded in the bottom section. The Se concentration difference in the top, middle and bottom sections of 1 year, 8 year and 20-year-old ash cores is noticeable suggesting that it is mobile. This mobility appears to be controlled by adsorption and desorption due to variations in the pore water pH. The acid neutralisation capacity results revealed that the Se release is dependent on the solution pH. Other likely factors that could influence Se mobility are inhomogeneity in ash cores, moisture content levels and point of saturation.

8.2.2.2 Molybdenum and chromium

Figure 8.5 shows Mo concentration trend in the exchangeable fraction of dry disposed ash cores at different age. The highest concentration of Mo is recorded in the 1-year-old fly ash indicating intense leaching has taken place in the older ashes. A somewhat low concentration of Mo is recorded in the top sections of 1 year and 8-year-old ash cores. Furthermore, the middle sections of 1-year-old and towards the end of middle section of 8-year-old ash cores. On the contrary, high concentration of Mo is recorded in the bottom sections of 1 year and 8-year-old ash cores. Table 6a&b showed Mo concentration within the ranged of 0.0009±0.0007-0.0015±0.0002 mg kg^{-1} in the exchangeable fraction of 1-year-old ash cores. The concentration of Mo in the exchangeable fraction of 8 year and 20-year-old ash ranged from 0.00010±0.00004-0.0008± 0.00003 mg kg^{-1} and 0.00048±0.00006-0.001±0.0005 mg kg^{-1} respectively.

A remarkable concentration difference of Mo in the top, middle and bottom sections suggest mobility due to adsorption and desorption caused by variations in the pore water pH. Mo release pattern in the dry disposed ash cores is controlled by the solution pH (see Figure 6.6b). Cr concentration in the exchangeable fraction of dry disposed fly ashes is shown in Figure 8.4. The highest concentration of Cr is recorded in the 1-year-old fly ash. However, the concentration of Cr in the exchangeable fraction of 1-year-old ash cores ranged from

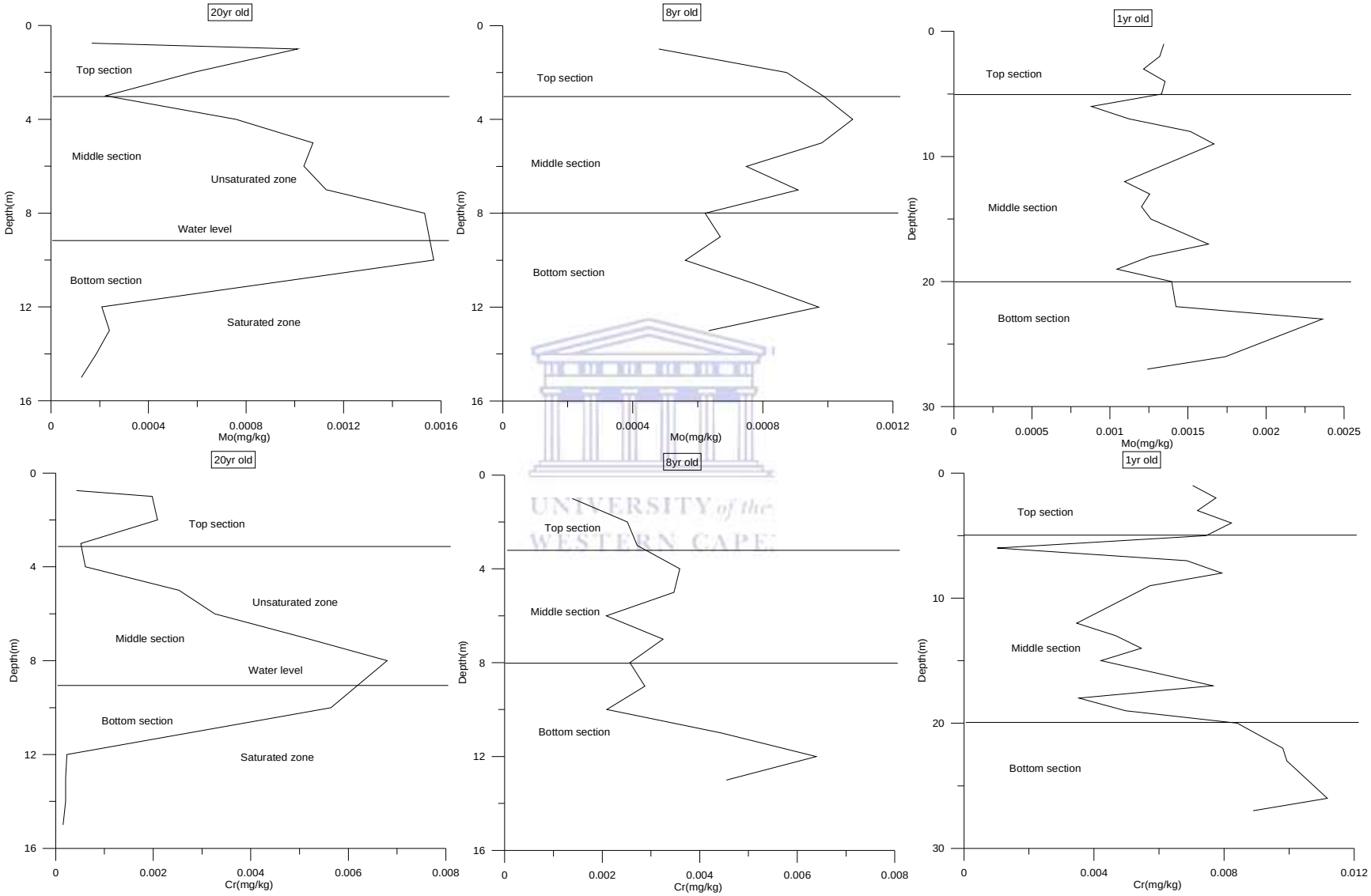

Figure 8.5. Molybdenum and chromium trend in exchangeable fraction of drilled cores of different ages and depths (n=3).

0.0031±0.0005-0.0088±0.0009 mg kg^{-1}. The concentration of Cr in the exchangeable fraction of 8 year and 20-year-old ash cores ranged from 0.0014±0.0003-0.0064±0.0005 mg kg^{-1} and 0.00015±0.00005-0.0068±0.0002 mg kg^{-1} respectively. Relatively low concentration of Cr is recorded in the top sections of 1 year, 8 year and 20-year-old ash cores. In addition, low concentration of Cr is recorded in the middle sections of 1 year and 8-year-old ash cores and bottom section of 20-year-old ash cores. In contrast, comparatively high concentration of Cr is recorded in the bottom sections of 1 year and 8-year-old ash cores and towards the end of the middle section of 20-year-old fly ash. A noticeable concentration difference in the top, middle and bottom sections of 1 year, 8 year and 20-year-old ash cores suggest mobility due to variations in the pore water pH (see Section 5.7). Acid neutralisation capacity results showed that chromium release is controlled by solution pH (Figure 6.6a).

8.2.2.3 Lead and boron

Figure 8.5 shows concentration profile of Pb in the exchangeable fraction of 20 yrs and 1-yr-old fly ash. The higher concentration of Pb is recorded in the 1-year-old ash cores. However, Pb concentration in the exchangeable fraction of 1-year-old ash ranged from 0.000014±0.0002-0.000018±0.00012 mg kg^{-1}. The Pb concentrations in the exchangeable fraction of 20-year-old ash cores ranged from 3.16E-06-0.00036 mg kg^{-1}. The low concentration of Pb in the exchangeable fraction of 1 year and 20-year-old ash cores suggests that fly ash have been leached. It has been established that Pb is one of the most important effect of fly ash leaching (Urgulu, 2004). Lead (Pb) was not detected in the exchangeable fraction of 8-year-old fly ash. Non-detection of Pb in the exchangeable fraction of 8-year-old ash indicates non availability of the Pb in the pore water for exchangeable on the adsorption sites. A fairly low concentration of Pb is recorded in the top and middle sections of 20 year and 1-year-old ash cores. In contrast, the bottom sections 20 year and 1-year-old ash cores exhibited a rather high concentration. The concentration difference in the top, middle and bottom sections of 20 year and 1-year-old ash cores is noticeable indicating that it is easily release. Its mobility is governed by the variations in the pore water pH. The acid neutralisation capacity results revealed that Pb release pattern is controlled by solution pH (see Figure 6.6b). It has been reported that Pb leaching in coal fly ash can be controlled by acidity and alkalinity of the ash pore water (Vitkova *et al*., 2009). It has also been reported that reduction in leaching is due to the neutralization of bottom ash pH and the

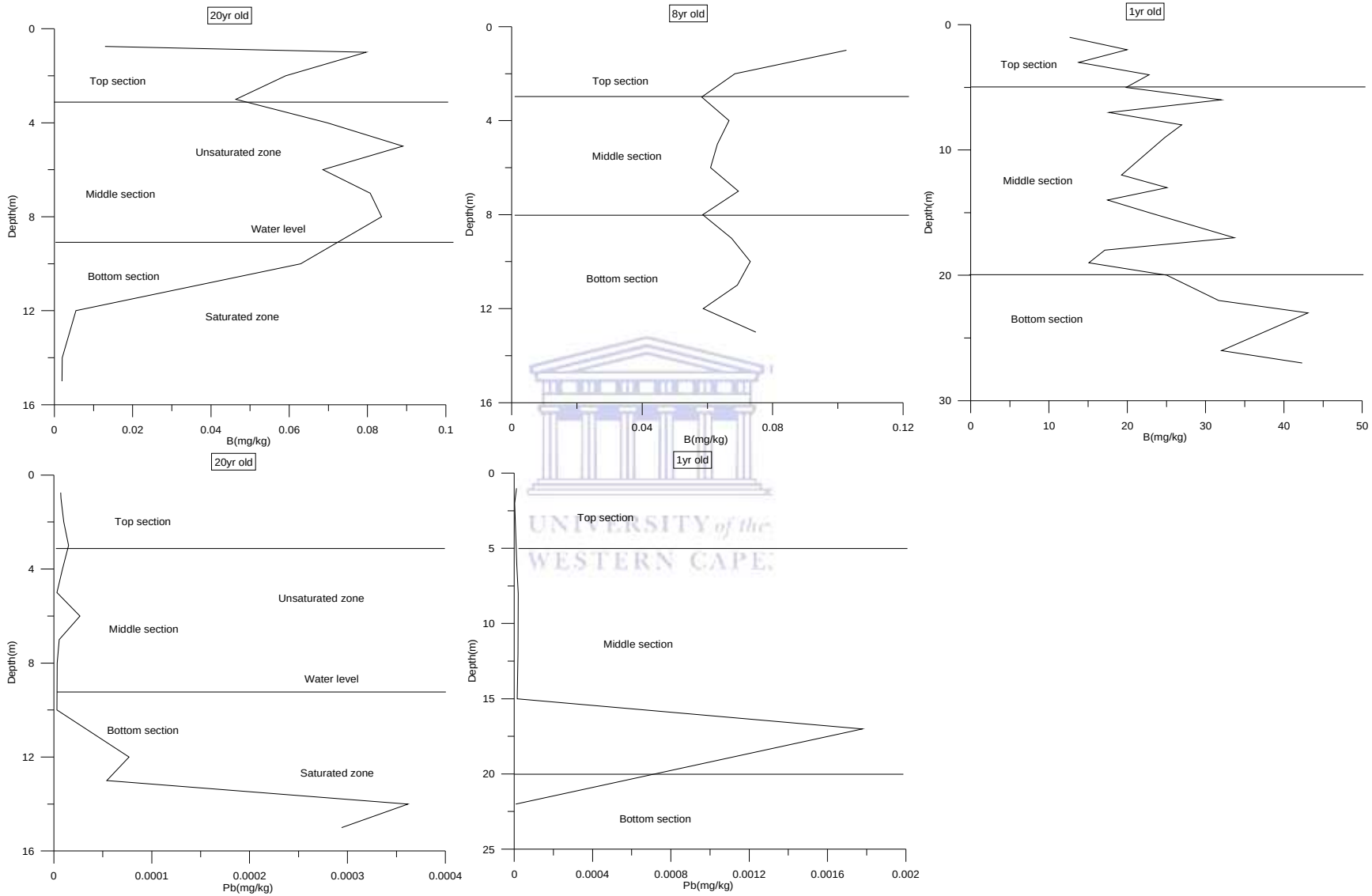

Figure 8.6. Boron and lead trend in exchangeable fraction of drilled cores of different ages and depths (Pb is not detected in the 8-year-old ash) (n=3)

formation of less soluble species of these elements (Cd, Pb, Cu, Zn and Mo) as weathering continues (Meima and Comans, 1999). The concentration of B in the exchangeable fraction of 1 year, 8 year and 20-year-old ash cores is shown in Figure 8.6. The highest concentration of B is recorded in the 1-year-old ash cores. The concentration trend of B in the exchangeable fraction show increasing response with increasing depth of 1-year-old ash cores. Its concentration in the exchangeable fraction of 1-year-old ash core samples ranged from 12.65±0.0002-284.96±0.0031 mg kg^{-1} (Table 8.2). Although, concentration of B in the exchangeable fraction of 8 year and 20-year-old ash cores ranged from 0.058±0.006-0.103±0.003 mg kg^{-1} and 0.013±0.004-0.089±0.005 mg kg^{-1} respectively. A relatively low concentration of B is recorded in the bottom sections of 8 year and 20-year-old ash cores. On the contrary, high concentration of B is recorded in the bottom section of 1-year-old ash cores. Furthermore, reasonably low concentration of B is recorded in the middle sections of 1 year and 8-year-old ash cores. Relatively high concentration of B is recorded in the top and middle sections of 20-year-old ash cores. Similarly high concentration of B is recorded in the top section of 8-year-old ash cores is influenced by mass transfer of leachate from top soil. In addition, comparatively high concentration of B is recorded in the bottom section of 20-year-old ash cores. The concentration difference of B in the top, middle and bottom sections highlighting mobility due to adsorption and desorption caused by variations in the pore water pH. It has been reported that B is present as surface oxide precipitates or incorporated in glassy matrix of fly ash (Hulett and Weinberger, 1980; Querol *et al*., 1995).

The important features in this section are trace metals showed mobility and marked downward movement. This is controlled by the adsorption and desorption due to variations in the pore water pH. Other factors such as in-homogeneity in ash cores, moisture content levels and point of contact with the ground water could also influence the mobility and downward movement.

8.2.3 Analysis of carbonate fraction

8.2.3.1 Arsenic and selenium

Figure 8.7 shows association of As with the carbonate fraction for fly ash of different ages. The highest concentration of As is recorded in the 1-year-old ash cores indicates less leaching has taken place within 1 year of ash dumping. However, As concentration in the carbonate fraction

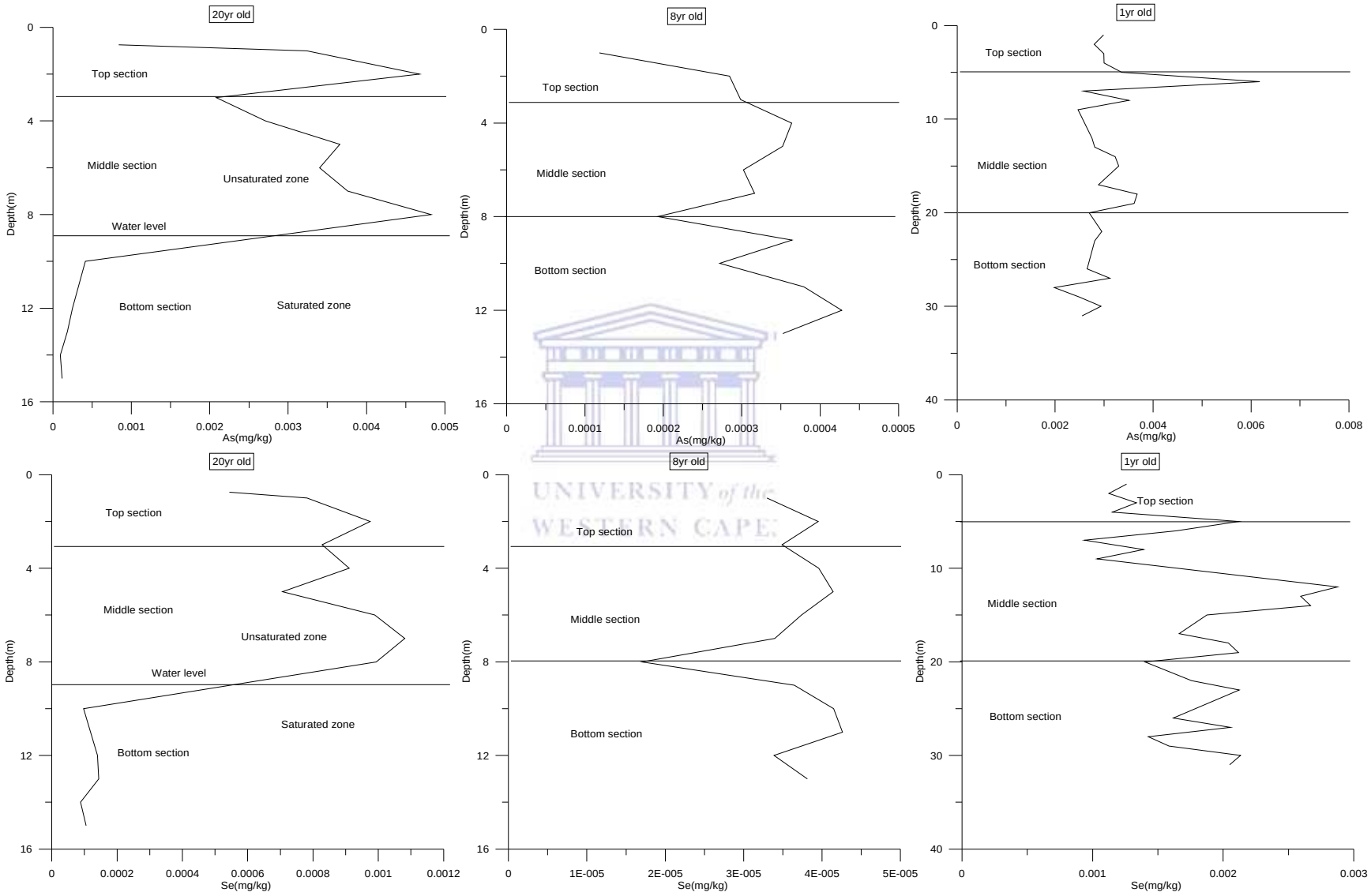

Figure 8.7. Arsenic and selenium trend in carbonate fraction of drilled cores of different ages and depths (n=3).

of 1-year-old ash cores ranged from 0.0022±0.0005-0.0033±0.00089 mg kg^{-1}. On the contrary, the concentration of As in the carbonate fraction of 8 year and 20-year-old ash cores ranged from 0.00012±0.00003-0.00043±0.00001 mg kg^{-1} and 9.21E-05±1.2E-06-0.0038±0.0002 mg kg^{-1} respectively. A fairly low concentration of As is recorded in the middle section of 1-year-old ash cores. Relatively low concentration of As is recorded in the top sections of 8 year and 1-year-old ash cores. Also in similar way, a fairly low concentration of As is recorded in the bottom sections of 1 year and 20-year-old ash cores suggest flushing down of As by advection forces. Relatively high concentration of As is recorded the top section of 20-year-old ash cores due to mass transfer of the leachates from top soil. Similarly, reasonably high As concentration is recorded in the middle section of 8 year and 20-year-old ash cores. The concentration difference of As in the top, middle and bottom sections of dry disposed fly ashes is noticeable suggesting mobility due to adsorption and desorption caused by variations in the pore water pH. Acid neutralisation results revealed that As release is pH dependent. Previous studies have shown that the concentration of As in solution can be reduced by the precipitation of calcium ortho arsenate ($Ca_3(AsO_4)_2$) at alkaline pH when considerable amounts of Ca is present in the solution (Zielinski *et al.*, 2007; Wang *et al.*, 2007). It has also been reported that As is captured by calcium-bearing minerals and hematite, and forms a stable complex of calcium or a transition metal of iron hydroxyl arsenate hydrate $[(M_2C)_2Fe_3(AsO4)_3(-OH)_4.10H_2O]$ in the fly ash (Goodarzi, 2006).

Figure 8.6 shows Se concentration profile in the carbonate fraction of fly ash of different ages. The highest concentration of Se is recorded in the 1-year-old ash cores indicates less leaching has taken place within 1 year of ash dumping. The concentration of Se in the carbonate fraction of 1-year-old ash cores ranged from 0.00093±6.2E-05-0.0026±1.3E-05 mg kg^{-1}. Although, concentration of Se in the carbonate fraction of 8 year and 20-year-old ash cores ranged from 1.7E-05±1.3E-06-4.3E-05±1.1E-07 mg kg^{-1} and 8.81E-05±2.3E-07-0.0011±0.00001 mg kg^{-1} respectively. A considerable high concentration of Se is also recorded in the middle section of 1-year-old fly ash and bottom section of 8-year-old ash cores. A rather low concentration of As is recorded in the top and bottom sections of 1-year-old ash cores; so also at the bottom section of 20-year-old ash cores. Comparatively high concentration of Se is recorded in the top and middle sections of 8 year and 20-year-old ash cores. A notable concentration difference in the top, middle sections and bottom sections of 1 year, 8 year and 20-year-old ash cores suggests

mobility due to adsorption and desorption caused by variations in the pore water pH. The acid neutralisation capacity results also revealed that the release pattern of Se is dependent on the solution pH (see Figure 6.6a).

8.2.3.2 Molybdenum and chromium

The concentration trend of Mo in the carbonate fraction of ash cores of different ages is shown in Figure 8.8. The highest concentration of Mo is recorded in the 8-year-old ash cores. The concentration of Mo in the carbonate fraction of 1 year and 20-year-old cores ranged from 0.0005±0.0001 - 0.001±0.001 mg kg^{-1} and 3.62E-05±2.1E-06-0.0063±0.0007 mg kg^{-1}. Relatively low concentration of Mo is recorded at the top section of 1-year-old ash cores. A comparatively high concentration of Mo is recorded in the middle sections of 1 year, 8 year and 20-year-old ash cores. A somewhat high concentration of Mo is recorded in the bottom sections of 1 year and 8-year-old ash cores. Moderately low concentration of Mo is recorded in the top and middle sections of 8-year-old ash cores. A fairly low concentration of Mo is recorded in the bottom section of 20-year-old ash cores. A considerable concentration difference of Mo in the 1 year, 8 year and 20-year-old ash cores suggests mobility due to variations in pore water pH. Mo release pattern in dry disposed fly ash is dependent on the solution pH (see Figure 6.6b).

The concentration trend of Cr in the carbonate fraction of fly ash of different ages is shown in Figure 8.8. The highest concentration of Cr is recorded in the 8-year-old ash cores. Cr concentration in the carbonate fraction of 8-year-old ash cores ranged from 0.00012±0.00001-0.00043±0.00003 mg kg^{-1}. Cr concentration in the carbonate fraction of 1 year and 20-year-old ash cores ranged from 0.0014-0.0078 mg kg^{-1} and 0.00034-0.0079 mg kg^{-1} respectively. Relatively high concentration of Cr is recorded in the top and middle section of 20-year-old ash cores. A considerably low concentration is recorded in the bottom section of 20-year-old ash cores. A relatively high concentration is recorded in the bottom section of 8-year-old ash cores compared with a moderately low concentration recorded in the top and middle sections. A relatively high concentration is recorded in the bottom section of 1-year-old ash cores compared with a fairly high concentration in the top and middle sections. Considerable concentration difference is recorded in the top, middle and bottom sections of

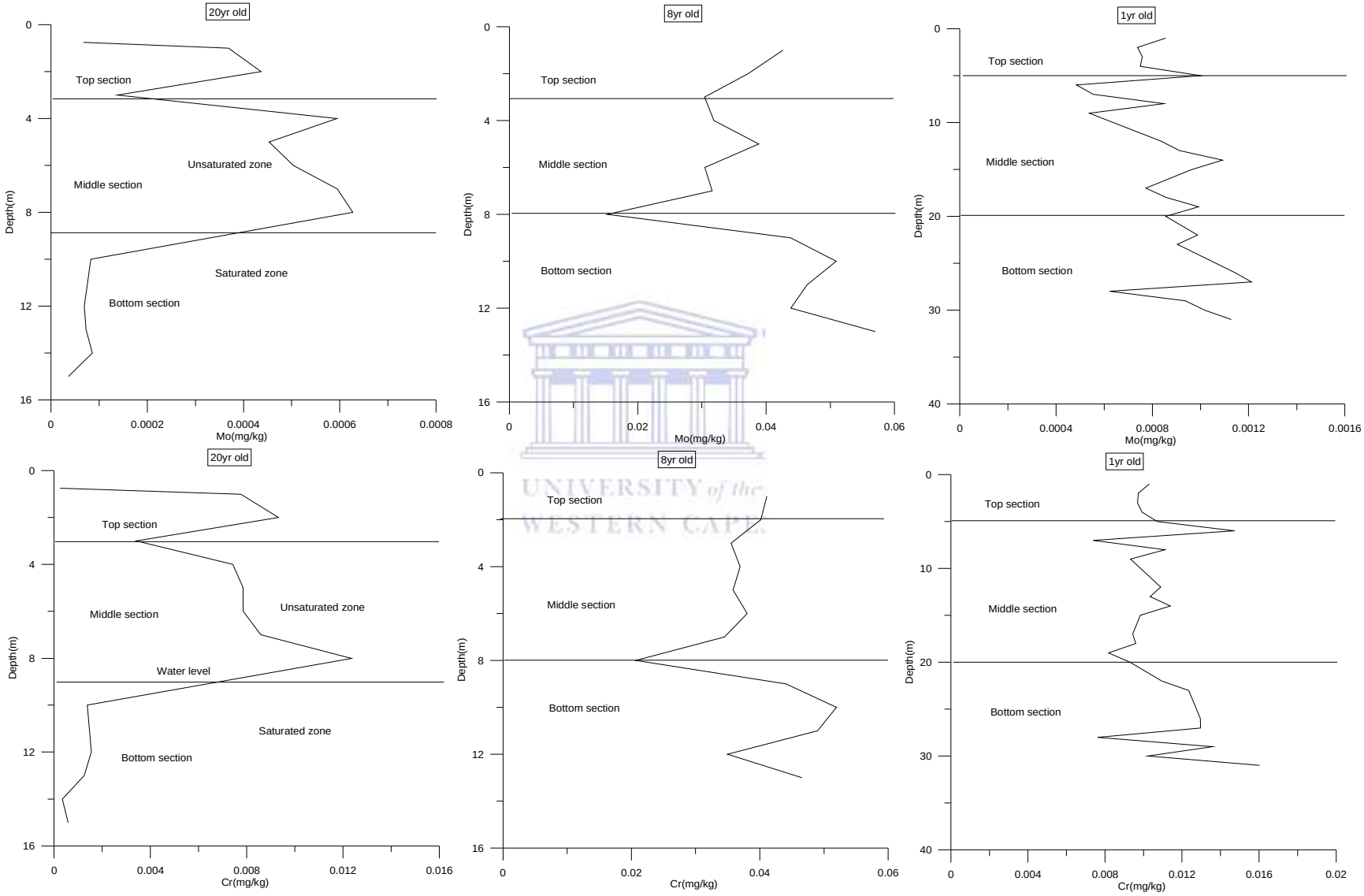

Figure 8.8. Molybdenum and chromium trend in carbonate fraction of drilled cores of different ages and depths (n=3).

1 year, 8 year and 20-year-old ash cores due to adsorption and desorption caused by variations in pore water pH.

8.2.3.3 Lead and boron

Figure 8.9 shows the concentration trend of Pb in carbonate fraction of fly ash of different ages. The highest concentration of Pb is recorded in 8-year-old ash cores. Pb concentration in the carbonate fraction of 8-year-old ash cores ranged from 2000±0.001 - 6200±0.013 mg kg^{-1}. The concentration of Pb in the carbonate fraction of 1 year and 20-year-old ash cores ranged from 0.0013±0.0006 - 0.0045±0.0001 mg kg^{-1} and 2.31E-06±1.1E-07 - 0.004±0.0001 mg kg^{-1} respectively. A considerable high concentration of Pb is recorded in the top and middle sections of 20-year-old ash cores. A rather low concentration of Pb is recorded in the top and middle sections of 1 year and 8-year-old ash cores. Conversely, a fairly high concentration of Pb is recorded in the bottom sections of 1 year and 8-year-old ash cores. A comparatively low concentration of Pb is recorded in the bottom section of 20-year-old ash cores. The concentration difference in the top, middle and bottom sections of 8 year and 20-year-old ash cores is noticeable; suggesting that Pb mobility is due to ash type and texture. Whereas, the subtle concentration difference in the top, middle and bottom sections of 1-year-old ash cores suggests that it is less mobile due to chemical alteration and mineralogical transformation (i.e. calcite formation). It has been reported that the leaching behavior of Pb was found to have a dependency relationship with the components of calcium, such as calcite, and calcium aluminates or calcium aluminosilicate (Wan *et al*., 2006).

Figure 8.8 shows concentration trend of B in carbonate fraction of fly ash of different ages. The highest concentration of B is recorded in the 1-year-old ash cores. The concentration of B in the carbonate fraction of 1-year-old ranged from 2.257±0.0024 - 284.96±0.0018 mg kg^{-1}. The concentration of B in the carbonate fraction of 8 year and 20-year-old ash cores ranged from 0.012±0.0003 - 0.038±0.001 mg kg^{-1} and 0.004±0.0001 - 0.037 ±0.0002 mg kg^{-1} respectively. A comparatively low concentration of B is recorded in the top and bottom sections of 1-year-old ash cores. A rather high concentration of B is recorded in the middle section of 1 year, 8 year and 20-year-old ash cores. A rather high concentration of B is recorded in the middle section of 1 year, 8 year and 20-year-old cores. Relatively low concentration of B is recorded in the bottom sections of 1 year and 20-year-old ash cores indicate overtime erosion by advection forces.

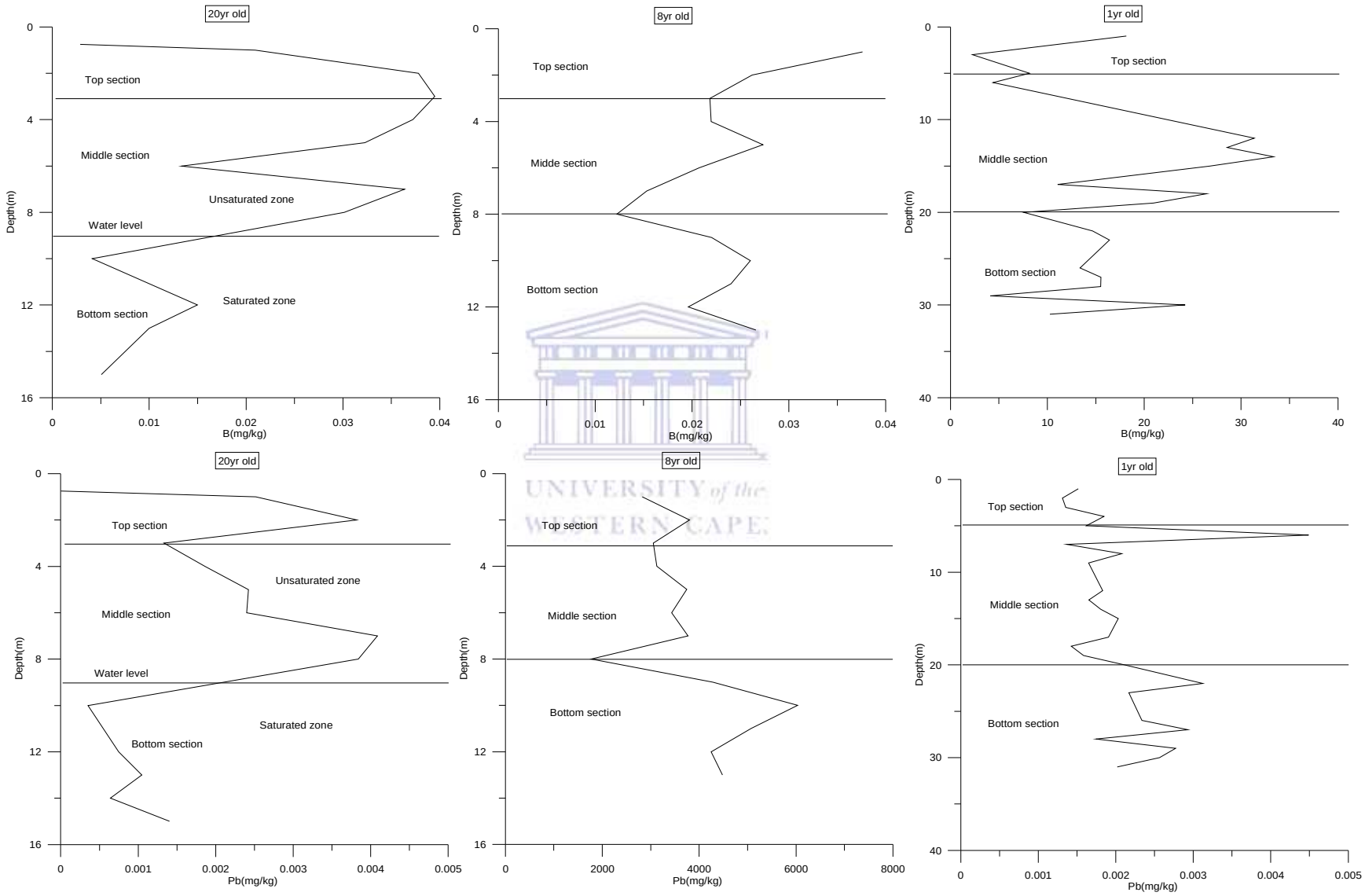

Figure 8.9. Boron and lead trend in carbonate fraction of drilled cores of different ages and depths (n=3).

The important features of this section are that all the trace metals show mobility and considerable downward movement in the carbonate fraction. Their mobility is due to the variations in the pore water pH. Other likely factors that could have influence their mobility are in-homogeneity of ash cores, moisture content levels and point of saturation.

8.2.4 Analysis of Fe and Mn fraction

8.2.4.1 Arsenic and selenium

Figure 8.10 depicts As concentration profile in the Fe and Mn fraction of fly ash of different ages. The highest concentration of As is recorded in the 20-year-old ash cores. Arsenic has concentration in the Fe and Mn fraction of 20-year-old ash cores ranged from 9.21E-05±1.2E-06 -0.0047±0.0001 mg kg^{-1}. The concentration in the Fe and Mn fraction of 8 year and 1-year-old ash cores ranged from 0.0003±3.9E-06 -1.517±0.0015 mg kg^{-1} and 1.2E-05±1.4E-06 - 0.00014±0.00001 mg kg^{-1} respectively. As concentration trend in the Fe and Mn fraction showed a decreasing response with increasing depth in the 1-year-old ash cores. A considerably low concentration of As is recorded in the bottom section and towards the end of middle section of 1-year-old ash cores. A moderately high concentration of As is recorded in the bottom section of 8-year-old ash cores and middle section of 1-year-old ash cores.

A comparatively low concentration of As is recorded in the top and middle sections of 8-year-old ash cores. In contrast, a relatively high concentration of As is recorded in the middle section and toward the end of top section of 20-year-old ash cores. A slight concentration difference in the top, middle and bottom sections of 1 year, 8 year and 20-year-old ash cores suggests mobility of arsenic in the dry disposed ash cores. The mobility of As in ash dump could be due to reduction process (Eh) which often cause precipitation and dissolution of iron hydroxides mineral phase. It has been reported that As is associated with some combination of iron oxide, oxyhydroxide, or sulphate (Zielinski *et al*., 2007). Figure 8.10 showed Se concentration trends in the dry disposed fly ash of different ages. The highest concentration of Se is recorded in the 20-year-old ash cores. The concentration of As in the Fe and Mn fraction of 20-years-old ash cores ranged from 8.81E-05±1.2E-06 - 0.001±0.0001 mg kg^{-1}. Although, concentration of Se in the Fe and Mn fraction of 1 year and 8-year-old ash cores ranged from 0.00019±2E-05 -0.0004±7.8E-05 mg kg^{-1} and 3.6E-06±1.2E07 - 1.6E-05±1.2-07 mg kg^{-1} in that order. A comparatively high concentration of Se is recorded in the top and middle sections of 1 year and 20-year-old ash cores.

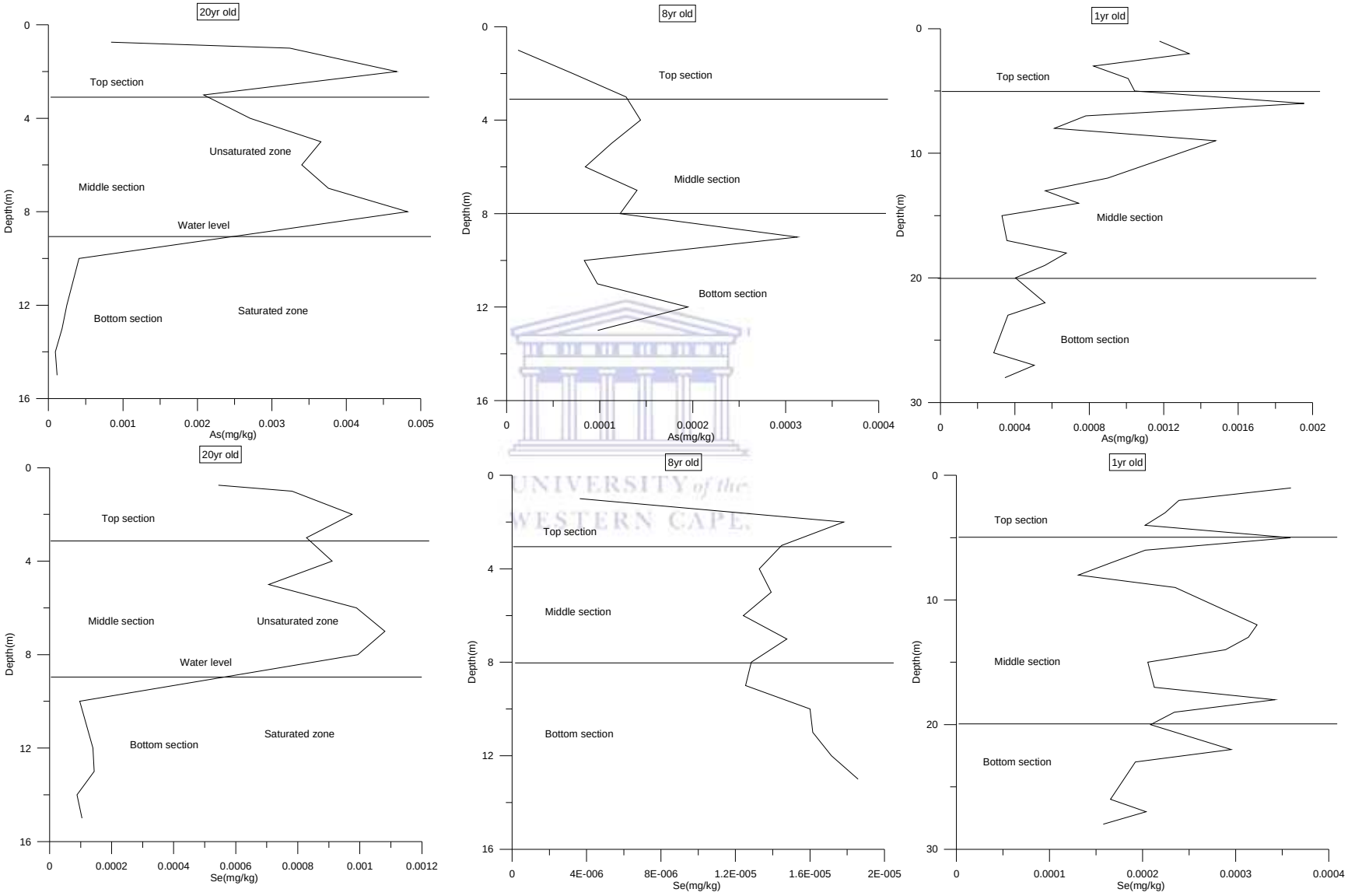

Figure 8.10. Arsenic and selenium trend in Fe and Mn fraction of drilled cores of different ages and depths (n=3).

A moderately high concentration of Se is recorded in the bottom section of 20-year-old and top section of 8-year-old ash cores. A considerable high concentration of Se is recorded in the middle and bottom sections of 8-year-old ash cores. Relatively low concentration of Se is recorded in the bottom section of 8-year-old and top section of 20-year-old ash cores. A slight concentration difference of Se in the top, middle and bottom section of 1 year, 8 year and 20-year-old ash cores suggests mobility of Se due to dissolution of secondary mineral phase (i.e. amorphous Fe-oxyhydroxide phase). Previous study had shown As and Se at the fly ash surface associated with hydroxylamine extractable amorphous iron (hydr.) oxides in the fly ash matrix (Van der Hoek and Comans, 1996).

8.2.4.2 Molybdenum and chromium

The concentration profile of Mo in the Fe and Mn fraction of fly ash of different ages is shown in Figure 8.11. The highest concentration of Mo is recorded in the 8-year-old ash cores. Mo concentration trend in the Fe and Mn fraction shows a decreasing response with increasing depth in the 1-year-old ash cores. Its concentration in the Fe and Mn fraction of 8 year and 1-year-old ash cores ranged from 0.00013±3.9E - 05-0.519±0.0001 mg kg^{-1} and 0.0003±0.00001 - 0.0199±0.0002 mg kg^{-1} respectively. Mo has concentration in the Fe and Mn fraction of 20-yrs-old fly ash ranged from 3.62E-05±1.3E-06 - 0.0006±0.00003 mg kg^{-1}. A fairly high concentration of Mo is recorded in the top and middle sections of 1 year and 20-year-old ash cores. In contrast, moderately low concentration of Mo is recorded in the bottom sections of 1 year and 20-year-old ash cores and towards the end of middle section of 1-year-old ash cores.

A relatively low concentration of Mo is recorded in the top soil leachate of top sections of 20-year-old ash cores. Similarly, a low concentration is recorded in the top section of 8-year-old ash cores. A somewhat high concentration of Mo is recorded in the middle and bottom sections of 8-year-old ash cores. A small concentration difference of Mo in the top, middle and bottom sections of 1 year, 8 year and 20-year-old ash cores suggests mobility due to reduction process which led to precipitation and dissolution of iron hydroxides or leaching of soluble major components of fly ash. Previous study has shown that Mo concentration can be controlled by Fe and Al in solution which reduces the leaching of Mo substantially at acidic condition as metal molybdates (Comans *et al*., 2000; Kukier *et al*., 2003). Cr concentration trend in the Fe and Mn fraction is depicted in the Figure 8.11. The highest concentration of Cr is recorded in the

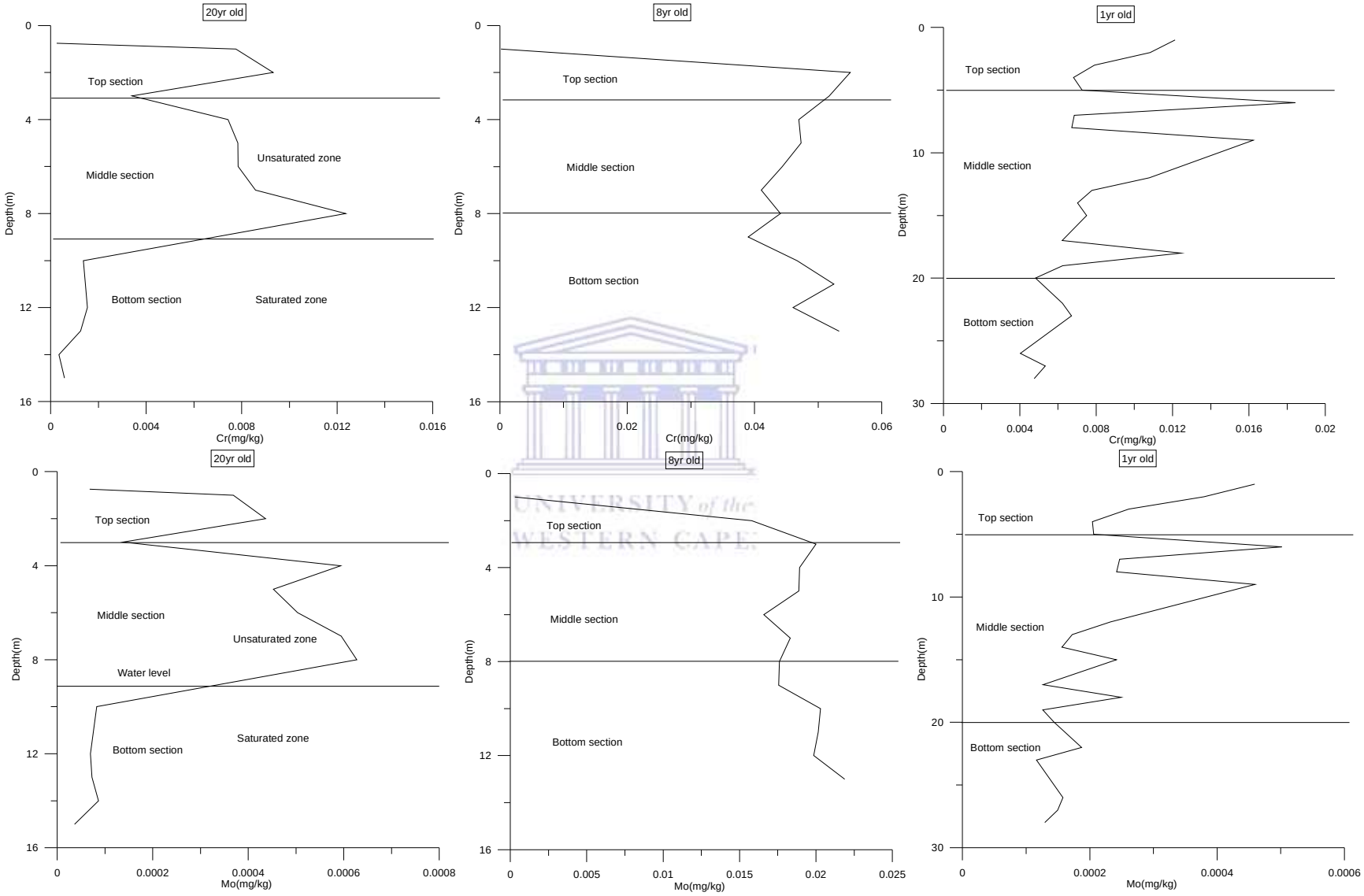

Figure 8.11. Molybdenum and chromium trend in Fe and Mn fraction of drilled cores of different ages and depths (n=3).

8-year-old ash cores suggesting that the greater proportion of MnO in 8-year-old ash cores (see Table 5.5) is probably used in conversion/oxidation of Cr (III) to Cr (VI). Rai *et al*. (1989) revealed the evidence of conversion of Cr (III) to Cr (VI) by the MnO in the fly ash. Cr has concentration in the Fe and Mn fraction of 8-year-old ash cores ranged from 0.00018±0.00002 - 0.055±0.001 mg kg^{-1}. The concentration of Cr in the Fe and Mn fraction of 1 year and 20-year-old ash cores ranged from 0.0048±0.0025 - 0.0112±0.0064 mg kg^{-1} and 0.0003±0.00002 - 0.012±0.0001 mg kg^{-1} respectively. Cr concentration trend in the Fe and Mn fraction showed a decreasing response with increasing depth in 1-year-old ash cores suggests mobility. A comparatively low concentration of Cr is recorded in the top and middle sections of 1 year and 20-year-old ash cores. In contrast, a fairly low concentration of Mo is recorded in the bottom sections of 1 year and 20-year-old ash cores. However, a considerably low concentration of Cr is recorded in the top section of 20-year-old ash cores suggests overtime leaching. Relatively high concentration of Cr is recorded in the middle and bottom sections of 8-year-old ash cores. A small concentration difference in the top, middle and bottom sections of 1 year, 8 year and 20-year-old ash cores suggests Cr mobility. Cr mobility in the dry disposed ash cores is possibly due to reduction process (Eh) which often led to precipitation and dissolution of less soluble amorphous Fe- oxyhydroxides (Donahoe, 2004).

8.2.4.3 Lead and boron

Figure 8.12 shows the leaching profile of Pb in the Fe and Mn fraction of fly ash of different ages. The highest concentration of Pb is recorded in the 8-year-old ash. The concentration of Pb in the Fe and Mn fraction of 8-year-old ash cores ranged from 16.61±0.002 - 1560.14±0.003 mg kg^{-1}. Although, Pb concentration in the Fe and Mn fraction of 1 year and 20-year-old ash cores ranged from 0.00029±2.4E-05 - 0.0176±0.0023 mg kg^{-1} and 2.31E-06±1.3E-07 - 0.0041±0.0003 mg kg^{-1} respectively. The concentration trend of Pb in the Fe and Mn fraction showed decrease response with increase depth of 1-year-old ash cores. A relatively low concentration of Pb is recorded in the bottom sections of 20-year-old ash cores; and towards the end of middle section and bottom section in 1-year-old ash cores. A rather high concentration of Pb is recorded in the middle and bottom sections of 8-year-old ash cores. A similar concentration trend is recorded in the top and middle sections of 20-year-old ash cores. Relatively low concentration of Pb is recorded in the top soil leachate of 20-year-old ash cores. A similar low concentration trend of

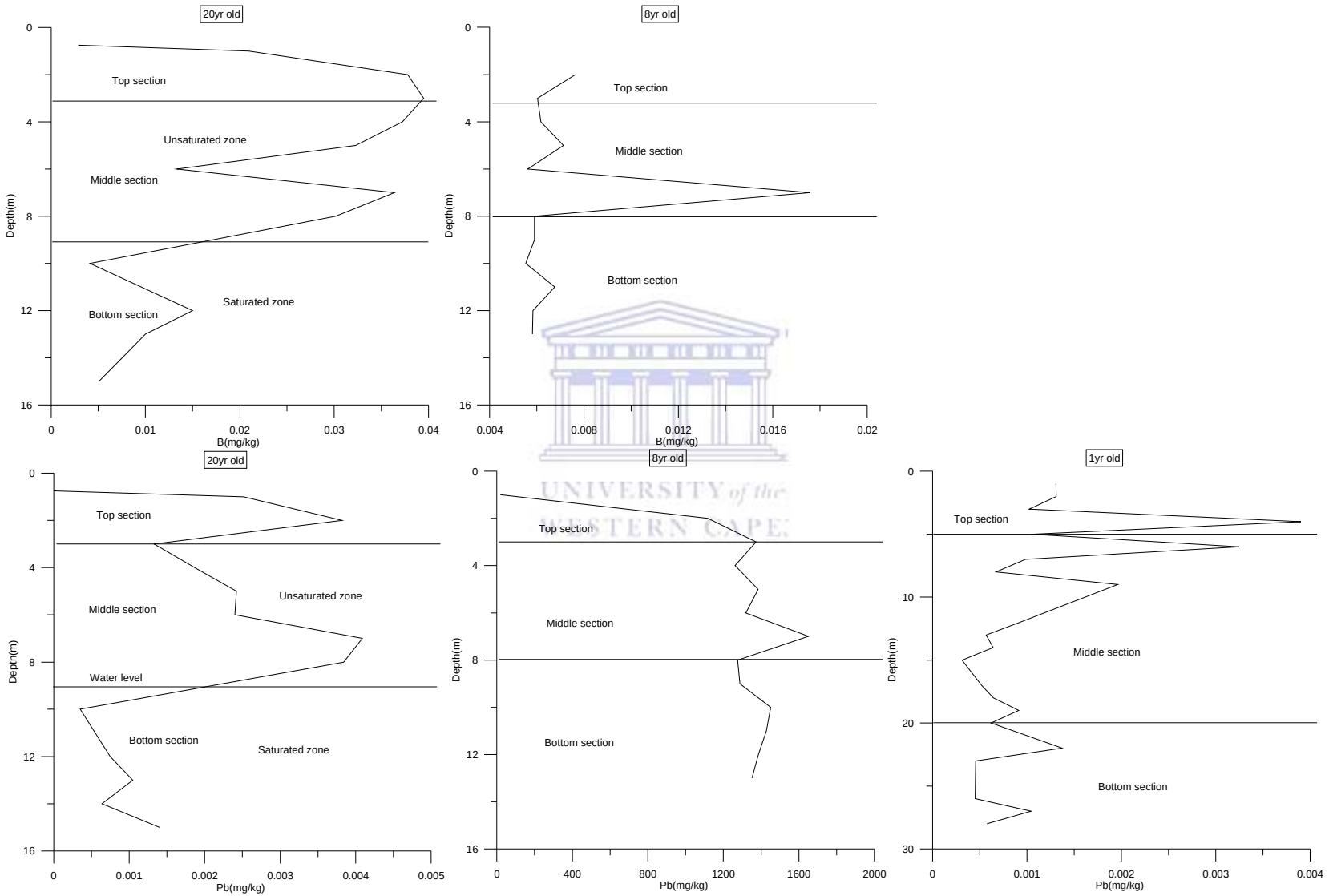

Figure 8.12. Boron and lead trend in iron and manganese fraction of drilled cores of different ages and depths (Boron was below detection limit in the 1-year-old) (n=3).

Pb is recorded in the top sections of 1 year and 8-year-old fly ash. Slight concentration difference occurs in the top, middle and bottom sections of 1 year, 8 year and 20-year-old ash cores suggests lead mobility in the dry disposed fly ashes. This mobility is due to the precipitation and dissolution of iron hydroxides caused by reduction process (change in Eh). Figure 8.12 shows the concentration trend of B in the Fe and Mn fraction of fly ash of different ages. A higher concentration of B is recorded in the 20-year-old ash cores. The concentration of B in the Fe and Mn fraction of 8 year and 20-year-old of ash cores ranged from 0.0056±0.0004 - 0.018±0.0001mg kg^{-1} and 0.0028±0.0002 - 0.015±0.0004 mg kg^{-1} respectively. The concentration of B in the Fe and Mn fraction of 1-year-old ash cores is below detection limits. A fairly low concentration of B is recorded in the bottom sections of 8 year and 20-year-old ash cores. A rather low concentration is also recorded in the top soil leachate of 20-year-old ash cores and top section of 8-year-old ash cores. On the contrary, a relatively high concentration is recorded in the part of top section and middle sections of 20-year-old ash cores. A similar trend is recorded in the middle section of 8-year-old ash cores. A slight concentration difference of boron amongst the top, middle and bottom sections of 8 year and 20-year-old ash cores suggests mobility which is due to precipitation and dissolution of amorphous Fe- oxyhydroxides caused by reduction process.

Important features of this section are that the trace elements showed slight mobility and downward movement in the Fe and Mn fraction. Their mobility patterns are influenced by precipitation and dissolution of less soluble amorphous Fe-oxyhydroxides due to reduction process (change in Eh). Factors such as in-homogeneity of ash cores, moisture content levels and point of contact with ground water.

8.2.5 Analysis of residual fraction

8.2.5.1 Arsenic and selenium

Figure 8.13 shows the concentration of As in residual fraction of fly ash of different ages. The highest concentration of As in the residual fraction is recorded in 20-year-old ash cores. The concentration of As in the residual fraction of 20-year-old ash cores ranged from 0.00091±0.00001 -0.0023±0.0003 mg kg^{-1}. However, concentration of As in the residual fraction of 1 year and 8-year-old ash cores ranged from 0.00027±0.0001 - 0.00039±0.00004 mg kg-1 and 0.00028±0.0003 - 0.00514±0.0076 mg kg^{-1} respectively.

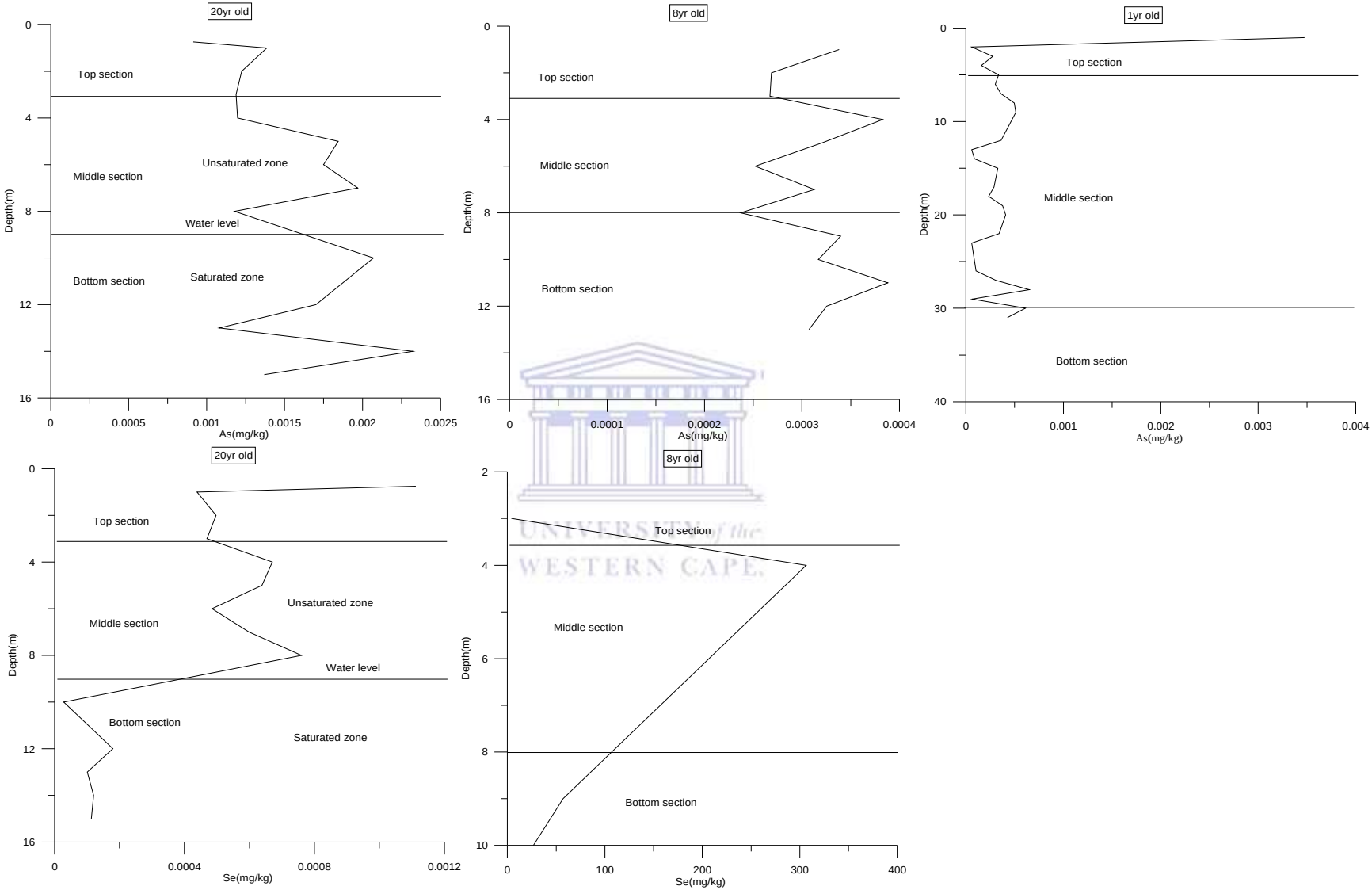

Figure 8.13. Arsenic and selenium trend in residual fraction of drilled cores of different ages and depths (Selenium is not detected in the 1-year-old ash cores) (n=3).

A fairly low concentration of As is recorded in the middle and bottom sections of 1-year-old ash cores. A comparatively high concentration of As is recorded in the middle and bottom sections of 20-year-old ash cores. A somewhat similar trend is recorded in the middle and bottom sections of 8-year-old ash cores. A relatively high concentration of As in the top sections of 1 year and 8-year-old ash cores is influenced by mass transfer of leachate from top soil. A relatively low concentration of arsenic in the top section of 20-year-old ash cores indicates overtime leaching. A slight concentration difference in the top, middle and bottom sections of 1 year, 8 year and 1-year-old ash cores suggests As mobility in the residual fraction ash cores.

The concentration of Se in the residual fraction of dry disposed fly ashes is shown in figure 8.13. The higher concentration of Se is recorded in the 8-year-old ash cores. The concentration of Se in the residual fraction of 8-year-old ash cores ranged from 3.99±0.001 - 56.99± 0.03 mg kg^{-1}. The Se concentration in the residual fraction of 20-year-old ash cores ranged from 2.81E-05±1.2E-06 - 0.00076±0.00003 mg kg^{-1}. Se concentration in the residual fraction of 1-year-old ash cores is below detection limits suggesting it has been considerably leached out. A rather low concentration of Se is recorded in the bottom and top sections of 8-year-old ash cores. In contrast, a comparatively high concentration is recorded in the middle section of 8-year-old ash cores. Se shows a fairly high concentration in the top and middle sections of 20-year-old ash cores. On the contrary, a somewhat low concentration of Se is recorded in the bottom section of 20-year-old ash cores. A slight concentration difference of Se amongst the top, middle and bottom sections of 8 year and 20-year-old ash cores indicates mobility due to dissolution of amorphous aluminosilicate mineral phase.

8.2.5.2 Molybdenum and chromium

Figure 8.14 depicts Mo concentration in the residual fraction of dry disposed fly ash of different ages. The higher concentration of Mo is recorded in the 20-year-old ash cores. Mo concentration in the 1 year and 20-year-old ash cores ranged from 7.49E-07±2.3E-08 – 0.00012± 0.00006 mg kg^{-1} and 6.66E-05± 1.2E-06 – 0.00062±0.00003 mg kg^{-1} respectively. Mo concentration in the residual fraction of 8-year-old ash cores is below detection limits indicating overtime intense leaching. A rather high concentration of Mo is recorded in the middle and bottom sections of 20-year-old ash cores. Conversely, a moderately low concentration is recorded in the top section of 20-year-old ash cores. A comparatively low concentration is recorded in the middle

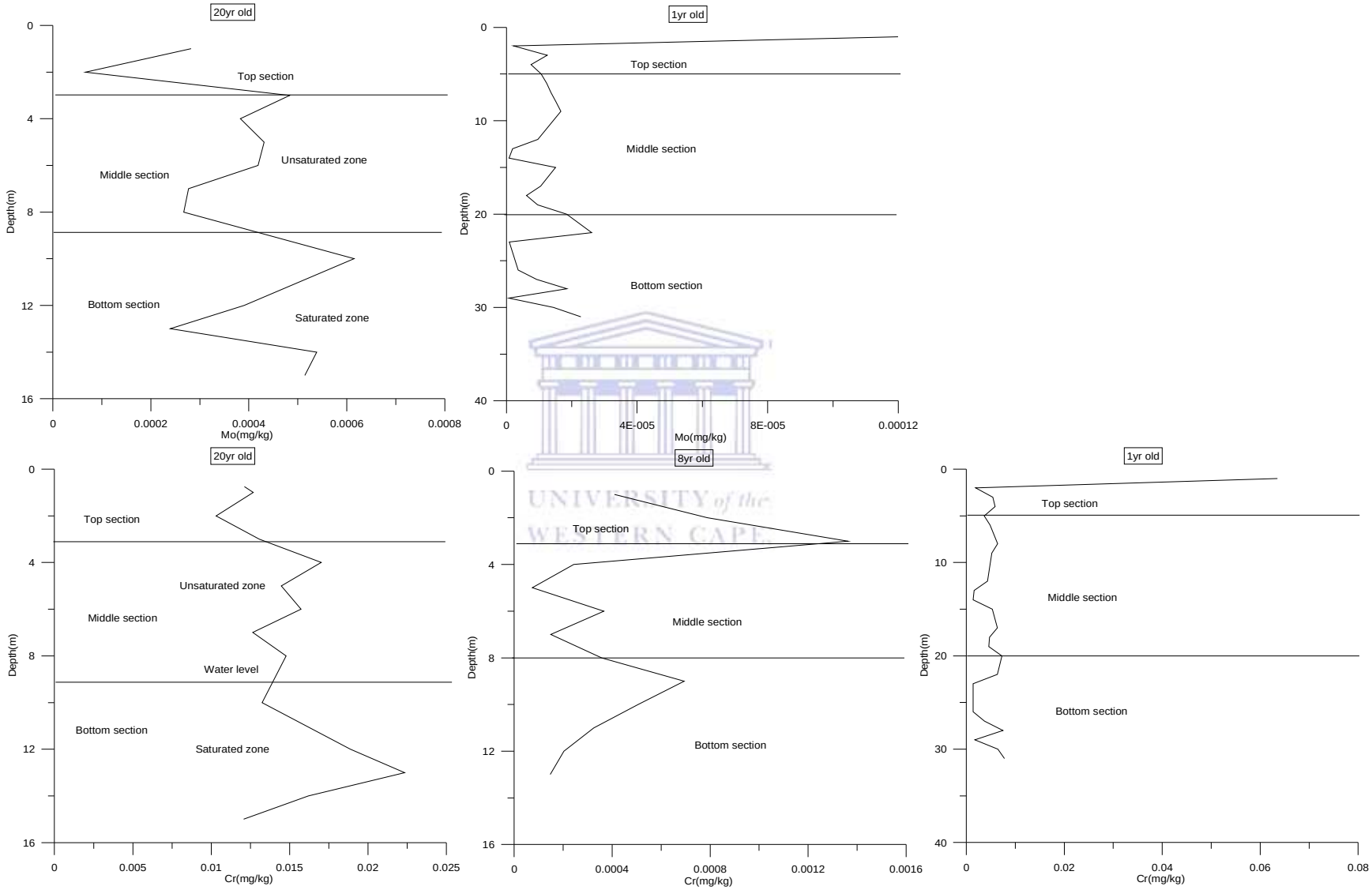

Figure 8.14. Molybdenum and chromium trend in residual fraction of drilled cores of different ages and depths (Molybdenum is not detected in the 8-year-old ash cores) (n=3).

and bottom section of 8-year-old ash cores. In contrast, a fairly high concentration is recorded in top section of 1-year-old ash cores due to mass transfer of leachate from top soil. Slight concentration difference of Mo amongst the top, middle and bottom sections of 8 year and 20-year-old ash cores suggest mobility in the residual fraction is controlled by dissolution of amorphous aluminosilicate phase. Cr concentration in the residual fraction of dry disposed fly ashes is shown in Figure 8.14. The highest concentration of Cr is recorded in 1-year-old ash cores. Cr concentration in the residual fraction of 1-year-old ash cores ranged from 0.0066±0.00045 - 0.0751±0.086 mg kg^{-1}. Whereas, Cr concentration in the 8 year and 20-year-old ranged from 7.4E-05±3.4E-06 – 0.00079±0.00005 mg kg^{-1} and 0.012±0.0006 - 0.018± 0.0007 mg kg^{-1} respectively. A rather low concentration of Cr is recorded in the top and middle sections of 20-year-old ash cores. On the contrary, a fairly high concentration of Cr is recorded in the bottom section of 20-year-old ash cores. A moderately low concentration of Cr is recorded in the middle section of 8-year-old ash cores. In contrast, a somewhat high concentration of Cr is recorded in the top and bottom sections of 8-year-old ash cores. Relatively low concentration of Cr is recorded in the middle and bottom sections of 1-year-old ash cores. Conversely, a fairly high concentration is recorded in the top section due to leachate from top soil. Slight concentration difference of Cr amongst the top, middle and bottom sections of 1 year, 8 year and 20-year-old ash cores indicating mobility of Cr in the residual fraction of ash cores.

8.2.5.3 Lead and boron

Figure 7.15 shows Pb concentration in the residual fraction of fly ash of different ages. The highest concentration of Pb in the residual fraction is recorded in 1-year-old ash cores. Pb concentration in the residual fraction of 1-year-old ash cores ranged from 31.77 – 415.77 mg kg^{-1}. Whereas, concentration of Pb in the residual fraction of 8 year and 20-year-old ash cores ranged from 6.88 – 37.55 mg kg^{-1} and 0.0011 – 0.0057 mg kg^{-1} respectively. A considerable low concentration of Pb is recorded in the top section of 1-year-old ash cores. At the same time, fairly high concentration of Pb is recorded in the middle and bottom sections of 1-year-old ash cores. A rather high concentration of Pb is recorded in the top and middle sections of 20-year-old ash cores. In contrast, a comparatively low concentration of Pb is recorded in the bottom section

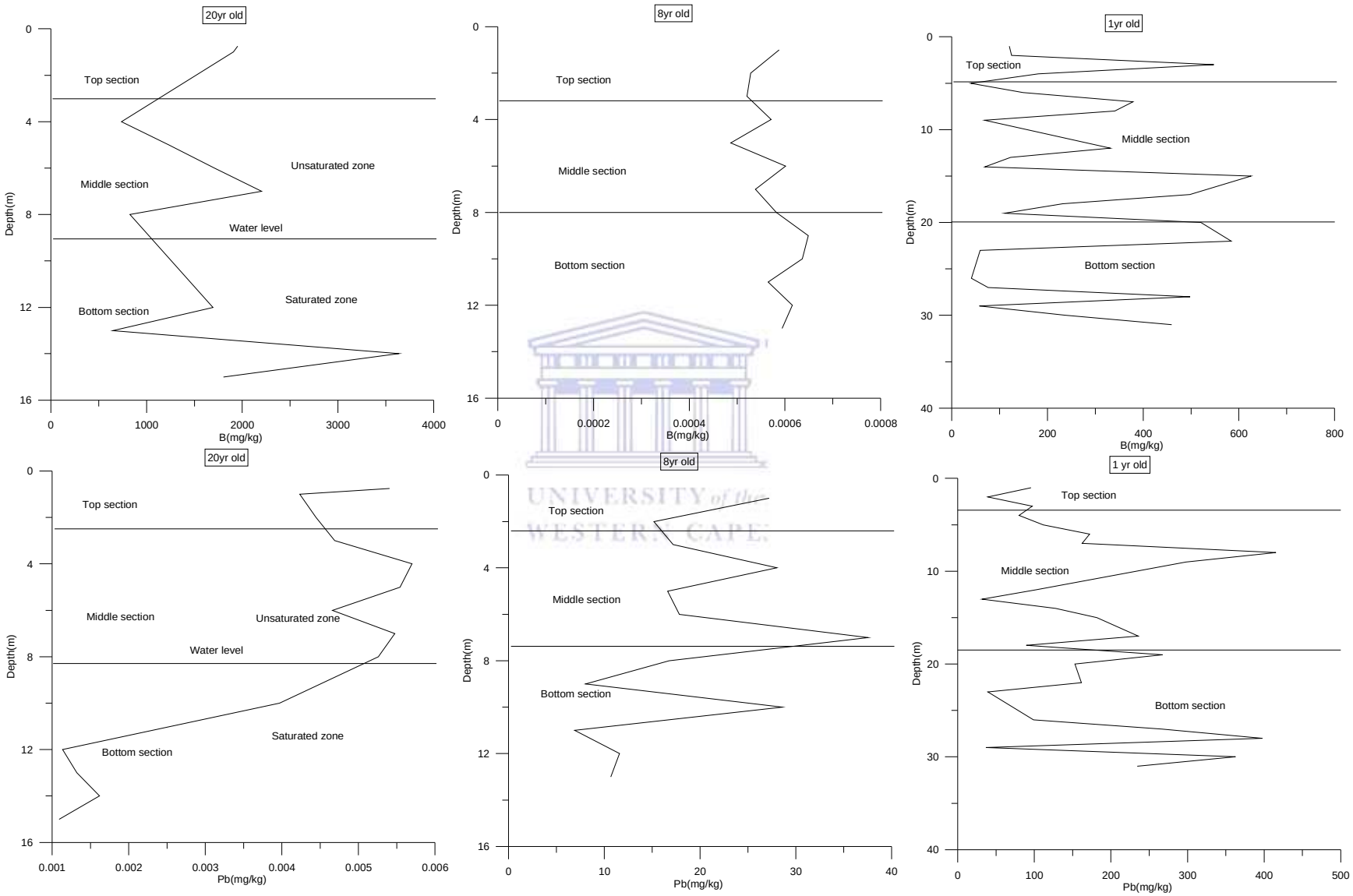

Figure 8.15. Boron and lead trend in residual fraction of drilled cores of different ages and depths (n=3).

of 20-year-old ash cores. Relatively high concentration of Pb is recorded in the top and middle section of 8-year-old ash cores. In contrast, a rather low concentration of Pb is recorded in the bottom section of 8-year-old ash cores. A considerable concentration difference of Pb in the top, middle and bottom sections suggest mobility in the residual fraction. The concentration of B in the residual fraction of dry disposed fly ashes is shown in Figure 7.15. The highest concentration of B is recorded in the 20-year-old ash cores. The concentration of B in the residual fraction of 20-year-old fly ash ranged from 647.53±0.07 – 3635.61±0.03 mg kg^{-1}. Whereas, concentration of B in the residual fraction of 1 year and 8-year-old ash cores ranged from 40.19±0.02 – 625.23±0.006 mg kg^{-1} and 0.00049 ± 0.00005 – 0.00064±0.00003 mg kg^{-1} respectively. The concentration of B is rather low in the top section of 1-year-old ash cores. On the contrary, a fairly high concentration of B is recorded in the middle and bottom sections of 1-year-old ash cores. A comparatively low concentration of B is recorded in the bottom sections of 8 year and 20-year-old ash cores. Whereas, a considerable high concentration of B is recorded in the top and middle sections of 8 year and 20-year-old ash cores. A clear and distinct concentration difference is recorded in the top, middle and bottom sections suggest mobility.

Important features of this section are trace metals in the residual fraction of ash cores showed slight mobility due to in-homogeneity in ash cores, moisture content levels and point of contact with the ground water system. The residual fraction is tentatively considered to contain mainly primary and secondary minerals (i.e. less soluble amorphous aluminosilicate phase), which may hold trace metals within their crystal structure. Under the conditions normally found in nature, probably these metals will be released in solution over a reasonable time span. Nevertheless As quick release from residual fraction of dry disposed ash is possible when come in contact with acid rain.

8.3 Distribution of trace elements in the five leached fractions

Most of the analytes discussed in the previous section show highest concentration in the 1-year-old ash cores. Accordingly, the concentration of each element leached in each fraction was calculated as a percentage of the total metal content and data obtained are presented in Figures 8.16 and 8.17. This section discusses the chemical partitioning of trace metals in 1-year-old ash.

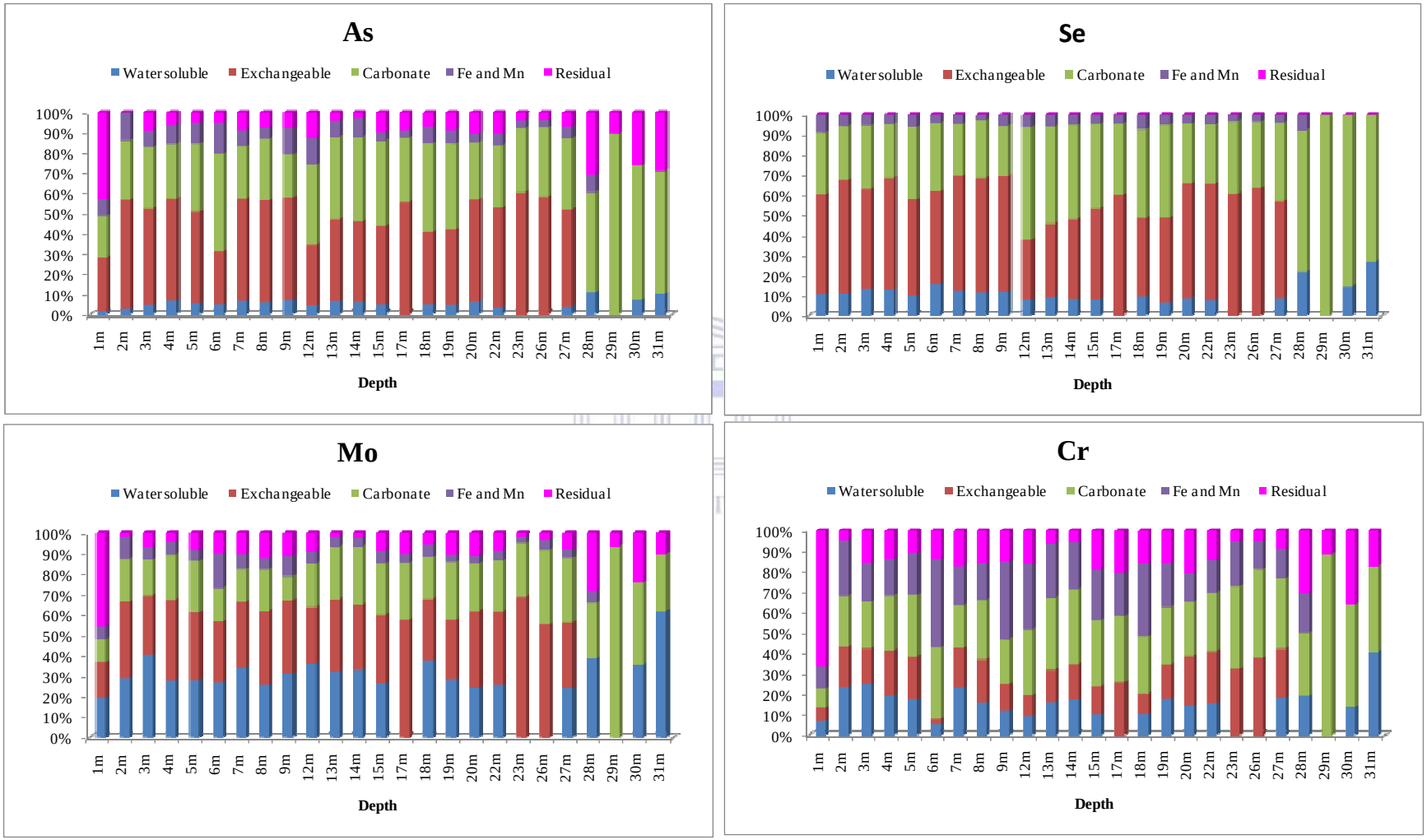

Figure 8.16. Distribution of As, Se, Mo and Cr in five fractions of 1-year-old ash cores.

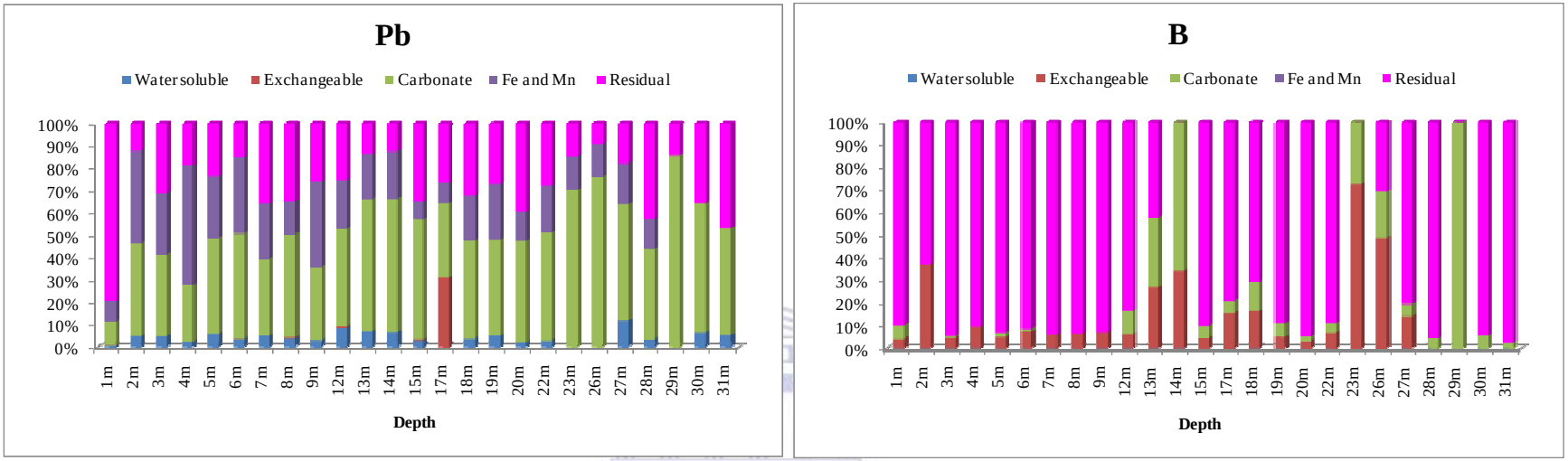

Figure 8.17. Pb and B distribution in five fractions of 1-year-old ash cores.

8.3.1 Water soluble fraction

Generally the weakly sorbed metal forms, mainly those retained on the dust surface by somewhat weak electrostatic interactions, are included in this water soluble fraction. The water soluble elements in fly ash are the most labile form that can be easily leached and readily reach the environment when fly ash is in contact with rain water or other water bodies (Yuan, 2009). As a result water soluble fraction is the most active part with regard to environmental risk on human beings and biomass. Therefore, water soluble fractions are of most environmental concern. Auspiciously, the amount and proportion of individual elements in water soluble fraction of 1-year-old ash core samples is very small. The percentage toxic metals leached in the water soluble fraction was in the following order: Mo (19.19-61.77%) > Cr (5.47-40.66 %) > Se (6.50-26.64 %) > As (1.48-10.87 %) > B (0.01-0.09 %) > Pb (2.31-11.89 %). Of the trace elements Cr and Mo show highest mobility in the 1-year-old fly ash samples. Highest percentage leached was achieved in the water soluble fraction. The presence of Cr compounds at coal ash disposal sites can contribute to the exposure of populations residing or working nearby through exposure to air containing particulates or mists of Cr (VI) compounds, through drinking water if soluble forms of Cr (VI) leach into groundwater, or through skin contact with soil at ash dump sites.

8.3.2 Exchangeable and carbonate fractions

The metals that occurred in this fraction may be thought to be present as co-precipitates with carbonate minerals and strongly-sorbed metal forms on the dust surface. The fraction is sensitive to pH changes, and metal release can be achieved through dissolution of a fraction of the solid material at low pH. The metals in this fraction can be released easily by ion-exchange processes and leach very easily when the environmental conditions are disturbed by pH change or Eh change. Heavy metals in the exchangeable fraction play a very significant role in the evaluation of the environment and always act as a pollution indicator for its environmental mobility and bioavailability (Yuan, 2009). The exchangeable fraction showed the relative abundance of the elements in the following sequence; B (3.37-72.41%) > Mo (17.71-68.61 %) > Se (29.70-63.48 %) > As (26.44-58.11 %) > Cr (2.42-37.60 %) > Pb (0.06-31.05 %). A marked amount of Pb is present in the exchangeable fraction of 1-year-old ash core samples. Conversely, Bodog *et al.* (1996) recognized the presence of small amount of Pb in the exchangeable fraction of fly ash samples. Considerable mobility of Mo, As, B and Se were observed in the exchangeable

fractions of 1-year-old ash cores. Jackson and Miller (1998) recognized that the predominant species of arsenic and selenium were As (V) and Se (IV), with As (III) detected in two low pH fly ashes. Shah *et al*. (2008) recognized forms of As^{3+} and Se^{4+} in the fly ash that was sampled in one Australian power station. It has been established that relatively high concentration of volatile elements (As, Se and Mo) in the water soluble and exchangeable fractions is due to vaporization, condensation and subsequent surface enrichment of fly ash particles during coal combustion process (Yinghui *et al*., 2008). The contributions in the carbonate fraction revealed percentage leached in the order of Se (24.95-100 %) > B (1.04-100 %) > Mo (11.28-93.49 %) > As (20.39-89.56 %) > Cr (9.29-88.24 %) > Pb (10.61-76.23 %). A rather notable amount of As, Se, Mo, B, Cr and Pb in carbonate fraction could be attributed to the formation or precipitation of calcite with sorbed arsenic in fly ash. Zielinski *et al*. (2007) established the association of As with a phase similar to calcium orthoarsenate in a highly alkaline fly ash. Galbreath and Zygarlicke (2004) documented that the high proportion of calcium oxide (CaO) in the coal fly ash can acts as a reactive capture of arsenic.

8.3.3 Iron and manganese fraction

It has been recognized that Fe and Mn oxides exist as nodules, concretions, cement between particles or simply as a coating on particles during the production process of fly ash in the boiler; a lot of toxic elements may be pooled into this fraction when the particles cool down in flue gas. These oxides can probably act as excellent scavengers for trace elements and are thermodynamically unstable under anoxic conditions (Yuan, 2009). It has been proven that most labile elements are found in association with oxides and salts such as sulphates, borates and arsenate (Querol *et al*., 1996; Zielinski *et al*., 2007). In the case of the Fe and Mn fraction, the percentage amount leached is as follows; Pb (8.29-53.50 %) > Cr (10.93-43.59 %) > Mo (3.373-16.82 %) > As (3.73-15.36 %) > Se (2.72-8.78 %). A fairly low percentage leached for As, Se, Mo and Pb are recorded in the Fe and Mn fraction of 1-year-old ash cores. This implies that moderately low percentage of As, Se and Mo is associated with Fe and Mn fraction compared with the other four fractions. This literally indicates that low leachability of As, Se and Mo in the Fe and Mn fraction is largely due to adsorption or co-precipitation with hematite (Fe_2O_3). Jegadesaan *et al*. (2008) had established that adsorption and or co-precipitation of metals with iron (hydr) oxides at neutral pH appeared to be the probable mechanisms controlling metal release. In addition, these trends agree with previously held opinion that the low relative

abundance of As, Se and Pb in the Fe and Mn fraction is due to co-precipitation or adsorption on precipitated iron oxides or Fe-oxyhydroxides (Al-Abed *et al*., 2006, Van der Hoek and Comans, 1996). Al-Abed *et al*. (2007) further acknowledged similarity in the As and Fe leaching profiles suggesting that the release of As was related to the dissolution of Fe in the low pH region. On the other hand, low relative abundance of As, Se and Mo in the Fe and Mn fraction of 1-year-old ash cores might possibly be due to alkaline nature of the fly ash. It has been proven that low metal leaching is possibly due to high pH resulting in low contamination of leachate or metal immobilization (Ugurlu, 2004, Al-Abed *et al*., 2006). Boron is below the detection limit in the Fe and Mn fraction of 1-year-old ash cores. Conversely, significantly high percentage of Cr is recorded in the Fe and Mn fraction of 1-year-old ash cores suggests that it could be easily released through reduction process.

8.3.4 Residual fraction

Metals in the residual fraction are safer for the environment owing to their lowest mobility and bioavailability. Primary and secondary mineral-containing metals in the crystalline lattice comprise the bulk of residual fraction (Gulmini *et al*., 1994). To extract elements in residual fraction is more difficult, because the structure of the crystalline lattice must be destroyed sufficiently by very strong acid or alkali (Yuan, 2009). The content of these metals in the residual fraction of the ash is significantly different. The percentage leached in the residual fraction of 1-yr-old ash cores has the following order; B (30.63-97.36 %) > Pb (9.09-79.46 %) > Cr (4.77-66.59 %) > As (2.84-43.51 %) > Mo (1.72-28.55%). Most of the B content was encountered in the residual fraction; it is assumed that this fraction was embedded in the mineral matrix of the 1-year-old ash core samples. A significant percentage of B and Pb are concentrated in the residual fraction of 1-year-old ash cores. This suggests that under natural settings, these metals will not be released in solution over a reasonable time span therefore they are not considering as environmental risk. This trend is in general agreement with the previous study on the chemical partitioning of Pb in coal fly ash. Wadge *et al*. (1987) established that approximately all the Pb content (98 %) was encountered in the residual fraction of coal fly ash and it was supposed that this fraction was entrenched in the mineral matrix. In this study Cr were mostly associated with the residual fraction of coal ash, this observation is consistent with the previous study on the Cr mobility in coal fly ash (Socˇo and Kalembkiewicz, 2009; Smichowski *et al*., 2008). Selenium showed moderately high concentration in the residual

fraction of 1-year-old ash cores. At the same time, molybdenum showed significantly low concentration in residual fraction of 1-year-old ash cores. A remarkable percentage of As is recorded in the residual fraction of 1-year-old ash cores. This suggests that under natural conditions As could only be release into the ground water underneath the ash dump over a reasonable time span.

8.4 Fractionation scheme and efficiency of fractionation for trace elements

Table 8.2 shows the statistical analysis for each element and the percent recovery descriptive statistics for each element. These analyses were performed to verify the accuracy of the analytical protocols. The one year old fly ash core which revealed highest concentration for the toxic metals investigated is used for statistical assessment of fractionation efficiency**.** Statistical analysis was carried out using SAS 9.2 (SAS Institute Inc. Cary, NC. USA), the output results are indicated in Table 8.2.

Table 8.2. Statistical analysis of five fractions in 25 sub samples from 1-year-old ash

COD descriptive statistics for each element						
Element	N Obs	Mean	Median	Stdv.Dev.	Mininum	Maximum
Arsenic	600	0.28	0.27	0.13	0.02	0.70
Boron	600	0.42	0.27	0.18	0.04	0.82
Chromium	600	0.28	0.28	0.13	0.04	0.68
Lead	600	0.38	0.40	0.16	0.03	0.73
Molybdenum	600	0.28	0.27	0.13	0.04	0.68
Selenium	600	0.14	0.15	0.06	0.00	0.28
Percent recovery descriptive statistics for each element						
Element	N Obs	Mean	Median	Stdv.Dev.	Mininum	Maximum
Arsenic	25	38.76	38.27	15.61	12.36	81.67
Boron	25	57.54	71.38	31.77	0.43	95.42
Chromium	25	19.66	16.08	15.86	7.48	82.31
Lead	25	74.39	72.86	16.22	51.49	116.88
Molybdenum	25	51.41	50.30	18.56	20.75	92.27
Selenium	25	25.47	24.91	13.09	8.12	76.98

The variations of elements concentration per fraction in the twenty five ash samples were assessed by means of the coefficient of divergence (COD). The COD is self normalizing. If two samples are similar in chemical composition the COD approaches zero, otherwise the COD approaches one (Smichowski *et al*., 2008). For the five fractions, we calculated 300 CODs

representing all possible combinations between the twenty-five ash samples. Table 8.1 presents the CODs for each toxic element, viz: As (COD=0.28±0.13), B (COD=0.42±0.18), Cr (COD=0.28±0.13), Pb (COD=0.38±0.16) and Mo (COD=0.28±0.13). This fact is corroborated with relatively high median value of COD for As (0.27±0.13), B (0.27±0.18), Cr (0.28±0.13), Pb (0.40±0.16) and Mo (0.27±0.13). The different leachability and COD observed for Cr and Pb in this study agreed with the work of (Bo'dog *et al*., 1999)].

Selenium has COD value of 0.14±0.06, indicating close similarities in the concentrations in the five fractions of the twenty-five ash samples. The low COD value of Se is corroborated with a low median value of COD (0.15±0.06). An overview of CODs values thus indicate that the concentrations of Se are rather closely similar in the five fractions considered in the twenty-five sub samples. Variations of As, B, Cr, Pb and Mo are most likely associated with minor variations in chemical composition of fly ash occasioned by the interactions of coal fly ash with carbon dioxide, atmospheric oxygen and percolated rain water. The fractionation scheme divided the total metal concentration in five partial concentrations (pseudo total); consequently the sum of five partial values of concentration (pseudo total) should coincide with the total metal concentration. The comparison between pseudo total concentration and the total metal concentration provides the performance of the extraction scheme. The control of efficiency in the sequential extraction procedure was defined in terms of the recovery.

All the recoveries were found to be good and acceptable considering the complexity of the matrix analyzed and the number of statistical manipulations performed.

The Table 8.2 compares the total content of each trace metal in the respective sample with the association of the trace element with the five fractions (namely water soluble fraction; exchangeable fraction, carbonate fraction, Fe and Mn and the residual fractions) tested. No marked differences were observed between the pseudo-total metal concentrations extracted with aqua regia and the sum of metals extracted by the sequential extraction procedure. Indicative of the good quality of the analytical work, the overall recovery rates (the sum of the four fractions expressed as percent of the independent total metal concentration) varied in the Pb (116.88 %) > B (95.42 %) > Mo (92.27 %) > Cr (82.31 %) > As (81.67 %) > Se (76.98 %). It should be noted that the trace elements partition between these different fractions to various extent

Table 8.3. Trace metals distribution in five step sequential scheme and total metal content in samples taken at various depths in 1 year old ash cores (*S1 = water soluble fraction, S2 = exchangeable fraction, S3 = carbonate fraction, S4 = iron and manganese fraction, S5 = residual fraction)*

1m depth												
Fractions	**As**	**As%**	**Se**	**Se%**	**Mo**	**Mo%**	**B**	**B%**	**Pb**	**Pb%**	**Cr**	**Cr%**
S1	0.0002±0.0003	1.37	0.0004±2.87E-05	9.77	0.0015±7.96E-06	19.76	0.037±0.00036	0.01	0.0001±9.11E-05	0.70	0.0076±4.05E-05	6.85
S2	0.0039±0.0007	26.62	0.0021±0.0003	51.32	0.0013±0.0002	17.13	12.651±0.0002	4.10	0.0000	0.08	0.0070±0.0008	6.31
S3	0.0029±0.0003	19.80	0.0013±0.0003	31.77	0.0008±6.82E-05	10.54	163.35±0.0001	5.88	0.0015±0.0003	10.49	0.0103±0.0002	9.28
S4	0.0012±0.0002	0.08	0.0004±7.8E-05	9.77	0.00045±7E-05	5.93	0.0000	0.00	0.0013±7.6E-05	9.09	0.0121±0.0004	10.90
S5	0.0063±0.0097	0.43	0.0000	0.00	0.0035±0.0044	46.11	277.64±0.0002	90.01	0.0114±0.015	79.75	0.0739±0.096	66.59
Pseudototal (mg/kg)	0.0146		0.0041		0.0076		308.4745		0.0143		0.1110	
Total metal content(mg/kg)	0.0156±0.0001		0.0046±3.3E-05		0.0083±0.0001		337.55±0.0003		0.0158±0.0002		0.1209±0.0001	
Variability (%)	5.93		9.96		8.93		8.61		9.61		8.17	
3m depth												
Fractions	**As**	**As%**	**Se**	**Se%**	**Mo**	**Mo%**	**B**	**B%**	**Pb**	**Pb%**	**Cr**	**Cr%**
S1	0.0004±0.0002	4.12	0.00055±0.0045	13.13	0.0017±0.0001	40.48	0.0400±0.0018	0.01	0.00018±0.0006	4.85	0.0105±0.0013	25.11
S2	0.0047±0.0001	48.45	0.0021±0.00019	50.12	0.0012±0.00034	28.57	13.79±0.00012	4.61	0.0000	0.00	0.0072±0.00012	17.22
S3	0.0029±0.00029	29.90	0.0013±0.0003	31.03	0.0008±0.00018	19.05	2.2574±0.0024	0.75	0.0014±0.0036	37.75	0.0097±0.0004	23.19
S4	0.0008±0.0019	8.25	0.0002±0.00012	4.77	0.00026±0.00012	6.19	0.0000	0.00	0.00102±0.00031	27.50	0.0079±0.00013	18.89
S5	0.0009±0.0004	9.28	0.000	0.00	0.00028±0.0003	6.67	283.049±0.0035	94.62	0.00116±0.00056	31.27	0.0066±0.00045	15.78
Pseudototal (mg/kg)	0.0000		0.0042		0.0042±0.00012		299.1324		0.0037		0.0418	
Total metal content(mg/kg)	0.010584±0.0018		0.0045±0.0002		0.0046±0.0013		323.425±0.00034		0.00401±0.00013		0.0462±0.00031	
Variability (%)	6.65		6.92		9.37		7.51		7.51		9.37	
5m depth												
Fractions	**As**	**As%**	**Se**	**Se%**	**Mo**	**Mo%**	**B**	**B%**	**Pb**	**Pb%**	**Cr**	**Cr%**
S1	0.5742±0.0057	97.62	0.0005±2.4E-05	9.62	0.0010±2.9E-05	12.82	0.0381±0.0014	9.98E-05	0.0002±0.0018	1.48	0.0055±0.0002	8.13
S2	0.004±0.0003	0.68	0.0025±0.0004	48.08	0.0012±9.3E-05	15.38	178.65±0.0001	4.68E-01	0.000	0.00	0.0067±0.0004	9.90
S3	0.0030±0.0005	0.51	0.0019±0.00045	36.54	0.0009±7.6E-05	11.54	73.41±0.00032	1.92E-01	0.0015±1.9E-05	11.07	0.00039±0.00014	0.58
S4	0.0009±0.0009	0.15	0.0003±7.6E-06	5.77	0.00018±3.5E-05	2.31	0.000	0.0E+00	0.00095±0.0003	7.01	0.0065±0.0015	9.60
S5	0.0061±0.0079	1.04	0.000	0.00	0.0045±0.0065	57.69	37919.71±0.0001	9.93E+01	0.0109±0.0145	80.44	0.0486±0.059	71.80
Pseudototal (mg/kg)	0.588		0.0052		0.0078		38171.81		0.01355		0.06769	
Total metal content(mg/kg)	0.6252±0.00013		0.0058±0.0002		0.0085±0.0013		39102.32±0.0003		0.01423±0.0003		0.069±0.0004	
Variability (%)	5.89		10.34		8.47		2.38		4.78		2.49	
7m depth												
Fractions	**As**	**As%**	**Se**	**Se%**	**Mo**	**Mo%**	**B**	**B%**	**Pb**	**Pb%**	**Cr**	**Cr%**
S1	0.00259±0.0036	14.24	0.0016±0.002	35.63	0.0055±0.00031	46.45	0.158496±0.207	0.0004	0.00081±0.0011	3.95	0.0309±0.041	24.66
S2	0.0045±0.0006	24.74	0.0019±0.0003	42.32	0.001±0.00013	8.45	158.93±0.00012	0.40	0.000	0.00	0.0062±0.0002	4.95
S3	0.0023±0.00026	12.64	0.00084±2.7E-05	18.71	0.00054±0.0005	4.56	0.000	0.00	0.0012±7.5E-06	5.85	0.0069±0.00085	5.51
S4	0.0007±0.00015	3.85	0.00015±5.9E-05	3.34	0.0002±3.5E-05	1.69	0.000	0.00	0.0009±0.00025	4.39	0.0062±0.0014	4.95
S5	0.0081±0.0103	44.53	0.000	0.00	0.0046±0.0059	38.85	39422.29±0.00013	99.60	0.0176±0.023	85.81	0.0751±0.086	59.94
Pseudototal (mg/kg)	0.01819		0.00449		0.01184		39581.38		0.02051		0.1253	
Total metal content(mg/kg)	0.0194±0.0108		0.0049		0.0130±0.0012		40010.01±0.0023		0.02201±0.00015		0.1322±0.00031	
Variability (%)	6.35		8.41		9.08		1.07		6.82		5.22	
9m depth												
Fractions	**As**	**As%**	**Se**	**Se%**	**Mo**	**Mo%**	**B**	**B%**	**Pb**	**Pb%**	**Cr**	**Cr%**
S1	0.00076±4E-05	0.05	0.00045±8.1E-05	11.00	0.0013±6.7E-05	0.25	0.0465±0.0015	0.0001	0.0002±4.96E-05	1.20	0.0045±0.0002	4.57
S2	0.0053±0.0005	0.35	0.0025±0.002	61.12	0.0015±0.0002	0.28	222.94±0.00019	0.68	0.000	0.00	0.0052±0.0008	5.28
S3	0.0022±0.0005	0.14	0.00093±6.2E-05	22.74	0.0005±0.0001	0.09	0.000	0.00	0.0015±0.0003	8.98	0.0084±0.0016	8.54
S4	1.517±0.0015	98.86	0.00021±3.9E-05	5.13	0.5193±0.0001	98.39	0.000	0.00	0.0018±0.00026	10.78	0.0146±0.004	14.84
S5	0.0093±0.0122	0.61	0.000	0.00	0.00514±0.0076	0.97	32649.41±0.00012	99.32	0.0132±0.0152	79.04	0.0657±0.075	66.77
Pseudototal (mg/kg)	1.53456		0.00409		0.5278		32872.3965		0.0167±0.0013		0.0984	
Total metal content(mg/kg)	1.632±0.0002		0.0043±0.0001		0.5431±0.0001		33997.23±0.0012		0.01811±0.0061		0.10311±0.023	
Variability (%)	5.98		5.1		2.82		3.31		7.79		4.57	

Table 8.3 contd. Trace metals distribution in five step sequential scheme and total metal content in samples taken at various depths in 1-year-old ash cores (*S1 = water soluble fraction, S2 = exchangeable fraction, S3 = carbonate fraction, S4 = iron and manganese fraction, S5 = residual fraction).*

12m depth												
Fractions	**As**	**As%**	**Se**	**Se%**	**Mo**	**Mo%**	**B**	**B%**	**Pb**	**Pb%**	**Cr**	**Cr%**
S1	0.0002±2.47E-05	1.40	0.00037±6.25E-05	7.31	0.0013±4.49E-05	33.85	0.0471465±0.00024	0.0002	0.00032±0.0003	2.38	0.0029±0.00014	3.56
S2	0.0019±0.00045	13.28	0.0018±0.0012	35.57	0.00098±0.00012	25.52	173.24025±0.0003	0.67	0.000018±0.00012	0.13	0.00312±0.0005	3.83
S3	0.0025±0.00013	17.47	0.0026±1.3E-05	51.38	0.00075±2.4E-05	19.53	282.317±0.0014	1.08	0.0017±0.00014	12.63	0.0098±0.0004	12.02
S4	0.00081±0.0004	5.66	0.00029±7.1E-05	5.73	0.00021±5.4E-05	5.47	0.000	0.00	0.00083±0.00014	6.17	0.0097±0.0034	11.90
S5	0.0089±0.0097	62.19	0.000	0.00	0.0006±0.00002	15.63	25584.24±0.00013	98.25	0.01059±0.0131	78.69	0.056±0.068	68.69
Pseudototal (mg/kg)	0.01431		0.00506		0.00384		26039.84±0.0017		0.013458		0.08152	
Total metal content(mg/kg)	0.0146±0.0001		0.00561±0.008		0.0039±0.0013		26532.94±0.0003		0.0142±0.00132		0.0904±0.0012	
Variability (%)	2.06		9.8		3.03		1.86		5.42		9.85	
15m depth												
Fractions	**As**	**As%**	**Se**	**Se%**	**Mo**	**Mo%**	**B**	**B%**	**Pb**	**Pb%**	**Cr**	**Cr%**
S1	0.0003±1.8E-05	1.83	0.0003±5.9E-05	7.52	0.00091±4.4E-05	12.47	0.0342±0.0017	7.4E-05	0.0001±7E-06	0.55	0.0028±3E-05	2.96
S2	0.0028±0.0015	17.07	0.0018±0.0008	45.11	0.0011±0.0003	15.07	205.409±0.00012	0.44	0.000014±0.0002	0.08	0.0038±0.0014	4.01
S3	0.0029±0.0007	17.68	0.0017±0.0003	42.61	0.00087±0.00024	11.92	205.409±0.0023	0.44	0.0018±0.00012	9.94	0.0089±0.0011	9.40
S4	0.0003±3.9E-06	1.83	0.00019±2E-05	4.76	0.00022±1.4E-06	3.01	0.000	0.00	0.00029±2.4E-05	1.60	0.0069±0.0002	7.29
S5	0.0101±0.014	61.59	0.000	0.00	0.0042±0.0062	57.53	45750.54±0.0002	99.11	0.0159±0.012	87.83	0.0723±0.093	76.35
Pseudototal (mg/kg)	0.0164		0.00399		0.0073		46161.3922		0.018104		0.0947	
Total metal content(mg/kg)	0.0170±0.0011		0.0042±0.002		0.0081±0.008		47351.432±0.001		0.0192±0.0016		0.1019±0.0091	
Variability (%)	3.77		4.33		9.87		2.51		5.80		7.09	
18m depth												
Fractions	**As**	**As%**	**Se**	**Se%**	**Mo**	**Mo%**	**B**	**B%**	**Pb**	**Pb%**	**Cr**	**Cr%**
S1	0.00035±3E-05	2.45	0.0004±5.7E-05	9.73	0.0014±3.5E-05	21.91	0.0342±0.0017	0.0001	0.00011±4E-05	0.74	0.0032±0.0003	3.35
S2	0.00271±0.0001	19.00	0.0016±0.0009	38.93	0.0011±0.0004	17.21	154.067±0.00012	0.60	0.000	0.00	0.0032±0.0009	3.35
S3	0.0033±0.00089	23.14	0.0018±0.0003	43.80	0.00077±0.00017	12.05	237.979±0.0019	0.93	0.0013±4.2E-05	8.79	0.0086±0.001	9.01
S4	0.0006±0.0004	4.21	0.00031±0.00015	7.54	0.00022±7E-05	3.44	0.000	0.00	0.00058±0.0005	3.92	0.0112±0.0064	11.74
S5	0.0073±0.0088	51.19	0.000	0.00	0.0029±0.0039	45.38	25130.193±0.0001	98.46	0.0128±0.016	86.54	0.0692±0.0876	72.54
Pseudototal (mg/kg)	0.01426		0.00411		0.00639		25522.27		0.01479		0.0954	
Total metal content(mg/kg)	0.0156±0.0081		0.0045±0.0012		0.0071±0.0012		26832.28±0.001		0.01567±0.0012		0.1034±0.0034	
Variability (%)	8.66		8.69		10.01		4.88		5.61		7.74	
22m depth												
Fractions	**As**	**As%**	**Se**	**Se%**	**Mo**	**Mo%**	**B**	**B%**	**Pb**	**Pb%**	**Cr**	**Cr%**
S1	0.0003±2.9E-05	1.79	0.0004±1.9E-05	7.31	0.00091±3.8E-05	14.26	0.0366±0.0007	0.0001	0.00017±9.9E-05	0.96	0.0054±0.0002	6.69
S2	0.0042±0.0004	25.00	0.0032±0.0003	58.50	0.0013±0.0002	20.38	284.96±0.0031	0.99	0.000	0.00	0.0088±0.0009	10.90
S3	0.0027±0.0001	16.07	0.0016±8.3E-05	29.25	0.00089±5.7E-05	13.95	284.96±0.0018	0.99	0.000	0.00	0.0099±0.0003	12.27
S4	0.0005±0.0003	2.98	0.00027±7E-06	4.94	0.00017±2.4E-05	2.66	0.000	0.00	0.0012±0.0012	6.79	0.0056±0.0015	6.94
S5	0.0091±0.0123	54.17	0.000	0.00	0.00311±0.005	48.75	28157.93±0.0011	98.02	0.0163±0.022	92.25	0.051±0.064	63.20
Pseudototal (mg/kg)	0.0168		0.00547		0.00638		28727.88		0.01767		0.0807	
Total metal content(mg/kg)	0.01822±0.0012		0.0061±0.0013		0.0067±0.0016		29361.73±0.0123		0.01923±0.0023		0.0890±0.0091	
Variability (%)	7.79		10.65		4.95		2.16		8.11		9.34	
27m depth												
Fractions	**As**	**As%**	**Se**	**Se%**	**Mo**	**Mo%**	**B**	**B%**	**Pb**	**Pb%**	**Cr**	**Cr%**
S1	0.0003±6.6E-05	1.89	0.0004±2.6E-05	10.0	0.0008±4.6E-05	11.71	0.0332±0.0017	0.0001	0.0006±0.0008	3.64	0.0061±0.006	8.80
S2	0.0028±0.0021	17.61	0.0016±0.012	40.0	0.0009±0.0007	13.18	250.47±0.0001	1.03	0.000	0.00	0.0058±0.0044	8.37
S3	0.0028±0.0003	17.61	0.0018±0.0004	45.0	0.0011±0.0001	16.11	139.61±0.0013	0.58	0.0026±0.0013	15.76	0.012±0.0008	17.32
S4	0.0028±0.0003	17.61	0.0002±3.4E-05	5.0	0.00013±3.9-05	1.90	0.000	0.00	0.0009±0.001	5.45	0.0048±0.0025	6.93
S5	0.0072±0.0094	45.28	0.000	0.00	0.0039±0.0057	57.10	23838.76±0.0002	98.39	0.0124±0.015	75.15	0.0406±0.048	58.59
Pseudototal (mg/kg)	0.0159		0.004		0.00683		24228.8732		0.0165		0.0693	
Total metal content(mg/kg)	0.0173±0.0012		0.0045±0.0012		0.00693±0.0034		25229.88±0.0023		0.0173±0.0013		0.075±0.0123	
Variability (%)	8.09		6.97		1.44		3.97		4.62		7.6	

(see Figures 8.16 and 8.17) and the associated mineral phase will determine the relative mobility or immobility of the element. There is variability (within 10 %) between sum of values obtained for different fractions (pseudo-total concentration) of As, B, Cr, Pb, Mo and Se and values obtained for the same sample extracted with total acid digestion (total metal concentration) (see Table 8.1).

8.5 Trace element patterns by age and depth of dry disposed fly ash

Table 8.4 shows the Spearman correlation coefficient (at 0.01 level significance) with the associated probability values of trace elements such as As, Mo, B and Pb by depth of dry disposed ash cores of different ages. The concentration trend of As showed negative strong correlation coefficient (*rho = -0.827 and p-values = <.0001*) with depth in the Fe and Mn fraction of 1-year-old dry disposed ash cores. This connotes decrease response with increase depth in the Fe and Mn fraction solubility of 1-year-old ash cores.

Table 8.4. Relationship of trace elements in different solubility with depth of weathered dry disposed ash cores

Spearman's correlation (Only correlations that are significantly different from 0 at the 0.01 level)										
Obs	Age	Solubility	Variable	As	Se	Mo	Cr	Pb	B	
1	1	Carbonate	Depth	-	-	0.56538	-	0.57846	-	
2	1	Exchangeable	Depth	-	-	-	-	-	0.55195	
3	1	Fe and Mn	Depth	-0.82722	-	-0.7437	-0.7109	-0.5799	-	
4	8	Carbonate	Depth	-	-	-	-	0.69231	-	
5	8	Exchangeable	Depth	-	-	-	-	-	-	
6	8	Water soluble	Depth	-	-	-	-	-	-	
7	20	Carbonate	Depth	-	-	-	-	-	-	
8	20	Exchangeable	Depth	-	-	-	-	-	-	
9	20	Fe and Mn	Depth	-	-	-	-	-	-	
10	20	Residual	Depth	-	-	-	-	-	-	
11	20	Water soluble	Depth	-	-	-	-	-	-	
Probability (p-values)										
Obs	Age	Solubility	Variable	PAs	PSe	PMo	PCr	PPb	PB	small p
1	1	Carbonate	Depth	-	-	0.0032	-	0.0025	-	0.00245
2	1	Exchangeable	Depth	-	-	-	-	-	0.0095	0.00107
3	1	Fe and Mn	Depth	<.0001	-	<.0001	0.0002	0.0047	-	2.1E-06
4	8	Carbonate	Depth	-	-	-	-	0.0087	-	1.4E-05
5	8	Exchangeable	Depth	-	-	-	-	-	-	0.00072
6	8	Water soluble	Depth	-	-	-	-	-	-	0.0037
7	20	Carbonate	Depth	-	-	-	-	-	-	0.00998
8	20	Exchangeable	Depth	-	-	-	-	-	-	0.00089
9	20	Fe and Mn	Depth	-	-	-	-	-	-	0.00998
10	20	Residual	Depth	-	-	-	-	-	-	0.0041
11	20	Water soluble	Depth	-	-	-	-	-	-	0.00527

**PAs= P-value associated with Spearman's rho correlation for arsenic.*

The concentration trend of Mo by depth showed a clear dissimilarity in both the carbonate, and Fe and Mn fractions of 1-year-old dry disposed ash cores. In the carbonate fraction, it shows strong correlation (*rho = 0.565 and p-value = 0.0032*) indicating increasing response with increasing depth of the 1-year-old dry disposed ash cores. This result suggests that dissolution of carbonate phase of 1-year-old ash cores due to considerable reduction in ash pore water pH. This has led to significant increase in concentration of As at deeper section of the dry disposed ash dump. The molybdenum concentration trend by depth in the Fe and Mn fraction showed negative correlation (*rho = -0.7437 and p-value = <.0001*) indicates decrease concentration trend with increase in depth of 1-year-old dry disposed fly ash due to overtime erosion. The concentration trend of Cr in Fe and Mn fraction, showed negative correlation (*rho = -0.7109 and p-value = 0.0002*) indicate a decrease in concentration with the corresponding increase in depth of 1-year-old dry disposed ash cores. Similarly, the concentration trend of Pb in the Fe and Mn fraction showed negative correlation (*rho = -0.5799 and p-value = 0.0047*) suggests decrease concentration with the corresponding increase in the depth of 1-year-old dry disposed ash cores. This suggests co-precipitation and adsorption of As, Cr, Pb and Mo by amorphous Fe-oxyhydroxide phase (i.e. less soluble secondary phase); thereby making these metals less available in the 1-year-old dry disposed ash cores.

In the carbonate fraction, the concentration of Pb showed strong correlations with depth in the 1-year-old (*rho = 0.5778 and p-value = -0.0025*) and 8-year-old ash cores (*rho = 0.6923 and p-value = 0.0087*) ash cores. These indicate increase concentration trends of Pb in the carbonate fractions of 1-year-old and 8-year-old ash cores with increase depth. This suggests carbonate phase dissolution due to reduction in pore water pH and subsequent transport by percolating rain water. This result trend is in general agreement with the previous study conducted on pulverized fuel ash by Lee and Spears (1997). The concentration trend of B in the exchangeable fraction showed strong correlation (*rho = 0.552 and p-value = 0.0095*) indicate increase concentration trend with increase in the depth of 1-year-old dry disposed fly ash. This result trend is in general agreement with the work conducted on pulverized fuel ash by Lee and Spears (1997).

The concentration trend of B in the exchangeable fraction showed strong correlation (*rho = 0.552 and p-value = 0.0095*) indicate increase concentration trend with increase in the depth of 1-year-old dry disposed fly ash. The result trends of Pb and B in the carbonate and exchangeable

fraction show that weathering/ageing could lead to the dissolution of carbonate and exchangeable fractions of ash cores; and subsequent transport with infiltrating rain water which in fact led to the concentration increase at the deeper section of the dry disposed ash cores.

Table 8.4 shows evidence of trace elements concentration (As, Mo, B, Cr and Se) trends in different mineral associations with time (age). Trace metals such as As, B and Mo showed enrichment in the residual fractions (i.e. dust) of older ash. The nicest result is for As (*rawp=1.2E-05 and fdrp =0.00073*) in the residual fraction of coal fly ash of different ages. Figure 1 showed strong positive correlation of the As concentration in the residual fraction of dry disposed ash cores with age of ash cores.

Table 8.5. Relationship of trace elements in different solubility medium with depth of dry disposed ash cores

Cases with evidence of trend over time								
Obs	Solubility	Table	DF	Value	Prob	raw p	bon p	fdr p
1	Exchangeable	Summary for Age * As	1	16.5035	<.0001	4.9E-05	0.00364	0.00073
2	Fe and Mn	Summary for Age * As	1	7.4556	0.0063	0.00632	0.47429	0.01824
3	Residual	Summary for Age * As	1	19.2373	<.0001	1.2E-05	8.7E-05	0.00073
4	Carbonate	Summary for Age * B	1	62.593	0.0124	0.01236	0.92659	0.02888
5	Exchangeable	Summary for Age * B	1	14.0565	0.0002	0.00018	0.0133	0.00111
6	Fe and Mn	Summary for Age * B	1	17.8432	<.0001	2.4E-05	0.0018	0.00073
7	Residual	Summary for Age * B	1	8.4571	0.0036	0.00364	0.27272	0.0124
8	Exchangeable	Summary for Age * Cr	1	9.2455	0.0024	0.00236	0.17705	0.00984
9	Exchangeable	Summary for Age * Mo	1	6.4273	0.0112	0.01124	0.84283	0.02809
10	Residual	Summary for Age * Mo	1	15.4525	<.0001	8.5E-05	0.00635	0.00088
11	Water soluble	Summary for Age * Mo	1	8.0694	0.0045	0.0045	0.33765	0.01468
12	Fe and Mn	Summary for Age * Se	1	7.9868	0.0047	0.00471	0.3534	0.01473

raw p= p-value; bonp= adjusted p-value by Bonferroni method; fdrp= adjusted p-value by false discovery rate method.

This literally implies that arsenic concentration increase with the increasing age of the dry disposed ash cores. This offers a unique trend that could be used as a marker for environmental and ecotoxicological studies. This suggests that the over time chemical interaction of ash cores with ingress CO_2 and infiltrating rain water which led to the transient secondary mineral formation (i.e. amorphous aluminosilicate) can caused co-precipitation and adsorption of arsenic in the coal fly ash. Thus, limits the mobility of the arsenic in the dry disposed ash cores.

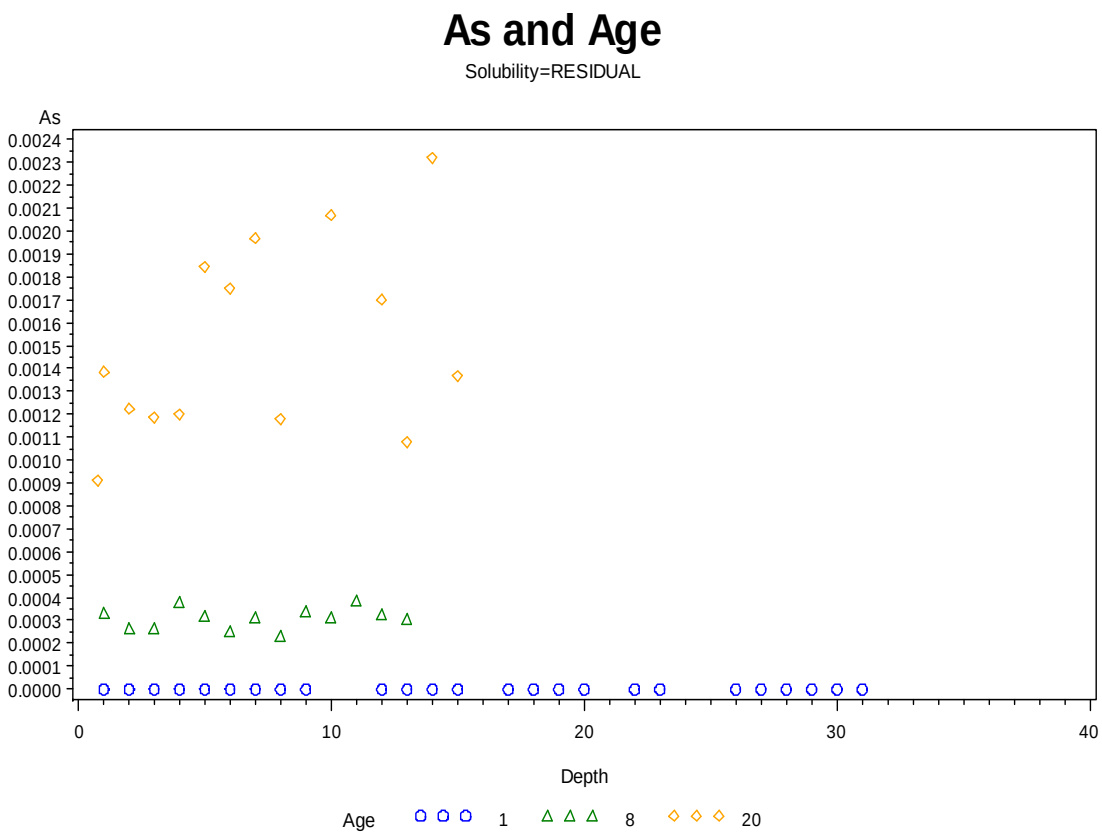

Figure 8.18. Relationship of As in residual fractions with the age of dry disposed ash cores.

This suggests that the older ash cores has propensity to have high concentration of arsenic than relatively young ash cores.

8.6 Summary and conclusions

The study has revealed that the mobility of toxic elements in ash cores do not only depend on the concentration, mode of occurrence but also on the chemical interactions of fly ash with ingressed CO_2, atmospheric oxygen and percolated rain water (which leads to pH variations in the ash profile). The following preliminary conclusions could be drawn from the study, for selected toxic elements in Tutuka fly ashes subjected to dry disposal.

- The leaching profile of the analytes in water soluble and exchangeable fractions (except Cr) of ash dump cores showed relatively higher concentration in 1-year-old ash cores. Low concentration in soluble fractions of these metals in older ashes could be due to co-

precipitation with secondary mineral phase (e.g. calcite and mica) that can capture metals from the pore water system of the ash cores.

- Statistical evaluation (CODs) showed that the extractability of the toxic elements from the five fractions of the fly ashes proved to be different. Percentage recoveries for all the labile elements in the ash samples varied from Se (76.98%) to Pb (116.88%).
- The average amount of toxic elements in the five-fractions of the 1-year-old cores is as follows: water soluble: Mo (26.61%) > Cr (14%) > Se (9.82) > As (4.66%) > Pb (4.05%) > B (0.02%), exchangeable: Se (42.33%) > As (37.92%) > Mo (30.69%) > B (13.68%) > Cr (15.86%) > Pb (1.31%), carbonate: Pb (47.05%) > Se (43.88%) > As (39.11%) > Cr (33.2%) > Mo (26.89%) > B (12.69%), iron and manganese: Cr (19.9%) > Pb (19.7%) > Mo (5.43%) > As (7.1%) > Se (4.58%) and residual: B (73.61%) > Pb (27.55%) > Cr (17.04%) > As (11.2%) > Mo (10.47%).
- The mobility and partitioning patterns of the toxic metals in the ash dumps showed that overtime, i.e. in the 8 year and 20-year-old ash cores, lower availability of toxic metals could indicate that the weathered dump may pose less of an environmental hazard to the environment than the 1-year-old ash cores, however, the fate of the elements that have already been lost to the environment from the ash during the aging process should be considered.
- The concentration of As in the residual fraction varied between 0.0003-0.00043 $mgkg^{-1}$ for 1-year-old ash cores to around 0.0003-0.0015 $mgkg^{-1}$ for 20-year-old ash cores. Thus 10.83 mass % of the total As was released from the residual fraction within 20 years of ash dumping. This showed that the older ash is enriched in arsenic; hence dust from the ash dump would be toxic to human health. This suggests that under the conditions normally found in nature, this metal will be released in solution over a reasonable time span (20 years). Nevertheless rapid release of arsenic from residual fraction could take place when dry disposed ash comes in contact with slightly acid rain hence it was considered as environmental risk.

- A modified sequential extraction scheme was not applied on multiple ash cores due to high cost of sample analysis.

CHAPTER NINE

Conclusions and Recommendations

This chapter summarizes the discussions, significant findings and conclusions of the results presented in the previous chapters. Recommendations for further research on some aspects are outlined.

9. Overview

This research has investigated the bulk chemistry, mineralogy, weathering patterns, chemical partitioning and mobility of inorganic elements, and acid susceptibility of dry disposed fly ash from Tutuka Power Station of different ages. In order to follow the alteration in the physico-chemical and mineralogical properties of fly ash during chemical weathering/ageing process, different analytical techniques were carried out as follows:

Both 2-week-old and weathered dry disposed ash cores were characterized with XRF, XRD, FT-IR and SEM/EDS techniques.

Weathering patterns in the ash dumps were investigated through comparison of pore water chemistry and triple acid leach (Total digestion method) of original ash core samples prior to the chemical sequential extraction scheme.

A comparison of the acid susceptibility of fresh ash versus of the weathered dry disposed ash core was investigated through the acid neutralization capacity (ANC) test.

The chemical partitioning and mobility of inorganic elements in dry disposed ash core was investigated and compared through the use of the modified sequential extraction scheme.

A general characterization of the weathered dry disposed fly ash was undertaking to ascertain the degree of weathering and its effect on the physico-chemical and mineralogical properties of dry disposed fly ash. Morphological and spectroscopic characterizations were used to determine the existence of microstructure and intrinsic properties of fresh ash and dry disposed ash cores. Procedures such as the modified chemical sequential extraction scheme and acid neutralisation capacity test (ANC) were applied to investigate the major and trace elements and mineralogical

phase distribution in dry disposed ash cores. In order to determine the major and toxic elements chemical partitioning, their mobility and their potential risk to surface and groundwater in the vicinity of the dry disposed ash dumps. The study has provided a platform for understanding various mechanisms that govern the release of inorganic elements in a dry disposed ash scenario based on a broad evaluation and comparison of mineralogy, bulk chemistry, morphology, spectroscopic acid susceptibility and chemical partitioning explored in this study.

9.1 Insight from physico-chemical and mineralogical analysis of weathered drilled ash cores

The characterization of fly ash is of importance because of the influence of its physical, chemical and mineralogical properties on the leachability of major and minor elements contained in it. The investigated ash dumps showed extreme in-homogeneity attributed to the ash type and texture. The in-homogenous irrigation of the ash dumps with high saline effluents (i.e. brine) was ascribed to variability in the moisture content levels of the ash cores. This heterogeneity nature of the ash dumps had a significant impact on the mobility of the elements in the ash dumps.

9.1.1 Pore water chemistry

The pH of the extracted pore water of the ash cores decreased over time due to carbonation and hydration process after disposal. Variation was observed in the pH values of pore water samples from various dry disposed ash core samples. This difference could be attributed to the variations in the concentrations of CaO, MgO, TiO_2 and Fe_2O_3 in the disposed fly ashes as confirmed by the XRF data. The analysis of extracted pore water also showed that several toxic elements, such as B, Cr, As, Mo, and Se, were soluble and leaching from the weathered ash over time. The core ash samples in contact with the atmosphere and those at the saturation point recorded the highest availability of soluble components, such as Mg, Ca, Fe, $K^{+,}$ $Na^{+,}$ B, Cr, As, Mo, and Se in pore water. Chloride and sulphate species in the pore water extract of weathered ash were at equilibrium with Na^+ and K^+ showed progressive leaching overtime. This positive correlation of Na^+ and K^+ in the easily mobilized fraction of dry disposed fly ashes suggests that these salts are readily dissolved and subsequently transported by infiltrating rain water. This implies that the dry disposed fly ashes are not holding salt (i. e. not a salt sink). This was further corroborated by the observed trend in the XRF results data.

9.1.2 Mineralogical composition by XRD/FTIR

XRD analysis of the dry disposed ash core samples indicated the complex nature of the fly ashes in terms of their mineralogical compositions. The major crystalline mineral phases of the Tutuka fly ashes of all ages were quartz (SiO_2) and mullite ($3Al_2O_3.2SiO_2$) with non-prominent peaks of lime (CaO), calcite ($CaCO_3$), mica, hematite (Fe_2O_3), enstatite, and anorthite. Apart from these phases, there could be other mineral phases that were not detected by XRD due to their low abundance or amorphous character or the masking effect of the crystalline mullite and quartz phases that are abundant in fly ash. The presence of minor phases in non-detectable concentrations or of amorphous nature could not be excluded. The XRD spectra do not revealed either small or abundant Na containing mineral phases like halite. The presence of minor amount of secondary minerals (i.e. calcite and mica) in all the weathered dry disposed ash core samples suggested the occurrence of hydration and carbonation processes at the ash dump site over time. This was attributed to ingress CO_2 causing chemical weathering due to reduction in pore water pH from 11.5-7.2 overtime. Nevertheless, FTIR analyses did not detect minor amount of secondary mineral phases in weathered dry disposed ash core samples. X-ray diffraction results showed significant loss of crystallinity in the weathered older ash cores. The mineralogy of the weathered ash cores did not reveal heterogeneity of mineral phases between the old ash cores. The mineral peak intensity by XRD showed variations in 1 year and 20-year-old ash cores which were ascribed to inhomogeneity of the ash dump in term of the texture, moisture content levels over time. The mineral peak intensity in the 8-year-old section of the ash dump showed anomalous trend which may be ascribed to in-homogenous brine irrigation. This showed that XRD analysis is not the best technique for detection of the mineralogical suite of ash dumps.

9.1.3 Elemental composition by XRF and total digestion

The total acid digestion and XRF analysis were carried out to evaluate the chemical compositions of the dry disposed ash cores from the Tutuka power station. Chemical compositional analyses revealed that selected, detected elements were present within the detectable limit (i.e. the concentrations of the elements detected in the fly ashes were high enough to be detected during analysis). The total acid digestion showed the relative concentration of major and trace elements in dry disposed ash cores. A large variability was observed showing ash core heterogeneity. Some of the major elements (i.e. Al, Si, Ca, Mg, Fe,

Mn, Na^+ and K^+) and trace elements (i.e. As, Se, Cr, Mo, B and Pb) showed enrichment or depletion in the dry disposed ash cores. The trends observed were mainly ascribed to extrinsic factors such as ash type, texture, moisture content levels and point of contact with groundwater. This observation was corroborated by the XRF analysis which showed depletion of soluble major components down the depth of ash dumps overtime.

It is noteworthy that the mass % of the major element Si varies through the depth of the core with an increase of nearly 3 %, to 58 mass % of SiO_2 at a depth of 6 m in the 1-year-old core whereas in the case of the 8-year-old core a 2 % increase of SiO_2 to a level of 57.5 mass % can be observed at levels between 4-8 m, showed dissolution of major components in the matrix of older ash cores.

Results of weathered ash cores showed SO_3 content varied 0.11-0.26% for 1-year-old ash cores to around 0.11-0.17% for 8-year-old ash cores. This showed that considerable leaching overtime of soluble salts (sodium sulphate) has taken place within 8 years of ash dumping.

Noticeable downward mobility of elements overtime was observed by X-ray fluorescence (XRF) for Ti, Mg, Al, S, Na^+, Si and Ca overtime was observed by XRF but K^+, Mn and Zn levels showed decreased down the depth of ash core. Trace metals such as Ni and Y downward mobility in the 1-year-old ash core whereas Ba, Pb, V, Sr and Cr decreased down the depth of ash core suggesting enrichment in surface layers of the 1-year-old ash core.

In the 1-year-old ash core, downward mobility of major elements such as Ti, K^+, Fe, Mg, Si, P and Ca was observed in the 20-year-old ash core. Whereas Al, Na^+ and Mn levels decrease down the depth of ash core indicate enrichment in surface layers due to loss of other major components from surface layers in the 20-year-old ash core. The trace metals such as Ba, Y and Zr showed considerable downward mobility (i.e. erosion overtime), but Ni, Sr, Pb, V, Cr and Co levels decrease down the depth of ash core suggest enrichment in surface layers of the 20-year-old ash core.

9.1.4 Morphology by SEM

The SEM micrograph of 2-week-old ash and 20-year-old ash core sample suggested that Tutuka fly ash particles were spherical in shape and also revealed some agglomerated particles. The

elemental composition by EDS quantitatively revealed that the elements in the fly ashes are predominantly Si, Al, Fe, Ca, Ba, K, C and O_2. The only trace element identified by EDS was barium; it was observed in only fresh ash sample typically associated with S and O_2. However, these elements identified by EDS cannot be conclusively used to identify the mineral compositions of the fly ashes due to the analysis volume limitations and contribution of signal from the underlying residual fly ash matrix. Thus EDS results are merely qualitatitive and allowed identification of major elements in micro regions of the ash. Thus specific microscopic morphological features could be associated with specific elements which might correspond with a mineral phase. The surface of the sphere as in the 2-week-old ash exhibits a smooth appearance produced by aluminosilicate glass but the 20-year-old core sample showed encrustation, etching and corrosion due to extensive weathering and alteration of ash morphology. The differences in the surface morphology observed between 2-week-old ash and 20-year-old ash core samples were in agreement with the XRD results, which confirmed the formation of small amounts of secondary mineral overtime in disposed ash core samples.

9.2 Acid susceptibility by ANC tests

The release of major and trace elements from weathered ash core samples did not only depend on mineralogy of the species in the fly ash, but also depended on other factors which included the pH of the ash/aqueous medium. The acid neutralisation capacity (ANC) tests were carried out on both fresh and 20-year-old unsaturated weathered core samples to determine the acid susceptibility, namely a change in the effect of pH on the release of elements from the fly ashes. The natural pH (pH of fresh ash in deionised water) of the Tutuka fresh fly ash was 11.5.

The ANC leaching test was not limited to leachant solutions of one particular pH value but considered the effect of leachant solutions of different final pH values on the leachability of elements from the fresh and unsaturated weathered core samples. This test was considered appropriate in determining the effect of leachant pH on the leachability of elements from fly ash since it evaluates the leachability of elements over a wide range of pH such as can be expected in the dry disposal scenario in the longer term. The concentration of major and trace elements such as Ca, Mg, Na, K, Se, Cr, and Sr increased in solution when pH was reduced. Thus, this showed that the mobility of these elements was pH dependent. Interestingly, trace elements such as Al, Mo, As and Pb exhibited maximum concentrations in leachates at intermediate pH values after

which reduction in their concentrations were observed at lower pH. This shows that the release of some of these elements was highest at intermediate pH values. The concentration of the major and trace elements found in ANC leachates of fresh ash were observed to be higher than the weathered unsaturated ash cores. This highlighted that long-term weathering led to the loss in concentration of these elements from weathered ash core samples.

The unsaturated weathered ashes showed lower buffering capacity at neutral pH (7.94-8.00) compared to unweathered (fresh) fly ash from the same power station. Thus, this shows that the formation of minor amount of secondary phases in weathered ash cores was due to chemical weathering which reduced its buffering capacity when compared to fresh ash. This was ascribed to the immediate initial high leaching/flushing of basic soluble buffering constituents such as CaO and MgO from fly ash at the dry disposal site at Tutuka within one year. The overall results of the acid susceptibility of the ash as determined by the ANC test suggests that both fresh ash and unsaturated weathered ashes will release a significant percentage of their elemental content when in contact with slightly acidic rain overtime. The ANC test revealed that as ash acidifies, higher concentrations of major and trace species would be released from fly ash and leaching was dependent on specific pH values. This shows that the acidification of the ash dump overtime could lead to considerable leaching of toxic elements into surface and groundwater in the vicinity of the ash dump. It is inevitable that ash pH will change overtime due to air pollution causing acid rain hence it can be expected that pH dependent leaching of numerous elements in ash will occur.

9.3 Mineralogical partitioning by chemical sequential extraction

A modified chemical sequential extraction was applied on the dry disposed weathered drilled ash core samples aged 1 year, 8 year and 20-year-old to determine mineralogical association of elements as a function of depth and age of ash dump. A modified chemical sequential extraction scheme was not applied on multiple ash cores due to high cost of sample analysis. The sequential extraction sequence includes water soluble, exchangeable, carbonate, Fe and Mn and residual fractions. The mineralogical partitioning of major and trace elements in various mineralogical fractions in weathered dry disposed ash core samples provided deep insight into various mechanisms that could affect mobility of elements from dry disposed weathered ash cores. A fairly high proportion of the average amount total Na^+ was contained in the water soluble

fraction (21%) of 1-year-old ash cores. Sodium concentration in the water soluble fraction showed a maximum of 878.82 mg kg^{-1} for 1-year-old ash cores to a maximum of 329.14 mg kg^{-1} for 20-year-old ash cores. This suggests that the 20-year-old ash is depleted in Na due to percolating rain water that dissolved and acts as a medium of transportation. The readily dissolved Na^+ may be in form of halite (NaCl) or sodium sulphate in the ash cores but the XRD analysis does not detect the presence of halite in the 1-year-old ash cores. Small proportion of average amount total Na^+ is contained in the exchangeable (11.26%), carbonate (2.6%) and Fe and Mn fractions (4.7%) of 1-year-old ash cores. Sodium concentration in the exchangeable fraction showed a maximum of 375.98 mg kg^{-1} for 1-year-old ash cores to a maximum of 169.94 mg kg^{-1} for 20-year-old ash cores. The Na^+ concentration in the carbonate fraction showed a maximum of 77.62 mg kg^{-1} for 1-year-old ash cores to a maximum of 11.40 mg kg^{-1} for 20-year-old ash cores. Sodium concentration in the Fe and Mn fraction showed a maximum of 16.52 mg kg^{-1} for 1-year-old ash cores to a maximum of 11.4 mg kg^{-1} for 20-year-old ash cores. These suggest that Na^+ is depleted in the exchangeable, carbonate fraction and Fe and Mn fractions of 20-year-old ash cores. Large proportion of average amount of total Na^+ was contained in the residual fraction (53.9%) of the 1-year-old ash cores. Sodium concentration in the residual fraction showed a maximum of 2704.41 mg kg^{-1} for 1-year-old ash cores to a maximum of 1083.48 mg kg^{-1} for 20-year-old ash cores. This moderately high proportion of total Na^+ in the residual fraction suggests they are present/exists in the less soluble phase.

Sodium showed depletion at the surface in the water soluble fraction of the 1 year, 8 year and 20-year-old ash cores highlighting mobility. However, sodium in the water soluble fraction showed enrichment/accumulation at the middle and bottom sections of the 3 drilled ash cores. Similar depletion/enrichment trend of Na^+ was observed in the exchangeable and carbonate fractions of 3 drilled ash cores. The vertical distribution pattern of Na^+ in the Fe and Mn and residual fractions is age dependent. The distribution pattern of Na^+ in the two fractions (Fe and Mn, and residual fractions) of 20-year-old ash showed depletion trend at the top section (surface) of the ash cores whereas enrichment/accumulation of Na^+ was observed at the bottom section. Sodium vertical distribution in the 1 year and 20-year-old ash cores showed incoherent enrichment and depletion patterns. The older ash core samples are depleted in Na^+ in the five extraction fractions when compared with relatively young ash core samples.

The proportion of average amount of total Ca contained in the water soluble fraction of 1-year-old ash core was 10.2%. This is the amount of Ca associated with minerals in the 1-year-old ash cores which can be readily dissolved by percolating water. Calcium concentration in the water soluble fraction showed a maximum of 2936.88 mg kg^{-1} for 1-year-old ash cores to a maximum of 1333.71 mg kg^{-1} for 20-year-old ash cores. This suggests relative depletion of Ca in the water soluble fraction 20-years-old ash cores due to chemical weathering. The exchangeable (37.04%) and carbonate (37.9%) fractions contained a somewhat high proportion of total Ca in the 1-year-old ash cores. Calcium concentration in the exchangeable fraction showed a maximum of 12145.99 mg kg^{-1} for 1-year-old ash cores to a maximum of 10328.26 mg kg^{-1} for 20-year-old ash cores. Calcium concentration in the carbonate fraction showed a maximum of 8862.76 mg kg^{-1} for 1-year-old ash cores to a maximum of 3437.88 mg kg^{-1} for 20-year-old ash cores. Calcium showed relative depletion in the exchangeable and carbonate fractions of 20-year-old ash cores due to chemical weathering. Calcium existed in the form of carbonate (calcite) and aluminosilicate (mica) minerals in the 1-year-old ash cores as revealed by XRD analysis. Considerable low proportion of average amount of total Ca in 1-year-old ash core was associated with Fe and Mn (7%) and residual (2.97%) fractions. Calcium concentration in the Fe and Mn fraction showed a maximum of 2051.22 mg kg^{-1} for 1-year-old ash cores to a maximum of 3437.88 mg kg^{-1} for 20-year-old ash cores. The calcium concentration in the residual fraction showed a maximum of 670.40 mg kg^{-1} for 1-year-old ash cores to a maximum of 1229.32 mg kg^{-1} for 20-year-old ash cores. These suggest enrichment in the Fe and Mn, and residual fractions of 20-year-old ash cores. This enrichment is attributed to formation of minor secondary phases (e.g. amorphous Fe-oxyhydroxides and amorphous aluminosilicate phases).

The vertical distribution pattern of Ca in the water soluble fraction of 3 drilled ash cores is age dependent. The enrichment of Ca in the water soluble fraction was observed in the surface of 1 year and 8-year-old ash cores whereas 1-year-old ash cores showed depletion trend. Calcium in the exchangeable and carbonate fractions showed depletion at the surface but a relative enrichment trend was observed at the bottom sections of the 3 drilled ash cores. The vertical distribution of calcium in the Fe and Mn fraction and residual fraction is age dependent. However, enrichment of Ca in the Fe and Mn fraction was observed in the middle sections of 3 drilled ash cores. Calcium in the residual fraction showed enrichment at the bottom sections of 8

year and 20-year old ash cores whereas enrichment of Ca was observed at the surface of 1-year-old ash cores.

The proportion of average amount of total As contained in the water soluble fraction of 1-year-old ash cores was 4.66%. This represents the amount of As associated with the readily dissolved salts in the 1-year-old ash cores. Arsenic concentration in the water soluble fraction showed a maximum of 0.00046 mg kg^{-1} for 1-year-old ash cores to a maximum of 0.00029 mg kg^{-1} for 20-year-old ash cores. Moderately high proportion of total As was contained in the exchangeable (37.92%) and carbonate (39.11%) fractions of 1-year-old ash cores. Arsenic concentration in the exchangeable fraction showed a maximum of 0.0043 mg kg^{-1} for 1-year-old ash cores to a maximum of 0.002 mg kg^{-1} for 20-year-old ash cores. The As concentration in the carbonate fraction showed a maximum of 0.0043 mg kg^{-1} for 1-year-old ash cores to a maximum of 0.0022 mg kg^{-1} for 20-year-old ash cores. These suggest the depletion of As in the water soluble, exchangeable and carbonate fractions of 20-year-old ash cores due to chemical weathering. Considerably low proportion of average amount of total As was contained in the Fe and Mn (7.1%) and residual (11.2%) fractions of 1-year-old ash cores. Arsenic concentration in the Fe and Mn fraction showed a maximum of 0.00076 mg kg^{-1} for 1-year-old ash cores to a maximum of 0.0022 mg kg^{-1} for 20-year-old ash cores. The As concentration in the residual fraction (non leachable portion) showed a maximum of 0.00043 mg kg^{-1} for 1-year-old ash core to a maximum of 0.0015 mg kg^{-1} for 20-year-old ash core. These suggest enrichment of the As in the Fe and Mn, and residual fraction of 20-year-old ash cores.

Arsenic in the water soluble fraction showed enrichment at the middle sections of the 3 drilled ash core but depletion trend was observed at the top and bottom sections. The vertical distribution of As in the exchangeable and carbonate fractions is age dependent. Arsenic in the exchangeable and carbonate fractions showed enrichment trend at the middle sections whereas depletion was observed at the surface and bottom sections of the 3 drilled ash cores. Arsenic in the Fe and Mn and residual fractions showed enrichment at the middle section but depletion trend was observed at the surface and bottom sections of 3 drilled ash cores. Arsenic in all the five extraction fractions showed relative enrichment in the older ash cores.

The proportion of average amount of total Se contained in the water soluble fraction of 1-year-old ash cores was 9.82%. This the amount of Se associated with the readily dissolved salts in the

1-year-old ash cores. Selenium concentration in the water soluble fraction showed a maximum of 0.00048 mg kg^{-1} for 1-year-old ash core to a maximum of 0.00041 mg kg^{-1} for 20-year-old ash core. Relatively high proportions of average amount of total Se were contained in the exchangeable (42.33%) and carbonate (43.88%) fractions of 1-year-old ash cores. Selenium concentration in the exchangeable fraction showed a maximum of 0.0024 mg kg^{-1} for 1-year-old ash core to a maximum of 0.0014 mg kg^{-1} for 20-year-old ash core. The concentration of Se in the carbonate fraction showed a maximum of 0.0018 mg kg^{-1} for 1-year-old ash core to a maximum of 0.0006 mg kg^{-1} for 20-year-old ash core. These suggest relative depletion of Se in the water soluble, exchangeable and carbonate fraction of 20-year-old ash core. Small proportion of total Se was contained in the Fe and Mn fraction of 1-year-old ash cores. Selenium concentration in the Fe and Mn fraction showed a maximum of 0.0004 mg kg^{-1} for 1-year-old ash core to a maximum of 0.0006 mg kg^{-1} for 20-year-old ash core. The proportion of average amount of total Se in the residual fraction of 1-year-old ash cores was below the detection limits. The concentration of Se in the residual fraction showed maximum of 0.0004 mg kg^{-1} for 20-year-old ash core. These suggest enrichment of Se in the Fe and Mn, and residual fractions of 20-year-old ash core.

The vertical distribution of Se in the water soluble fraction, exchangeable, carbonate, Fe and Mn, and residual fractions of 1-year-old ash cores are age dependent. The 20-year-old ash cores showed enrichment at the surface and middle section but 1 year and 8-year-old ash cores showed enrichment at the middle and bottom section. Selenium in the exchangeable, carbonate, and Fe and Mn fractions showed depletion at the surface of 3 drilled ash cores. Selenium showed enrichment in the water soluble fraction, exchangeable, carbonate, and Fe and Mn fractions of the relatively young ash cores.

The proportion of average amount of total toxic elements in residual fraction of 1-year-old ash cores is as follows; B (73.61%), Cr (17.01%), Pb (27.55%) and Mo (10.47%). Thus, the result showed B, Cr, Mo and Pb are enriched in the residual fractions of older ash core samples. The vertical distribution of these toxic elements in the residual fractions of 3 drilled ash cores is age and depth dependent.

9.4 Integration of findings

This study revealed that the leaching of species from dry disposed ash core samples depended on various factors which include: physical and chemical characteristics, relative abundance of each element and mineralogical composition of the fly ashes, the availability of species in the ash core, and more importantly the pore water pH of the ash system. The in-homogeneity of ash dump in term of elemental composition and mineralogical association was also seen by variation in ash type and texture, and moisture content levels which had a significant impact upon the mobility patterns of the chemical species. The age of the ash dump (i.e. degree of chemical weathering) also had a large impact on the mobility patterns of the major and trace elements in the dry disposed ash scenario, an older section of the Tutuka dry disposed dump showed extensive and deep weathering with loss of specific more soluble components.

The results of the sequential extractions showed that factors such as (i) reduction in the pore water pH overtime (ii) the influence of the top soil leachate on weathered ash cores (iii) the intersection of core ash with the groundwater level leading to dissolution of hydrated mineral phases and ultimate diffusion of metals into the groundwater system. (iii) the precipitation and dissolution of transient secondary hydrated mineral (compounds) (iv) in-homogeneity in ash cores (vi) moisture content could contribute to the extraction/mobility patterns of the elements in the sequential fractionation of core ash samples taken from dry disposed ash in landfill at different stages of weathering. Nonetheless, relatively quick and longer term leaching as well as transformation of mineral phases and the association of specific metals with different phases at different stages of weathering were observed to occur within the depths of the Tutuka ash disposal.

The sequential extraction scheme employed in this study proved to be adequate for purpose of determining mineralogical partitioning of the constituents elements and can therefore be applied in similar research studies. Development of the Tessier et al., procedure (with water extraction as the first step) is recommended, because the release of soluble As, Se, Cr, Mo, B and Pb is of environmental concern for possible groundwater contamination. The limitation of the present study is that the presence of sulfur as various metal sulfides would be expected in fly ashes. Therefore, it seems to be necessary to add more extraction steps with properly selected extractants, including more aggressive reagents. Other limitation is the lack of multiple cores due

to high cost of sample analysis. Management issues such as inconsistent placement of ash in the dumps, poor choice of ash dump site, in-homogeneity in brine irrigation, no record of salt load put on the ash dumps and lack of proper monitoring requires improvement.

9.5 Main scientific contributions of the dissertation

The Na_2O content of the Tutuka ash cores was low and varied between 0.6-1.1 mass % for 1-year-old ash cores to around 0.6-0.8 mass % for 8-year-old ash cores. Na_2O levels were higher in 1-year-old ash compared to 8-year-old ash and observed trends indicate that ash is weathering quickly (within a year) and Na^+ is leached from the ash dump immediately; thus the dry disposal ash placement method does not result in a sustainable salt sink for Na-containing species over time. The non-leachable portion of the total Na^+ content (namely that contained in the residual fraction) in the 1-year-old ash core samples under conditions found in nature ranged between 5-91 %. The considerable variability in the non leachable Na^+ components in older ash showed metastability of the mineral phases with which insoluble Na^+ associates overtime.

Toxic elements such as As, Cr, B, Mo and Pb was enriched in older ash cores. For instance arsenic concentration in the residual fraction (non leachable portion) showed a maximum of 0.00043 mg kg^{-1} for 1-year-old ash core to a maximum of 0.0015 mg kg^{-1} for 20-year-old ash core. This suggests that the 20-year-old ash cores are enriched in the As thus dust from the ash dump would be toxic human health.

9.6 Recommendations

This study revealed overall leaching and mobility of the chemical species in the dry disposed fly ash dumps at Tutuka power station. Therefore better management of ash dumps is recommended in minimising the risk ash dumps pose to human health. The best practice should be protection of ash dumps from the ingress of CO_2 and percolating rain water after disposal. Management issues such as inconsistent placement of ash in the dumps, poor choice of ash dump site, in-homogeneity in brine irrigation, no record of salt load put on the ash dumps and lack of proper monitoring requires improvement.

9.7 Future work

- Future work that relates to groundwater hydraulics, how leached contaminants from ash dump interact with water table and where it decants in the catchment?

- Investigation of other ash disposal techniques.
- Reuse of fly ash instead of disposal.
- Improving rehabilitation of the ash dumps.
- Preventing ingress of CO_2 and percolating water at the ash dump sites.

9.8 Output from the dissertation

9.8.1 Contribution at conferences

S. A. Akinyemi, A. Akinlua, W. M. Gitari and L. F. Petrik. 2009. Mineralogy and mobility patterns of chemical species in weathered fly ash. Paper presentation at International Conference on Coal Science and Technology, Cape Town.

9.8.2 Manuscripts and publication authored from PhD study

(i). **S. A. Akinyemi**, A. Akinlua, W. M. Gitari and L. F. Petrik. 2011. Mineralogy and mobility patterns of chemical species in weathered coal fly ash. Energy Sources, Part A, 33:768–784.

(ii) **S. A. Akinyemi**, A. Akinlua, W. M. Gitari, R. O. Akinyeye and L. F. Petrik. 2011. The leachability and chemical speciation of major elements at different stages of weathering in coal fly ash. Coal Combustion and Gasification Products 3, 1-13.

(iii) **S. A. Akinyemi**, A. Akinlua, O. I. Ojo, W. M. Gitari, R. O. Akinyeye and L. F. Petrik. Mineralogy and mobility pattern of trace metals in brine irrigated dry disposed, weathered coal fly ash. Energy Sources, Part A: Recovery, Utilization, and Environmental Effects. [Accepted manuscript; Manuscript ID-UESO-2011-0294].

(iv) **S. A. Akinyemi**, A. Akinlua, W. M. Gitari N. Khuse, P. Eze, R. O. Akinyeye and L. F. Petrik. Inorganic metal leaching and acid susceptibility of weathered, dry disposed fly ashes. Journal of Environmental Management. [Manuscript ID-JEMA-D-11-00863] is currently under review.

(v) **S. A. Akinyemi**, A. Akinlua, W. M. Gitari, R. O. Akinyeye and L. F. Petrik. 'Mobility and chemical partitioning of toxic elements in dry disposed coal fly ash at different stages of weathering'. Applied Geochemistry. [Manuscript ID: APGEO-S-11-00231] is currently under review.

(vi). **S. A. Akinyemi**, A. Akinlua, O. I. Ojo, W. M. Gitari, R. O. Akinyeye and L. F. Petrik. Chemical partitioning and mobility of elements in dry disposed weathered ash conditioned with high saline effluents. FUEL [Manuscript ID: JFUE-D-11-00824] is currently under review.

REFERENCES

Abollino, O., Giacomino, A., Malandrino, M., Mentasti, E., Aceto, M., Barberis, R. 2006. Assessment of Metal Availability in a Contaminated Soil by Sequential Extraction. Water, Air, and Soil Pollution, 137: 315–338.

Abreu, M. F., de, Berton, R. S., Andrade, J. C. de. 1996. Comparison of methods to evaluate heavy metals in organic wastes. Commun Soil Sci Pl Anal., 27: 1125-1135.

Abu-Samra, A., Steven Morris, J., Koirtyohann, S. R. 1975. Wet ashing of some biological samples in a microwave oven. Anal. Chem., 47: 1475–1477.

Adriano, D. C., Page, A. L., Elseewi, A. A., Chang, A. C., Straughan, I. 1980. Utilization and disposal of fly ash and other coal residues in terrestrial ecosystems: A review. J. Environmental Quality 9: 333-344.

Adriano, D. C., Page, A. L., Elseewi, A. A., Chang, A. C. 1982. Cadmium availability to sudangrass grown on soils amended with sewage sludge and fly ash. J Environ Qual., 11:197–203.

Adriano, D. C., Weber, J., Bolan, N. S., Paramasivam, S., Bon-Jun K and Sajwan, K. S. 2002. Effects of high rates of Coal Fly Ash on Soil, Turfgrass, and Groundwater Quality. Water, Air, and Soil Pollution, 139: 365–385.

Adriano, D. C., Woodford, T. A., Ciravolo, T. G. 1978. Growth and elemental composition of corn and bean seedlings as influenced by soil application of coal ash. J. Environ. Qual., 7: 416-421.

Adriano, D. C., Page, A. L., Elseewi, A.A., Chang, A. C. and Straughan I. 1980: Utilization and disposal of fly ash and other coal residues in terrestrial ecosystems: A review. J. Environ. Qual., 9: 333-344.

Ahmaruzzaman, A. 2010. A review on the utilization of fly ash. Progress in Energy and Combustion Science, 36: 327–363.

Aitken, R. L., Bell, L. C. 1985. 'Plant uptake and phytotoxicity of boron in australian fly ashes', Plant and Soil, 84: 245–257.

Akinyemi, S. A., Akinlua, A., Gitari, W. M. and Petrik L. F. 2011. Mineralogy and Mobility Patterns of Chemical Species in Weathered Coal Fly Ash. Energy Sources, Part A, 33:768–784.

Aktar, Md. W. 2007. Fly Ash Use in Agriculture: a Perspective. http://www.articlesbase.com/science-articles/fly-ash-use-in-agriculture-a-perspective. 273459. html. Retrieved on January 24, 2011.

Al-Abed, S. R., Hageman, P. L., Jegadeesan, G., Madhavan, N., Derrick Allen, D. 2006. Comparative evaluation of short-term leach tests for heavy metal release from mineral processing waste. Science of the Total Environment, 364: 14–23.

Al-Abed, S. R., Jegadeesan, G., Purandare, J. and Allen, D. 2007. Arsenic release from iron rich mineral processing waste: Influence of pH and redox potential. Chemosphere, 66: 775-782.

Alborés, A. F., Cid, B. P., Gómez, E. F. and López, E. F. 2000. Comparison between sequential extraction procedures and single extractions for metal partitioning in sewage sludge samples. Analyst, 125: 1353-1357.

Al-Harahsheh, M., Kingman, S., Somerfield, C., Ababneh, F. 2009. Microwave-assisted total digestion of sulphide ores for multi-element analysis. Analytica Chimica Acta, 638: 101–105.

Aljoe, W., Buckley, T. D., and Pflughoeft-Hassett, D. F. 2007. National synthesis report on regulations, standards, and practices related to the use of coal combustion products. Available at http: // www.undeerc.org/carrac/Assets/TB-FinalNationalSummaryReport.pdf

Alloway, B. J. 1995. Heavy metal in soils. 2nd edition, Blackie Academic and Professional.

Alonso, J. L., Wesche, K. 1991. Characterisation of Fly Ash, In: Fly Ash in Concrete-Properties and Performance, K. Wesche (Ed), First Edition, E & FN Spon, London, 8pp.

American Coal Ash Association, 2001. Proceedings of the 14th International Symposium on Management and Use of Coal Combustion Products (CCPs), San Antonio, TX, January 22-26, 2001: Alexandria, VA, American Coal Ash Association, 19 p.

American Society for Testing and Materials; 1993. ASTM C 618: Standard speciation for fly ash and raw or calcined natural pozzolan for use as a mineral admixture in Portland cement concrete. In: *Annual Book of ASTM Standards*. Philadelphia, PA.

American Society for Testing Materials; 2005. ASTM standard specification for coal fly ash and raw or calcined natural pozzolan for use in concrete (C618-05). In: *Annual book of ASTM standards*, concrete and aggregates, vol. 04.02.

Amrhein, C., Haghnia, G. H., Kim, T. S., Mosher, P. A., Gagjena, R. C., Amanios, T., De La Torre, L. 1996. Synthesis and Properties of Zeolites from Coal Fly Ash. Environmental Science and Technology, 30:735-742.

Andini, S., Cioffi, R., Colangelo, F., Grieco, T., Montagnaro, F., Santoro, L. 2008. Coal fly ash as raw material for the manufacture of geopolymer-based products. Waste Management, 28: 416–423.

Annandale, J. G., Jovanovic, N. Z., Tanner, P. D., Benade, N., and Du Plessis, H. M. 2002. The sustainability of irrigation with Gypsiferous Mine Water and Implications for the Mining Industry in South Africa. Mine Water and the Environment, 21: 81-90.

API-IA, 1995. Standard methods for the examination of water and wastewater, 19th ed., APHAAWWA-WPCF, Washington DC.

Arunachalam, J., Ernons, H., Krasnodebska, B., Mohl, C. 1996. Sequential extraction studies on homogenized forest soil samples. The Science of the Total Environment, 181: 147-159.

Asokan, P., Saxena, M., Asolekar, S.R., 2005. Coal combustion residues – environmental implications and recycling potentials. Resources, Conservation and Recycling, 43: 239–262.

ASTM C618-08 Standard Specification for Coal fly ash and Raw or Calcined Natural Pozzolan for use in Concrete. ASTM International. Retrieved on 2008-09-18.

ASTM, 1988. Annual book of standards-construction: cement, lime, gypsum, vol. 04.01. Philadelphia: American Society for Testing and Materials.

Ayrault, S., Bonhomme, P., Carrot, F., Amblard, G., Sciarretta, M. D., Galsomies, L. 2001. Multianalysis of Trace Elements in Mosses with Inductively Coupled Plasma–Mass Spectrometry Biol. Trace Elem. Res., 179: 177-184.

Azzie, B. A-M. 2002: Coal mine waters in South Africa: Their geochemistry, quality and classification. PhD Thesis, University of Cape Town, South Africa.

Baba, A., Gurdal, G., Sengunalp, F., Ozay, O., 2008. Effects of leachant temperature and pH on leachability of metals from fly ash. A case study: Can thermal power plant, province of Canakkale, Turkey. Environ. Monit. Assess., 139: 287–298.

Bakharev, T. 2005. Resistance of geopolymer materials to acid attack. Cement and Concrete Research, 35: 658–670.

Bandopadhyay, A. K. 2010. "A study on the abundance of quartz in thermal coals of India and its relation to abrasion index: Development of predictive model for abrasion", International Journal of Coal Geology, 84: 63-69.

Barona, A., Arangniz, I., and Elias, A. 1999. Assessment of Metal Extraction, Distribution and Contamination in Surface Soils by a 3-Step Sequential Extraction Procedure. Chemosphere, 39: 1911-1922.

Barona, A., Aranquiz, I., Elias, A. 2001. Metal associations in soils before and after EDTA extractive decontamination: implications for the effectiveness of further clean-up procedures. Environmental Pollution, 113:79-85.

Barona, A., Romero, F. 1996. Distribution of metals in soils and relationships among fractions by principal component analysis. Soil Technology, 8: 303-319.

Barrer, R.M. 1982. Hydrothermal chemistry of zeolites. Academic Press, London, 360 p.

Basham Kim and Clark Micheal, France Tim, and Harriso Patrick. 2007. What is fly ash? Fly ash is a by-product from burning pulverised coal in electric power generating plants. Concrete Construction Magazine.

Basham, K., Clark, M., France, T., and Harrison, P. 2007. What is fly ash? Fly ash is a by-product from burning pulverized coal in electric power generating plants. Concrete Construction Magazine, November 15.

Bates, J. B. 1978. Fourier Transform Infrared Spectroscopy; Ferraro, J. R., Baaile, L. J., Eds.; Academic Press: New York.

Batley, G. E., Gardner, D. 1977. Sampling and storage of natural waters for trace metal analysis, Water Res., 11:745–756.

Baxtar, L. L., Hardeety, D. R. 1993. The Fate of Mineral Matter during Pulverized Coal Combustion: Quarterly Report for July-September 1992; Sandia National Laboratories: Livermore, CA.

Bayat, O. 1998. Characterization of Turkish fly ashes. Fuel, 77: 1059-1066.

Beauchemin, D. 2008. Inductively Coupled Plasma Mass Spectrometry. Anal. Chem., 80: 4455–4486.

Beizile, N., Pierre Lecomte, P., Tessier, A. 1989. Testing Readsorption of Trace Elements during Partial Chemical Extractions of Bottom Sediments. Environ. Sci. Technol., 23:1015-1020.

Bengtsson, L. & M. Enell, 1986. Chemical analysis. In Berglund, B. E. (ed.), Handbook of Holocene Palaeoecology and Palaeohydrology. John Wiley & Sons Ldt., Chichester, 423-451.

Benjamini, Y. and Hochberg, Y. 1995. "Controlling the False Discovery Rate: A Practical and Powerful Approach to Multiple Testing," Journal of the Royal Statistical Society, B, 57, 289-300.

Bern, J., 1976. Residues from power generation: processing, recycling and disposal. In: Land Application of Waste Materials. Soil Conservation Society of America, Ankeny, Iowa, pp. 226–248.

Berrow, M. L., Stein, W. M. 1983. Extraction of metals from soils and sewage sludges by refluxing with aqua regia. Analyst, 108: 277-285.

Bettinelli, M., U. Baroni, U. and Pastorelli**,** N. 1989. Microwave oven samle dissolution for the analysis of environmental and biological materials. Analytica Chimica Acta, 225: 159-174.

Bezuidenhout, N., 1995. Chemical and mineralogical changes associated with leachate production at Kriel power station ash dam. Unpublished M.Sc Thesis, University of Cape Town.

Bhanarkar, A. D., Gavane, A. G., Tajne, D. S., Tamhane, S. M., P. Nema, P. 2008. Composition and size distribution of particules emissions from a coal-fired power plant in India. Fuel, 87: 2095–2101.

Biester, H. and Scholz, C. 1997. Determination of Mercury Binding Forms in Contaminated Soils: Mercury Pyrolysis versus Sequential Extractions. Environ. Sci. Technol., 31: 233-239.

Bigham, J. M., Schwertmann, U., Carlson, L., Murad, E. 1990. A poorly crystallized oxyhydroxysulfate of iron formed by bacterial oxidation of Fe (II) in acid mine waters. Geochim Cosmo Acta, 54: 2743–2758.

Bilski, J. J., Alva, A. K., Sajwan, K. S., 1995. Fly ash. In: Rechcigl, J.E. (Ed.), Soil Amendments and Environmental Quality. Lewis, Boca Raton, pp. 237–363.

Bing¨ol, D., Akc¸ay, M. 2005. Determination of trace elements in fly ash samples by FAAS after applying different digestion procedure. Talanta, 66: 600–604.

Bin-Shafique, S., Benson, C. H., Edil, T. B. Hwang, K. 2006. Leachate concentrations from water leach and column leach tests on fly ash-stabilized soils, Environ. Eng. Sci., 23: 53–67.

Bo'dog I., Polya'k Csiko Z., 'Nyi, S. and Hlavay, J. 1996. Sequential extraction procedure for the speciation of elements in fly ash samples. J. Microchem., 54: 320-330.

Boonjob, W., María Rosende, M., Manuel Miró, M., Cerdà, V. 2009. Critical evaluation of novel dynamic flow-through methods for automatic sequential BCR extraction of trace metals in fly ash. Anal. Bioanal. Chem., 394: 337–349.

Bordas, F., Bourg, A. C. M. 1998. A critical evaluation of sample pretreatment for storage of contaminated sediments to be investigated for the potential mobility of their heavy metal load. Water Air Soil Pollut., 103: 137–149.

Borovec, Z. 1996. Evaluation of the concentrations of trace elements in stream sediments by factor and cluster analysis and the sequential extraction procedure. The Science of the Total Environment, 177: 237-250.

Bosch, G. L. 1990. The mineralogy and chemistry of pulverised fuel ash produced by three South African fly ashes, Ph.D. Thesis, University of Cape Town, Cape Town.

Brannvall, E., Andreas, L., Diener, S., Tham, G and Lagerkvist, A., 2009. Influence of accelerated ageing on acid neutralization capacity and mineralogical transformations in refuse derived-fuel fly ashes. Twelfth International Waste Management and Landfill Symposium, Sardinia.

Brannvall, E., Andreas, L., Diener, S., Tham, G., Lagerkvist, A. 2009. Influence of accelerated ageing on acid neutralization capacity and mineralogical transformation in refused derived fuel fly ashes. Proceedings Sardinia, Twelfth International Waste Management and Landfill Symposium S. Margherita di Pula, Cagliari, Italy.

Breger, I. A. 1958. Geochemistry of coal. Economic Geology, 53: 823-841.

Breslin, V. T., Duedall, I. W. 1983. The behavior of fly-ash derived arsenic in sea water. Marine Chemistry, 13: 341-355.

Bruder-Hubscher V., Lagarde F., Leroy M. J. F., Coughanowr C., Engeuhard F. 2002. Application of a sequential extraction procedure to study the release of elements from municipal solid waste incineration bottom ash, Anal. Chim. Acta., 451: 285-295.

Brunori, C., Cremisini, C., D'Annibale, L., Massanisso, P., Pinto, V. 2005. A kinetic study of trace element leachability from abandoned mine-polluted soil treated with SS-MSW compost and red mud. Comparison with results from sequential extraction. Anal. Bioanal. Chem., 381: 1347–1354.

Buckley, T. D., Pflughoeft-Hassett, D. F. 2007. National Synthesis Report on Regulations, Standards, and Practices Related to the use of Coal Combustion Products. Energy & Environmental Research Center (EERC) Final Report, 65 pp.

Burgers, C. L. 2002. Synthesis and characterization of sesquioxidic precipitates formed by the reaction of acid mine drainage with fly ash leachate. Unpublished M.Sc Thesis, University of Stellenbosch, South Africa.

Cabral, A. R. and Lefebvre, G. 1998. Use of Sequential Extraction in the Study of Heavy Metal Retention by Silty Soils. Water, Air, and Soil Pollution, 102: 329–344.

Cadle, A. B., Cairncross, B., Christie, A. D. M. and Roberts, D. L. 1993. The Karoo Basin of South Africa: type basin for the coal-bearing deposits of Southern Africa. International Journal of Coal Geology, 23:117-157.

Campbell, A. 1999. Chemical, physical and mineralogical properties associated with the hardening of some South African fly ashes, Ph.D. Thesis, University of Cape Town, Cape Town.

Campos, E., Barahona E., Lachica, M., Migorance, M. D. 1998. A study of the analytical parameters important for the sequential extraction procedure using microwave heating for Pb, Zn and Cu in calcareous soils. Analytica Chimica Acta, 369: 235-243.

Carapeto, C. and Purchase, D. 2000. Use of Sequential Extraction Procedures for the Analysis of Cadmium and Lead in Sediment Samples from a Constructed Wetland. Bull. Environ. Contam. Toxicol., 64: 51-58.

Carlson, C. L., Adriano, D. C. 1993. Environmental impacts of coal combustion residues. Journal of Environmental Quality, 22: 227–247.

Catuneanu, O., Elango, H. N. 2001. Tectonic control on fluvial styles: the Balfour Formation of the Karoo Basin, South Africa. Sedimentary Geology, 140: 291-313.

Catuneanu, O., Hancox, P. J., Rubidge, B. S. 1998. Reciprocal flexural behavior and contrasting stratigraphies: a new basin development model for the Karoo retroarc foreland system south Africa. Basin Res., 10: 417-439.

Chang, C., Wang, C., Mui, D.T., Chiang, H. 2009. Application of methods (sequential extraction procedures and high-pressure digestion method) to fly ash particles to determine the element constituents: A case study for BCR 176. Journal of Hazardous Materials, 163: 578-587.

Chao, T. T. 1972. Selective Dissolution of Manganese Oxides from Soils and Sediments with Acidified Hydroxylamine Hydrochloride. Soil Science Society of America, 36: 764-768.

Chao, T. T. and Zhou, L. 1983. Extraction techniques for selective dissolution of amorphous iron oxides from soils and sediments. J. Soil Sci. Sot. Am. Proc., 47: 225-232.

Chapman, H. D. 1965. Cation-exchange capacity. In: C. A. Black (ed.) Methods of soil analysis - Chemical and microbiological properties. Agronomy, 9: 891-901.

Chen, Y., Shah, N., Huggins, F. E., Huffman, G. P. 2005. Characterisation of Fine and Ultrafine Fly Ash by Electron Microscopy Techniques. World of Coal Ash (WOCA), April 11-15 Lexington, Kentucky, USA.

Cherkauer, D. S. 1980. The effect of Flyash Disposal on a Shallow Ground-Water System. Ground Water, Vol. 18: 544-550.

Cherry, D. S. and Guthrie, R. K. 1977. Toxic metal concentration in surface waters from coal ash. Water Res. Bull. 13: 1227 – 1236.

Chimenos, J. M., Fernández, A. I., Nadal, R., Espiell, F. 2000. Short-term natural weathering of MSWI bottom ash. Journal of Hazardous Materials, B79: 287–299.

Chlopecka, A., Adriano, D. C. 1996. Mimicked in situ stabilization of metals in a cropped soil: bioavailability and chemical forms of zinc. Environ. Sci. Technol. 30, 3294–3303.

Choi S. K., Lee S, Song Y. K., Moon H. S. 2002. Leaching characteristics of selected Korean fly ashes and its implications for the groundwater composition near the ash disposal mound. Fuel, 81: 1083-1090.

Chomchoei, R., Shiowatana, J., Pongsakul, P. 2002. Continuous-flow system for reduction of metal readsorption during sequential extraction of soil. Analytica Chimica Acta, 472: 147–159.

Chou, J. D., Wey, M. Y., Chang, S. H. 2009. Evaluation of the distribution patterns of Pb, Cu and Cd from MSWI fly ash during thermal treatment by sequential extraction procedure. Journal of Hazardous Materials, 162: 1000–1006.

Coal Ash (WOCA) Conference, Lexington, Kentucky, May 4–7.

Coetzee, P. P., Gouws, K., Pluddemann, S., Yacoby, M., Howell, S., Drijver, L. D. 1995. Evaluation of sequential extraction procedures for metal speciation in model sediments. Water S. A Vol. 21: 51-60.

Cohen, A. D. 1970. "An Allochthonous Peat Deposit from Southern Florida," Geological Society of America Bulletin, Vol. 81: 2477-2482.

Comans, R. N. J. Meima J. A. and Geelhoed, P. A. 2000: Reduction of contaminant leaching from MSWI bottom ash by addition of sorbing components. Waste Management 20: 125-133.

Cope, F. 1962. The development of a soil from an industrial waste. Transactions of the International Soil Science Society Conference, IV: 859–863.

Criado, M. Ferna´ndez-Jime´nez, A. Palomo, A. 2007. Alkali activation of fly ash: Effect of the SiO_2/Na_2O ratio Part I: FTIR study. Microporous and Mesoporous Materials 106. 180-191.

Crowell, J. C. and Frakes, L. A. 1972. Late Palaeozoic glaciation: Part V, Karoo Basin, South Africa. Bull. Geol. Soc. Am., 83: 2887-2912.

Cultrone, G., Sebastia´n, E., Elert, K., de la Torre, M. J., Cazalla, O., Rodriguez-Navarro, C. 2004. Influence of mineralogy and firing temperature on porosity of bricks. J. Eur. Ceram. Soc., 24:547–564.

Dakyns, J. R. 2009. VIII.-Origin of coal, Cambridge Univ Press. 8: 135-135.

Daniel, M. 1991. African coat supply prospects, lEA Coal Research, London, 83 pp.

Daniels, J. L and Das, G. P. 2006. Leaching behavior of lime-fly ash mixtures, Environ. Eng. Sci., 23: 42–52.

Das, A. K., Chakraborty , R., Cervera, M. L., de la Guardia, M. 1995. Metal speciation in solid matrices. Talanta, 42: 1007-1030.

Das, A. K., Chakraborty, R., Miguel de la Guardia, M., Cervera, M. L., Goswami, D. 2001. ICP-MS multielement determination in fly ash after microwave-assisted digestion of samples. Talanta, 54: 975–981.

Davidson, C. M., Duncan, A. L., Littlejohn, D., Ure, A. M., Garden, L. M. 1998. A critical evaluation of the three-stage BCR sequential extraction procedure to assess the potential mobility and toxicity of heavy metals in industrially-contaminated land. Analytica Chimica Acta, 363: 45-55.

Davidson, C. M., Wilson, L. E., Ure, A. M. 1999a. Effect of sample preparation on the operational speciation of cadmium and lead in freshwater sediment. Fresenius J Anal Chem., 363:134–136.

Davidson, C. M., Ferreira, P. C. S., Ure, A. M. 1999b. Some sources of variability in application of the three-stage sequential extraction procedure recommended by BCR to industrially-contaminated soil. Fresenius J Anal Chem., 363: 446–451.

Davison, R. L., Natusch, D. F. S., Wallace, J. R. and Evans Jr., C. A. 1974, 'Trace elements in fly ash – Dependence of concentration on particle size', Environ. Sci. Technol., 8: 1107–1113.

De Beer, J. J., Van Zijl, J. S. V. and Gough, D. I. 1982. The Southern Cape Conductive Belt (South Africa) : its composition, origin and tectonic significance. Tectonophysics, 83: 205-225.

De Groot A. J., Zzschuppe, K. H., Salomons, W. 1982. Standardization of methods of analysis for heavy metals in sediment. Hydrobiologia, 92: 689-695.

de Groot, G. J., Wijkstra, J., Hoede, D. and van der Sloot, H. A. 1989. Leaching characteristics of selected elements from coal fly ash as a function of the acidity of the contact solution and the liquid/solid ratio, ASTM International., pp.70-183.

de Wit, M. J., Ransome, I. G. D. 1992. Regional inversion tectonics along the southern margin of Gondwana. In: de Wit, M. J., Ransome, I.G.D. (Eds.). Inversion Tectonics of the Cape Fold Belt, Karoo and Cretaceous Basins of Southern Africa. Balkema, Rotterdam, pp. 15-21.

Dhir, R. K., Jones, M. R. 1999. Development of chloride-resisting concrete using fly ash. Fuel, 78:137–142.

Digioia, Anthony, M., Jr. and William, L. N. 1997. ”Fly ash as Structural Fill”. Proceedings of the American Society of Civil Engineers. Journal of the Power Division, New York, NY.

Dijkstra, J. J., van der Sloot, H. A. and Comans, R. N. J., 2006. The leaching of major and trace elements from MSWI bottom ash as a function of pH and time. Applied Geochemistry, 21: 335–351.

Ding, M., Geusebroek, M., van der Sloot, H. A. 1998. Interface precipitation affects the resistance to transport in layered Jarosite/fly ash. Journal of Geochemical Exploration, 62: 319–323.

Dionex, 1998: Application notes on conductivity detection. Dionex DX-120 Ion Chromatography Operator’s Manual, Dionex. Overview of principles behind conductivity and concentration relation of ionic solutions, as well as description of auto self-regenerating suppression module, and eluent composition for anion analysis.

Donahoe, R. J. 2004. Secondary mineral formation in coal combustion byproduct disposal facilities: implications for trace element sequestration. In: Gieré R, Stille P editors. Energy, waste and the environmental: a geochemical perspective. Geological Society, London, Special Publications, 236: 641–658.

Doran, J. W., Martens, D. C. 1972. Molybdenum availability as influenced by application of fly ash to soil. J. Environ. Qual., 1: 186–189.

Drever, I. J. 1997. The geochemistry of natural waters: surface and ground water environments, 3rd Edition, Published by Prentice Hall, Inc., Englewood Cliffs, NJ.

Dudas, M. J. 1981. Long-Term Leachability of Selected Elements from Fly Ash. Environmental Science & Technology, 15: 841-843.

Earles, H. V., Marsh, J. S. and Cox, K. G. 1984. The Karoo Igneous Province: an introduction. In : Erlank A. J. (Ed.), Petrogenesis of the Volcanics Rocks of the Karoo Province. Geological Society of South Africa. Special Publication, 13: 1-26.

Eary, L. E., Dhanpat, R., Mattigod, S. V., Ainsworth, C. C. 1990. Geochemical factors controlling the mobilization of inorganic constituents from fossil fuel combustion residues: II. Review of the minor elements. J Environ Qual., 19:202–214.

Eble, C. F., and Hower, J. C. 1997. Coal quality trends and distribution of potentially hazardous trace elements in Eastern Kentucky coals. Fuel, 76: 711 715.

Eisenberg, S., Tittlebaum, M., H. Eaton, H., Soroczak, M. 1986. Chemical characteristics of selected fly ash leachates, J. Environ. Sci. Health Part A, 21: 383–402.

El-Mogazi, D., Lisk, D. J. and Weinstein, L. H. 1988. A review of physical, chemical, and biological properties of fly ash and effects on agricultural ecosystems The Science of the Total Environment, 74: 1-37.

Elseewi, A. A., Page, A. L., Grimm, S. R. 1980. Chemical characterization of fly ash aqueous system. J. Environ. Qual., 9:224.

Elseewi, A.A., Page, A.L., 1984. Molybdenum enrichment of plants grown on fly ash treated soils. J. Environ. Qual., 13: 394–398.

Erol, M., Küc_ükbayrak, S., Ersoy-Mericboyu, A., Ulubas, T. 2005. Removal of Cu^{2+} and Pb^{2+} in aqueous solutions by fly ash. Energy Convers Manage., 46: 1319–1331.

Eskom abridged annual report 2009. Available at www.eskom.co.za, Accessed on 23rd May 2010.

Essenhigh, R. H., 1976. 16th Symp. (Int.) on Combust., p.353, The Combustion Institute, Pittsburgh, PA.

Fail, J. L., Jr, and Wochok, Z. S. 1977. Soybean growth on fly ash-amended strip soil mine spoils. Plant Soil, 48: 472-484.

Fan, Y., Zhang, F. S., Zhu, J., Liu, Z. 2008. Effective utilization of waste ash from MSW and coal co-combustion power plant—Zeolite synthesis. Journal of Hazardous Materials, 153: 382–388.

Fang, Y., Chen, Y., Silsbee, M. R., Roy, D. M. 1996. Microwave sintering of fly ash Materials Letters, 27: 155-159.

Farrah, H., Pickering, W. F. 1993. Factors influencing the potential mobility and bioavailability of metals in dried lake sediments. Chem. Spec. Bioavail., 5:81-96.

Fatoba, O.O., 2011. Chemical Interactions and mobility of species, Unpublished PhD thesis, University of the Western Cape, Cape Town, South Africa.

Fatoba, O.O., 2007. Chemical compositions and leaching behaviour of some South African fly ashes, Unpublished M.Sc thesis, University of the Western Cape, Cape Town, South Africa.

Feng, S., Wang, X., Wei, G., Peng, P., Yang, Y., Cao, Z. 2007. Leachates of municipal solid waste incineration bottom ash from Macao: Heavy metal concentrations and genotoxicity. Chemosphere, 67: 1133–1137.

Fernandez-Carrasco, L., Vazquez, E. 2009. Reactions of fly ash with calcium aluminate cement and calcium sulphate. Fuel, 88. 1533-1538.

Fernández-Turiel, J. L., Cabañas, M., Querol, X., López-Soler, A. 1994. Mobility of heavy metals from coal fly ash, Environ. Geol., 23: 264-270.

Fernando, L. A., Heavner, W. D., Gabrielli, C. C. 1986. Closed-Vessel Microwave Dissolution and Comprehensive Analysis of Steel by Direct Current Plasma Atomic Emission Spectrometry. Anal. Chern., 58: 511-512.

Ferraiolo, G., Zilli, M., Converti, A. 1990. Fly Ash Disposal and Utilisation. J. Chem. Tech. Biotechnology, 47: 281-305.

Filippidis A., Georgakopoulos**,** A. 1992. Mineralogical and chemical investigation of fly ash from the Main and Northern lignite fields in Ptolemais, Greece. Fuel, 71: 373-376.

Fischer, G. L., Chang, D. P. Y., Brummer M. 1979. Fly ash collected from electrostatic precipitators, microcrystalline structures and the mystery of spheres. Science, 192:553–555.

Fishman, N. S., Rice, C. A., Breit, G. N., Johnson, R. D. 1999. Sulfur bearing coatings on fly ash from a coal-fired power plant: composition, origin, and influence on ash alteration. Fuel, 78: 187–196.

Foner, H. A., Robl, T. L., Hower, J. C., Graham, U. M. 1999. Characterization of fly ash from Israel with reference to its possible utilization. Fuel, 78: 215–223.

Font, O., Moreno, N., Querol, X., Izquierdo, M., Alvarez, E., Diez, S., Elvira, J., Antenucci, D., Nugteren, H., Plana, F., López, A., Coca, P., Peña, F. G. 2010. X-ray powder diffraction-based method for the determination of the glass content and mineralogy of coal (co)-combustion fly ashes Fuel, 89: 2971–2976.

Förstner, U. 1993. Metal speciation-general concepts and applications. Intern. J. Environ. Anal. Chem., 51: 5–23.

Fourie, A., Blight, G. Bhana, Y., Harris, R., Barnard, N. 1997. The geotechnical properties of dry dumped and hydraulically placed power station fly ash. Reference: Proc. 2nd International Conference on Mining and Industrial Waste Management. Midrand, South Africa, 10pp.

Francis W. (1961) 'Coal, its formation and composition' 2nd Ed., Edward Arnold, London.

Fraser, J. L., Lum, K. R. 1983. Availability of Elements of Environmental Importance in Incinerated Sludge Ash. Environ. Sci. Technol., 17 : 52-54.

Frenzel, W. 1995. Microanalytical concept for multicomponent analysis of airborne particulate matter. Fresenius' Journal of Analytical Chemistry, 340: 525-533.

Fritz, J. S. 2005. Factors affecting selectivity in ion chromatography. Journal of Chromatography A, 1085: 8–17.

Fruchter, J. S., Rai, D., Zachara, J. M. 1990. Identification of solubility-controlling solid phases in a large fly ash field lysimeter, Environ. Sci. Technol., 24: 1173–1179.

Fuentes, A., Llorens, M., Saez, J., Soler, A., Aguilar, M. I., Ortuno, J. F., Meseguer, V. F. 2004. Simple and sequential extractions of heavy metals from different sewage sludges. Chemosphere, 54: 1039–1047.

Fulekar, M. H., Dave, J. M. 1986. Disposal of fly ash-An environmental problem. Inter. J. Environ. Stud., 26: 191-215.

Furr, A. K., Parkinson, T. F., Bache, C. A., Gutenmann, W. H., Wszolek, P. C., Irene S. Pakkala, I. S. and Lisk, D. J." 1979. Multielement Analysis of Municipal Sewage Sludge Ashes. Absorption of Elements by Cabbage Grown in Sludge Ash-Soil Mixture. Environmental Science & Technology, Volume 13: 1503-1506.

Fytianos, K., Tsaniklidi, B., Voudrias, E. 1998. Leachability of heavy metals in Greek fly ash from coal combustion, Environ. Int., 24: 477–486.

Galbreath, K. C., Zygarlicke, C. J. 2004. Formation and chemical speciation of arsenic-, chromium-, and nickel-bearing coal combustion PM2.5. Fuel Processing Technology, 85:701-726.

Gao, P., Lu, X., Lin, H, Li, X., Hou, J. 2007. Effects of fly ash on the properties of environmentally friendly dam concrete. Fuel, 861: 208–211.

Garavaglia, R. and Caramuscio, P., 1994. Coal Fly-Ash Leaching Behaviour and Solubility Controlling Solids. In: Goumans, J. J. J. M., van der Sloot, H. A., Aalbers, Th. G. Editors, Environmental Aspects of Construction with Waste Materials, Elsevier Science, Amsterdam.

Geiger, W. M. and Raynor, M. W. 2009. ICP-MS: A Universally Sensitive GC Detection Method for Specialty and Electronic Gas Analysis. ICP-MS: Available at http://spectroscopyonline.findanalytichem.com/spectroscopy/ICP-MS/ICP-MS-AUniversally-Sensitive-GC-Detection-MMethod/ArticleStandard/Article/detail. Accessed on November 18, 2010.

Geladi, P., Adams, F. 1979. The determination of beryllium and manganese in aerosols by atomic absorption spectrometry with electrothermal atomization. Analytica Chimica Acta, 105: 219-231.

Georgakopoulos, A., Filippidis, A., Kassoli-Fournaraki, A., Iordanidis, A., Fernandez- Turiel, J.-L., Llorens, J. F. 2002. Leachability of major and trace elements of fly ash from Ptolemais power station, Northern Greece. Energy Sources, 24: 103–113.

Ghodrati, M., Sims, J., Vasilas, B. 1995. Evaluation of fly ash as a soil amendment for the Atlantic Coastal Plain: 1. Soil hydraulic properties and elemental leaching. Water Air Soil Pollut., 81: 349-361.

Giampaolo, C., Lo Mastro, S., Polettini, A., Pomi, R., Sirini, P. 2002. Acid neutralisation capacity and hydration behaviour of incineration bottom ash–Portland cement mixtures. Cement and Concrete Research, 32: 769–775.

Gismera, M. J., Lacal, J., da Silva, P., Garcia, R., Teresa Sevilla, M. T., Jesu´s, R. Procopio, J. R. 2004. Study of metal fractionation in river sediments. A comparison between kinetic and sequential extraction procedures. Environmental Pollution, 127: 175–182.

Gitari, M. W., Fatoba, O. O., Nyamihingura, A., Petrik, L. F., Vadapalli, V. R. K., Nel, J., October, A., Dlamini, L., Gericke, G., and Mahlaba, J. S. 2009a. Chemical weathering in a dry ash dump: an insight from physicochemical and mineralogical analysis of drilled cores. World of 295 Coal Ash (WOCA) Conference, Lexington, Kentucky.

Gitari, W. M., Fatoba, O. O., Petrik, L. F., Vadapalli, V. R. K. 2009b. Leaching characteristics of selected South African fly ashes: Effect of pH on the release of major and trace species. Journal of Environ. Sci. and Health, Part A: Toxic/Hazardous Substances and Environmental Engineering, 1532-4117, 44: 206 – 220.

Gitari, M. W., Petrik, L. F., Etchebers, O., Key, D. L., Iwuoha, E., Okujeni, C. 2006. Treatment of acid mine drainage with fly ash: removal of major contaminants and trace elements. J. Environ. Sci. Health – Part A, 41:1729–1747.

Gitari, M. W., Petrik, L. F., Etchebers, O., Key, D. L., Iwuoha, E., Okujeni C. 2007. Passive neutralization of acid mine drainage by fly ash and its derivatives: a column leaching study. Fuel, 87:1637-1650.

Gitari, W. M., Petrik, L. F., Etchebers, O., Key, D. L., Okujeni, C. 2008. Utilization of fly ash for treatment of coal mines wastewater: Solubility controls on major inorganic contaminants. Fuel, 87: 2450–2462.

Glass, G. K. and Buenfeld, N. R. 1999. Differential acid neutralisation analysis. Cement and Concrete Research 29, 1681–1684.

Gleyzes, C., Tellier, S., Astruc, M. 2002. Fractionation studies of trace elements in contaminated soils and sediments: a review of sequential extraction procedures. trends in analytical chemistry, 21: 451-467.

Gleyzes, C., Tellier, S., Sabrier, R., Astruc, A. 2001. Arsenic characterisation in industrial soils by chemical extractions. Environ. Technol., 22: 27-38.

Go´mez Ariza, J. L., Gira´ldez, I., Sa´nchez-Rodas, D., E. Morales, E. 2000. Selectivity assessment of a sequential extraction procedure for metal mobility characterization using model phases. Talanta, 52:545–554.

Gómez-Ariza, J. L., Giráldez, I., Sánchez-Rodas, D., Morales, E. 1999. Metal readsorption and redistribution during the analytical fractionation of trace elements in oxic estuarine sediments. Analytica Chimica Acta, 399: 295–307.

Goodarzi, F. 2006. Characteristics and composition of fly ash from Canadian coal-fired power plants. Fuel, 85:1418–1427.

Goodarzi, F., Huggins, F. E. 2001. Monitoring the species of arsenic, chromium and nickel in milled coal, bottom ash and fly ash from a pulverized coal-®red power plant in western Canada. J. Environ. Monit., 3: 1-6.

Green, J. B., Manahan, S. E., 1978. Determination of acid-base and solubility behavior of lignite fly ash by selective dissolution in mineral acids. Analytical Chemistry, 50: 1975–80.

Griffiths, P. R., de Haeeth, J. A. 1986. Fourier Transform Infrared Spectrometry; John Wiley & Sons: New York.

Grisafe, D. A., Angino, E. E., Smith, S. M. 1988. Leaching characteristics of a high-calcium fly ash as a function of pH: a potential source of selenium toxicity. Applied Geochemistry, 3: 601-508.

Grochowiak, K. S., Gołaś, J., Jankowski, H., Koziński, S. 2004. "Characterization of the coal fly ash for the purpose of improvement of industrial on-line measurement of unburned carbon content". Fuel, 83: 1847-1853.

Gulmini, M., Ostacoli, G., Zelano, V. and Torazzo, A. 1994. Comparison between microwave and conventional heating procedures in Tessier's extractions of calcium, copper, iron and manganese in Lagoon sediment. Analyst, 119: 2075-2080.

Güngör, H. and Elik, A. 2007. Comparison of ultrasound-assisted leaching with conventional and acid bomb digestion for determination of metals in sediment samples. Microchemical Journal, 86: 65–70.

Gutenmann, W. H., Bache, C. A., Youngs, W. D. and Lisk, D. J. 1978. Selenium in fly ash. Science, 191: 966-967.

Gutierrez, B., C. Pazos, C., J. Coca, J. 1993. Characterization and leaching of coal fly ash, Waste Manage. Res., 11: 279–286.

Haddad, P. R. 2004. Ion chromatography. Anal. Bioanal. Chem., 379: 341–343.

Haddad, P. R., Nesterenko, P. N., Buchberger, W.2008. Recent developments and emerging directions in ion chromatography. Journal of Chromatography A, 1184: 456–473.

Hall, G. E. M., Vaive, J. E., Beer, R. and Hoashi, M. 1996. Selective leaches revisited, with emphasis on the amorphous Fe oxyhydroxide phase extraction. Journal of Geochemical Exploration, 56: 59-78.

Halstead, W. J. 1986. Use of Fly Ash in Concrete. National Highway Research Program Synthesis of Highway Practice #127. Washington, DC: Transportation Research Board.

Hareeparsad, S., Tiruta-Barna, L., Brouckaerta, C. J. and Buckleya, C. A. 2010. Quantitative geochemical modelling using leaching tests: Application for coal ashes produced by two South African thermal processes. Journal of Hazardous Materials, xxx: xxx–xxx.

Hatanpaa, E., Kajander , K., Laitinen, T., Piepponen, S., Revitzer, H. 1997. A study of trace element behavior in two modern coal-fired power plants I. Development and optimization of trace element analysis using reference materials. Fuel Processing Technology, 51: 205-217.

Haynes, R. J. 2009. Reclamation and revegetation of fly ash disposal sites – Challenges and research needs. Journal of Environmental Management, 90: 43–53.

Hendrikson, T. A. 1975 (Ed.), Synthetic Fuels Data Handbook, Cameron Engineers, Inc., Denver, C.O. 1975.

Henry, W. W., Knapp, K. T. 1980. Compound forms of fossil fuel fly ash emissions, Environ. Sci. Technol., 4: 450–456.

Heiri, O., Lotteri, A. F., Lemcke, G. 2001. Loss on ignition as a method for estimating organic and carbonate content in sediments: reproducibility and comparability of results. Journal of Paleolimnology, 25**:** 101–110.

Hill, G. R. 1972. Chemical Technology, 296p.

Hirner, A. V. 1992. Trace element speeiatiori in soils and sediments using sequential chemicai extraction methods. Int. J. Environ. Anal. Chem., 46: 77-85.

Hobbs, M. L., Radulovic, P. T. and Smoot, L. D. 1993. Combustion and gasification of coals in fixed-beds. Prog. Energy Combust. Sci., Vol. 19: 505-586.

Hodgson, F. I. D. 1999. Physical properties of the ash generated at the Tutuka Power station. Unpublished Report to Eskom.

Hodgson, F. I. D. and Krantz, R. M. 1998. Investigation into groundwater quality deterioration in the olifants river catchment above the Loskop Dam with specialized investigation in the Witbank dam sub-catchment. WRC Report No. 291/1/98. Water Research Commission P.O.Box 824, Pretoria 0001.

Hodgson, L., Dyer, D., Brown, D. A., 1982. Neutralization and dissolution of high calcium fly ash. Journal of Environmental Quality, 11: 93–98.

Holcombe, L. J. 1985. Variability of Elemental Concentrations in Power Plant Ash Environ. Sci. Technol., Vol. 19: 615-620.

Holler, H., Wirshing, U. 1985. Zeolites formation from fly ash. Fortschr. Mineral., 63:21-34.

Hollis, J. F., Keren, R. and Fal, M. 1988: Boron release and sorption by fly ash as affected by pH and particle size. J. Environ Qual, 17:181-185.

Horowitz, A. J. 1991. A primer on sediment-trace element chemistry. Chelsea. Lewis Publication Incorporation.

Howard, J. L., Vandenbrink, W. J. 1999. Sequential extraction analysis of heavy metals in sediments of variable composition using nitrilotriacetic acid to counteract resorption. Environmental Pollution, 106: 285-292.

Hower, J. C., Robertson, J. D., Thomas, G. A., Amy S. Wang, A. S., Schram, W. H., Graham, U. M., Rathbone, R. F. and Rob, T. L. 1996. Characterization of fly ash from Kentucky power plants. Fuel, Vol. 75: 403-411.

Hower, J. C., Robl, T. L., Thomas, G. A. 1999. Changes in the quality of coal combustion by-products produced by Kentucky power plants, 1978 to 1997: consequences of Clean Air Act directives. Fuel, 78:701–712.

Huang, S. J., Chang, C. Y., Mui, D. T., Chang, F. C., Lee, M. Y., Wang, C. F. 2007. Sequential extraction for evaluating the leaching behavior of selected elements in municipal solid waste incineration fly ash. Journal of Hazardous Materials, 149: 180–188.

Huffman**,** G. P., Huggins**,** F. E., Shah**,** N., Jianmin Zhao**,** J. 1994. Speciation of arsenic and chromium in coal and combustion ash by XAFS spectroscopy. Fuel Processing Technology, 39: 47-62.

Huggins, F. E., Najih, M., Gerald P. and Huffman, G. P. 1999. Direct speciation of chromium in coal combustion by-products by X-ray absorption fine-structure spectroscopy. Fuel, 78: 233–242.

Huggins, F. E., Senior, C. L., Chu, P., Ladwig, K. and Huffman, G. P. 2007. Selenium and Arsenic Speciation in Fly Ash from Full–Scale Coal-Burning Utility Plants. Environ. Sci. Technol., 41: 3284-3289.

Hulett L. D. and Weinberger, A. J. 1980. Some etching studies of the microstructure and composition of large aluminosilicate particles in fly ash from coal-burning power plants. American Chemical Society, 14: 965-970.

Ilic, M., Cheeseman, C., Sollars, C., Knight, J. 2003. Mineralogy and microstructure of sintered lignite coal fly ash. Fuel, 82: 331–336.

Inada, M., Eguchi, Y., Enomoto, N. and Hojo, J. 2005. Synthesis of zeolite from coal fly ashes with different silica–alumina composition. Fuel, 84: 299–304.

ISO, 1995. Soil quality, Extraction of trace elements soluble in aqua-regia, ISO 11466.

Iwashita, A., Nakajima, T., Takanashi, H., Ohki, A., Fujita, Y. and Yamashita, T. 2007. Determination of trace elements in coal and coal fly ash by joint-use of ICP-AES and atomic absorption spectrometry. Talanta, 71: 251–257.

Iwashita, A., Nakajima, T., Takanashi, H., Ohki, A., Fujita, Y. and Yamashita, T. 2006. Effect of pre-treatment conditions on the determination of major and trace elements in coal fly ash using ICP-AES. Fuel, 85: 257–263.

Iwashita, A., Sakaguchi, Y., Nakajima, T., Takanashi, H., Ohki, A., Kambara, S. 2005. Leaching characteristics of boron and selenium for various coal fly ashes. Fuel, 84: 479–485.

Iyer, R. 2002. The surface chemistry of leaching coal fly ash. Journal of Hazardous Materials, B93: 321–329.

Jackson, B. P., Miller, W. P. 1998. Arsenic and selenium speciation in cola fly ash extracts by ion chromatography-inductively coupled plasma mass spectrometry. Journal of Analytical Atomic Spectrometry, 13: 1107-1112.

Jala, S., Goyal, D. 2006. Fly ash as a soil ameliorant for improving crop production-a review. Bioresource Technology, 97: 1136–1147.

James**,** R. H. and Palmer**,** M. R. 2000. The lithium isotope composition of international rock standards. Chemical Geology, 166: 4319-326.

Jankowski, J., Ward, C.R., French, D. and Groves, S. 2006. Mobility of trace elements from selected Australian fly ashes and its potential impact on aquatic ecosystems. Fuel, 85: 243-256.

Janos Beer and Cutler Cleveland, C. (Topic Editor) "Fossil fuel power plant". In: Encyclopedia of Earth. Eds. Cutler J. Cleveland (Washington, D.C.: Environmental Information Coalition, National Council for Science and the Environment). [First published in the Encyclopedia of

Earth May 17, 2010; Last revised Date May 17, 2010; Acessed January 9, 2011 <http://www.eoearth.org/article/Fossil fuel power plant.

Janos, P., Wildnerova´, M. and Loucˇka, T. 2002. Leaching of metals from fly ashes in the presence of complexing agents. Waste Management, 22: 783–789.

Jegadesaan G., Al-Abed S. R. and Pinto P. 2008. Influence of trace metal distribution on its leachability from coal fly ash. Fuel, 87: 1887-1893.

Jin, Q., Liang, F., Zhang, H., Zhao, L., Huan, Y., Song, D. 1999. Application of microwave techniques in analytical chemistry. trends in analytical chemistry, 18: 479-484.

Jo, H. Y., Min, S. H., Lee, T. Y., Ahn, H. S., Lee, S. H., Hong, J. K. 2008. Environmental feasibility of using coal ash as a fill material to raise the ground level. Journal of Hazardous Materials, 154: 933–945.

Johnson, M. R., Van Vuuren, C. J., Hegenberger, W. F., Key, R. and Shoko, U. 1996. Stratigraphy of the Karoo Supergroup in southern Africa: an overview. Journal of African Earth Sciences, 23: 3-15.

Junor, R. S. 1978. Control of wind erosion on coal ash. Journal of the Soil Conservation Service of New South Wales, 34: 8-13.

Johnson, C. A., Brandenberger, S. and Baccini, P. 1995. Acids neutralizing capacity of municipal waste incinerator bottom ash, Environ. Sci. Technol., 29: 142–147.

Johnson, M. R. 1991. Sandstone petrography, provenance and plate tectonic setting in Gondwana context of the south-eastern Cape Karoo Basin. S. Afr. Tydskr. Geol., 94: 137-154.

Kaakinen, J. W., Jorden, R. M., Lawasani, M. H., West, R. E. 1975. Trace element behaviour in a coal-fired power plant. Environ. Qual., 6: 862-869.

Kalembkiewicz, J. Sitarz-Palczak, E. Zapala, L. 2008. A study of the chemical forms or species of manganese found in coal fly ash and soil. J. Microchem., 90: 37-43.

Kalnicky D.J., Singhvi R. 2001. Field portable XRF analysis for environmental samples. Journal of Hazardous Materials, 83: 93-122.

Kanazu T, Ito K, Takahasi M. JIS A 6201. 1998. Fly ash for use in concrete. Electr. Power Civ. Eng., 274: 50-55.

Karayigit, A. I., Onacak, T., Gayer, R. A., Goldsmith, S. 2001. Mineralogy and geochemistry of feed coals and their combustion residues from the Cayirhan Power Plant, Ankara, Turkey. Applied Geochemitry, 16: 911-919.

Kazi, T. G., Jamali, M. K., Kazi, G. H., Arain, M. B., Afridi, H. I., Siddiqui, A. 2005. Evaluating the mobility of toxic metals in untreated industrial wastewater sludge using a BCR sequential extraction procedure and a leaching test. Anal. Bioanal. Chem., 383: 297–304.

Kersten, M., Forstner, U. 1986. Chemical fractionation of heavy metals in anoxic estuarine and coastal sediments. Water Sci. Technol., 18: 121-130.

Kesley, J. W., Kottler, B. D., Alexander, M. 1997. Selective Chemical Extractants to Predict Bioavailability of Soil-Aged Organic Chemicals. Environ. Sci. Technol., 31: 214-217.

Keyser, T. R., Natusch, D. F. S., Evans, C. A., Linton R. W. 1978. Characterizating the surface of environmental particles. Environ Sci Technol., 12: 768–773.

Khan M. R. and Khan, M. W. 1996. Effect of fly ash on growth and yield of tomato. Environmental Pollution, 92: 105-111.

Khanra, S., Mallick, D., Dutta, S. N., Chaudhuri, S. K. 1998. Studies on the phase mineralogy and leaching characteristics of coal fly ash water, air, and soil. Pollution, 107: 251–275.

Kheboian, C and Bauer, C. F. 1987. Accuracy of Selective Extraction Procedures for Metal Speciation in Model Aquatic Sediments. Analytical Chemistry, 59**:** 1417-1425.

Kim, A. G. 2006. The effect of alkalinity of Class F PC fly ash on metal release. Fuel, 85: 1403–1410.

Kim, A. G., Kazonich, G. 2004. The silicate/non-silicate distribution of metals in fly ash and its effect on solubility. Fuel, 83: 2285–2292.

Kim, A. G., Kazonich, G., Dahlberg, M. 2003. Relative solubility of cations in Class F fly ash. Environmental Science Technology, 37: 4507-4518.

Kim, N. D., Fergusson, J. E. 1991. Effectiveness of a commonly used sequential extraction technique in determining the speciation of cadmium in soils. The Science of the Total Environment, 105: 191-209.

Kim, Y. J., Lee, D. H., Osako, M. 2002. Effect of dissolved humic matters on the leachability of PCDD/F from fly ash—laboratory experiment using Aldrich humic acid, Chemosphere, 47: 599–605.

Kimmel, W. 1983. The impact of acid mine drainage on the stream ecosystem. In Pennsylvania Coal: Resources, Technology, and Utilization. Pennsylvania, PA: The Pennsylvania Academy of Science, 425-437.

Kirby, C. S. and Rimstidt, J. D. 1994. Interaction of Municipal Solid Waste Ash with Water Environ. Sci. Technol., 28: 443-457.

Kot, A., Namiesnèik, J. 2000. The role of speciation in analytical chemistry. trends in analytical chemistry, 19: 69-79.

Koukouzas, N., Ha¨ma¨la¨inen, J., Papanikolaou, D., Tourunen, A., Ja¨ntti, T. 2007. Mineralogical and elemental composition of fly ash from pilot scale fluidised bed combustion of lignite, bituminous coal, wood chips and their blends. Fuel, 86: 2186–2193.

Koukouzas, N. K., Zeng, R., Perdikatsis, V., Xu, W., Emmanuel K. Kakaras, E. K. 2006. Mineralogy and geochemistry of Greek and Chinese coal fly ash. Fuel, 85: 2301–2309.

Kramer, J. R. and Allen, H. E. 1988. Metal Speciation: Theory, Analysis and Application. Lewis, Chelsea, Mich., 320 pp.

Kruger, R. A. 1997. Fly ash beneficiation in South Africa: creating new opportunities in the market-place. Fuel, 76: 777-779.

Kukier, U., Ishak, C.F., Summer M.E., Miller, W. P. 2003. Composition and element solubility of magnetic and non-magnetic fly ash fractions. Environ. Pollut., 122 : 255-266.

Kukier, U., Sumner, M. E. 1996. Boron availability to plants from coal combustion byproducts. Water, Air, and Water Pollution, 87: 93–110.

Kutchko, B. G. and Kim, A. G. 2006. Fly ash characterization by SEM–EDS. Fuel, 85: 2537–2544.

La Force, M. J. and Fendorf, S. 2000. Solid-Phase Iron Characterization During Common Selective Sequential Extractions. Soil Sci. Soc. Am. J., 64: 1608–1615.

Laban, K. L. and Atkin, B. P. 1999. The determination of minor and trace element associations in coal using a sequential microwave digestion procedure. International Journal of Coal Geology, 41: 351–369.

Laforce, M. J., Hansel, C. M., Fendorf, S. 2000. Arsenic Speciation, Seasonal Transformations, and Co-distribution with Iron in a Mine Waste-Influenced Palustrine Emergent Wetland. Environ. Sci. Technol**.**, 34: 3937-3943.

Lau, S. S. S., Fang, M., Wong, J. W. C. 2001. Effects of Composting Process and Fly Ash Amendment on Phytotoxicity of Sewage Sludge. Arch. Environ. Contam. Toxicol., 40: 184–191.

Lecuyer, I., Bicocchi, S., Ausset, P., Leferre, R. 1996. Physico-chemical characterization and leaching of desulphurization coal fly ash. Waste Manage, Res, 14: 15-28.

Lee, M. K., Saunders, J. A. 2003, Effect of pH on metals precipitation and sorption: Field bioremediation and geochemical modeling approaches, Vadose Zone J., 2: 177-185.

Lee, S., Spears, D. A. 1997. Natural weathering of pulverized fuel ash and pore water evolution. Applied Geochemistry, 12: 367-376.

Leleyter, L., Probst, J. L. 1999. A new sequential extraction procedure for the speciation of particulate trace elements in river sediments. Int. J. Environ. Anal. Chem., 73: 109-128.

Li, X., Coles, B. J., Ramsey, M. H., Thornton, I. 1995. Sequential extraction of soils for multielement analysis by ICP-AES. Chemical Geology, 124: 109-123.

Lin, C. F., Hsi, H. C. 1995. Resource Recovery of Waste Fly Ash: Synthesis of Zeolite-like Materials. Environ. Sci. Technol., 29: 1109-1 117.

Lin, R. B., Shih, S. M. 2003. Characterization of Ca $(OH)_2$/fly ash sorbents for flue gas desulfurization. Powder Technology, 131: 212– 222.

Lin, Y. K. 1971. Compressibility, strength, and frost susceptibility of compacted fly ash. PhD thesis, University of Michigan, Michigan.

Lingling, X., Wei, G., Tao, W., Nanru, Y. 2005. Study on fired bricks with replacing clay by fly ash in high volume ratio. Constr. Build Mater., 19: 243–247.

Liu, G., Vassilev, S. V., Gao, L., Zheng, L., Zicheng Peng, Z. 2005. Mineral and chemical composition and some trace element contents in coals and coal ashes from Huaibei coal field, China. Energy Conversion and Management, 46: 2001–2009.

Lo, H., Liao, Y. 2007. The metal-leaching and acid-neutralizing capacity of MSW incinerator ash co-disposed with MSW in landfill sites, Journal Hazardous Material, 142: 512-9.

Lo, I. M. C. and Yang, X. Y. 1998. Removal and redistribution of metals from contaminated soils by sequential extraction method. Waste Management, 18: 1-7.

Lo, J. M. and Sakamoto, H. 2005. Comparison of the Acid Combinations in Microwave-assisted Digestion of Marine Sediments for Heavy Metal Analyses. Anal. Sci., 21: 1181-184.

Lohtia R. P., Joshi, R. C. 1995. Mineral admixtures**.** In Concrete Admixtures Handbook-Properties, Science, and Technology, edn 2. Edited by Ramachandran VS. Park Ridge, N J: Noyes Publications; 657- 739. London.

Long, Y. Y., Hu, L. F., Wang, J., Fang, C. R., He, R., Hu, H., Shen, D. S. 2009. Effect of sample pretreatment on speciation of copper and zinc in MSW. Journal of Hazardous Materials, 168: 770–776.

Lopez-Sanchez, J. F., Sahuquillo, A., Fiedler, H. D., Rubio, R., Rauret, G., Muntau, H., Quevauviller, Ph. 1998. CRM 601, A stable material for its extractable content of heavy metals. Analyst, 123:1675-1677.

Loyaux-Lawniczak, S., Perafait, P., Ehrhardt, J., Lecomte, P., Genin, J. 2000. Trapping of Cr by Formation of Ferrihydrite during the Reduction of Chromate Ions by Fe(II)-Fe(III) Hydroxysalt Green Rusts. Environ. Sci. Technol., 34: 438-443.

Lu, S. G., Chen, Y. Y., Shana, H. D., Bai, S. Q. 2009. Mineralogy and heavy metal leachability of magnetic fractions separated from some Chinese coal fly ashes. Journal of Hazardous Materials, 169: 246–255.

Lucey, J. A., Vintro´, L. L., Boust, D., Mitchell, P. I., Gouzy, A. L., Bowden, L. 2007. A novel approach to the sequential extraction of plutonium from oxic and anoxic sediment using sodium citrate to inhibit post-extraction resorption. Journal of Environmental Radioactivity, 93: 63-73.

Luque-Garcı´a, J. L. and Luque de Castro, M. D. 2003.Where is microwave-based analytical equipment for solid sample pre-treatment going? Trends in Analytical Chemistry, 22: 90-98.

Ma, Y. B., Uren, N. C. 1998. Transformations of heavy metals added to soil-application of a new sequential extraction procedure. Geoderma, 84:157–168.

Machulla, G., Zikeli, S., Kastler, M., Jahn, R., 2004. Microbial biomass and respiration in soils derived from lignite ashes: a profile study. Journal of Plant Nutrition and Soil Science, 167: 449–456.

Mackowsky, M-Th. 1968. Coal and Coal Bearing Strata. Editors O.G. Murchison and T.S. Westroll. Oliver and Boyd.

Mahlaba, J. S., Kearsley, E. P., Richard A. Kruger, R. A. 2011. Physical, chemical and mineralogical characterisation of hydraulically disposed fine coal ash from SASOL Synfuels. Fuel, xxx: xxx–xxx.

Maiz, I., Arambarri, I., Garcia, R., Millan, E. 2000. Evaluation of heavy metal availability in polluted soils by two sequential extraction procedures using factor analysis. Environmental Pollution, 110: 3-9.

Maiz, I., Esnaola, M. V., Millian, E. 1997. Evaluation of heavy metal availability in contaminated soils by a short sequential extraction procedure. The Science of the Total Environment, 206:107-115.

Malhotra, V. M., Valimbe, P. S., Wright, M. A. 2002. Effects of fly ash and bottom ash on the frictional behaviour of composites. Fuel, 81: 235-244.

Margu´i, E., Salvadó, V., Queralt, I., Hidalgo, M. 2004. Comparison of three-stage sequential extraction and toxicity characteristic leaching tests to evaluate metal mobility in mining wastes. Analytica Chimica Acta, 524: 151–159.

Marrero, J., Polla, G., R. J., Rebagliati, Plá, R., Gómez, D., Smichowski, P. 2007. Characterization and determination of 28 elements in fly ashes collected in a thermal power plant in Argentina using different instrumental techniques. Spectrochimica Acta Part B, 62: 101–108.

Martens, D.C., Schnappinger Jr., M.G., Doran, J.W., Zelazny, L.W., 1970. The plant availability of potassium in fly ash. Soil Sci. Soc. Am. Proc., 34: 453–456.

Matjie, R. H., Li, Z., Ward, C. R., French, D. 2008. Chemical composition of glass and crystalline phases in coarse gasification ash. Fuel, 87: 857-869.

Mattigod, S. V., Dhanpat, R., Eary, L. E., Ainsworth, C. C. 1990a. Geochemical factors combustion residues: I. Review of the major elements. Journal of Environmental Quality, 19:188–201.

Mattigod, S. V., Rai, D., Eary, L. E. and Ainsworth, C. C.: 1990b ‘Geochemical factors controlling the mobilization of inorganic constituents from fossil fuel combustion residues: 1. Review of the major elements’, J. Environ. Qual., 19: 188–201.

Matuslewlcz, H. 1994. Development of a High Pressure/Temperature Focused Microwave Heated Teflon Bomb for Sample Preparation. Anal. Chem., 66: 751-755.

McCarthy, G. J., Swanson, K. D., Keller, L. P., and Blatter, W. C. 1984. Mineralogy of western fly ash Cement and Concrete Research, 14: 471-478.

McQuaker, N. R., Brown, D. F. and Kluckner, P. D. 1979. Digestion of Environmental Materials for Analysis by Inductively Coupled Plasma-Atomic Emission Spectrometry. Analytical Chemistry, 51: 1082-1084.

Measurements and Testing Newsletter, Vol. 1 (1), 1993.

Mehlich, A. 1938. Use of triethanolamine acetate-barium hydroxide buffer for the determination of some base exchange properties and lime requirement of soil. Soil Sci. Soc. Am. Proc. 29: 374-378.

Mehta, P. K. 1986. Effect of fly ash composition on sulfate resistance of cement. J Am Concr Ins., 83: 994-1000.

Meima, J. A., Comans, R. N. J. 1999. The leaching of trace elements from municipal solid waste incinerator bottom ash at different stages of weathering. Applied Geochemistry, 14: 159-171.

Melaku, S., Dams, R., Moens, L. 2005. Determination of trace elements in agricultural soil samples by inductively coupled plasma-mass spectrometry: Microwave acid digestion versus aqua regia extraction. Analytica Chimica Acta, 543: 117–123.

Melquiades, F. L., Appoloni, C. R. 2004. Application of XRF and field portable XRF for environmental analysis. Journal of Radio analytical and Nuclear Chemistry, 262: 533 – 541.

Menghistu, M. T. 2010. Development of a numerical model for unsaturated/saturated hydraulics in Ash/Brine systems. Unpublished PhD Thesis, University of Free State, South Africa.

Menon, M. P., Ghuman, G. S., James, J., Chandra, K., Adriano, D. C. 1980. Physico-chemical characteristics of water extracts of different coal ashes and fly ash amended composts. Water Air Soil Pollut., 50: 343–53.

Mester, Z., Angelone, M., Brunori, C., Cremisini, C., Muntau, H., Morabito, R. 1999. Digestion methods for analysis of fly ash samples by atomic absorption spectrometry. Analytica Chimica Acta, 395: 157-163.

Mester, Z., Cremisini, C., Ghiara, C., Morabito, R. 1998. Comparison of two sequential extraction procedures for metal fractionation in sediment samples. Anal. Chim. Acta., 359: 133-142.

Meyers, James F., Raman Pichumani and Bernadette S. Kapples. 1976. Fly ash. A Highway Construction material. Federal Highway Administration Report No. FHWA-IP-76-16, Washington.

Midgley, D. C., Pitman, W. V., and Middleton, B. J. 1994. Surface Water Resources of South Africa 1990. WRC Report No 298/1.4/94.

Mishra, S. R., Kumar, S., Wagh, A., Rho, J. Y., Gheyi, T. 2003. Temperature-dependent surface topography analysis of Illinois class F fly ash using ESEM and AFM. Materials Letters, 57: 2417-2424.

Mittra, B. N., Karmakar, S., Swain, D. K., Ghosh, B. C. 2005. Fly ash-a potential source of soil amendment and a component of integrated plant nutrient supply system. Fuel, 84: 1447–1451.

Mizutani, S., Yoshida, T., Sakai, S and Takatsuki, H. 1996. Release of metals from MSW I Fly Ash and availability in Alkali condition. Waste Management, 16: 537-544.

Moitsheki, L. J., Matjie, R. H., Baran, A., Mooketsi, O. I., Schobert, H. H. 2010. Chemical and mineralogical characterization of a South African bituminous coal and its ash, and effect on pH of ash transport water. Minerals Engineering, 23: 258–261.

Mokobia C. E., Ogundare F.O., Inyang E. P., Balogun F. A., Jonah S. A. 2008. Determination of the elemental constituents of a natural dolerite using NIRR-1. Applied Radiation and Isotopes, 66: 1916-1919.

Mollah, M. Y. A., Promreuk, S., Schennach, R., D. L. Cocke, D. L., Gu¨lerc, R. 1999. Cristobalite formation from thermal treatment of Texas lignite fly ash. Fuel, 78:1277–1282.

Moreno, N., Querol, X., Ayora, C., Pereira, C. F., Janssen- Jurkovicova. 2001. Utilization of Zeolites Synthesized from Coal Fly Ash for the Purification of Acid Mine Waters. Environ. Sci. Technol., 35: 3526-3534.

Mossop, K. F., Davidson, C. M. 2003. Comparison of original and modified BCR sequential extraction procedures for the fractionation of copper, iron, lead, manganese and zinc in soils and sediments. Analytica Chimica Acta , 478 :111–118.

Moutsatsou, A., Stamatakis, E., Hatzitzotzia, K., Protonotarios, V. 2006. The utilization of Ca-rich and Ca–Si-rich fly ashes in zeolites production. Fuel, 85: 657–663.

Mukhopadhyay, P. K.1994. Vitrinite reflectance as Maturity Parameter; Chapter 1 in *Vitrinite reflectance as a maturity parameter*; Mukhopadhyay P.K.; Dow W.G. Eds; ACS Symposium Series 570, American Chemical Society.

Murayama, N., Yamamoto, H., Shibata, J. 2002. Mechanism of zeolite synthesis from coal fly ash by alkali hydrothermal reaction. Int. J. Miner. Process., 64: 1–17.

Muriithi, G. N., 2009. CO_2 sequestration using brine impacted fly ash. Unpublished M.Sc thesis, Earth Sciences Department, University of the Western Cape, South Africa.

Muriithi, G. N., Gitari, W. M., Petrik, L. F., Ndungu, P. G., 2010. Carbonation of brine impacted fractionated coal fly ash: Implications for CO_2 Sequestration. Journal of Environmental Management, 92: 655-664.

Nadkarni, R. A. 1980. Multitechnique Multielemental Analysis of Coal and Fly Ash. Anal. Chem., 52: 929-935.

Nadkarni, R. A. 1984. Applications of Microwave Oven Sample Dissolution in Analysis. Analytical Chemistry, 56: 2233-2237.

Naik, T. R., Singh, S. S., Ramme, B. W. 1998. Mechanical properties and durability of concrete made with blended fly ash. ACI Mater J., 95:454–462.

Navarro, C. R., Agudo, E. R., Luque, A., Navarro, A. B. R., Huertas, M. O. 2009. "Thermal decomposition of calcite: Mechanisms of formation and textural evolution of CaO nanocrystals", American Mineralogist, 94: 578-593.

Narukawa, T., Riley, K. W., French, D. H., Chiba, K. 2007. Speciation of chromium in Australian fly ash. Talanta, 73: 178–184.

Nathan, Y., Dvorachek, M., Pelly, I., Mimran, U. 1999. Characterization of coal fly ash from Israel. Fuel, 78: 205–213.

National Academy Press, 1980. Trace Element Geochemistry of Coal Resource Development Related to Environmental Quality and Health. US National Committee for Geochemistry. Washington, DC. Illinois State Geological Survey Circular # 499, 1977. Relative Abundance of Selected Elements in Eastern Bituminous Coal. Urbana, IL: US Geological Survey.

Natusch, D. F. S., Bauer, C. F., Matusiewicz, H., Evans, C. A., Baker, J., Loth, A., Linton, R. W. and Hopke, P. K.: 1975, in T. E. Hutchinson (ed.), Proc. of Int. Conf. on Heavy Metals in Environment, Part 2, Toronto, Ontario, Canada, 2: 553–575.

Nemati, K., Abu Bakar, N. K., Bin Abas, M. R., Sobhanzadeh, E., Low, K. H. 2010. Comparative study on open system digestion and microwave assisted digestion methods for metal determination in shrimp sludge compost. Journal of Hazardous Materials, 182: 453–459.

Novozamsky, I., Lexmond, Th. M., Houba, V. J. G. 1993. A single extraction procedure of soil for evaluation of uptake of some heavy metals by plants. Int. J. Environ. Anal. Chem., 51: 47–58.

Nyamhingura, A. 2009. Characterization and Chemical Speciation Modelling of Saline Effluents at Sasol Synthetic Fuels Complex-Secunda and Tutuka Power Station. Unpublished M.Sc Thesis, Chemistry Department, University of the Western Cape, South Africa.

Ojha, K., Pradhan, C. N. and Samanta, A. N. 2004. Zeolite from fly ash: synthesis and characterization. Bull. Mater. Sci., 27: 555-564.

Ojo, O. I. 2009. Mineralogy and chemical mobility in some weathered ash dump sites, South Africa. Unpublished M.Sc Thesis, Earth Sciences Department, University of the Western Cape, South Africa.

Pacifico, R., Adamo, P., Cremisini, C., Spaziani, F., Ferrara, L. 2007. A Geochemical Analytical Approach for the Evaluation of Heavy Metal Distribution in Lagoon Sediments. J Soils Sediments, 7: 313 – 325.

Page, A. L., Elseewi, A. A., Straughan, I. R. 1979. Physical and chemical properties of fly ash from coal-fired power plants with special reference to environmental impacts. Residue Rev., 71: 83-120.

Palomo, A., Macı´as, A., Blanco, M. T., Puertas, F. 1992. Physical, Chemical and mechanical characterization of geopolymers. In: Proceedings of the 9th International Congress on the Chemistry of Cement, New Delhi, India, 5: 505–511.

Parkhurst, D. L., Appelo, C. A. J. 1999. User's guide to PHREEQC (Version 2) - A computer program for speciation, batch-reaction, one-dimensional transport, and inverse geochemical calculations: U.S. Geological Survey Water-Resources Investigations Report 99-4259: 312 p.

Paya, J., Monzo, J.., Borrachero, M. V. and Peris-Mora, E. 1995. Mechanical and Treatment of Fly Ashes. Part I: Physico-chemical Characterization of Ground Fly Ashes. Cement and Concrete Research 25: 1469-1479.

Pe´rez-Bendito, D., Rubio, S, editors. 1999. Environmental analytical chemistry. Comprehensive analytical chemistry series, vol. 32. Amsterdam: Elsevier; p. 709.

Pérez-López, R., Nieto, J. M., Almodóvar, G. R. 2007a. Utilization of fly ash to improve the quality of the acid mine drainage generated by oxidation of a sulphide-rich mining waste: column experiments. Chemosphere, 67:1637–1646.

Pérez-López, R., Cama, J., Nieto, J. M., Ayora, C. 2007b. The iron-coating role on the oxidation kinetics of a pyritic sludge doped with fly ash. Geochim. Cosmochim. Acta., 71:1921–34.

Petaloti, C., Triantafyllou, A., Kouimtzis, T., Samara, C. 2006. Trace elements in atmospheric particulate matter over a coal burning power production area of western Macedonia, Greece. Chemosphere 65: 2233–2243.

Petit, M. D., Rucandio, M. I. 1999. Sequential extractions for determination of cadmium distribution in coal fly ash, soil and sediment samples. Anal. Chim. Acta., 401: 283-291.

Petrik, L. F., Gitari, W. M., Etchebers, O., Nel, J., Vadapalli, V. R. K., Fatoba, O. Nyamihingura, A., Akinyemi, S. A. and Antonie, M. J. 2008. Towards the Development of Sustainable Salt Sinks: Fundamental Studies on the Co-Disposal of Brines within Inland Ash Dams. UWC, Final Report to ESKOM/SASOL, South Africa.

Petrik, L., Hendricks, N., Ellendt, N. and Burgers, C. 2007. Toxic element removal from water using Zeolite adsorbents made from solid waste residues. Water Research Commission, WRC Report No. 1546/1/07, University of the Western Cape, South Africa.

Petrik, L. F., White, R. A., Klink, M. J., Somerset, S. V., Burgers, L. C., Fey, V. M. 2003. Utilization of South African fly ash to treat acid coal mine drainage, and production of high quality zeolites from the residual solids. International Ash Utilization Symposium, Lexington, Kentucky, USA.

Pickering, W. F. 1986. Metal ion speciation-soils and sediments (a review). Ore Geology Reviews, 1: 83-146.

Plank, C. O., Martens, D. C., 1973. Amelioration of soils with fly ash. Soil Water Conservation, 28: 177-186.

Plank, C. O., Martens, D. C., 1974. Boron availability as influenced by application of fly ash to soil. Soil Sci. Soc. Am. Proc., 38: 974–977.

Polat, M., Eli, L., Ithamar, P., Haim, C. 2002. Chemical neutralization of acidic wastes using fly ash in Israel. J Chem Tech Biotechnol., 77: 377–381.

Popovic, A., Djordjevic, D., Polic, P. 2001. Trace and major element pollution originating from coal ash suspension and transport processes. Environment International, 26: 251-255.

Potgieter-Vermaak, S. S., Potgieter, J. H., Monama, P., Van Grieken, R. 2006. Comparison of limestone, dolomite and fly ash as pre-treatment agents for acid mine drainage. Miner Eng., 19:454–462.

Potts, P. J., Ellis, A. T., Holmes, M., Kregsamer, P., Streli, C., Weste, M., Wobrauschekd, P. 2000. X-ray fluorescence spectrometry. J. Anal. At. Spectrom., 15: 1417-1442.

Prasad, B., Banerjee, N. N., Dhar, B. B. 1996. Environmental assessment of coal ash disposal: a review. J Sci Ind Res India, 55:772–780.

prEN14429. 2003. Leaching behaviour test – Influence of pH on leaching with initial acid/base addition – Horizontal standard.

Puccio, M. 1983. Le Ceneri de carbone. ITEC, Milan.

Pueyo, M., Mateu, J., Rigol, A., Vidal, M., Lo´pez-Sa´nchez, J. F., Rauret, G. 2008. Use of the modified BCR three-step sequential extraction procedure for the study of trace element dynamics in contaminated soils. Environmental Pollution, 152: 330-341.

Querol. X., Moreno, N., Umana, J. C., Alastuey, A., Hernandez, E., Lopez-Soler, A., Plana, F. 2002. Synthesis of zeolites from coal fly ash: an overview. International Journal of Coal Geology, 50: 413-423.

Querol, X., Umaña, J. C., Alastuey, A., Ayora, C., Lopez-Soler, A. and Plana, F. 2001. Extraction of soluble major and trace elements from fly ash in open and closed leaching systems. Fuel, 80: 801-813.

Querol, X., Umana, J. C., Plana, F., Alastuey, A., Lopez-Soler, A., Medinaceli, A., Valero, A., Domingo, M. J., Garcia-Rojo, E. G. 1999. Synthesis of Zeolites from Fly Ash in a Pilot Plant Scale. Examples of Potential Environmental Applications. International Ash Utilization Symposium, Centre for Applied Energy Research, University of Kentucky, Paper # 12.

Querol, X., Alastuey, A., Lopez-Soler, A., Plana, F., Andreas, J. M., Juan, R., Ferrer, P., Ruiz, C. R. 1997. A Fast Method for Recycling Fly Ash: Microwave-Assisted Zeolite Synthesis. Environ. Sci. Technol., 31: 2527-2533.

Querol, X., Juan, R., Lopez-Soler, A., Fernandez-Turiel, J. L. and Ruiz, C. R., 1996. Mobility of trace elements from coal and combustion wastes. Fuel, 75: 821-838.

Querol, X., Fernández-Turiel, J. L., Lopez-Soler, A. 1995a. Trace elements in coal and their behaviour during combustion in a large power station. Fuel, 74: 331.

Querol, X., Alastuey, A., Jose L. Fernandez-Turiel, J. L., Lopez-Soler, A. 1995b. Synthesis of zeolites by alkaline activation of ferro-aluminous fly ash. Fuel, 74: 1226-1231.

Quevauviller, Ph., Rauret, G., tipez-SBnchez, J. F., Rubio, R. Ure', A., Muntau, H. 1997. Certification of trace metal extractable contents in a sediment reference material (CRM 601)

following a three-step sequential extraction procedure. The Science of the Total Environment, 205: 223-234.

Quevauviller Ph, Rauret, G., Muntau, H., Rubio, R., tipez- Sgnchez, J. F., Fiedler, H, Griepink, B. 1994. Evaluation of a sequential extraction procedure for the determination of extractable trace metal contents in sediments. Fresenius J. Anal. Chem., 349: 808-814.

Quevauviller, Ph., Donard, O. F. X., Maier, E. A., Griepink, B. 1992. Improvements of speciation analyses in environmental matrices. Mikrochim. Acta, 109: 169-190.

Quina, M. J., Bordado, J. C. M., Quinta-Ferreira, R. M. 2009. The influence of pH on the leaching behaviour of inorganic components from municipal solid waste APC residues. Waste Management 29: 2483–2493.

Radojević Miroslav and Vladimir, B. N. 1999. "Practical environmental analysis". The Royal Society of Chemistry, pp. 353-355.

Rai, D., Ainsworth, C. C., Early, L. E., Mattigod, S. V., Jackson, D. R. 1987. A critical review. In: Inorganic and Organic Constituents in Fossil Fuel Combustion Residues, Vol. 1. Electric Power Research Institute. Report EA-5176.

Rai, D., Eary, L. E., Zachara, J. M. 1989. Environmental Chemistry of Chromium. The Science of the Total Environment, 86: 15-23.

Raksasataya, M., Langdon, A. G., Kim, N. D. 1996. Assessment of the extent of lead redistribution during sequential extraction by two different methods. Analytica Chimica Acta, 332: 1-14.

Ram, C. L., Srivastava, K. N., Tripathi, C., Ramesh, T. K., Sanjay, S. K., Awadhesh, J. K., Sangeet, M. E. R., Mitra, S. 2007: Leaching behaviour of lignite fly ash with shake and column tests. Environmental Geology, 51:1119-1132.

Rao, C. R. M., Sahuquillo, A. Lopez Sanchez, J. F. 2008. A Review of the Different Methods Applied in Environmental Geochemistry For Single and Sequential Extraction of Trace Elements in Soils and Related Materials. Water Air Soil Pollut., 189: 291–333.

Rapin, F., Tessier, A., Campbell, P. G. C., Carignan, R. 1986. Potential artifacts in the determination of metal partitioning in sediments by a sequential extraction procedure, Environ. Sci. Technol., 20: 836–840.

Rauret, G., Lopez-Sanchez, J. F., Sahuquillo, A., Barahona, E., Lachica, C., A.M. Ure, A. M., Davidson, C. M., Gomez, A., Lu¨ck, D., Bacon, J., Yli-Halla, M., Muntau, H., Quevauviller, Ph. 2000. Application of a modified BCR sequential extraction (three-step) procedure for the determination of extractable trace metal contents in a sewage sludge amended soil reference material (CRM 483), complemented by a three-year stability study of acetic acid and EDTA extractable metal content J. Environ. Monit., 2: 228-233.

Rauret, G., López-Sánchez, J. F., Sahuquillo, A., Rubio, R., Davidson, C., Ure, A., Quevauviller, Ph. 1999. Improvement of the BCR three-step sequential extraction procedure prior to the certification of new sediment and soil reference materials. . Environ. Monit., 1: 57-61.

Reardon, E. J, Czank, C. A., Warren, C. J., Dayal, R., Johnson. H. M. 1995. Determining controls on element concentrations in fly ash leachate. Waste Management and Research, 13: 435-450.

Reidelbach, J.A. 1970. An industrial evaluation of fly ash bricks. In: The US Department of the Interior, Bureau of Mines, Information Circular Number 8488. Washington, DC: US Department of the Interior.

Rohrman, F. A. 1971. Analyzing the effect of fly ash on water pollution. Power, 115: 76-77.

Rönkkömäki, H., Pöykiö, R., Nurmesniemi, H., Popov, K., Merisalu, E., Tuomi, T., Välimäki, I. 2008. Particle size distribution and dissolution properties of metals in cyclone fly ash. International Journal of Environmental Science and Technology, 5: 485-494.

Roy, W. R., Griffin, R. A. 1984. Illinois Basin Coal Fly Ashes.2.Equlibria relationships and qualitative modelling of ash–water reactions, Environ. Sci. Technol., 18: 739–742.

Roy, W. R., Griffin, R. A. 1982. A proposed classification system for coal fly ash in multidisciplinary research. Journal of Envir. Qual., 11: 563-568.

Rubio, R., Ure, A. M. 1993. Approaches to sampling and sample pretreatments for metal speciation in soils and sediments, Int. J. Environ. Anal. Chem., 51: 205–217.

Sahuquillo, A, Rigol, A., Rauret, G. 2003a. Overview of the use of leaching/extraction tests for risk assessment of trace metals in contaminated soils and sediments. Trends in Analytical Chemistry, 22: 152-159.

Sahuquillo, A., Rauret, G., Rehnert, A., Muntau, H. 2003b. Solid sample graphite furnace atomic absorption spectroscopy for supporting arsenic determination in sediments following a sequential extraction procedure. Analytica Chimica Acta, 476: 15–24.

Sahuquillo, A., LoÂpez-SaÂnchez, J. F., R. Rubio, R., G. Rauret, G., Thomas, R. P., Davidson, C. M., Ure, A. M. 1999. Use of a certified reference material for extractable trace metals to assess sources of uncertainty in the BCR three-stage sequential extraction procedure. Analytica Chimica Acta, 382: 317-327.

Saikia, N., Kato, S and Kojima, T. 2006a. Behavior of B, Cr, Se, As, Pb, Cd, and Mo present in waste leachates generated from combustion residues during the formation of ettringite. Environmental Toxicology and Chemistry. 25: 1710–1719.

Saikia, N., Kato, S., Kojima, T. 2006b. Compositions and leaching behaviours of combustion residues. Fuel, 85: 264–271.

Sakorafa, V., Burragato, F., Michailidis, K., 1996. Mineralogy, geochemistry and physical properties of fly ash from the Megalopolis lignite fields, Peloponnese, Southern Greece. Fuel 75: 419–23.

Samara, C. 2005. Chemical mass balance source apportionment of TSP in a lignite-burning area of Western Macedonia, Greece. Atmospheric Environment, 39: 6430–6443.

Sandroni, V. and Smith, C. M. M. 2002. Microwave digestion of sludge, soil and sediment samples for metal analysis by inductively coupled plasma–atomic emission spectrometry. Analytica Chimica Acta, 468: 335–344.

Sandroni, V., Smith, C. M. M., Donovan, A. 2003. Microwave digestion of sediment, soils and urban particulate matter for trace metal analysis. Talanta, 60: 715-723.

Sastre, J., Sahuquillo, A., Vidal, M., Rauret, G. 2002. Determination of Cd, Cu, Pb and Zn in environmental samples: microwave-assisted total digestion versus aqua regia and nitric acid extraction. Analytica Chimica Acta, 462: 59–72.

Satapathy, L. N. 2000. A study on the mechanical, abrasion and microstructural properties of zirconia fly ash material. Ceramics International, 26: 39-45.

Schakelford, C. D. 2000. Journal of Hazardous Materials, 76: Vii-Viii.

Scheckel, K. G., Impellitteri, C. A., Ryan, J. A., Mcevoy, T. 2003. Assessment of a Sequential Extraction Procedure for Perturbed Lead-Contaminated Samples with and without Phosphorus Amendments. Environ. Sci. Technol., 37: 1892-1898.

Scheetz, B. E. and Earle, R. 1998. Utilisation of fly ash. Current Opinion in Solid State & Material Science, 3:510-520.

Schmu¨cker, M., MacKenzie, K. J. D. 2005. Microstructure of sodium polysialate siloxo geopolymer. Ceramic International, 31: 433–437.

Schnappinger Jr., M. G, Martens, D. C., Plank, C. O. 1975. Zinc availability as influenced by application of fly ash to soil. Environ. Sci. Technol., 9: 258–261.

Schollenberger, C. J. 1927. Exchangeable hydrogen and soil reaction. Sci., 35:552-553.

Schopf, J. M. 1948. Variable coalification; the processes involved in coal formation. Economic Geology; 43: 207-225.

Schramke, J. A. 1992. Neutralization of alkaline coal fly ash leachates by CO_2 (g). Applied Geochemistry, 7: 481–492.

Schure, M. R., Soitys, P. A., Natusch, D. F. S. and Mauneys, T. 1985. Surface Area and Porosity of Coal Fly Ash/ Environ. Sci. Technol., 19: 82-86.

Scott, A. C. 2002. Coal petrology and the origin of coal macerals: a way ahead? International Journal of Coal Geology, 50: 119-134.

Seferinog˘lu, M., Paul, M., Sandstro¨m, A°., Ko¨ker, A., Toprak, S., Paul, J. 2003. Acid leaching of coal and coal-ashes. Fuel, 82: 1721–1734.

Seoanne, S. and Leiros, C. M. 2001. Acidification-Neutralization processes in a lignite Mine Spoil Amended with Fly ash or Limestone. Environmental Quality, 30: 1420-1431.

Shah, P., Strezov, V., Nelson, P. F. 2009. Speciation of chromium in Australian coals and combustion products. Fuel, xxx: xxx–xxx.

Shah, P., Strezov, V., Prince, K., Nelson, P. F. 2008. Speciation of As, Cr, Se and Hg under coal fired power station conditions. Fuel, 87: 1859-1869.

Shan, X.Q., Chen, B., 1993. Evaluation of sequential extraction for speciation of trace metals in model soil containing natural minerals and humic acid. Anal. Chem., 65: 802–807.

Shefsky, S. 1997. Comparing Field Portable X-Ray Fluorescence (XRF) To Laboratory Analysis of Heavy Metals In Soil. Presented at the International Symposium of Field Screening Methods for Hazardous Wastes and Toxic Chemicals. Las Vegas, Nevada, USA (January 29-31).

Shiowatana, J., Tantidanai, N., Nookabkaew, S., Nacapricha, D. 2001. A flow system for the determination of metal speciation in soil by sequential extraction. Environment International, 26: 381-387.

Siddique, R. 2004. Performance characteristics of high-volume Class F fly ash concrete. Cem Concr Res., 34: 487–493.

Silva, L. F.O., Ward, C. R., Hower, J. C., Izquierdo, M., Waanders, F., Oliviera, M. L. S., Li, Z., Hatch, R. S., Querol, X. 2010. Mineralogy and Leaching Characteristics of Coal Ash a Major Brazilian Power Plant. Coal Combustion and Gasification Products, 2: 51-65.

Singh, D. N. and Kolay, P. K. 2002. Simulation of ash-water interaction and its influence on ash characteristics. Progress in Energy and Combustion Science, 28, 267-299.

Singh, R. P., Gupta, A. K., Ibrahim, M. H., Mittal, A. K. 2010. Coal fly ash utilization in agriculture: its potential benefits and risks. Rev Environ Sci Biotechnol., 9: 345–358.

Skvarla J., 1998. A study on the trace metal speciation in the Ruzin reservoir sediment. Acta Montanistica Slovaca, Rocnik 3: 177-182.

Smeda, A., Zyrnicki, W., 2002. Application of sequential extraction and the ICP-AES method for study of the partitioning of metals in fly ashes. Microchemical, 72: 9-16.

Smichowski, P., Polla, G., Gomez, D., Fernandez Espinosa, A. J., Lopez, A. C. 2008. A three step sequential metal fractionation scheme for fly ashes collected in an Argentine thermal power plant. Fuel, 87: 1249-1258.

Smith, R. M. H., Eriksson, P. G., Botha, W. J. 1993. A review of the stratigraphy and sedimentary environments of the Karoo-aged basins of Southern Africa. Journal of African Earth Sciences, Vol. 16: 143-169.

Snyman, C. P. and Botha, W. J. 1993. Coal in South Africa. Journal of African Earth Sciences, 16: 171-180.

Snyman, C. P., Barclay, J. 1989. The coalification of South African coal. International Journal of Coal Geology, 13: 375-390.

So˘co, E., Kalembkiewicz, J. 2007. Investigations of sequential leaching behavior of Cu and Zn from coal fly ash and their mobility in environmental conditions. J. Hazard. Mat., 145: 482–487.

Soc˘o, E. and Kalembkiewicz, J. 2009. Investigations on Cr mobility from coal fly ash. Fuel, 88: 1513–1519.

Sokol, E. V., Maksimova, N. V., Volkova, N. I., Nigmatulina, E. N., Frenkel, A. E. 2000. Hollow silicate microspheres from fly ashes of the Chelyabinsk brown coals (South Urals, Russia). Fuel Processing Technology, 67: 35–52.

Solem-Tishmack, J. K., McCarthy. G. J. 1995. High-Calcium Coal Combustion by products: Engineering Properties, Entrringite Formation and Potential Application in Solidification and Stabilisation of Selenium and Boron. Cement and Concrete. Research, 25: 658-670.

Soong, Y., Fauth, D. L., Howard, B. H., Jones, J. R., Harrison, D. K., Goodman, A. L., Gray, M. L., Frommell, E. A. 2006. CO_2 Sequestration with brine solution and fly ashes. Energy Conversion and Management, 47: 1676-1685.

South African Coal Report cc. 2001. South African Coal Statistics and Marketing Manual.

Spears, D. A., Lee, S. 2004. Geochemistry of leachates from coal ash. In: Giere´ R, Stille P, editors. Energy, waste and the environment: a geochemical perspective. Geological Society of London, Special Publications, 236: 619–639.

Spears, D. A. 2000. Role of clay minerals in UK coal combustion. Applied Clay Science, 16: 87–95.

Spears, D. A. and Martinez-Tarazona, M. R. 1993. Geochemical and mineralogical characteristics of a power station feed-coal; Eggborough, England, Int. J. Coal Geol., 22: 1-20.

Speight, J. G. 1994. The Chemistry and Technology of Coal (2nd Ed.), Marcel Dekker, New York.

Stach, E., MacKowsky, M-Th, Teichmuller, M., Taylor, G. H., Chandra, D., Teichmuller, R., Murchison, D. G., Zierke, F. Stachs 1982. Textbook of Coal Petrology, edn 3. Berlin: Gebruder Bantraeger; pp.535.

Stalikas, C. D., Pilidis, G. A., Tzouwara-Karayanni, S. M. 1999. Use of a sequential extraction scheme with data normalization to assess the metal distribution in agricultural soils irrigated by lake water. The Science of the Total Environment, 236: 7-18.

Stanislav V. Vassilev, S. V., Yossifova, M. G., Vassileva, C. G. 1994. Mineralogy and geochemistry of Bobov Dol coals, Bulgaria International Journal of Coal Geology, 26: 185-213.

Steenari, B. M., Schelander, S., O. Lindqvist, O. 1999a. Chemical and leaching characteristics of ash from combustion of coal, peat and wood in a 12 MW CFB – a comparative study. Fuel, 78: 249-258.

Steenari, B.-M., Karlsson, L. G., Lindqvist, O. 1999b. Evaluation of the leaching characteristics of wood ash and the influence of ash agglomeration. Biomass and Bioenergy, 16: 119-136.

Steenari, B. M., Lindqvist, O. 1997. Stabilisation of Biofuel Ashes for Recyling to Forest Soil. Biomass and Bioenergy, 13: 39-50.

Steenbruggen, G., Hollman, G. G. 1998. The synthesis of zeolites from fly ash and the properties of the zeolite products. Journal of Geochemical Exploration, 62: 305–309.

Stephens, S. R., Alloway, B. J., Parker, A., Carter, J. E., Hodson, M. E. 2001. Changes in the leachability of metals from dredged canal sediments during drying and oxidation. Environmental Pollution, 114: 407-413.

Stevenson, R. J., McCarthy, G. J. 1985. Mineralogy of Fixed-Bed Gasification Ash Derived from North Dakota Lignite. Mat. Res. Soc. Symp. Proc. Vol. 65.

Stewart, B. R., Daniels, W. L., Jackson, M. L. 1997. Evaluation of leachate quality from co-disposed coal fly ash and coal refuse. J Environ Qual., 26: 1417–1424.

Stucki, J. W. 2006. Chapter 8. Properties and behavior of iron in clay minerals. Development in Clay Science, 1: 423-475.

Stumm, W., Morgan, J. J. 1981. Aquatic Chemistry (2nd edn). John Wiley, New York.

Sutherland, R. A. 2002. Comparison between non-residual Al, Co, Cu, Fe, Mn, Ni, Pb and Zn released by a three-step sequential extraction procedure and a dilute hydrochloric acid leach for soil and road deposited sediment. Applied Geochemistry, 17: 353–365.

Sutherland, R. A., Tack, F. M. G. 2003. Fractionation of Cu, Pb and Zn in certified reference soils SRM 2710 and SRM 2711 using the optimized BCR sequential extraction procedure. Advances in Environmental Research, 8: 37–50.

Sutherland, R. A., Tack, F. M. G., Tolosa, C.A., Verloo, M. G. 2000. Operationally defined metal fractions in road depositedsediment, Honolulu, Hawaii. J. Environ. Qual., 29: 1431–1439.

Swami, K., Judd, C. D., Orsini, J., Yang, K. X., Husain, L. 2001. Microwave assisted digestion of atmospheric aerosol samples followed by inductively coupled plasma mass spectrometry determination of trace elements. Fresenius J Anal Chem., 369: 63–70.

Swanepoel, J. C., Strydom, C. A. 2002. Utilization of fly ash in a geopolymeric material. Applied Geochemistry, 17: 1143-1148.

Tack, F. M., Verloo, M. G. 1996. Impact of single reagent extraction using NH4OAc-EDTA on the solid phase distribution of metals in a contaminated dredged sediment. The Science of the Total Environment, 178: 29-36.

Talmi, Y and Andren, A. W. 1974. Determination of Selenium in Environmental Samples Using Gas Chromatography with a Microwave Emission Spectrometric Detection System. Analytical Chemistry, 46: 2122-2126.

Tam, N. F. Y., Yao, M. W. Y. 1999. Three Digestion Methods to Determine Concentrations of Cu, Zn, Cd, Ni, Pb, Cr, Mn, and Fe in Mangrove Sediments from Sai Keng, Chek Keng, and Sha Tau Kok, Hong Kong. Bull. Environ. Contam. Toxicol., 62: 708-716.

Tan, L. C., Choa, V., Tay, J. H. 1997. The influence of pH on mobility of heavy metals from municipal solid waste incinerator fly ash. Environmental Monitoring and Assessment, 44: 275-284.

Tang, X. Y., Katou, H., Suzuki, K., Ohtani, T. 2011. Air-drying and liming effects on exchangeable cadmium mobilization in contaminated soils: A repeated batch extraction study. Geoderma, 161: 18–29.

Teichmuller T. M., Teichmuller, R. 1975. The geologic basis of coal formation. In Stach's Textbook of Coal Petrology. Edited by Murchison D. G., Taylor G. H., Zierke E Berlin-Stuttgart: Gebruder Borntrager: 5-53.

Tessier, A., Campbell,P. G. C., Bisson, M. 1979. Sequential extraction procedure for the speciation of particulate traces metals. Analy. Chem., 51: 844-850.

Tessier, A. 1992. Sorption of trace elements on natural particles in oxic environments. In: Buffle, J. and Van Leeuwen, H.P., Editors, 1992. Environmental Particles, Environmental Analytical and Physical Chemistry Series, J. Lewis Publishers, Boca Raton, F L, 425–453.

Tessier, A. Campbell, P. G. C. 1988. Comments on the Testing of the Accuracy of an Extraction Procedure for Determining the Partitioning of Trace Metals in Sediments. Anal. Chem., 60: 1475-1476.

Tessier, A., Campbell, P. G. C., Bisson, M. 1982. Particulate trace metal speciation in stream sediments and relationships with grain size: implications for geochemical exploration. J. Geochem. Exploration, 16: 77-104.

Theis, T. L., Richter, R. O. 1979. Chemical Speciation of Heavy Metals in Power Plant Ash Pond Leachate. Environ. Science and Tech., 13: 219-224.

Theis, T. L. and Wirth, J. L. 1977. Sorptive Behavior of Trace Metals on Fly Ash in Aqueous Systems Environmental Science & Technology, 11: 1096-1100.

Tikalsky P. J., Carrasquillo, P. M., Carrasquillo, R. L. 1988. Strength and durability considerations affecting mix proportions of concrete containing fly ash. ACI Mater J., 85:505–511.

Tiruta-Barna L., Rakotoarisoa, Z. and Mehu, J. 2006. Assessment of the multi-scale leaching behavior of compacted coal ash. Hazardous Material, B137: 1466-1478.

Tiruta-Barna, L., Inyim, A., Barna, R. 2004. Long-term prediction of the leaching behaviour of pollutants from solidified wastes. Advance in Environmental Research, 8: 697-711.

Totland, M., Jarvis, I., Jarvis, K. E. 1992. An assessment of dissolution techniques for the analysis of geological samples by plasma spectrometry. Chemical Geology, 95: 35-62.

Townsend, W. N., Hodgson, D. R. 1973. Edaphological problems associated with deposits of pulverized fuel ash. In: Hutnik, R.J., Davis, G. (Eds.), Ecology and Reclamation of Devastated Land, vol. 1. Gordon and Breach, New York.

Tu¨zen, M. 2003. Determination of heavy metals in soil, mushroom and plant samples by atomic absorption spectrometry. Microchemical Journal, 74: 289–297.

Tyrrell, E., Shellie, R. A., Hilder, E. F., Pohl, C. A., Haddad, P. R. 2009. Fast ion chromatography using short anion exchange columns. Chromatogr. A, 1216: 8512–8517.

Ugurlu, A. 2004. Leaching characteristics of fly ash. Environ. Geol., 46: 890–895.

Uhrberg, R. 1982. Acid Digestion Bomb for Biological Samples. Analytical Chemistry, 54: 1906-1908.

Unsworth, J. F., Barratt, D. J., Park, D., Titchener, K. J. 1988. Ash formation during pulverized coal combustion. 2. The significance of crystalline anorthite in boiler deposits. Fuel, 67: 632-642.

Ure A, Quevauviller Ph, Muntau H, Griepink B. 1993. Speciation of heavy metals in soils and sediments. An account of the improvement and harmonization of extraction techniques undertaken under the auspices of the BCR of the Commission of the European Communities. Int J Environ. Anal. Chem., 51: 135-151.

Usero, J., Gamero, M., Morillo, J., Gracia, I. 1998. Comparative Study of Three Sequential Extraction Procedures for Metals in Marine Sediments. Environment International, 24: 487-496.

Valentim, B. V., Hower, J. C. 2010. Influence of feed and sampling systems on element partitioning in Kentucky fly ash. Int. J. of Coal Geology., 82: 94-104.

Van Bekkum, H., Flanigen, E. M., Jansen, J. C. 1991. Introduction to Zeolite Science and Practice. Elsevier, Amsterdam.

Van benschoten, J. E., Reed, B. E., Matsumoto, M. R., McGarvey, P. J. 1994. Metal removal by soil washing for an iron oxide coated sandy soil. Water Environment Research, 66: 168-174.

Van den Berg, J. J., Cruywagen, L., De Necker, E., Hodgson, F. D. I. 2001. The suitability and impact of power station fly ash for water quality control in coal opencast mine rehabilitation. Report to the Water Research Commission, WRC Report No.745/1/01.

Van der Hoek, E. E., Coman, R. N. J. 1999. Speciation of As and Se during leaching of Fly Ash. Stud. in Environ. Sci., 60: 467-476.

Van der Hoek, E. E. and Comans, R. N. J. 1996**.** Modeling Arsenic and Selenium Leaching from Acidic Fly Ash by Sorption on Iron (Hydr) oxide in the Fly Ash Matrix. Environ. Sci. Technol., 30: 517-523.

Van der Hoek, E. E., Bonouvrie, P. A., Comans, R. N. J. 1994. Sorption of As and Se in mineral components of fly ash, relevance for leaching processes. Appl. Geochem., 9: 406-412.

Van der Merwe, L., Kempster, P. I., Van Vliet, H. R., Van Staden, J. F. 1994. A pH-dependent sequential extraction procedure to determine mobilization and transport of metals in sediments. Water Research Commission-S Africa, 20: 27-34.

van Jaarsveld, J. G. S., van Deventer, J. S. J. 1999. Effect of the Alkali Metal Activator on the Properties of Fly Ash-Based Geopolymers. Ind. Eng. Chem. Res., 38: 3932-3941.

van Jaarsveld, J. G. S., van Deventer, J. S. J., Lukey, G. C. 2003. The characterization of source materials in fly ash-based geopolymers. Materials Letters, 57: 1272–1280.

Van Jaarsveld, J. G. S., Van Deventer, J. S. J., Lorenzen, L., 1996. The potential use of geopolymeric materials to immobilize toxic metals: part 1. Theory and applications. Miner. Engin., 10: 659–669.

van Jaarsveld, J. G. S., van Deventer, J. S. J., Lukey, G. C., 2002. The effect of composition and temperature on the properties of fly ash and kaolinite based geopolymers. Chemical Engineering Journal, 89: 63–73.

Vassilev S. V. and Vassileva, C. G. 2007. A new approach for the classification of coal fly ashes based on their origin, composition, properties and behaviour. Fuel, 86: 1490-1512.

Vassileva, C. G., Vassilev, S. V. 2006. Behaviour of inorganic matter during heating of Bulgarian coals 2. Sub bituminous and bituminous coals Fuel Processing Technology, 87: 1095–1116.

Vassilev, S .V., Vassileva, C. G. 2005a. Methods for characterization of composition of fly ashes from coal-fired power stations: A critical overview. Energy Fuels, 19: 1084–98.

Vassileva, G. G., Vassilev, S. V. 2005b. Behaviour of inorganic matter during heating of Bulgarian coals 1. Lignites. Fuel Processing Technology, 86: 1297-1333.

Vassilev, S. V., Vassileva, C. G. 1998. Comparative chemical and mineral characterization of some Bulgarian coals. Fuel Processing Technology, 55: 55–69.

Vassilev, S. V., Kitano, K. and Vassileva, C. G. 1997a. Relations between ash yield and chemical and mineral composition of coals. Fuel, 76: 3-8.

Vassilev, S. V., Vassileva, C. G. 1997b. Geochemistry of coals, coal ashes and combustion wastes from coal-fired power stations. Fuel Processing Technology, 51: 19-45.

Vassilev, S. V., Kitano, K. and Vassileva, C. G. 1996a. Some relationships between coal rank and chemical and mineral composition. Fuel, 75: 1537-1542.

Vassilev S.V., Vassileva C. G. 1996b. Occurrence, abundance and origin of minerals in coals and coal ashes. Fuel Proc. Technol., 48: 85-106.

Vassilev, S. V., Vassileva, C. G. 1996c. Mineralogy of combustion wastes from coal-fired power stations. Fuel Process Technol., 47: 261–280.

Vassilev, S. V. 1994. Trace elements in solid waste products from coal burning at some Bulgarian thermoelectric power stations. Fuel, 73: 367-374.

Veschetti, E., Maresca, D. Cutilli, D., Santarsiero, A., Ottaviani, M. 2000. Optimization of H_2O_2 action in sewage sludge microwave digestion using Delta pressure vs. temperature and pressure vs. time graphs, Microchem. J., 67: 171-179.

Visser, J. N. J. and Loock, J. C. 1987. Ice margin influence on glaciomarine sedimentation in the Permo-Carboniferous Dwyka Formation from the southwestern Karoo, South Africa. Sedimentology, 34: 929-941.

Visser, J. N. J. 1986. Lateral lithofacies relationships in the glacigene Dwyka Formation in the western and central parts of the Karoo Basin. Trans. Geol. Soc. S. Afr., 89: 373-383.

Vitkova, M., Ettler V., Sebek, O., Mihaljevic, M., Grygar, T., Rohovec, J. 2009. The pH-dependent leaching of inorganic contaminants from lead smelter fly ash. J. of Hazard. Mat., 167: 427-433.

Wadge, A. and Hutton, M. 1987. The leachability and chemical speciation of selected trace elements in fly ash from coal combustion and refuse incineration. Environmental pollution, 86: 85-99.

Wan, X., Wang, W., Ye, T., Guo, Y., Gao, X. 2006. A study on the chemical and mineralogical characterization of MSWI fly ash using a sequential extraction procedure Journal of Hazardous Materials, B134: 197–201.

Wang, J., Teng, X., Wang, H., Ban, H. 2004a. Characterizing the metal adsorption capability of a Class F coal fly ash. Environ Sci Technol., 38: 6710-6715.

Wang, J., Nakazato, T., Sakanishi, K.,Yamada, O., Tao, H., Saito, I. 2004b. Microwave digestion with HNO_3/H_2O_2 mixture at high temperatures for determination of trace elements in coal by ICP-OES and ICP-MS. Analytica Chimica Acta, 514: 115–124.

Wang, J., Wang, T., Burken, J.G., Chusuei, C.C., Ban, H., Ladwig, Huang, C.P. 2008. Adsorption of arsenic (V) onto fly ash: A speciation-based approach. Chem., 72: 381-388.

Wang, S., Wu, H. 2006. Environmental-benign utilization of fly ash as low-cost adsorbents. Journal of Hazardous Materials, B136: 482–501.

Wang, T., Su, T., Wang, J., Ladwig, K. 2007. Calcium effects on Arsenic (V) Adsorption onto Coal fly ash. World of Coal Ash (WOCA) Covington, Kentucky.

Wang, Z., Shan, X. Q., Zhang, S. 2002. Comparison between fractionation and bioavailability of trace elements in rhizosphere and bulk soils. Chemosphere, 46: 1163–1171.

Ward, C. R., French, D. 2006. Determination of glass content and estimation of glass composition in fly ash using quantitative X-ray diffratometry. Fuel, 85:2268-2277.

Warren, C. J., Dudas, M. J. J. 1985. Formation of secondary minerals in artificially weathered fly ash. Environ. Qual. 14, 405-410.

Warren, C. J., Dudas, M. J. 1984. Weathering processes in relation to leachate properties of alkaline fly ash. Environmental Quality, 19: 188-201.

White, A. F. 1984. Weathering characteristics of natural glass and influences on associated water chemistry. Journal of Non-Crystalline Solids, 67: 225-244.

White, S. C., Case, E. D. 1990. Characterization of fly ash from coal-fired power plants. Journal of Materials Science, 25: 5215–5219.

Wilbur, S. 2009. Universal Quantification-The Uncelebrated Strength of ICP-MShttp://spectroscopyonline.findanalytichem.com/spectroscopy/Atomic+Perspectives+Column/Universal-Quantification-mdash-The-Uncelebrated St/ArticleStandard/Article/detail/597218. Accessed on November 18, 2010.

Wittridge, N. J., Knutsen, R. D., Gerneke, D. A., Sewell, B. T. 2007. Application notes for the Leica S440 Scanning Electron Microscope at the Electron Microscope Unit, University of Cape Town, South Africa.

Xu, L., Guo, W., Wang, T., Yang, N. 2005. Study on fired bricks with replacing clay by fly ash in high volume ratio. Constr. Build. Mater., 19: 243–247.

Yan, J., Moreno, L., I. Neretnieks, I. 1999. The neutralization behavior of MSWI bottom ash on different reaction systems, Waste Management, 19: 339–347.

Yan, J., Neretnieks, I. 1995. Is the glass phase dissolution rate always a limiting factor in the leaching processes of combustion residues? The Science of the Total Environment, 172: 95-118.

Yeyehis, M. B., Shang, J. Q., Yanful, E. K. 2009. Chemical and mineralogical transformation of coal fly ash after land filling. World of Coal Ash (WOCA) Conference-May-4-7 in Lexington, KY, USA.

Yinghui, L., Chuguang, Z., Quanhai, W. 2008. Speciation of Most Volatile Toxic Trace Elements during Coal Combustion. Dev. in Chem. Eng. and Min. Proc., 11: 381-394.

Yuan, C. G. 2009. Leaching characteristics of metals in fly ash from coal-fired power plant by sequential extraction procedure. Microchim. Acta., 165:91-96.

Yunusa, I. A. M., Eamus, D., DeSilva, D. L., Murray, B. R., Burchett, M. D., Skilbek, G. C., Heidrich, C. 2006. Fly-ash: an exploitable resource for management of Australian agricultural soils. Fuel, 85: 2337–2344.

Zevenbergen, C., Bradley, J. P., van Reeuwijk, L. P., Shyam, A. K., Hjelmar, O., Comans, R. N .J. 1999a. Clay formation and metal fixation during weathering of coal fly ash. Environmental Science and Technology, 33: 3405–3409.

Zevenbergen, C., Bradley, J. P., van Reeuwijk, L. P., and Shyam, A. K. 1999b. Clay formation during weathering of alkaline coal fly ash. Paper no. 14. International Ash Utilization Symposium, Centre for Applied Energy Research, University of Kentucky.

Zevenbergen, C., van Reeuwijk L. P., Bradley, J. P., Comans, R. N. J., Schuiling, R. D. 1998. Weathering of MSWI bottom ash with emphasis on the glassy constituents. Journal of Geochemical Exploration, 62: 293-298.

Zevenbergen C., VanReeuwijk L. P., Bradley J. P., Bloemen P. and Comans R. N. J., 1996. Mechanism and conditions of clay formation during natural weathering of MSWI bottom ash. Clays and Clay Minerals, 44: 546-552.

Zevenbergen, C., Vander Wood, T., Bradley, J. P., Van Der Broeck, P. F. C. W. Orbons, A. J., Van Reeuwijk, L. P. 1994. Morphological and Chemical Properties of MSWI Bottom Ash with Respect to the Glassy Constituents. Hazardous Waste and Hazardous Materials, 11: 371-383.

Zhu, B., Alva, A. K. 1993. Distribution of trace metals in some sandy soils under citrus production. Soil Sci. Soc. Am. J., 57: 350–355.

Zielinski, R. A., Foster, A. L., Meeker, G. P., Brownfield, I. K. 2007. Mode of occurrence of arsenic in feed coal and its derivative fly ash, Black Warrior Basin, Alabama. Fuel, 86: 560-572.

Zikeli, S., Kastler, M., Jahn, R. 2005. Classification of anthrosols with vitric/andic properties derived from lignite ash. Geoderma, 124: 253–265.

Arsenic Standard: http://www.sos-arsenic.net/english/contamin/1.html of 2nd August, 2010.

http://www.chem.agilent.com/en-us/products/instruments/icp-ms/pages/gp455.aspx.Accessed October 5, 2009)

http://www.marscigrp.org/elconv.html. Accessed Aril 21, 2009

http://www.icr.org/article/origin-coal/. Accessed November 24, 2010

http://www.mbendi.com/indy/ming/coal/af/sa/p0005.htm#5. Accessed December 10, 2010

http://www.sierraclub.org/coal/downloads/Seleniumfactsheet.pdf. Accessed December 12, 2010

http://www.eskom.co.za/annreport09/abridged/index.html. Accessed February 9, 2011

APPENDIX

Appendix A. Analytical techniques

The various standard analytical techniques employed in this study are as follows; pH, EC and TDS measurements, X-ray fluorescence (XRF), Ion chromatography (IC); analytical spectroscopic techniques namely Induced coupled plasma optical emission spectroscopy (ICP-OES), Induced coupled plasma atomic emission spectroscopy(ICP-AES) and Induced coupled plasma mass spectroscopy (ICP-MS); X-ray diffraction (XRD), Fourier transform infra red spectroscopy (FT-IR), morphological technique which was mainly using scanning electron microscopy (SEM), and up flow percolation test (Column leaching test). In the following their working principles are discussed.

i. pH measurements

The pH of a solution is a measure of the hydrogen ion [H^+] concentration in solution which defines the acidity or alkalinity of the solution. It is measured on a continuous scale from 0 - 14. The scale is logarithmic. The pH value of a given solution is a measure of the activity of the hydrogen ion (H^+) in that solution.

Figure Ai. Hanna HI 991301 pH meter with portable pH/EC/TDS/Temperature probe.

The pH measurement involves comparing the potential of solutions with unknown hydrogen ion [H^+] to a known reference potential. This is done when the indicating electrode, which is sensitive to the hydrogen ion, develops a potential directly related to potential directly related to the hydrogen concentration in the solution, and the reference electrode provides a stable potential against which the indicating electrode can be compared. The pH meter converts the potential (voltage) ratio between a reference half-cell and an indicating half-cell to pH values. In acidic or alkaline solutions, the voltage on the outer membrane surface changes proportionally to changes in [H^+]. The pH meter detects the change in potential and determines [H^+] of the unknown sample (Fatoba, 2007). The pH of all the drilled core samples in this study was measured by using a Hanna HI 991301 pH meter with portable pH/EC/TDS/Temperature probe (Figure. Ai). The pH meter was calibrated before use with buffer solution of pH 4.0 and 7.0. Duplicate sample measurements were done at room temperature.

ii. Electrical conductivity (EC) measurement

Electrical conductivity measurements focuses on salts - or their ions when dissolved in water - which are conductors of an electrical current. Conductivity is measured by a probe that applies voltage between two electrodes, spaced a known distance apart, and records the drop in voltage. This drop reflects the resistance of the water, which is then converted to conductivity. Thus, conductivity is the inverse of resistance and is measured as the amount of conductance over a certain distance. Electrical conductivity is normally measured in mS/cm or μS/cm, or in μmhos/cm (1 mS/cm = 1000 μmhos/cm). The electrical conductivity (EC) measurement of the samples was determined using a Hanna HI 991301 pH meter with portable pH/EC/TDS/Temperature probe (Figure Ai). The meter was calibrated before use by using a standard of 12.88 mS/cm at room temperature. Duplicate samples measurements were taken at room temperature.

iii. Total dissolved solids (TDS)

Total dissolved solids (TDS) is an expression of the combined content of all inorganic and organic substances contained in a liquid which are present in a molecular, ionized or micro-granular (colloidal sol) suspended form (Fatoba, 2007). Electrical conductivity of water is directly related to the concentration of dissolved ionized solids in the water. Ions from the

dissolved solids in water create the ability for that water to conduct an electrical current, which can be measured using a conventional conductivity meter. When correlated with laboratory TDS measurements, electrical conductivity provides an approximate value for the TDS concentration, usually to within ten percent accuracy (Azzie, 2002). The total dissolved solids (TDS) of all the samples in this study were estimated using a Hanna HI 991301 pH meter with portable pH/EC/TDS/Temperature probe (Figure Ai). The pH meter was calibrated and duplicate samples measurements were taken at room temperature.

iv. Bulk chemical composition by X-ray fluorescence (XRF)

X-Ray fluorescence spectroscopy is one of the first commercially available instrumental techniques for elemental analysis. It is commonly used for the qualitative and quantitative elemental analysis of solid environmental, geological, biological, industrial and other samples. X-ray fluorescence (XRF) is the emission of characteristic secondary (or fluorescent) X-rays from a material that has been excited by bombarding with high energy X-rays or gamma rays.

Figure Aii. Phillips PANalytical pw1480 X-ray spectrometry using Rhodium tube as X-ray source.

An inner shell electron is excited by an incident photon in the X-ray region. Emission of the innermost electron leaves a vacancy in the inner shell. The vacancy created is filled by an electron from a higher shell. Its most important disadvantage is that analyses are usually restricted to elements heavier than fluorine and that a large sample is required (Kalnicky and Singhvi, 2001). Procedures for sample preparation vary considerably in the cases of in situ or intrusive measurements. Solid samples such as rock minerals must be polished to achieve surface homogeneity (uniform grain size), while powdery materials are usually pressed into pellets.

The XRF analysis was carried out according to the experimental procedure recognized in the study carried out by Akinyemi *et al.* (2011). The representative samples were taken at an interval of 1m depth along the drilled cores in Tutuka ash dumps. The fresh ash and drilled core samples were oven-dried at 100 °C for 12 hours to determine the adsorbed water prior to analysis, and pulverized to a uniform size grained powder. The powder samples were then mixed with a binder (ratio of 1: 9 in grams of C-wax and EMU powder) at a ratio of 2: 9 (2 gram binder and 9 gram sample). The powder mixture was then pelletized at a pressure of 15 Kbars for 1 minute. Loss on ignition experiment was performed prior to major element analysis and for accuracy of the analytical results. A Phillips PANalytical PW1480 X-ray fluorescence spectrometer using a Rhodium Tube as the X-ray source was used (Figure Aii). The technique reports concentration as % oxides for major elements and ppm for minor elements. Elements reported as % oxides were converted as % elements using element conversion software downloaded at www.marscigrp.org/elconv.html. The XRF analyses were done at the Geology department of the University of the Western Cape.

v. Mineralogical analysis quantitative and qualitative by X-ray diffraction (XRD)

In an X-ray diffraction measurement, a crystal is mounted on a goniometer and gradually rotated while being bombarded with X-rays, producing a diffraction pattern of regularly spaced spots known as reflections (Figure Aiii). The two-dimensional images taken at different rotations are converted into a three-dimensional model of the density of electrons within the crystal using the mathematical method of Fourier transforms, combined with chemical data known for the sample. The diffraction pattern is recorded and then analyzed or "solved" to reveal the character of the crystal. This analytical technique is extensively used in chemistry and biochemistry to determine the structures of an immense variety of molecules, as well as inorganic compounds,

DNA, and proteins. When single crystals are not obtainable, related investigative techniques such as powder diffraction or thin film x-ray diffraction together with lattice refinement algorithms for instance Rietveld refinement perhaps used to extort similar, though less complete, information about the character of the crystal. The spacing in the crystal lattice can be determined using Bragg's law ($n\lambda=2d\sin\theta$)**.** The electrons that surround the atoms, rather than the atomic nuclei themselves, are the entities that physically interact with the incoming X-ray photons. If the angles of incidence (θ) and the wavelength (λ) are known, the spacing d of the reflecting atomic planes can be determined using the above equation. The lattice spacing is characteristic of the mineral, thus, the X-ray diffraction method can be used for the identification of minerals and for the analysis of mixtures of minerals and hence it was used for this purpose in the study. X-ray diffraction is mainly used to describe the bulk mineralogy of the fly ash.

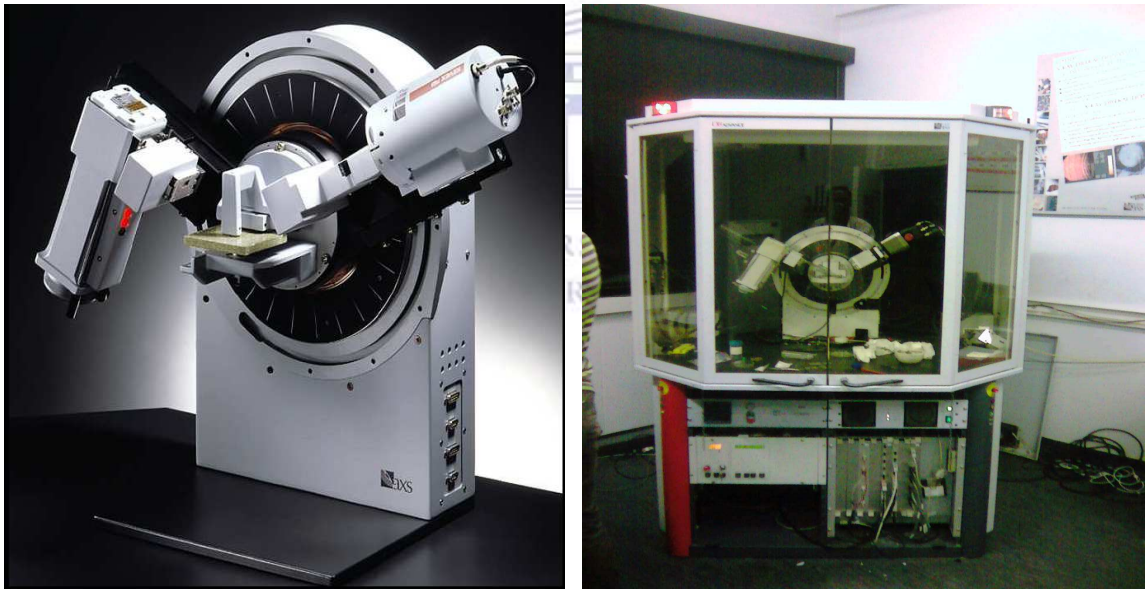

Figure Aiii. Phillips PANalytical XRD instrument with pw 3830 X-ray generator operated at 40 kV and 25 mA.

The mineralogical compositions of the fresh and drilled core ash samples were qualitatively determined according to the experimental procedure documented in the study carried out by Akinyemi *et al*. (2011). A Philips PANalytical instrument equipped with a pw 3830 X-ray generator operated at 40 kV and 25 mA was used (Figure Aiii). Both fresh ash (2-week-old) and weathered ash samples were oven dried at 105 ºC for 12 hours to remove the adsorbed water. The samples were pressed into rectangular aluminium sample holders using an alcohol wiped

spatula and then clipped into the instrument sample holder. The representative samples for different depths and ages were step-scanned from 5 to 85 degrees 2-theta-scale at intervals of 0.02 and counted for 0.5 seconds per step. The quantitative XRD analysis was carried out according to the following experimental procedure. After addition of 20 % (Aldrich 99.9 %) for quantitative determination of amorphous compounds, and micronizing in a McCrone micronizing mill, the fresh and 20-year-old core ash samples (taken at 9 m depth) were prepared for XRD analysis using a back loading preparation method. They were analysed with a PANalytical X'Pert Pro powder diffractometer with X'Celerator detector and variable divergence- and fixed receiving slits with Fe filtered Co-Kα radiation (located at XRD Analytical & Consulting, Pretoria, South Africa). The phases were identified using X'Pert Highscore plus software. The relative phase amounts (weight %) was estimated using the Rietveld method (Autoquan Program).

vi. Fourier Transform Infra-Red Analysis of drilled core samples

Infrared spectrometry (IR) is a standard analytical tool that utilizes the fact that chemical bonds between unlike atoms can absorb IR light and cause vibrations of the bonds. The IR wavelength absorbed is characteristic of a particular bond in a particular molecule or mineral and can be measured by an FT-IR spectrometer. The different functional groups (SO_4^{2-}, OH^-, NO_3^-, O-Si-O) can be identified in unknown material by comparison with published charts. Bond vibrations are of two main types; stretching vibrations in which the bond-length changes and bending (deformation) vibrations in which bond angles change. Most modern FT-IR instruments produce plots with wave number (units: cm^{-1}) on the abscissa and percent transmission (or absorbance) on the ordinate. The results were compared with published data for the purpose of identification of the functional groups. Fourier transform infrared (FTIR) emission spectroscopy is one technique that provides surface species information at high temperatures for both crystalline and amorphous phases (Griffiths and de Haeeth, 1986). Investigators have used this technique to investigate the structure of high temperature inorganic melts (Bates, 1978) and the thermal transformations of common coal minerals, including quartz, kaolinite, calcite, and anhydrite (Baxtar and Hardeety, 1992).

Figure Aiv. Perkin Elmer Spectrum 100 series (FT-IR spectrometer), Universal ATR accessory spectrometer.

The FT-IR analysis was done according to the procedure recognized in the study carried out by Akinyemi *et al*. (2011). The FT-IR analysis of all samples in this work was carried out on a Perkin Elmer Spectrum 100 series (FT-IR spectrometer), Universal ATR accessory spectrophotometer (located in the Chemistry Department, University of the Western Cape). Dried and powdered drilled core samples were pressed into a transparent diamond disc (Figure Aiv). Thereafter pressure was applied through force gauge and scanned 4 times over the wave number range 4000 cm^{-1} to 380 cm^{-1}. The results were compared with published data for the purpose of identification of the functional groups.

vii. Scanning electron microscopy-energy dispersion spectroscopy

As pointed out by Vassilev and Vassileva (2005a), Scanning Electron Microscopy (SEM) is one of the best and most widely used techniques for the chemical and physical characterization of fly ash. SEM, using a focused electron beam to scan the surface of a sample, generates a variety of signals. SEM images have a characteristic three-dimensional appearance due to the manner in which the images are created. It is useful for judging the surface structure and morphology of samples. Specimen beam interactions in the SEM produces a number of scattering events which may either be elastic or inelastic. For crystalline specimen, some of the elastically scattered

electrons are diffracted and may be back scattered to form a pattern on the phosphor screen strategically placed within the specimen chamber. In order to obtain a significant yield of the diffracted electrons, the specimen is tilted at a high angle (usually 70 º) with respect to the horizontal axis. The video image of the electron back scattered diffraction is captured using a computer containing a MATROX IP8 frame store. Once the pattern of the image has been captured, the position of at least 3 zones is marked and the software is indexed by the software routine. The pattern is then replotted and the results confirmed. The process allows for approximately 60 crystal orientations per hour (Wittridge et al., 2007).

The fly ash samples were oven-dried at 105 °C for 12 hours in preparation for the analysis. Aluminium SEM stubs were covered with carbon graphite glue, and a small amount of each sample was sprinkled onto the stub. Once the glue had dried, but still sticky; a small amount of powder was sprinkled onto the stub. The excess powder was tapped off, the stubs were coated with carbon in an evaporation coater; the glue was completely dried. Each sample was then mounted into specimen holders and the morphology, texture and chemistry of the samples were analyzed from backscattered electron as well as secondary electron images. The scanning electron microscope / electron dispersive x-ray spectroscopy (SEM / EDX) analysis was carried out with analytical Leica/Leo S440 Scanning Electron Microscope equipped with a Fissons Quantum EDS detector, using Sigma software. The samples were viewed at 20 KV at a working distance of about 25 mm and the EDS spectrum was collected over 60 seconds. And an FEI Nova Nano SEM 230(both instruments are located at Electron Microscope Unit, University of Cape Town, South Africa), equipped with an Oxford X- max detector and INCA software was used for the elemental analysis (quantitative work by energy dispersive X-ray analyses). The EDS analysis was carried out at 20 Kv and 5 mm working distance.

viii. Ion chromatography (IC)

Ion chromatography is a form of liquid chromatography where retention is predominantly controlled by ionic interactions between the ions of the solute and counter ions that are situated in, or on, the stationary phase. For example, to separate organic acids, it is the negatively charged acid ions that need to be selectively retained. It follows that the stationary phase must contain immobilized positively charged cations as counter ions to interact with the acid ions to retain them. Alternately, to separate cations, the stationary phase must contain immobilized anions as

counter ions with which the cations can interact (Fritz, 2005). Ion exchange stationary phases are available in mainly two forms. One form (probably the most popular) consists of cross-linked polystyrene polymer beads of an appropriate size which have been suitably treated to link ionic groups to the surface. The other form is obtained by chemically bonding ionic groups to silica gel by a process similar to that used to produce bonded phases. These materials are called ion exchange media, a term which has given rise to the term "ion exchange chromatography" as an alternative to ion chromatography.

Ionic substances can also be adsorbed on the surface of a reverse phase media and act as an adsorbed ion exchanger. The mobile phase is made to contain a small percentage of a soluble organic ionic material (e.g. tetrabutyl ammonium dihydrogen phosphate or n-octyl sulphonate). These substances are adsorbed onto the surface by dispersive interactions between the alkyl groups of the agent and those of the bonded phase and act as counter ions (Dionex, 1998). Ion chromatography is an analytical method of choice for inorganic anions and cations (Haddad, 2004). The instrument can separate and determine anions such as chloride, chlorate, nitrate, chromate sulfate, thiocyanate and perchlorate (Tyrell et al., 2009). It uses ion-exchange resins to separate atomic or molecular ions based on their interaction with the resin.

Figure Av. Ion chromatography system-Dionex ICS-1600 (RFIC).

Its greatest utility is for analysis of anions for which there are no other rapid analytical methods (Dionex, 1998). The instrument analyzes aqueous samples for quantities of common anions such as fluoride, chloride, nitrite, nitrate and sulphate in parts per million (ppm) and parts per billion (ppb) for common cations like lithium, sodium and potassium using conductivity detectors. The Ion Chromatography (IC) unit was first calibrated with a certified reference standard solution and then recalibrated after every 10 samples. Reference value of standards are: F = 20.07 mg/L; Cl = 30.04 mg/L; Br = 100.3 mg/L; NO_3 = 100.2 mg/L; NO_2 = 99.9 mg/L; PO_4^{3-} = 150.2 mg/L; SO_4^{2-} = 150.1 mg/L. Average values are: F = 20.05 mg/L; Cl = 29.95 mg/L; Br = 100.6 mg/L; NO_3 = 100 mg/L; NO_2 = 100.35 mg/L; PO_4^{3-} = 149.15 mg/L: SO_4^{2-} = 150.15 mg/L. Common application areas of IC include environmental analysis, clinical analysis, and industrial analysis, bio analysis (Haddad *et al*., 2008; Haddad, 2004) just to mention a few. The leachates of the fly ashes were filtered through a 0.45 μm membrane filter with the aid of a vacuum pump to remove suspended solids. SO_4^{2-}, Cl^-, NO_3^- and PO_4^{3-} were analyzed in the leachates using a Dionex DX-120 ion chromatograph with an Ion Pac AS14A column and AG14-4 mm guard column (located at Soil Science Department, University of Stellenbosch, South Africa) and Dionex ICS-1600 (Figure Av) (located at Chemistry Department, University of the Western Cape, South Africa).

ix. Inductively coupled plasma mass spectroscopy (ICP-MS)

ICP-MS originally was designed primarily to replace atomic absorption and ICP-optical emission instrumentation for analysis of metals in aqueous and organic matrices (Geiger and Raynor, 2009). The Inductively Coupled Plasma Mass Spectroscopy (ICP-MS) was introduced commercially in 1983 (Beauchemin, 2008), the basic design is still the same today. ICP-MS gives very high sensitivity for the determination of elements and it is good at separating isotopes of the same element. It is well-suited to detecting very small amounts of material, in the parts per billion (ppb) to the parts per trillion (ppt) range. The dynamic range is typically ten orders of magnitude and data reduction is relatively simple. Rapid data acquisition and data reduction enables the measurement of large numbers of samples in a short period of time. ICP-MS is the technique of choice for trace element analysis of natural waters, and can be used in analyzing minerals and rocks after digestion. One of the major short coming of ICP-MS technique is its susceptibility to matrix effects (Beauchemin, 2008).

Figure Avi. ICP Optical Emission Spectrometer (Varian 710-ES).

In general, liquid samples are introduced by a peristaltic pump (brings the liquid sample in at about 1 mL per minute), to the nebulizer where the sample aerosol is formed. A double-pass spray chamber ensures that a consistent aerosol is introduced into the plasma. Argon (Ar) gas is introduced through a series of concentric quartz tubes which form the ICP. The torch is located in the center of an RF coil, through which RF energy is passed. The intense RF field causes collisions between the Ar atoms, generating high-energy plasma. Thus, the ICP portion of the technique, or the "inductively coupled plasma" aspect, continues to supply radio frequency energy to the argon gas, forming more ions, and making more plasma. The sample aerosol is instantaneously decomposed in the plasma (plasma temperature is in the order of 6000-10000 K) to form analyte atoms which are simultaneously ionized (Wilbur, 2009). The ions produced are extracted from the plasma into the mass spectrometer region which is held at high vacuum (typically 10-4 Pa). The vacuum is maintained by differential pumping: the analyte ions are extracted through a pair of orifices known as sampling and skimmer cones. The analyte ions are then focused by a series of ion lenses into a quadrupole mass analyzer, which separates the ions based on their mass charge ration.

Finally, the ions are measured using an electron multiplier, and are collected for each mass number (http://www.chem.agilent.com/en-us/products/instruments/icp-ms/pages/gp455.aspx). In this study, samples to be analyzed were filtered with 45 µm membrane filter paper to remove

suspended solids and refrigerated before analysis. Major and trace elements were analyzed using ICP-OES (Varian 710-ES) (Figure Avi), ICP-AES (Varian Liberty) and ICP-MS (Agilent 7500 ce). The inductively coupled plasma mass spectrometry (ICP-MS) and the inductively couple plasma atomic emission spectrometry (ICP-AES) were calibrated twice daily using multi-element standards, with a calibration verification standard analyzed directly after the calibration and control standards for every 12 samples run by the ICP-MS and every 20 samples for the ICP-AES. Internal standards were used to correct for instrument drift in ICP-MS.

x. Up-flow percolation test (Column leaching test)

The test was carried out according to European standard method prEN14405 (prEN14405, 2003). This method involves packing the material to be tested in a column in a standardized manner (Fatoba, 2007), and the leachant is percolated in an up-flow direction through the column at a specified flow-rate to attain a fixed liquid/solid (L/S) ratios. This method was used to determine the release of constituents from fly ash packed in a column after a specific volume of leachant had percolated through it. A continuous vertical up-flow was used in this study so that the column would be properly saturated with the leachant and preferential percolation of the leachant would also be avoided. The method is designed to give insight into the components of solids (fly ash) that are readily soluble and would be easily washed away when ash contacts water, and evaluate the effect of possible secondary mineral formation on the release of species.